

Advances in Science, Technology & Innovation
IEREK Interdisciplinary Series for Sustainable Development

Mabrouk Boughdiri · Beatriz Bádenas · Paul Selden
Etienne Jaillard · Peter Bengtson · Bruno R. C. Granier *Editors*

Paleobiodiversity and Tectono-Sedimentary Records in the Mediterranean Tethys and Related Eastern Areas

Proceedings of the 1st Springer Conference of the
Arabian Journal of Geosciences (CAJG-1), Tunisia 2018

Advances in Science, Technology & Innovation

IEREK Interdisciplinary Series for Sustainable
Development

Editorial Board Members

Anna Laura Pisello
Dean Hawkes
Hocine Bougdah
Federica Rosso
Hassan Abdalla
Sofia-Natalia Boemi
Nabil Mohareb
Saleh Mesbah Elkaffas
Emmanuel Bozonnet
Gloria Pignatta
Yasser Mahgoub
Luciano De Bonis
Stella Kostopoulou
Biswajeet Pradhan
Md. Abdul Mannan
Chaham Alalouch
Iman O. Gawad

Series Editor

Mourad Amer

Advances in Science, Technology & Innovation (ASTI) is a series of peer-reviewed books based on the best studies on emerging research that redefines existing disciplinary boundaries in science, technology and innovation (STI) in order to develop integrated concepts for sustainable development. The series is mainly based on the best research papers from various IEREK and other international conferences, and is intended to promote the creation and development of viable solutions for a sustainable future and a positive societal transformation with the help of integrated and innovative science-based approaches. Offering interdisciplinary coverage, the series presents innovative approaches and highlights how they can best support both the economic and sustainable development for the welfare of all societies. In particular, the series includes conceptual and empirical contributions from different interrelated fields of science, technology and innovation that focus on providing practical solutions to ensure food, water and energy security. It also presents new case studies offering concrete examples of how to resolve sustainable urbanization and environmental issues. The series is addressed to professionals in research and teaching, consultancies and industry, and government and international organizations. Published in collaboration with IEREK, the ASTI series will acquaint readers with essential new studies in STI for sustainable development.

More information about this series at <http://www.springer.com/series/15883>

Mabrouk Boughdiri • Beatriz Bádenas
Paul Selden • Etienne Jaillard
Peter Bengtson • Bruno R. C. Granier
Editors

Paleobiodiversity and Tectono-Sedimentary Records in the Mediterranean Tethys and Related Eastern Areas

Proceedings of the 1st Springer Conference
of the Arabian Journal of Geosciences
(CAJG-1), Tunisia 2018

Editors

Mabrouk Boughdiri
Faculty of Sciences of Bizerte
University of Carthage
Amilcar, Tunisia

Beatriz Bádenas
Earth Science Department
University of Zaragoza
Zaragoza, Spain

Paul Selden
University of Kansas
Lawrence, KS, USA

Etienne Jaillard
University of Grenoble Alpes
Grenoble, France

Peter Bengtson
Institute of Earth Sciences
Heidelberg University
Heidelberg, Germany

Bruno R. C. Granier
University of Bretagne Occidentale
Brest, France

ISSN 2522-8714 ISSN 2522-8722 (electronic)
Advances in Science, Technology & Innovation
IEREK Interdisciplinary Series for Sustainable Development
ISBN 978-3-030-01451-3 ISBN 978-3-030-01452-0 (eBook)
<https://doi.org/10.1007/978-3-030-01452-0>

Library of Congress Control Number: 2018958939

© Springer Nature Switzerland AG 2019

This work is subject to copyright. All rights are reserved by the Publisher, whether the whole or part of the material is concerned, specifically the rights of translation, reprinting, reuse of illustrations, recitation, broadcasting, reproduction on microfilms or in any other physical way, and transmission or information storage and retrieval, electronic adaptation, computer software, or by similar or dissimilar methodology now known or hereafter developed.

The use of general descriptive names, registered names, trademarks, service marks, etc. in this publication does not imply, even in the absence of a specific statement, that such names are exempt from the relevant protective laws and regulations and therefore free for general use.

The publisher, the authors and the editors are safe to assume that the advice and information in this book are believed to be true and accurate at the date of publication. Neither the publisher nor the authors or the editors give a warranty, express or implied, with respect to the material contained herein or for any errors or omissions that may have been made. The publisher remains neutral with regard to jurisdictional claims in published maps and institutional affiliations.

This Springer imprint is published by the registered company Springer Nature Switzerland AG
The registered company address is: Gewerbestrasse 11, 6330 Cham, Switzerland

Preface

The Austrian geologist Eduard Suess (1831–1914) considered the Tethys Ocean as connecting eastern and southern Asia with the Middle East and Europe through the Himalayas. It persisted from mid-Permian and vanished in the Paleocene and was an epicontinental sea, transgressed and regressed frequently, covering northern India to southern Siberia, from the present Pacific coastal area to Italy. At least since the earliest Mesozoic, the Tethys and its shallow marine margins occupied dominant surfaces of the Earth. Their evolution implies major events in the history of our planet as the Tethys represented, mainly, one of the most important components of the global climatic system. Through times, organisms adapted to resistant or precarious ecosystems and their diversity are preserved within various sedimentary rocks now incorporated into mountain ranges issued from the Tethys. Paleontological and sedimentological studies supporting paleogeographic and paleoclimatic reconstructions are continuously evidencing various key events of the Tethys and Earth history. Paleobiogeographic distributions, determined by multiple geographically disparate samples spanning their time range, allow precise bio-stratigraphy and long-distance interregional correlations. Considerations of various sedimentary facies analyses and depositional environment reconstructions are required for paleogeographic interpretations and cross-checking interactions between the paleoenvironment components and possible mitigating discrepancies. Much of the evidence for the Tethys history of environmental change has been derived from detailed geological observations across North Africa and the Middle East, across Europe, and central and eastern Asia. Still, more findings can be gleaned from drilling into the sedimentary archives beneath the present day oceans.

This proceedings volume is based on the best papers accepted for presentation during the 1st Springer Conference of the Arabian Journal of Geosciences (CAJG-1), Tunisia 2018. The book offers new paleontological, biostratigraphic, and sedimentological studies by experienced researchers mainly from research institutes in the Mediterranean and Middle East region. Main topics include: palaeontology, biostratigraphy, sedimentology, paleoclimatology, and geomorphology. This volume gives new insights into paleobiodiversity and major biological tools for biostratigraphy, patterns, mechanisms, and processes of Meso-Cenozoic sedimentation in the Mediterranean and Middle East. Included are case studies which particularly highlight the major controlling factors of Tethyan biosphere-geosphere interactions as inferred from the Mediterranean and Middle East regions.

Amilcar, Tunisia
Zaragoza, Spain
Lawrence, USA
Grenoble, France
Heidelberg, Germany
Brest, France
July 2018

Mabrouk Boughdiri
Beatriz Bádenas
Paul Selden
Etienne Jaillard
Peter Bengtson
Bruno R. C. Granier

Acknowledgements

Our appreciation is extended to the authors of the papers for their hard and diligent work in producing high-quality contributions. We would like to thank the reviewers of the papers for their in-depth reviews and great efforts in improving the quality of the papers. Also, thanks are extended to Amjad Kallel who supervised and handled the evaluation process, to Sahbi Moalla who handled the submission and evaluation system for the ten conference proceedings volumes, and to the publishing staff of Springer headed by Nabil Khélifi, Senior Editor for their efforts and contributions in completing this conference proceedings volume. All the above-mentioned efforts were very important in making this book a success.

About the 1st Springer Conference of the Arabian Journal of Geosciences (CAJG-1), Tunisia 2018



The *Arabian Journal of Geosciences (AJG)* is a Springer journal publishing original articles on the entire range of Earth sciences in partnership with the Saudi Society for Geosciences. The journal focuses on, but not limited to, research themes which have regional significance to the Middle East, the Euro-Mediterranean, Africa, and Asia. The journal receives on average 2000 submissions a year and accepts around 500 papers for publication in its 24 annual issues (acceptance rate 25%). It enjoys the participation of an editorial team of 100 international associate editors who generously help in evaluating and selecting the best papers.

In 2008, Prof. Abdullah Al-Amri, in close partnership with Springer, founded the Arabian Journal of Geosciences (AJGS). In this year, the journal celebrates its tenth anniversary. On this occasion and to mark this event, the Founder and Editor-in-Chief of the AJGS Prof. Al-Amri organized in close collaboration with Springer the 1st Conference of the Arabian Journal of Geosciences (1st CAJG) in Hammamet, Tunisia, from November 12 to 15, 2018 (www.cajg.org).

The conference was an occasion to endorse the journal's long-held reputation for bringing together leading authors from the Middle East, the Euro-Mediterranean, Africa, and Asia who work in the wide-ranging fields of Earth sciences. The conference covered all cross-cutting themes of Geosciences and focused principally on the following ten tracks:

- Track 1. Climate, paleoclimate and paleoenvironmental changes
- Track 2. Geoinformatics, remote sensing, geodesy
- Track 3. Geoenvironmental engineering, geomechanics and geotechnics, geohazards
- Track 4. Geography, geoecology, geoarcheology, geotourism
- Track 5. Geophysics, seismology
- Track 6. Hydrology, hydrogeology, hydrochemistry
- Track 7. Mineralogy, geochemistry, petrology and volcanology
- Track 8. Petroleum engineering and petroleum geochemistry
- Track 9. Sedimentology, stratigraphy, palaeontology, geomorphology, pedology
- Track 10. Structural/petroleum/mining geology, geodynamics, marine geology

The dynamic four-day conference provided more than 450 attendees with opportunities to share their latest unpublished findings and learn the newest geoscience studies. The event also allowed attendees to meet and discuss with the journal's editors and reviewers.

More than 950 short contributing papers to the conference were submitted by authors from more than 70 countries. After a pre-conference peer review process by more than 500 reviewers, 700 papers were accepted. These papers were published as chapters in the conference proceedings by Springer.

The conference proceedings consist of ten edited volumes, each edited by the following group of *Arabian Journal of Geosciences* (AJGS) editors and other guest editors:

Volume 1. Patterns and Mechanisms of Climate, Paleoclimate, and Paleoenvironmental Changes from Low-Latitude Regions

Zhihua Zhang (AJGS Editor): Beijing Normal University, Beijing, China

Nabil Khélifi (AJGS Editor): Earth Sciences Editorial Department, Springer, Heidelberg, Germany

Abdelkader Mezghani (Guest Editor): Norwegian Meteorological Institute, Norway

Essam Heggy (Guest Editor): University of Southern California and Jet Propulsion Laboratory, Caltech, USA

Volume 2. Advances in Remote Sensing and Geo Informatics Applications

Hesham M. El-Askary (Guest Editor): Schmid College of Science and Technology at Chapman University, USA

Saro Lee (AJGS Editor): Korea Institute of Geoscience and Mineral Resources, Daejeon, South Korea

Essam Heggy (Guest Editor): University of Southern California and Jet Propulsion Laboratory, Caltech, USA

Biswajeet Pradhan (AJGS Editor): University of Technology Sydney, Sydney, Australia

Volume 3. Recent Advances in Geo-Environmental Engineering, Geomechanics and Geotechnics, and Geohazards

Amjad Kallel (AJGS Editor): ENIS, University of Sfax, Tunisia

Zeynal Abiddin Erguler (AJGS Editor): Dumlupinar University, Kutahya, Turkey

Zhen-Dong Cui (AJGS Editor): China University of Mining and Technology, Xuzhou, Jiangsu, China

Ali Karrech (AJGS Editor): The University of Western Australia, Australia

Murat Karakus (AJGS Editor): University of Adelaide, Australia

Pinnaduwa Kulatilake (AJGS Editor): Department of Materials Science and Engineering, The University of Arizona, USA

Sanjay Kumar Shukla (AJGS Editor): School of Engineering, Edith Cowan University, Perth, Australia

Volume 4. Exploring the Nexus of Geocology, Geography, Geoarcheology and Geotourism: Advances and Applications for Sustainable Development in Environmental Sciences and Agroforestry Research

Haroun Chenchouni (AJGS Editor): University of Tebessa, Algeria

Ezzoura Errami (Guest Editor): Chouaib Doukkali University, El Jadida, Morocco

Fernando Rocha (Guest Editor): University of Aveiro, Portugal

Luisa Sabato (AJGS Editor): Università degli Studi di Bari "Aldo Moro", Bari, Italy

Volume 5. On Significant Applications of Geophysical Methods

Narasimman Sundararajan (AJGS Editor): Sultan Qaboos University, Muscat, Oman

Mehdi Eshagh (AJGS Editor): University West, Trollhättan, Sweden

Hakim Saibi (AJGS Editor): United Arab Emirates University, Al-Ain, Abu Dhabi, UAE

Mustapha Meghraoui (AJGS Editor): Université de Strasbourg, Strasbourg, France

Mansour Al-Garni (AJGS Editor): King Abdulaziz University, Jeddah, Saudi Arabia

Bernard Giroux (AJGS Editor): Centre Eau Terre Environnement, Québec, Canada

Volume 6. Advances in Sustainable and Environmental Hydrology, Hydrogeology, Hydrochemistry and Water Resources

Helder I. Chaminé (AJGS Editor): School of Engineering (ISEP), Polytechnic of Porto, Portugal

Maurizio Barbieri (AJGS Editor): University of Rome La Sapienza, Italy

Ozgur Kisi (AJGS Editor): Ili State University, Tbilisi, Georgia

Mingjie Chen (AJGS Editor): Sultan Qaboos University, Muscat, Oman

Broder J. Merkel (AJGS Editor): TU Bergakademie Freiberg, Freiberg, Germany

Volume 7. Petrogenesis and Exploration of the Earth's Interior

Domenico Doronzo (AJGS Editor): Consejo Superior de Investigaciones Científicas, Spain

Emanuela Schingaro (AJGS Editor): Università degli Studi di Bari Aldo Moro–UniBa, Italy

John S. Armstrong-Altrin (AJGS Editor): The National Autonomous University of Mexico, Mexico

Basem Zoheir (Guest Editor): Benha University, Egypt and University of Kiel, Germany

Volume 8. Advances in Petroleum Engineering and Petroleum Geochemistry

Santanu Banerjee (AJGS Editor): Indian Institute of Technology Bombay, Mumbai, India

Reza Barati (AJGS Editor): The University of Kansas, Lawrence, KS, USA

Shirish Patil (Guest Editor): Saudi Aramco and King Fahd University of Petroleum and Minerals, Dhahran, Saudi Arabia

Volume 9. Paleobiodiversity and Tectono-Sedimentary Records in the Mediterranean Tethys and Related Eastern Areas

Mabrouk Boughdiri (AJGS Editor): University of Carthage, Amilcar, Tunisia

Beatriz Bádenas (AJGS Editor): University of Zaragoza, Zaragoza, Spain

Paul Selden (AJGS Editor): University of Kansas, Lawrence, KS, USA

Etienne Jaillard (Guest Editor): University of Grenoble Alpes, France

Peter Bengtson (AJGS Editor): University of Heidelberg, Heidelberg, Germany

Bruno R. C. Granier (AJGS Editor): University of Bretagne Occidentale, Brest, France

**Volume 10. The Structural Geology Contribution to the Africa-Eurasia Geology:
Basement and Reservoir Structure, Ore Mineralisation and Tectonic Modelling**

Federico Rossetti (Guest Editor): Università Roma Tre, Roma, Italy

Ana Crespo Blanc (Guest Editor): University of Granada, Spain

Federica Riguzzi (Guest Editor): National Institute of Geophysics and Volcanology, Roma, Italy

Estelle Leroux (Guest Editor): IFREMER, Unité Géosciences Marines, Plouzané, France

Kosmas Pavlopoulos (Guest Editor): Sorbonne University Abu Dhabi, Abu Dhabi, UAE

Olivier Bellier (Guest Editor): CEREGE, Aix-en-Provence, France

Vasilios Kapsimalis (Guest Editor): Institute of Oceanography, Hellenic Centre for Marine Research, Anavyssos, Greece

About the Conference Steering Committee

General Chair



Abdullah Al-Amri: Founder and Editor-in-Chief of AJGS, King Saud University, Saudi Arabia

Conference Supervisor



Nabil Khélifi: Senior Publishing Editor, Springer Middle East and North African Program Springer, a part of Springer Nature, Heidelberg, Germany

Scientific Committee Chair

François Roure: Guest of Editorial Board of AJGS, IFP—
Energies Nouvelles, France



Walter D. Mooney: Guest of Editorial Board of AJGS, US
Geological Survey Western Region, USA

Local Organization Chair

Mabrouk Boughdiri: Associate Editor of AJGS, University of
Carthage, Amilcar, Tunisia

Evaluation Chair



Amjad Kallel: Assistant Editor of AJGS, ENIS, University of Sfax, Tunisia

Publication Chair



Biswajeet Pradhan: Associate Editor of AJGS, University of Technology Sydney, Sydney, Australia



Essam Heggy: Guest of Editorial Board of AJGS, University of Southern California and Jet Propulsion Laboratory, Caltech, USA

Program Chair

Hakim Saibi: Associate Editor/Assistant Editor of AJGS, United Arab Emirates University, Al-Ain, Abu Dhabi, UAE



Domenico Doronzo: Associate Editor/Assistant Editor of AJGS, Consejo Superior de Investigaciones Cientificas, Spain

Communication Chair

Mohamed Ksibi: Guest of Editorial Board of AJGS, ISBS, University of Sfax, Tunisia

English Language Advisory Committee

Abdelmajid Dammak: ENIS, University of Sfax, Tunisia

Chokri Khalaf: FMS, University of Sfax, Tunisia

Dhouha Mabrouk: FLSHS, University of Sfax, Tunisia

Mohamed Elbahi: ENIS, University of Sfax, Tunisia

Sami Shami: ENIS, University of Sfax, Tunisia

Yasmine Basha: FLSHS, University of Sfax, Tunisia

Conference Manager



Mohamed Sahbi Moalla: Coordinator of AJGS, ISET,
University of Sfax, Tunisia

Contents

Part I Keynote

- Phanerozoic Global Sea-Level Changes: Evidences from Tunisia
Illustrating how Eduard Suess' Concepts (Gondwana, Tethys, Eustasy)
are Still Relevant** 3
Mohamed Soussi
- Facies Architecture in Carbonate Ramps: Learned Lessons from Jurassic
Cases Studies in the Iberian Basin** 7
Beatriz Bádenas
- An Early Anthropocene Analog: The Geomorphology and Hydrology
of the Rio Bravo Watershed in the Belize Tropics** 11
Tim Beach, Sheryl Luzzadder-Beach, Samantha Krause, and Colin Doyle

Part II Palaeontology—Systematics

- Similarity Analysis of Ostracoda Faunas in West-Tethyan During
the Upper Pliensbachian-Lower Toarcian** 17
Choukri Soulimane, Abbas Marok, and Matías Reolid
- Cladistic approach for phylogenetic reconstruction testing the subfamily
Reineckiinae (Saida, western Algeria)** 21
Fatiha Douas Bengoudira, Abdia Touahria, and Abbes Sebane
- Rudists in the Revised Bivalvia ‘*Treatise Online*’** 25
Peter W. Skelton, Eulàlia Gili, Thomas Steuber, Robert Scott, and Simon Mitchell
- Morphological variability of *Polyconites hadriani* (Hippuritida, Bivalvia)
in the Aptian carbonate platforms of the western Maestrat Basin,
eastern Iberia** 29
Eulàlia Gili, Enric Pascual-Cebrian, Peter W. Skelton,
and Telm Bover-Arnal
- Description of a New Genus of Radiolitidae (Bivalvia, Hippuritida)
with Canals in the Calcitic Shell Layer** 33
Valentin Rineau and Loïc Villier
- Similarities and Differences of *Orbitoides* & *Omphalocyclus* Microspheric Forms
with Selected Examples from Northern Iraq and Turkey and Their New
Morphometric Data** 37
Muhittin Görmüş, Qahtan Ahmed Al Nuaimy, and Engin Meriç
- Cretaceous *Paleodictyon* Trace Fossils: Evolutionary Mimicry Tactic
Versus Burrowing: Examples from the Kurdistan Region,
Northeastern Iraq** 41
Kamal Haji Karim and Polla Azad Khanaqa

First Titanosauriform Teeth from the Early Cretaceous of Tunisia	45
Jihed Dridi	
Mesopelagic Fish Size Reduction in Response to the Messinian Salinity Crisis	49
Konstantina Agiadi	
Middle Miocene <i>Giraffokeryx</i> (Giraffidae) with Marks of Enamel Hypoplasia from Dhok Bun Amir Khatoon, Punjab, Pakistan	53
Muhammad Akbar Khan and Muhammad Asim	
Dental Morphology and Palaeoecological Implications of <i>Brachypotherium</i> (Rhinocerotidae) of the Middle Miocene Siwaliks (Pakistan)	57
Amtur Rafeh, Abdul Majid Khan, Rana Manzoor Ahmad, and Muhammad Akhtar	
Systematic Study of the New Remains of <i>Propotamochoerus Hysundricus</i> (Suidae, Mammalia) from the Late Miocene-Early Pliocene Middle Siwaliks (Pakistan)	61
Sadaf Aslam, Abdul Majid Khan, Rana Manzoor Ahmad, Ayesha Iqbal, and Muhammad Akhtar	
Systematics and Palaeo-Environmental Implications of <i>Hexaprotodon Sivalensis</i> (Hippopotamidae, Mammalia) from the Plio-Pleistocene Upper Siwaliks (Pakistan)	65
Ayesha Iqbal, Abdul Majid Khan, Rana Manzoor Ahmad, Muhammad Akbar Khan, and Muhammad Akhtar	
Part III Biostratigraphy	
Bajocian Ostracods from the Krachoua Formation (Beni Kheddache, Southern Tunisia): Implications for Biostratigraphy and Paleocology	71
Lassad Tiss, Khaled Trabelsi, and Fekri Kammoun	
Paleobathymetric Influence on the Distribution of Ammonite and Foraminifer Settlements in the Callovian of the Saïda Region (Western Algeria)	75
Abdia Touahria and Abbes Sebane	
First Calpionellid Biozonation of the Berriasian Reference Section of Jebel Ben Younes (Gafsa Basin, South Central Tunisia): Updated Age Attribution and Geodynamic Consequences	79
Rafika Ferchichi, Ichrak Cherif, Mabrouk Boughdiri, Sana Ben Nsir, Néjib Bahrouni, and Mohamed Faouzi Zagrarni	
Berriasian Ammonite and Calpionellid Associations from the North-South Range of Central Tunisia: Updated Biozonation, Regional Geodynamic Context and Paleobiogeography	83
Sana Ben Nsir, Mabrouk Boughdiri, Ichrak Cherif, Néjib Bahrouni, Rafika Ferchichi, and Asma Zrelli	
Barremian-Albian (Lower Cretaceous) Rudist Chronostratigraphy, Caribbean Province North America	87
Robert Scott, Whitney Campbell, Brian Diehl, Xin Lai, Allison Porter, and Yulun Wang	
Mid-Cretaceous Rudist Assemblage from the Lhasa Block, Tibet (China)	91
Xin Rao, Peter W. Skelton, Shin-ichi Sano, Jingeng Sha, and Bin Wan	
Tethyan Non-rudist Associations from the Cretaceous Rudist Formations in Northern Egypt	95
Yasser Salama and Gouda Abdel-Gawad	

New Biostratigraphic Scheme from the Cenomanian-Turonian of South Algeria	99
Madani Benyoucef, Djamila Zaoui, Mohammed Adaci, Mohamed Lassad Guendouz, Abdelkader Mennad, and Mustapha Bensalah	
Ostracods of the Cenomanian-Turonian Transition (<i>Whiteinella archaeocretacea</i> Zone) in the Ksour and Amour Mountains (Saharan Atlas, Algeria): Paleobiogeographic Implication	103
Mustapha Benadla, Abbas Marok, and Matías Reolid	
Cenomanian Foraminiferal Biostratigraphy of the Aures Basin (Northeastern Algeria)	107
Aida Bensekhria, Ramdane Marmi, and Abdelouahab Yahiaoui	
An Integrated Biostratigraphy of the Cenomanian-Turonian Transition at Kasserine Area in Central Tunisia: Implication from Khanguet Esslougui Section	113
Zaineb Elamri, Sherif Farouk, and Doha Alouani	
Micropaleontological Study of the Contact Between Kometan and Shiranish Formations from Dokan Area, Northern Iraq	117
Ibrahim Al-Shareefi, Omar Al-Badrani, and Aseel Yousif	
Planktonic Foraminiferal Evidence of Upper Cretaceous in the Well “A” (Gulf of Hammamet Area, Northeastern Offshore Tunisia)	121
Ezzedine Saïdi and Dalila Zaghib-Turki	
Paleocene Benthic Foraminifera and <i>Neoeponides duwi</i> Event from Dineigil Area, South-Western Desert, Egypt	125
Mohamed Youssef	
Upper Eocene (Priabonian) Larger Foraminifera from the Deh-Rashti Section, Rafsanjan City, Southeastern Iran	129
Tayebeh Ahmadi	
The Tortonian–Messinian Transition in Saïs basin, South Rifian corridor (Morocco), Biostratigraphical and Paleoenvironmental Implications	133
Soukaina Targhi, Nadia Barhoun, Naima Bachiri Taoufiq, Mohamed Achab, and Abdallah Ait Salem	
Early Pliocene Gastropods of Southern Pacific Coast of Mexico: Taxonomy and Paleogeography	137
Catalina Gómez-Espinosa, Claudia Ortiz-Jerónimo, Luis Antonio Flores-de-Bois, and Oscar Talavera-Mendoza	
Composition of the Pliocene Meiofauna from Punta Maldonado Formation, Guerrero (Mexico)	141
Frank Raúl Gío-Argaez, Catalina Gómez-Espinosa, Luis Antonio Flores-de-Bois, Delfina Cruz-Flores, and Sergio Salgado-Souto	
Part IV Sedimentology	
Gravel Bed River Scouring Analysis Downstream of Block Ramps	147
Karol Plesiński and Artur Radecki-Pawlik	
Diagenesis and Reservoir Quality of Glacio-Lacustrine Sandstones: An Example from the Upper Carboniferous-Lower Permian Al Khlata Formation in Wadi Daïqa, Northern Oman	151
Mohamed A. K. El-Ghali, Nasayaba Al-Hinai, Kothar Mandhari, and Junaid Khan	

Stromatolitic Origin of Laminar Crusts in Palustrine Environments (Pleistocene of Borj Edouana Unit, Northwestern Tunisia)	155
Ildefonso Armenteros, Naoufel Ghannem, and Kamel Regaya	
Sedimentary Characteristics of the Fourth Member of Cretaceous Nenjiang Formation in the Southern Songliao Basin, Northeast of China	159
Jinkai Wang, Jinliang Zhang, and Jun Xie	
The Dolomitization in the Deltaic System of Meloussi Formation (Upper Berriasian-Valanginian) in Jebel Meloussi (Central Tunisia)	163
Najwa Khlifi, Jamel Tourir, and Anna Travé	
Integrated Sequence Stratigraphy of the Middle Jurassic (Bajocian-Callovian) Chiltan Formation in the Lower Indus Basin, Pakistan	167
Sajjad Ahmad, Abdul Wahab, Suleman Khan, Muhammad Sadiq, Kamil Qureshi, and Zaid Khan	
Factors Controlling Oncoid Distribution in the Inner Areas of a Late Kimmeridgian Carbonate Ramp (Northeast Spain)	171
Cristina Sequero, Beatriz Bádenas, and Marcos Aurell	
Diagenetic Evolution of Upper Jurassic-Lower Cretaceous Berdiga Formation, NE Turkey: Petrographic and Geochemical Evidence	175
Merve Özyurt, Ihsan S. Al-Aasm, and M. Ziya Kirmaci	
Rudist Mud Mounds and Biostromes from Upper Cretaceous of Istria (Croatia)	179
Alan Moro, Alceo Tarlao, and Giorgio Tunis	
Early Cretaceous Oceanic Anoxic Events in Rudist-Bearing Succession, North Egypt	183
Yasser Salama and Gouda Abdel-Gawad	
Late Cretaceous Transgressive-Regressive Cycles Including Rudist-Rich Units in Central Tunisia	187
Mohamed Hédi Negra and Jalel Jaballah	
Sedimentology and Petrophysics of Turonian-Coniacian Rudist Rich-Reservoir Rocks, Offshore Tunisia	191
Senda Boughalmi, Mohamed Hédi Negra, Yves Géraud, Sonia Ben Alaya, and Danièle Grosheny	
Depositional Facies, Sequence and Diagenesis of the Middle-Upper Eocene in Jebel Cherahil (Central Tunisia)	195
Zahra Njahi-derbali and Jamel Tourir	
Paleozoic Reservoir Systems in the Ghadames and Jefarah Basins, Tunisia	199
Adel Jabir, Adrian Cerepi, Corinne Loisy, and Jean-Loup Rubino	
The Albian-Cenomanian Transition in Central Tunisia: Insights from Jebel Mrhila	203
Etienne Jaillard, Jean-Louis Latil, and Naser Raisossadat	
Sequence Stratigraphic Analysis of the Middle Paleocene-Middle Eocene in the Sulaimani District (Kurdistan Region), North Iraq	207
Fadhil Ameen and Fawzi Mardan	
Palynological study of the Pliensbachian-Toarcian transition of the Traras Mountains (northwestern Algeria)	211
Louisa Samar, Abbas Marok, and Choukri Soulimane	

Stratal Geometries and Patterns: A New Lower-Upper Cretaceous Depositional Model of the Levant Shelf, Syria	217
Hussam Ghanem and Hans-Joachim Kuss	
Foraminiferal and Geochemical Input to OAE 2 Event at Jebel Bou Arif (Aures, Eastern Algeria)	221
Abdia Touahria, Abdelmoumen Garah, Abbes Sebane, and Fatiha Hadji	
Carbonate Deposit Microfacies and Carbonatogenesis of Abiod Formation (Campanian/Maastrichtian) in Jebel Kebar (Central Tunisia)	225
Manel Zidi, Jamel Tourir, Frédéric Boulvain, and Abderrazak El Albani	
The Eocene–Oligocene Climate Transition in the Southern Tethys: Calcareous Nannofossil Response and Element Geochemistry	229
Jihede Haj Messaoud, Chokri Yaich, Johannes Monkenbusch, and Nicolas Thibault	
Sedimentology and Geochemistry of the Chouabine Phosphate Succession (Upper Paleocene-Lower Ypresian) in El Guettar Area (Gafsa Region, Central Tunisia)	233
Wejdène Slimène, Jamel Tourir, Lotfi Khélil, Zied Saiid, and Nabil Fatteh	
Thin-Bedded Turbidites of the Numidian Flysch, North Africa and Southern Europe	237
Dorrik Stow, Sami Riahi, Bouabdellah Menzoul, Urval Patel, Bayonle Omoniyi, and Melissa Johansson	
Deepwater Sediment Facies and Sole Marks of the Numidian Flysch, Algeria	241
Bouabdellah Menzoul, Dorrik Stow, Mohammed Adaci, Miloud Benhamou, Hicham Mahdjoub Araibi, Mustapha Bensalah, and Madani Benyoucef	
Part V Tectonics and Sedimentation	
Evaluation of Sediment Transport Rate of the Kizilirmak River Basin on the Tectonically Active North Anatolian Fault Zone (NAFZ), Turkey	247
Gulcan Sarp	
Paleoseismological Indices Recognized in the Great Kabylia Region (Algeria)	251
Nadia Sidi Said, Azzeddine Benhamouche, Sahra Aourari, Djamel Machane, and Sid Ali Kechid	
New Insights of the Early Cretaceous Syn-Rift Sedimentation in the Mecella Structure (Northeastern Atlas of Tunisia): Geodynamic Evolution	255
Nejla Sekatni Aïch and Mohamed Gharbi	
The Main Late Cretaceous Tectonic Episodes Controlling the Deposition of Rudist-Rich Platform Carbonates in Central Tunisia	259
Jalel Jaballah and Mohamed Hédi Negra	
Lower Albian Sequence Stratigraphy of the South Tethyan Margin: The Tajerouine Area, Tunisia	263
Abir Chihaoui, Etienne Jaillard, and Jean-Louis Latil	
Stratigraphic Differentiation of the Zagros Foreland Basin Sequence, Kurdistan Region, (Northern Iraq): Impacts on Oil Accumulations	267
Basim Al-Qayim	

Paleogene Calciclastic Deposits in Southern Tunisia	271
Moez Ben Fadhel, Mohsen Henchiri, Njoud Gallala, Rim Zammali, Ahlem Amri, Asma Chermiti, and Mohamed Ben Youssef	
Lower to Middle Miocene Deposits of North-East Tunisia: Implied Facies Evolution and Tectonic-Sedimentary Control	275
Nadia Gaaloul, Wissal Ghazzay, and Saloua Razgallah	
Geologic Origins of the North American Shale-Gas Revolution: Can it Happen Elsewhere?	279
Frank R. Ettensohn	
Part VI Geomorphology—Quaternary Geology	
Thermodynamic Consideration on Volcanic Landforms	285
Naoto Kaneko and Hiroyuki Nagahama	
Quantitative Study of the Geomorphic Evolution of Shilin County, Yunnan Province, China, Based on Classic Theory and Method	289
Yuhui Li and Zhiqiang Ding	
Karst Landforms as Possible Lithological and Paleo-Climatic Markers in an Unnamed Crater in Northern Sinus Meridiani, Mars	293
Davide Baioni	
Boron Characterization and Distribution in Particle-Size Fractions Separated from a Semi-arid Tunisian Soil	297
Ahlem Tlili, Imene Dridi, Rafla Attaya, and Moncef Gueddari	
A Study of Ammonium Adsorption on Clay Soil (Siliana, Northern Tunisia)	301
Manel Allani, Abdessatar Hatira, and Hatem Ibrahim	
Assessing Heavy Metal Distribution and Contamination of Soil in Ogere Trailer Terminal, Ogun State (Southwestern Nigeria)	305
Olutoyin Adeola Fashae, Adeyemi Oludapo Olusola, and Paulina Orekan	
Spectroscopic and Chromatographic Characterization of the Composition of Organic Matter in Arid Salt-Affected Soils Under Different Vegetation Cover, Southeastern Tunisia (Gabes and Medenine)	309
Zohra Omar, Abdelhakim Bouajila, Jalloul Bouajila, Rami Rahmani, Houda Besser, and Younes Hamed	
Soil Salinity Dynamic and Water Quality in a Ramsar Saline Inland Wetland: Case Study—Bazer-Sakra Sabkha, Setif (North-East Algeria)	315
Yacine Louadj, Ahcene Semar, Salah Belghemmaz, Nasser-Eddine Soualili, and Nazim Soualili	
Impact of Catchments Morphology and Lithology on Stream Channels System in High Mountains of Arid Zone (Example of High Atlas, Morocco)	319
Elżbieta Rojan, Maciej Dłuzewski, Joanna Rotnicka, Kazimierz Krzemien, Lukasz Kokosinski, and Ewelina Niklas	
Classification and Prediction of Channel Morphology Within Selected Third-Order Basins (Southwestern Nigeria)	323
Adeyemi Oludapo Olusola, Olutoyin Adeola Fashae, and Adetoye Faniran	
Pool and Riffle Sequences and Morphology of Lower Alaknanda River in Srinagar Valley (Garhwal Lesser Himalaya), India	327
Sapna Semwal and Devi Datt Chauniyal	

Quaternary Fluvial Terraces of the Oued El Gourzi (Batna, NE Algeria): Sedimentology and Characteristics of the Depositional Environment	331
Fouad Djaiz, Nabil Defafli, Bachir Lamouri, Abdallah Boushaba, and Imen Chairat	
Characterization of Sand Particles in Arid Areas	335
Abdulsalam Alhazza, Shorouq Ahmad, and Ali Al-Dousari	
Aeolian Sand Transport Rate Over Windward and Lee Slopes of Small Reversing Dunes, Southern Morocco	339
Maciej Dłuzewski and Joanna Rotnicka	
Grain Size Analysis for the Study of Wave Energy in the Vicinity of Breakwaters: Case of the Coast of Ain Taya (Algiers)	343
Mohamed Bouhmadouche, Yacine Hemdane, and Farid Atroune	
Recent Geochemical and Grain Size Distribution of Terrestrial Sediment in Coastal Area from the Watershed of Medjerda River, Gulf of Tunis	347
Thouraya Benmoussa, Oula Amrouni, Laurent Dezileau, Gil Mahé, Domenico Chiarella, and Saâdi Abdeljaouad	
Multidisciplinary Approaches for the Study of Sediment Discharges to the Mediterranean Sea to Mitigate the Impact of Climate and Anthropogenic Activities on Coastal Environments	353
Oula Amrouni, Gil Mahé, Saâdi Abdeljaouad, Hakim Abichou, Abdallah Hattour, Nejmeddine Akrouf, Chrystelle Bancon-Montigny, Thouraya Benmoussa, Kerim Ben Mustapha, Lassâad Chouba, Domenico Chiarella, Michel Condomines, Laurent Dezileau, Claudine Dieulin, Nadia Gaaloul, Ahmed Ghadoum, Abderrouf Hzami, Nabil Khelifi, Samia Khsiba, Fatma Kotti, Mounir Medhioub, Hechmi Missaoui, François Sabatier, Alberto Sánchez, Alessio Satta, Abdelaziz Sebei, and Wième Ouertani	

About the Editors



Prof. Mabrouk Boughdiri holds a B.Sc. in Geology (1988) from El Manar University of Tunis (Tunisia), a M.Sc. in Palaeontology and Stratigraphy (1989) from the Bourgogne University of Dijon (France), a Ph.D. in Palaeontology and Stratigraphy (1994) from the Claude Bernard University of Lyon (France) and a Habilitation in Geology (2006) from El Manar University of Tunis. He is currently a Professor of Palaeontology and Stratigraphy and the Chair of the Doctorate Commission at the Faculty of Sciences of Bizerte (University of Carthage, Tunisia). He is also the President of the Tunisian National Commission of Geological Sciences, the President of the National Commission of Co-built LMD formation at Tunisian universities and the President of the Tunisian Association of Palaeontology and Stratigraphy. Since 2008, he has been a voting member of the International Commission of Stratigraphy (Subcommission of Jurassic Stratigraphy) and, until 2016, an active member of the international Berriasian Working Group for the Jurassic-Cretaceous boundary at the International Subcommission on Cretaceous Stratigraphy (ISCS). He has received one national prize and two international awards for scientific excellence. His research interests focus on Upper Jurassic-Lower Cretaceous ammonite, calpionellid and radiolarian palaeontology, biostratigraphy and paleobiogeography, mainly from the South-Tethyan Margin of the Maghreb and neighboring provinces. He has participated in (and conducted) many national and international research projects, the most recent of which involved comparative Jurassic bio-, chemo-, and magnetostratigraphy of the Iberian Peninsula and the Maghreb. He has co-published many research articles in international indexed and refereed journals and chaired and/or co-organized four international thematic meetings. In 2015, he joined the AJGS as an Associate Editor responsible for evaluating submissions in the fields of Palaeontology and Life History.



Dr. Beatriz Bádenas obtained a 5-year B.Sc. in Geology (1991) and a Ph.D. in Stratigraphy (1999) at the Earth-Science Department of the University of Zaragoza (Spain), where she teaches courses in Stratigraphy and Sedimentology since 1998. Her research interests mainly focus on Sedimentology and Sequence and cyclostratigraphic analyses of marine carbonate sediments, with special emphasis on sedimentary processes and facies heterogeneities from coastal to hemipelagic sediments. She is currently working in a multidisciplinary research project on the palaeoenvironmental reconstructions of the Jurassic and Cretaceous in the Iberian Plate. She has co-published near 100 research articles in international indexed and refereed journals. Since 2011, she is member of the editorial board of the journals edited by the Geological Society of Spain, and from 2016, she is Associate Editor of Stratigraphy and Sedimentology of the Arabian Journal of Earth Sciences.



Dr. Paul Selden gained the B.Sc. (Hons) in Geology and Zoology in 1975. He then went up to the University of Cambridge, Darwin College, where he achieved a Ph.D. in 1979, working with Prof. Harry Whittington. His career has been in university teaching, first (1979–1981) at the University of London, Goldsmiths' College, then at the University of Manchester (1981–2005). He left the latter institution (as Reader in Palaeontology in the School of Earth, Atmospheric and Environmental Sciences) and joined the Natural History Museum in London as a Scientific Associate (and now holds an Honorary Research Fellowship there). In 2007, he started a new position as Distinguished Professor in Invertebrate Palaeontology and Director of the Paleontological Institute, at the University of Kansas, USA. His research interests are in fossil arthropods, mainly Chelicerata. He has served as Vice President of the Palaeontological Association and the Palaeontographical Society, President of the British Arachnological Society, International Society for Arachnology, and the Manchester Geological Association. He has also served as Editor of Palaeontology, and presently serves as Editor of the Treatise on Invertebrate Palaeontology, Paleontological Contributions, and Arachnology, and as Associate Editor for PALAIOS. In 2016, he joined the AJGS as an Associate Editor responsible for evaluating submissions in the fields of Palaeontology.



Etienne Jaillard is Senior Researcher at the French «Institut de Recherche pour le Développement» (IRD). He is specialized in sedimentary geology and uses it for understanding continental margins and their geodynamic setting. He worked about 5 years in the Western Alps, 20 years in the Andes, and since 15 years, he studies sedimentation, tectonics, and paleoenvironments in North Africa. He is the author of about 70 international publications, and contributed to the redaction of several books.



Dr. Peter Bengtson studied Historical Geology, Palaeontology, Sedimentology, Stratigraphy, Mineralogy, and Chemistry at Uppsala University in Sweden and at “Universidade Federal do Rio Grande do Sul” in Porto Alegre, Brazil. He holds a B.Sc. (1969) in Geology, an M.Sc. (1974), a Ph.D. (1977) and a D.Sc. (1978) in Historical Geology and Palaeontology from Uppsala University. From 1975 to 1989, he was employed by Uppsala University as a Research Associate, Assistant Professor and Associate Professor. From 1990 until his retirement in 2010, he worked at Heidelberg University in Germany as a full Professor of Palaeontology. At Uppsala and Heidelberg, he has been teaching mainly Invertebrate Palaeontology and Biostratigraphy and led field courses in the marine Cretaceous of Brazil, Germany, France, and Ukraine, the Lower Paleozoic and Mesozoic of Sweden, and the Neoproterozoic to Lower Paleozoic of Newfoundland, Canada. From 1975 to 1985, he was Project Secretary of IGCP Project 58 “Mid-Cretaceous Events” (MCE) and from 1995 to 2001, he was Co-Leader of IGCP Project 381 “South Atlantic Mesozoic Correlations” (SAMC). During 1978–1980, he was Editor-in-Chief of the journal *Geologiska Föreningens i Stockholm Förhandlingar* (GFF), Co-Editor of the newsletter MCE News (1975–1985), Co-Editor of the newsletter SAMC News (1995–2001), and Co-Editor of the journal *Gaea heidelbergensis* (1995–2011). From 1981 to 1982, he served as a board member of the European Life Science Editors association (ELSE). From 1980 to 1990, he was on the editorial board of the journal *Cretaceous Research* and since 2000 on the editorial board of the journal *Revista Brasileira de Paleontologia*. From 1995 to 2000, he was Chairman of the Turonian Working Group of the International Subcommittee on Cretaceous Stratigraphy, voting member of the German Subcommittee for Cretaceous Stratigraphy (1996–2006), voting member of the International Subcommittee on Cretaceous Stratigraphy (1998–2006), and board member of the German National Committee for the IGCP (2000–2006). He has organized and co-organized 15 international conferences. His principal research interests are Cretaceous palaeontology, biostratigraphy, and biogeography with focus on marine Mollusca of the Southern Hemisphere,

geological and palaeontological terminology and nomenclature, and stratigraphic principles and procedures. He has carried out extensive fieldwork in Brazil, Sweden and Antarctica and has further field experience from Norway, Denmark, Germany, Austria, the Czech Republic, England, France, Italy, Spain, Portugal, Greece, Ukraine, Georgia, Gabon, Canada, Argentina, and Colombia. He has published and co-authored more than 250 original articles, monographs, textbooks, edited books, special issues, and conference abstracts. In 2016, he joined the AJGS as an Associate Editor responsible for evaluating submissions in the fields of Biostratigraphy, Invertebrate Macropaleontology, and Palaeoecology.



Dr. Bruno R. C. Granier holds a B.Sc. in Sedimentary Geology (1981) from P. Sabatier University, Toulouse (France), a M.Sc. in Geodynamics (1983), a Ph.D. in Stratigraphy (1987) as well as a D.Sc. (Habilitation) in Earth Sciences (2003) from Sorbonne University—UPMC, Paris (France). Before joining academe, he worked over a decade and a half for the oil industry. In 1991, he joined Total as Senior Carbonate Sedimentologist at its Scientific and Technical Research Centre in Saint-Rémy-lès-Chevreuse (France). There, he coordinated studies on Angola and Libya, and was responsible for carbonate studies on France, Qatar, and Yemen. In 1995, he was seconded to ADMA-OPCO in Abu Dhabi (United Arab Emirates), as a Petrography Expert. In 2001, he was back in Paris—La Défense with Total in the reservoir division where he dealt with the carbonate reservoirs of the Congo, Angola, along with the bituminous sands of Alberta. Since 2004, Dr. Granier is a full Professor and the Chairperson in Paleontology and Sedimentology at the University of Western Brittany—UBO, Brest (France). Since 2007, he is also an Adjunct Research Associate with the Department of Ecology and Evolutionary Biology at the University of Kansas in Lawrence (USA). Since 2011, he is a “Pesquisador Associado” with the UNESPetro at the “Centro de Geociências Aplicadas ao Petróleo” of the “Universidade Estadual Paulista” in Rio Claro—SP (Brazil). In summer 2015, he was awarded a Franco-Brazilian professorship at the UNESP. Since 2013, he is also an Adjunct Researcher at the Faculty of Sciences II—Fanar Campus of the Lebanese University in Beirut (Lebanon). He has authored or co-authored some 150 research papers and 50 technical reports. He serves as an Editor or Associate Editor some journals such as *PALAIOS*, *Carnets Geol.* and *Studia UBB*. He was and he is still an active member of several not-for-profit associations (Emirates Society of Geosciences, International “Fossil Algae” Association, International Subcommittee on Cretaceous Stratigraphy, etc.) and also chaired invited sessions at international meetings. From 2007 to 2011, he was the Chair of the

French Committee on Stratigraphy (CFS) and as such he organized the International Congress STRATI2010 in Paris on behalf of the CFS. In 2016, he joined the AJGS as an Associate Editor responsible for evaluating submissions in the fields of Stratigraphy, Sedimentology, Carbonate Reservoir Geology and Micropaleontology.

Part I
Keynote

Phanerozoic Global Sea-Level Changes: Evidences from Tunisia Illustrating how Eduard Suess' Concepts (Gondwana, Tethys, Eustasy) are Still Relevant

Mohamed Soussi

Abstract

This key note is given in honor of the Austrian geologist Eduard Suess, born in London, August 20, 1831 and died in Vienna in April 26, 1914. It aims to illustrate, using some key selected stratigraphic intervals from the Tunisian geological archive, **how Edward Suess's concepts are still relevant** and is also planned to briefly introduce the most important features of the Geology of Tunisia for the guests of the CAJG Conference, November 2018)

This key note is given in honor of the Austrian geologist Eduard Suess, born in London, August 20, 1831 and died in Vienna in April 26, 1914. It aims to illustrate, using some key selected stratigraphic intervals from the Tunisian geological archive, **how Edward Suess's concepts are still relevant** and is also planned to briefly introduce the most important features of the Geology of Tunisia for the guests of the CAJG Conference, November 2018). Some of these features are in relation with the Gondwanan super continent development and fragmentation while other are connected to the Tethyan Ocean developed between the Gondwana to the south and Eurasia to the north during the Mesozoic before the onset of its closure during the Cenozoic.

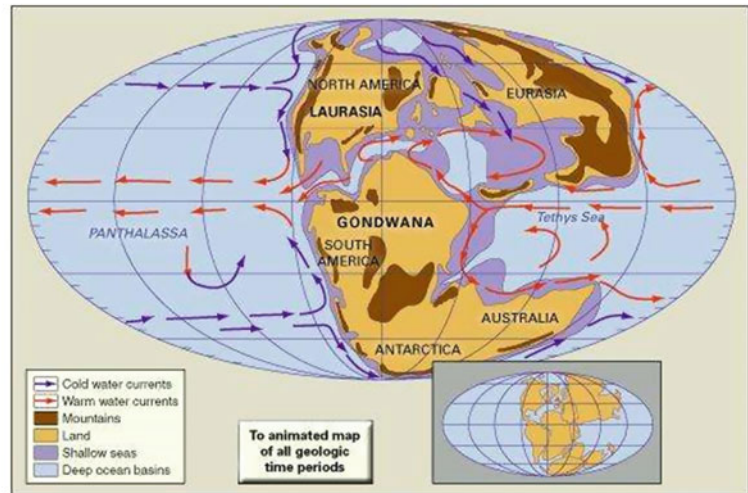
Indeed, it will be shown progressively during the presentation that the major events that accompanied the history of the Geology of Tunisia fit perfectly the line of thoughts that Eduard Suess had at the end of the nineteenth century

especially about the role played by sea level fluctuations in the build of the stratigraphic archive. This conference also brings additional arguments to his theory which continues to impact our kind of reasoning, even if this conveys new modern terms created to explain more the process controlling the global Earth's dynamics especially the global plate tectonics and the eustatic movement theories. Among the concepts and ideas, proposed for the first time by this imminent "geoscientist", based on his exploration and geological investigations of distant regions of the world, some are retained for the purpose of our conference:

- (1) The hypothesis of the existence, 500 million years ago, of an ancient supercontinent named Gondwana or Gondwanaland (Eduard Suess 1885). This "megacontinent" eventually split into several continents which are Africa, South America, Australia, Antarctica, the Indian subcontinent and the Arabian Peninsula.
- (2) The hypothesis of the existence of an inland sea designated the "Tethys" (with reference to the Greek Goddess of the Sea) situated between Gondwana to the South and Laurasia to the North (Eduard Suess 1893).
- (3) the creation of the term Eustasy, (Edward Suess, in 1988, translated and published in English in 1906) to describe the rises and falls of sea level (eustatic movements) as a major factors controlling the development of transgressive and regressive events correlatable worldwide.

The above three concepts among other important ideas, mainly related to tectonics (genesis of the Alps and the introduction of the concept of the east African rift fracture in 1881, etc....) have been detailed in his famous and monumental, three volume treaty entitled "*The Face of the Earth*" (1885–1909) just before Wegener's Continental drift theory presented in 1912 and also the establishment of the theory of plate tectonic in the 1960s which greatly changed the line of thinking of geologists about the dynamic evolution of the Planet.

M. Soussi (✉)
Sedimentary Basins and Petroleum Geology Laboratory
(LR18ES07), Faculty of Sciences,
University of Tunis El Manar, Tunis, Tunisia
e-mail: Mohamed.Soussi@fst.utm.tn



1 Why Tunisia Can Be Considered as Good Example Supporting Eduard Suess's Concepts?

1. Tunisia is situated in a remarkable situation between Africa and Europe. Indeed, with its Atlasic and Tellian domains, situated to the north and displaying intensive deformation typical of the Alpine Orogenic system stretching from Morocco to the West into the Himalayan ranges from China to the East and its relatively stable Saharan platform domain, belonging to a cratonic domain situated in the south, Tunisia can be considered as useful relay or bridge between South America, Africa and Europe that can serve for any attempt of geological reconstruction between these continents through geological time.
2. Its Phanerozoic stratigraphic record can be split into two Megacycles. The first one, which extends between 590 and 251 Ma (**Paleozoic**), is encountered in the Ghadames Basin (southern Tunisia) currently buried under the desert (Oriental Erg) while the second Megacycle, comprising the Mesozoic and the Cenozoic (=251 Ma) is well exposed in the Saharan platform domain to the south and in the Atlasic foreland belt system (Central and North of Tunisia) to the north. These two major megacycles, labeled "Gondwanian" and "Tethyan" respectively are separated by a major unconformity resulting of the Hercynian deformation and Pangea supercontinent

formation that occurred in the late Carboniferous (299 Ma). Their composition is dominantly (99%) represented by sedimentary rocks accumulated in superimposed basins developed during the Paleozoic and the Mesozoic.

The sediments of the Gondwanian cycle are Paleozoic in age and are recognized and well characterized thanks to the numerous boreholes targeting the prolific petroleum systems of North Africa (Algeria, Tunisia and Libya). They are mainly composed of siliciclastic deposits (sandstones and shales), deposited either in fluvio-deltaic to coastal shallow marine settings, and constituting fair to good hydrocarbon reservoirs and intra seal formation or deposited in offshore settings, during major maximum transgressive events (Middle Ordovician, Silurian and Devonian organic-rich facies), and constituting the primary source of the prolific petroleum systems of the Sahara of North Africa. However, the sediments of the Tethyan super-cycle which unconformably rest above the deformed Paleozoic series in the Ghadames basin, are formed at the base by dominantly fluvial sandstones and shales ("Trias Argilo-Gréseux" = TAGI) constituting the main productive hydrocarbon reservoir in southern Tunisia. The latter is in turn overlain by the Upper Triassic- Lower Jurassic evaporitic (limestones, dolomites, salts and gypsum) acting as efficient seal at regional scale. These rocks are well exposed along the Saharan platform domain (Dahar). The geological investigations conducted on this Phanerozoic archive, which

covers a long period of 600 Ma, by numerous geologists of different disciplines, in southern, central and northern Tunisia, during much more than one century, allowed the collection of a huge surface and subsurface information.

This large information, when properly gathered and synthesized can be used in regional stratigraphic correlations and paleogeographic reconstructions of the domains situated between the North Africa to the south, the Europe to the north as well as of the vanished Tethyan Ocean which was situated between and between as ingeniously hypothesized by Eduard Suess 135 years back.

For the purpose of this conference, only some key periods, illustrating the way by which the Phanerozoic global sea level changes and associated transgressive and regressive events have been recorded in Tunisia, as part of the Gondwana and the Tethyan domains, will be presented. The main facts used for the conference are gathered from data collected thanks to my personal works, the works of my team or other works conducted in collaboration with colleagues around the world during the implementation of academic or industrial projects such as the Peri-Tethys Program. In the Conference we will focus on the following three main aspects each of which is connected to the Eduard Suess's concepts

2 Henceforth Tunisia Is a Key Part of the Northern Gondwana Supercontinent as Inferred from Paleontological New Finds

Recent intensive excavations undertaken in 2012 and 2014 in southern and central Tunisia by a multidisciplinary team composed of Tunisian and Polish researchers allowed to discover an important diagnostic ichnofauna (Dinosaur foot prints within the Triassic and Jurassic strata of the Saharan platform and the Early Cretaceous strata of central Atlas Tunisia) as part of the northern Gondwana supercontinent. The new finds confirm that northwest and northeast Africa might have been an important corridors for the exchange of fauna between Euramerica in the northern part and Gondwana in the southern part of the Pangea supercontinent.

Furthermore, paleobiogeographically, the fauna (conchostromatolites, ostracods, fishes, etc....) and flora (charophytes) recently discovered in the lower Cretaceous rocks (Barremian, Aptian and Albian non marine and marginal marine rocks) by the researchers of our team with the collaboration of well known experts from Poland, China, Switzerland, USA and Austria, clearly shows good relations with South America, Europe/West Africa.

Moreover, comparative studies strongly suggest that the migration of this fauna between eastern south America/west Africa and Asia was ensured via numerous northern African Peri-Tethyan islands (such as the Early Cretaceous Kairouan islands of central Tunisia). As a consequence, it is thought that these exposed lands could have worked as bridges for fauna migration.

3 Tunisia Is Part of the Vanished Tethyan Ocean Which Presence Was Hypothesized by Eduard Suess in 1893

As outlined above, the stratigraphic archive of Tunisia is composed of two well separated supercycles named as "Gondwanian and Tethyan". The tethyan cycle records the progressive break-up of the Pangea that start occurring since Late Carboniferous and continued throughout the Mesozoic when North Africa became a broad Tethyan facing passive continental margin.

From the Triassic-Jurassic Cretaceous succession, which records synrift, post rift phases and passive margin development, will be presented the paleogeographic maps of key periods:

- the Syn-rift Permian clastics and reefal carbonates. They are currently well exposed in the northern part of the Saharan platform (Jebel Tebaga of Medenine). The latter represent the unique Permian marine rocks in North Africa
- the Triassic fluvial deposits (TAGI reservoir) and overlying transgressive retrograding evaporitic facies deposited in large and subsident sag basin. They act as efficient seal at regional scale. These two kind of facies constitute the main ingredients of the major prolific petroleum system of North Africa in which the Silurian Hot shales act as the principal source rock.
- the Jurassic (Callovian-Oxfordian) facies which represent the deepest sedimentary recorded in the different paleogeographic domains of Tunisia. In northern Tunisia the Callovo-Oxfordian facies are represented by the well known "Ammonitico-rosso facies" developed on pelagic swells laterally relayed in the deepest part of the sedimentary system (basin) by typical radiolaritic facies.
- the Cretaceous deep marine organic-rich facies of central and northern Tunisia which are coeval their analogues Oceanic Anoxic Events well documented worldwide. The latter constitute the principal source of the petroleum systems of the Pelagian block.

4 Sea Level Changes as Recorded in the Ghadames Basin, the Saharan Platform and Atlas Tunisia (Third Suess' Concept)

For the Paleozoic sea level, falls and rises will be treated the Ordovician/Silurian deposits of Ghadames basin as glacio-eustatic example controlled by the growth and decay of ice sheet. While, regarding the Mesozoic, throughout the Saharan Platform of southern Tunisia, the Mesozoic deposits are mainly composed of siliciclastic and/or evaporitic deposits including shallow marine carbonate platform sediments constituting good markers in the landscape as they can

be traced continuously over several kilometers. Using the modern sequence stratigraphic approach we will demonstrate that the main six carbonate episodes of the Mesozoic of the Saharan platform perfectly coincide with the major second order highest eustatic pulses of Haq chart (2014). This can be explained by the fact that in the Saharan platform local tectonism had a little effect on the sedimentation control. Instead, the examples taken from the Jurassic and Cretaceous of Atlas Tunisia, where tectonic were relatively important, show how the interaction between the global sea level signatures and intra-platform local deformation, is important in the development of reduced stratigraphic successions characterized by frequent unconformities and gaps.

Facies Architecture in Carbonate Ramps: Learned Lessons from Jurassic Cases Studies in the Iberian Basin

Beatriz Bádenas

Abstract

High-frequency sequences (HFSs) recorded in shallow platform carbonates represent key “building blocks” to decipher how and where carbonate sediments were created and accumulated in response to internal and external mechanisms. This keynote illustrated the usefulness of the HFSs to improve understanding of the facies heterogeneities in shallow-water carbonate ramp successions. Learned lessons in this topic from the analysis of three distinct Jurassic carbonate ramps in the Iberian Basin (NE Spain) will be explained. The studied ramps illustrate the facies heterogeneities generated by the interaction of distinct depositional facies arrangements (facies mosaic vs. facies belts) to changing internal and external factors.

Keywords

High-frequency • Sequences • Facies heterogeneities • Carbonate ramp • Jurassic

1 Introduction

The facies architecture and the degree of the facies heterogeneities of the carbonate platform successions depends on internal and external factors (tectonics, climate) controlling the facies arrangement during deposition and the changes in sediment accumulation and accommodation through time. A high-resolution record of these heterogeneities can be obtained from the recognition and the correlation of the high-frequency sequences (HFSs) as they are the elementary “building blocks” containing the detailed information of the vertical and lateral facies stacking.

The usefulness of the combined facies and the HFSs analyses to decipher facies heterogeneities is illustrated from three

different Jurassic carbonate ramps in the Iberian Basin (NE Spain): (1) a non-skeletal dominated homoclinal ramp (upper Sinemurian), (2) a microbial/siliceous sponge-dominated distally steepened ramp (Bajocian), and (3) an homoclinal ramp with coral-microbial reefs (upper Kimmeridgian). The HFSs were identified in individual logs as the smaller stratal/facies packages bounded by discontinuity (erosive or omission) surfaces that may be (or not) accompanied by a sharp facies change. Physical tracing in continuous outcrops or correlation of logs by using key HFS boundaries allowed the lateral and vertical distribution of facies to be deciphered.

2 Case Studies

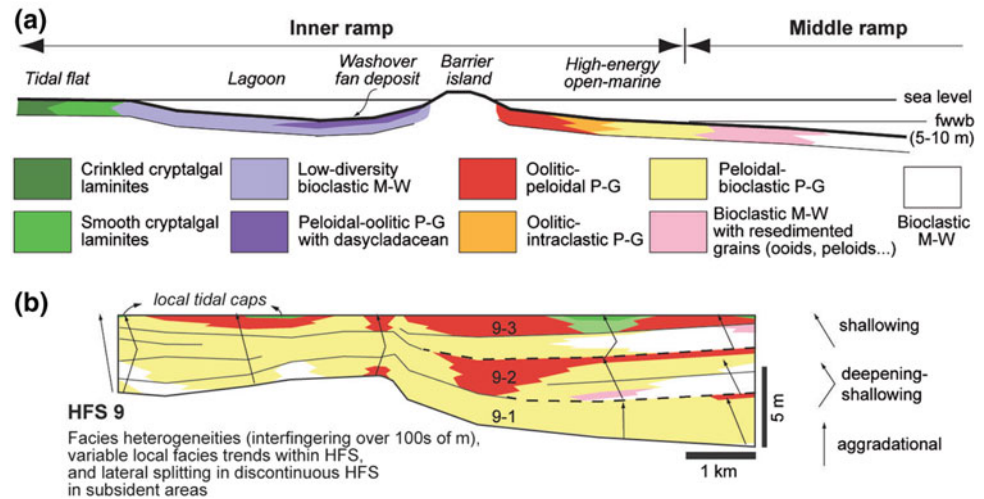
2.1 Upper Sinemurian Ramp

The upper Sinemurian successions exposed in a 12 km long continuous outcrop near the village of Almonacid allow recognizing the inner to middle ramp areas of a non-skeletal dominated homoclinal ramp [1]. A barrier-island system developed between a low-energy coastal area (tidal flat with cryptalgal laminites and muddy lagoon) and a high-energy inner ramp domain dominated by oolitic and peloidal sand blankets passing offshore to lime muds (Fig. 1a). Key data indicating the existence of low-lying barrier islands are: (1) sharp facies contrast (muddy vs. grainy sediments) in the inner ramp; (2) overwash (washover) deposits in the lagoon and backwash intraclastic deposits in high-energy areas; (3) local tidal caps in the grainy facies.

The correlation of the HFSs and facies reveals that the most prominent facies heterogeneities (interfingering over 100 s of metres) are recorded in high-energy inner ramp facies as a result of the lateral migration of sand bodies and the heterogeneous subsidence controlling the generation of discontinuous HFSs (Fig. 1b). Observations at a broader (intrabasin) scale shows that the high degree of heterogeneity of both the HFSs and the facies [2].

B. Bádenas (✉)
Department of Earth Sciences, University of Zaragoza, 50009
Zaragoza, Spain
e-mail: bbadenas@unizar.es

Fig. 1 a Sedimentary model of the upper Sinemurian ramp (fwwb: fair-weather wave base; M: mudstone; W: wackestone; P: packstone; G: grainstone). **b** Facies heterogeneities in high-frequency 9 (HFS 9)



2.2 Bajocian Ramp

The outcrop near the village of Moscardón represents a ~1 km-long depositional-dip oriented exposure of the Bajocian microbial/siliceous sponge-dominated facies [3]. The physical mapping of the HFSs and facies indicates the ramp was distally steepened with two main facies belts separated by a low-angle (7–10°) slope located around storm wave base (Fig. 2a). The shallow ramp domain was the locus of deposition of intraclastic-bioclastic (sponge rich) grainy facies which underwent episodic stabilization by microbial crusts. Microbial-sponge patches and lens-shape mounds intercalated with sponge-rich muddy limestones dominated the ramp slope and deep ramp.

The different stacking of the HFSs in response to long-term relative sea-level variations controlled the present facies distribution including two prominent sedimentary features: (1) large microbial-sponge mounds (~30 m-thick and 50–100 m-wide) formed locally at the toe of the slope as a result of the aggradational stacking of successive HFSs (microbial-sponge boundstones) during the stage of accommodation gain (Fig. 2b); (2) the shallow grain-supported facies accumulated preferentially (thicken) down dip as a result of the sharp progradation and filling of the available accommodation space over the ramp slope.

2.3 Upper Kimmeridgian Homoclinal Ramp

The outcrops located in Sierra de Albarracín expose the inner to mid ramp areas of the upper Kimmeridgian storm-dominated homoclinal carbonate ramp [4–6]. The inner ramp to proximal middle ramp included lagoon and high-energy (shoal and foreshoal) areas with a broad spectrum of non-skeletal facies. A wide range of bioconstructions, mainly coral-microbial buildups with patch and

pinnacle morphology, grew from inner to middle ramp, intercalated with both grainy and muddy facies (Fig. 3a).

Lateral tracing of the HFSs at outcrop-scale and over a long-distance area (20 × 20 km) reflects that the bioconstructions and grainy facies varied laterally and vertically throughout the successive HFSs as a result of the variable hydrodynamic conditions and the terrigenous input and the relative sea-level variations (Fig. 3b). In particular, the non-skeletal grainy facies record a high degree of facies heterogeneities both in deep and strike direction with interfingering of 100 s of metres to few kilometers.

3 Learned Lessons

The facies architecture of the three studied ramps illustrate variable facies heterogeneities as a result of the response of distinct depositional facies distributions (facies mosaics vs. facies belts) to changing internal and external factors:

- (1) Inner ramp facies mosaics linked to a barrier-island system and differential subsidence controlled the high degree of facies heterogeneities in the upper Sinemurian homoclinal ramp.
- (2) More homogenous facies belts of shallow grainy facies and deeper sponge-rich muddy sediments and bioherms were recorded in the distally steeped Bajocian ramp; however, the heterogeneity increased in stages of relative sea-level rise as a result of the stacking of microbial-sponge bioherms to form large mounds at the toe of the slope.
- (3) Inner to mid ramp facies mosaics of grainy facies and bioconstructions characterized the upper Kimmeridgian homoclinal ramp. In this case, a high degree of facies heterogeneities of both facies types are recorded as they changed throughout deposition (i.e. facies partitioning)

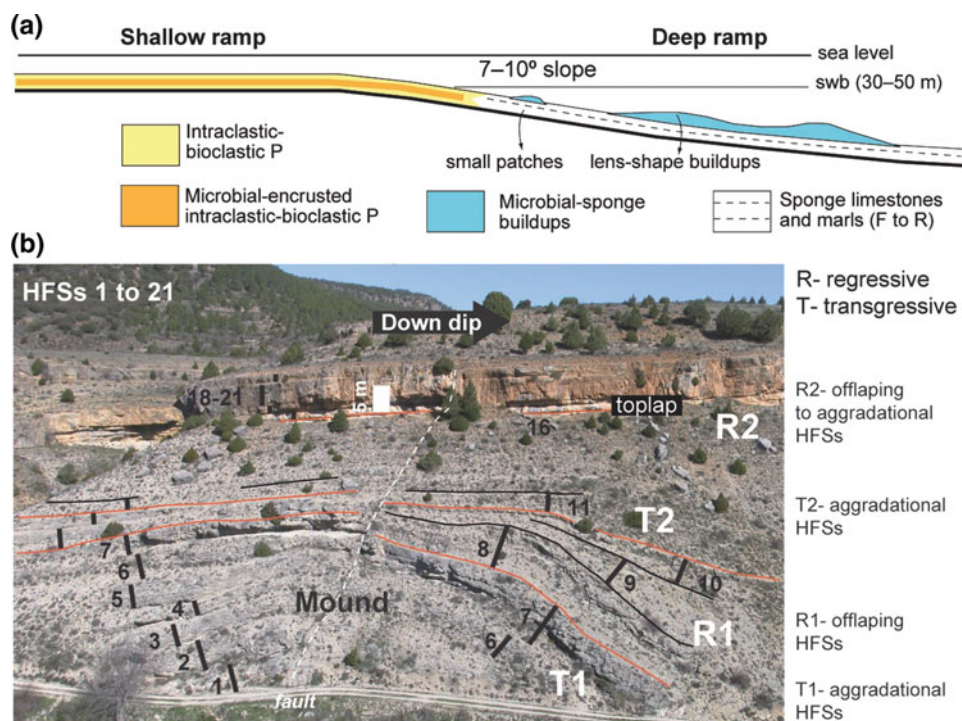


Fig. 2 a Sedimentary model of the Bajocian ramp (swb: storm wave base; P: packstone; F: floatstone; R: rudstone). b Variable stacking of high-frequency sequences (HFS) depending on the long-term relative sea-level variations

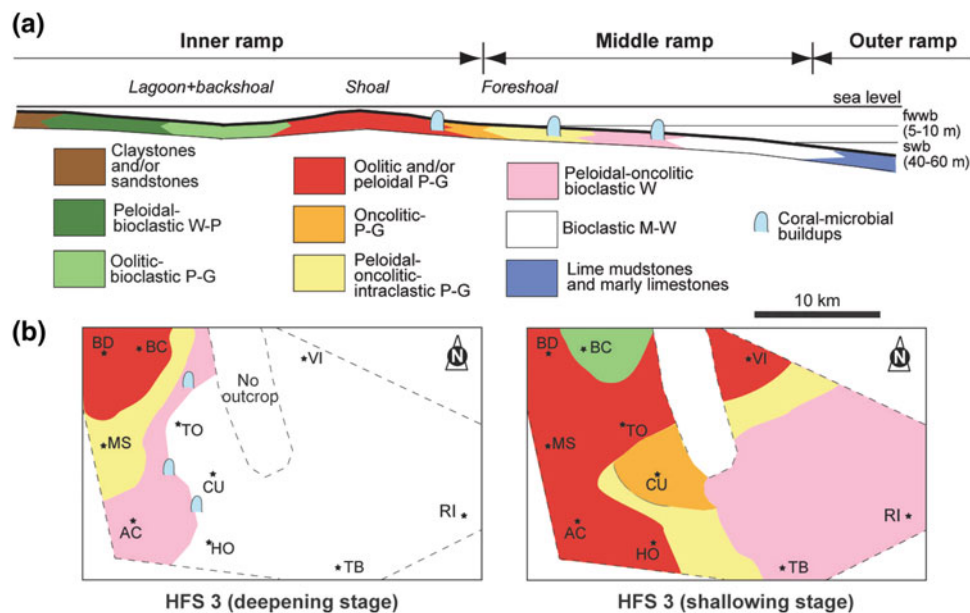


Fig. 3 a Sedimentary model of the upper Kimmeridgian ramp (fwwb: fair-weather wave base; swb: storm wave base; M: mudstone; W: wackestone; P: packstone; G: grainstone). b Facies distribution in high-frequency sequence 3 (HFS 3)

in response to the variable hydrodynamic conditions and the terrigenous input and the relative sea-level variations.

Only with the identification and the correlation of the HFSs and their constituent facies, the detailed lateral and vertical facies heterogeneities of shallow carbonate ramp successions can be properly deciphered.

References

1. Bádenas, B., Aurell, M., Bosence, D.: Continuity and facies heterogeneities of shallow carbonate ramp cycles (Sinemurian, Lower Jurassic, NE Spain). *Sedimentology* **57**(4), 1021–1048 (2010)
2. Aurell, M., Bádenas, B.: Análisis comparado de secuencias de alta frecuencia en plataformas carbonatadas con subsidencia diferencial (Sinemuriense, Cordillera Ibérica). *Revista de la Sociedad Geológica de España* **28**(1), 77–90 (2015)
3. Aurell, M., Bádenas, B.: Facies architecture of a microbial-siliceous sponge-dominated carbonate platform: the Bajocian of Moscardon (Middle Jurassic, Spain). *Geol. Soc. Spec. Publ.* **418**, 155–174 (2015)
4. Bádenas, B., Aurell, M.: Facies models of a shallow-water carbonate ramp based on the distribution of non-skeletal grains. *Facies* **56**(1), 89–110 (2010)
5. Alnazghah, M.H., Bádenas, B., Pomar, L., Aurell, M., Morsilli, M.: Facies heterogeneity at interwell-scale in a carbonate ramp, Upper Jurassic, NE Spain. *Mar. Pet. Geol.* **44**, 140–163 (2013)
6. San Miguel, G., Aurell, M., Bádenas, B.: Occurrence of high-diversity metazoan- to microbial-dominated bioconstructions in a shallow Kimmeridgian carbonate ramp (Jabaloyas, Spain). *Facies* **63**(3), 13 (2017)



An Early Anthropocene Analog: The Geomorphology and Hydrology of the Rio Bravo Watershed in the Belize Tropics

Tim Beach, Sheryl Luzzadder-Beach, Samantha Krause, and Colin Doyle

Abstract

The fluviokarst Rio Bravo watershed of Belize Central America is about 400 km². More importantly, it has global implications for the long-term human alteration of a tropical forest. We have studied this watershed's geomorphology and archaeology since 1995. We have documented many ancient Maya modifications like terraces, wetland canals and fields, and reservoirs. We have recently been able to quantify canals and wetland field complexes. We have found four main agricultural zones that date back as early as 2000 BP but came to fruition from 1300 to 1000 BP, at the end of Maya Classic and the beginnings of the Post Classic. These canal complexes extended the known area of wetlands and altered river and karst geomorphology in this watershed.

Keywords

Anthropogenic geomorphology • Early anthropocene • Soils • Geoarchaeology

1 Introduction

This paper is a comparison of the natural and anthropogenic factors that have formed ancient Maya canals of the trans-boundary Rio Bravo watershed between Guatemala, Belize, and Mexico. Studies have consistently found greater and earlier human impacts on the Maya region over the last three decades. The Maya altered slopes both positively and negatively [1], built many reservoirs, made roads, and constructed canals and wetland fields [2]. All of these alterations created an early form of the Anthropocene both on the geomorphology of this tropical forest region and at the global level through increased greenhouse gas emissions [3].

T. Beach (✉) · S. Luzzadder-Beach · S. Krause · C. Doyle
Department of Geography and the Environment, The University of
Texas at Austin, Austin, TX 78712, USA
e-mail: beacht@austin.utexas.edu

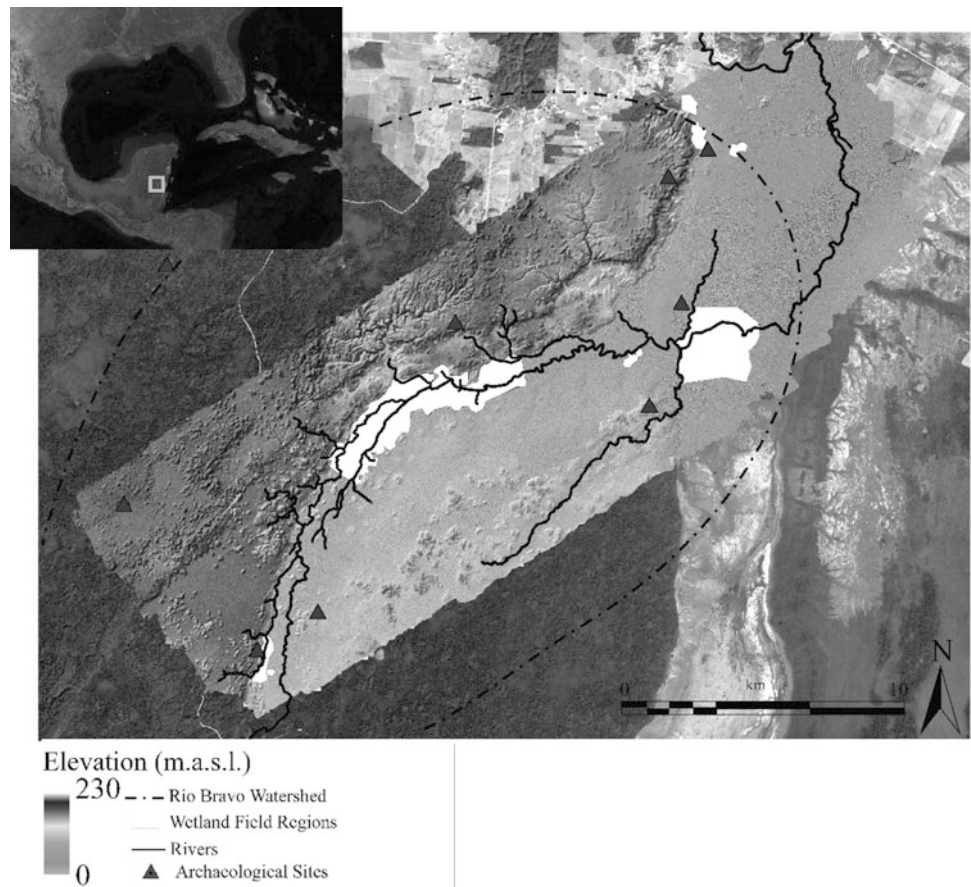
Here, we focus on the anthropogenic geomorphology of the Rio Bravo watershed because it provides a time capsule of the ancient human impacts sealed by a millennium of reforestation in a remnant tropical forest preserve.

2 Settings, Materials and Methods

Most of the Maya Lowlands is an internally draining karst region with roughly 400 m of regional relief and intensely wet and dry precipitation. Fluvial and fluviokarst systems drain the edges of this landscape from mostly low limestone uplands, with small inputs from igneous and metamorphic terrains. Thus far, most fluvial researchers have studied areas near archaeological projects. The current study reviews the investigations conducted across the region as well as those on the Rio Bravo watershed of Belize and Guatemala (Fig. 1). The Rio Bravo drains a largely primary tropical forest today, but was partly deforested, especially around ancient Maya cities and farms from 3000 to 1000 BP, during the Preclassic through Terminal Classic periods. Several studies estimate that 30–40% of forest survived through the Maya period in a landscape of cities, roads, dams, diversions, canals, and terraces. Like other ancient societies, the Maya created regional Anthropocenes with some global impacts [3].

From 1995 to 2018, we studied the watershed by aerial survey and pedestrian survey through remote and dense tropical forest accessed by archaeological survey trails. We studied soils, ecology, and geo-archaeology in the floodplain, the terraces, and the slopes, especially around archaeological sites to understand the ancient land uses and the scales of their impacts. We studied multiproxy evidence for these sites including radiocarbon dating, sediment stratigraphy, pollen and charcoal, and geochemistry that included carbon isotope analysis of soil humin in order to study the plant sources of the organic matter.

Fig. 1 Wetland field areas of the Rio Bravo Watershed



3 Results

There are three main regions of the ancient canals in this watershed of ca. 400 km². In the upper watershed, where the fluviokarst system has eroded a stream valley into a structural graben, canals and wetland fields lie near the foot of the ancient Maya village of Chawak. Soil and water chemistry indicates that these soils built up slowly by fluvial aggradation from flooding. Excavations, here, indicate that in the Classical period Maya built terraces, canals, and raised fields within this deepest section of the tilted graben. AMS dating and charcoal analysis of excavated stratigraphy indicate that the ancient Maya burned the forest and built canals and fields in the Late Classic (ca. 1300 years BP) changing this slowly aggrading wetland floodplain into intensive agricultural system. Nevertheless, Chawak's wetland fields and terraces declined rapidly in the Terminal Classic by 1100 years BP. The laser scanning imagery suggests that the area of the wetland farming is larger but we have not been able to field-verify these new areas [4].

This imagery system suggests that in a broad swath of the Rio Bravo's middle valley, canals and fields occupy many hectares of the floodplain wetlands. We have accessed these field systems only for a few days of field work to verify their rectilinear forms and connect them with the Late Classic Maya artifacts from 1300 to 1100 years BP. Preliminary excavations and geochemical analyses of this area shows that the water sources, the soils of the floodplain in this area and the farther downstream also have a significant input of gypsum precipitating into soils as a result, thereby aggrading the soils and creating excess sulfate that limited the crop growth.

At the Birds of Paradise fields (Fig. 2), the River is just downstream from its canyon sides meandering across the coastal plain, and a large area of canals crisscrosses the floodplain in a zone where two major tributaries converge [2, 5]. Here we have excavated 20 units from as deep as 4.4 m to the surface, estimating aggradation rates of the floodplain of ca. 1 mm yr⁻¹ over 4 millennia by mostly floodplain sedimentation, gypsum deposition, and human field raising. We also found evidence of large scale field burning, canal



Fig. 2 The birds of paradise wetland agroecosystems in the Rio Bravo floodplain of Belize, CA

construction, and intensive wetland farming that is widely dated to 1300 to about 1000 years BP. Multiple lines of evidence from pollen, phytoliths, macrobotanicals, charcoal, and 40 radiocarbon dates indicate that ancient polycultural systems with crops like maize, fruit trees, and root crops along with the protein harvesting from mollusks, fish, and deer. Artifacts and economic pollen also show that this wetland field complex and two ancient cities at its margins either had reoccupations or continued occupations into the Post Classic about 1000 years BP.

At the fourth zone near the mouth of the Rio Bravo, a group of ancient villages lie in the midst of wetland field complexes at the base of the Rio Bravo escarpment. More than 20 excavations provide evidence of the wetland agriculture as early as the Late Preclassic (2300 to 1700 years BP) and possibly as late as the Post Classic about 1000 years BP. Similar crop and protein harvesting evidence as at BOP exists for these wetland fields, but the evidence starts as earlier as 2000 BP. Moreover, water sources are higher in calcium and sulfate, and the soils have horizons of nearly pure gypsum aggradation, partly caused by ancient humans altering canals and water flow [2, 3].

4 Discussion

The ongoing multiproxy studies of geoarchaeology and paleoecology are refining our understanding of the intensity and the chronology of human management of this one key watershed of the Maya tropical forest. More broadly, newly

acquired Lidar imagery from many other parts of the Maya Lowlands is showing that the intensity of the Maya Anthropocene in Rio Bravo watershed may be an apt microcosm of much of this area. This adds to the growing evidence from many other tropical forests that is showing much earlier impacts by humans on soils, geomorphology, and ecologies.

5 Conclusion

In the Rio Bravo watershed, the ancient Maya altered their fluviokarst system by clearing slopes, causing erosion, and building terraces, reservoirs, roads, and canal and wetland field complexes. These new features altered the geomorphology, hydrology, and ecosystems in negative and positive ways that presage the Anthropocene both in terms of regional impacts on millennial timescales and globally through increasing greenhouse gases by burning forests and expanding wetlands. The intensive human impacts in the Rio Bravo watershed of the Maya region is a microcosm of the growing evidence for earlier intensive land use changes around the world.

References

1. Beach, T., Luzzadder-Beach, S., Cook, D., Krause, S., Doyle, C., Eshleman, S., Wells, G., Dunning, N., Brennan, M., Brokaw, N., Cortes-Rincon, M., Hammond, G., Terry, R., Trein, D., Ward, S.: Stability and instability on maya lowlands tropical hillslope soils. *Geomorphology* **305**, 185–208 (2018)

2. Luzzadder-Beach, S., Beach, T., Dunning, N.: Wetland fields as mirrors of drought and the Maya abandonment. *Proc. Natl. Acad. Sci.* **109**, 3646–3651 (2012)
3. Beach, T., Luzzadder-Beach, S., Cook, D., Dunning, N., Kennett, D., Krause, S., Terry, R., Trein, D., Valdez, F.: Ancient Maya impacts on the earth's surface: an early anthropocene analog? *Quat. Sci. Rev.* **124**, 1–30 (2015)
4. Beach, T., Luzzadder-Beach, S., Krause, S., Walling, S., Dunning, N., Flood, J., Guderjan, T., Valdez, F.: 'Mayacene' floodplain and wetland formation in the Rio Bravo Watershed of Northwestern Belize. *The Holocene* **25**(10), 1612–1626 (2015)
5. Beach, T., Luzzadder-Beach, S., Dunning, N., Jones, J., Lohse, J., Guderjan, T., Bozarth, S., Millsbaugh, S., Bhattacharya, T.: A review of human and natural changes in Maya Lowlands wetlands over the Holocene. *Quat. Sci. Rev.* **28**, 1710–1724 (2009)

Part II

Palaeontology—Systematics

Similarity Analysis of Ostracoda Faunas in West-Tethyan During the Upper Pliensbachian-Lower Toarcian

Choukri Soulimane, Abbas Marok, and Matías Reolid

Abstract

The purpose of this work is to calculate the similarity and distance indices of ostracod faunas for Upper Pliensbachian-Lower Toarcian which has made it possible to compare nine (09) Basins belonging to paleobiogeographic provinces of Western Tethys. This comparison for each chronological interval shows stability over the three chronological intervals of the ostracods from Traras and Lusitanian Basin. A displacement often occurs from the Beni Snassen (BSB), Iberian Cordillera (IC), Aquitanian (AB), the Central High Atlas Basins (CHA) and finally the remoteness of Paris, Southern Germany and Umbria-Marche Basins.

Keywords

Ostracod faunas • Upper Pliensbachian-Lower toarcian • Similarity • Distance • Western tethys

1 Introduction

In order to quantify the relationship between ostracods from different basins and palaeobiogeographic provinces of Western Tethys, the multivariate method (calculation of similarity and distance indices) was used. This method tested mainly on ammonites [14] is better adapted to the quality of ostracods data that will be analyzed during the Upper Pliensbachian (Emaciatum Zone)-Lower Toarcian (Polymorphum-Levisoni Zones) interval.

C. Soulimane (✉) · A. Marok
Department of Earth and Univers Sciences, University of Tlemcen, 119 Tlemcen, Algeria
e-mail: soulimanec@yahoo.fr

M. Reolid
Departamento de Geología, Universidad de Jaén, Campus Las Lagunillas Sn, 23071 Jaén, Spain

2 Materials and Methods

The analyzed data come from nine (09) different basins (Fig. 1): Central High Atlas (CHA) [9], Beni Snassen Basin (BSB) [7], Traras Basin (TB) [17], Paris Basin (PB) [5], Aquitanian Basin (AB) [1, 2], Iberian Cordillera (IC) [4, 11], Lusitanian Basin (LB) [6, 8, 13, 15], Umbria-Marche Basin (UMB) [3], and South Germany (SG), [12, 16]. To avoid falling into the contradictions between the specific and the generic structures, only the generic treatment (42 genera are analyzed) are used. This binary processing is generated by BG-Index ver. 1.1 β software [10] in order to compare the similarity or dissimilarity degree between each pair of lists generated by the database. In this analysis, the degree is calculated by similarity (Jaccard and Dice coefficients) or distance indices (Bray-Curtis coefficient) from a chronological point of view by performing calculation intervals by interval (Emaciatum, Polymorphum and Levisoni Zones).

3 Results and Discussion

The results will be illustrated in phenogram and hierarchical association diagram form and that will allow us to order the different basins according to a similarity gradient.

- Chronological interval 1 (Emaciatum Zone): During Upper Pliensbachian interval (Figs. 2a, 3a), the treatment shows a proximity between three Basins. These are Traras (TB) and Lusitanian Basins (LB) that share 5 genera in common (*Bairdia*, *Bairdiacypris*, *Liasina*, *Ogmoconcha*, *Polycope*) which linked Beni Snassen Basin (BSB). On the other side, the new typology which is emerging during this period concerns the rapprochement between ostracods of Aquitanian (AB) and Southern German Basins (SG) which share 13 genera in common (41%) of the list represented Emaciatum zone.

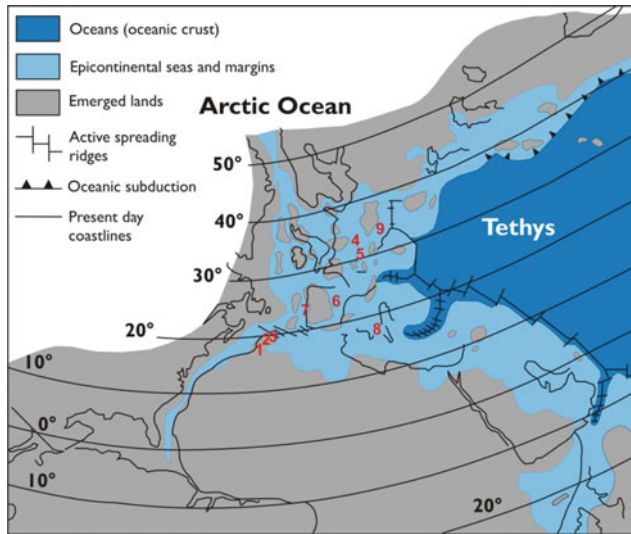


Fig. 1 Palaeogeographic location of the analysed areas. Morocco [1: Central High Atlas (CHA), 2: Beni Snassen Basin (BSB)], Algeria [3: Traras Basin (TB)], France [4: Paris Basin (PB), 5: Aquitanian Basin (AB)], Spain [6: Iberian Cordillera (IC)], Portugal [7: Lusitanian Basin (LB)], Italy [8: Umbria-Marche Basin (UMB)], Germany [9: South Germany (SG)]

The distance separating the ostracods and the three Basins: Central High Atlas (CHA) with 9%, Paris Basin (PB) with 16% and Umbria-Marche (UMB) with 19% is maximal. It corresponds at isolation (low similarity gradient).

- Chronological interval 2 (Polymorphum Zone): At the Lower Toarcian (Polymorphum Zone) (Figs. 2b, 3b), a new topology change takes place. The Basin of the Iberian Cordillera (IC) is attached to the Traras (TB) -Lusitanian (LB) which results in the presence of 8 common genera (23%) (*Bairdia*, *Bairdiacypris*, *Isobrythocypris*, *Liasina*, *Ogmoconcha*, *Ogmoconchella*, *Paracypris*, *Polycope*). There is a resemblance between the ostracods of Central High Atlas (CHA), Aquitanian (AB) and Paris Basins (PB). The three Basins share 3 genera in common (*Bairdia*, *Kinkelinella*, *Pontocyprilla*). Finally, the remoteness of the ostracods from the 3 Basins belongs to different paleobiogeographic provinces. These are Umbria-Marche (UMB), Beni Snassen (BSB) and Southern Germany (SG).
- Chronological interval 3 (Levisoni Zone): During this interval (Figs. 2c, 3c), the general topology is modified

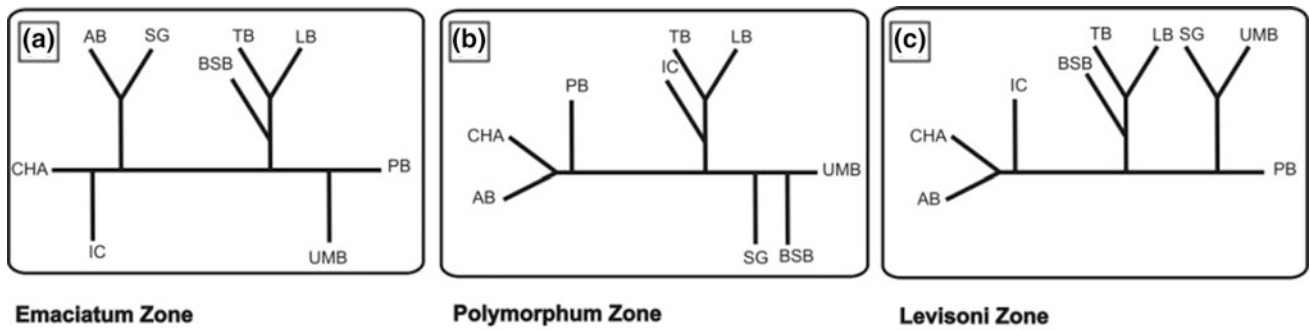


Fig. 2 Phenogram reconstituted by chronological intervals

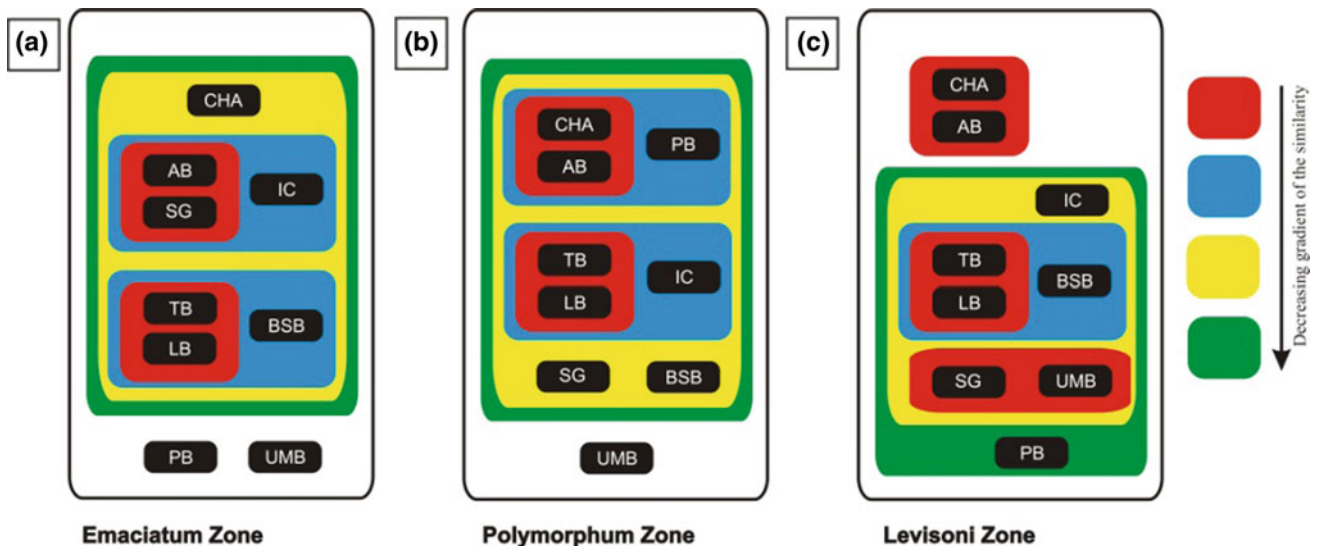


Fig. 3 Hierarchical associations diagrams between areas by chronological intervals

by the rapprochement, this time, with the ostracods from south Germany (SG) and Umbria-Marche (UMB) (*Bairdia*, *Cardobairdia*, *Polycope*). For the other Basins, the similarity gradient is the same as the Polymorphum Zone.

4 Conclusions

From this quantitative study of ostracods biodiversity, we were able to clear stability for the Upper Pliensbachian-Lower Toarcian period from the three chronological intervals of the ostracods of the Traras (TB) and Lusitanian Basins (LB) which probably facilitated by the presence of the communicative ways. On the other side, we remarked a frequent displacement of Beni Snassen (BSB), Iberian Cordillera (IC), Central High Atlas (CHA) and Aquitanian Basins (AB) with at the same time the remoteness of the ostracods from the Paris Basin (PB), southern Germany (SG) and Umbria-Marche (UMB).

References

1. Andreu, B., Bodergat, A.M., Brunel, F., Colin, J.P., Cubaynes, R.: Ostracodes du Carixien supérieur-Domérien (Jurassique inférieur) du Quercy, Bassin d'Aquitaine. France. *Paleontographica (A)* **250**, 68–122 (1998)
2. Andreu, B., Qajoun, A., Cubaynes, R.: Ostracode du Toarcien du Quercy (Bassin d'Aquitaine, France): Systématique. *Biostratigraphie et Paleobiogeographie*. *Geobios* **28**, 209–240 (1995)
3. Arias, C.: Upper Domerian and Lower Toarcian Ostracoda from the Umbria-Marche Basin. Central Italy. *Boll Soc Paleontol Ital* **32**, 367–383 (1993)
4. Arias, C.: Extinction pattern of marine Ostracoda across the Pliensbachian-Toarcian boundary in the Cordillera Ibérica, NE Spain. *Causes Consequences*. *Geobios* **42**, 1–15 (2009)
5. Bodergat, A.M., Donze, P., Nicollin, J.P., Ruget, C.: Répartition biostratigraphique des microfaunes toarciennes (Foraminifères et Ostracodes) en bordure du Bassin de Paris. *Les Cahiers de l'Institut Catholique de Lyon* **14**, 103–123 (1985)
6. Boomer, I., Ainsworth, N.R., Exton, J.: A re-examination of the Pliensbachian and Toarcian Ostracoda of Zambujal, west-central Portugal. *Micropaleontology* **17**, 1–14 (1998)
7. Boudchiche, L.: Etude Micropaléontologique du Domérien, Toarcien et Bajocien du Massif des Béni-Snassen Orientaux (Maroc nord-oriental). Ph.D. Thesis Université de Lyon 1, 187 (1986)
8. Cabral, M.C., Loureiro, I.M., Duarte, L.V., Azerêdo, A.C.: Registo da extinção dos Metacopina (Ostracoda, Crustacea) no Toarciano de Rabaçal, região de Coimbra. *Com Geol 100 Esp I*:63–68 (2013)
9. El Kamer, A., Boutakiout, M., Elmi, S., Sadki, D., Ruget, C.: Foraminifères et ostracodes du Lias supérieur et du Bajocien de la Ride de Talghemt (Haut-Atlas central, Maroc). *Bulletin de l'Institut Scientifique, Rabat, section Sciences de la Terre* **21**, 31–41 (1998)
10. Escarguel, G.: BG-Index version 1.1β. Programme et notice d'utilisation. Laboratoire de Paléontologie, Université Claude Bernard (2001)
11. Gómez, J.J., Arias, C.: Rapid warming and ostracods mass extinction at the Lower Toarcian (Jurassic) of central Spain. *Mar. Micropaleontol.* **74**, 119–135 (2010)
12. Harloff, J., Jäger, J.: Ostracoden aus dem Lias der Kalkalpen Bayern und Norditrols. *Stuttgarter Beiträge zur Naturkunde. Geologie und Paläontologie Série B* (205), 1–63 (1994)
13. Loureiro, I.M., Cabral, M.C., Duarte, L.V., Azerêdo, A.C.: Ostracodos do Toarciano de Rabaçal (região de Coimbra): novos dados biostratigráficos. *e-Terra* **17**, 1–4 (2010)
14. Marok, A., Sebane, A., Henriques, M.H., Sadki, D., Hadji, F.: Analyse de similarité des faunes d'ammonites dans la Téthys occidentale au cours de l'Aalénien supérieur-Bajocien inférieur. *Bulletin du Service Géologique National* **21**(3), 229–245 (2010)
15. Pinto, S., Cabral, M.C., Duarte, L.V.: Preliminary data on the ostracod fauna from the Lower Toarcian of Peniche. *Ciências da Terra* **16**, 37–43 (2007)
16. Riegraf, W.: Microfauna, Biostratigraphie und Fazies im Unteren Toarcium Südwest-Deutschlands und Vergleiche mit benachbarten Gebieten. *Tübinger Mikropaläontologische Mitteilungen* **3**, 1–232 (1985)
17. Soulimane, C., Reolid, M., Marok, A.: Ostracod assemblages from the uppermost Pliensbachian and Lower Toarcian of the Traras Mountains (Tlemcen Domain, north Algeria). *Arab. J. Geosci.* **10** (18) (2017)

Cladistic approach for phylogenetic reconstruction testing the subfamily Reineckiinae (Saida, western Algeria)

Fatiha Douas Bengoudira, Abdia Touahria, and Abbes Sebane

Abstract

The cladistic analysis appears as one of the most useful methods to reconstruct the phylogeny of fossil taxa. The Step capital of the cladistic analysis is the recognition of homology assumptions and monophyletic clades reconstruction. The study area is located around the city of Saida in the eastern segment of Tlemcen area (Algerian North west). This work is based on the study of the ammonite fauna Callovo- Oxfordian harvested in the Training Clays Saida (Sidon, western Algeria). This study provides new additional information to prior knowledge. In order to reconstruct the phylogenetic relationships across the subfamily Reineckiinae (Family Reineckeidae), a cladistic approach based on morphological arguments was carried out. The genres of ammonites grouped in the subfamily Reineckiinae studied: (*Rehmannia* Schirardin 1956, *Reineckeia* Bayle, 1878 and *Collotia* De Grossouvre 1917) undoubtedly constitute separate branches. The genus *Rehmannia* appears as a type strain in the subfamily Reineckeinae. It gives birth to the genres of *Reineckeia* and *Collotia*. The results of this analysis confirm the classical model proposed by Cariou (Upstairs Callovian in the Central West of France 790, 1980 [1]).

Keywords

Ammonite • Callovian-Oxfordian • Phylogenetic Reineckeinae • Cladistic

1 Introduction

The studied area is located 150 km SW of the city of Oran (Fig. 1). It corresponds to an elongated mountainous region WSW - ENE whose bedrock is essentially composed of

F. D. Bengoudira (✉) · A. Touahria · A. Sebane
Faculty of Geology and Universe Science, University Benahmed
Mohamed, Oran, Algeria
e-mail: fatiha.douas@yahoo.fr

Jurassic and cretaceous. It sometimes reveals the Triassic and Paleozoic basement.

The family Reineckeidae consists of two geographically disjoined subfamilies: the pacific Neuqueniceratinae and the Tethyanian Reineckeinae. It presumably represents a lateral branch derived from the Pacific strain that penetrated the tethys through the opening phase of the lower Callovian scarring at the beginning of the formation of the North Atlantic. The objective of this work is to reconstruct the phylogenetic relationships across the subfamily Reineckiinae.

2 Materials and Methods

The cladistic analysis is conducted in order to propose the hypotheses of the phylogenetic relationships across the subfamily Reineckeinae. It is based on the study of the specimens collected by Touahria [2] in the Saida region (western Algeria). The extracted sample leads to the selection of the 15 taxa (species) of the subfamily Reineckiinae. The genus of *Rehmannia* is represented by: (*R. (L)cf. hungarica* until 1907, *R. (L)richei* Fleming, 1911, *R. (L)reissi (macroconch Form)* Steinmnn 1881, *R. (L)reissi (microconque Form)* Steinmnn 1881, *R. (L)corrugis* Bourquin, 1968 and *R. (L)intermedia* Bourquin, 1968). The other of the *Reineckeia* is represented by: (*R. (R)anceps* Reinecke, 1818, *R. (R)anceps elmii* Bourquin, 1968, *R. (R)nodosa* until 1907, *R. (R)stuebeli* Steinmann, 1881). The genus of *Collotia* is represented by: (*C. multicosata* Petitclerc, 1915, *C. gigantea* Bourquin, 1988, *Collotia bourquini* Cariou, 1984, *C. nivernensis (macroconch form)* Bourquin, 1968 and *C. nivernensis (microconque form)* Bourquin, 1968.

Board: Morphological characteristics and states of characters selected for cladistic analysis.

Six morphological characteristics are taken into account (Board). They describe the geometrical characteristics of the shell. The states are coded for adult specimens. All seems to

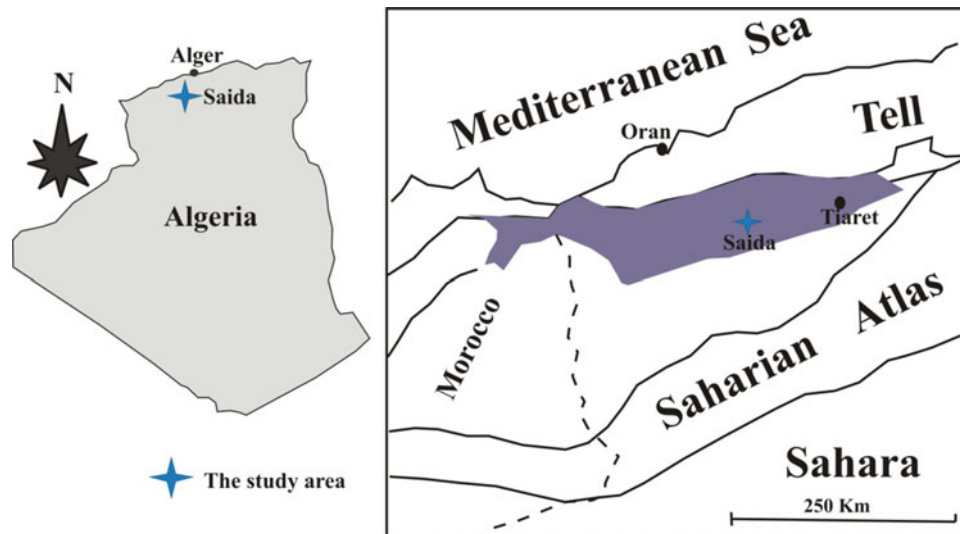


Fig. 1 Location of the study area

No morphological characters and states						
A. Winding type shell: 0 (evolute), 1 (slightly involute), 2 (frankly involute).						
B. Section of the towers: 1 (oval), 2 (slightly compressed), 3 (highly compressed).						
C. Compression of the shell: 0 (thickness / height ratio <1), 1 (W / O ≥ 1).						
D. Depth of the umbilicus: 0 (shallow), 1 (average depth), 2 (deep).						
E. Form of the shell: 0 (flat) 1 (icon snake).						
F. Shell size 1 (largest), 2 (average), 3 (small)						
Personal references	A	B	C	D	E	F
<i>Rehmannia (Loczyceras) cf. hangarica</i> Till 1907	0	3	0	0	0	2
<i>Rehmannia (Loczyceras) richei</i> Fleming, 1911	0	3	0	0	0	2
<i>Rehmannia (Loczyceras) reissi (macroconch)</i> Steinmann 1881	0	3	0	0	0	2
<i>Rehmannia (Loczyceras) reissi (Microconch)</i> Steinmann 1881	0	3	0	0	0	2
<i>Rehmannia (Loczyceras) corrugis</i> Bourquin, 1968	0	3	0	0	0	2
<i>Rehmannia (Loczyceras) intermedia</i> Bourquin, 1968	0	1	0	0	0	2
<i>Reineckeia (Reineckeia) anceps</i> Reinecke, 1818	0	2	1	2	1	1
<i>Reineckeia (Reineckeia) anceps elmii</i> Bourquin, 1968	0	2	1	2	1	1
<i>Reineckeia (Reineckeia) nodosa</i> Till 1907	0	2	1	2	1	1
<i>Reineckeia (Reineckeia) stubeli</i> Steinmann, 1881	0	2	1	2	1	2
<i>Collotia multicostata</i> Petitclerc, 1915	0	3	0	1	0	0
<i>Collotia gigantea</i> Bourquin 1988	0	1	0	1	0	0
<i>Collotia bourquini</i> Cariou 1984	0	3	0	1	0	0
<i>Collotia nivernensis (macroconch)</i> Bourquin, 1968	0	1	0	1	0	0
<i>Collotia nivernensis (Microconque)</i> Bourquin, 1968	0	1	0	1	0	0

Fig. 2 Matrix characters for 15 species of Réineckeinae

be a description of base that may apply to 15 taxa taken in Reineckiinae.

The matrix characters (Fig. 2) is treated with the PAST sparingly software (Paleontological statistic analyzed) version 3.20. The characters are considered unordered, undirected and unweighted. The matrix contains only informative character. The search for the most parsimonious trees is done with the “heuristic” search option that produced 6 trees.

3 Results

The parsimony trees show an index of coherence of a 0.8 and a 0.86 retention value revealing the presence of homoplasies. The topologies of these 5 trees are quite similar and differ only on particular nodes. The Conflict and the coherence between these minimum parsimonious trees can be analyzed and synthesized by calculating the consensus trees.

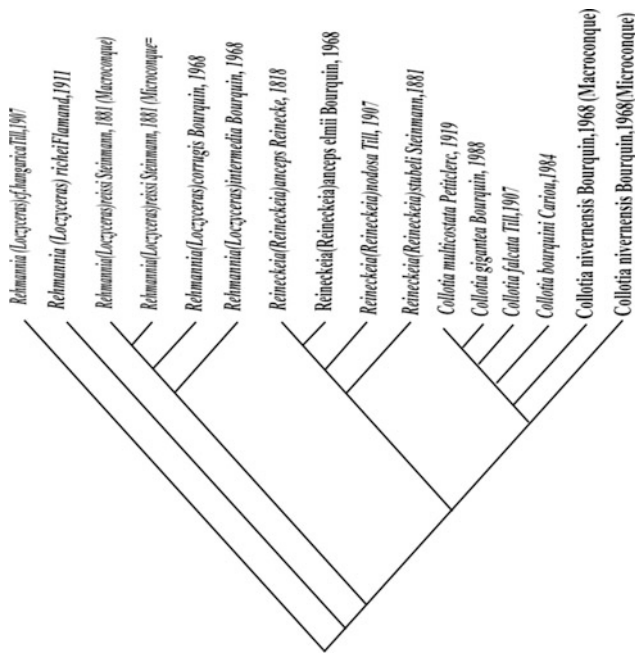


Fig. 3 Phylogeny supposed studied genera (Cladistic approach: strict consensus tree)

The strict consensus tree (Fig. 3) indicates that three types studied (*Rehmannia*, *Reineckeia* and *Collotia*). They are three different branches. This finding confirms the studied group.

The resulting phylogram (Fig. 4) shows that three types studied (*Rehmannia*, *Reineckeia* and *collotia*) which belong to 3 different lines. The *Rehmannia* strain appears as a type of the subfamily of the Reineckeinae which gives birth to its gender and the genders of *Reineckeia* and *Collotia*.

4 Discussion

Today, much of the phylogenetic reconstructions in ammonites are built by using the heterogeneous methods and the eclectic, phylogenetic relationships that are based on these eclectic methods. Even though they can be considered as reasonable, they have theoretical and practical weaknesses. More recently, authors have shown that the cladistic method can offer an operational alternative for the reconstruction of the phylogeny of this group.

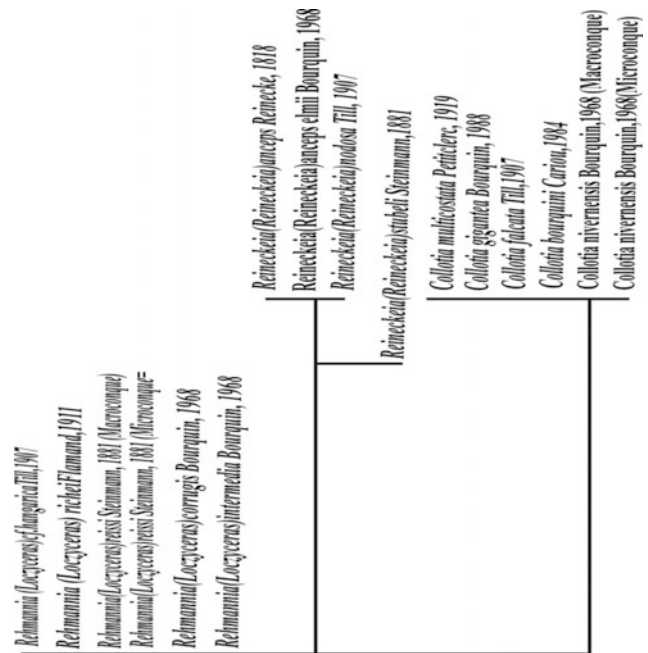


Fig. 4 Phylogram studied genera (Cladistic analysis)

5 Conclusion

Comparing the previously mentioned results with the classical approach to the phylogeny proposed by Cariou [2], certain analogy in the evolutionary history of the studied Reineckeinae is noted. The Cladistic analysis confirms the polyphyletism group, the studied genera *Rehmannia*, *Reineckeia* and *Collotia*. Undoubtedly, they constitute separate lineages. The genus *Rehmannia* appears as a type strain in the subfamily Reineckeinae which later gives rise to the genres of the *Reineckeia* and *Collotia*.

References

1. Cariou, E.: Upstairs Callovian in the central West of France. Thesis Univ. Poitiers, No. 325, Part 1, 37 p., 32 fig., 2 pl. - Part 2, Issue. 1, 361 p., 121 text. Fig., 34 tabl.; fasc. 2, 790 p., 244 text. fig., 70 tabl.; fasc. 3, pl. I-LXIX (1980)
2. Touahria, A.: Biostratigraphy of Callovian around Sidon (western Algeria). The Reineckeidae (Ammonitina, Perisphinctaceae). 3rd thesis Cycle, University of Lyon, 152 p., (Unpubl.) (1979)

Rudists in the Revised Bivalvia ‘*Treatise Online*’

Peter W. Skelton, Eulàlia Gili, Thomas Steuber, Robert Scott, and Simon Mitchell

Abstract

The background to the preparation of the rudist sections for the ongoing complete revision of the Bivalvia volumes of the ‘*Treatise on Invertebrate Palaeontology*’ is described. The progress on publication is reported. The plans for further work are outlined. Three introductory chapters on rudists have already been published in ‘*Treatise Online*’ (University of Kansas, Paleontological Institute). Future work will be devoted to the preparation of the taxonomic descriptions of genera and a synoptic example of which is provided for the genus *Pachytraga*.

Keywords

Rudists • Taxonomy • Evolution • Palaeoecology • Stratigraphy

1 Introduction

Nearly four decades after the publication of the original Bivalvia volumes of the ‘*Treatise on Invertebrate Palaeontology*’ [3, 11], a proposal for a complete revision was launched

in 2006 by Joe Carter and Roger Thomas at the International Congress on Bivalvia. It was held in Barcelona [6]. For the rudist bivalves (Order Hippuritida), this proposal was timely as extensive taxonomic, palaeoecological and stratigraphical work on them had been done in the interim and was to follow—much of it published in proceedings from a series of international rudist conferences in: Belgrade, former Yugoslavia, 1988 [16]; Rome and Bari, Italy, 1990 [13]; México, D.F., México, 1993 [1]; Marseille, France, 1996; [7]; Erlangen, Germany, 1999 [5]; Rovinj, Croatia, 2002 [18]; Austin, Texas, USA, 2005 [12]; İzmir, Turkey, 2008 [9]; Kingston, Jamaica, 2011 [8]; and Barcelona, Spain, 2014 [10]. An informal group was formed in 2008 for the task of preparing the rudist part of the revised Bivalvia *Treatise* for which an outline classification was proposed by Skelton and adopted by Carter et al. [2]. A revised version of that scheme [14] provides the systematic basis for the published and projected chapters on rudists as described below.

2 Progress with Publication to Date

Three introductory chapters on rudists have been published in *Treatise Online, Part N (Revised) Mollusca 6, Bivalvia, Vol. 1*. Chapter 26A [15] covers their shell structure, anatomy and evolution, including systematics and palaeogeographical history. Chapter 26B [4] reviews rudist palaeoecology. Finally, Chapter 26C [17] documents the stratigraphical ranges and the diverse dynamics of rudist genera <http://paleo.ku.edu/tronline/treatiseonline.html>.

These chapters show how, despite confinement to sessile epifaunal life habits, rudists achieved considerable taxonomic diversity (>160 genera currently recognized), coupled with exceptional morphological disparity in relation to both shell growth geometry and structural modification of the two shell layers that all rudists possessed—an outer layer of fibrillar prismatic calcite and an aragonitic inner shell. This morphological exuberance reflects their adaptive diversity, particularly in response to modes of sedimentation, in

P. W. Skelton (✉)
The Open University, Milton Keynes, MK7 6AA, UK
e-mail: pwskelto@waitrose.com

E. Gili
Universitat Autònoma de Barcelona, 08193 Bellaterra, Spain

T. Steuber
Khalifa University of Science and Technology, Abu Dhabi, UAE

R. Scott
Precision Stratigraphy Associates and The University of Tulsa,
Cleveland, OK 74020, USA

S. Mitchell
The University of the West Indies, Mona, Kingston, Jamaica

Table 1 Illustrative taxonomic data, for genus *Pachytraga*. LV, left valve; RV, right valve

Genus, author, date, full reference	<i>Pachytraga</i> Paquier, Victor 1900. Recherches géologiques dans le Diois et les Baronnies orientales. Allier frères, Grenoble. 402 + viii p., 12 figs., Pls. 1–3 and 7–8 + geological map. [Name made available on p. 189.]
Type species, author, date, full reference	<i>Sphaerulites paradoxa</i> Pictet, François J. and Gustave Campiche, 1869. Description des fossiles du terrain Crétacé de Sainte-Croix. Matériaux pour la paléontologie suisse (5) 9:352 p. [By monotypy, in Paquier, 1900.]
Type locality; stratigraphic horizon; geological age	Swiss Jura, Regny, plaine de Rocailles; erratic block of Urgonian limestone; presumed Early Aptian
Junior synonym(s) of type species, with author, date and full reference(s)	<i>Pachytraga lapparenti</i> Paquier, Victor, 1905. Les Rudistes urgoniens, Deuxième partie—série Inverse. Mémoire de la Société géologique de France, Paléontologie, 29:49–102. [= Subjective synonym: Skelton, Peter W. & Jean-Pierre Masse, 1998. Revision of the Lower Cretaceous rudist genera <i>Pachytraga</i> Paquier and <i>Retha</i> Cox (Bivalvia: Hippuritacea), and the origins of the Caprinidae. Geobios, Mémoire Spécial 22:331–370.]
Generic junior synonym(s) and misspellings with author, date and full reference(s)	None
Generic diagnosis [N.B., <i>excluding</i> character data for inclusive higher taxa—Superfamily Caprinoidea d’Orbigny, 1847 and Family Caprinidae d’Orbigny, 1847 [14]— <i>Derived</i> : ligament invaginated, shell uncoiled, with RV cylindro-conical and LV capuloid; LV posterior myophore inwardly inclined, rooted on posterior valve wall, and separated from body cavity by accessory cavity, which is demarcated internally by lamina connecting anterior tooth to postero-ventral margin; RV posterior myophore a robust vertical plate attached to lamina connecting central tooth to postero-ventral valve margin, separated from posterior valve wall by narrow cavity, and traversing commissural plane to face posteriorly onto LV posterior myophore. <i>Primitive</i> : outer shell layer thin, with fine radial riblets on RV; LV teeth unequal (posterior much smaller than anterior).]	Commissure rounded sub-trapezoidal, with prominent anterior carina; dorso-ventral diameter > antero-posterior diameter. Internally, RV: posterior ectomyophoral cavity undivided or radially divided at depth by thin laminar partitions; anterior myophore may be separated from valve wall by narrow cavity, which may also be radially subdivided as incipient pallial canals; no ventral canals. LV: posterior and/or anterior myophore(s) may be separated from valve wall by shallow gutter(s), which may also be subdivided by thin radial partitions; pallial canals, if present, outside <i>either</i> anterior <i>or</i> posterior myophore, but not both, and absent ventrally. No tabulae present in either valve. [Comment: diagnostic characters that are universal for genus are all relatively primitive within Caprinidae, of which it is thus the basal member.]
Description of type species, including depository, accession numbers and available data on type specimens	Six syntype specimens in Pictet & Campiche (1869), Pl. 150, Figs. 1–6; deposited in Musée d’histoire naturelle, Geneva, with lot number AIII-36-11001. [LV figured as Pl. 150, Fig. 2a, b designated as lectotype by Skelton and Masse, 1998 [7].]
Description (as above) of other reference species for genus	Skelton and Masse, 1998 [7]
Illustrations of type (and reference species) of genus, with repository and accession numbers of all illustrated specimens (TIFF or eps)	Skelton and Masse, 1998 [7]
Illustrations of type (and reference species) of generic junior synonym(s)	(Not applicable)
History of usage (optional)	Six species assignments rejected by Skelton and Masse, 1998 [7].
Geographic/palaeogeographic distribution	Mediterranean to Arabian Tethys; Cuba, Japan?
Stratigraphic range with species author(s) and full references	<i>First</i> , basal Hauterivian: <i>P. tubiconcha</i> Astre, Gaston, 1961. <i>Pachytraga</i> tubuleux du Barrémien du Doubs. Bulletin de la Société d’Histoire Naturelle de Toulouse 96:205–222 (Skelton and Masse, 1998). <i>Last</i> , topmost Lower Aptian: <i>P. cf. paradoxa</i> (Skelton and Masse, 1998)

Dedication: to the memory of Stefan Götz, our fellow co-author, of Chapter 26B, whose tragically early death robbed us of an outstandingly able colleague and a good friend

addition to other factors. From a Late Jurassic origin to an abrupt demise at the close of the Cretaceous, they underwent a series of evolutionary radiations, becoming widely distributed across the shallow marine, carbonate-dominated shelves and platforms spread along the equatorially

encircling Tethyan-Atlantic-tropical Pacific oceanic belt. These radiations were checked by episodic extinctions linked with crises in the growth of their hosting carbonate platforms and shelves, most notably in the mid-Valanginian, Early to mid-Aptian, and Late Cenomanian.

3 Future Publication Tasks

Beyond these three introductory chapters, the task of preparing taxonomic descriptions for each genus—the essential purpose of the *Treatise*—has yet to be accomplished. To achieve consistency of format and to avoid overlap, it will be necessary to appoint a single person, or at most a few people, to coordinate the data for each family, but the more people with specialist expertise who are able to contribute to the work, the sooner publication can be achieved. Potential volunteers are therefore invited to contact the corresponding author, stating for which taxon or taxa they could supply data and/or illustrations. As an illustrative guide to the information ideally required, Table 1 summarises the data for a single genus, *Pachytraga*. Of course, some genera will prove not to have such a relatively uncontentious and recently revised taxonomy as this example, thus requiring some extra bibliographic, and/or primary descriptive work—for example, to resolve issues of priority, types and synonymy.

References

- Alencáster, G., Buitrón-Sánchez, B.E. (eds.): Número dedicado a la tercera Conferencia internacional sobre Rudistas. *Revista Mexicana de Ciencias Geológicas* **12**(2), 316 (1996)
- Carter, J.G., others: A synoptical classification of the Bivalvia (Mollusca). *University of Kansas Paleontological Contributions* **4**, 1–47 (2011)
- Cox, L.R., others: *Treatise on Invertebrate Paleontology, Part N, Mollusca 6 Bivalvia*, vol. 1, pp. i–xxxviii, N1–N489; vol. 2, pp. N491–N952. University of Kansas and Geological Society of America, Lawrence, Kansas (1969)
- Gili, E., Götz, S.: Part N, Revised, vol. 2, Chapter 26B: Paleocology of rudists. *Treatise Online* **103**, 1–29, 22 fig. (2018)
- Höfling, R. (ed.): Contributions to the 5th International Congress on Rudists. *Courier Forschungsinstitut Senckenberg* **247**, 245 (2004)
- Malchus, N., Pons, J.M. (eds.): International Congress on Bivalvia: Abstracts. *Organisms Diversity and Evolution* **6**, Electronic Supplement 16, part 1, 1–82. © Gesellschaft für Biologische Systematik (2006). <http://senckenberg.de/odes/06-16.htm>. Accessed 29 April 2018
- Masse, J.-P., Skelton, P.W. (eds.): Quatrième Congrès international sur les rudistes. *Geobios, Mémoire spécial* **22**, 427 (1998)
- Mitchell, S.F., James-Williamson, S.A. (eds.): Rudists 2013—Papers presented at the Ninth International Congress on Rudist Bivalves, 18th to 25th June, 2011, and selected other papers. *Caribbean J. Earth Sci.* **45**, 132 (2013). <http://caribjes.com/caribjesbackissues.html>. Accessed 29 April 2018
- Özer, S., Sari, B., Skelton, P.W. (eds.): Jurassic-Cretaceous Rudists and Carbonate Platforms. *Turkish J. Earth Sci.* **19**(5), ii + 527–669; (6), ii + 671–798 (2010)
- Pons, J.M., Vicens, E. (eds.): Tenth International Congress on Rudist Bivalves, Scientific Program and Abstracts. *Universitat Autònoma de Barcelona*, 36 p. (2014)
- Stenzel, H.B.: *Treatise on Invertebrate Paleontology, Part N, Mollusca 6 Bivalvia*, vol. 3, p. i–iv, N953–N1224. University of Kansas and Geological Society of America, Lawrence, Kansas (1971)
- Scott, R.W. (ed.): *Cretaceous Rudists and Carbonate Platforms: Environmental Feedback*. SEPM Special Publication 87, Tulsa, Oklahoma, 257 p. (2007)
- Sirna, G. (ed.): The Second International Conference on Rudists. *Geologica Romana (nuova serie)* **28**, Università degli studi di Roma “La Sapienza”, 372 p. (1992)
- Skelton, P.W. Rudist classification for the revised Bivalvia volumes of the ‘*Treatise on Invertebrate Paleontology*’. *Caribbean J. Earth Sci.* **45**, 9–33 (2013a; with nomenclatural correction, p. 34, 2013b)
- Skelton, P.W.: Part N, Revised, Volume 1, Chapter 26A: Introduction to the Hippuritida (rudists): Shell structure, anatomy, and evolution. *Treatise Online* **104**, 1–37, 19 fig. (2018)
- Sladić-Trifunović, M. (ed.): Proceedings—First International Conference on Rudists, 1988. Memorial Publication, Union of Geological Societies of Yugoslavia, Belgrade, 322 p. (2002)
- Steuber, T., Scott R.W., Mitchell S.F., Skelton, P.W.: Part N, Revised, Volume 1, Chapter 26C: Stratigraphy and diversity dynamics of Jurassic–Cretaceous Hippuritida (rudist bivalves). *Treatise Online* **81**, 1–17, 7 fig., 1 table (2016)
- Velić, I., Vlahović, I. (eds.): *Geologia Croatica* **56/2** (2003), **57/1** and **57/2** (2004), including papers from 5th International Rudist Congress, 331 p. (2003–2004)

Morphological variability of *Polyconites hadriani* (Hippuritida, Bivalvia) in the Aptian carbonate platforms of the western Maestrat Basin, eastern Iberia

Eulàlia Gili, Enric Pascual-Cebrian, Peter W. Skelton, and Telm Bover-Arnal

Abstract

This investigation is aimed to study the morphological variability of the polyconitid rudist, *Polyconites hadriani*, from the Aptian carbonate platforms of the western Maestrat Basin, in Iberia. The individuals of the platform top to upper slope carbonates differ from those of the slope deposits in the size and external shape of the shell. Therefore, the populations of these two distinct platform habitats were compared by morphometric measures (dorso-ventral commissural diameter and antero-posterior commissural diameter). The results of the morphometric analysis showed that shell size and shell form were correlated with depth. (1) Larger shells occur in the slope deposits while smaller shells in the shallower platform top to upper slope settings; (2) commissural outline is compressed dorso-ventrally in the individuals from the platform top to upper slope environments and in half the individuals from the slopes, whereas the commissural outline is compressed antero-posteriorly in the other half of the slope group. It is suggested that phenotypic plasticity allowed *P. hadriani* to adapt shell growth to the different ecological conditions prevailing in the two habitats.

Keywords

Rudists • *Polyconites* • Morphological variability
Aptian • Iberia

1 Introduction

The polyconitid rudist, *Polyconites hadriani* Skelton et al. [1], was a common inhabitant of carbonate platforms of Aptian age in the Galve sub-basin of the western Maestrat Basin in the eastern Iberian Chain [2–4]. Although *P. hadriani* was widespread in the platforms, its most favoured habitats were the platform margins and proximal slopes [1, 5].

Polyconites shells from these two platform settings show variation in size and external form. The present paper addresses the relationship between the environmental and the morphological variability in *P. hadriani*.

The studied polyconitids came from platform top to upper slope carbonates of two uppermost Lower Aptian platforms, the highstand Camarillas-El Morrón platform [2, 6] and the succeeding Las Mingachas lowstand platform [3, 6]; and from the slope carbonates of the uppermost Lower Aptian La Serna isolated highstand platform [4, 7] and from lowermost Upper Aptian highstand slope carbonates in the localities of Las Mingachas [3, 6], Barranco de las Corralizas [2] and Barranco de La Serna [2, 4].

The preliminary results of the current study are presented below.

2 Materials and Methods

Description of the Polyconitid. The shell of *Polyconites hadriani* is highly inequivalve. The right valve has an elongated asymmetrical conical form with the ventral flank relatively more extended than the dorsal flank. The left valve is operculiform. Commissural outline varies from rounded to

E. Gili (✉)
Universitat Autònoma de Barcelona, 08193 Bellaterra
(Cerdanyola del Vallès), Spain
e-mail: eulalia.gili@uab.cat

E. Pascual-Cebrian
Institute of Earth Sciences Jaume Almera, ICTJA-CSIC, 08028
Barcelona, Spain

P. W. Skelton
The Open University, Milton Keynes, MK7 6AA, UK

T. Bover-Arnal
Universitat de Barcelona, 08028 Barcelona, Spain

oval with antero-posterior or dorso-ventral long axis. Adult shell length rarely exceeded 80 mm. Commissural diameters (antero-posterior and dorso-ventral) may approach 70 mm. *P. hadriani* was an elevator, growing more or less embedded in the sediment or attached to other individuals, thereby forming clusters of imbricated shells. (See [1] for an accurate description of the species.)

Sampling. Specimens were collected in two distinct depositional settings of the carbonate platforms: platform top to upper slope carbonates (n = 2 sites) and in slope carbonates (n = 4 sites). A total of 111 shells were used: 31 from platform top to upper slope deposits and 80 from slope deposits.

Analysis. For each individual the following measurements were done: dorso-ventral commissural diameter, Comm Diam d/v; antero-posterior commissural diameter, Comm Diam a/p. Graphs were created in Microsoft Excel. Linear trend lines were used to guess the general trend of the data. ANOVA test for equal means: differences for both variates highly significant (for Comm Diam d/v, $p = 2.8 \times 10^{-9}$; for Comm Diam a/p, $p = 0.0002157$).

We thank Mükerrerem Fenerci-Masse for the ANOVA test.

3 Results

The largest specimens of *Polyconites hadriani* are found in slope facies (Fig. 1), both in the slope carbonates of the uppermost Lower Aptian La Serna platform and in the lowermost Upper Aptian highstand slope deposits (Fig. 2).

Commissural outline varies in shape from rounded, less commonly, to oval. Specimens from platform top to upper slope facies usually have an oval commissural outline with an antero-posterior long axis. Approximately half of the slope *Polyconites* also have the commissural outline compressed dorso-ventrally, but the other half have an oval commissural outline with dorso-ventral long axis (Fig. 1).

4 Discussion

The morphometric overlap between these stratigraphically and geographically contiguous populations leaves no doubt that they all belong to a single species. Whereas Fig. 2 rules out any significant difference between the stratigraphically older (latest Early Aptian) and younger (earliest Late Aptian) samples from similar slope settings, Fig. 1 shows a clear distinction between the two different settings—slope, and platform-top to upper slope, respectively, for which the simplest explanation would be ecophenotypic differentiation due to different conditions in the two settings.

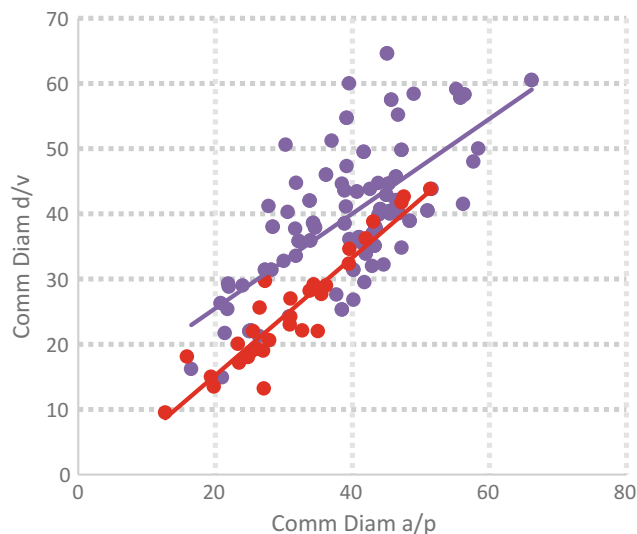


Fig. 1 Bivariate scatter plot of commissural diameters (measured in mm) in 111 specimens of *Polyconites hadriani*. Comm Diam d/v, dorso-ventral commissural diameter; Comm Diam a/p, antero-posterior commissural diameter. Blue = specimens from the uppermost Lower Aptian slope of La Serna platform and lowermost Upper Aptian highstand slopes; red = specimens from platform top to upper slope carbonates of uppermost Lower Aptian Camarillas-El Morrón and Las Mingachas platforms

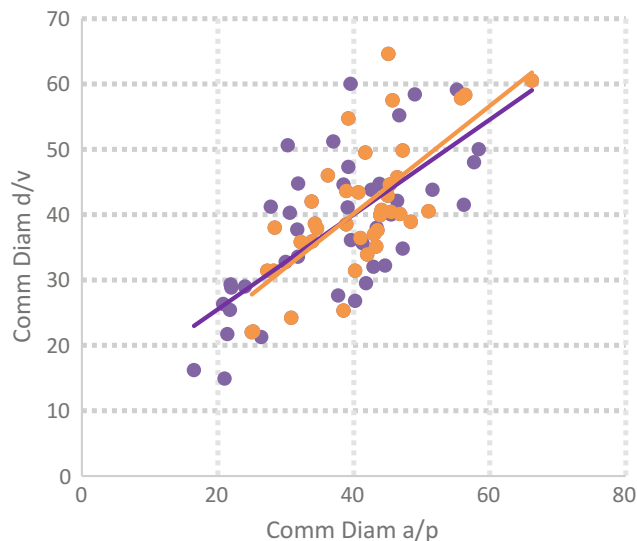


Fig. 2 Bivariate scatter plot of commissural diameters (measured in mm) in 80 slope specimens of *Polyconites hadriani*. Comm Diam d/v, dorso-ventral commissural diameter; Comm Diam a/p, antero-posterior commissural diameter. In this figure, the blue points from Fig. 1 have been sub-divided into uppermost Lower Aptian (yellow) and lowermost Upper Aptian (purple)

There are many possible causal factors for such ecophenotypic differentiation in sessile epifaunal bivalves, though one likely factor identified in a comparative study of living

and fossil oysters is that of the differences in ambient primary productivity [8]. Further work is needed to test this hypothesis in the present case.

References

1. Skelton, P.W., Gili, E., Bover-Arnal, T., Salas, R., Moreno-Bedmar, J.A.: A new species of *Polyconites* from the uppermost Lower Aptian of Iberia and the early evolution of polyconitid rudists. *Turkish J. Earth Sci.* **19**, 557–572 (2010)
2. Bover-Arnal, T., Moreno-Bedmar, J.A., Salas, R., Skelton, P.W., Bitzer, K., Gili, E.: Sedimentary evolution of an Aptian syn-rift carbonate system (Maestrat Basin, E Spain): effects of accommodation and environmental change. *Geol. Acta* **8**, 249–280 (2010)
3. Bover-Arnal, T., Salas, R., Skelton, P.W., Gili, E., Moreno-Bedmar, J.A.: The Aptian carbonate platforms of the western Maestrat Basin: a textbook example of four systems tract-based sequence stratigraphy. In: Arenas, C., Pomar, L., Colombo, F. (Eds.), 28th IAS Meeting, Zaragoza. Sociedad Geológica de España, Geo-Guías vol. 7, pp. 27–64 (2011)
4. Bover-Arnal, T., Pascual-Cebrian, E., Skelton, P.W., Gili, E., Salas, R.: Patterns in the distribution of Aptian rudists and corals within a sequence-stratigraphic framework (Maestrat Basin, E Spain). *Sed. Geol.* **321**, 86–104 (2015)
5. Gili, E., Skelton, P.W., Bover-Arnal, T., Salas, R., Obrador, A., Fenerci-Masse, M.: Depositional biofacies model for post-OAE1a Aptian carbonate platforms of the western Maestrat Basin (Iberian Chain, Spain). *Palaeogeogr. Palaeoclimatol. Palaeoecol.* **453**, 101–114 (2016)
6. Bover-Arnal, T., Salas, R., Moreno-Bedmar, J.A., Bitzer, K.: Sequence stratigraphy and architecture of a late Early-Middle Aptian carbonate platform succession from the western Maestrat Basin (Iberian Chain, Spain). *Sed. Geol.* **219**, 280–301 (2009)
7. Bover-Arnal, T., Löser, H., Moreno-Bedmar, J.A., Salas, R., Strasser, A.: Corals on the slope (Aptian, Maestrat Basin, Spain). *Cretac. Res.* **37**, 43–64 (2012)
8. Johnson, A.L.A., Liquorish, M.N., Sha, J.: Variation in growth rate and form of a Bathonian (Middle Jurassic) oyster in England, and its environmental implications. *Palaeontology* **50**, 1155–1173 (2007)

Description of a New Genus of Radiolitidae (Bivalvia, Hippuritida) with Canals in the Calcitic Shell Layer

Valentin Rineau and Loïc Villier

Abstract

The species *Radiolitella pulchellus* (Vidal 1876) from Campanian-Maastrichtian of Spain (provinces of Lleida and Barcelona) and France (Dordogne) is revised and re-described. The genus *Radiolitella* gathers all the Radiolitidae where the floors formed by the growth lamellae disappear and the cells take the appearance of canals. *R. pulchellus* is the only taxon with canals in the calcitic layer of the left valve while canals of the other *Radiolitella* species are found on the right valve. This major difference suggests that the genus *Radiolitella* should be redefined with species having canals on the left valve moved to a new genus. A new species is proposed based on an unpublished specimen from the Toucas collection which belongs to them as a group.

Keywords

Rudist bivalves • Late cretaceous • *Radiolitella* Radiolitidae • Canals

1 Introduction

Radiolitidae were abundant and diversified on the shallow carbonate platforms during the middle-upper Cretaceous. Amongst them, the genus *Radiolitella* is defined by Douvillé [1] and by the presence of the canals in the calcitic layer.

Those canals in the calcitic layer are not all homologous. They are investigated in *Radiolitella* suggesting the polyphyly of the genus. We propose to split the species assigned to *Radiolitella* into two genera: (i) the genus *Radiolitella* based on, keeping together the species having several rows of large polygonal canals in the calcitic layer in the right valve and (ii) a new genus based on the species *Radiolitella*

pulchellus (Vidal 1876) as well as a new species in which the canals in the calcitic layer are arranged in a single row on the left valve.

2 Materials and Methods

The re-description of the fossil shells is based on a literature survey and on the specimens held in Sorbonne Université (SU) and Muséum National d'Histoire Naturelle (MNHN) collections. Two specimens from Dordogne (France) are held in the Toucas collection (SU): one from Beaumont-du-Périgord (MNHN.F.J07088; upper Campanian) and the other from Douville (MNHN.F.J07091; locality of Saint-Mamet in Toucas 1907 [4]; upper Campanian). A third specimen of the Toucas collection belonging to the same genus has been found (SU 2017.0.58.3); however, no information is available on its locality.

3 Results

The specimens of *R. pulchellus* are highly inequivalve with an almost opercular left valve (a few millimeters deep) and a conical right valve. The apex of the left valve is close to the center and slightly dorsal. The apex of the right valve is acuminate and curved on the ventral-posterior side. The surface of the shell is smooth with two radial bands limited by three round ribs. The shells of *R. pulchellus* have an average height of 40 mm and a diameter ranging from 20 to 30 mm (the dorso-ventral side being slightly compressed compared to the anteroposterior side).

The species was initially described as *Sphaerulites pulchellus* on the base of the external shape of the shell (Fig. 1): “*Valva superior opercular plana, de contorno ovalado ó subangulos, adornada de estrechas y numerosas arrugas radiales muy aproximadas*” [5: 109]. Thereafter, Toucas assigned the species to *Praeradiolites* but suggested it may belong to the genus *Radiolitella* on the basis of the presence

V. Rineau (✉) · L. Villier
UMR 7207 CR2P, Sorbonne Université/CNRS/MNHN/UPMC,
43 rue Buffon, 75231 Paris Cedex 05, France
e-mail: valentin.rineau@mnhn.fr

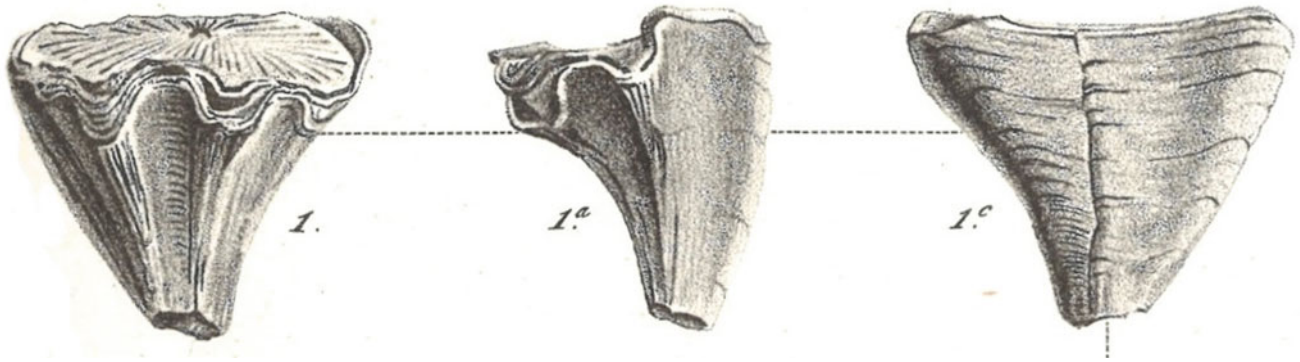


Fig. 1 First illustration of *Radiolitella pulchellus* in Vidal 1876 originally assigned to *Sphaerulites* with the canals in the calcitic layer of the left valve interpreted as costae

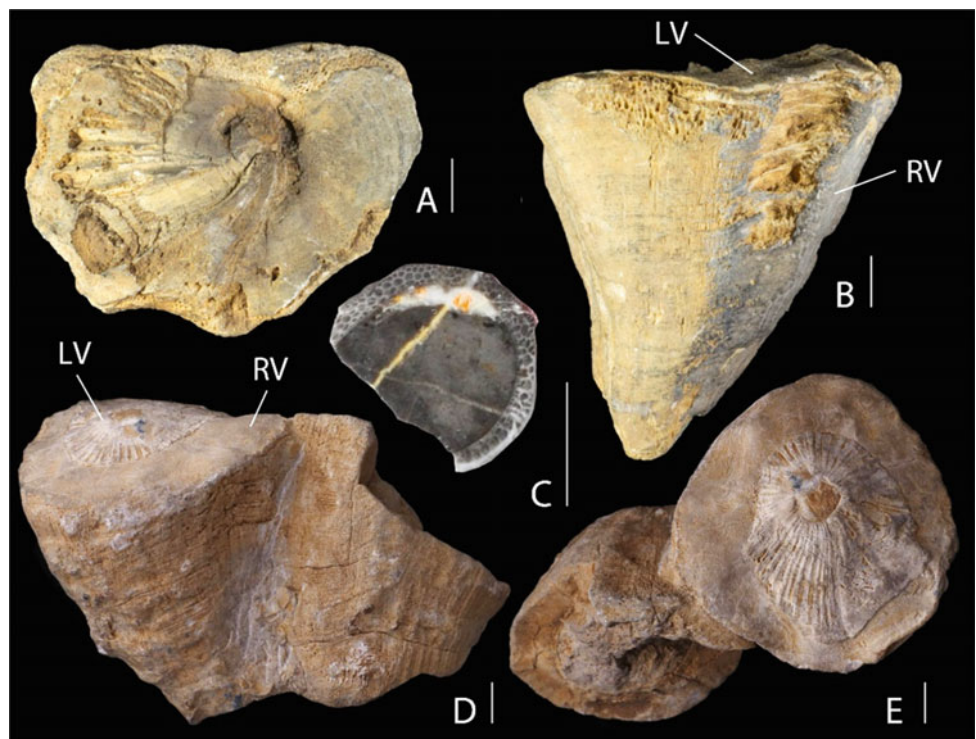
of canals in the calcitic shell layer without saying on which valve it is [4]. Toucas briefly describes the upper valve: “*la valve supérieure est plane et radiée*” [4: 39]. Pons [2] formally assigned *R. pulchellus* to *Radiolitella*. He unambiguously described the canals as being on the right valve: “*Ya Toucas (1907) había señalado la presencia de canales en la valva inferior; en sección se observan estos perfectamente, por lo que no cabe duda la atribución de esta especie al género Radiolitella*” [2: 73].

Following Toucas the left valve is described without canals but only with “*ornamentada con finas costillas radiales*” [2: p. 73].

The re-description of the syntypes and Toucas specimens clarifies the nature of the left valve canals. The left valve carries a single layer of canals and a triangular cross-section that radiate from the apex (Fig. 2a). These canals take a groove-like appearance when the outermost part of the calcitic layer is either dissolved or broken. Very fine striations are present in the width of the canals. The Toucas specimens (Fig. 2b) show the celluloprismatic layer (polygonal cells) situated only on the right valve.

We found an unpublished specimen in the Toucas collection that represent a new species (SU 2017.0.58.3; Fig. 2d, e) related to *R. pulchellus*. The specimen is a cluster

Fig. 2 Photographies of specimens of *Radiolitella*. **a, b**—*Radiolitella pulchellus* figured in Toucas 1907 (MNHN.F.J07091; Douville, Périgord, France; upper Campanian). **c**—*Radiolitella* sp. figured in Douville 1904 and shown the characteristic polygonal canals of the right valve (EM 15876; Sierra de Cadi, Spain). **d, e**—specimen related to *Radiolitella pulchellus* but belonged to a distinct species (SU 2017.0.58.3). Legends: LV, left valve; RV, right valve. Scale bar: 5 mm



of two individuals (one has the two valves preserved while the other missed the left one). The largest specimen is the most completed measuring 80 mm in height. However, its apex of the right valve is broken. The individual had to measure about 120 mm in all. The left opercular valve does not measure more than 3 mm in height. A row of canals, circular in section, is present in the calcitic layer of the left valve. The right valve is characterized by the arrangement of the celluloprismatic layer with horizontal floors with a width of 5 mm and a shallowness of less than 1 mm as far as ribs are concerned.

4 Discussion

R. pulchellus is not related to other *Radiolitella*. We propose to assigned *R. pulchellus* to a new genus of Radiolitidae defined on the presence of a row of canals in the calcitic layer of the left valve. These canals are non-homologous to the several rows of polygonal canals (Fig. 2c) in the calcitic layer of the right valve found in other species of *Radiolitella*: *R. forojuliensis*, *R. guiscardiana*, *R. secunda*, *R. mirabilis*, and *R. maestrichtiana*. It is not homologous to the canals found in several Radiolitidae taxa especially in the Jouffinae (where canals are in the aragonitic layer or in the right valve).

The presence of canals in the calcitic layer of the left valve is unusual in Rudists except in Hippuritidae where they are associated with external pores. The occurrence of similar canals in the left valve of Radiolitidae can be explained by two evolutionary scenarios that require future testing in cladistic analysis:

- It illustrates a kinship relationship between *R. pulchellus* and Hippuritidae where *R. pulchellus* shows a stage in the development of the canal-pore system with (i) the development of canals followed by (ii) the appearance of pores. In modern phylogenetic scenarios, the origin of the canal/pore system in terms of homology is unknown.
- The most likely scenario is where canals evolved independently in the Hippuritidae and some Radiolitidae species result in a morphological convergence [3].

5 Conclusion

The various species of *Radiolitella* endorse different combinations of characters. The genus may be polyphyletic. Two groups can be defined from the location and structure of the canal in the calcitic layer of the shell:

- A first group of species with canals in the right valve that might result from the loss of floors in the celluloprismatic layer and comprise *R. forojuliensis*, *R. guiscardiana*, *R. secunda*, *R. mirabilis*, *R. maestrichtiana*.
- A second group with canals in the left valve associates *R. pulchellus* and a new species to be described from a specimen of the Toucas collection.

References

1. Douvillé, H.: Sur quelques rudistes à canaux. Bulletin de la Société géologique de France 4(4), 519–538 (1904)
2. Pons, J.M.: Estudio estratigráfico y paleontológico de los yacimientos de rudistidos del Cretácico sup. del Prepirineo de la Prov. de Lerida. Universidad Autónoma de Barcelona, Publicaciones de Geología (3), 105 (1977)
3. Skelton, P.W., Smith, A.B.: A preliminary phylogeny for rudist bivalves: sifting clades from grades. Geological Soc. Lond. Spec. Publ. 177(1), 97–127 (2000)
4. Toucas, A.: Etudes sur la classification et l'évolution des Radiolitidés. Mémoires de la Société géologique de France. Paléontologie (36), 119 (1907)
5. Vidal, L.M.: Note acerca del sistema Cretáceo de los Pireneos de Cataluña. Boletín de la Comisión del Mapa geológico de España 4, 257–372 (1878)

Similarities and Differences of *Orbitoides* & *Omphalocyclus* Microspheric Forms with Selected Examples from Northern Iraq and Turkey and Their New Morphometric Data

Muhittin Görmüş, Qahtan Ahmed Al Nuaimy, and Engin Meriç

Abstract

Aqra Formation sediment outcrops are widespread in the northern Iraq. There are different formations in various localities of Turkey which contain rich *Orbitoides* and *Omphalocyclus* genera. Megalospheric (A) forms are particularly predominant in the Campanian-Maastrichtian aged siliciclastic and carbonate sediments. External and internal parameters of both genera are correlated in selected specimens to bring out differences and similarities especially on microspheric forms of *Orbitoides* and *Omphalocyclus*. New morphometric data on more than one hundred individual equatorial thin sections from the carbonate samples of the Aqra Formation show that microspheric individuals of *Omphalocyclus* include semicircular equatorial chamberlets at the initial part. On later parts thick walled rectangular shaped chamberlets are shown. In contrast, microspheric individuals of *Orbitoides* mainly comprise semicircular and semi rectangular equatorial chamberlets. Biometrical data on the *Orbitoides* tests from the Aqra Formation show population abundance of *Orbitoides megaliformis* and *O. gruenbachensis*.

Keywords

Aqra Formation • N Iraq • Turkey • *Orbitoides* *Omphalocyclus* • Biometry

1 Introduction

Although there have been many previous studies on systematics, morphometric data, microborings and biostratigraphy of *Orbitoides* and *Omphalocyclus* genera in Turkey and Iraq (see Görmüş, [5] for additional references), similarities and differences of microspheric forms between these genera are not well documented. Hinte [6], Gorsel [4], Caus et al. [2] introduce species identifying criteria for the *Orbitoides* genus. Neumann [8] gives details of its species. Özcan [9] and Al Nuaimy [1] carried out their studies on biometrical data of the genus *Omphalocyclus* from Turkey and Iraq. More recently, Georgescu and Almogi-Labin [3] discuss the initial part of Cretaceous orbitoidal forms. However, these are the first records on biometrical data on the *Orbitoides* genus while new data of microspheric forms from northern Iraq are the first records (Fig. 1).

The aims of the study are basically to compare microspheric forms of the *Orbitoides* and *Omphalocyclus* genera as well as to present preliminary morphometric data and abnormal views of the *Orbitoides* genus from the Aqra Formation, Maastrichtian in age.

2 Materials and Methods

Equatorial thin sections of *Orbitoides* and *Omphalocyclus* were prepared in the geology department laboratory of the Ankara University. More than one hundred new thin sections from carbonates of the Aqra Formation in the northern

M. Görmüş (✉)

Engineering Faculty, Geology Department, Ankara University, Ankara, Turkey
e-mail: mhtngrms@gmail.com

Q. A. Al Nuaimy

Northern Technical University/Technical College, Kirkuk, Iraq

E. Meriç

Moda Hüseyin Bey Sokak, No: 15/4 34710, Kadıköy, Istanbul, Turkey



Fig. 1 Significant localities of *Orbitoides* and *Omphalocyclus* in Turkey and northern Iraq

Iraq were analyzed and photographed under SEM and research microscopes. Internal and external parameters were measured for the megalospheric forms of both genera. In particular, microspheric forms based on the previous literature and obtained data were evaluated.

3 Results

3.1 Comparison of Microspheric Forms of *Orbitoides* and *Omphalocyclus*

Both genera are usually seen in the same paleoenvironmental sediments. Although the distinguished differences are clear in their A forms, the interpretation of B forms is unclear. The initial parts of A forms of both genera seem to be similar (Fig. 2a, b). It is assumed that individuals having rectangular to semi-rectangular shaped chamberlets are B forms of *Omphalocyclus*. They are compared with its megalospheric characterized form (Fig. 2c, d). The initial part of the B forms of *Omphalocyclus* does not include an embryo. The first protoconch is tiny and unclear due to the micritic fillings (Fig. 2c, d). *Orbitoides* B forms include shaped equatorial chamberlets ranging from regular, to semi-circular and to

semi-rectangular (Fig. 2e). Microspheric individuals of both genera have mainly larger test sizes (Fig. 3); meanwhile, small sized ones are not unusual.

3.2 Morphometric Data on the *Orbitoides* Genus

In particular, internal parameters of the *Orbitoides* genus were measured and evaluated in light of its species' descriptions according to Gorsel [4]. Due to a convenient preservation of embryos, they give more reliable descriptive data of species. They are as follows: embryo size, embryo wall thickness, and the number of auxiliary chamberlets changes in different *Orbitoides* species. It is noted that the *Orbitoides* population in the Aqra Formation is considered as both *Orbitoides megaliformis* and *Orbitoides gruenbachensis*. Embryo sizes of *Orbitoides megaliformis* are between 0.6 and 0.75 mm. They are 0.75 and 1 mm in the *Orbitoides gruenbachensis* (Fig. 3). *Orbitoides gruenbachensis* includes a larger embryo by having a large protoconch in addition to a thicker embryonic wall. Microspheric forms of *O. gruenbachensis* and *O. megaliformis* are also different from each other with the views of equatorial chamberlets [7].

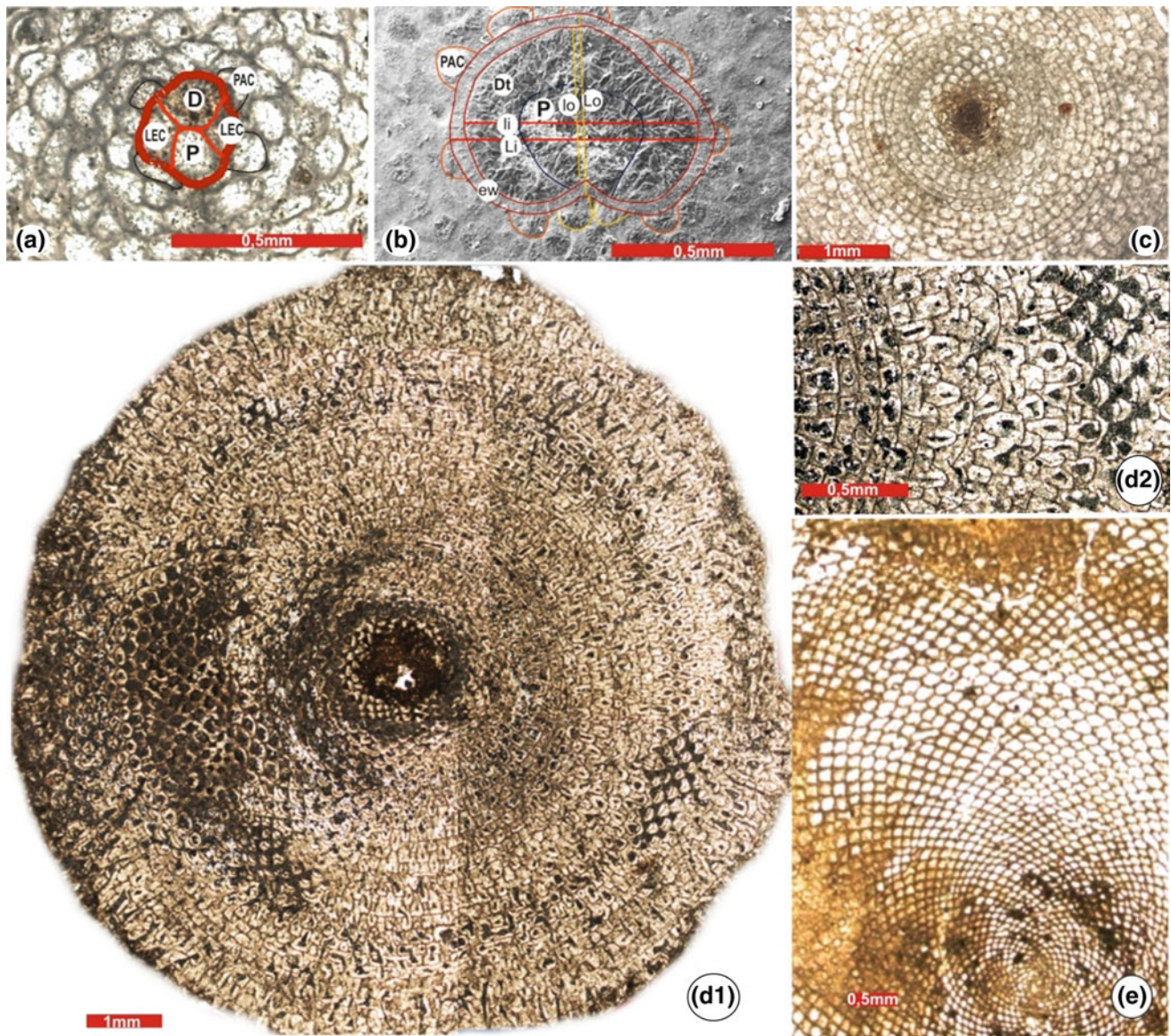


Fig. 2 Initial parts of megalospheric forms of *Omphalocyclus* (a) and *Orbitoides apiculatus* (b), microspheric forms of *Omphalocyclus* (c, d) and *Orbitoides* (e), P. protoconch, D. deuteroconch, LEC. lateral

embryonic chambers, PAC. Principal auxiliary equatorial chamberlets, Li. outer length, li. inner length, Lo. outer width, lo. inner width, ew. embryo wall thickness, A, c–d from Iraq, B. from Turkey

4 Discussion

Previous literature starting from the beginning of the century to recent work on the *Omphalocyclus* and *Orbitoides* has brought out many details of both genera [5]. The current study focuses only on the microspheric forms of the genera and the new preliminary biometric data on the *Orbitoides* from the northern Iraq.

5 Conclusion

New morphometric data and observations from the the Aqra Formation in the northern Iraq and Turkey prove that microspheric individuals of *Omphalocyclus* and *Orbitoides* are different from each other. *Orbitoides* richness is more than *Omphalocyclus*. Their microspheric occurrences are about 1or 2 percentage of the population. Biometrical data

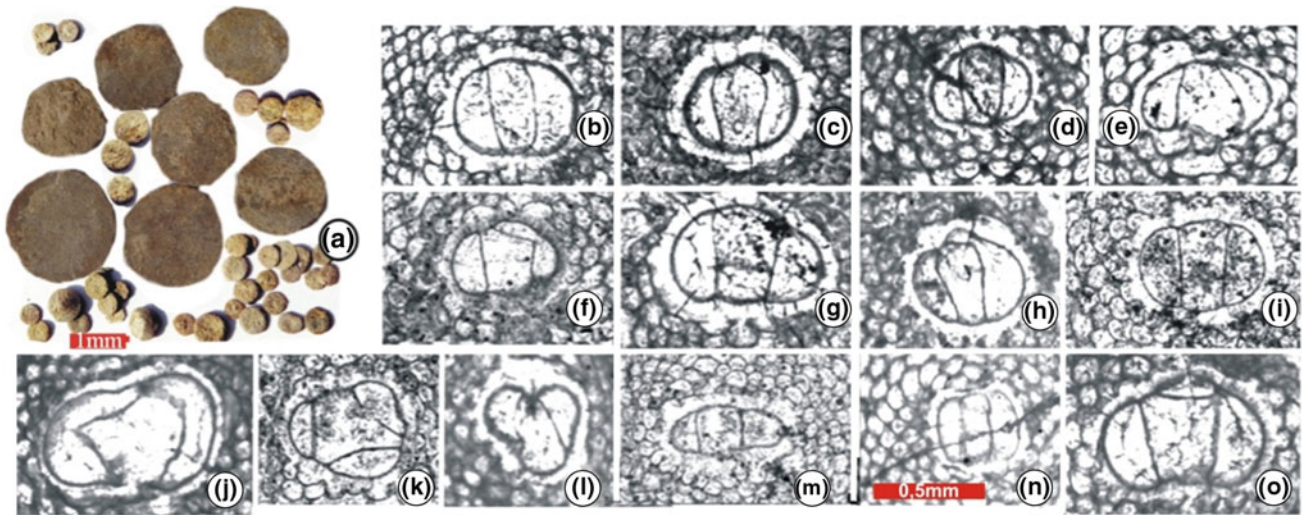


Fig. 3 External views of A and B forms of Maastrichtian orbitoidal forms from the northern Iraq (a) and various shaped embryonic views of *Orbitoides* sp. (k, l), *Orbitoides megaliformis* (b-i, m, n), *O. gruenbachensis* (o, j)

on the *Orbitoides* tests indicate a population abundance of *Orbitoides megaliformis* and *O. gruenbachensis* in the Maastrichtian carbonate platforms of the northern Iraq.

References

1. Al Nuaimy, Q.A.: New quantitative data on *Omphalocyclus* from the Maastrichtian in Northern Iraq. *J. Afr. Earth Sci.* **138**, 319–335 (2018)
2. Caus, E., Bernaus, J.M., Gomez-Garrido, A.: Biostratigraphic utility of species of the genus *Orbitoides*. *J. Foramin. Res.* **26**(2), 124–136 (1996)
3. Georgescu, M.D., Almoji-Labin, A.: New data to suport the phylogenetic relationship between the serial planktonic foraminifera (Family Heterohelicidae Cushman, 1927) and some large sized benthic foraminifera (Family Orbitoididae Schwager, 1876) of the Late Cretaceous. *Revue de Paléobiologie, Genève* **27**(1), 15–24 (2008)
4. Gorsel, J.T. Van: Late Cretaceous Orbitoidal Foraminifera. In: Hedley, R.H., Adams, C.G. (eds.) *Foraminifera*, 1–120. Akademik Press, London (1978)
5. Görmüş, M.: Türkiye *Orbitoides*'lerindeki çalışmalar ve olağan olmayan görünümler In: Gormus, M., Demircan, H. (eds.) 16 PCG Proceedings, 25–28 October 2015, pp. 87–100 (2015)
6. Hinte, J.E. Van: A cretaceous time scale. *Bull. Amer. Assoc. Petrol. Geol.* **60**(4), 498–516 (1976)
7. Meriç, E., Görmüş, M.: *Orbitoides gruenbachensis* Papp'ın Maastrichtian (Geç Kretase) Tetis Okyanusu'ndaki paleocoğrafik yayılımı. *TJK Bülteni* **42**(2), 1–11 (1999)
8. Neumann, M.: Le Genre “*Orbitoides*” I. Reflexion sur les Especies Primitives Attribuees a'ce Genre. *Rev. Micropaleont.* **29**(4), 220–261 (1987)
9. Özcan, E.: Morphometric analysis of the genus *Omphalocyclus* from the Late Cretaceous of Turkey: new data on its stratigraphic distribution in Mediterranean Tethys and description of two new taxa. *Cretac. Res.* **28**, 621–641 (2007)

Cretaceous *Paleodictyon* Trace Fossils: Evolutionary Mimicry Tactic Versus Burrowing: Examples from the Kurdistan Region, Northeastern Iraq

Kamal Haji Karim and Polla Azad Khanaqa

Abstract

The present study is set out not only to discuss but also to propose possible new functions (origins) of *Paleodictyon*. This function is a kind of protection against predation and not related to food habit or burrowing as concluded in previous studies. The organism achieving this protection by making its shape and size resemble (mimic) hard corals to decisive attacker organism. This protective operation happens through the hard corals which are found in the same basin with the traces. The study attributes the origin of trace to the evolutionary mimicry by which the previous dispute about the origin of the *paleodictyon* will be improved or ended.

Keywords

Paleodictyons • Hexagonal coral • Trace fossils
Tanjero formation • Zagros foreland basin
Mimicry • Organism camouflage • Sandstone

1 Introduction

The *Paleodictyons* are complex grazing and patterned feeding/dwelling structures which occur below the sediment/water interface [1, 2]. They include several behavioral buildings such as burrowing and nutritional strategies in food-restricted deep-sea environments Seilacher [3]. They are observable on the event beds either at deep-sea turbidites or

shallow-water storm beds in environments characterized by high-sedimentation rates [4]. Lan and Chen [5] have recorded *Paleodictyon* from a near shore paleo-environmental setting in the Guadalupian of the Carnarvon Basin; Western Australia. Similar traces are also discernible in modern deep seas [6]. However, there is growing evidence that the active eco-space of *Paleodictyon* trace makers are extended into shallow marine environments [4].

2 Methodology and Materials

This paper deals with record of *Paleodictyons* and corals' samples in Maastrichtian Foreland Basin and Early Cretaceous Arabian Passive Margin from Zagros Orogenic Belt, Kurdistan Region, NE Iraq. The authors have found the *paleodictyons* samples in four localities which are Lower Dokan, Upper Dokan, Arbat and Shameran (near Bani Bolan village) areas. They have indicated them by green X letters in the Fig. (1a). They occur in the lower part of Tanjero Formation (turbidite facies), which consists of a succession (about 400 thick) of thick alternation, of medium to thin beds and of sandstone and calcareous shales. The *Paleodictyons* are found on the soles of 3–15 cm thick Bouma sequence sandstone beds that are deposited on submarine fans in deep basin. The authors found the coral samples in the same foreland basin. They are compared analytically with *Paleodictyons* in term of shape and size.

3 Results

3.1 *Paleodictyons* and Coral in the Same Basin

In the Tanjero Formation, Karim [7] described *paleodictyons* for the first time. They comprised horizontal net of hexagonal meshes and have the size of honeycombs. They are observable on the lower surface of fine and medium grain

K. H. Karim (✉)

Department of Geology, University of Sulaimani, Sulaymaniyah, Iraq

e-mail: kamal.karim@univsul.edu.iq

P. A. Khanaqa

Kurdistan Institution for Strategic Studies and Scientific Research, Sulaymaniyah, KRG, Iraq

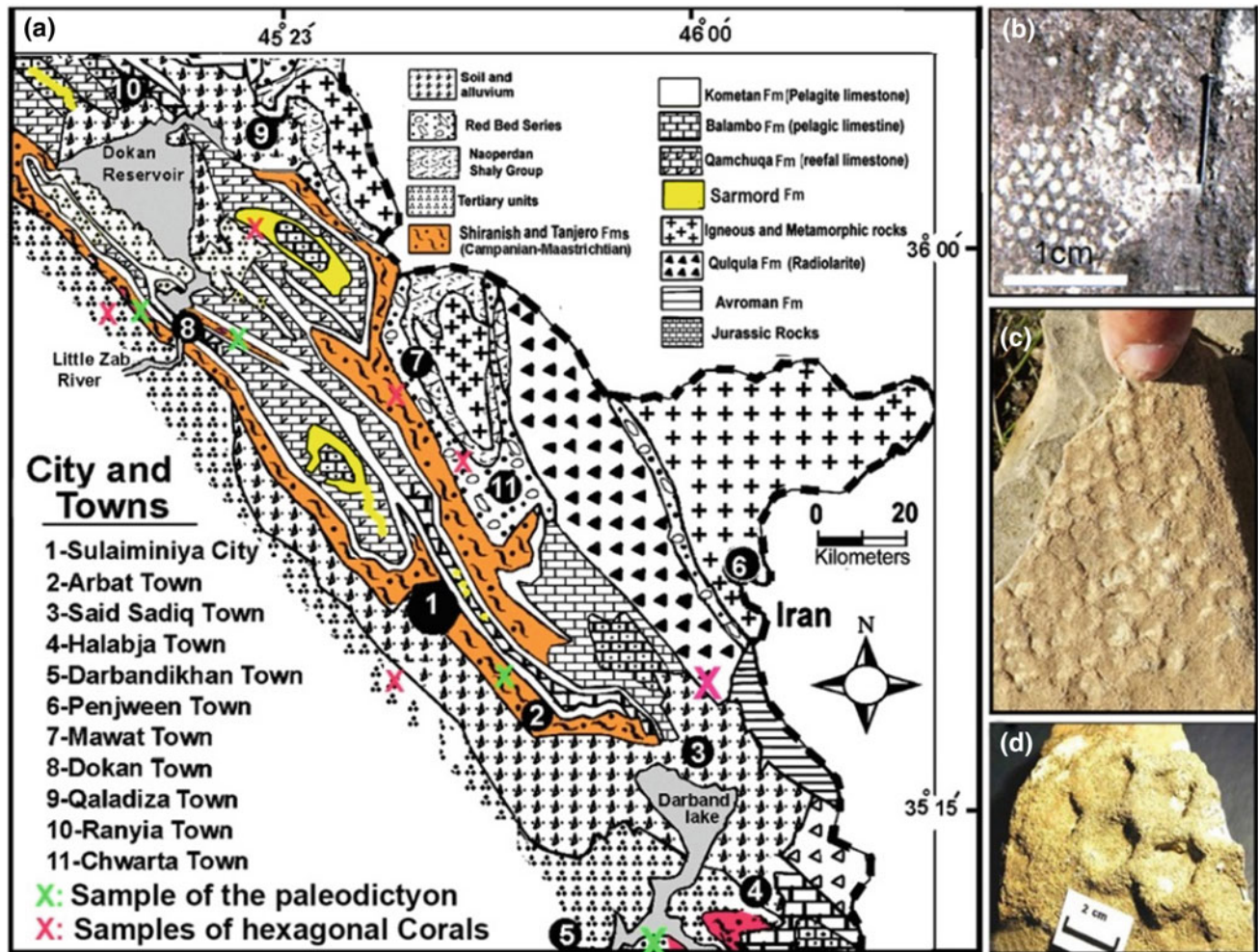


Fig. 1 a Geological map of the studied area shows the location of corals and paleodictyons (Modified from Karim et al. 2011) [8]. b Occurrence of Paleodictyons on overturned slabs of fine grain

sandstone of Tanjero Fm in the Lower Dokan, c on medium grain sandstone in Upper Dokan and d on coarse grain sandstone beds in Arbat area

clastic sediments. The width and depth of a single mesh are 2–10 and 1–4 mm respectively while the large one occurs on the overturned surface of coarse sandstone (Fig. 1b, c and d).

3.2 Corals in the Neo-Tethys (Present Western Zagros)

The occurrences of coral in Zagros Foreland basins are more common than paleodictyons. The present study has recorded many hexagonal coral colonies in the carbonate of the margin at the contact between Sarmord (Valanginan-Barremian) and Qamchuqa (Cenomanian-Aptian) Formations (Fig. 2a). Additionally, they occur in the foreland basin in the Aqra Formation in Dokan and Chwarta areas and in Kolosh & Sinjar Formations (Paleocene) (Fig. 2b).

4 Discussion

Rona et al. [6] discussed possible constructional burrow and sponge body fossil as two explanations for the origin of paleodictyon. The present study proposes new functions for the paleodictyon shapes attributes them to the habit of mimicry between paleodictyon and corals. Parris [9] has cited mimicry as a common method among animals for the protection against predation. This habit is a method by which one animal mimics the shape of another strong animal for protection against any predator (<https://en.wikipedia.org/wiki/Mimicry>). The present proposal depends on the four facts. The first refers to the similarity between the shapes and sizes of the coral and paleodictyon meshes: even the depth and diameter of one cell (or mesh) of both are nearly equal (Figs. 1b, c, d and 2). The second comes into being of both

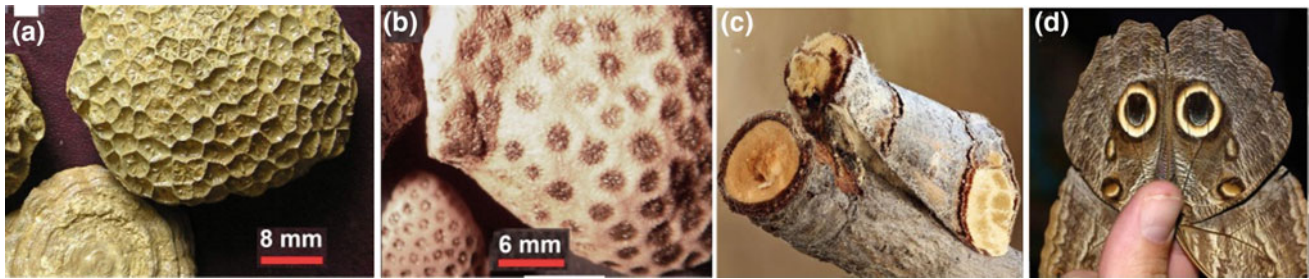


Fig. 2 a and b hexagonal coral colonies in the Neo-Tethys Sea, during Valanginian, and the Paleocene basin respectively, c a moths in the attitude of mimicry and camouflage, a the buff-tip moth (*Phalera*

bucephala) avoids predators by hiding itself as a broken stick during rest <https://www.pinterest.com/pin/42784265185274640/>, d a moth looks like owls to mimic a larger animal

organisms during the Cambrian period and has survived to the recent time. The third is a survival both paleodictyons and corals in the same basin (e.g. Neo-Tethys basin) but in different depths. In this respect, Fursich et al. [4] discussed *Paleodictyon* traces in shallow environment. Moreover, he documents another example of a shallower-water occurrence of the same ichnofossil in Paleozoic rocks.

Therefore, both the coral and the trace can exist in deep and shallow water especially gravel-sized bio-clasts of hexagonal coral could be reworked into deep water by submarine mass wasting, including debris flow and sliding, as seen in Dokan area near the contact between Kolosh and Tanjero Formations. Although corals are mainly restricted to shallow marine water but Freiwald et al. [10] found deep water corals that survive more than 500 m below sea surface. The fourth fact is a mimicry record among the organisms in the literature by which an organism mimics signal properties of another organism to confuse a third organism. The reasons of the mimicry are protection, feeding, and mating [11]. There are two classical types of defensive mimicry: Batesian and Müllerian. Both involve aposematic coloring or warning signals to avoid being attacked by a predator [12]. Examples of the coral and paleodictyon in which soft organism mimics hard body or stronger organism as it is observable in the Fig. (2c and d) showing two types of moths. At the evolutionary level, the proposed mimicry between paleodictyons corals is a genetic and natural selection by which all the earlier paleodictyons shapes become extinct except the hexagonal shape due to its resemblance to hard coral.

The criticism against the present study is related to the occurrence of the paleodictyons mesh below sediment/water surface. It is assumed that it is not observable by predators such as fishes. The justification of this critic is proven through the restriction of the trace to event beds either in deep-sea turbidites or shallow-water storm beds in an environments

characterized by high-sedimentation rates [4]. In these turbulent waters, the removing of the overlying veneer of soft sediments is a common process. Additionally, swimming and moving predators, near the surface of sediment, can generate turbulences and thus uncover the traces. Another justification is that recent paleodictyons are identifiable (expressed) on the sediment surface. Rona et al. [6] showed this identification and expression by publishing many photos.

5 Conclusion

The functions (origins) of *Paleodictyons* are changed from planned for food habit and burrowing to protection from predation against invaders by resembling (mimic) hard corals. The study attributes the origin of the traces to the evolutionary mimicry by which the previous dispute about the origin of the paleodictyon will be improved or ended.

References

1. Seilacher, A.: Biogenic sedimentary structures. In: Imbrie, J., Newell, N. (eds.) *Approaches to Paleocology*, pp. 296–316. Wiley, New York (1964)
2. Wetzel, A.: Recent bioturbation in the deep South China Sea: a uniformitarian ichnologic approach. *Palaios* **23**, 601–615 (2008)
3. Seilacher, A.: Evolution of trace fossil communities. In: Hallam, A. (ed.), *Patterns of Evolution, as Illustrated by the Fossil Record*, pp. 359–376. Elsevier (1977)
4. Fursich, F.T., Taheri, J., Wilmsen, M.: New occurrences of the trace fossil *Paleodictyon* in shallow marine Environments: examples from the Triassic-Jurassic of Iran. *Palaios* **22**, 408–416 (2007)
5. Lan, Z., Chen, Z.Q.: *Paleodictyon* from a near shore paleoenvironmental setting in the Guadalupian (Middle Permian) of the Carnarvon Basin, Western Australia *AUSTRALIAN J. Earth Sci.* **57**, 1–15 (2010)
6. Rona, P.A., Seilacher, A., Vargas, C., Gooday, et al.: *Paleodictyon nodosum*: a living fossil on the deep-seafloor. *Deep-Sea Research II* **56**, 1700–1712 (2009)

7. Karim, K.H.: Environment of Tanjero Formation as inferred from sedimentary structures, Sulaimanyia area, NE-Iraq. (KAJ) Kurd. Acad. J. **4**(1),12–30 (2006)
8. Karim, K.H., Koyi, H., Baziany, M., Hessami, K.: Significance of angular unconformities between Cretaceous and Tertiary strata in the north western segment of the Zagros fold–thrust belt, Kurdistan Region. NE-Iraq. Geol. Mag. **148**(5–6), 925–939 (2011)
9. Parris A.C.: Adaptive Rhetoric: Evolution, Culture, and the Art of Persuasion. Routledge, Rylor and Francis Grou, New York, London (2014)
10. Freiwald, A, Fosså, J. H. Grehan, A. Koslow, T., Roberts, J. M.: Cold-Water Coral Reefs. United Nations Environment Programme–World Conservation Monitoring Centre, Cambridge (2004)
11. Endler J.A: An overview of the relationships between mimicry and crypsis. Biol. J. Linn. Soc. **16**, 25–31 (1981)
12. Holmgren, H., Enquist, M.: Dynamics of mimicry evolution. Biol. J. Lin. Soc. **66**, 145–158 (1999)

First Titanosauriform Teeth from the Early Cretaceous of Tunisia

Jihed Dridi

Abstract

The fossil record of titanosauriform dinosaurs from southern Tunisia is extremely poor. It mainly consists of incomplete specimens that were described from Early Cretaceous fluvial to foreshore deposits of the Tataouine Basin. In the present contribution, I describe new teeth from the Chenini Member in the North of the governorate of Tataouine. The combination of the morphological characters shared by the crowns supports an attribution to titanosauriforms. Although there is no evidence for their autochthony, due to the high energy of the depositional environment, these specimens provide new and valuable information on the dental morphology of the North African titanosauriforms. They confirm their wide palaeo-geographic distribution and at the same time support previous hypotheses about a sporadically connected routes for sauropods between Africa and Europe at the end of the Early Cretaceous.

Keywords

Teeth • Titanosauriform • Early cretaceous
Palaeogeography • Tunisia

1 Introduction

Sauropods are one of the most successful groups of dinosaurs which were widely distributed throughout the terrestrial ecosystems [10]. In southern Tunisia, sauropod remains were collected at three distinct vertebrate-bearing horizons along the Dahar cliff. However, most of these fossils are largely disarticulated and, in most instances, give evidence of taphonomic distortion with one exception. An early

J. Dridi (✉)
Musée de la Géologie, Service Patrimoine Géologique, Office
National des Mines, 24 Rue de l'Énergie, La Chargaia, 2035
Tunis, Tunisia
e-mail: jihed-dridi@live.fr

Cretaceous rebbachisaurid, *Tataouinea hannibalis* is known from a partial post-cranial skeleton [5]. Here, the first titanosauriform teeth from the “Intercalaire Continental” of southern Tunisia with new insights into the coexistence of two distinct sauropod groups during the late Early Cretaceous are described.

2 Geographical and Geological Settings

The fossils described herein were surface collected at the Bir Miteur locality. It is situated approximately 30 km in the north of Tataouine. The locality is part of a chain of escarpments that sporadically edges the Dahar Plateau. This steep relief was substantially affected and fashioned by hydraulic erosion. It exposes a sedimentary sequence that dates from the Late Jurassic to the Late Cretaceous. The fossil layer occurs in the Chenini Member of the Aïn El Guettar Formation which is Aptian-Albian in relation to age. The Chenini Member displays fossiliferous conglomeratic deposits with large petrified tree trunks supporting the presence of an extended marginal alluvial plain. The Chenini Member yields one of the most diverse vertebrate assemblages in the Tataouine Basin. The vertebrate remains, which were highly re-worked, pertain to various marine such as brackish, freshwater and continental taxa including actinopterygians, sarcopterygians, hybodontids, chelonians, crocodylomorphs, pterosaurs and dinosaurs [3, 4].

3 Materials and Institutional Abbreviations

The specimens were collected during the course of two geological field trips aiming at identifying the exceptional geological sites in southern Tunisia. They have been identified and housed in the Museum of Geology of the Office National des Mines (ONM) under the following accession numbers: ONM TM 1 and ONM TM 2.

4 Systematic Palaeontology

Dinosauria Owen, 1842
 Sauropoda Marsh, 1878
 Titanosauriformes Salgado, Coria and Calvo, 1997
 Specimens. ONM TM 1; ONM TM 2

Description: here, new isolated tooth crowns of titanosauriform sauropods are described. The specimens can be classified into two distinct morphotypes:

Morphotype 1: ONM TM 1 is a nearly complete leaf-like tooth crown. It is asymmetric with a moderately sharp apex and a wide basal cross section (maximum apicobasal height 1.5 cm and mesiodistal width 0.8 cm). It is labiolingually compressed. The lingual face is slightly concave; however, the labial face is convex at the mid-height of the crown. There are two distinct curvatures: a lingual curvature visible in mesial view and another one occurring distally near the apical region of the crown. The crown is the broadest. It is close to the tip. The basal section gives a lenticular shape. The mesial and distal edges are narrow. They display smooth carinae which extend from the base to the apex. These carinae bear series of small denticles which have been worn off during transportation. Only some serrations are preserved at the base of the distal carina and in the apical region of the mesial one. Tooth enamel ornamentation is composed of five well-pronounced apicobasally directed ridges which anastomose in the apical region of the lingual face. There is a deep groove between the lingual ridges and the mesial carina. It produces the mesio-lingual flange of the crown. A distal groove is also visible. However, it is markedly shallower than that of the mesial side. The mesial edge bears a low-angled wear facet. A mesio-lingual wear facet occurs apically with a smoothening of the tip of the crown. Microscopically, very fine and irregular enamel wrinkles and scratches are visible on the labial surface of the crown. In basal view, the enamel is markedly thick and the root canal is extremely narrow compared to the mesiodistal and labiolingual widths. It runs into the mid-height of the crown. A hardly distinguishable constriction is present between the crown and the root.

Morphotype 2: ONM TM 2 is a preserved functional tooth crown. It is small but slightly larger than the previous specimen. It was not entirely freed from the matrix which partially hides its basal region. ONM TM 2 has an overall spatulate shape. It is compressed at the labiolingual level. However, the labial and lingual faces are convex. Only a very slight mesial curvature is visible. The basal sectional view of the crown gives an elliptical shape with prominent mesial and distal flanges. These flanges consist of carinae which appear smooth and continuous from the base to the apex. Denticles are hardly distinguishable on both mesial and distal carinae. The labial and the lingual faces are ornamented with apicobasal ridges which originate at the base of the crown. They vanish towards its tip. They are

more pronounced labially than lingually. Two mesial and distal grooves are present on the labial face of the crown. The enamel surfaces display fine apicobasally directed and anastomosed wrinkles with shallow scratches and small sub-circular pits. Two wear facets are identified: the first one consists of a small apical wear facet visible in lingual view; whereas, the second extends along the distal side of the crown. It bears fine and discontinuous wrinkles which seem to be restricted to the basal half of the crown.

5 Discussion

The specimens were compared to several sauropod teeth described and figured in previous publications. They display a combination of morphological features which has been only diagnosed in titanosauriforms. Titanosauriformes have an overall small spatulate tooth crowns which are asymmetric mesiodistally, markedly compressed labiolingually and enlarged mesiodistally at the mid-height of the crown. The maxillary teeth are often more cylindrical than the premaxillary ones. The thick enamel displays apicobasally aligned ridges which are more visible lingually than labially [6]. The presence of the constriction between the crown and the root is reminiscent of Titanosauria. The teeth differ from those of the Early Cretaceous titanosauriforms from Malawi (*Malawisaurus* and *Karongasaurus*) which demonstrate extreme morphological variation among titanosaurian teeth [6]. The noticeable asymmetry in ONM TM 1 is likely due to its position as a right premaxillary tooth [1]. ONM TM 2 has a relatively lower distal curvature and a deeper mesio-lingual groove. These characteristics are reminiscent of an upper right maxillary tooth [9].

Rebbachisaurids and titanosauriforms have been previously reported from Aptian-Albian series of many localities of the Continental Africa. They are shown as they were widely dispersed. Rebbachisaurid remains have also been discovered in the Early-Late Cretaceous of Morocco (with the genus *Rebbachisaurus*). They represent the latest record of this clade confirming their distribution in Western Africa. However, the titanosauriform dinosaurs were more widespread in Africa and survived until the Late of Maastrichtian [8]. Skeletal remains referred to basal titanosaurian sauropods were also found in the Aptian-Albian and the Albian deposits of France and the Italian peninsula respectively. They indicate a possible Afro-Eurasian route for their ancestors [2, 7]. These discoveries are in agreement with those of Titanosauriformes in the northern margin of Gondwana and previous hypotheses of a possible land bridge that would have sporadically connected Africa to Europe allowing for faunal exchanges between these two landmasses [2]. It is suggested that the advanced European titanosaurs would be

the radiation of the late Early Cretaceous basal titanosaurs, which may have had a Gondwanan origin.

6 Conclusion

The occurrence of the Titanosauriformes in North Gondwana confirms the faunal continuity between Africa and southern Europe. Even though they were poorly diverse at the end of the Early Cretaceous, the morphological variations among sauropod teeth support the coexistence of several taxa which shared the same environment. The diversification among the terrestrial plants during this period is an indication of a productive ecosystem. These large terrestrial animals would have avoided competitive exclusion by partitioning their resources. By the Late Cretaceous, the decrease in rebbachisaurid diversity and their post-Cenomanian loss is contemporaneous with significant peaks in biodiversity observed among the Titanosauria [8].

References

1. Amiot, R., Kusuhashi, N., Xu, X., Wang, Y.Q.: Isolated dinosaur teeth from the Lower Cretaceous Shaihai and Fuxin formations of northeastern China. *J. Asian Earth Sci.* **39**(5), 347–358 (2010)
2. Dal Sasso, C., Pierangelini, G., Famiani, F., Cau, A., Nicosia, U.: First sauropod bones from Italy offer new insights on the radiation of Titanosauria between Africa and Europe. *Cretac. Res.* **64**, 88–109 (2016)
3. Dridi, J., Hassine, M., Ouaja, M.: La richesse paléontologique et paléobotanique du Sud-Est tunisien: Archive unique du paléo-océan téthysien. *Annales des Mines et de la Géologie* **47**, 98–113 (2017)
4. Fanti, F., Contessi, M., Franchi, F.: The « Continental Intercalaire » of southern Tunisia: stratigraphy, paleontology and paleoecology. *J. Afr. Earth Sci.* **73–74**, 1–23 (2012)
5. Fanti, F., Cau, A., Hassine, M., Contessi, M.: A new sauropod dinosaur from the Early Cretaceous of Tunisia with extreme avian-like pneumatization. *Nat. Commun.* **4**, 2080 (2013)
6. Gomani, E.M.: Sauropod dinosaurs from the Early Cretaceous of Malawi, Africa. *Palaeontol. Electron.* **8**, 27A (2005)
7. Le Loeuff, J., Suravech, S., Buffetaut, E.: A new sauropod dinosaur from the Albian of Le Havre (Normandy, France). *ORYCTOS* **10**, 23–30 (2013)
8. Mannion, P.D., Barrett, P.M.: Additions to the sauropod dinosaur fauna of the Cenomanian (early Late Cretaceous) Kem Kem beds of Morocco: Palaeobiogeographical implications of the mid-Cretaceous African sauropod fossil record. *Cretac. Res.* **45**, 49–59 (2013)
9. Martinelli, A., Garrido, A., Forasiepi, A., R. Paz, E., Gurovich, Y.: Notes on fossil remains from the Early Cretaceous Lohan Cura Formation, Neuquén Province, Argentina. *Gondwana Res.* **11**, 537–552 (2007)
10. Upchurch, P., Barrett, P.: *Phylogenetic and Taxic Perspectives on Sauropod Diversity*. University of California Press, In the Sauropods (2005)

Mesopelagic Fish Size Reduction in Response to the Messinian Salinity Crisis

Konstantina Agiadi

Abstract

The Messinian salinity crisis (MSC) has already strongly affected the Mediterranean ecosystems from the beginning of the Messinian. Here, the Tortonian, Messinian, and Zanclean size distributions of the most common mesopelagic fish species are compared in order to test the hypothesis that the MSC impacted the size and hence the biomass of Mediterranean mesopelagic fish in the late Miocene. The results suggest that, with appropriate data, a size reduction can be detected during the Messinian that is possibly connected to the MSC restriction of Mediterranean–Atlantic connection. Indeed, these preliminary data suggest an increase otolith size of *Ceratoscopelus* in the Zanclean.

Keywords

Otolith • Miocene • Size distribution • Zanclean • Mediterranean

1 Introduction

In the Late Miocene, the Mediterranean experienced strong environmental disturbances due to the restriction of the basin's connection to the Atlantic Ocean from the Tortonian/Messinian boundary (7.24 Ma) and the culmination toward the Messinian salinity crisis (MSC; 5.97–5.33 Ma) [1]. Fully marine conditions were established

once more at the beginning of the Pliocene [2]. These events had a profound effect on the marine ecosystems manifesting through massive endemism, extinctions and the final re-introduction of the marine species [3].

Fish respond to the environmental stress through various mechanisms including the distribution range shifts and the lifestyle adaptations [4]. Here, we test the hypothesis that mesopelagic fish size was reduced as a physiological response to the Late Messinian restricted oceanographic conditions in the Mediterranean by comparing the size distribution of the selected species as reflected in the fossil assemblages of the pre-evaporitic Messinian against those for the same species in the Tortonian and the Pliocene.

2 Materials and Methods

The size distribution of the typical marine mesopelagic fish species from the Tortonian until the Messinian is obtained by measuring the otolith length of the adult specimens found in six eastern Mediterranean localities (Fig. 1, Table 1).

Otoliths are the aragonitic incremental stone-like structures in the inner ear of Teleost fish that facilitate sound and balance perception [9]. They have species-specific morphology and are commonly found in marine and lake sediments thereby forming a valuable tool for the reconstruction of the past fish faunas [10]. The Otolith length was used here as a direct measure of the fish length and biomass as evidenced by numerous previous studies [11]. Due to space restrictions, only the results for four species are presented here.

3 Results

The results pertaining to the most abundant and common species in all assemblages, *Ceratoscopelus maderensis*, support the initial hypothesis. Indeed, both Tortonian and

K. Agiadi (✉)

Faculty of Geology and Geoenvironment, Department of Historical Geology and Paleontology, National and Kapodistrian University of Athens, Panepistimioupolis, 15784 Athens, Greece
e-mail: kagiadi@geol.uoa.gr

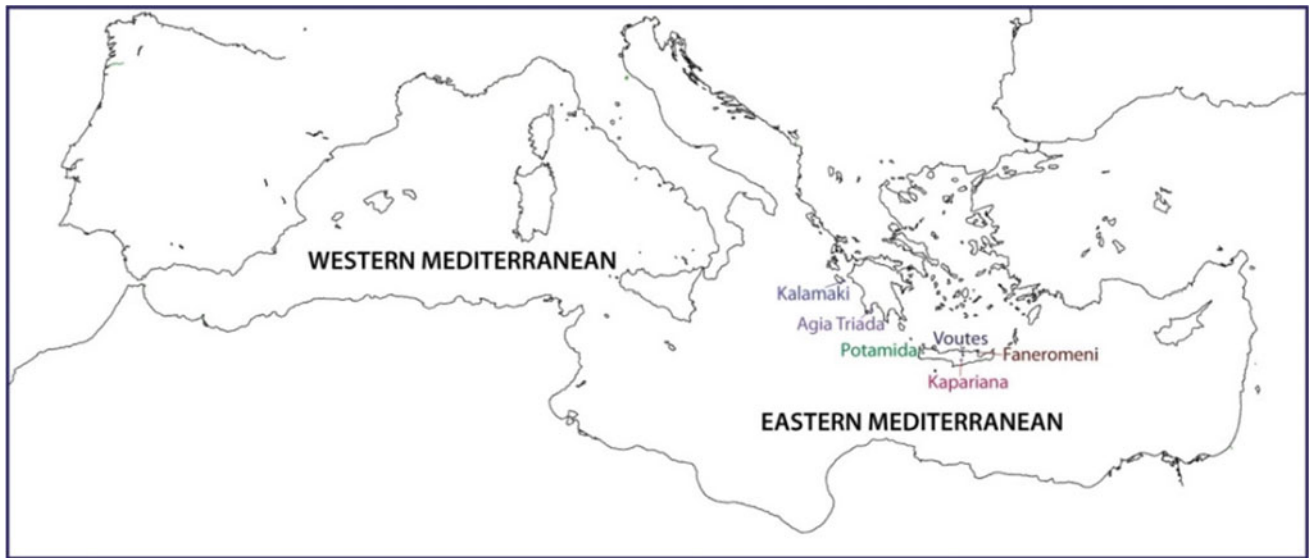


Fig. 1 Map of the Mediterranean Sea with the localities where the material for present analysis was found. Potamida [5], Kapariana, Faneromeni, Kalamaki [6], Voutes [7], Agia Triada [8]

Table 1 The measured otolith material of the four species presented here

Species	Locality	Age (Ma)	Number of specimens
<i>Ceratoscopelus maderensis</i>	Potamida	7.36–6.72	10
<i>Ceratoscopelus maderensis</i>	Kapariana	6.83–6.64	3
<i>Ceratoscopelus maderensis</i>	Faneromeni	6.70–6.64	1
<i>Ceratoscopelus maderensis</i>	Agia Triada	5.00	1
<i>Ceratoscopelus maderensis</i>	Voutes	3.80–3.64	30
<i>Diaphus cavallonis</i>	Faneromeni	7.58–6.72	20
<i>Diaphus cavallonis</i>	Potamida	7.51–6.72	37
<i>Diaphus cavallonis</i>	Kalamaki	6.26–6.09	8
<i>Diaphus cavallonis</i>	Voutes	3.80–3.64	38
<i>Hygophum hygomii</i>	Potamida	7.36–6.72	12
<i>Hygophum hygomii</i>	Faneromeni	7.24–6.83	1
<i>Hygophum hygomii</i>	Agia Triada	5.00	1
<i>Hygophum hygomii</i>	Voutes	3.80–3.64	17
<i>Myctophum fitchi</i>	Faneromeni	7.58–7.45	1
<i>Myctophum fitchi</i>	Potamida	7.36–6.72	3
<i>Myctophum fitchi</i>	Voutes	3.78–3.66	6

Zanclean specimens are larger than Messinian specimens of this species (Fig. 2). Furthermore, in the Zanclean, the specimens are much larger than the Tortonian ones as well. The same appears to be true for the extinct species *Diaphus cavallonis* although the signal is not as clear as it may be expected. The results for *Hygophum hygomii* and *Myctophum fitchi* are inconclusive probably due to the limited number of the examined specimens (Table 1) (Fig. 2).

4 Discussion

Fish size reduction is a well-known physiological response to the environmental disruptions such as the modern climate change. The observations reported here support the validity of the initial hypothesis. However, the results differ depending on the number of the examined specimens and on

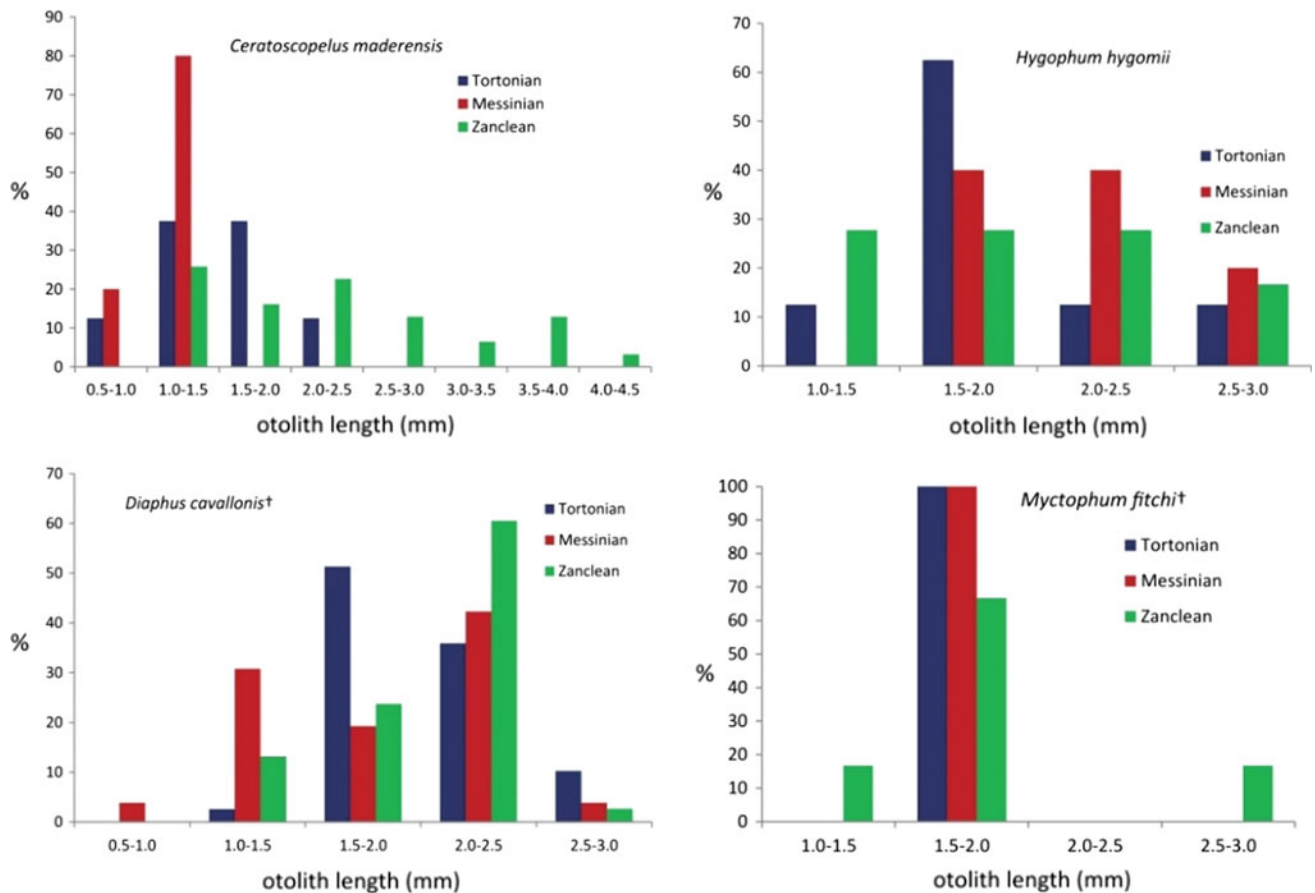


Fig. 2 Otolith size distributions for four very common mesopelagic fish species from the Tortonian until the Zanclean † indicates currently extinct species

whether or not the species was endemic such as *Myctophum fitchi* and *Diaphus cavallonis*, which were probably better-adapted to the Mediterranean restricted conditions than *Ceratoscopelus maderensis* that has a worldwide distribution until today.

5 Conclusion

In order to test the hypothesis that the restricted oceanic circulation possibly increasing the stratification and/or the salinity in the Mediterranean just before the MSC onset affected the mesopelagic fish by inducing a reduction in their size, we compared otolith size distributions from typical mesopelagic fish. The results support the validity of this hypothesis, although they seem to vary depending on the number of the measured otoliths and the distribution and ecology of the examined species. Nevertheless, this hypothesis deserves a further inquiry by examining more species and material.

Acknowledgements This research has been co-funded by the European Social Fund and the Greek National Funds through the action “Postdoctoral Research Fellowships” of the program “Human Resource Development, Education and Lifelong Learning” 2014–2020 which is implemented by the State Scholarships Foundation (I.K.Y.).

References

1. Hsü, K.J., Ryan, W.B.F., Cita, M.B.: Late Miocene desiccation of the Mediterranean. *Nature* **242**(5395), 240–244 (1973)
2. Krijgsman, W., Hilgen, F.J., Raffi, I., Sierro, F.J., Wilson, D.S.: Chronology, causes and progression of the Messinian salinity crisis. *Nature* **400**(6745), 652–655 (1999)
3. Roveri, M., et al.: The Messinian salinity crisis: past and future of a great challenge for marine sciences. *Mar. Geol.* **352**, 25–58 (2014)
4. Cheung, W.W.L., et al.: Shrinking of fishes exacerbates impacts of global ocean changes on marine ecosystems. *Nat. Clim. Change* **3**(3), 254 (2013)
5. Agiadi, K., et al.: Connectivity controls on the late Miocene eastern Mediterranean fish fauna. *Int. J. Earth Sci.* **106**(3), 1147–1159 (2017)

6. Karakitsios, V., et al.: A record of the Messinian salinity crisis in the eastern Ionian tectonically active domain (Greece, eastern Mediterranean). *Basin Res.* **29**(2), 203–233 (2017)
7. Agiadi, K., Koskeridou, E., Triantaphyllou, M., Girone, A., Karakitsios, V.: Fish otoliths from the Pliocene Heraklion Basin (Crete Island, Eastern Mediterranean). *Geobios* **46**(6), 461–472 (2013)
8. Koskeridou, E., Giamali, C., Antonarakou, A., Kontakiotis, G., Karakitsios, V.: Early Pliocene gastropod assemblages from the eastern Mediterranean (SW Peloponnese, Greece) and their palaeobiogeographic implications. *Geobios* **50**(4), 267–277 (2017)
9. Schulz-Mirbach, T., et al.: In-situ visualization of sound-induced otolith motion using hard X-ray phase contrast imaging. *Sci. Rep.* **8**(1), 3121 (2018)
10. Nolf, D.: *Otolithi Piscium*, vol. 10. G. Fischer Verlag, Stuttgart (1985)
11. Paxton, J.R.: Fish otoliths: do sizes correlate with taxonomic group, habitat and/or luminescence? *Philos. Trans. R. Soc. Lond. B Biol. Sci.* **355**(1401), 1299–1303 (2000)

Middle Miocene *Giraffokeryx* (Giraffidae) with Marks of Enamel Hypoplasia from Dhok Bun Amir Khatoon, Punjab, Pakistan

Muhammad Akbar Khan and Muhammad Asim

Abstract

Giraffokeryx punjabiensis are ascribed from Dhok Bun Amir Khatoon (DBAK), district Chakwal, Punjab, Pakistan. The newly recovered material includes two maxillary fragments: three mandibular rami and seven isolated teeth. The preserved specimens enhance the knowledge about *G. punjabiensis*. It can be used as a reference material in the future. Some specimens show a clear sign of the enamel hypoplasia as a nutritional and ecological stress indicator for the middle Miocene giraffids of Dhok Bun Amir Khatoon. The existence of *G. punjabiensis* along with *Dorcatherium* and suid suggests the presence of wet meadows, floodplain and open woodland at the time of the middle Miocene deposition in Dhok Bun Amir Khatoon, Lower Siwalik Subgroup.

Keywords

Giraffidae • Ruminantia • Siwaliks • Palaeontology • Taxonomy

1 Introduction

In the Siwaliks, the giraffids are represented by four sub-families: Bohlininae, Giraffinae, Sivatheriinae and Giraffokerycinae. *Progiraffa* is sited in the subfamily Bohlininae

[1]. Giraffinae is represented by the genus of *Giraffa*. Sivatheriinae is represented by the genera of *Bramatherium*, *Helladotherium* and *Sivatherium* [2]. Giraffokerycinae contains the genus of *Giraffokeryx* [3]. Bohlininae is documented from geologically older strata [4]. The fossil record of Giraffokerycinae and Giraffinae seems to be former than Sivatheriinae [5]. The giraffids appeared in the Kamli Formation of lower Siwaliks and relatively plentiful in the basal part of the Chinji Formation. Three genera of giraffid are found from the lower Siwaliks of Pakistan i.e. *Giraffokeryx*, *Giraffa* and *Progiraffa*.

The fossil remains of Giraffokerycinae designated in this manuscript were recovered from the outcrops of DBAK village (Lat. 32° 47' N; Long. 72° 55' E), the Chakwal district, northern Pakistan. The outcrops comprise reddish shales, red and brown siltstones and grey sandstones dumped in a fluvial environment [6, 7]. The material provides additional information about the middle Miocene giraffids of Pakistan with enamel hypoplasia as a stress indicator.

2 Materials and Methods

The hills near DBAK village (Chinji Formation), district Chakwal, Punjab, Pakistan, was extensively visited to collect the middle Miocene giraffids. For the systematic study, they were prepared by washing and cleaning in the laboratory with the help of fine needles and brushes. The various kinds of gums were used to assemble the broken parts.

The detailed morphometric characters and systematic positions of the specimens were described and discussed. The specimens catalogue number (e.g. 17/225) consists of numerator (collection year) and denominator (serial number). The photographs were taken and manipulated in adobe Photoshop to make a plate. The tooth terminology and measurement protocols follow [8].

M. A. Khan (✉) · M. Asim
Dr. Abu Bakr Fossil Display & Research Centre, Department of
Zoology, University of the Punjab, Lahore, Pakistan
e-mail: akbar.zool@pu.edu.pk

3 Systematic Palaeontology

Giraffokeryx punjabiensis Pilgrim, 1910

3.1 Description

Upper dentition: The premolar series is extremely worn and well preserved including the roots (Fig. 1). The length of premolar series is 62 mm. The median rib is heavy and slightly broken. The morphology of the P3 is more apparent than the P2. Small and narrow fossettes are ornamented with spur. The parastyle is prominent but the metastyle is weak. A thick cingulum is positioned at the posterior wall of the tooth. Ribs are strong.

The maxillary fragment is not well preserved. However, it covers the roots of almost all the cheek teeth. The cheek teeth are moderately worn and well preserved. The M1 is mostly worn among the cheek teeth. The prefossette is smaller and narrower than the postfossette that is divided posteriorly due to the presence of a thin spur. The metastyle is less developed than para- and mesostyles. The cingulum covers the molar labio-lingually. The M2 has a large and deep islet at the posthypocrista. Like the M1, the metastyle is the least developed; whereas, the parastyle, mesostyle and anterior median rib are thick and heavy. A large cingulum is located at the base of the preprotocrista; whereas, the small cingula are present at the base of the pre- and posthypocristae. The M3 is smaller than M2. A small spur is present at the anterior wall of the anterior fossette; whereas, a deep islet is present at the posthypocrista.

Lower dentition: It includes two hemimandibles, one mandible fragment and isolated dentitions (Fig. 1). The

corpus is fragile and cracked at various places in the hemimandibles. The complete cheek teeth series is preserved. The p2 is the least worn while the m1 is the most worn. Both the anterior and posterior valleys of the p2 are well developed. The conids are noticeable. The median valley is the broadest while the posterior valley is blocked by a tubercle. A cingulid is present at the base of the paraconid labially. A deep groove is present labially. The p4 is molariform. The posterior fossette is smaller than the anterior one. The stylids are less conspicuous. A heavy cingulid is present near the base of the preprotoconid. The median valley is small.

The m1 is in late wear, partially broken with less developed stylid, prominent anterior cingulid and strong median basal pillar. The anterior fossette is broader than the posterior one. The m2 is also partially broken. The stylids are more developed than the m1. The metastylid and mesostylid are divergent. Fossettes are broader. The strong cingulid is present at the preprotocristid. The median basal pillar covers the base of the median valley. The hypoconulid is well developed in the m3. The cingulid is present at the base of the preprotoconid.

3.2 Comparison

The studied data show a clear resemblance to *Giraffokeryx* [9–12]. Their measurements coincide with the previously studied specimens of *G. punjabiensis* [10, 12]. The antero-posterior length and crown width are almost similar. The slight disparity is due to the intraspecific variations. The presence of the above mentioned morphological characters and metric values are helpful to allocate the specimens under study to *G. punjabiensis*.

Fig. 1 Representative dentition of *Giraffokeryx punjabiensis*.

a upper dentition P3-M3;
b Lower dentition p2-m3



4 Discussion

From the Siwaliks, *G. punjabiensis* was documented as a single valid species of the genus *Giraffokeryx* [10, 12]. It is well-represented and well recorded species of the lower Siwaliks and basal portion of Nagri Formation. It coincides with the emergence of the Siwalik hipparionine [6, 10]. *G. punjabiensis* has also been verified from the Greco-Irano-Afganian state. The existence of this species in the Greco-Irano-Afganian state suggests that in the middle Miocene, the Himalayan Mountains was not a geographical obstacle for its spreading. This species inhabited a vast range from the Subcontinent to the Greco-Irano-Afganian state.

In the lower Siwaliks, the small sized giraffids were linked with the middle Miocene artiodactyls [10]. The tragulid *Dorcatherium* were likely to be reliant on grasses, allied with wet meadow, floodplains, or permanent drainage. The giraffes and suids are commonly existed in open woodlands and assumed to be mixed feeders. *G. punjabiensis* suggests the presence of woodland in Dhok Bun Amir Khatoon at the time of deposition during the middle Miocene.

5 Conclusion

During the middle Miocene, small-sized giraffids were represented by two species in lower Siwalik: *Giraffa priscilla* and *Giraffokeryx punjabiensis*. *G. punjabiensis* was only a single species of the genus *Giraffokeryx* in the Siwaliks. This species is recognized from Chinji (middle Miocene) to Nagri Formations (early late Miocene) of the Siwaliks and entirely vanished about 10 Ma from the Subcontinent. The presence of *G. punjabiensis* in Greco-Irano-Afganian state suggests that in the middle Miocene, the Himalayan Mountains was not a geographical obstacle for its spreading. As a species, it inhabited a vast range from the Subcontinent to the Greco-Irano-Afganian state.

References

1. Solounias, N.: Family Giraffidae. In: The Evolution of Artiodactyls, vol. 257 (2007)
2. Khan, M.A., Akhtar, M., Irum, A.: Bramatherium (Artiodactyla, Ruminantia, Giraffidae) from the Middle Siwaliks of Hasnot, Pakistan: biostratigraphy and palaeoecology. *Turk. J. Earth Sci.* **23** (3), 308–320 (2014)
3. Bhatti, Z.H., Khan, M.A., Akhtar, M.: Hydaspathierium (Artiodactyla, Giraffidae) from the Dhok Pathan Formation of the Middle Siwaliks, Pakistan: New Collection. *Pak. J. Zool.* **44**(3), 799–808 (2012)
4. Barry, J.C., Cote, S., MacLachy, L., Lindsay, E.H., Kityo, R., Rajpar, A.R.: Oligocene and early miocene ruminants (Mammalia, Artiodactyla) from Pakistan and Uganda. *Palaeontol. Electron.* **8** (1), 1–29 (2005)
5. Colbert, H.: Distributional and phylogenetic studies on Indian fossil mammals II: the correlation of the Siwaliks of India as inferred by the migrations of Hipparion and Equus. in *Am. Mus. Novitates.* (1935). Citeseer
6. Barry, J.C., Morgan, M.L.E., Flynn, L.J., Pilbeam, D., Behrensmeyer, A.K., Raza, S.M., Khan, I.A., Badgley, C., Hicks, J., Kelley, J.: Faunal and environmental change in the late Miocene Siwaliks of northern Pakistan. *Paleobiology* **28**(2 Supplement), 1–71 (2002)
7. Cheema, I.U.: Phylogeny and evolution of Neogene murine rodents from the Potwar Plateau of Pakistan and Azad Kashmir with special emphasis on zoogeographic diversification and stratigraphic implications. University of the Punjab, Lahore (2003)
8. Gentry, A.W., Roessner, G.E., Heizmann, E.P.: Suborder Ruminantia. In: Rössner, G.E., Heissing, K. (eds.) *The Miocene Land Mammals of Europe*, pp. 225–258. Dr. Friedrich Pfeil, München. (1999)
9. Pilgrim, G.E.: The Fossil Giraffidae of India. *Memoirs of the Geological Survey of India: Palaeontologia Indica, New Series.* 4 (1), 38.(1911)
10. Colbert, E.H.: Siwalik mammals in the American Museum of Natural History. *Transactions of the American Philosophical Society*, vol. 26. American philosophical Society (1935)
11. Khan, M., Akhtar, M., Iqbal, M.: The late miocene artiodactyls in the dhok pathan type locality of the dhok pathan formation, the middle siwaliks, Pakistan. *Pak. J. Zool. Suppl. Ser.* **10**, 1–90 (2010)
12. Aftab, K., Khan, M.A., Babar, M.A., Ahmad, Z., Akhtar, M.: Giraffa (Giraffidae, Mammalia) from the lower siwaliks of Pakistan. *J. Anim. Plant Sci.* **26**(3), 833–841 (2016)

Dental Morphology and Palaeoecological Implications of *Brachypotherium* (Rhinocerotidae) of the Middle Miocene Siwaliks (Pakistan)

Amtur Rafeh, Abdul Majid Khan, Rana Manzoor Ahmad, and Muhammad Akhtar

Abstract

New dental remains of rhinoceros species have been discovered from the Middle Miocene deposits of the Siwaliks of Pakistan. The specimens have been identified as *Brachypotherium perimense* and *Brachypotherium fatehjangense* based on their comparative morphometric analysis. The hypsodonty and thick enamel of the studied samples are the indicators of the presence of grazing community feeding on coarse grasses during Middle Miocene times in the Siwalik region. This newly discovered dental material adds up additional information about the Middle Miocene faunal composition of family Rhinocerotidae that can play role in tracing out the community structure during this epoch in the Asian region. The ecological implications of the *Brachypotherium* genus towards the changing Middle Miocene climatic condition on the basis of enamel hypoplasia is also discussed in this article.

Keywords

Siwaliks • Chinji formation • Dental remains
Enamel hypoplasia • *B. fatehjangense*

1 Introduction

Brachypotherium is a genus of the family Rhinocerotidae that is reported in Europe, Asia and Africa (Falconer and Cautley [6]). The newly discovered dental remains of the *Brachypotherium* genus belong to the Middle Miocene (Chinji Formation) deposits of the Siwaliks. The Chinji Formation (Lower Siwaliks) is widely exposed in the Potwar Plateau of Northern Pakistan. The lithological properties of

the formation are red clay due to the bright red and brown orange siltstone interbedded with ash-gray sandstone. Its chronological age ranges from 14.2 to 11.2 Ma. [10].

2 Materials and Methods

The collected material includes the lower jaw fragment and the isolated maxillary and mandibular dental remains. The specimens being collected during different expeditions are housed in the Paleontological Collections of the University of the Punjab, Lahore (PUPC). The measurements were taken by Vernier Caliper in millimeters. The morphometric characters of the newly discovered material were compared with the characters of all the reported species in the Middle Miocene epoch of the Siwaliks of Pakistan. The dental terminology that is used to describe the newly recovered material has been taken from Heissig [7].

3 Results

In the studied samples of *B. perimense* upper first premolar (PUPC 69/519) Length = 32 mm, Width = 28 mm has the same morphology as it was described by Khan [10]. The right lower fourth molar (PUPC 68/833) Length = 48 mm, Width = 31 mm is highly crowned with thick enamel. Only anterior and posterior cingula are present that are weak and high in position. Many shallow and deep vertical and horizontal cracks are observed. The buccal side of the conids is not quite straight but slightly curved. A shallow buccal fold is present. It is up to the middle of the crown. The buccal wall becomes nearly flattened until the crown base. The protoconid ridge is higher than the rest of the crown. The lophids are sharply ridged on the top but abruptly end to a thick base. The metaconid is very slightly constricted from outside while the inner side is flattened. The trigonid basin is widely opened and shallow. It has a V-shape while the talonid basin is U-shaped (Fig. 1).

A. Rafeh · A. M. Khan (✉) · R. M. Ahmad · M. Akhtar
Department of Zoology, University of the Punjab, Lahore,
Pakistan
e-mail: majid.zool@pu.edu.pk

PUPC 67/90 (Length = 52 mm) is a lower tooth. It is identified as the right first molar. It has late early wear with less degree of preservation. The lingual side is not preserved and the walls of the conids on the lingual side are broken. The enamel is shiny on the buccal side. The anterior part has two deep cracks. The buccal fold is shallow. It flattens on reaching the base of the crown. Some small enamel ridges indicate a very weak anterior cingulum with a large span covering the both edges of the lingual and the buccal sides. A very slightly appearing cingulum can be seen on the posterior side. The paralophid is thin, short and slightly curved inward. The base of the metaconid on the lingual side seems to be slightly swollen. The trigonid basin is U-shaped while the talonid basin is angularly V-shaped (Fig. 1).

The specimen of *B. fatehjangense* (PUPC 87/113) is incomplete in terms of the right lower ramus bearing only a single tooth, m2 (length 45 mm; width 25 mm) and the remains of the anterior conids is of m3. The ramus also bears the base of the ascending ramus. The outline of the anterior conids is circular. The trigonid basin is U-shaped while the talonid is angularly V-shaped. The entoconid has broken enamel. It appears swollen when the traces are observed. The anterior cingulum is high but not very prominent in appearance while the posterior cingulum is lower in position. The buccal groove has eroded enamel; however, the traces indicate a deep fold (Fig. 2). This specimen is incomplete in terms of the right lower ramus bearing only a single tooth, m2 and the remains of the anterior conids is of m3. The ramus also bears the base of ascending ramus. The tooth is quite hypsodont and in early middle wear. The outline of the anterior conids is circular. The trigonid basin is U-shaped while the telonid is angularly V-shaped. The entoconid has broken enamel. It appears swollen when the traces are observed. The anterior cingulum is high but not very prominent in appearance while the posterior cingulum is lower in position. The buccal groove has eroded enamel; however, the traces indicate a deep fold. The overall condition of the ramus is poor with many cracks and smaller and larger pits.

4 Discussion

4.1 Comparison with Reported Literature

Antoine and Welcomme [9] have reported the *Brachypotherium* genus from the Early Miocene deposits of the Bughti Hills, Baluchistan, Pakistan. The species *B. fatehjangense* is reported from Early to Late Miocene in South

Asian countries of India, Pakistan, and Thailand [7]. Colbert [4] identified *B. perimense* from Chinji, Nagri and Dhok Pathan formations of the Siwaliks. Heissig [7] also found this species in Kamli strata. A wide distribution of *B. perimense* is reported from Late Middle Miocene to Early Late Miocene by Barry et al. [1]. According to these stratigraphic ranging by different authors for the *Brachypotherium* genus, both *B. fatehjangense* and *B. perimense* were the present species during the Middle Miocene in the Siwalik region. The studied samples recovered from the Middle Miocene deposits of the Siwaliks also endorse the existence of both species during this geological time interval. The comparative study of the recovered sample with the reported literature also has supported the view pointed out by Ducrocq et al. [5]. Their view was basically an indication of the fact that South–East Asia and Pakistan belonged to the same biogeographical province during the Middle Miocene. Colbert [4] indicated *B. perimense* as large sized and hypsodont species. This species is distinct from the other rhinoceroses of the Siwaliks because of its massive size [11]. The studied material also point out the same idea that *B. perimense* is a larger size species as compared to *B. fatehjangense*. The *Brachypotherium* genus along with its existence in the Siwaliks had its biogeographic distribution in the other regions like Central as well as Western Europe and Turkey. It indicates the faunal affinities of the Siwalik Middle Miocene mammals with the European mammals.

4.2 Palaeoecological Implication

Heissig [8] indicated *B. perimense* as the peak representative at the time of the climatic transition. However, their population was reduced during the most humid and arid geological intervals of Siwalik. This species appeared again in less humid conditions in the Nagri Formation. Thus, it can be observed that the animals surviving the humid conditions are often smaller in size as the reported data and the discovered material showed. The *B. perimense* was a large size species that could not survive well in the humid Middle Miocene conditions. Enamel hypoplasia is a dental defect that can point out to an ecological stress faced by the mammals. According to Badgley et al. [3], the Middle Miocene was the period of intense climatic change. It is a period of stress which is due to rapid and irregular climate changes at 13 Ma and which resembles that of 17 Ma changes. The increased ratio of the mammals' appearance

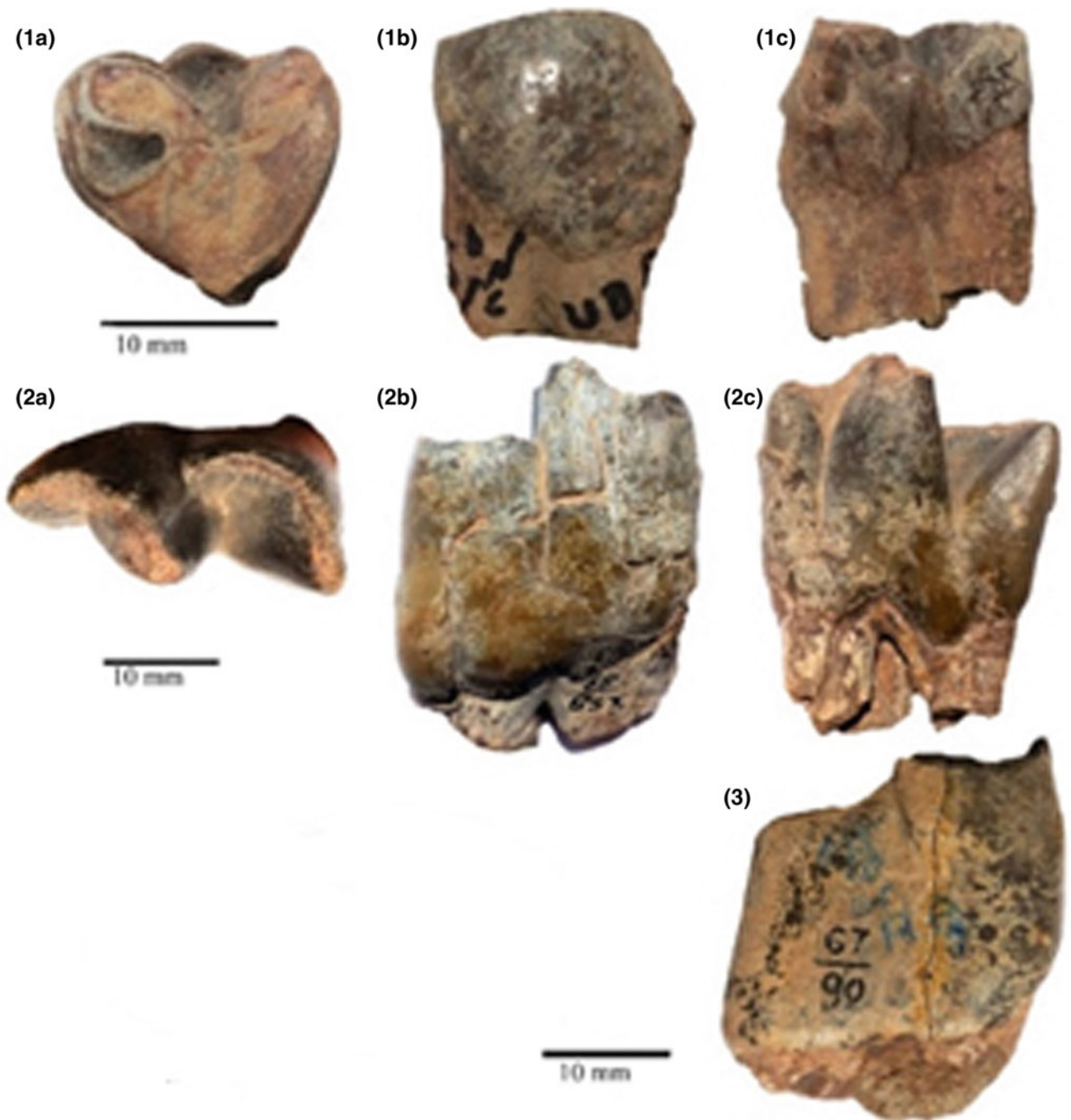


Fig. 1 *Brachytherium perimense*. 1. PUPC 69/519 IP1, 2. PUPC 68/833 rp4, 3. PUPC 67/90 rm1 (a = occlusal view, b = buccal view, c = lingual view)

and disappearance during this period indicates a rapid change in environment. It is ultimately responsible for the nutritional and the ecological stress for the Middle Miocene species (Barry and Flynn [1, 2]. Both studied Middle

Miocene rhino species had a high occurrence of the enamel hypoplasia that shows a strong impact of the Middle Miocene climatic variation on the Siwalik rhinos of this chronological interval.

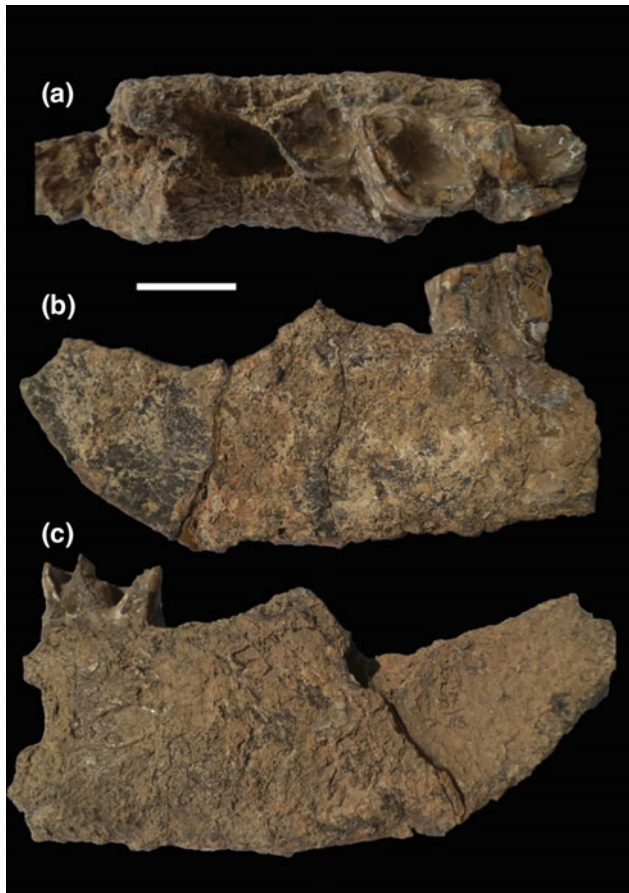


Fig. 2 *Brachypotherium fatehjangense* PUPC 87/113, A right mandibular ramus with m2 and rudiments of anterior conids of m3 (a = occlusal view, b = buccal view, c = lingual view)

5 Conclusion

The discovered dental material shows that *B. perimense* and *B. fatehjangense* are the species of the family Rhinocerotidae that were the members of the Middle

Miocene community of the Siwalik of Pakistan. The associated families of the Middle Miocene epoch of the Siwalik region of Pakistan with these rhino species are bovids, suids, anthracotheroides, tragulids and giraffids.

References

1. Barry, J.C., Morgan, M., Flynn, L., Pilbeam, D., Behrensmeyer, A.K., Raza, S., Khan, I.A., Badgely, C., Hicks, J., Kelley, J.: Faunal and environmental change in the late Miocene Siwaliks of northern Pakistan. *Paleobiology* **28**, 1–72 (2002)
2. Barry, J.C., Flynn, L.J.: Key biostratigraphic events in the Siwalik sequence. In: *European Neogene mammal chronology*. Springer, US, p. 557–571 (1990)
3. Badgley, C., Barry, J.C., Morgan, M.E., Nelson, S.V., Behrensmeyer, A.K., Cerling, T.E., Pilbeam, D.: Ecological changes in Miocene mammalian record show impact of prolonged climatic forcing. *Proc. Natl. Acad. Sci.* **105**, 12145–12149 (2008)
4. Colbert, E. H.: Siwalik mammals in the American Museum of Natural History. *Trans. Am. phil. Soc., n.s.*, **26**, 1–401 (1935)
5. Ducrocq, S., Chaimanee, Y., Suteethorn, V., Jaeger, J.J.: Age and paleoenvironment of Miocene mammalian faunas from Thailand. *Palaeogeogr. Palaeoclimatol. Palaeoecol.* **108**, 149–163 (1994)
6. Falconer, H., Cautley, P.T.: *Fauna Antiqua Sivalensis*, pp. 72–75. Folio Atlas, London (1847)
7. Heissig, K.: Pala ontologische und geologische Untersuchungen im Tertiär von Pakistan, 5. Rhinocerotidae (Mamm.) aus den unteren und mittleren Siwalik Schichten. *Bayerische Akademie der Wissenschaften Mathematisch Naturwissenschaftliche Klasse, Abhandlungen, Neue Folge* **152**, 1–112 (1972)
8. Heissig, K.: Change and Continuity in Rhinoceros faunas of Western Eurasia from the Middle to the Upper Miocene, pp. 35–37. EEDEN, Stará Lesná (2003)
9. Antoine, P.O., Welcomme, J.L.: A new rhinoceros from the Lower Miocene of the Bugti Hills, Baluchistan, Pakistan: the earliest elasmotheriine. *Palaeontology* **43**(5), 795–816 (2000)
10. Khan, A.M.: *Taxonomy and Distribution of Rhinoceroses from the Siwalik Hills of Pakistan*, p. 134. University of the Punjab, Lahore (2009)
11. Lydekker, R.: *Siwalik Rhinocerotidae*. *Pal. Indica* (X), II, Pt., 1: 1–62 (1881)

Systematic Study of the New Remains of *Propotamochoerus Hysundricus* (Suidae, Mammalia) from the Late Miocene-Early Pliocene Middle Siwaliks (Pakistan)

Sadaf Aslam, Abdul Majid Khan, Rana Manzoor Ahmad, Ayesha Iqbal, and Muhammad Akhtar

Abstract

New fossil remains of *Propotamochoerus hysundricus* have been studied from the Dhok Pathan and Padhri localities of the Middle Siwaliks of Pakistan. *Propotamochoerus hysundricus* is among one of the best known Siwalik suids with complete skulls, mandibles and isolated specimens. This species is most commonly found suid in the Dhok Pathan and Nagri units of the Siwaliks. The genus *Propotamochoerus* in Siwaliks is represented only by single species *Propotamochoerus hysundricus*. The chronological range of the species is about 10-06 million years ago. The probable ancestor of *Propotamochoerus* is *Hyotherium* of Chinji Formation about 11 million years ago. The primitive *Propotamochoeroides* were near to the *Palaeochoerus* and were treated as precursor of other suinae.

Keywords

Propotamochoerus hysundricus • Dhok pathan Formation • Nagri Formation • Suinae

1 Introduction

Propotamochoerus hysundricus (Stehlin) is large species of *Propotamochoerus* with large canine flanges, elongated premolars, thick P^{2-3} , P^3 having elongated lingual ridges and M^1 having additional accessory conules and grooves. The described material is collected from the localities of Padhri and Dhok Pathan areas of the middle Siwaliks of Potwar Plateau, Pakistan. The Padhri village is located 57 km in west from the River Jhelum, Punjab Pakistan. Topographic characters include water channels, levees and palaeosol of different length and width. During the last

S. Aslam · A. M. Khan (✉) · R. M. Ahmad · A. Iqbal · M. Akhtar
Department of Zoology, Quaid-e-Azam Campus, University of the Punjab, Lahore, Pakistan
e-mail: majid.zool@pu.edu.pk

100 years, it is considered a famous area for Miocene fossil collection. The village Dhok Pathan is situated in Chakwal district of northern Pakistan (Lat. 33° 07'N: Long. 72° 14'E). It represents complete sequence of Siwaliks and yield highly diversified mammalian fauna. Lithologically, the included Siwaliks outcrops contain orange red clay stone, light red sandstone and conglomerates [1].

2 Materials and Methods

PUPC 99/1, right mandibular piece having m2-3; PUPC 99/3, skull having left teeth row P1-4 and M1-3; PUPC 97/40, left mandible with snout and broken ascending ramus having p3.4; PUPC 97/41, left mandible having p3-4 and m1-3; PUPC 95/15 consists of lm1-3; PUPC 97/90, an isolated lc1; PUPC 02/69, a left mandibular fragment bearing m1-3; PUPC 15/28, skull having palate with right and left tooth row; PUPC 15/38, mandible bearing rI1-P3 and II1-2; PUPC 94/65, left mandibular ramus bearing p4-m2; PUPC 92/5, an isolated rm3; PUPC 16/86, an isolated lower left fourth premolar; PUPC 92/3, an isolated rC1; PUPC 16/75, an isolated ri2; PUPC 16/73, an isolated rm2; PUPC 16/103, left mandibular ramus having p3-m3; PUPC 16/85, an isolated lm3; PUPC 16/104, an isolated II2. The fossils are put up in the Dr. Abu Bakr Fossil Display and Research Center of the Department of Zoology, University of the Punjab, Lahore, Pakistan. The measurements of the specimens were taken with the help of metric Vernier Calipers in millimeters (mm). Tooth length and width were measured at occlusal plane.

3 Results

3.1 Upper Dentition

Second incisor is long and high crowned tooth with well-developed lingual cingulum. The Upper first canine is with visible dentine on top and shiny enamel. It is pointed

Fig. 1 *Propotamochoerus hysudricus*, Upper Dentition PUPC 99/3; skull having left teeth row P1-M3



Table 1 Cranial measurements (mm) of studied *Propotamochoerus hysudricus*

PUPC 99/3	Measurements (mm)
Length of skull: tip of praemaxilla to back of occipital crest	260
Bizygomatic width	+150
Width of orbita	60
Distance between posterior nasal and foramen magnum	270
Condyllo-basal length	225
Length of palatine	135
Length of P1-M3	113.5
Length of M1-M3	62.5

forwards and downwards. Root is longer than crown height. Its section appears roughly rounded. Its enamel is rugose. Second upper premolar is a higher, larger, and wider version of P1. The main cusp is large and slightly inflated. P3 is larger and stronger copy of P2. The principal cusp is large, centrally placed and inflated. Prominent anterior accessory cusp and cingulum present. P4 is more molarized tooth than P3. It consists of two labial cusps and a single lingual cusp. All cusps are more or less equal in height. In M1 median basal pillar is present on buccal side of median valley. Protocone and paracone secondarily fused to form protoloph similarly hypocone and metacone are secondarily fused to form metaloph. M2 is larger than M1. Anterior, median and posterior accessory cusps are also present. Median basal pillar is well developed on the buccal side of median valley. M3 has expanded posterior accessory cusp and a cingulum forming a talon. Lingual side of cusps is higher than buccal side. Cingulum forms a complete whorl around the tooth. Median basal pillar present on buccal side of median valley. Anterior, median and posterior accessory

cusps are visible. Talon is closer to lingual side than buccal side so that the rear half of the tooth narrows considerably from buccal to lingual side.

3.2 Lower Dentition

Third premolar is simple with single main cusp having well developed anterior and posterior accessory cusps associated with cingulum. It is two rooted. Cingulum is expanded on buccal side. Fourth premolar is a molarised tooth and it is distinctly bifurcated and birooted. First molar is simple with moderately thick enamel. Central accessory cusp is present in it. Protoconid and paraconid are simple and blunt. Protoconid is fused with medial accessory cusp. Median basal pillar is present. In Second molar accessory cusp is present. Lower third molar is similar to m2 but is a larger version of m2. Moderate quantity of cingulum is present anteriorly, forming anterior accessory cusps. Posteriorly cingulum expands to form posterior accessory cusp and

talonid. Its enamel is shiny. It is a short paper so dental features of the studied species are diagrammatically represented by single selected sample (Fig. 1) and only cranial measurements are given in Table 1.

4 Discussion

The bunodont dentition and the possession of more than one accessory conules/conulids in all specimens suggest their inclusion in the family Suidae. Dental morphology of molars and premolars indicate that all the specimens belong to *Propotamochoerus* genus. According to Pickford [3], the genus *Propotamochoerus* in the Siwaliks is represented by only a single species *P. hysudricus*. The skull which was assigned by Pilgrim into *P. salinus*, belongs to *Hyotherium* (*Sensu soemmeringi*). The skulls of *Propotamochoerus hysudricus* and the modern African *Potamochoerus* are of about the same size and are very similar to each other. The difference between the two lies in the position and size of the orbit which is more centrally placed and smaller in *Propotamochoerus hysudricus* (Pilgrim [4]). The upper premolar is present in *P. hysudricus* but absent in the *Potamochoerus* genus (Colbert [2]). Several evolutionary trends including variations in size, in complexity and hypsodonty of premolars, changes in enamel thickness of molars have been noticed in this species. The probable ancestor of *Propotamochoerus* is about 11 Ma old *Hyotherium* of Chinji Formation. 11 Ma is the time for the initiation of the Late Miocene. The average species duration decreased significantly in the Late Miocene due to an increase in the

frequency of the environmental disturbances. The evolutionary changes made by *Propotamochoerus* over *Hyotherium* includes the addition of the saggittal cusplets in P4, increase in size, alteration in the shape of anterior zygomata and squaring off of the snout section. Its closest relatives are found in Eurasia. *Korynochoerus palaeochoerus* is very close to *Propotamochoerus*.

5 Conclusion

The studied specimens show affinities with *P. hyotherioides* based on tooth morphology and measurements. So it is concluded that the species described here is *P. hyotherioides*. Along with this Siwalik species, from other regions the reported species of *Propotamochoerus* genus are *P. palaeochoerus*, *P. hyotherioides*, *P. wui*, *P. provincialis* and a MN11-13 form of Europe.

References

1. Barry, J.C., Morgan, M.E., Flynn, L.J., Pilbeam, D., Behrensmeier, A.K., Raza, S.M., Khan, I.A., Badgley, C., Hicks, J., Kelley, J.: Faunal and environmental change in the late Miocene's Siwaliks of Northern Pakistan. *Paleobiology* **18**, 1–71 (2002)
2. Colbert, E.H.: Siwalik mammals in the American museum of natural history. *Bull. Am. Phil. Soc.* **26**, i–x, 1–401 (1935)
3. Pickford, M.: Revision of the Miocene Suidae of the Indian subcontinent. *Munchen Geowiss. Abh.* **12**, 36–43 (1988)
4. Pilgrim, G.E.: The fossil Suidae of India. *Pal. Indica*, ns, **8** (4), 1–65 (1926) (Pls.,-IXX)

Systematics and Palaeo-Environmental Implications of *Hexaprotodon Sivalensis* (Hippopotamidae, Mammalia) from the Plio-Pleistocene Upper Siwaliks (Pakistan)

Ayesha Iqbal, Abdul Majid Khan, Rana Manzoor Ahmad, Muhammad Akbar Khan, and Muhammad Akhtar

Abstract

The specimens discussed in this paper were collected from the Tatrot Formation of the Upper Siwaliks of Pakistan. The sample comprises isolated upper premolar, molars and a complete mandible. Based upon the comparative morphological affinities with the previously reported fossil material of Hippopotamidae from the Siwalik region, the newly recovered specimens are recognized as belonging to *Hexaprotodon sivalensis*. These samples showed differences both in morphology and size when compared to living *Hippopotamus amphibius* and *Hexaprotodon liberiensis*.

Keywords

Artiodactyla • Hippopotamus • Tatrot • Pinjor Pliocene • Pleistocene

1 Introduction

The Siwalik rocks of Pakistan are considered as highly fossiliferous fluvial depositional sediments having a stratigraphic age from 18.3 to 0.6 Ma. Lithologically, the Upper Siwalik sediments are composed of tedious alterations of sandstones, fine and coarse grained elements, siltstones and conglomerates [8]. The Upper Siwaliks includes Tatrot, Pinjor and Boulder conglomerate strata having a stratigraphic age from 3.3 to 0.6 Ma [4]. The *Hexaprotodon sivalensis* is known from the Siwaliks of Pakistan with an estimated age range of 5.9 and 2.2 Ma [1].

2 Materials and Methods

Our samples include; one isolated upper premolar, two upper molars and a complete mandible that were collected from the Tatrot Formation of the Upper Siwaliks of Pakistan. The standard protocols were used for the preparation of the fossils in the laboratory. The fossils are generally well preserved showing occlusal morphology. However, some parts are worn and broken. The terminology of the tooth crown and the measurements has been adopted from Boisserie [2]. The measurements were taken in millimeters with the help of the error free Vernier caliper.

Abbreviations: Million years ago (Ma), Upper Premolar/Molar (P/M), Lower Premolar/Molar (p/m), Lower incisor (i) and Hexaprotodon (Hex)

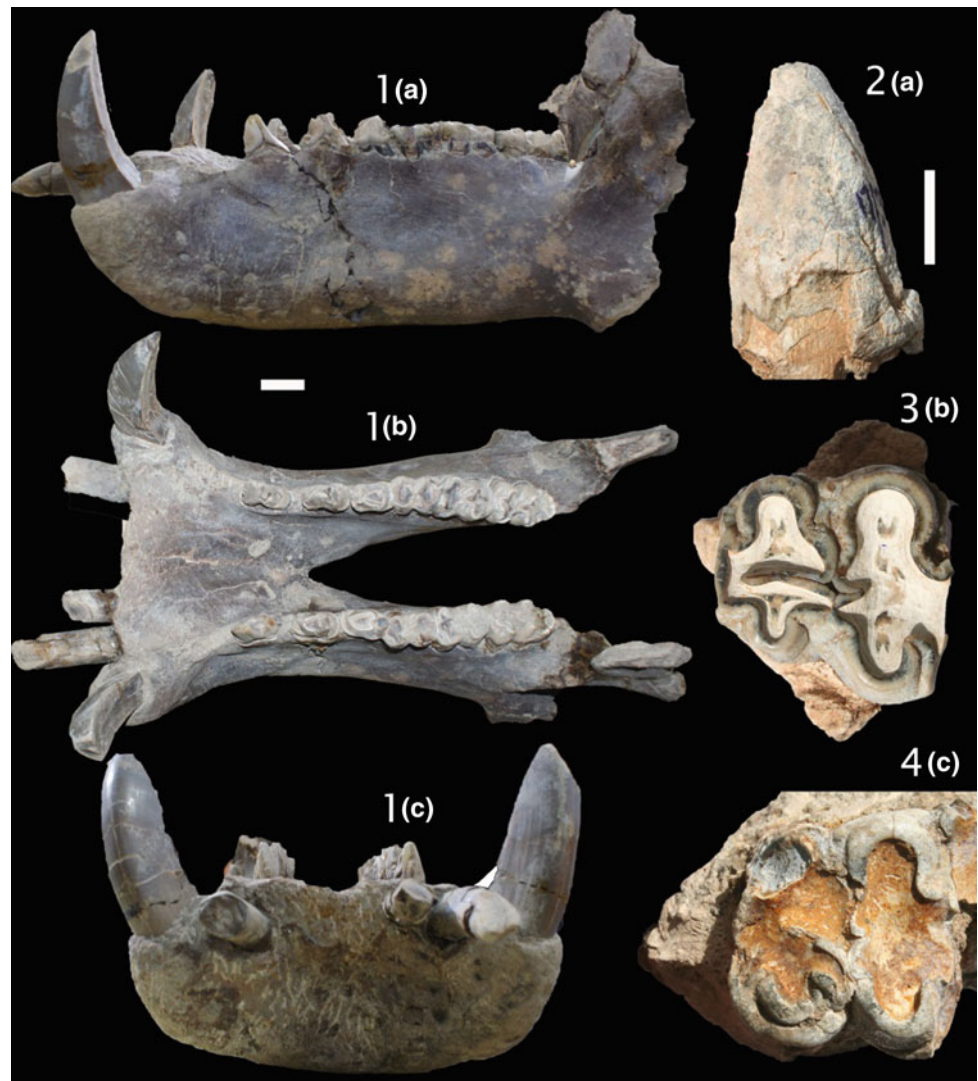
3 Results

The upper premolars are conical in shape having a prominent cingulum. A wear facet is prominent and located at the tip of upper premolars. The enamel pattern of the upper molars is basically trefoil in shape. The transverse valleys are broad and prominent at the occlusal surface of the molars. A thick and continuous cingulum is present at both surfaces (labial and lingual) of the crown. The M2 is complete. It shows clear tri-foliated cusps. The cingulum is prominent especially at the lingual side. The cingulum in M3 is basically weaker as compared to M2 (Fig. 1).

The lower incisors are less curved, cylindrical, and less circular. The lower canines are relatively well-striated and shiny with shallow grooves. They are slightly rectangular and narrower at the buccal and lingual side. The lower premolars length is typically greater than the width but the height is less at the anterior as compared to the posterior side. They have rugosity and a main cusp protoconid is present. The p1 is generally not preserved but sometime present in the mandibles in the form of small rudimentary

A. Iqbal · A. M. Khan (✉) · R. M. Ahmad · M. A. Khan
M. Akhtar
Department of Zoology, Quaid-e-Azam Campus,
University of the Punjab, Lahore, Pakistan
e-mail: majid.zool@pu.edu.pk

Fig. 1 The newly discovered samples of *Hexaprotodon sivalensis*; 1a–c The complete mandible. This specimen is taken from another article from our Research fellow, Khan [7], 2a Upper second premolar, 3b Upper second molar, 4c Upper third molar, Scale is equal to 20 mm



circular alveoli. The p4 is basically wider with circular roots as compared to other premolars. Thus, it can easily be distinguished. In p3 the grooves can be seen on the labial side and a small wear facet present on the anterior side. The lower molars are robust with thick enamel rugosity. The metaconid is fused with the protoconid. This feature is basically present in m1. The entoconid and hypoconid are united with each other. The cingulum is absent; whereas, an accessory buccal cusp is located in the central valley but bend toward the hypoconid. In m2, the hypoconid is larger in size than rounded entoconid and an accessory labial cusp close to the protoconid is present; whereas, the cingulum is absent. In m3, the protoconid is relatively larger than the metaconid while the hypoconid is larger than entoconid. The cingulum and the accessory cusps are absent. A robust talonid is present at the posterior side (Fig. 1). All these characters of the discovered dental remains and the comparison of their measurements with the reported

measurements of *Hexaprotodon sivalensis* confirm that the studied material belongs to *Hexaprotodon sivalensis*.

4 Discussion

4.1 Comparison with the Reported Literature

The comparative morphometric analysis of the included samples taken from the available literature shows that the *Hexaprotodon sivalensis* is differentiated from the Myanmar species *Hexaprotodon iravaticus* for their larger body size, wider and shorter robust mandibular symphysis as compared to *Hex. iravaticus*. Moreover, the *Hex. iravaticus* is comparatively different from *Hex. sivalensis* in having lesser developed cingulum, narrow muzzle, tapered mandible at the anterior side. The lower third incisor (i3) is less in height than the lower canine, molars with less expanded tri-foliated

cusps and lower p4 with short cusplets [5]. The *Hex. iravaticus* is considered as a younger species than the large Siwalik species *Hex. sivalensis* [1]. In comparison with the molars, both species *Hex. sivalensis* and *Hex. iravaticus* have a correlative degree of hypsodonty. In *Hex. sivalensis*, the enamel pattern of the molars are more complex, more longitudinal enamel ridges and larger in size. The outer trefoil loops are more expanded than *Hex. iravaticus*. The outer loops of *Hex. iravaticus* molars are not pushed out more to enclose the transverse valleys. The basal accessory pillars are not well developed as in *Hex. sivalensis* [3]. The living representative of the genus *Hexaprotodon* is *Hexaprotodon liberiensis* and it is also called pygmy hippopotamus. Geographically, this species is present in four countries of the West Africa that are Liberia, Guinea, Sierra Leone and Ivory Coast.

4.2 Palaeo-Environmental Implications

Enamel hypoplasia is a dental defect that can be used to trace out the impact of the ecological stress on the different extant as well as extinct mammalian families. The occurrence of EH is significantly high $p > 0.05$ in *Hexaprotodon sivalensis* during the Upper Late Pliocene interval of the Siwaliks. The high level of stress faced by *Hex. sivalensis* during Pliocene interval may be due to the intense glaciation events during the Upper Pliocene to Pleistocene epoch as reported by Jansen et al. [6]. Along with the glaciation stress another stress faced by this amphibious taxon was the depletion of water bodies during the Pliocene as Quade et al. [9] reported the dry environmental condition after 09 Ma and the increase in the aridity during Pliocene.

5 Conclusion

The studied specimens are showing affinities to *Hex. sivalensis* based on tooth morphology and measurements. Consequently, it is concluded that the species described here

is *Hex. sivalensis*. Bovids, cervids, giraffids, suids, anthracotheroides and equids are the mammalian groups that were present along with *Hex. sivalensis* in the Tatrot Formation of the Siwaliks of Pakistan.

References

1. Barry, J.C., Morgan, M.E., Flynn, L.J., Pilbeam, D., Behrensmeyer, A.K., Raza, S.M., Khan, I.A., Badgley, C., Hicks, J., Kelley, J.: Faunal and environmental change in the late Miocene's Siwaliks of Northern Pakistan. *Paleobiology* **18**, 1–71 (2002)
2. Boisserie, J.R., Zazzo, A., Merceron, G., Blondel, C., Ignaud, P., Likius, A., Mackaye, H.T., Brunet, M.: Diets of modern and late Miocene hippopotamids: evidence from carbon isotope composition and microwear of tooth enamel. *Palaeogeogr. Palaeoclim. Palaeoecol.* **221**, 153–174 (2005)
3. Colbert, E.H.: Distributional and phylogenetic studies on Indian fossil mammals. IV. The phylogeny of the Indian Suidae and the origin of the Hippopotamidae. *Am. Mus. Novit.* **799**, 1–24 (1935)
4. Dennell, R.W., Coard, R., Turner, A.: The biostratigraphy and magnetic polarity zonation of the Pabbi Hills, northern Pakistan: an upper Siwalik (Pinjor stage) upper Pliocene-lower Pleistocene fluvial sequence. *Palaeogeogr. Palaeoclimatol. Palaeoecol.* **234**(2), 168–185 (2006)
5. Htike, T.: Review on the taxonomic status of *Hexaprotodon iravaticus* (Mammalia, Artiodactyla, and Hippopotamidae) from the Neogene of Myanmar. *Shwebo Univ. Res. J.* **III**(1) (2012)
6. Jansen, E., Sjöholm, J., Bleil, U., Erichsen, J.A.: Neogene and Pleistocene glaciations in the northern hemisphere and late Miocene–Pliocene global ice volume fluctuations: evidence from the Norwegian Sea. In: *Geological history of the polar oceans: arctic versus antarctic*, pp. 677–705. Springer, Dordrecht (1990)
7. Khan, M.A.: *Hexaprotodon* (Mammalia: Hippopotamidae) from the Pinjor Formation of Bhimber, Azad Kashmir, Pakistan. *Pakistan J. Zool.* **50**(2), 1367–1372 (2018)
8. Pilbeam, D.R., Behrensmeyer, A.K., Barry, J.C., Shah, S.M.I.: Miocene sediments and faunas of Pakistan. 45 pp. Postilla. No. 179 (1979)
9. Quade, J., Cerling, T.E., Bowman, J.R.: Development of Asian monsoon revealed by marked ecological shift during the latest Miocene in northern Pakistan. *Nature* **342**(6246), 163 (1989)

Part III
Biostratigraphy

Bajocian Ostracods from the Krachoua Formation (Beni Kheddache, Southern Tunisia): Implications for Biostratigraphy and Paleocology

Lassad Tiss, Khaled Trabelsi, and Fekri Kammoun

Abstract

Ostracods and charophytes are considered as biological indicators of the environments in the Middle Jurassic strata of southern Tunisia. The biostratigraphic and Palaeoecology studies of the Krachoua Formation undertaken from the region of Beni Kheddache are based on the ostracodfauna and charophyte flora. A Bajocian age is assigned to the upper part of the Krachoua Formation. It consists of a multi-specific ostracod association dominated by the following three genera, *Limnocythere*, *Bisulcocypris*, and *Theriocynoecum* which reflect appropriate palaeoecological conditions with a salinity decrease. This is due to the influx and installation of a freshwater pond occasionally developed and enhanced by humid climate coupled to a sea level fall. The occurrence of these species towards the top of Krachoua Formation is synchronous with the increase of silt and clay associated to vertebrate bones reflecting a regressive tendency within a transgressive/regressive sedimentary sequence within a Middle Jurassic long-term regressive cycle.

Keywords

Ostracods • Biostratigraphy • Palaeoecology
Southern tunisian • Krachoua

1 Introduction

The complex biological organization of marine benthic ostracods together with their small size and high mobility enables them to react quickly to environmental change. It is for this reason that they are often used to monitor pollution both in marine and fresh water with the discovery and description of Southern Tunisia ostracods. The aim behind the present study is to propose new interpretations on palaeoecology and biostratigraphy of these species Gondwana. Tunisian ostracods found in the Middle Jurassic provided a new stratigraphical, paleoecological and paleoenvironmental information of the Krachoua fossiliferous strata in Beni Kheddache region.

The studied specimens are recovered from the Krachoua Formation assigned to Bajocian [1, 2]. They are sampled in the “Kef el Anéba” section (Béni Kheddache area), 30 km to the West of Medenine city.

The Krachoua formation has a total thickness of 50 m. It lies unconformably on the top of the “Dolomie informe”. It is mainly composed of the alternation of metric carbonates beds (dolomitic at the base and calcareous to the top) intercalated of marls, evaporites, and sands levels of a marginal marine environment [2–4].

2 Materials and Methods

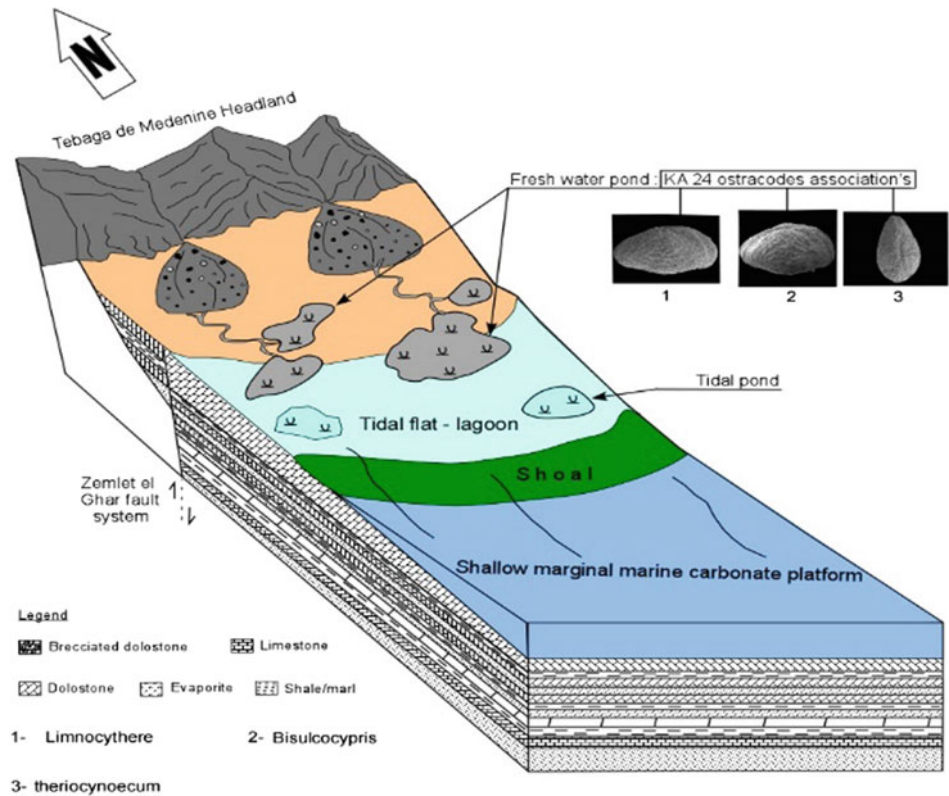
Bulk samples were collected from the consolidated marly-limestone level KA 23 and marlstone KA 24 of the Krachoua Fm. Marlstone samples were treated following a traditional sieving method; whereas, limestone samples were treated by using acetolysis. The efficiency of this later method, first advocated by Nötzold (1965) and applied by Trabelsi et al. [5–8] to recovery well-preserved charophytes and ostracods from hard calcareous rocks. It consists in taking the sample of calcareous rock perfectly dried and mechanically comminuted in fragments about 1 and 3 mm

L. Tiss (✉) · K. Trabelsi · F. Kammoun
Faculté des Sciences de Sfax, LR GEOGLOB, Université de Sfax,
B-P 802, 3038 Sfax, Tunisia
e-mail: lassad.tiss.etud@fss.usf.tn; tisslassad30@gmail.com

L. Tiss · K. Trabelsi · F. Kammoun
Sfax University, 3029 Sfax, Tunisia

K. Trabelsi
Faculté des Sciences de Tunis, Université de Tunis El Manar II,
UR11 ES15, CP 2092 Tunis, Tunisie

Fig. 1 Simplified diagram presented a palaeoenvironmental reconstruction of krachoua formation in Bajocian



across and adding similar amounts of anhydrous acetic acid and anhydrous copper sulfate (acid attacks in an exothermic reaction). After the neutralization by ammonia, the residue is treated with ultra-sound. Then, it is washed and rinsed. The selected specimens were imaged by using Scanning Electron Microscope (SEM).

3 Results

New micropaleontological, stratigraphical and palaeoecological data have been obtained. In fact, the present work gives the rich associations of the Ostracods and charophytes of the middle Jurassic (Bajocian-Callovian) of Tunisia (North Africa). This assemblage consists mainly of different genera from the limnic ostracods, *Limnocythere*, *Bisulco-cypris*, and *Theriocynoecum*, and the *Porochara* and *Aclistochara* genus of charophytes.

3.1 Stratigraphical Implication

The associations of ostracods and charophytes supply a new tool for the chronostratigraphic analysis of the Krachoua formation. Indeed, ostracods collected in Krachoua indicate that this series is Bajocian in age. It is in agreement with the results of Kammoun and Mette [2, 4].

3.2 Paleoecologic Implication

In the present work, the studied locality (J. Kef El Aneba, southern Tunisia) evolved as a tidal to freshwater environment during the Bajocian as indicated by the ostracods and charophytes associations. From the paleoenvironmental view point, the charophyte assemblage from Krachoua formation and ostracods is paucispecific and dominated by genus *Porochara* and *Aclistochara africana*. This assemblage is reminiscent of

similar assemblages from the Lower Cretaceous of Spain, Germany and Switzerland that were usually attributed to brackish water [9–12]. In addition, some ostracods and charophytes of freshwater environment found in the middle layers of the Krachoua formation demonstrate that the studied area has known an emersion reflecting regressive tendency of this transgressive/regressive sedimentary sequence within a Middle Jurassic long-term regressive cycle according to Haq [13] (Fig. 1).

4 Discussion

The studied ostracods and the associated microfossils represent a new tool for the stratigraphical and paleoecological interpretation of the Jurassic deposits of the Krachoua formation in this region.

The rich ostracod fauna from the Middle Jurassic of southern Tunisian Atlas, discovered in Krachoua formation, gives us new important insights into the environmental deposit type and the related eustatic control of the sedimentary sequences from which it has extracted.

5 Conclusion

Middle Jurassic (Bajocian) ostracods are first described from the Krachoua Formation of Kef El Annéba section (Beni Kheddache area, southern Tunisian Atlas). Taphonomic and palaeoecological interpretations enhance our understanding of the depositional environment of these strata onset. Our interpretations support previous reconstructions in line with marginal-marine deposition where salinity variations were mainly controlled by long- and short-term climatic changes as well as global sea level fluctuations.

References

1. Enay, R., El Asmi, K., Soussi, M., Mangold, Ch., Hantzpergue, P.: Un *Pachyerymnoceras* arabe dans le Callovien, supérieur du

- Dahar (Sud tunisien), nouvel élément de datation du membre Ghomrassène (formation Tataouine); corrélations avec l'Arabie Saoudite et le Moyen-Orient. *C. R. Geosci.* **334**, 1157–1167 (2002)
2. Kammoun, F.: Le Jurassique du Sud tunisien, témoin de la marge africaine de la Tethys; stratigraphie, sédimentologie et micropaléontologie. Thèse 3ème cycles (1988)
3. M'Rabet, A., Ben Ismail, M.H., Soussi, M., Turki, M.: Jurassic rifling and drifting of North African Margin and their sedimentary responses in Tunisia. In: 2nd International Geological Congress (abstracts), pp. 473–414. Washington, U.S.A. (1990)
4. Mette, W.: Palaeoecology and palaeobiogeography of the Middle Jurassic ostracods of southern Tunisia. *Palaeogeogr. Palaeoclimatol. Palaeoecol.* **131**, 65–111 (1997)
5. Trabelsi, K., Sames, B., Salmouna, A., Piovesan, E.K., Ben Rouina, S., Houla, Tour, J., Soussi, M.: Ostracods from the marginal coastal Lower Cretaceous (Aptian) of the Central Tunisian Atlas (North Africa): paleoenvironment, biostratigraphy and paleobiogeography. *Revue de Micropaléontologie* (2015)
6. Trabelsi, K., Colin, J.P., Tour, J., Soussi, M.: Cypridea Bosquet, 1952 (Ostracoda) in the early Albian of Tunisia. *J. Micropaleontol.* (2011)
7. Trabelsi, K., Tour, J., Soulie-Märsche, I., Martín-Closas, C., Soussi, M., Colin, J.P.: Découverte des charophytes de l'Albien dans la Formation Kebar (Tunisie centrale): Implications paléocologiques et paléobiogéographiques. *Ann. Paléontol.* **96**, 117–133 (2010)
8. Trabelsi, K., Soussi, M., Tour, J., Houla, Y., Abbes, C., Martín-Closas, C.: Charophyte biostratigraphy of the non-marine Lower Cretaceous in the Central Tunisian Atlas (North Africa): Palaeobiogeographic implications. *Cretac. Res.* **67**, 66–83
9. Grambast-fessard, N., Ramalho, M. M.: Charophytes du Jurassique supérieur du Portugal. *Rev. Micropaléontol.* **28**, 58–66 (1986)
10. Mojon, P. O.: Les formations mésozoïques à charophytes (Jurassique moyen-Crétacé inférieur) de la marge téthysienne nord-occidentale (Sud-Est de la France, Suisse Occidentale, Nord-Est de l'Espagne). *Sédimentologie, Micropaléontologie, Biostratigraphie. Géol. Alpine, Mém. Hors-Série* **41**, 386
11. Mojon, P. O., Haddoumi, H., Charriere, A.: Nouvelles données sur les charophytes et ostracodes du Jurassique moyen-supérieur-Crétacé inférieur de l'Atlas marocain. *Cah. Géol. (Notebooks on Geology)* **3**, 1–39 (2009)
12. Schudack, M. E.: Die charophyten im oberjura und unterkreide Westeuropas. Mit einer phylogenetischer Analyse der Gesamtgruppe. *Berl. Geowiss. Abh. (A)* **8**, 1–209 (1993)
13. Haq, B.U.: Jurassic sea-level variations: a reappraisal. *GSA Today* **28**(1), (2017). CC-BY-NCGSA

Paleobathymetric Influence on the Distribution of Ammonite and Foraminifer Settlements in the Callovian of the Saïda Region (Western Algeria)

Abdia Touahria and Abbes Sebane

Abstract

Saïda clay formation (NW Algeria) of Callovian-Oxfordian age is widespread in the Tlemcenian Domain. In the Saïda region, its lower limit is placed above a general gap of the upper Bathonian age. Its upper limit is overlaid by the first coarser sandstone beds (Bou-Medine Sandstone Fm) belonging to the Oxfordian. The Saïda clays rest on a slab of limestone with iron-rich stromatolitic ovoids that coincide with sedimentation resumption and fed by the arrival of an abundant clay-sandstone material. It is composed of a rhythmic alternation of clays and sandstone rich in sedimentary figures and structures. The monotony is sometimes broken by calcareous beds intercalations and often fossiliferous (ammonites) considered as biostratigraphical benchmark levels of lower, middle and upper Callovian. In this area fine-grained sandstone with rhizocorallium level divides the formation into two members. Foraminifera collected in the marly levels are *Nodosariidae*-rich which are associated with other families such as *Spirillinidae*, *Lituolidae*, *Epistominidae*, *Saccaminidae*, *Hormosinidae*, *Nebucularidae* and *Textulariidae*. Their vertical distribution enabled us to highlight three micro-faunal (foraminifera) renewals.

Keywords

Saïda clays • Callovian-Oxfordian • Reference levels Ammonites • Foraminifera • Rhizocorallium

1 Introduction

In the Oued Rhoua section, located about fifteen kilometers North-East of the Saïda city (Fig. 1), three successive fossiliferous levels (Fig. 2) were located and made it possible to

A. Touahria (✉) · A. Sebane
Faculty of Earth and Universe Sciences, Laboratory GeoBaBise,
University of Oran 2 Ahmed Benahmed, Bir El Djir, Algeria
e-mail: touahria_abdia@yahoo.fr

date the formation. The first level delivers ammonites of the lower Callovian (Gracilis Zone, layer 16) while the second which is highly condensed, contains Middle Callovian ammonites (Coronatum Zone, layer 21). The third one is subdivided into six centimetric layers, yielded upper Callovian ammonites (Athleta Zone, layer 32). A Rhizocorallium benchmark level (layer 38) at which divides the “Saïda clays” in two members was noted.

The palaeontological study of ammonites (*Perisphinctidae*, *Oppeleiidae*, *Reineckeidae*, *Phylloceratidae* and *Lytoceratidae*) shows a discontinuous and incomplete succession. This is explained by a rhythmic sedimentation; it is composed of clays and sandstones associated with intercalations of reference levels and condensed limestone with ammonites.

2 Materials and Methods

Sampling was done during various field trips. Macro-fauna (ammonites) consists mainly of internal molds often poorly preserved which have been released from their gangue in order to better observe the ornamentation and winding of the shell. As for the micro-fauna (foraminifera), the collected marl samples were washed in sieves (mesh size of 500, 250, 125 and 60 μ). The sieve residues were dried and observed under a binocular microscope for determination.

3 Results

Outside the ammonites (*Perisphinctidae*, *Oppeleiidae*, *Reineckeidae*, some *Phylloceratidae* and *Lytoceratidae*) macro-fauna is extremely poor. It is composed of belemnite rostrums and some poorly preserved brachiopods (Fig. 2).

Collected foraminifera in the marly levels were rich in *Nodosariidae*. They were associated with other families such as *Spirillinidae*, *Lituolidae*, *Epistominidae*, *Saccaminidae*, *Hormosinidae*, *Nebucularidae* and *Textulariidae*. Their distribution was controlled by bathymetric variations.

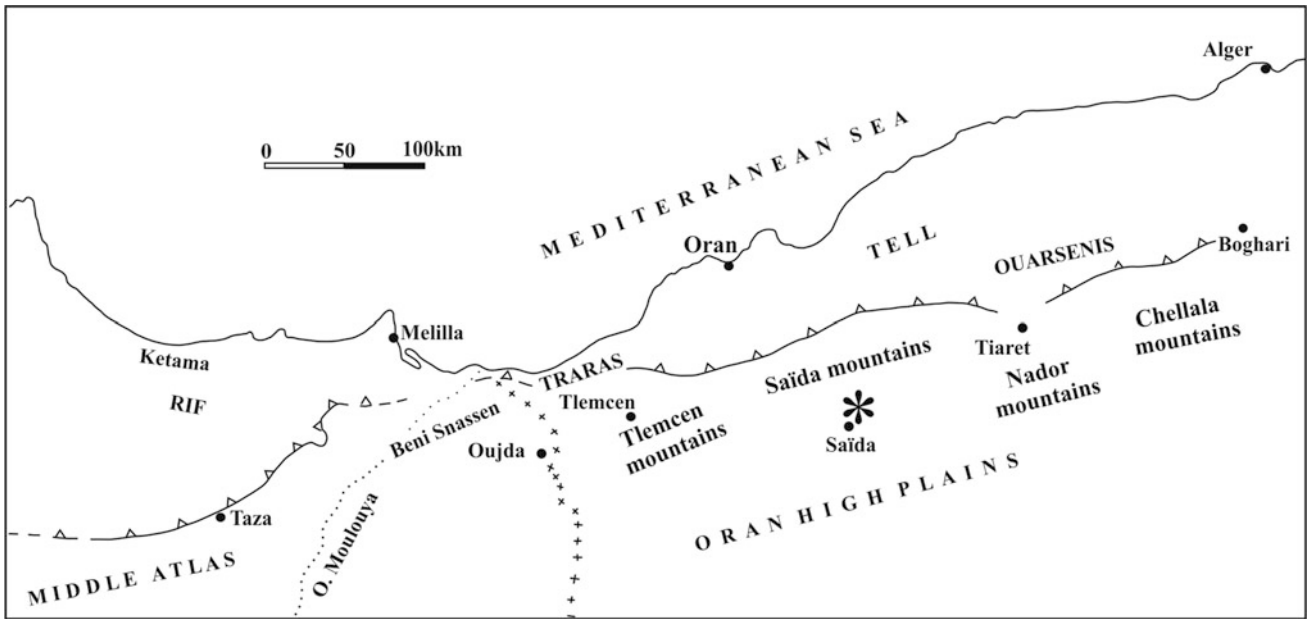


Fig. 1 Study region location

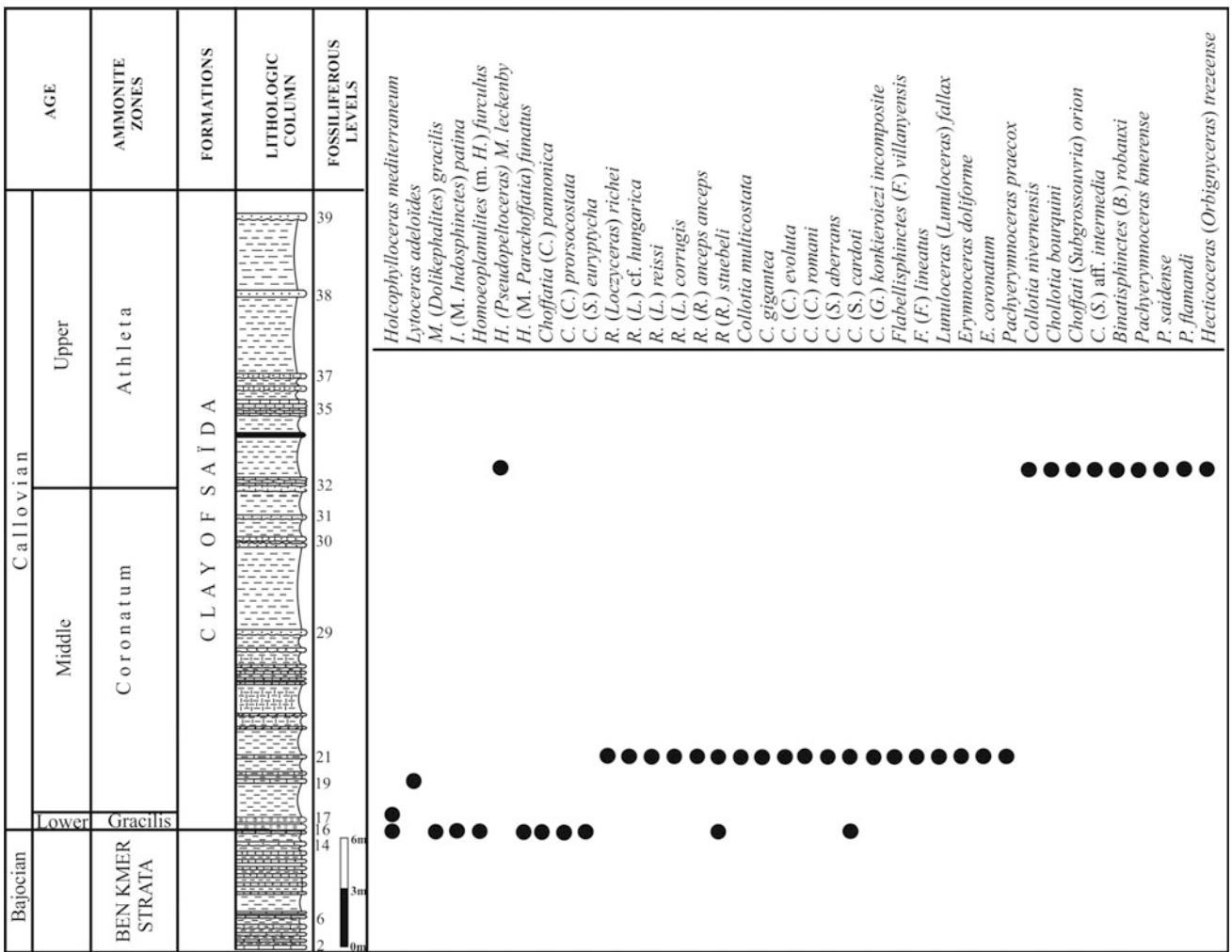


Fig. 2 Oued Rhoua lithostratigraphic section

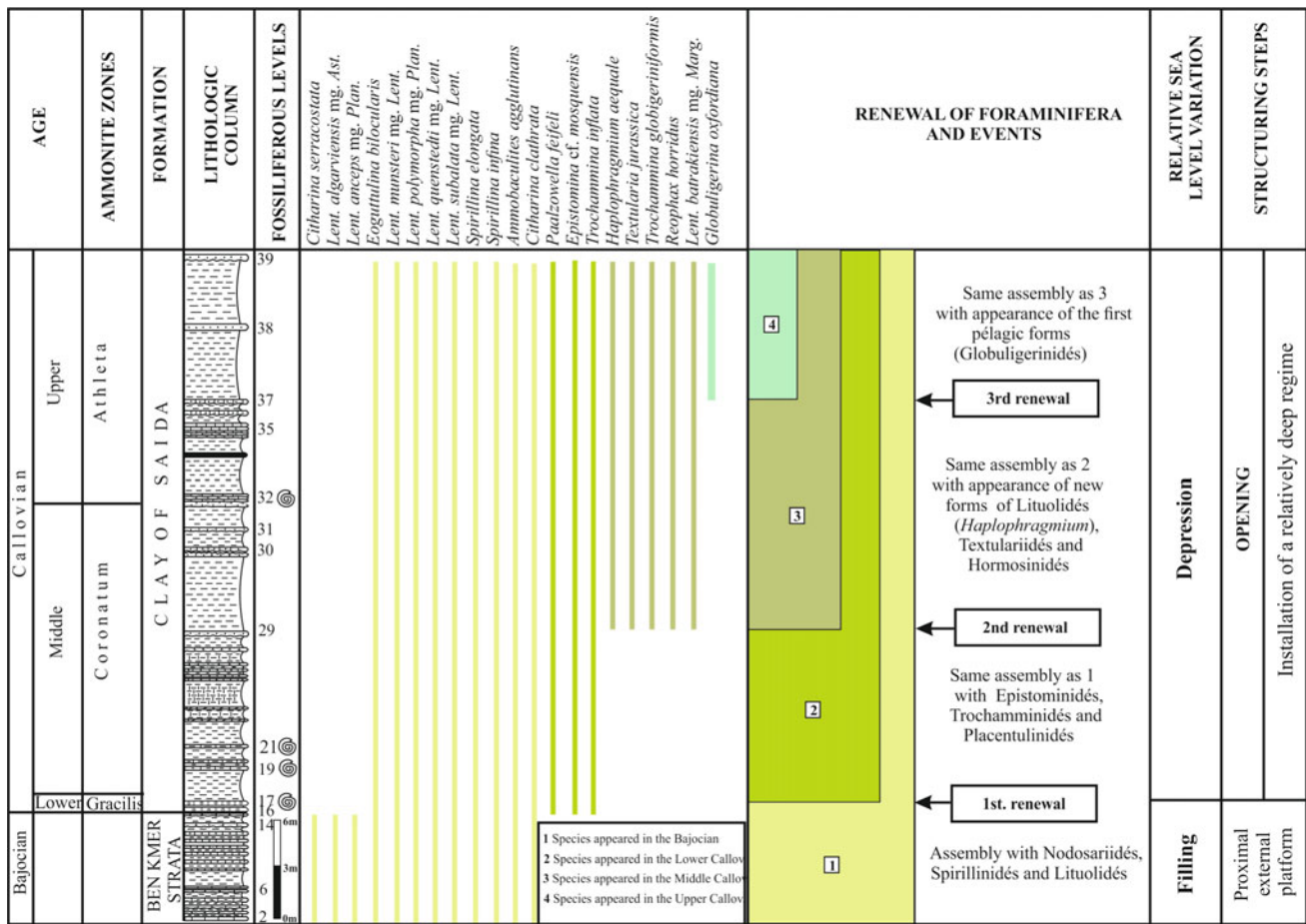


Fig. 3 Vertical distribution and renewal of foraminifera settlements

Compared with calcareous hyaline forms, belonging to the abundant *Nodosariidea* family in the shallower environment, Bajocian limestones dominates (“Ben Kmer Formation”). The agglutinated forms such as *Réophax* and *Ophthalmidae* develop in deeper environments rich in terrigenous material.

The foraminiferal vertical distribution revealed three micro-faunal renewals: the first occurred after a filling phase and began in the lower Callovian. The second and the third occurred during the deepening and the opening of the basin during the middle and upper Callovian (Fig. 3).

4 Discussion

The clays of Saïda result from an attempt to install a turbid regime whose influence becomes stronger until the lower Oxfordian. They are divided into many sequences defined as slices of sediments between two successive discontinuity surfaces. The lower part of the sandstone beds (soles of sequence) carries sedimentary figures such as load casts, flute casts, groove and chevron casts, prod and bounce casts

[1]. Three fault families, N120, N70 and N20, inherited from the Hercynian structures replayed several times before and during the atlasic orogeny [2]. Faults N70 were active during Jurassic sedimentation. This syndimentary activity resulted from rhythmic deposits. Deepening is interspersed with detrital sedimentation stops and the resumption of carbonate sedimentation which has led to the establishment of ammonite fossiliferous levels. The foraminiferal renewals occurred during the beginning of the deepening sequences.

5 Conclusion

The formation of Saïda Clays is rhythmic: it can be explained by the filling sequences which globally follow each other in a strato- and grano-decreasing way as the basin deepens. Ammonite levels are generally at the top of the filling sequences. The vertical distribution and the renewal of the foraminiferal fauna reflect the instability of the basin which would result from the strong tectonic activity during the Callovian and Oxfordian. The results obtained from the

distribution of foraminiferal and ammonite settlements confirm the Callovian and Oxfordian palaeogeography.

It should be noted that on the shores of the Tiffrit resistant mole, the Saïda clays are not thick (50 m). They thicken quickly towards the North and the West thanks to a strong tectonic activity and the set of synsedimentary faults responsible for the variation in thickness of the formation Mangold and Touahria [2].

References

1. Mangold, C., Benest M., Elmi, S.: Les « Argiles de Saïda » (Callovo-oxfordien d'Oranie, Algérie): âge et milieu de dépôt. C. R. Acad. Sc. Paris, 279(1974)
2. Mangold, C., Touahria, A.: Structure des Djebel Ben-Kmer et Modzab près de Saïda (Algérie). 4ème Réun.annu. Sci. Terre, Paris, S.G.F., 279 (1976)

First Calpionellid Biozonation of the Berriasian Reference Section of Jebel Ben Younes (Gafsa Basin, South Central Tunisia): Updated Age Attribution and Geodynamic Consequences

Rafika Ferchichi, Ichrak Cherif, Mabrouk Boughdiri, Sana Ben Nsir, Néjib Bahrouni, and Mohamed Faouzi Zagrarni

Abstract

Three sections from the Jebel Ben Younes reference outcrops are wisely sampled. Gathered macrofossils (ammonites, echinoderms, brachiopods) and calpionellid associations allow us to propose a first biozonation and update the age of the Sidi Khalif Formation (= Fm) in the Gafsa basin. A Lower-Middle Berriasian age is assigned to this lithostratigraphic unit. It is topped by a major discontinuity from which the Barremian Sidi Aïch Fm unconformably rests on. This hiatus is interpreted as the result of differential bottom topography structured under the synsedimentary control of the Southward-bordering Gafsa fault.

Keywords

Berriasian • Calpionellids • Biozonation
Gafsa basin • Geodynamics

1 Introduction

Located within a transitional zone between the North-South Axis (Central Tunisia), to the North, and the northern Chott Range, to the South; the Berriasian series of Jebel (= J.) Ben

Younes in the Gafsa region is of a particular interest. It allows an N-S correlation between two distinct paleogeographic domains around the Jurassic-Cretaceous boundary interval.

Discovered by Thomas [1] on the southern flank of J. Ben Younes, close to the major NW-SE trending Gafsa fault, this particular outcrop consists of a marly succession with intercalated limestones bearing mainly echinids, brachiopods and bivalvs. This author assigned a “Neocomian” age to the section of J. Ben Younes that was mapped after and under the same stratigraphic attribution by Solignac [2]. A more recent lithostratigraphic attribution (BouHedma and SidiAïchFms) was given to this same series by subsequent thematic works on the Gafsa area geology (e.g. [3–5]). Slimane et al. [6] established a 1/100000 scale of a geological map including the J. Ben Younes section within the Sidi Khalif Formation (Upper Tithonian-Berriasian) on the basis of an age assignment published four years after [7]. These authors proposed a detailed biostratigraphic study by means of benthic foraminifera, ostracods, brachiopods, echinids, ammonites and calpionellids that led to the characterization of the Ammonite Jacobi zone formerly included within the Upper Tithonian substage.

Our first examination of the ammonite and calpionellid assemblages listed by [7, Fig. 2] from the J. Ben Younes section, highlighted an age discrepancy between the distribution of listed taxa and the age attributed. In fact, for a given level, determined ammonite species indicate a Middle Berriasian age (Occitanica ammonite zone); whereas, calpionellid associations plead in favor of a rather Upper Tithonian age (Durangites ammonite zone). For each paleontological group, the assemblages identified by [7] do not support the proposed biozonation. This prompted us to revisit the J. Ben Younes

R. Ferchichi · I. Cherif · M. Boughdiri (✉) · S. B. Nsir
Faculty of Sciences of Bzerte, Earth Science Department,
University of Carthage, 7021 Bizerte, Jerzouna, Tunisia
e-mail: mab_boughdiri@yahoo.fr;
Mabrouk.Boughdiri@fsb.mu.tn

N. Bahrouni
National Geological Survey, ONM (Tunisian National Office of
Mines), La Charguia, Tunis, Tunisia

M. F. Zagrarni
Higher Institute of Water Sciences and Technology (ISSTEG),
University of Gabès, Gabès, Tunisia

section and propose the updated biozonal chart presented in this work. Consequently, a correlation with nearby lateral equivalents from the J. Bou Hedma section of the North South Axis of central Tunisia allows us to reconstruct the regional geodynamic context and the main controlling factors.

2 Settings

The J. Ben Younes consists of a NW-SE anticline limited to the south by the major N120 trending Gafsa fault. On the one hand, the northern flank of this anticline and its eastern periclinal termination crop out. On the other hand, the southern flank is collapsed beyond the quaternary deposits of the area. The youngest Lower Cretaceous outcrops correspond to the clay, sandstone and dolomite alternations of the Sidi Aïch Formation (Barremian-Lower Aptian).

The sections dealt with in the current study represent an examination of the region located to the south of the northern flank of the J. Ben Younes anticline. They are served by a track bifurcating from the GP3 Gafsa-Metlaoui main road.

3 Materials and Methods

The Ben Younes sections were systematically sampled bed by bed. A total of 81 carbonate samples were collected for calpionellid and microfacies analyses. All the thin sections were observed and photographed under Leica polarized light microscope with a Nikon digital camera. Observations and micropalaeontological identifications were carried out at the magnifications of 60X and 100X. Rare ammonite specimens, brachiopods, echinoderms and bivalves were collected from four ammonite-bearing levels. More than 30 macrofossils specimens were collected. The set of thin-slides and gathered macrofossils are stored at the Department of Earth Sciences of Bizerte. The calpionellid biozonation referred to the standard of Remane et al. [8] complemented by more recent data of [9–11]. Ammonite/Calpionellid zone correlations are due to Le Hégarat and Remane [12] and Hoedemaker et al. [13].

4 Results: Calpionellid Biozonation and Age of the Study Sections

The calpionellid bearing beds of the J. Ben Younes sections span the Upper part of the Alpina subzone and the Remaniella and Elliptica (*p.p*) subzones of calpionellids. These are

correlated with the Grandis (upper Lower Berriasian) and Subalpina (lower Middle Berriasian) subzones of ammonites. The top of the section is marked by a major discontinuity through which the Barremian Sidi Aïch Fm and the overlying units uncomfortably rest on the here-dated Sidi Khalif Fm.

5 Discussion

Our results can confirm those of the “Tithonian” age (Jacobi subzone) attributed by Ben Youssef et al. [7] to the J. Ben Younes sections which are no longer justified. The lithological succession and thickness presented by these authors show the superposition of two similar subsections (Fig. 1).

In fact, these same-aged subsections are separated by a senestral strike-slip fault leading to their apparent succession in the field. As a consequence, their sequential stratigraphy and identified discontinuities within the J. Ben Younes section are wrongly correlated.

On the other hand, our investigations confirm the results of Ben Youssef et al. [7] concerning the existence of a major hiatus expressed by the major topmost discontinuity of the section. Indeed, this discontinuity materializes the lack of the Meloussi, Boudinar and BouHedma Formations outcropping in neighboring sections.

On this same subject, two divergent points of view were adopted to highlight the geodynamic role played by the Gafsa major fault during the onset of Lower Cretaceous sedimentary series. The first assigned a passive role to this accident referring to seismic data. However, the second pleads in favor of its relevant synsedimentary control of facies distribution.

The correlation of the Upper Jurassic-Lower Cretaceous outcrops and well data from the Gafsa area show that: (1) in the Ben Younes section, the upper Sidi Khalif Fm (Lower-Middle Berriasian) is uncomfortably overlain by the Sidi Aïch Fm dated as Barremian; (2) in J. Sidi Aïch and Orbata, the total thickness of the Meloussi, Boudinar and Bouhedma Fms exceeds 1000 m. These correlations supported by field observations allow us to interpret this major hiatus as due to a differential bottom topography structured under the regional tectonic control of the Gafsa fault corridor. During Berriasian times, the current J. Ben Younes latitude corresponds to the apex of a tilted block at the intersection of N-S and NW-SE lineaments. This structuring can be related to Neocimmerian tectonics whose signatures are already identified at a regional scale ([14, 15]).

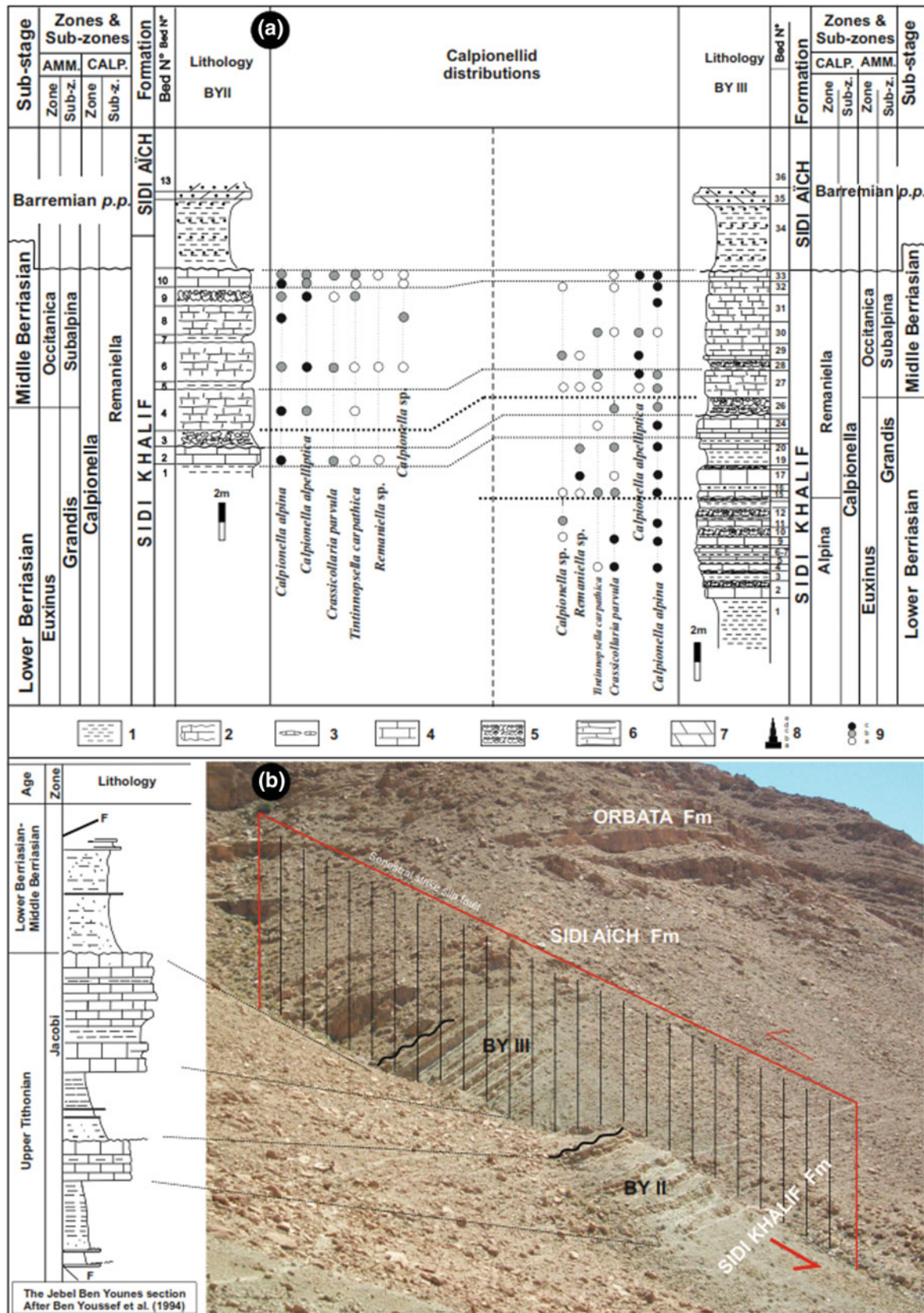


Fig. 1 The sections BY III and BYII from the J. Ben Younes (Gafsa basin). **a.** Lithological succession, faunal distribution and biozonation. 1. marls, 2. limestone beds with irregular surfaces, 3. limestone nodules/pinching out beds, 4. well stratified limestones, 5. nodular

limestone, 4. Chalky limestone, 5. Dolomite, 8–9. abundance of calpionellids. **b.** Field photograph of the sections correlated to the section proposed by Ben Youssef et al. [7]

6 Conclusion

The biostratigraphy of the Sidi Khalif Fm in J. Ben Younes is updated here. Calpionellid associations indicate a Lower-Middle Berriasian age. The top of the unit corresponds to a major discontinuity related to a hiatus of the Upper Berriasian-Lower Barremian time interval. Future works will be probably focusing on wider biozonation and correlations of the Sidi Khalif Fm with its lateral equivalents of J. Ben Younes. N-S and E-W transect correlations are of a particular relevance. The aim behind them is to replace the Jurassic-Cretaceous boundary of Tunisian successions and to bear signatures in a wider geodynamic context within the Maghrebian Tethyan margin.

References

1. Thomas, Ph.: Essai d'une description géologique de la Tunisie; 2ème partie: Stratigraphie des terrains paléozoïques et mésozoïques. Impr. Nat. Paris (1908)
2. Solignac, M.: Carte géologique au 1/200 000 de gafsa. Publ. Serv. Mines Tunisie
3. Burollet, P.F.: Contribution à l'étude stratigraphique de la Tunisie centrale. *Ann. Mines et Géol. Tunisie* **18**, 1–345 (1924/1956)
4. M'rabet, A.: Stratigraphie, sédimentation et diagenèse carbonatée des séries du Crétacé inférieur de Tunisie centrale. *Annales Mines et Géologie* **30**, 1–412 (1987)
5. Zargouni, F.: Tectonique de l'Atlas méridional de Tunisie. Evolution géométrique et cinématique des structures en zone de cisaillement, pp. 1–292. Thesis univ. Strasbourg, France (1985)
6. Slimane F., Rabia M.C., Zerai, N.: Carte géologique de Gafsa au 1/100000; N°. 66. Publ. ONM. Tunisie (1991)
7. Ben Youssef, M., Memmi, L., Rabiaa, M.C., Slimane, F.: Caractérisation de la Zone à Jacobi (Tithonique supérieur) au jebel Ben Younés (Atlas méridional): cadre maghrébin et conséquences paléogéographiques. *Notes Serv. Géol. Tunisie* **60**, 11–20 (1994)
8. Remane J., Borza K., Nagy I., Bakalova-Ivanova D., Knauer J., Pop G., Tardi-Filacz, E.: Agreement on the subdivision of the standard calpionellid zones defined at the second Planktonic Conference, Roma 1970. *Acta Geologica Hungarica* **29**, 5–14 (1986)
9. Olóriz, F., Caracuel, J.E., Lopez-Marques, B., Rodriguez-Tovar, F. J.: Asociaciones de Tintinnoides en facies ammonítico rosso de la Sierra Norte (Mallorca). *Revista española de Paleontología* **7**, 77–93 (1995)
10. Pop, G.: Calpionellidevolutive events and their use in biostratigraphy. *Romanian Journal of Stratigraphy* **76**, 7–24 (1994)
11. Reháková, D., Michalík, J.: Evolution and distribution of calpionellids—the most characteristic constituents of Lower Cretaceous Tethyan microplankton. *Cretaceous Research* **18**, 493–504 (1997)
12. Le Hégarat, G., Remane, J.: Tithonique supérieur et Berriasien de la bordure Cévenole. Corrélations des ammonites et des calpionelles. *Geobios* **1**, 7–70 (1968)
13. Hoedemaeker, P.J., Janssen, N.M.M., Casellato, C.E., Gardin, S., Reháková, D., Jamrichová, M.: Jurassic/Cretaceous boundary in the Río Argos succession (Caravaca, SE Spain). *Rev. Paléobiol.* **35** (1), 111–247 (2016)
14. Tlig, S.: The upper jurassic and lower cretaceous series of southern Tunisia and northwestern Libya revisited. *J. Afr. Earth Sci.* **110**, 100–115 (2015)
15. Bahrouni, N., Houla, Y., Soussi, M., Boughdiri, M., Ben, Ali W., Nasri, A., Bouaziz, S.: Discovery of Jurassic ammonite-bearing series in Jebel Bou Hedma (South-Central Tunisian Atlas): implications for stratigraphic correlations and paleogeographic reconstruction. *J. Afr. Earth Sci.* **113**, 101–113 (2016)

Berriasian Ammonite and Calpionellid Associations from the North-South Range of Central Tunisia: Updated Biozonation, Regional Geodynamic Context and Paleobiogeography

Sana Ben Nsir, Mabrouk Boughdiri, Ichrak Cherif, Néjib Bahrouni, Rafika Ferchichi, and Asma Zrelli

Abstract

Six Berriasian sections from Central Tunisia were wisely sampled bed by bed. Hundreds of gathered ammonite specimens and observed calpionellid associations allowed an updated biozonation of the Sidi Khalif Formation on the “North-South Axis” of the area. This Fm spans all the Berriasian stage. Respective ammonite- and calpionellid-bioevents were correlated and the proposed regional chart fits the Mediterranean Tethys standards. These bioevents and corresponding limits of the biostratigraphic units were the object of a long-distance correlation with well dated European sections, wisely calibrated with magnetostratigraphic data. The upper Tithonian and Berriasian biogeographic distribution of ammonite genera allows the reconstruction of population dynamics and confirms the existence of two potential seaways for faunal exchanges. These peri-Gondwanian routes consist of the Hispanic corridor as part of the proto-Atlantic ocean to the West, and an eastern seaway joining the Indo-Malgasian territory with Somalia and Mozambique.

Keywords

Ammonites • Calpionellids • Berriasian
Central Tunisia • Biozonation • Paleobiogeography

1 Introduction

The Lowermost Cretaceous series of Central Tunisia have been the object of relatively wise biostratigraphic investigations at least since the fifties ([1–4] among others). The first ammonite

S. Ben Nsir · M. Boughdiri (✉) · I. Cherif · R. Ferchichi · A. Zrelli
Faculty of Sciences of Bizerte, Earth Science Department,
University of Carthage, 7021 Jerzouna, Tunisia
e-mail: mabrouk.boughdiri@fsb.rnu.tn;
mab_boughdiri@yahoo.fr

N. Bahrouni
National Office of Mines, Geological Survey, La Chargaia, Tunis,
Tunisia

and calpionellid biozonation in the area is mainly due to [5] which proposed a first integrated ammonite and calpionellid biostratigraphic scheme. M’rabet [6, 7] represents an adaptation of the same reference scale for the Lowermost Cretaceous succession of the Sidi Khalif Formation. The last two decades is marked by punctual contributions on the Berriasian biostratigraphy with scarce illustrations of faunas [8–14]. No updated synthesis is proposed and no sufficient ammonite and calpionellid figurations are available. This work attempts to synthesize the Berriasian biozonation from central Tunisia, to discuss previous works and to replace the Sidi Khalif Formation in its regional geodynamic context. Stratigraphically, well located ammonites from numerous Tethyan sections allowed us to discuss the dynamics of ammonite populations and favorable seaways for potential faunal exchanges.

2 Methods and Materials

The study sections were sampled along the North-South Axis of Central Tunisia between the villages of Faiedh to the South and Nasrallah to the North. More than two hundred ammonite specimens were sampled bed by bed. For calpionellid identification and abundance evaluation, three hundred thin sections were analyzed under a Leica polarized optic microscope adapted to a Canon camera. All ammonite specimens were cleaned by using suspended-motor electric and/or pneumatic engraver pens.

3 Results and Discussion

3.1 Biozonations

The following zones and subzones were identified. For ammonites, the Euxinus Zone is subdivided into two subzones: the Jacobi and Grandis subzones. Up section, the Occitanica Zone base is defined mainly by the first occurrence (FO) genus *Tirnovella* particularly *Tirnovella*

BENABDESSALEM (2015, Tabl. 11)				BENZAGGAGH (2000; Fig. 94, p. 190)				REMANE (1963, Fig. 18)	REMANE (1985, Fig. 15)			REMANE <i>et al.</i> (1986, Fig. 1) *	
Marker bioevents		Calp.	Ammonite Zones and Subzones (SUBTAGES)		Calp.	Marker bioevents		Marker bioevents	calpionellid Zones and Subzones		Bio-events	AGE	
F.O. <i>Calpionellopsis simplex</i>		D1	Boissieri (p.p.)	Paramim.	D1	Appearance of <i>Calpionellopsis simplex</i>		First <i>Calpionellopsis simplex</i>	Calpionellopsis simplex	D1	Calpionellopsis	7	BERRIASIAN
Tintinnopsella carpathica more frequent than <i>Calpionella alpina</i>		C2	Occitanica	Dalmasi	C2	Large <i>T. carpathica</i> (T.c.); Inversion of abundance C.a. vs T.c.		Transition to large <i>Tintinnopsella carpathica</i> and rapid expansion	Calpionella	C	Calpionella elliptica	6	
F.O. <i>Calpionella elliptica</i>		C1	(BER. MOY.)	Privasens.	C1	Appearance of <i>C. ellipt.</i>		«Explosion» of <i>Calpionella alpina</i> with small spherical varieties		B	Remaniella	5	
F.O. <i>Calpionella alpeptica</i>		B3	Euxinus (BER. INF.)	Subalp.	B3	Appearance of <i>C. alpeptica</i>		Predominance of <i>Crassicollaria brevis</i> in relation to <i>Cr. intermedia</i>	Intermedia (p.p.)	A3	Crassicollaria (p.p.)	4	
F.O. <i>Remaniella duranddelgai</i>		B2		Grandis	B2	Appearance of <i>Remaniella</i> (div. sp.)				3	Calpionella alpina	3	
«Bloom» of <i>C. alpina</i>		B1	Durangites (p.p.)	Jacobi	B1	«Explosion» of spherical forms of <i>C. alpina</i> (C.a)							
					A (pp)								

Fig. 1 Calpionellid biozonations: correlations and marker bioevents. **Legend.** * In the synthetic biozonation of [22], the three columns correspond to standard zones of de Rome after the Sümeg meeting (left column), zones and subzones from SE France (middle) and those of [23]. For correlations with other charts, the same authors [22] refer to

Remane [20, 21]. Marker bioevents: 3. «explosion» of *C. alpina* and transition to small globular forms; 4. First *Remaniella*; 5. First *C. elliptica*; 6. Transition to large *T. carpathica*; 7. First *Calpionellopsis simplex*

occitanica and *Tirnovella subalpina*. This latter marks the base of the Alpina subzone. The Boissieri Zone is defined by the FO of the index species *Fauriella boissieri*.

For calpionellids, the defined Calpionella Zone corresponds to the zone B of Remane [19]. Four subzones have been identified: the Alpina, Remaniella, Elliptica and Longa Subzones. The base of the overlying Calpionellopsis Zone is traced considering few *Calpionellopsis* specimens determinable only at the genus level: all observed to the topmost of the study sections.

3.2 Regional Correlations and Geodynamic Context

To the south of the studied area, the Upper Tithonian successions are known in the J. Rheouis section. Along the North-South Axis, the Sidi khalif Fm spans the whole Berriasian stage and all the studied section can be easily correlated. To the North, in the J. Haouareb area, lower Upper Jurassic series are of Ammonitico Rosso-type, they are overlain by Kimmeridgian-Tithonian carbonate units intercalating breccias and slumps [15]. A 30-cm single bed outcropping within a ravine crossing the uppermost part of the covered Sidi Khalif Fm yields the Upper Berriasian specimens. During the Berriasian, the northern part of the North-South Axis has acted as a high resistant block separated by: (1) the Haouareb ombilicus to the North and (2) a subsiding zone covering the J. Rheouis and neighboring latitudes to the South. This domain has been structured in

favor of a synsedimentary distensional tectonics where major bordering fault had played an important role.

3.3 Paleobiogeography

Paleobiogeographic distribution of ammonites around the Jurassic-Cretaceous transition shows two particularities: (1) to the West, Mediterranean taxa arriving to Mexico and extending to the Peru, Argentina and Chile platforms. (2) Taxa of Caribbean affinities found in India and in Arabia to the East. In areas from northern latitudes, only sporadic arrivals of Tethyan faunas have been reported from the Berriasian of the Boreal Realm.

During the Jurassic-Cretaceous transition, the co-occurrence of south-American taxa and their Mediterranean affinity conspecific specimens can be interpreted as “passive” migration of faunas via two possible seaways: (1) Tethyan afflux across the Protoatlantic ocean of planktonic ammonite larva. (2) The “Indo-Malgasian route”, proposed by Cecca [16], links South Africa and Patagonia to the Tethys via Mozambique, Somalia and Eastern India.

3.4 Discussion

This paper proposes to discuss recent biozonations of the Sidi Khalif Fm in Central Tunisia. These were based on an alpha-numerical chart of calpionellid biostratigraphy proposed by [17, 18].

Our Fig. 1 correlates the calpionellid biozonation charts proposed by different authors. This correlation takes into account all the identical bioevent markers identified from different regions.

It clearly appears that the base of B3 zone of Benzaggagh et al. ([18] and references therein) is well correlated with that of Elliptica Subzone of [24], therefore correlatable to the Subalpina subzone of ammonites as confirmed by [11]. Benzaggagh [17] wrongly interpreted the base of the Elliptica subzone of Pop as equivalent to that of the zone C of Remane (= C1 + C2 of [17, 18]).

We consider the C1 subzone of Benzaggagh [17, 18] and Benzaggagh et al. [18] as a very small transitional interval, spanning the extreme base of the Remane C zone. For practical reasons, the subzone C2 of these authors can be admitted with a sufficient margin of tolerance as an equivalent of almost all of Remane C zone. The extreme base of the latter is excluded. Their subzones B3 and C1 are thus of a limited practical value for calpionellid biozonation around the Lower Berriasian-Middle Berriasian transition.

4 Conclusion

The integrated biozonation of the Sidi Khalif Fm in Central Tunisia identified three zones and four subzones of ammonites within the Berriasian stage. Accompanying or relaying calpionellid associations served to distinguish all zones and subzones of the reference standards for the Tethyan domain. The diachronism of the Sidi Khalif Fm in central Tunisia is interpreted here as due to an irregular structuring of the Upper Jurassic basement into tilted blocks, a mosaic of swells and depressions receiving Tithonian and Berriasian prograding sediments. Future works may be focused on other paleontological tools (nannofossils, dinokysts) to calibrate the biostratigraphy of some relatively thick marl levels of the Sidi Khalif Fm devoid of calpionellids and ammonites. A further sequential stratigraphy of the same sections could also be an aim at the analysis of spatio-temporal distribution of both the facies and the basin structure.

References

1. Castany, G.: Etude géologique de l'Atlas tunisien oriental. Ann. Mines Géologie **8**, 1–632 (1951)
2. Burolet, P.F.: Contribution à l'étude stratigraphique de la Tunisie centrale. Ann. Mines et Géol. Tunisie **18**, 1–345 (1956)
3. Memmi, L.: Succession de faunes dans le Tithonique supérieur et le Berriasien du Jebel Nara (Tunisie centrale). Bull. Soc. Géol. France **9**, 267–272 (1967)
4. Bonnefous, J.: Contribution à l'étude stratigraphique et paléontologique du Jurassique de Tunisie (Tunisie septentrionale et centrale, Sahel, zone des Chotts). Thèse Université Paris VI, pp. 1–397 (1972)
5. Busnardo, R., Donze, P., Khessibi, M., Le Hegarat, G., Memmi, L., M'rabet, A.: La formation Sidi Kralif (Tithonien Berriasien) en Tunisie centrale, synthèse stratigraphique et sédimentologique. Annales des mines et de la géologie, Tunis **31**, 115–122 (1985)
6. M'rabet, A.: Stratigraphie, sédimentation et diagenèse carbonatée des séries du Crétacé inférieur de Tunisie centrale. Annales des Mines et de la Géologie, Tunis, pp. 1–405 (1987)
7. Memmi, L.: Le Crétacé inférieur (Berriasien-Aptien) de Tunisie. Biostratigraphie, paléogéographie et paléoenvironnements. Thèse Université Claude Bernard Lyon 1, France (1989)
8. Boughdiri, M.: Les genres d'ammonites *Durangites* et *Protacanthodiscus* (Tithonien supérieur) dans la Téthys occidentale (SE Espagne, SE France, Algérie et Tunisie). Stratigraphie, Paléontologie et Biogéographie. Thèse Université Claude Bernard, Lyon I, pp. 1–268 (1994)
9. Enay, R., Boughdiri, M., Le Hégarat, G.: *Durangites*, *Protacanthodiscus* et formes voisines du Tithonien supérieur-Berriasien dans la Téthys méditerranéenne (SE France, Espagne, Algérie et Tunisie). Comptes Rendus Acad. Sci. Paris sér. 2a (327): 425–430 (1998)
10. Boughdiri, M., Enay, R., Le Hégarat, G., Memmi, L.: *Hegarites* gen. nov. Himalayitidé nouveau du Tithonien supérieur de la coupe du J. Rhéouis (Axe Nord-Sud, Tunisie centrale). Précisions stratigraphiques, approche phylétique et signification biogéographique. Revue de Paléobiologie, Genève **18**(1), 105–121 (1999)
11. Ben Abdesslem-Mahdaoui, S.: Le passage Jurassique supérieur-Crétacé inférieur. Etude de l'évolution verticale des calpionelles et de la microfaune associée en Tunisie septentrionale. Thèse Université de Tunis El Manar Faculté des Sciences de Tunis, pp. 1–263 (2015)
12. Maalaoui, K., Zargouni, F.: The lower and middle berriasian in central tunisia: integrated ammonite and calpionellid biostratigraphy of the Sidi Kralif formation. Acta Geol. Pol. **66**(1), 43–58 (2016)
13. Maalaoui, K., Zargouni, F.: Biozones de calpionelles et d'ammonites du Berriasien inférieur et moyen de la Formation Sidi Khalif au JebelMeloussi Tunisie centrale. Revue de Paléobiologie **35**(1), 373–384 (2016)
14. Maalaoui, K., Zargouni, F.: Biostratigraphical study around the Jurassic/Cretaceous boundary in Central Tunisia, zonal schemes and correlation. J. Afr. Earth Sc. **125**(2017), 166–176 (2017)
15. Soussi, M.: Le Jurassique de la Tunisie atlasique. Stratigraphie, dynamique sédimentaire, paléogéographie et intérêt pétrolier. Docum. Labo. géol. Lyon **157**, 1–363 (2002)
16. Cecca, F.: Paleobiogeography of Tethyan ammonites during the Tithonian (latest Jurassic). Paleogeography, Paleoclimatology, Palaeoecol. **147**, 1–37 (1999)
17. Benzaggagh, M.: Le Malm supérieur et le Berriasien dans le Prérif interne (Rif, Maroc): biostratigraphie, lithostratigraphie, paléogéographie et évolution tectono-sédimentaire. Documents du Laboratoire de Géologie de Lyon **152**, 1–374 (2000)
18. Benzaggagh, M., Cecca, F., Schnyder, J., Seyed-Emami, K., Majidifard, M.R.: Calpionelles et microfaunes pélagiques du Jurassique supérieur-Crétacé inférieur dans les Formations Shal et Kolor (Montagnes du Talesh, chaîne de l'Elbourz, Nord-Ouest Iran). Répartition stratigraphique, espèces nouvelles, révision systématique et comparaisons régionales. Annales de Paléontologie **98**, 253–301 (2012)
19. Remane, J.: Les Calpionelles dans les couches de passage Jurassique-Crétacé de la fosse vocontienne. Travaux du Laboratoire de Géologie de la Faculté des Sciences de Grenoble **39**, 25–82 (1963)

20. Remane, J.: Calpionellids. In: Bolli, H.M., Saunders, J.B., Perch-Nielsen, K. (eds.) *Plankton Stratigraphy*, pp. 555–572. Cambridge University Press (1985)
21. Remane, J.: Calpionellids and the Jurassic-Cretaceous boundary. *Acta Geol. Hung.* **29**, 15–26 (1986)
22. Remane, J., Borza, K., Nagy, I., Bakalova-Ivanova, D., Knauer, J., Pop, G., Tardi-Filacz, E.: Agreement on the subdivision of the standard calpionellid zones defined at the IInd Planktonic Conference Roma 1970. *Acta Geol. Hung.* **29**, 5–14 (1986)
23. Allemann, F., Catalano, R., Fares, F., Remane, J.: Standard calpionellid zonation (Upper Tithonian-Valanginian) of the western Mediterranean province. In: Farinacci, A. (ed.) *Proceedings of the II Planktonic Conference, Roma 1970*, vol. 2, pp. 1337–1340 (1971)
24. Pop, G.: Calpionellid evolutive events and their use in biostratigraphy. *Rom. Ian J. Strat.* **76**, 7–24 (1994)

Barremian-Albian (Lower Cretaceous) Rudist Chronostratigraphy, Caribbean Province North America

Robert Scott, Whitney Campbell, Brian Diehl, Xin Lai, Allison Porter, and Yulun Wang

Abstract

The Bivalvia Family Caprinuloideidae in the North American Caribbean Province defines seven Barremian-Albian biozones. This rudist clade diversified from one early Barremian species into six assemblages with a total of thirty-two species. The early Aptian and middle Albian assemblages experienced extinction following OAEs 1a, 1b and 1c. Each associated with terrigenous flooding cycles. The latest Albian assemblage was followed by OAE 1d and flooding by an early Cenomanian terrigenous depositional system.

Keywords

Caprinuloideidae biozones • Early Cretaceous • Comanchean • Texas-Mexico

1 Introduction

North American Barremian-Albian carbonate facies host diverse Hippuritida (Rudists) that define precise biostratigraphic zones. Barremian-Albian biostratigraphy of the great Comanche Shelf that embraced the proto-Gulf of Mexico has been correlated with European stages by ammonites and planktic foraminifera [1]. However, the shelf margin carbonates inhibited ammonites and instead hosted a rich, diverse rudist and benthic foraminifer assemblage.

R. Scott (✉) · B. Diehl · A. Porter
University of Tulsa, Tulsa, OK 74104, USA
e-mail: rwscott@cimtel.net

W. Campbell
Laredo Petroleum, Tulsa, OK 74119, USA

X. Lai
Research Institute of Petroleum Exploration & Development-Langfang, Hebei, 065007, China

Y. Wang
School of Geology, Oklahoma State University,
Stillwater, OK 74078, USA

Rudist zones were first proposed [2] updated [3] and revised [4–6]. This status report is based on new outcrop and core data. It summarizes the existing Caprinuloideidae ranges in Texas and northern Mexico. These ranges are integrated with ammonite and foraminifer ranges and calibrated to the most recent numerical time scale [7, 8].

2 Methods

Rudist taxon ranges were correlated with standard European Barremian-Albian stages by one of two methods: (1) taxa have been reported in lithostratigraphic units that have been correlated by regional mapping; or (2) specific rudist-bearing sections have been graphically correlated with the revised Cretaceous Chronostratigraphic Database (CRETCSDB17) which has been re-scaled to the 2016 Geologic Time Scale [8].

Global ammonite and foraminifer ranges are calibrated in CRETCSDB17 from Tethyan reference sections outside of the Caribbean Province [9, 10]. Comanchean sections have been correlated with these sections so that provincial rudists and benthic foraminifer ranges can be integrated. The numerical ages are calibrated by the interpretations of the rates of the sediment accumulation based on the first and the last occurrences (FO, LO).

Comanchean sections are interrupted by widespread disconformities that reflect regional terrigenous drowning events (Ap SB PR 1; Ap SB PR 2, Al SB Gr 1, Al SB FR 1, Al SB WA 1, Ce TS WA 6) [1, 5] (Fig. 1). The numerical ages are constrained by the radioisotope ages in associated sections [8].

3 Results

Seven Caprinuloideidae biozones subdivide the Barremian-Albian strata in North American carbonate facies (Fig. 1). These zones are correlated with ammonite zones and the First Appearance Datums (FADs) of foraminifera [9–11].

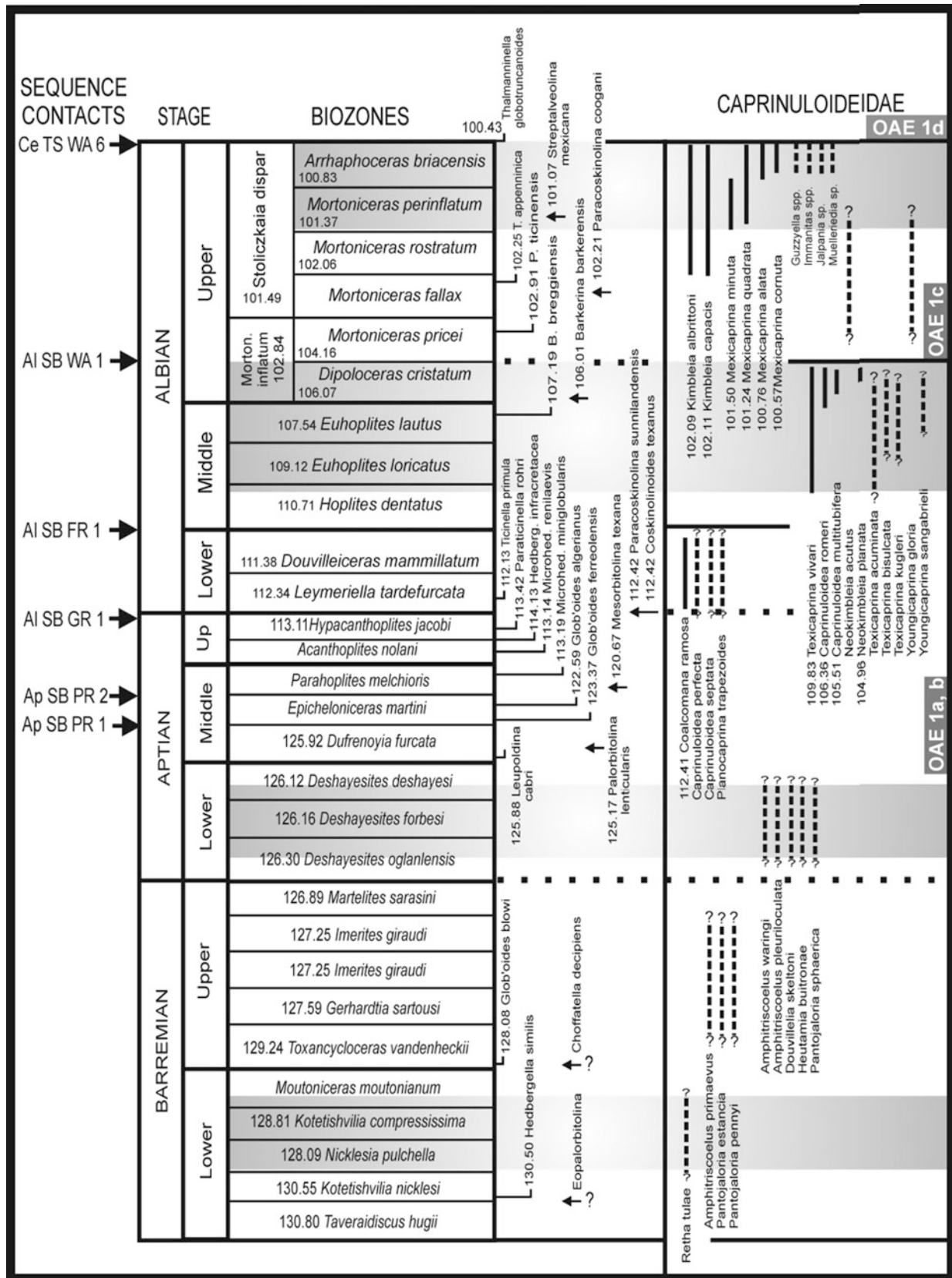


Fig. 1 Barremian-Albian chronostratigraphy Texas-Northern Mexico Comanche shelf. Ammonite and planktic Foraminifera zones [9]; mega-annages are calibrated in CRETCSD17 with the 2016 Geologic Time Scale [7]. Solid range bars based on ranges in key

lithostratigraphic sections; dashed range bars based on taxa reported in lithostratigraphic units not in CRETCSD17. Question marks indicate uncertain correlation with ammonite zones

The *Retha tulae* Range Zone correlates approximately with the lower Barremian ammonites and the FADs of *Eopalorbitolina* and *Hedbergella similis*.

The *Pantojaloria estancia* Assemblage Zone correlates approximately with the upper Barremian ammonites and the FADs of *Choffatella decipiens* and *Globigerellinoides blowi*.

The *Amphitricoeus waringi* Assemblage Zone correlates approximately with the lower Aptian ammonites. No middle-upper Aptian rudist zones have been recognized yet as in the Caribbean Province.

The *Coalcomana ramosa* Range Zone spans lower Albian shelf carbonates and the major part of the Trinity Group.

The *Caprinuloidea romeri* Assemblage Zone characterizes the middle and the basal upper Albian ammonite zones. On the Comanche Shelf, this includes the Fredericksburg Group and the correlative strata.

The *Kimbleia albrittoni* Assemblage Zone correlates with the middle upper Albian *Mortoniceras rostratum* Zone and the FADs of *Thalmaninella appenninica* and *Paracoski-nolina coogani* in the middle part of the Washita Group.

The *Mexicaprina quadrata* Assemblage Zone correlates with the uppermost Albian ammonite zones and the FAD of the benthic foraminifera *Streptalveolina mexicana*.

4 Conclusion

The Bivalvia Family Caprinuloideidae in the North American Caribbean Province defines seven Barremian-Albian biozones. This rudist clade diversified from one species in the early Barremian to seven in the early Aptian. Following OAE 1a, they were virtually extinct during the middle-late Aptian. In the beginning of the early Albian, four species occupied the Comanchean carbonate shelf. Nine middle Albian species populated the shelf. In the late Albian following OAE 1c on the shelf, two species diversified into ten species by the end of the late Albian.

References

1. Scott, R.W., Benson, D.G., Morin, R.W., Shaffer, B.L., Oboh-Ikuenobe, F.E.: Integrated Albian-lower Cenomanian chronostratigraphy standard, Trinity River Section, Texas: U.S. Gulf Coast. Cretaceous Stratigraphy and Paleocology Perkins Memorial, vol. 1, pp. 277–282 (2003)
2. Coogan, A.: Early and middle Cretaceous Hippuritacea (Rudists) of the Gulf coast. In: Bebout, D.G., Loucks, R.G. (eds.) Cretaceous Carbonates of Texas and Mexico, Report of Investigations, vol. 89, pp. 32–70. University of Texas Bureau of Economic Geology (1977)
3. Scott, R.W., Filkorn, H.F.: Barremian—Albian rudist zones, U.S. Gulf coast. In: Scott, R.W. (ed.) Cretaceous Rudists and Carbonate Platforms: Environmental Feedback, vol. 87, pp. 167–180. SEPM Special Publication, Tulsa, Oklahoma (2007)
4. Mitchell, S.F.: A revision of selected Lower Cretaceous American caprinoid rudists: Implications for phylogeny and biostratigraphy. Caribbean Journal of Earth Science **45**, 47–75 (2013)
5. Scott, R.W.: Cretaceous chronostratigraphic database: construction and applications. Carnets Geol. **14**(1), 1–13(2014). <http://paleopolis.rediris.es/cg/uk-index.html>. Accessed 20 Jan 2015
6. Scott, R.W., Campbell, W., Hojnacki, R., Wang, Y., Lai, X.: Albian rudist biostratigraphy (Bivalvia), Comanche shelf to shelf margin, Texas. Carnets Geol. **16**(21), 513–541 (2016). <http://paleopolis.rediris.es/cg/uk-index.html>. Accessed 20 Jan 2015
7. Ogg, J.G., Ogg, G.M., Gradstein, F.M.: A Concise Geologic Time Scale 2016. Elsevier, Amsterdam (2016)
8. Scott, R.W., Oboh-Ikuenobe, F.E., Benson, D.G., Jr., Holbrook, J. M., Alnahwi, A.: Cenomanian-Turonian flooding cycles: U.S. Gulf Coast and Western interior. Cretac. Res. **98**, 191–210 (2018). <http://www.doi.org/10.1016/j.cretres.2018.03.027>. Accessed 20 May 2015
9. Reboulet, S., Rawson, P.F., Moreno-Bedmar, et al.: Report on the 4th international meeting of the IUGS Lower Cretaceous ammonite working group, the “Kilian Group” (Dijon, France, 30th August 2010). Cretac. Res. **32**, 786–793 (2011)
10. Cherchi, A., Schroeder, R.: The *Praeorbitolina/Palorbitolina* association: an Aptian biostratigraphic key-interval at the southern margin of the Neo-Tethys. Cretac. Res. **39**, 70–77 (2013)
11. Mitchell, S.F., Green, R.: Field Trip 1: Lower Cretaceous rudists of the Benbow Inlier, central-north Jamaica (Saturday, 18 June 2011). In: The Ninth International Congress on Rudist Bivalves 18th to 25th June, 2011, Kingston, Jamaica, Abstracts, Articles and Field Guides. UWI Mona Contributions to Geology, vol. #6, pp. 29–36 (2011). ISSN 0799-0162

Mid-Cretaceous Rudist Assemblage from the Lhasa Block, Tibet (China)

Xin Rao, Peter W. Skelton, Shin-ichi Sano, Jingeng Sha, and Bin Wan

Abstract

A total of four rudist taxa had been distinguished from the Sangzugang Formation and the Langshan Formation of the Lhasa block, Tibet by Rao et al. [4, 5]. They are *Auroradiolites biconvexus* [5], *Magallanesia rutogensis* [5], *Eoradiolites* cf. *hedini* and *Sellaea* sp. The genus *Auroradiolites* was established for a group of SW Asian to the Pacific endemic radiolitids that featured by an entirely compact outer shell layer. The geological range of this rudist assemblage is Late Aptian to Albian. The mid-Cretaceous SW Asian-Pacific province was recognized based on the occurrence of endemic rudist taxa *Auroradiolites* and the accompanying polyconitid lineage, *Horiopleura haydeni*—*Praecaprotina*—*Magallanesia*.

Keywords

Lhasa block • Sangzugang Formation
Langshan Formation • Rudist
SW Asian/Pacific faunal province

1 Introduction

Rudists are sessile mollusks that belong to the Order Hippuritida and differ from other bivalves by their bizarre shell shape. They lived in the margins of the

X. Rao (✉) · J. Sha · B. Wan
State Key Laboratory of Palaeobiology and Stratigraphy, Nanjing Institute of Geology and Palaeontology and Center for Excellence in Life and Palaeoenvironment, Chinese Academy of Sciences, 39 East Beijing Road, Nanjing, 210008, China
e-mail: xinrao@nigpas.ac.cn

P. W. Skelton
School of Environment, Earth and Ecosystem Sciences, The Open University, Milton Keynes, MK7 6AA, UK

S. Sano
Department of Earth System Science, Graduate School of Science and Engineering for Research, University of Toyama, 3190 Gofuku, Toyama-Shi, Toyama, 930-8555, Japan

Tethyan-Atlantic-tropical Pacific oceans from the Oxfordian to the end of Cretaceous [8]. In mid-Cretaceous times, the Lhasa Block was situated on the northern margin of the eastern Tethys. Shallow marine carbonate deposits were widely distributed there [10]. Abundant rudists from the mid-Cretaceous Langshan Formation and the Sangzugang Formation of the Lhasa Block had been described. Most of them were established as new species that belong to the genus *Praeradiolites* [1, 7, 9], then assigned these *Praeradiolites* species to *Eoradiolites*, Rao et al. [4, 5] revised these radiolitids and reported three other rudist species subsequently. This short paper is a brief summary of the rudists from the Lhasa Block that described by Rao et al. [4, 5] and unreported discoveries (Fig. 1).

2 Geological Setting

The Tibetan plateau is composed of a series of terranes or blocks that drifted northward and accreted to the Asian continent. From north to south these are: the Songpan-Ganzi, the Qiangtang, the Lhasa and the Tethyan-Himalayan blocks which were separated by the Jinsha, the Bangong-Nu and the Indus-Yarlung sutures respectively [11, 12]. In mid-Cretaceous times, the Lhasa block had already converged with the Qiangtang block then situated on the north margin of the eastern Tethys Ocean [10]. Shallow marine rudist-bearing deposits were widely distributed over the Lhasa block at that time represented by the Langshan Formation in its northern part and the Sangzugang Formation in scattered outcrops along its southern margin [2] (Fig. 2).

3 Results

There are four rudist taxa in general that have been recognized and described by Rao et al. [4, 5]: *Auroradiolites biconvexus* [5], *Magallanesia rutogensis* [5], *Eoradiolites* cf. *hedini* and *Sellaea* sp.

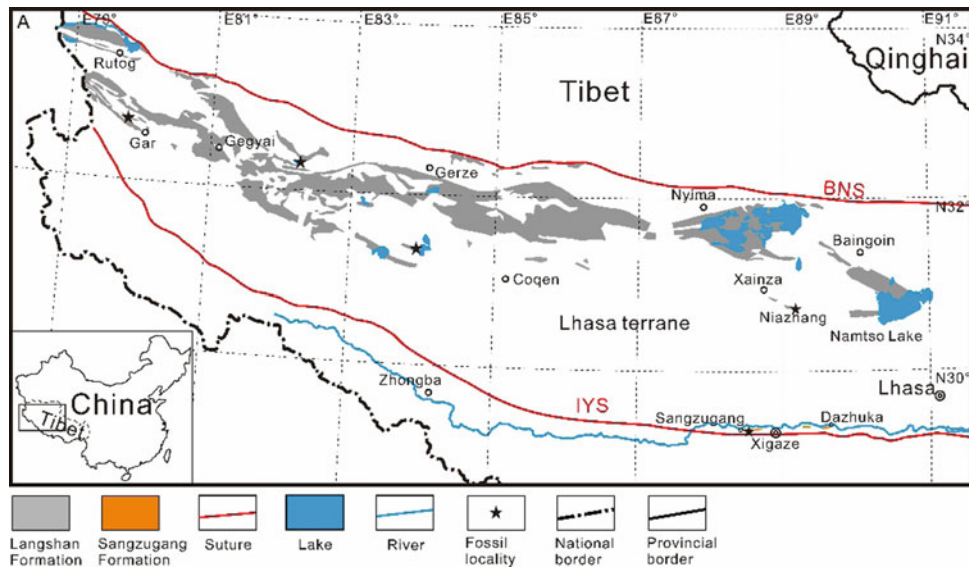


Fig. 1 The distributions of the Langshan and Sangzugang formations in the Lhasa block

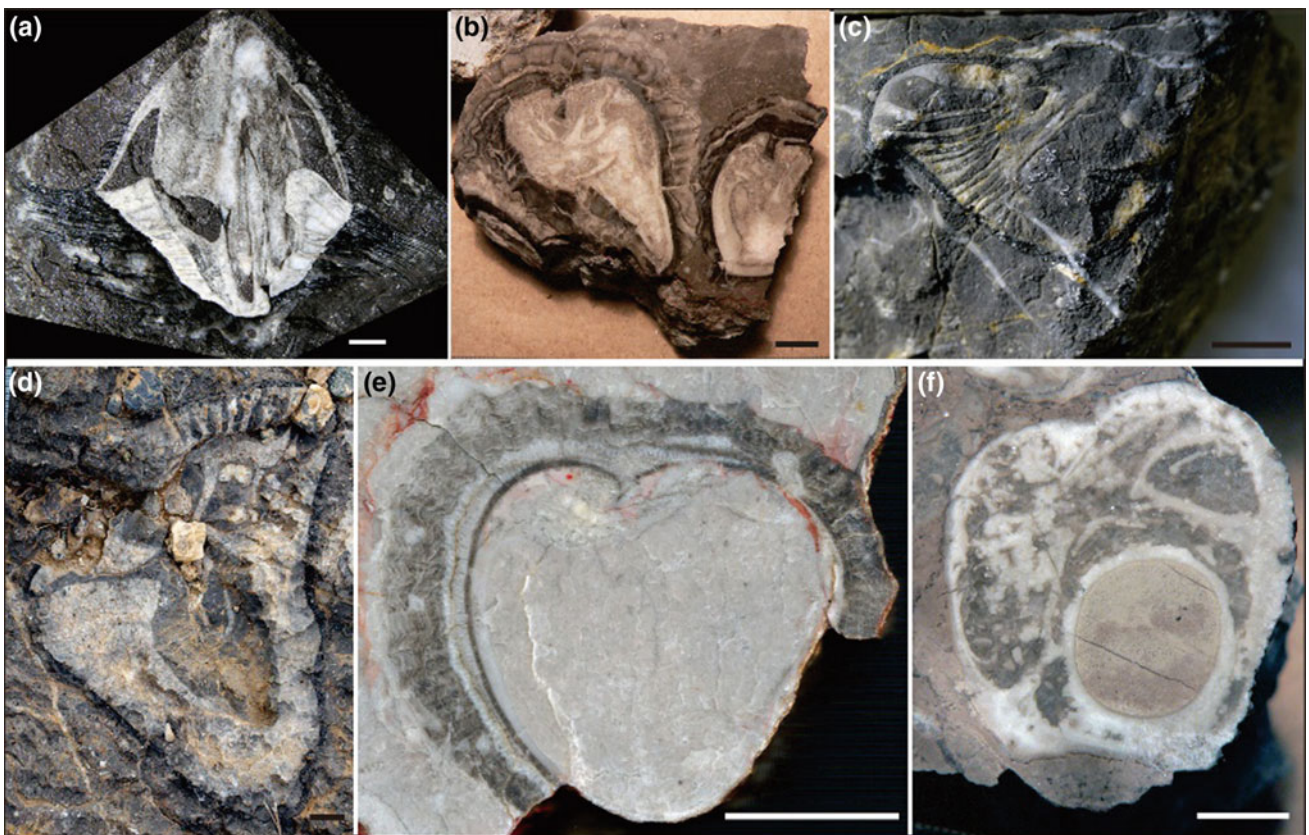
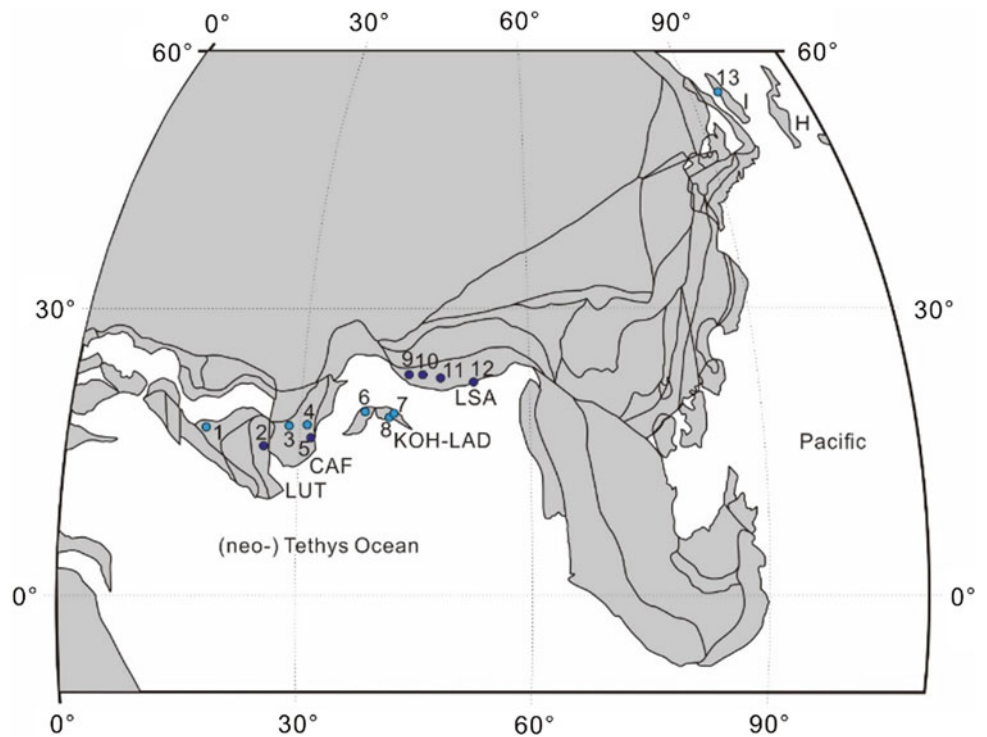


Fig. 2 Rudist specimens from the Sangzugang Formation and Langshan Formation. **a–b**, *Auroradiolites biconvexus*. **c–d**, *Magallanesia rutogensis*. **e**, *Eoradiolites cf. hedini*. **f**, *Sellaea* sp. All scale bars represent 10 mm

Auroradiolites was established for a group of SW Asian to Pacific endemic radiolitids which were assigned to the *Prearadiolites* [1, 9] originally. Then, they have been

transferred to *Eoradiolites* [6, 7]. *Auroradiolites* differs from *Eoradiolites* mainly by the entirely compact outer shell layer, slightly or strongly convex left valve (LV), and

Fig. 3 Palaeogeographical map for 113 ma showing the reconstructed situations of the fossil localities bearing *Auroradiolites*. Light blue dots represent *A. gilgitensis* and dark ones *A. biconvexus*. LUT, Lut block; CAF, Central Afghanistan; KOH-LAD, Kohistan-Ladakh terrane; LSA, Lhasa block; I, Ishikari terrane; H, Hidaka terrane



strongly developed myocardial apparatus and invaginated ligament. Compared with the type species *A. gilgitensis* (Douville 1926), the Tibetan *A. biconvexus* [9], which has been reported from both the Langshan Formation and the Sangzugang Formation, is characterized by a more convex LV and obviously radially undulation in the ol of right valve (RV) (Fig. 3).

Magallanesia rutogensis is featured by the rather thick ol, subequal teeth, and the single row of pallial canals that subdivided the posteroventral cavity of the LV. It has been reported from the Langshan Formation by Rao et al. [5]. Recently, it was also been found from the Sangzagang Formation.

Eoradiolites cf. *hedini*, which was recorded from the Langshan Formation, is characterized by mixed compact and cellular calcitic ol, short, truncated ligamentary inflating in the RV and a slightly convex LV. Rao et al. [5] recorded some small radiolitid specimens from the Langshan Formation that show celluloprismatic structure in most part of the ol. They assigned them to *Eoradiolites* cf. *dauidsoni*. Rao et al. [4] revised these specimens and concluded that they possibly just representing relatively juvenile form of *Eoradiolites* cf. *hedini*. This kind of small *Eoradiolites* cf. *hedini* specimens were also founded from the Sangzugang Formation co-occurring with *A. biconvexus*.

Sellaea sp., which was described from both the Langshan Formation and the Sangzugang Formation, shows typical

features of a relatively thin ol, an erect posterior myophore and adjacent broad posterior ectomyophoral cavity in the RV.

4 Discussion

The rudist biostratigraphic correlation between the Sangzugang Formation and the Langshan Formation indicates that the rudist assemblage of these two formations is similar. Both include *Auroradiolites biconvexus*, *Eoradiolites* cf. *hedini*, *Magallanesia rutogensis* and *Sellaea* sp. the geological range of this rudist assemblage is Late Aptian to Albian. This age was also confirmed by the orbitolinid study of the Sangzugang Formation and the Langshan Formation [4, 5].

Masse and Gallo Maresca [3] first summarized the distribution of the mid-Cretaceous radiolitids from the Southwest Asian regions, which were assigned to *Auroradiolites* subsequently. Sano and Masse [6] described some *A. gilgitensis* specimens from late Early to Late Aptian shallow marine limestones in the Yezo Group, central Hokkaido. They revealed a faunal connection between the northwestern Pacific and Southwest Asia in the late Aptian. Rao et al. [4, 5] described the Late Aptian to Albian rudist fauna from the Sangzugang Formation and the Langshan Formation of the Lhasa block. They characterized the mid-Cretaceous SW

Asian-Pacific province on the basis of *Auroradiolites* and the accompanying polyconitid lineage, *Horiopleura haydeni*—*Praecaprotina*—*Magallanesia*.

5 Conclusion

Auroradiolites biconvexus [5], *Magallanesia rutogensis* [5], *Eoradiolites* cf. *hedini* and *Sellaea* sp were found from both the Langshan Formation and the Sangzugang Formation of the Lhasa Block, Tibet. The geological range of this rudist assemblage is Late Aptian to Albian. The mid-Cretaceous SW Asian-Pacific province was recognized based on the occurrence of endemic rudist taxa *Auroradiolites* and the accompanying polyconitid lineage, *Horiopleura haydeni*—*Praecaprotina*—*Magallanesia*.

References

- Gou, Z.H., Shi, H.: Rudists (Bivalvia) from the Cretaceous of Tibet, China, with descriptions of new species. In: Johnson, P.A., Haggart, J.W. (eds.). *Bivalves: An Eon of Evolution—Paleobiological Studies Honoring Norman D. Newell*. University of Calgary Press, Calgary, Canada, vol. 461, pp. 255–266 (1998)
- Leier, A.L., Decelles, P.G., Kapp, P., Gehrels, G.E.: Lower Cretaceous strata in the Lhasa Terrane, Tibet, with implications for understanding the early tectonic history of the Tibetan Plateau. *J. Sediment. Res.* **77**, 809–825 (2007)
- Masse, J.-P., Gallo Maresca, M.: Late Aptian radiolitidae (rudist bivalves) from the Mediterranean and Southwest Asiatic regions: taxonomic, biostratigraphic and palaeobiogeographic aspects. *Palaeogeogr. Palaeoclimatol. Palaeoecol.* **128**, 101–110 (1997)
- Rao, X., Skelton, P.W., Sano, S., Cai, H., Pan, Y., Sha, J.: Discovery of *Auroradiolites* (Bivalvia: Hippuritida) in the Sangzugang formation of the Xigaze Forearc Basin, Tibet and the Palaeogeographical distribution of the Genus. *Pap. Palaeontol.* **3** (2), 297–315 (2017)
- Rao, X., Skelton, P.W., Sha, J., Cai, H., Iba, Y.: Mid-Cretaceous rudists (Bivalvia: Hippuritida) from the Langshan formation, Lhasa block, Tibet. *Pap. Palaeontol.* **1**, 401–424 (2015)
- Sano, S., Masse, J.-P.: First record of a primitive radiolitid rudist from Japan. *Paleontological Res.* **17**, 317–324 (2013)
- Scott, R.W., Wan, X.Q., Sha, J.G., Wen, S.X.: Rudists of Tibet and the Tarim Basin, China: significance to Requeniidae phylogeny. *J. Paleontol.* **84**, 444–465 (2010)
- Skelton, P.W.: Rudist classification for the revised Bivalvia volumes of the 'Treatise on Invertebrate Paleontology'. *Caribb. J. Earth Sci.* **45**, 9–33 (2013)
- Yang, Z., Nie, Z., Wu, S., Liang, D.: Cretaceous rudists from Ngari, Xizang (Tibet), autonomous region, China and their geologic significance. *Acta Geol. Sin.* **56**, 293–301 (1982)
- Zhang, K.J.: Cretaceous palaeogeography of Tibet and adjacent areas (China): tectonic implications. *Cretac. Res.* **21**, 23–33 (2000)
- Zhang, Z.M., Dong, X., Santosh, M., Zhao, G.C.: Metamorphism and tectonic evolution of the Lhasaterrane, Cent. Tibet. *Gondwana Res.* **25**(1), 170–189 (2014)
- Zhu, D.C., Zhao, Z.D., Niu, Y.L., Dilek, Y., Hou, Z.Q., Mo, X.X.: The origin and pre-Cenozoic evolution of the Tibetan plateau. *Gondwana Res.* **23**, 1429–1454 (2013)

Tethyan Non-rudist Associations from the Cretaceous Rudist Formations in Northern Egypt

Yasser Salama and Gouda Abdel-Gawad

Abstract

The Cretaceous marine successions of North Egypt are rich in rudists and their associations. The Egyptian rudists are generally recorded from late Barremian to Turonian carbonate ramp sections in North Egypt. These sections are best exposed in Sinai with limited occurrence in north Eastern and Western Deserts. Approximately 65 rudist species were recorded during this interval. These rudists were reported in thirteen levels and eight sub-levels alternated or associated with fossiliferous horizons rich in algae, benthic foraminifera, ostracodes, coralline sponges, corals, bivalves, gastropods, ammonites, brachiopods, bryozoan and echinoids. The study is a focus on stratigraphic distribution, occurrences and paleoecology of algae, orbitolinid and alveolinid foraminifera, coralline sponges, corals, *Chondrodonta*, oysters, nerineids and actaeonellids. The majority of the non-rudist associations occur as banks or biostromes.

Keywords

Cretaceous • Egypt • Non-rudists • Stratigraphy
Paleoecology

1 Introduction

The Cretaceous rudists of Egypt has attracted attention of the paleontologists from [1, 2]; however, the accompanying fossils have not been adequately studied. Therefore, this study is concerned with the non-rudist associations from different locations in northern Egypt (Fig. 1). Detailed stratigraphic distribution, systematic description, facies and

sequence stratigraphy of these rudist-bearing rocks were recently presented in two publications [2, 3]. The recorded rudist levels and sub-levels are associated with non-rudist fossiliferous beds. The majority of these non-rudist groups were systematically studied by previous workers. This paper aims to highlight some stratigraphical and paleoecological significance of algae, orbitolinid and alveolinid foraminifera, coralline sponges, corals, *Chondrodonta*, oysters, nerineas and actaeonellids. The ammonites biozones determine the late Barremian to Turonian age of these rudists and their associations especially from Sinai outcrops.

2 Materials and Methods

The Rudists and non-rudist association are collected from sections related to Rizan Aneiza, Halal, Raha, Galala, Wata and Abu Roash formations exposed in north Egypt sections (Fig. 1). The study includes the fieldwork and sampling of the rudists and their associated fauna. All the fossil specimens are preserved in The Geology Department, Beni-Suef University

3 Results

Algae (Fig. 1): the identified Cretaceous calcareous algae are represented by red, udoteacean and dasycladacean algae. These algae include the following species *Montiella elitzae* (Bakalova), *Neomeris* sp., *Salpingoporella* sp., *Arabicodium* sp., *Bacinella irregularis* Radoičić, *Lithocodium aggregatum* Elliott, *Boueina hochstetteri* Toulou, *Halimeda* sp., *Sporolithon rude* (Lemoine), *Permocalculus* sp., *Marinella lugeoni* Pfender and *Solenopora* sp. The first record for a problematic *Porocystis globularis* (Giebel) characterized the upper Cenomanian deposits.

Orbitolinid and alveolinid foraminifera (Fig. 2): the significant associations of orbitolinid and alveolinid foraminifera include *Orbitolina* (*Conicorbitolina*) *conica*

Y. Salama · G. Abdel-Gawad (✉)
Faculty of Science, Geology Department, Beni-Suef University,
Bani Sweif, Egypt
e-mail: gabdelgawad@bsu.edu.eg

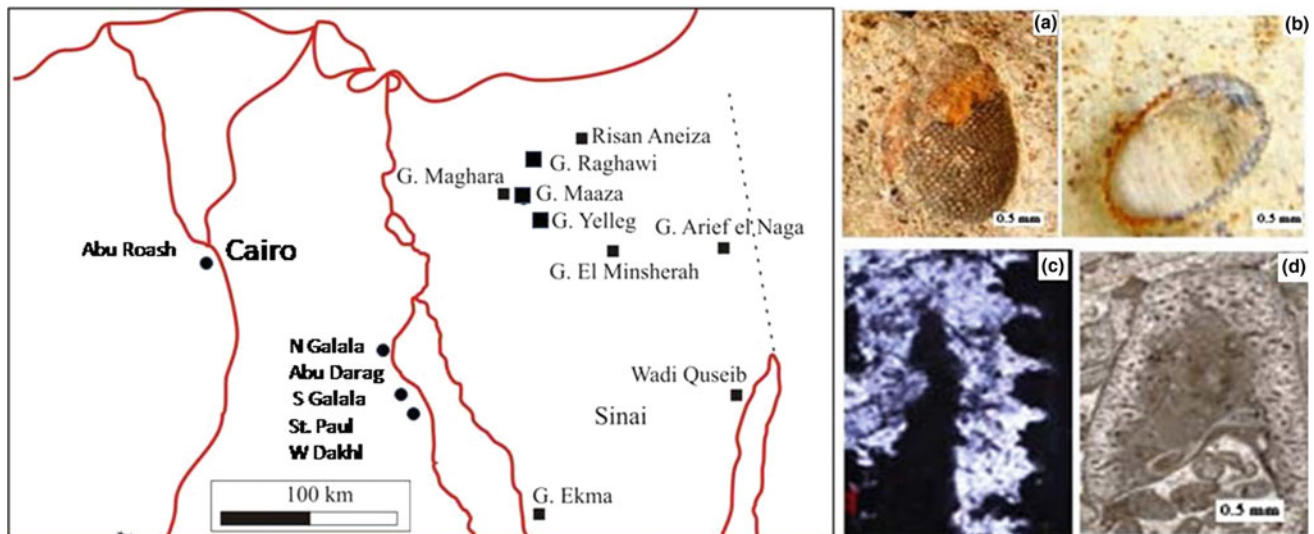


Fig. 1 Location map for some rudist-bearing sections in north Egypt at the left side. On the right **a–d** Calcareous algae, **a–c** Problematic *Porocystis globularis* (Giebel) Upper Cenomanian, El Hamra section Sinai; **d** *Boueina* sp. Albian, Raghawi section Sinai

(d'Archiac), *Orbitolina* (*Conicorbitolina*) *cuvillieri* (Moullade), *Orbitolina* (*Mesorbitolina*) *parva* Douglass, *Orbitolina* (*Mesorbitolina*) *subconcava* Leymerie, *Orbitolina* (*Mesorbitolina*) *texana* (Roemer), *Orbitolina* (*Orbitolina*) *birmanica* Sahni, *Orbitolina* *qatarica* Henson, *Palorbitolina* *lenticularis* (Blumenbach), *Praealveolina* *cretacea* Reichel, *Praealveolina* *tenuis* Reichel and *Praeretia* *cuvillieri* Deloffre and Hamaoui. **Coralline sponges and corals** (Fig. 2): the identified mid-Cretaceous coralline sponge species belong to *Millestroma*, *Steineria*, *Shuqraia* and *Actinostromarianina*. Colonial and solitary corals of variable morphotypes are abundant in the Aptian rocks of Gabal Abu Ruqum, north Sinai [4] with limited occurrence in the Cenomanian and Turonian rocks [5]. Corals belong to the genera *Parasmilia*, *Micrabacia*, *Montlivatia*, *Eugyra*, *Stylina*, *Thecosmilia*, *Thamnastrea*, *Fungiastrea*, *Leptoria*, *Actinastrea* and *Ellipsocoenia* are reported from Aptian-Albian of North Sinai. The Cenomanian and Turonian corals are represented by *Aspidiscus*, *Thecosmilia*, *Fungiastrea*, *Ellipsosmilia*, *Phylloconia*, *Neophyllia*, *Astraeofungia*, *Rennensismilia*, *Phyllocoenia* and *Polytremacis* [7]. **Nerineids and Actaeonellids** (Fig. 2): the recorded species are *Nerinella* *algarbiensis* Choffat, *Nerinea* *fleuriausa* d'Orbigny, *Nerinea* *cretacea* Conrad, *Nerinea* *gemmifera* Coquand, *Nerinea* *requieniana* d'Orbigny, *Neoptyxis* *olisiponensis* (Sharpe), *Actaeonella* *delgadoi* Choffat and *Trochactaeon* *salomonis* (Fraas). **Chondrodonta and oysters** (Fig. 2): non-rudist bivalves belong to the genera *Gervillaria*, *Certostereon*, *Neithea* and *Trigonia* that

dominated the Aptian-Albian rocks of north Sinai. Species related to *Ceratostreon*, *Chondrodonta*, *Costagyra*, *Ilymatogyra*, *Rastellum*, *Rhynchostreon* dominate the Cenomanian rocks.

4 Discussion

Paleoecologically, the non-rudist bivalvia such as *Chondrodonta* *joannae* (Choffat) formed a biostrome capping for the rudist horizon during the Cenomanian. The shells were accumulated parallelly to the bedding. Similar *Chondrodonta* beds are described from the Albian of N. America [6], Upper Cenomanian of Middle East and Italy [7, 8]. *Chondrodonta* shells were often uprooted from the substrate during storm episodes. This is indicated by their oriented shells parallel to the bedding and strongly packed bivalve shells. They were transported and reworked as channel lags [7]. However, the analysis of the xenomorphic area in the studied shells from SE Themed, East Sinai agree with the interpretation that concluded the growth of the *Chondrodonta* shells inclined to the substrate [8]. Stratigraphically, the orbitolinid foraminifers are distributed in the Aptian to Early Cenomanian marine deposits. The Late Aptian deposits are characterized by the first appearance of the radiolitic rudists and the genus *Mesorbitolina*. The occurrence of gastropod *Actaeonella* *delgadoi* Choffat designates the Middle Albian age. The first appearance of *Orbitolina* (*Conicorbitolina*) *conica* (d'Archiac) marked the



Fig. 2 Associated non-rudist fauna: **a** *Praealveolina* sp., Cenomanian, Minshera, Sinai; **b** *Mesorbitolina* sp., Albian, Raghawi, Sinai; **c** *Actinostromarianina*, Cenomanian, Abu Darag area; **d** *Millestroma nichlsoni* Gregory., Upper Turonian, Abu-Roash; **e** *Thecosmilia* cf. *tommassii* Prever; **f** *Aspidiscus cristatus*, Cenomanian, Themed, Sinai;

g *Phyllocoenia toucasi*, Upper Turonian, Abu Roash **h** “*Parasmilia*” sp., Cenomanian, Themed, Sinai; **i** *Trochactaeon salomonis*, Turonian, Abu Roash; **j** *Nerinea gemmifera*, Cenomanian, Minshera; **k** *Chondrodonta joannae*, Cenomanian, Themed

Albian-Cenomanian boundary in north Sinai. The ranges of *Praealveolina cretacea* Reichel and *Praealveolina tenuis* Reichel span the Middle to Late Cenomanian age [9]. Thus, the first occurrence of these benthic foraminifers in north Sinai successions indicates late Middle Cenomanian age. Here is a new observation showing that a focus is needed on the future studies on the revision of the earliest definitions that have question marks especially the algae group. “*Globulipora*” *africana* Peron, 1893 is identified as species belonged to a cyclostomate bryozoan, calcareous algae or calcisponges [10] from the Cenomanian deposits. The studied Upper Cenomanian materials (Fig. 1) agree well with the morphologic characters of *Porocystis globularis* (Giebel) that are identified as the reproductive body of a “seaweed” from the lower Cretaceous of Texas.

5 Conclusion

The studied non-rudist tethyan groups are associated with the Cretaceous rudist assemblages. This study highlighted the record of algae, orbitolinid and alveolinid foraminifera, coralline sponges, corals, *Chondrodonta*, oysters, nerineas and actaeonellids. The paleoecologic and the biostratigraphic significance of *Chondrodonta*, Orbitolinids and alveolinids are briefly discussed. The systematic position of a problematic “*Globulipora*” *Africana* Peron, 1893 is adopted as algae like *Porocystis globularis* (Giebel) from Lower Cretaceous of Texas. Finally, systematic update for corals, coralline sponges and nerineids for the Egyptian materials are recommended.

References

1. Douvillé, H.: Etudes sur les Rudistes. Rudistes de sicile, d Algerie, d Egypt, du Liban et de la perse. Mém. Soc. Geol. France **41**, 1–83 (1910)
2. Salama, Y., Grammer, M., Saber, S., El-Shazley, S., Abdel-Gawad, G.: Sequence stratigraphy and rudist facies development of the upper Barremian-lower Cenomanian platform, Northern Sinai. Egypt. Acta Geologica Sinica (English Edition) **92**, 286–310 (2018)
3. Salama, Y., Abdel-Gawad, G., Saber, S., El-Shazly, S., Grammer, M., Özer, S.: Chemostratigraphy of the Cenomanian-Turonian shallow-water carbonate: new correlation for the rudist levels from north Sinai. Egypt. Arab. J. Geosci. **9**(20), 755 (2016)
4. Gameil, M., Aly, M.F.: Aptian corals from gabal Abu Ruqum, North Sinai, Egypt: taxonomy and adaptive morphotypes. In: 7th International Conference on the Geology of the Arab World, pp. 265–284, Cairo (2004)
5. Abdel-Gawad, G.I., Gameil, M.: Cretaceous and Palaeocene coral faunas in Egypt and Greece. Coral Res. Bull. Dresd. **4**, 1–36 (1995)
6. Scott, R.W.: Models and stratigraphy of Mid-Cretaceous reef communities, Gulf of Mexico. SEPM, Concepts in Sedimentol. Paleontol. **2**, 102p. 51 figs, Tulsa (1990)
7. Dhondt, A.V., Dieni, I.: Rudist-associated Cretaceous bivalves. Saito Ho-on Kai Spec. Pub. **3**, 193–200 (1991) (Proceeding of Shallow Tethys 3, Sendai, 1990)
8. Hannaa, W., Fürsich, F.T.: Palaeoecology and environmental significance of benthic associations from the Cenomanian-Turonian of eastern Sinai. Egypt. Beringeria **42**, 93–138 (2012)
9. Calonge, A., Caus, E., Bernaus, J.M., Aguilar, M.: Praealveolina (Foraminifera) species: a tool to date Cenomanian platform sediments. Micropaleontology **48**, 53–66 (2002)
10. Abdel Gawad, G.I.: Some upper cretaceous coralline sponges from Egypt. Egypt. J. Paleont. **1**, 299–325 (2001)

New Biostratigraphic Scheme from the Cenomanian-Turonian of South Algeria

Madani Benyoucef, Djamila Zaoui, Mohammed Adaci, Mohamed Lassad Guendouz, Abdelkader Mennad, and Mustapha Bensalah

Abstract

The Cenomanian-Turonian rocks of South Algeria (Saharan Atlas and Sahara) are widely distributed, well exposed and display beds extremely rich in ammonites and other macrofossils as well as in microfauna and forming laterally traceable horizons. They are subdivided into four ammonite zones: *Neolobites vibrayeanus* Zone, *Nigericeras gadeni* Zone, *Vascoceras cauvini* Zone and *Pseudotissotia nigeriensis-Choffaticeras sinaiticum* Zone. The Cenomanian/Turonian boundary coincides with the base of the *Pseudotissotia nigeriensis-Choffaticeras sinaiticum* Zone. The lower-middle Cenomanian and middle-upper Turonian are barren of ammonites.

Keywords

Cenomanian-Turonian • Algeria • Saharan atlas Sahara • Ammonites • Biostratigraphy

1 Introduction

Due to its position during Late Cretaceous, Algeria was heavily influenced palaeogeographically the gradual constriction of Tethys to the north. Consequently, two different palaeogeographic domains were developed: a deep-marine basin named the Tellian trough in the north, and a carbonate platform in the south including the Saharan Atlas and the Saharan Platform. The Cenomanian–Turonian (C–T) outcrops of the south Algeria are widely distributed. They display beds extremely rich in ammonites, other macrofossils, and microfauna, forming laterally traceable horizons.

A biostratigraphic scheme is proposed to date this succession based on the vertical distribution of ammonites that are mainly preserved as internal moulds. The first occurrence (FO) and the last occurrence (LO) of the identified fossils were used to define the biostratigraphic zonal limits accurately.

2 Biostratigraphic Scheme

The biozones defined herein are an important and necessary step in establishing a standard zonation for the Algerian Cenomanian-Turonian succession and its inter-regional correlation. Based on both, the occurrence of the index species and the similarity in their characteristic assemblages, we propose a correlation between the south Algerian zonal scheme used in the present work (see below) and the standard ammonite zones in addition to those previously established by various authors for well-dated Cenomanian–Turonian sections in other key areas along the southern Tethysian margin. The description of the proposed biozones is given from base to top.

M. Benyoucef (✉)
Faculty of Natural and Life Sciences, University Mustapha
Stambouli of Mascara, 29000 Mascara, Algeria
e-mail: benyoucefmadad@gmail.com

D. Zaoui · M. Adaci · M. L. Guendouz · A. Mennad · M. Bensalah
Earth and Universe Sciences, Research Laboratory no 25,
Abou-Bekr Belkaid University, 13000 Tlemcen, Algeria
e-mail: zaouidjm@gmail.com

M. Adaci
e-mail: med.adaci@gmail.com

M. L. Guendouz
e-mail: med.lassad@yahoo.fr

A. Mennad
e-mail: abdelkademennad@gmail.com

M. Bensalah
e-mail: mus.bensalah@yahoo.fr

2.1 Zone C1—*Neolobites vibrayeanus* Total-Range Zone

The C1 zone represents the total range of the zonal species *Neolobites vibrayeanus* (d'Orbigny). It represents the oldest identified ammonite zones and the most fossiliferous interval recorded in south Algeria. It characterizes the early late Cenomanian. The C1 zone, as defined herein, is equivalent to the *N. vibrayeanus* Zone recognized in North Africa, Middle East, Niger and Spain. In addition, this zone corresponds to the European *Calycoceras* (*Proeucalycoceras*) *guerangeri* Zone.

2.2 Zone C2—*Nigericeras gadeni* Interval Zone

This zone includes the acme of the nominate species. The zone's base is coincident with the first occurrence (FO) of *Nigericeras gadeni*. The zone's top is defined by the FO of *Vascoceras* aff. *glabrum* (Barrér). Associated ammonoid fauna include *Metengonoceras dumbli* (Cragin). The *Nigericeras gadeni* Zone defined herein can be correlated with the upper part of the *Metoicoceras geslinianum* Zone (= *Burroceras clydense* Subzone) defined in Egypt, Tunisia and NW-Europe [7].

2.3 Zone C3—*Vascoceras cauvini* Interval Zone

The lower boundary of the zone is defined by the LO of *Nigericeras gadeni* (Chudeau) and the upper boundary is coincident with the LO of *Vascoceras* aff. *glabrum*. It rests on the *Nigericeras gadeni* Zone and is followed, directly and unconformably, by the *Pseudotissotia nigeriensis-Choffaticeras sinaiticum* Zone which is considered as the first lower Turonian zone in the studied area. The C3 zone is rich in ammonites and yields *Vascoceras* aff. *glabrum* (Barber), *Fikaites subtuberculatus* (Collignon), *Fikaites laffitei* (Collignon), *Pseudaspidoceras pseudonodosoides* (Choffat), *Pseudaspidoceras grecoi* (Collignon), *Rubroceras burroense* Cobban, Hook and Kennedy, *Vascoceras gamai* (Choffat) and *Vascoceras cauvini* (Chudeau). The *Vascoceras cauvini* Zone is now considered as one of the uppermost Cenomanian zones in the Tethysian realm. It is also equivalent to the standard *Neocardioceras juddii* Zone of the Boreal realm and of the *Buttoceras clydense*, *Neocardioceras juddii* and *Nigericoceras scotti* zones of USA [4].

2.4 Zone T1—*Pseudotissotia nigeriensis-Choffaticeras sinaiticum* Interval Zone

The lower boundary of the zone is coincident with the FO of *Pseudotissotia nigeriensis* (Woods), its upper boundary is

defined by the LO of the *Choffaticeras sinaiticum* (Douvillé). It is placed above the uppermost Cenomanian *Vascoceras cauvini* Zone and below an interval barren of ammonites. Rich ammonite assemblages are found in this zone: *Fagesia peroni* Pervinquier, *Pseudotissotia nigeriensis* (Woods), *Choffaticeras parvielleri* (Pervinquier), *Choffaticeras Meslei* (Péron), *Choffaticeras sinaiticum* (Douvillé), *Choffaticeras* sp., *Eotissotia simplex* (Barber), *Hoplitoides wohltmanni* (von Koenen) and *Kamerunoceras turoniense* (d'Orbigny). The lower Turonian indicative *Choffaticeras* and other ammonite species are recognized in North Africa, West Africa, France, the Middle East, and Madagascar. The *Choffaticeras* interval of south Algeria is correlative to the *Choffaticeras segne* Zone of Egypt [1] and Jordan [2]. It corresponds to the *Choffaticeras* interval of Robaszynskiet al. [10] defined in Tunisia, to the *Pseudotissotia nigeriensis* Zone of Niger and Nigeria [9]. The *Pseudotissotia nigeriensis-Choffaticeras sinaiticum* Zone is equivalent to the *Vascoceras* (*Greenhornoceras*) *birchbyi* subzone of the *Watinoceras coloradoense* Zone in the standard ammonite Zones.

3 Cenomanian–Turonian Boundary

Hancock [7] suggested that the base of the Turonian should be chosen at the bottom of the *Pseudaspidoceras flexuosum* ammonite Zone. In the Tethysian realm, [6] defined the base of the Turonian on the base of the *Watinoceras coloradoense* ammonite assemblage Zone which is placed above the *Pseudaspidoceras flexuosum* Zone in the Western Interior Basin, United States. In this later, the C/T boundary is defined at the base of Bed 86 in the Rock Canyon Anticline which in this section coincides with the FO of *Watinoceras devonense*. Unfortunately, *Watinoceras devonense* has not been found, to date, in south Algeria as like for most Cenomanian-Turonian sections in other countries; e.g., the Westphalia sections in north-west Germany [8]. In the south Algeria, the first appearance of the mid-lower Turonian ammonites (*Pseudotissotia nigeriensis-Choffaticeras sinaiticum* Zone) immediately above the uppermost Cenomanian deposits (*Vascoceras cauvini* Zone) is viewed as a good indicator of a stratigraphic gap between the Cenomanian and Turonian deposits. The lowermost Turonian ammonite zone that is missing in the south Algeria is the equivalent of the lower and the middle parts of the standard *Watinoceras coloradoense* ammonite zone.

The mid-lower Turonian *Pseudotissotia nigeriensis-Choffaticeras sinaiticum* Zone is very rich in pelagic fauna (ammonites, planktonic foraminifers and roveacrinoids). It thus characterizes an overlapping accumulation episode that was apparently related to a submarine non-deposition during an early Turonian maximum flooding event (e.g., maximum

flooding K140 of Sharland et al. [11] on the Arabian Plate). As observed in the Sahara Platform, a sharp discontinuity surface marked by ferruginous hard-ground containing ammonites, oysters and burrows documents a hiatus between the extinction of Cenomanian ammonites and the appearance of early Turonian ammonites [14]. Such a hiatus of this magnitude was also reported in the Saharan Atlas [5], in Sinai in Egypt [3], in northern Peru, in the eastern part of the Central Andean Basin of Bolivia and in the Sergipe Basin in Brazil [12]. Stratigraphic gaps around the Cenomanian-Turonian boundary are also well-known from some Cretaceous basins in Europe [13].

References

1. Abdel-Gawad, G.I., El Qot, G.M., Mekawy, M.S.: Macrobiostratigraphy of the upper Cretaceous succession from southern Galala, eastern desert, Egypt. In: 2nd International Conference on the Geology of the Tethys, vol. 2., pp. 329–349, Cairo University (2007)
2. Aly, M.F., Smadi, A., Abu Azzam, H.: Upper Cenomanian-Lower Turonian ammonites of Jordan. *Rev. Paléobiol.* **27**(1), 43–71 (2008)
3. Bauer, J., Kuss, J., Steuber, T.: Sequence architecture and carbonate platform configuration (Late Cenomanian–Santonian), Sinai Egypt. *Sedimentol.* **50**, 387–414 (2003)
4. Bengtson, P.: The Turonian stage and substage boundaries. *Bulletin de l'Institut Royal des Sciences Naturelles de Belgique. Sci. Terre* **66** (supp), 69–79 (1996)
5. Benyoucef, M., Mebarki, K., Ferré, B., Adaci, M., Bulot, L.G., Desmares, D., Villier, L., Bensalah, M., Frau, C., Ifrim, C., Malti, F.-Z.: Litho- and biostratigraphy, facies patterns and depositional sequences of the Cenomanian-Turonian deposits in the Ksour mountains (Saharan Atlas, Algeria). *Cretac. Res.* **78**, 34–55 (2017)
6. Birkelund, T., Hancock, J.M., Hart, M.B., Rawson, P.F., Remane, J., Robaszynski, F., Schmid, F., Surlyk, F.: Cretaceous stage boundaries—proposals. *Bull. Geol. Soc. Den.* **33**, 3–20 (1984)
7. Hancock, J.M.: Ammonite scales for the Cretaceous system. *Cretac. Res.* **12**, 259–291 (1991)
8. Lehmann, J.: Integrated stratigraphy and palaeo environment of the Cenomanian-Lower Turonian (Upper Cretaceous) of Northern Westphalia North Germany. *Facies* **40**, 25–70 (1999)
9. Meister, C., Alzouma, K., Lang, J., Mathey, B.: Les ammonites du Niger (Afrique occidentale) et la transgression transsaharienne au cours du Cénomanién-Turonien. *Geobios* **25**, 55–100 (1992)
10. Robaszynski, F., Caron, M., Dupuis, C., Amédéo, F., González Donoso, J.-M., Linares, D., Hardenbol, J., Gartner, S., Calandra, F., Deloffre, R.: A tentative integrated stratigraphy in the Turonian of central Tunisia: formations, zones and sequential stratigraphy in the Kalaat Senan area. *Bull. Cent. Rech. Explor. Prod. Elf-Aquitaine* **14**, 213–384 (1990)
11. Sharland, P.R., Archer, R., Casey, D.M., Davies, R.B., Hall, S.H., Heward, A.P., Horbury, A.D., Simmons, M.D.: Arabian plate sequence stratigraphy. *GeoArabia Journal Special Publication 2*, Gulf Petro Link, Bahrain, p. 371 (2001)
12. Walter, S., Herrmann, A.D., Bengtson, P.: Stratigraphy and facies analysis of the Cenomanian–Turonian boundary succession in the Japarutuba area, Sergipe Basin, Brazil. In: P. Bengtson (ed.): *Mesozoic palaeontology and stratigraphy of South America and the South Atlantic, Part II*, *Journal of South American Earth Sciences* **19**(3), 273–283 (2005)
13. Wilmsen, M.: Late Cretaceous nautilids from northern Cantabria, Spain. *Acta Geol. Pol.* **50**(1), 29–43 (2000)
14. Zaoui, D., Tchenar, S., Benyoucef, M., Meister, C., Adaci, M., Piuz, A., Mebarki, K., Bensalah, M., Gabani, A., Mahboubi, M.: Le Cénomano-Turonien dans la Hamada du Tinrhert (Sahara, Algérie): résultats préliminaires. *Rev. Paléobiol.* **35**(2), 541–559 (2016)

Ostracods of the Cenomanian-Turonian Transition (*Whiteinella archaeocretacea* Zone) in the Ksour and Amour Mountains (Saharan Atlas, Algeria): Paleobiogeographic Implication

Mustapha Benadla, Abbas Marok, and Matías Reolid

Abstract

The ostracods study of the Cenomanian-Turonian transition in the Ksour and Amour Mountains (Saharan Atlas, Algeria) enables us to identify two faunal assemblages characterizing the *Whiteinella archaeocretacea* Zone. These assemblages of 9 genera were compared with those often basins which belonging to different paleobiogeographic provinces in order to look for possible similarity between basins. The obtained results show an isolation of the Ksour and Amour Mountains compared to the considered basins.

Keywords

Ostracods • Cenomanian-Turonian • Ksour and amour Mountains • Saharan atlas • Algeria • Paleobiogeography

1 Introduction

Through the ostracods study of the Cenomanian-Turonian transition in the Ksour and Amour Mountains (Saharan Atlas, Algeria), an attempt is made, for the first time, to characterize the *Whiteinella archaeocretacea* Zone and to look for the probable presence of exchanges and migrations between the study basins and certain basins of the North African and Southern European margins. In this study, concerning biogeographic quantification, the analytical method was based on the qualitative data being processed by the software BG-Index ver. 1.1 β [8].

M. Benadla (✉) · A. Marok
Department of Earth and Univers Sciences,
University of Tlemcen, P.O. Box 119 Tlemcen, Algeria
e-mail: benadla_mustapha@yahoo.fr

M. Reolid
Departamento de Geología, Universidad de Jaén,
Campus Las Lagunillas S/N, 23071 Jaén, Spain

2 Materials and Methods

The chronological interval study consists essentially of limestone layers and some marly interlayers. Twenty (20) samples of marl (500 g per sample) were washed, sieved (250, 125 and 63 μm) and sorted. Ostracods determination was based mainly on Bassoullet and Damotte [5] and Andreu et al. [3] works. Biogeographic data processing was performed by the BG-Index versoftware. 1.1 β [8].

3 Results and Discussion

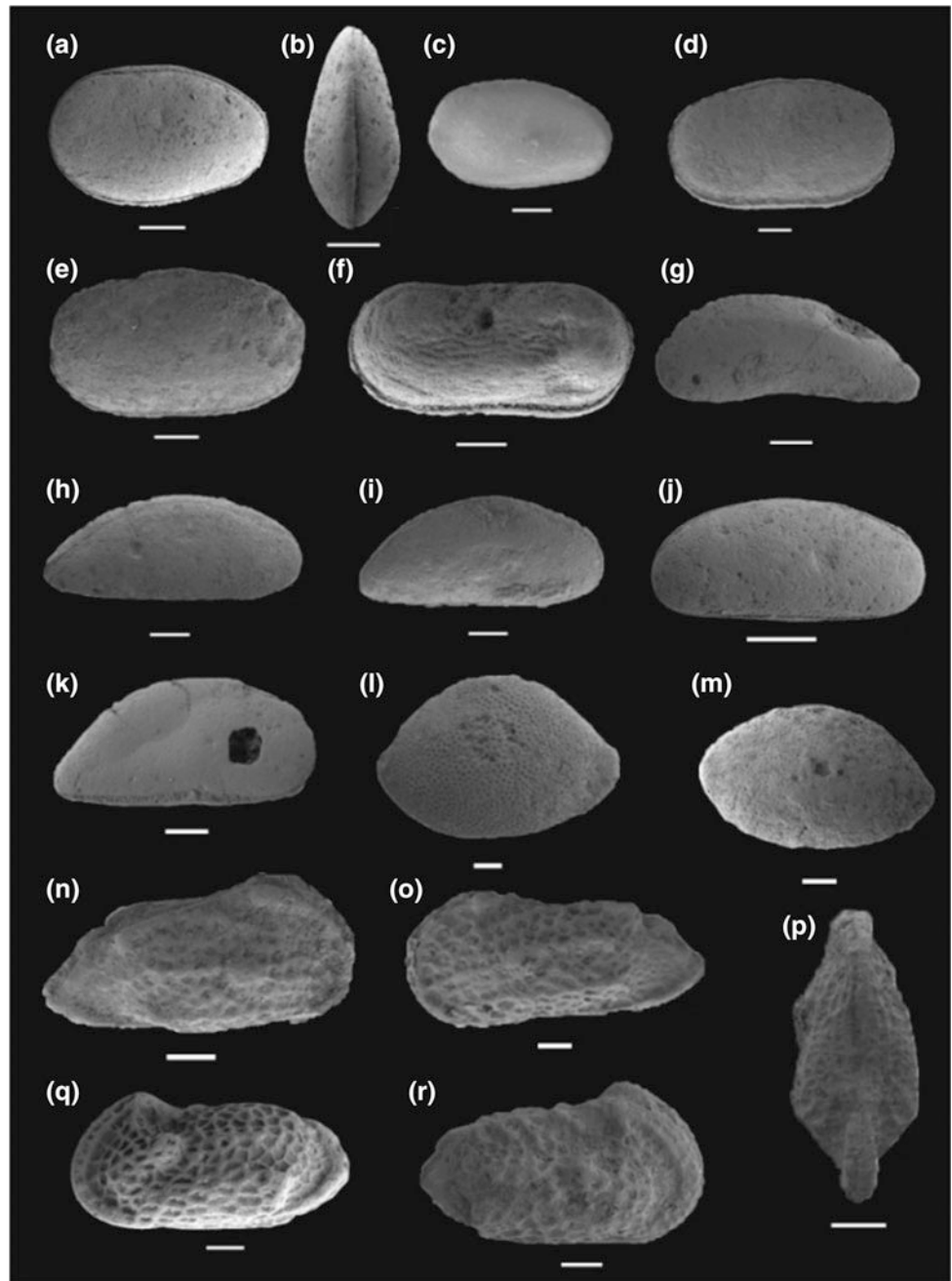
The ostracofauna of the upper Cenomanian-lower Turonian in the Ksour and Amour Mountains has been studied and figured out by Bassoullet and Damotte [5] and Benadla (works in progress). Several species determined for the first time remain endemic.

3.1 Ostracod Distribution in the Study Basins

From a biostratigraphic point of view, two assemblages of ostracods could be found in the *Whiteinella archaeocretacea* Zone.

- the first, rich and diverse group, consists of *Cytherella* gr. *ovate* (Roemer) (Fig. 1a, b), *Cytherella* gr. *parallela* (Reuss), *Cytherella gigantosulcata* (Rosenfeld) (Fig. 1c), *Cytherella* sp.1 (Fig. 1d, e), *Cytherelloidea* sp. (Fig. 1f), *Paracypris dubertreti* (Damotte & Saint-Marc) (Fig. 1g), *Paracypris mdaourensis* (Bassoullet & Damotte) (Fig. 1h, i), *Bythocypris* sp. (Fig. 1j), *Macrocypris* sp. (Fig. 1k), *Bairdia* sp.1 (Fig. 1l), *Bairdia* sp.2 (Fig. 1m), *Cythereis ziregensis* (Bassoullet & Damotte), *Cythereis mdaourensis* (Bassoullet & Damotte) (Fig. 1n, p), *Cythereis* sp.1 (Fig. 1q), *Cythereis* sp.2 (Fig. 1r). This species assemblage indicates an upper Cenomanian age. At the North

Fig. 1 Ostracods from Ksour and Amour basins. **a**, **b** *Cytherella* gr. *ovate* (Roemer); **c** *Cytherella gigantosulcata* (Rosenfeld); **d**, **e** *Cytherella* sp. 1.; **f** *Cytherelloidea* sp.; **g** *Paracypris dubertreti* (Damotte & Saint-Marc); **h**, **i** *Paracypris mdaourensis* (Bassoullet & Damotte); **j** *Bythocypris* sp.; **k** *Macrocypris* sp.; **l** *Bairdia* sp. 1; **m** *Bairdia* sp. 2; **n**, **p** *Cythereis mdaourensis* (Bassoullet & Damotte); **q** *Cythereis* sp.1; **r** *Cythereis* sp. 2. Scale bars = 100 μ m



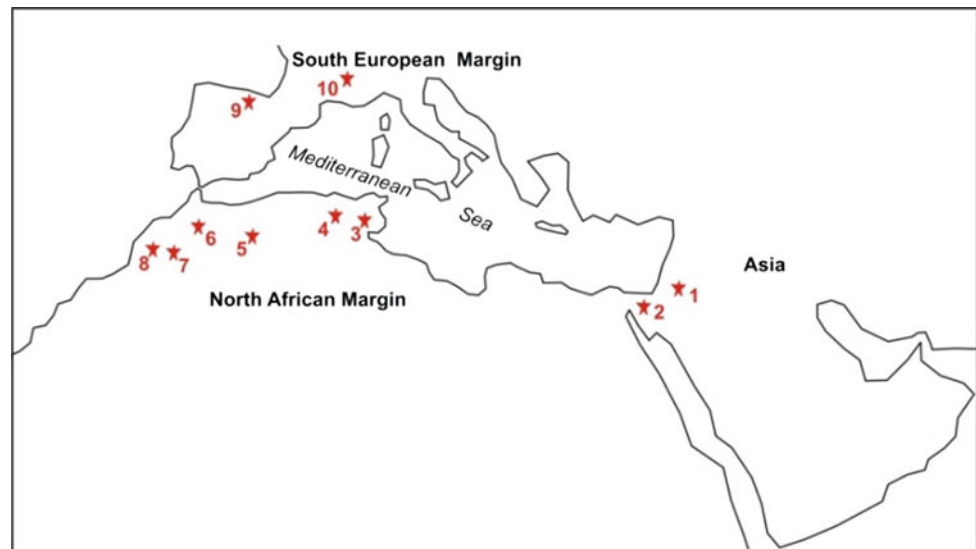
Africa scale, this recognized association in the Western Saharan Atlas corresponds to *Cythereis algeriana* Zone defined in Tunisia [6] and in Egypt [11].

- The second group, which is very rich but not very diverse, consists of *Cytherella* sp. 2, *Cythereis magnei*, *Cytherelloidea* sp. This association indicates a lower Turonian age and corresponds to *Cythereis mdaourensis* Zone [6].

3.2 Qualitative Comparison of the Taxonomic Composition Between Basins

Here, the ostracods similarity are analyzed by comparing ten basins belonging to different palaeobiogeographic provinces (Fig. 2): Central Jordan [12], Sinai basin [7, 15], Central Tunisia [14], Tébessa Basin [13], Ksour and Amour

Fig. 2 Geographic location of the analysed areas. 1: Central Jordan, 2: Sinai basin (Egypt), 3: Central Tunisia, 4: Tébessa Basin, 5: Ksour and Amour Mountains (Algeria), 6: Middle Atlas, 7: Central High Atlas, 8: Preafrican basin (Morocco), 9: Northern Spain, 10: SE France



Mountains (study basin), Middle Atlas [1, 10], Central High Atlas [1], Preafrican basin [9], Northern Spain [4] and SE France [2]. In this biogeographic quantification analysis, only the generic contents was used. These contents will be written in a binary matrix (Presence/Absence). The obtained results have allowed us to see a rapprochement between the Southern European basins. For the other basins, remoteness and isolation are probably dictated by physiography.

4 Conclusion

The taxonomic data submitted to the BG-Index ver. 1.1 β [8] shows no biogeographic gradient between the northern margin basins of Africa. The general topology during the *Whiteinella archaeocretacea* Zone is marked by the binary similarity between Egyptian and Jordanian basins where the similarity index is high with reference to exchanges and migrations.

References

- Andreu, B.: Cretaceous ostracode biochronology of Morocco. *Eclogae Geol. Helv.* **95**, 133–152 (2002)
- Andreu, B., Bilotte, M.: Ostracodes du Cenomanien supérieur et du Turonien de la zone sous-pyrénéenne orientale (Corbières méridionales, SE France). *Systématique, biostratigraphie, paléoécologie et paléobiogéographie. Rev. Micropaléontologie* **49**, 55–73 (2006)
- Andreu, B., Lebedel, V., Wallez, M.J., Lézin, C., Ettachfni El M.: The upper Cenomanian lower Turonian carbonate platform of the Preafrican Trough, Morocco: Biostratigraphic, paleoecological and paleobiogeographical distribution of ostracods. *Cretac. Res.* **45**, 216–246 (2013)
- Barroso-Barcenilla, F., Pascual, A., Peyrot, D., Rodriguez-Lazaro, J.: Integrated biostratigraphy and chemostratigraphy of the upper Cenomanian and lower Turonian succession in Puentevedy, Iberian Trough Spain. *Proc. Geologists' Assoc.* **122**, 67–81 (2011)
- Bassoullet, J.P., Damotte, R.: Quelques ostracodes nouveaux du Cénomano-Turonien de l'Atlas Saharien occidental (Algérie). *Rev. Micropaléontologie* **12**(3), 130–144 (1969)
- Bismuth, H., Boltenhagen, C., Donze, P., Le Fevre, Saint-Marc, J. P.: Le Crétacé moyen et supérieur du Djebel Semmama (Tunisie du Centre-Nord): Microstratigraphie et évolution sédimentologique. *Bull. Cent. Rech. Explor.-Prod. Elf-Aquitaine* **5**, 193–267 (1981)
- El-Nady, H., Abu-Zied, R., Ayyad, S.: Cenomanian-Maastrichtian ostracods from Gabal Arif El-Naga anticline, Eastern Sinai Egypt. *Rev. Paléobiologie* **27**(2), 533–573 (2008)
- Escarguel, G.: BG. Index version 1.1 β . Programme et notice d'utilisation (2001)
- El Ettachfni, M., Andreu, B.: Le Cénomanién et le Turonien de la Plate-forme Préafricaine du Maroc. *Cretac. Res.* **25**, 277–302 (2004)
- El Ettachfni, M., Souhel, A., Andreu, B., Caron, M.: La limite Cénomanién—Tutroniéndans le Haut Atlas central. *Maroc. Geobios* **38**, 57–68 (2005)
- Ismail, A.A.: Correlation of Cenomanian-Turonian ostracods of Gebel Shabraweet with their counterpart in Egypt, North Africa and the Middle East. *Neues Jahrbuch, Geologische und Paläontologische-Monatshefte* **9**, 513–533 (2001)
- Morsi, A.M., Wendler, J.E.: Biostratigraphy, palaeoecology and palaeogeography of the middle Cenomanian-early Turonian levant platform in central Jordan based on ostracods. *Geol. Soc. Spec. Publ.* **341**, 187–201 (2010)
- Ruault-Djerrab, M., Ferré, B., Kechid-Benkherouf, F., Djerrab, A.: Etude micropaléontologique du Cénomano-Turonien dans la région de Tébessa (NE Algérie): implications paléoenvironnementales et recherche de l'empreinte de l'OAE2. *Revue de Paléobiologie* **31**(1), 127–144 (2012)
- Salmouna, D.J., Chaabani, F., Dhari, F., Mzoughi, M., Salmouna, A., Zijlstra, H.B.: Lithostratigraphy analysis of the Turonian-Coniacian Bireno and Douleb carbonate members in Jebels Berda and Chemsî, Gafsa basin, central-southern Atlas of Tunisia. *J. Afr. Earth Sci.* **100**, 733–754 (2010)
- Shahin, A., Elbaz, S.: Cenomanian-Early Turonian of the shallow marine carbonate platform sequence at west central Sinai: Biostratigraphy, paleobathymetry and paleobiogeography. *Revue micropaléontologie* **56**, 103–126 (2013)

Cenomanian Foraminiferal Biostratigraphy of the Aures Basin (Northeastern Algeria)

Aida Bensekhria, Ramdane Marmi, and Abdelouahab Yahiaoui

Abstract

The lower-upper Cenomanian boundaries interval of Nouader site in the Aures Basin has been undertaken for the first time by using foraminifera. Lithologically, the study section is divided into two formations (Fahdene and Bahloul respectively) and one member (Annaba). Biostratigraphically, five foraminifera Biozones were identified and calibrated: (1) IZ of *Thalmaninella brotzeni* (Sigal 1948) Biozone, (2) IZ of *Thalmaninella reicheli* (Mornod 1950) Biozone; (3) TRZ of *Rotalipora cushmani* (Morrow 1934) Biozone, (4) PRZ of *Whiteinella archaeocretacea* (Passagno 1967) Biozone; and (5) TRZ of *Helvetoglobotruncana helvetica* (Boli 1945) Biozone. The sequence of the index species occurs in the same order in both Tethyan (Northeastern Algeria and Central Tunisia) and indeed elsewhere in the Boreal-realms. It indicates that they are robust assemblage zones and subzones that can be recognized on both the north and south sides of the Tethys.

Keywords

Cenomanian • Aures basin • Foraminifera
Biostratigraphy • Algeria

1 Introduction

Within the Aures basin, a thick marly sedimentation was developed in the center and reduced carbonated at the SW end Laffite [13]. The basin corresponds to a subsiding basin

A. Bensekhria (✉) · A. Yahiaoui
State Key Laboratory of Natural Hazards and Regional Planning,
Institute of Earth Sciences and Universe, University of Batna 2,
Batna, Algeria
e-mail: a.bensekhria@univ-batna2.dz; ; m_bouhata12@yahoo.fr

A. Bensekhria · R. Marmi
State Key Laboratory of Geology and Environment, University of
Mentouri Brothers, Constantine 1, Constantine, Algeria

according to Guiraud [15] which is a characteristic of a poorly oxygenated environment (anoxic even). On one part, it is favorable to the preservation of organic matter. On the other part, the Cenomanian exists in all great anticlines of this massif. It is characterized by a powerful marly series which has not been revised since the works of Laffite [13]. Moreover, it has not been studied in details yet. The boundaries of the Cenomanian substages have not been formally defined. Consequently, they cannot be determined. The finding G will then be compared with those obtained in neighboring regions (Central Tunisia and NW of Europe).

2 Geographical and Geological Settings

The Auresian realm represents the eastern part of the Atlas Basin which extends into Tunisia as the Tunisian Atlas [8, 11] (Fig. 1). The Aures Basin is characterized by a system of tilted blocks bounded by NW-SE to WNW-ESE trending faults. Otherwise, NE-SW faults located within the basin are characterized by transtensional movements [9, 12, 13, 15]. The studied deposits are only of sedimentary nature, dating middle Cretaceous (Cenomanian) and are generally very thick. This fact can be explained by the significant transgression that affected the region during the Cenomanian (details on regional geology are provided, for example: by [1, 2, 4, 5, 7–10, 12, 13, 15])

3 Methodology

A regular sampling step was conducted from 5 to 10 m. 20 thin sections in all were made in limestone levels for microfacies study. The soft levels (marls) were taken for a standard washing with hydrogen peroxide (soaking) and screened through two sieves of different mesh. They are respectively of 2 mm and 63 μ . Planktonic and benthic foraminifera have been systematically isolated and determined. The used biozonations are those of Caron [6, 14] and more recently of Amédéo and Robaszynski [3]. The species

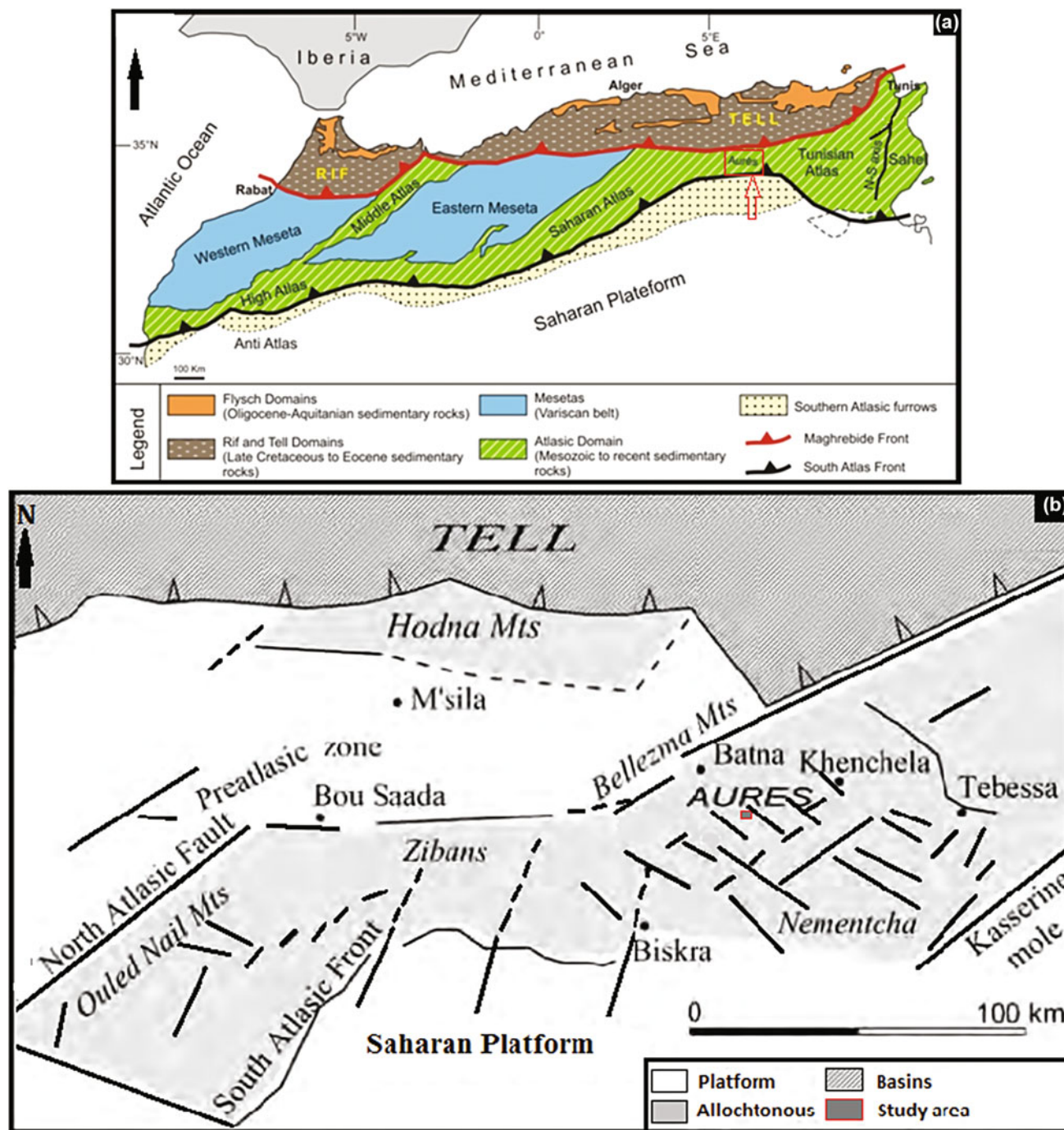


Fig. 1 a Geological sketch of the Maghreb. b Paleogeographic map of oriental atlassic domain and location of the study area (Herkat and Guiraud 2006)

are named in accordance with the enacted rules in the International Code of Zoological Nomenclature (CINZ).

4 Results and Discussion

Five biozones of lower Cenomanian-lower Turonian have been identified (Fig. 2).

- *IZ of Thalmanninella brotzeni Biozone*: (= *globotruncanoides*) sensu Robaszynski and Caron in 1995 dating from lower Cenomanian to lower middle Cenomanian and containing: *H. planispira* (Tappan 1940), *H. delrioensis* (Carsey 1926), *H. simplex* (Morrow 1934), *Heterohelix* sp., *Guembelitrasi* sp., *Globigerinelloides* sp., *Praeglobotruncanadelrioensis* (Plummer 1931), *Th. Montsalvensis* (Mornod 1949), *Th. Appenninica* (Renz

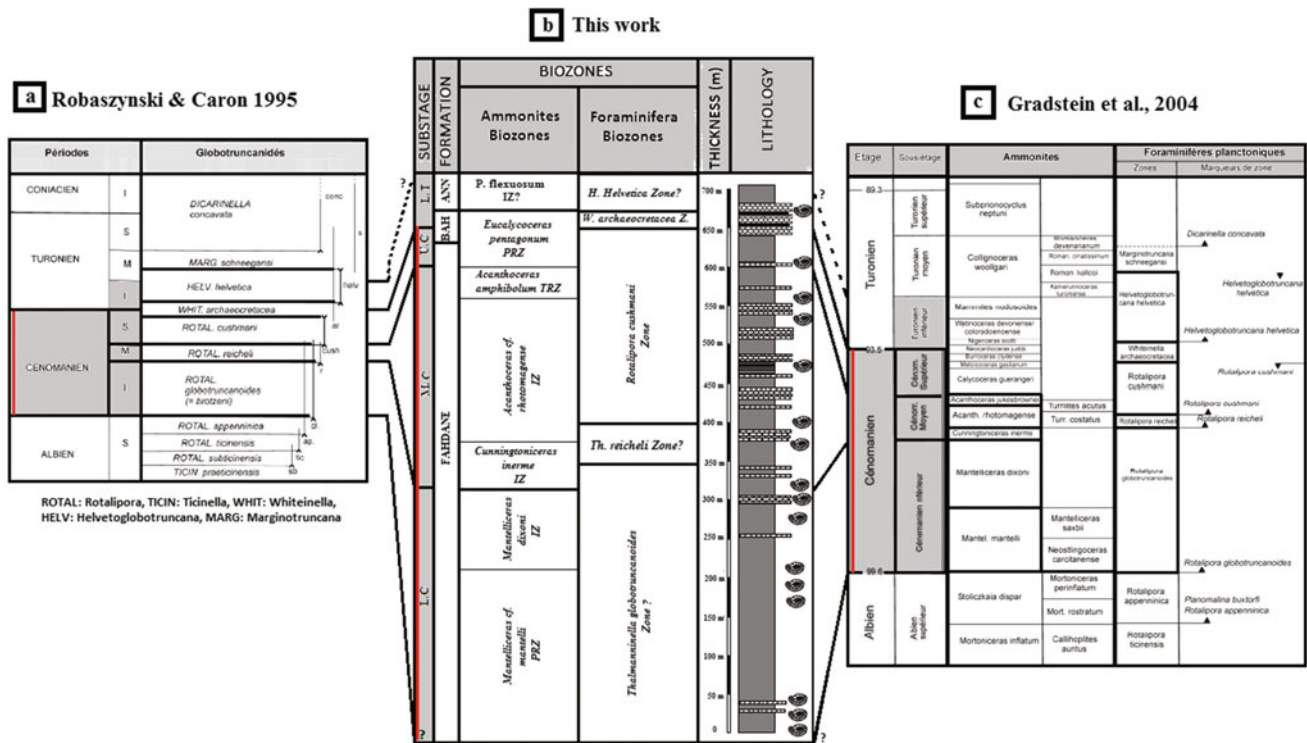


Fig. 2 Calibration of Cenomanian limits and Biozones of Nouader site a Middle cretaceous biozones by planktonic foraminifera (Robaszynski and Caron 1995); b Ammonites and planktonic foraminiferal biozones (this work); c Middle Cretaceous Biozones by Ammonites and planktonic Foraminifera [20]. Sub-stages: L.C: lower Cenomanian,

M.C: middle Cenomanian, U.C: upper Cenomanian, L.T: Lower Turonian. Formation: BAH: Bahloul, Member: ANN: Annaba. Concerned Biozones are highlighted in black. Red line highlights the Cenomanian stage

1936), *Th. Balernaensis* (Gondolfi 1957), *Th. Brotzeni* (Sigal 1948) and *P. stephani* (Gondolfi 1942).

- IZ of *Thalmanninella reicheli* Biozone (middle Cenomanian): the first occurrence of *Tahlmanninella reicheli* (Fig. 3b) was at sample number 77' associated with: *Praeglobotruncana delrioensis*, *Th. montsalvensis*, *H. simplex*, *Praeglobotruncanastephani*, *Heterohelix mormani* (Cushman 1938), *Hedbergellaplnispira*, *Th. appenninica*, *Th. globotruncanoides*, and *Hedbergella delrioensis*. The last occurrence falls in Sample 87.
- TRZ of *Rotalipora cushmani* Biozone (middle to upper Cenomanian): This biozone is defined by the appearance of the index species (Fig. 3d) after the last occurrence of the species: *Th. appenninica* and *Th. brotzeni*, accompanied by that of the first *whiteinella* (*Whiteinella baltica* (Douglas et Rankin, 1969), then *W. brittonensis* (Loeblich et Tappan 1961) and *W. paradubia* (Sigal 1952)) and a little higher up by that of *P. gibba* (Klaus 1960).

These few species come to diversify the previous assembly. Some forms have disappeared (*Th. appenninica*, *Th. montsalvensis*, *Th. brotzeni*).

- PRZ of *Whiteinella rhaeocretacea* Biozone (upper Cenomanian to lower Turonian): it is characterized by the presence of many species of the genus *Whiteinella* including *W. rhaeocretacea* and *W. paradubia*. The carinated forms are absent. Previous species persist with the exception of *P. delrioensis*. There are also *P. gibba* and *H. globulosa* (Ehrenberg 1840). *Whiteinella rhaeocretacea* Biozone was known in numerous pre-Atlantic basins [16–19]. It coincides with anoxic period materialized by rich organic carbon sediments.
- TRZ of *Helvetoglobotruncana helvetica* Biozone (lower Turonian): its first appearance is observed in thin section of 117 sample associated with *Hedbergella sp.*, *Heterohelix sp.*, *Heterohelix globulosa*, *Globigerinelloides sp.*, *Whiteinella sp.*, *Whiteinella baltica*, *Lunatriella sp.*, and *W. praelhelvetica* (Trujillo 1960).

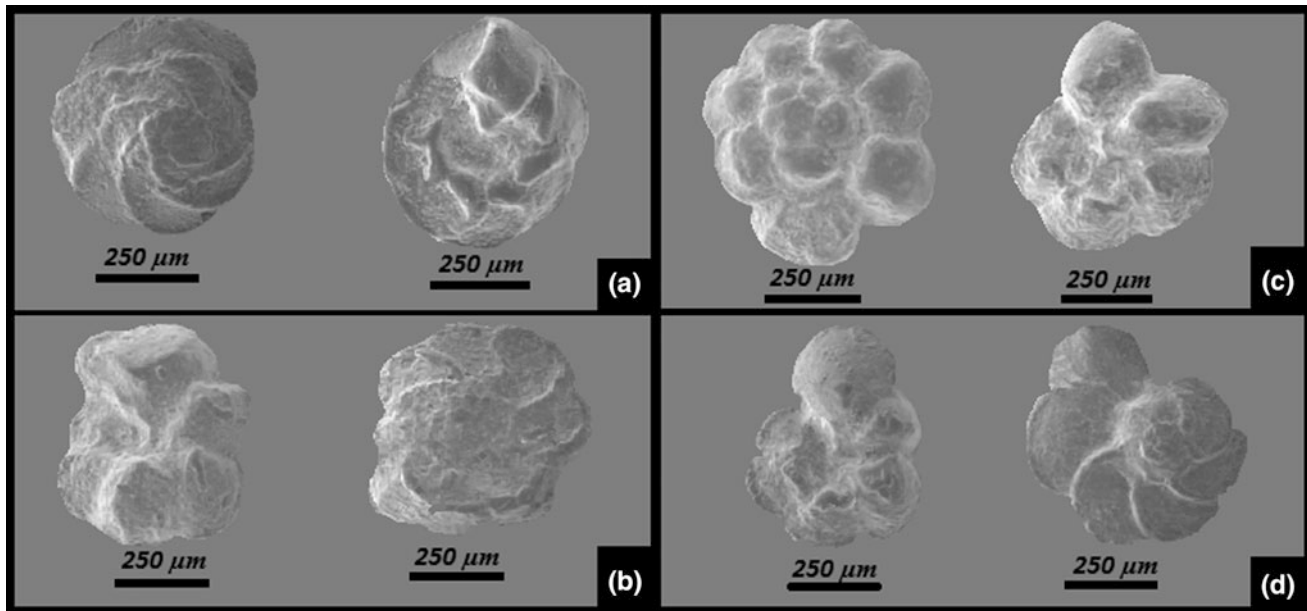


Fig. 3 Some index foraminiferaphotoes. **a** *Thalmanninella greenhornensis* is taken from sample 106; **b** *Thalmanninella reicheli* from sample 83; **c** *Rotalipora montsalvensis* found in sample 75; **d** *Rotalipora cushmani* first occurrence in sample 88

5 Conclusion

- Five foraminifera biozones were identified: (1) *Thalmanninella brotzeni* Biozone, (2) *Thalmanninella reicheli* Biozone; (3) *Rotalipora cushmani* Biozone, (4) *Whiteinella archaeocretacea* Biozone; and (5) *Helvetoglobotruncana helvetica* Biozone.
- A comparison of the planktonic foraminifera biozones of the Boreal and Tethyan domains shows numerous affinities between the two realms: five planktonic foraminifera biozones are common.

References

1. Addoum, B.: L'Atlas Saharien Sud-Oriental. Cinématique des plis chevauchements et reconstitution du bassin du Sud-Est constantinois (confins algéro-tunisiens), pp. 1–158. Thesis, University of Paris Sud, Orsay, France (1995)
2. Aissaoui, D.: Les structures liées à l'accident sud-atlasique entre Biskra et le Dj. Mandra (Algérie). Evolution géométrique et cinématique, pp. 1–145. Thesis, University of Strasbourg, France (1985)
3. Amédro, F., Robaszynski, F.: Zonation by ammonites and foraminifers of the Vraconnian-Turonian interval: a comparison of the Boreal and Tethyan domains (NW Europe/Central Tunisia). Carnets de Géologie/Notebooks on Geology, Brest, Letter 2008/02 (CG2008_L02), pp. 1–5 (2008)
4. Bureau, D.: Approche sédimentaire de la dynamique structurale: Evolution mésozoïque et devenir orogénique de la partie septentrionale du fossé saharien (sud-ouest constantinois et Aurès-Algérie), vol. 6, pp. 1–779. Thesis 2, University of Pierre & Marie Curie, Paris, France (1986)
5. Bertraneu, J.: Contribution à l'étude géologique des Monts du Hodna. (1) Le massif du Bou Taleb. Bulletin du Service Géologique de l'Algérie **4**, 189 (1955)
6. Caron, M.: Cretaceous planktonic foraminifera. In: Bolli, H. M., Saunders, J. B., Perch-Nielsen, K., (eds.) Plankton Stratigraphy, pp. 11–86. Cambridge University Press, Cambridge (1985)
7. Emberger, J.: Esquisse géologique de la partie orientale des Monts des OuladNail, Atlas Saharien, vol. 27, p. 400. Publications du Service de la Carte Géologique de l'Algérie (1960)
8. Ghandriche, H. (1991). Modalités de la superposition de structures de plissements chevauchements d'âge alpin dans les Aurès (Algérie), pp. 1–189. Thesis, University of Paris XI, France
9. Guiraud, R.: Evolution post-Triasique de l'Avant pays de la chaîne alpine en Algérie d'après l'étude du Bassin du Hodna et des régions voisines, pp. 1–270. Thesis, University of Nice, France (1973)
10. Herkat, M.: La sédimentation de haut niveau marin du Crétacé supérieur de l'Atlas saharien oriental et des Aurès. Stratigraphie séquentielle, analyse quantitative des biocénoses, évolution paléogéographique et contexte géodynamique, pp. 1–802. Thesis, University of Algiers USTHB, Algeria (1999)
11. Herkat, M., Guiraud, R.: The relationships between tectonics and sedimentation in the Late Cretaceous series of the eastern Atlas domain (Algeria). J. Afr. Earth Sci. **46**, 346–370 (2006)
12. Kazi Tani, N.: Evolution géodynamique de la bordure nord-africaine: le domaine intraplaque nord- algérien. Approche megaséquentielle, pp. 1–871. Thesis, University of Pau (1986)
13. Laffitte, R.: Thesis, Sciences Paris. Bulletin du Service Géologique de l'Algérie, série 1. Etude géologique de l'Aurès, vol. 11, pp. 484, 1 carte au 1/200000 (1939)
14. Robaszynski, F., Caron, M.: Foraminifères planctoniques du Crétacé: commentaire de la zonation Europe-Méditerranée. Bull. Société Géologique Fr. **166**(6), 681–692 (1995)
15. Vila, J.M.: La chaîne alpine d'Algérie orientale et des confins algéro-tunisiens, pp. 1–665. Thesis, University of Pierre & Marie Curie, Paris 6, France (1980)

16. Noemi, A.F., Allison, P.: Events of Cenomanian—Turonian succession, Southern Mexico. *J. Iber. Geol.* **31**(1), 35–50 (2005)
17. Robaszynski, F., FaouziZagrarni, M., Caron, M., Amédéo, F.: The global bio-events at the Cenomanian-Turonian transition in the reduced Bahloul Formation of Bou Ghanem (central Tunisia). *Cretac. Res.* **31**, 1–15 (2010)
18. Ruault-Djerrab, M., Ferré, B., Kechid-Benkherouf, F.: Etude micropaléontologique du Cénomano-Turonien dans la région de Tébessa (NE Algérie): implications paléoenvironnementales et recherche de l’empreinte de l’OAE2. *Rev. Paléobiologie, Genève* **31**(1), 127–144 (2012)
19. Ruault-Djerrab, M., Kechid-Benkherouf, F., Djerrab, A.: Données paléoenvironnementales sur le Vraconnien/Cénomaniens de la région de Tébessa (Atlas Saharien, nord-est Algérie). Caractérisation de l’OAE2. *Ann. Paléontologie* **100**, 343–359 (2014)
20. Gradstein, F.M., Ogg, J.G., Smith, A.G., Bleeker, W., Lourens, L. J.: A new geologic time scale, with special reference to the Precambrian and Neogene. *Episodes* **27**(2), 83–100 (2004)

An Integrated Biostratigraphy of the Cenomanian-Turonian Transition at Kasserine Area in Central Tunisia: Implication from Khanguet Esslougui Section

Zaineb Elamri, Sherif Farouk, and Doha Alouani

Abstract

An integrated biostratigraphic study by means of planktonic foraminifera and macrofauna has been developed for the Cenomanian-Turonian (C/T) transition in the Khanguet Esslougui section. Several important bioevents of ammonites are recorded in this section from older to younger (FOs of *Calycoceras cenomanense*, *Vascoceras cauvini* and *Pseudaspidoceras pseudonodosoides*) and planktic foraminifera (LO of *Rotalipora cushmani*, FOs of *Withenella archaeocretacea* and *Helvetoglobotruncana helvetica*). The base of the studied section is characterized by the black shale which occurs within the upper part of the *Rotalipora cushmani* Zone and matches with the Oceanic Anoxic Event 2 (OAE 2). The Cenomanian/Turonian boundary is detected within the *Withenella archaeocretacea* biozone (PRZ) above directly the ammonite zone of *Pseudaspidoceras pseudonodosoides*.

Keywords

Cenomanian/turonian • Biostratigraphy
Kasserine • Tunisia

1 Introduction

In central Tunisia, the C/T successions are characterized by continuous outcrops that are rich in macrofauna and foraminifera. Several authors have discussed the C/T in Tunisia

[1, 3, 4, 6–13, 15–17]. To improve the stratigraphic resolution at a regional scale, it is important to integrate the planktic foraminiferal and the biostratigraphic ammonites. The Khanguet Esslougui section is characterized by high species richness in pelecypods, echinoids, ammonites and planktic foraminifera.

2 Materials and Methods

A total of 65 samples were placed in spaced interval from 0.5 to 1 m and collected from the exposed study section at Khanguet Esslougui in the Kasserine area (Fig. 1). For foraminiferal study, the dry samples were washed following the classic micropaleontological procedure by using approximately 50 g of dry rock samples. The studied assemblages of macrofauna comprises three species of ammonites, two species of gastropods, twelve species of pelecypods, five species of echinoids and one species of inoceramids.

3 Results

In the Khanguet Esslougui section, the Cenomanian-Turonian was subdivided into four lithologic units (Kh1, Kh2, Kh3 and Kh4) within the Bahloul Formation [2].

Kh1: marl with “black shales”; Kh2: marl rich in pelecypods with some beds of platy limestone; Kh3: alternation of marl and limestone rich in gastropods and ammonites and Kh4.

The upper Cenomanian-lower Turonian interval deposits cover three biozones: *Rotalipora cushmani* biozone, *Withenella archaeocretacea* biozone and *Helvetoglobotruncana helvetica* biozone.

The middle part of this section is rich in pelecypods (*Lopha syphax*, *Ilymatogyra africana*, *Ceratostreon flabelatum*). Few specimens of ammonites are present in this interval (*Calycoceras cenomanensis*). The upper part is

Z. Elamri (✉)

Kairouan University, 3100 Kairouan, Tunisia
e-mail: zaineb_amri@yahoo.fr

S. Farouk

Egyptian Petroleum Research Institute, 11727 Nasr City, Egypt

D. Alouani

Gafsa University, 2112 Gafsa, Tunisia

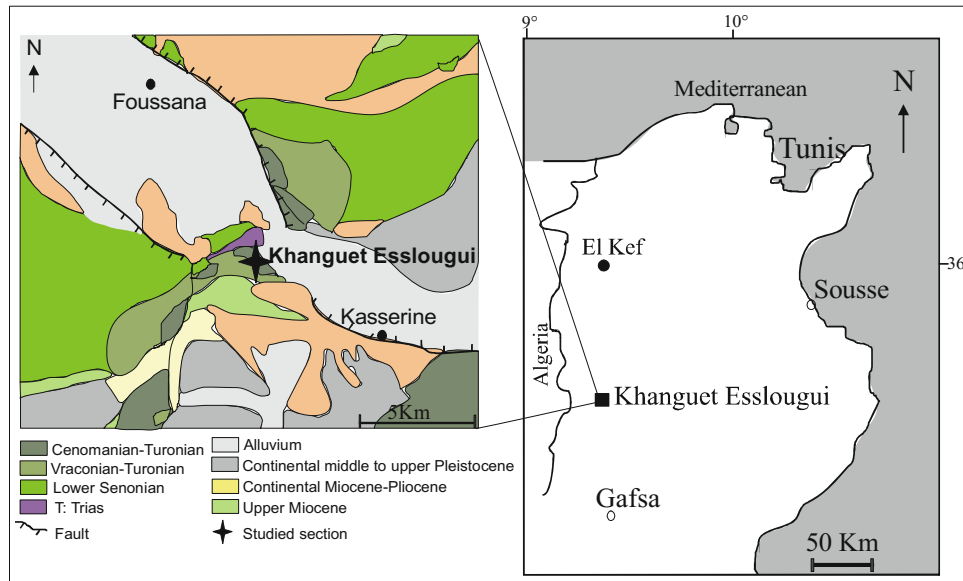


Fig. 1 Location and geological map of the studied section

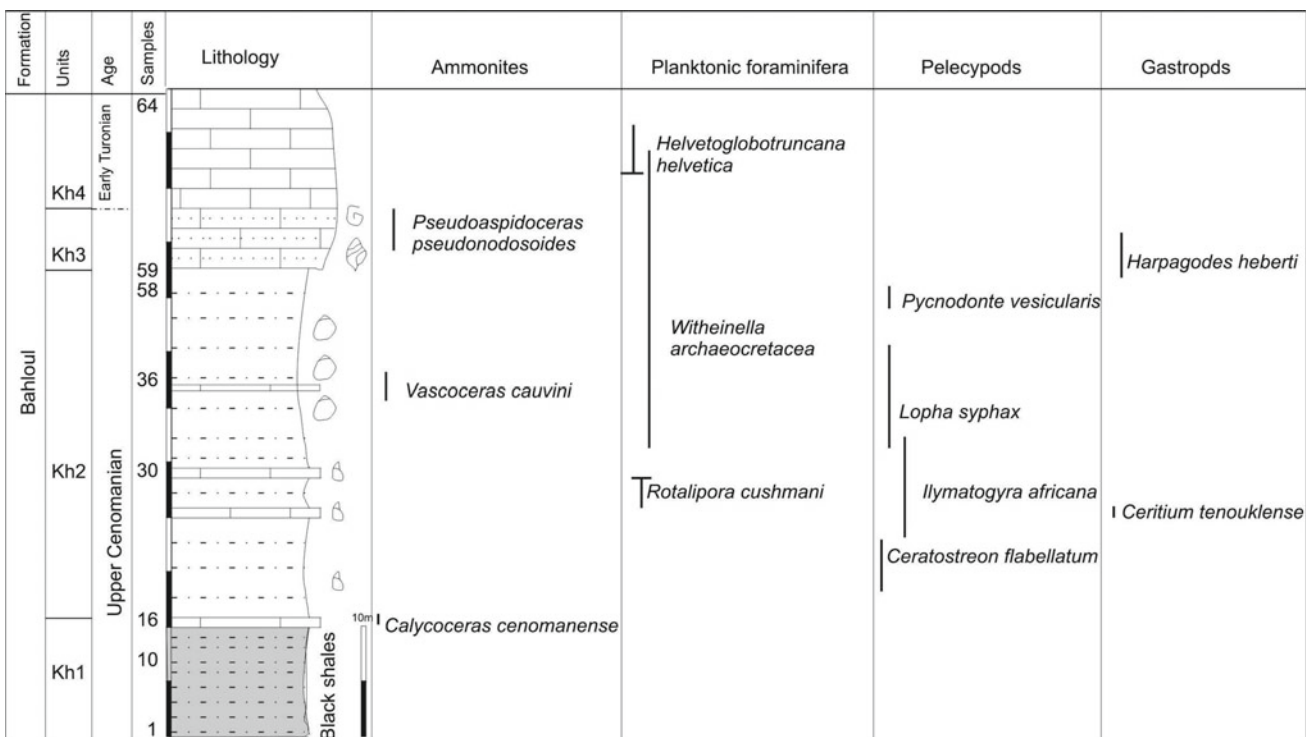


Fig. 2 Ammonites, foraminifera, pelecypods and gastropods bioevents in the Cenomanian-Turonian transition in the Khanguet Esslougui section

composed of an alternation of marl and limestone rich in gastropods (*Harpagodes heberti*). Some Cenomanian ammonite species are recorded such as *Vascoceras cauvini* and *Pseudoaspidoceras pseudonodosoides* (Fig. 2). The benthic foraminifera and ostracods become abundant in the upper part.

4 Discussion

Khanguet Esslougui section occurs in paleo-high area where the shallowest dominated macrofaunal content are reported above the black shales interval. The shallower macrofaunal

content is similar to that recorded in shallower basins such as in Egypt and south Jordan [5]. Black shales deposits reflect the oceanic anoxic event (OAE2) which is recorded in different deeper basins such as Algeria [6] and Tunisia [4, 13, 14]. It is absent in shallow basins such as Egypt. However, it increases towards the deeper basins [5]. The relative abundance of foraminifera shows high relative abundance of planktonic foraminifera in the lower part of the interval deposits during the Kh1 and Kh2 in upper Cenomanian [17]. It reflects a transgressive phase. In fact, benthic foraminifera shows high abundance in the Kh 3 and Kh 4. The Cenomanian/Turonian boundary is placed in the *Witheimella archaeocretacea* Zone (Fig. 2) which is in agreement with [8, 11, 17]. The Bahloul Formation is ascribed to the upper Cenomanian-lower Turonian interval [5, 8, 10].

5 Conclusion

The Cenomanian-Turonian Bahloul Formation in the Khanguet Esslougui section comprises three planktonic foraminifera biozones of upper Cenomanian-lower Turonian age: the *Rotalipora cushmani* biozones, *Witheimella archaeocretacea* Biozone and *Helvetoglobotruncana helvetica* biozone. The C/T boundary is located in the middle part of the *Witheimella archaeocretacea* Biozone. Three marker Cenomanian species of ammonites are present in this section named *Calycoceras cenomanensis*, *Vascoceras cauvinii* and *Pseudoaspidoceras pseudonodosoides*.

References

1. Abdallah, H., Sassi, S., Meister, C., Souissi, R.: Stratigraphie séquentielle et paléogéographie à la limite Cénomanién-Turonien dans la région de Gafsa-Chotts (Tunisie centrale). *Cretac. Res.* **21**, 35–106 (2000)
2. Burolet, P.F.: Contribution à l'étude stratigraphique de la Tunisie centrale. *Ann. Mines Geol. Tunis* **18**, 350 (1956)
3. Chaabani, F., Razgallah, S., Bonze, P., Belayouni, H.: L'épisode anoxique du passage Cénomanién-Turonien au Jebel Berda (Tunisie centro-méridionale): Stratigraphie et géochimie. *Notes du Service Géologique de Tunisie* **60**, 21–33 (1994)
4. Caron, M., Dall'Agnolo, S., Accarie, H., Barrera, E., Kauffman, E. G., Amédéo, F., Robaszynski, F.: High-resolution stratigraphy of the Cenomanian-Turonian boundary interval at Pueblo (USA) and wadi Bahloul (Tunisia): stable isotope and bio-events correlation. *Geobios* **39**, 171–200 (2006)
5. Farouk, S., Ahmad, F., Powell, J.H.: Cenomanian-Turonian stable isotope signatures and depositional sequences in northeast Egypt and central Jordan. *J. Asian Earth Sci.* **134**, 207–230 (2017)
6. Grosheny, D., Chikhi-Aouimeur, Ferry, S., Benkherouf-Kechid, F., Jati, M., Atrops, F., Redjimi-Bourouiba, W.: The upper Cenomanian-Turonian of the Saharan Atlas (Algeria). *Bulletin de la Société géologique de France* **179**, 593–603 (2008)
7. Layeb, M.: Étude géologique, géochimique et minéralogique, régionale, des faciès riches en matière organique de la formation Bahloul d'âge Cénomano-Turonien dans le domaine de la Tunisie Nord-Centrale, Thèse, Doct, Tunis (1990)
8. Maamouri, A.L., Zaghbib-Turki, D., Matmati, M.F., Salaj J.: La Formation Bahloul en Tunisie centro-septentrionale: variations latérales, nouvelle datation et nouvelle interprétation en terme de stratigraphie séquentielle. *J. Afr. Earth Sci.* **18**(1), 37–50 (1994)
9. Meister, C., Abdallah, H.: Précision sur les successions d'ammonites du Cénomanién-Turonien dans la région de Gafsa. *Tunis. Cent. -Sud. Rev. Paléobiologie* **24**, 111–199 (2005)
10. Negra, M.H., Zagrani, M.F., Hanini, A., Strasser, A.: The filament event near the Cenomanian-Turonian boundary in Tunisia: filament origin and environmental signification. *Bull. Soc. Géol. France* **182**(6), 507–519 (2011)
11. Rami, A., Zaghbib-Turki, D., Elouardi, H.: Biostratigraphie (Foraminifères) et contrôle tectono sédimentaire du Crétacé supérieur dans la région de Mejez El Bab (Tunisie septentrionale). *Geol. Méditerranéenne* **24**(1-2), 101–123 (1997)
12. Razgallah, S., Philip, J., Thomel, G., Zaghbib-Turki, D., Chaabani, F., Ben Haj Ali, N., M'rabet, A.: La limite Cénomanién-Turonien en Tunisie centrale et méridionale: biostratigraphie et paléoenvironnements. *Cretac. Res.* **15**, 507–533 (1994)
13. Robaszynski, F., Caron, M., Dupuis, C., Amédéo, F., Gonzalez-Donoso, J.M., Linares, D., Hardenbol, J., Gartner, S., Calandra, F., Deloffre, R.: A tentative integrated stratigraphy in the Turonian of Central Tunisia: formations, zones and sequential stratigraphy in the Kalaat Senan area. *Bull. Cent. Rech. Explor.-Prod. Elf Aquitaine* **14**, 213–384 (1990)
14. Robaszynski, F., Zagrani, M.F., Michèle Caron, M., Francis Amédéo, F.: The global bio-events at the Cenomanian-Turonian transition in the reduced Bahloul Formation of Bou Ghanem (central Tunisia). *Cretac. Res.* **31**, 1–15 (2010)
15. Salaj, J. Microbiostratigraphie du Crétacé du Paléogène de la Tunisie septentrionale et orientale (hypostratotypes tunisiens). Institut Géologique Dionyz Stur Bratislava, 238 p., 64 pl. (1980)
16. Soua, M., Zaghbib-Turki, D., Ben Jemia, H., Smaoui, J., Boukadi, A.: Geochemical record of the Cenomanian-Turonian anoxic event in Tunisia: is it correlative and isochronous to the biotic signal? *Acta Geol. Sin.* **85**, 801–840 (2011)
17. Zaghbib-Turki, D., Soua, M.: High resolution biostratigraphy of the Cenomanian-Turonian interval (OAE2) based on planktonic foraminiferal bioevents in North-Central Tunisia. *J. Afr. Earth Sci.* **78**, 97–108 (2013)

Micropaleontological Study of the Contact Between Kometan and Shiranish Formations from Dokan Area, Northern Iraq

Ibrahim Al-Shareefi, Omar Al-Badrani, and Aseel Yousif

Abstract

Nine samples of carbonate rocks from the contact between Kometan and Shiranish Formations from Dokan area, Northern Iraq are studied in terms of micropaleontology. The study showed different assemblages of microfauna such as ostracode, planktonic foraminifera and calcareous nannofossils which are observed by using thin sections in addition to the picked species. According to the identified species, the top of the Kometan Formation is early Campanian while the base of the Shiranish Formation is middle Campanian and the contact between them is unconformable.

Keywords

Kometan formation • Shiranish formation
Campanian • Micropaleontology • Iraq

1 Introduction

Kometan Formation was first described by Dunnington 1953, in Bellen et al. [1]. The type section is located about 400 m northwest of Kometan village, north of Ranyia town, northern Iraq. According to Bellen [1] the formation is 36 m thick. It consists of thinly bedded, light grey limestone with chert nodules and glauconite.

Shiranish Formation was first described by Henson [2] from the high folded zone of northern Iraq near the village of Shiranish Islam, northeast of Zakho [1]. It consists of a bipartite lithological division. The lower parts are composed of thin bedded marly limestone while its upper part composed of blue marl.

The studied section is located to the northwest of Sulaimaniya city within the southwestern limb of Sarah anticline (Fig. 1). This section represents 3 m of carbonate rocks. It belongs to the contact between Kometan and Shiranish Formations. The contact includes 1 m of the base of the Shiranish Formation and the top of Kometan Formation. The aim behind this study is to list the microfauna in the section by indicating its age and even to identify the nature of the contact between the two formations.

2 Materials and Methods

A total of nine upper Cretaceous rock samples are selected for the study of micropaleontology (Ostracode, planktonic foraminifera, calcareous nannofossils). The ostracode and foraminifera are studied by applying the standard method of the separation of species from samples (by using the Hydrogen peroxide). The species above the two groups are studied as picked specimens (under the reflected binocular microscope). Another method is conducted which consists of using the thin sections (under transmitted microscope). The calcareous nannofossils are extracted by using the method (H) from Armstrong and Brasier [3].

3 Results

The micropaleontological study has identified three different assemblages of microfauna includes four species of ostracode, *Bythocypris gohrbdonti*, *Bythocypris windhami*, *Abyssocypris adunca*, *Argilloecia taylorensis*. The identified fauna contain fourteen species of the planktonic foraminifera which are *Archaeoglobigerina blowi*, *Archaeoglobigerina cretacea*, *Globigerinelloides ultramicra*, *Globotruncana arca*, *Globotruncana bulloides*, *Globotruncana lapparenti*, *Globotruncana ventricosa*, *Globotruncanita elevate*, *Globotruncanita stuartiformis*, *Hedbergella delrioensis*,

I. Al-Shareefi · O. Al-Badrani (✉) · A. Yousif
Department of Geology, College of Science, University of Mosul,
Mosul, Iraq
e-mail: omarbadrani@yahoo.com

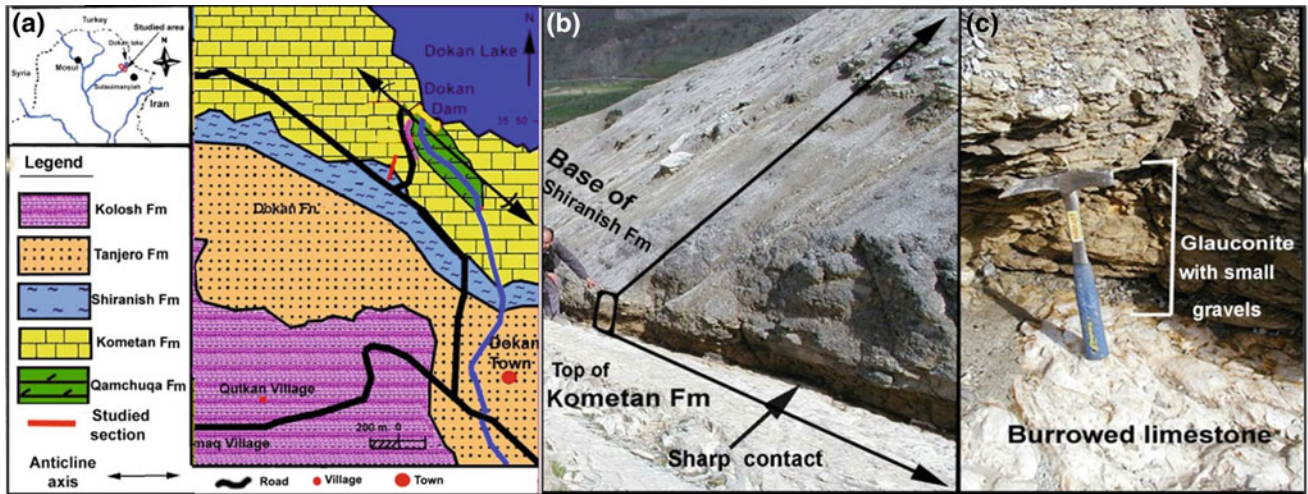


Fig. 1 a Location map of the studied area [8], b Sampled section, c Close up view of the contact between Kometan and Shiranish formations

Hedbergella holmdelensis, *Heterohelix reussi*, *Heterohelix striata*, *Rosita fornicate*.

Calcareous nannofossils are represented by thirteen species which are: *Calculites obscurus*, *Calculites ovalis*, *Cyclagelosphaera deflandre*, *Eiffellithus eximius*, *Eiffellithus turriseiffelii*, *Lucianorhabdus cavyeuxii*, *Lithraphidites praequadrata*, *Micula concave*, *Micula swastika*, *Quadrum*

cf. sissingh, *Reinrandites cf. levis*, *Stradneria crenulates*, *Watznaueria bioporta* (Fig. 2).

All the ostracode species are restricted to the bottom of the Shiranish formation (Middle Campanian) whereas the Kometan Formation (Early Campanian) was barren from species. This absence is due to the stiff lithology by which most species carapaces are crushed during the preparation of

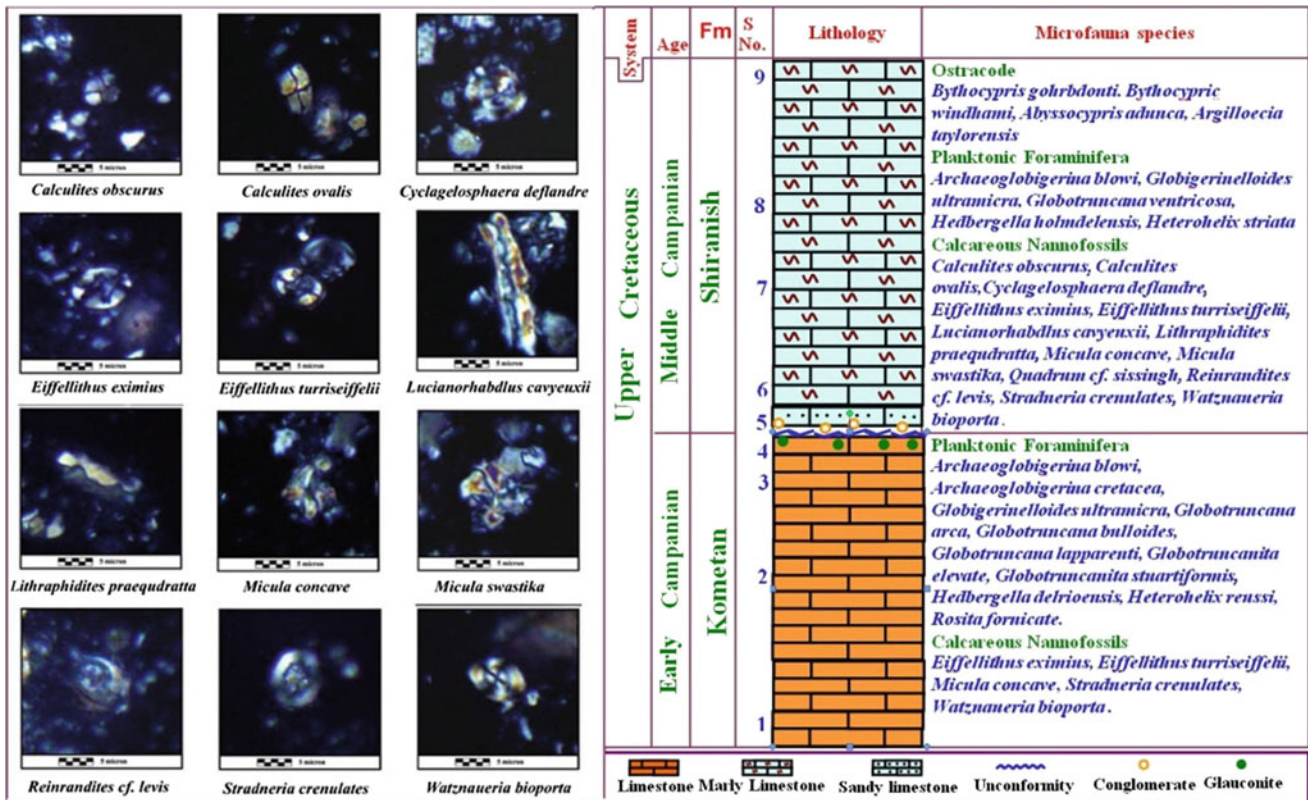


Fig. 2 Distribution of microfauna in the studied stratigraphic section (without scale)

the hard limestone of the Kometan Formation. The ostracode species indicate a paleo-environment that extended from middle shelf—outer shelf.

The Planktonic foraminifera are abundant and diverse in both Formations. The best recognized species is *Globotruncanita elevata* which is the best indicator species in the kometan formation due to its records by many previous studies in Iraq within the early Campanian age such as Al-Tamemi [4], Hamoudi [5]. In addition to that, this species considered the index species for the Early campanian biozone by many authors such as Al-Khafaf [6]. In general, the planktonic foraminifera assemblage in this Formation indicate middle shelf and tend to be a shallow environment comparatively.

In the Shiranish Formation many species are there. However, the presence of the *Globotruncana ventricosa* is the best indicator of the biozonal marker for the Campanian. In terms of calcareous nannofossils, thirteen species have been identified and have appeared in both Formations. Five of them continued from the top of the Kometan Formation to the base of the Shiranish Formation. In general, these species signify the early-middle Campanian [7]. It is important to mention that there are burrows which refer to the Glossifungites ichnofacies and (some burrowing trace fossils of *Chondrite*). It is a sign for a hard ground that indicates the shallowing during the deposition at the top of the Kometan Formation. These traces are known from the marine environments.

Other observations are recognized at the top of the Kometan Formation such as the existence of the Glouconite whether it is filling the burrows or as a thin layers between limestone beds. The conglomerate also presents the base of the Shiranish Formation. With regard to the above mentioned observations and in spite of the discontinuities, some species ranges indicate short loss of time. The upper contact of the Kometan Formation is unconformable with overlain Shiranish Formation.

4 Conclusion

Three different assemblages of microfauna have been recognized. They are as follows ostracode, foraminifera, and nannofossil. Based on the microfauna the age of the studied section is determined by the Early Campanian for the Kometan Formation; whereas, the Shiranish formation is by the Middle Campanian.

There are signs of hard ground that appeared at the top of the Kometan Formation such as burrows. It refers to Glossifungites ichnofacies and some burrowing trace fossils of *Chondrite*. This is indicative of the shallowing during the sedimentation. The lower contact of the Shiranish Formation is unconformable with the underlain Kometan Formation.

References

1. Bellen, R.C., Dunnington, H.V., Wetzel, R., Morton, D.M.: Lexique stratigraphique international, vol. 3 Asie, Fascicule 10a. Centre National de la Recherche Scientifique (CNRS), Paris, 1–333 (1959)
2. Henson, F.R.S.: Cretaceous and tertiary reef formation and associated sediments in Middle East. AAPG Bull. **34**(2), 215–238 (1950)
3. Brasier, A.H.: Microfossils, 296 pp. Black Well Publishing, Oxford (2005)
4. Al-Tamemi, F.M.: Micropaleontological study of Kometan Formation for determination of the paleoenvironment. Unpublished M.Sc. Thesis, University of Baghdad, 174 pp (1986)
5. Hammoudi, R.A.: Stratigraphy of the Turonian-Early Campanian depositional subsycle from selected wells in Iraq. Unpublished Ph. D. Thesis, University of Mosul, 215 pp (1995)
6. Al-Khafaf, A.O.: Stratigraphy of Kometan Formation (upper cretaceous) in Dokan-Endezah area, Northeastern Iraq. Unpublished M.Sc. Thesis, University of Mosul, 79 pp (2005)
7. Perch-Nielsen, K.: Mesozoic calcareous nannofossils. In: Bolli, H. M., Saundes, J.B., Perch-Nielsen, K. (eds.) Plankton Stratigraphy, pp. 427–554. Cambridge University Press, Cambridge (1985)
8. Taha, Z.A., Karim, K.H.: New ideas about Gulneri Shale formation (early Turonian) in Dokan area, Kurdistan Region, NE-Iraq. Iraqi Bull. Geol. Min. **5**(2), 29–39 (2009)

Planktonic Foraminiferal Evidence of Upper Cretaceous in the Well “A” (Gulf of Hammamet Area, Northeastern Offshore Tunisia)

Ezzedine Saïdi and Dalila Zaghib-Turki

Abstract

The Gulf of Hammamet area, lying in the extreme northeastern offshore Tunisia, is characterized by several discontinuities through the Mesozoic and Cenozoic series. These discontinuities had affected the thickness distribution of deposited sequences in the area such as the El Haria Formation (Fm.), which is supposed in the literature to be locally, partially or totally eroded. A number of geological works based on geophysics, seismic and log data in the Gulf of Hammamet area consider the existent part of the El Haria Fm. as a whole sequence, attributed to the Palaeocene when it is partially eroded. Hence, the focus on the planktonic foraminiferal stratigraphic range in the present work revealed the existence of a Late Cretaceous unit of the El Haria Fm., spanning ~25 m of marls overlying the limestones of the chalky and fractured Abiod Fm. This does not exclude the existence of discontinuities that can affect the Abiod-El Haria interval but confirms the existence of a Late Campanian unit (First Downhole Occurrence of *Radotruncana subspinosus*) that can probably be unconformably overlaid by a Late Maastrichtian unit (First Downhole Occurrence of Late Maastrichtian foraminifera).

Keywords

Gulf of Hammamet • Late Maastrichtian
Late Campanian • El Haria • *Radotruncana subspinosus*

1 Introduction

The Late Cretaceous Abiod and El Haria Formations [5, 10] are among the most widespread formations in Tunisia. Nevertheless, a number of discontinuities affect these formations in several localities especially in the Gulf of Hammamet (GH) area [1, 4, 7], where the El Haria Formation (Fm.) is documented to be locally, partially or totally eroded [1, 4, 7]. Therefore, this marly formation is chronologically attributed to the Palaeocene [1, 4] in high zones where its thickness is reduced and does not exceed 50 m [6, 7]. Accordingly, the present work aims to characterize biostratigraphically the existing El Haria Fm. in the area by studying the stratigraphic range of the planktonic foraminifera from the well “A”, located in the eastern part of the Gulf of Hammamet area, lying offshore northeastern Tunisia on the margin of the Pelagian Sea.

2 Materials and Methods

The planktonic foraminiferal assemblages which were picked out from the well “A” cutting samples are herein analyzed in order to characterize biostratigraphically the crosscut El Haria Formation. Therefore, 10 samples were taken from the 30.5 m-thick studied interval. Sufficient amount from each sample was soaked in H₂O₂ solution, washed through a set of Afnor sieves (63–630 µm), sonically agitated, dried in oven at a temperature below 50 °C, and then sorted for picking out typical foraminifera.

The planktonic foraminiferal occurrences were carefully examined throughout the studied interval by taking the existence of caved specimens into consideration. Taxonomic identification was carried out by using mainly the works of [2, 9, 14]. Selected specimens were photographed by using a scanning electron microscope.

E. Saïdi (✉)

Petroleum Services Department, Tunisian Public Oil Company-ETAP, Petroleum Research and Development Centre-CRDP, 2035 Tunis, Tunisia
e-mail: ezzedine.saïdi@etap.com.tn

D. Zaghib-Turki

Faculty of Sciences, Department of Geology, University of Tunis El Manar, Campus Universitaire, El Manar, 2092 Tunis, Tunisia

more, the planktonic foraminiferal range evidenced the occurrence of a Late Campanian-Early Maastrichtian hiatus in the studied well “A”. At last, we intend to carry out further biostratigraphical analysis in the surrounding wells for the purpose of delimitating the lateral extent of each identified unit and to better understand the chronological history and architecture of the Gulf of Hammamet basin during the Late Cretaceous.

References

1. Abidi, O., Inoubli, M.H., Sebei, K., Boussiga, H., Amiri, A., Hamdi Nasr, I.: Geodynamic framework and petroleum potential of the cap Bon—Gulf of Hammamet province—Tunisia. In: Search and Discovery Article #30368. AAPG International Conference & Exhibition, Istanbul, Turkey (2014)
2. Arz, J.A.: Los foraminíferos planctónicos del Campaniense y Maastrichtiense: biostratigrafía, cronostratigrafía y eventos paleoecológicos. Thesis, Universidad de Zaragoza, Zaragoza, Spain, pp. 1–419 (1996)
3. Arz, J.A., Molina, E.: Late Campanian and Maastrichtian biostratigraphy and chronostratigraphy based on planktonic foraminifera in temperate and subtropical latitudes (Spain, France and Tunisia). *Neues Jahrb für Geol P-A* **224**, 161–195 (2002)
4. Ben Ferjani, A., Burolet, P. F., Mejri, F.: Petroleum Geology of Tunisia. *Entreprise Tunisienne d’Activités Pétrolières*, pp. 1–194, Tunisia (1990)
5. Burolet, P.F.: Contribution à l’étude stratigraphique de la Tunisie centrale. *Ann. Mines Géologie* **18**, 1–293 (1956)
6. Ferchichi, A., El Ghali, A.: Apport des données géologiques et géophysiques à l’évaluation géopétrolière du champ de Birsa: Tunisie orientale. *Géologie Fr.* **1**, 3–10 (2017)
7. Hezzi, I.: Caractérisation géophysique de la plateforme de Sahel, Tunisie nord-orientale et ses conséquences géodynamiques. Thèse Université Rennes 1, pp. 1–174 (2014)
8. Molina, E., Alegret, L., Arenillas, I., Arz, J.A., Gallala, N., Hardenbol, J., Von Salis, K., Steurbaut, E., Vandenbeghe, N., Zaghbib-Turki, D.: The global boundary stratotype section and point for the base of the Danian stage (Paleocene, Paleogene, “Tertiary”, Cenozoic) at El Kef, Tunisia: original definition and revision. *Episodes* **29**(4), 263–278 (2006)
9. Nederbragt, A.J.: Late Cretaceous biostratigraphy and development of Heterohellicidae (planktic foraminifera). *Micropaleontology* **37**(4), 329–372 (1991)
10. Negra., M.H.: Les dépôts de plate-forme à bassin du Crétacé supérieur en Tunisie septentrionale (Formation Abiod et faciès associés). Stratigraphie, sédimentation, diagenèse et intérêt pétrolier. Thèse de Doctorat es-Sciences, Université de Tunis, pp. 1–649 (1994)
11. Odin, G.S.: Définition d’une limite multicritère; stratigraphie du passage Campanien-Maastrichtien du site géologique de Tercis (Landes, SW France). *Comptes Rendus Geosci.* **334**, 409–414 (2002)
12. Ogg, J.G., Ogg, G.: Late Cretaceous time scale (65–100 Ma time-scale) (2004). https://engineering.purdue.edu/stratigraphy/charts/Timeslices/3_Late_Cret.pdf
13. Premoli Silva, I., Verga, D.: Practical manual of Cretaceous planktonic foraminifera. In: Verga, D., Rettori, R. (eds.), International School on Planktonic Foraminifera, 3rd Course: Cretaceous. Universities of Perugia and Milan, Tipografia Pontefelcino, Perugia, Italy, 283 p (2004)
14. Robaszynski, F., Caron, M., Gonzalez Donoso, J. M., Wonders, A. A.H.: Atlas of late Cretaceous globotruncanids. *Rev. Micropaléontol.* **26**, 145–305 (1984)
15. Saïdi, E., Zaghbib-Turki, D.: Prediction of the Abiod reservoir’s top in northern Tunisia applying a high resolution foraminiferal biostratigraphy. In: Proceedings of the 13th Tunisian Petroleum Exploration and Production Conference, ETAP Memoir, vol. 35, pp. 357–369, Tunisia (2015)
16. Saïdi, E., Zaghbib-Turki, D.: Planktonic foraminiferal biostratigraphy and quantitative analysis during the Campanian-Maastrichtian transition at the Oued Necham section (Kalâat Senan, central Tunisia). *Turk. J. Earth Sci.* **25**(6), 538–572 (2016)
17. Saïdi, E.: Foraminifères de l’intervalle Campanien terminal-Maastrichtien inférieur en Tunisie septentrionale et centrale: Taxonomie, Biostratigraphie et Paléoécologie. Thèse Université de Tunis El Manar, pp. 1–173 (2017)

Paleocene Benthic Foraminifera and *Neoponides duwi* Event from Dineigil Area, South-Western Desert, Egypt

Mohamed Youssef

Abstract

Seventy-three rock samples from Dineigil area were used to study the paleo-environments of the Paleocene interval. The foraminiferal assemblage is typically dominated by the Midway-type fauna. The Velasco-type fauna of Paleocene were absent. The foraminiferal distribution of the Paleocene sequence from the study area indicates the deposition from inner to middle neritic environment (50–100 m depth). *Neoponides duwi* event in the Paleocene of Egypt comprises an abundant occurrence of *N. duwi* with the common occurrence of *Siphogenerinoides eleganta*, costate lenticulinids, and *Stainforthia* spp in the latest Danian. The *N. duwi* event gives the evidence that *Neoponides duwi* live in restricted environments characterized by oxygen deficiency and rich food resources.

Keywords

Paleocene • Benthic foraminifera • Dineigil
South Western desert • Egypt

1 Introduction

Dramatic shifts in climate system and carbon cycle have been recorded in Paleocene [18]. A series of hyper-thermal events were recorded in Paleocene: Paleocene/Eocene Thermal Maximum (PETM) ~55 Ma [20]; the Latest

Danian Event (LDE) ~61.7 Ma [5]; the Danian/Selandian transition event ~61.7 Ma [12]; the mid Paleocene Biotic Event (MPBE) ~58.2 Ma [3].

Egyptian sections thus provide a detailed record of biologic and chemical changes through the Paleocene (e.g. [4]). The high-resolution paleo-environmental studies of benthic foraminiferal on the Paleocene of central Egypt are generally scarce (e.g. [9, 16]). Most of studies were focused on the Danian/Selandian transition (e.g. [6, 15]); Paleocene—Eocene Thermal Maximum (e.g. [2, 19]). The present study gives meticulous information of the benthic foraminifera that have prevailed during the Paleocene in Dineigil Area near Dineigil well (Fig. 1) in south-western desert. Qualitative and quantitative analyses of benthic foraminifera are conducted.

2 Geological Setting, Lithology, Studied Section, and Methods

Egypt can be subdivided structurally into Stable and unstable shelves. The Stable shelf is composed of two basins. One is situated in the western part of the country. It is covered by the Dakhla basin. The other is in the eastern part of the country. It is covered by the upper Nile basin. The lithological sequence consists of three units: the Kiseiba Formation (base), the Kurkur Formation, and the Garra Formation (top). The present study deals with the Kurkur Formation, and the Garra Formation. The studied sequence is composed of shale and limestone (Kurkur Fm), limestone beds with shale and marl intercalations (Garra Fm). The age of the studied interval is Danian-Selandian [8].

The area under investigation lies in the face of the Sinn EL-Kaddab Escarpment, east of Dungul Oasis and Western Desert, Egypt. The Dineigil section is a composite section of five subsections as follow:

M. Youssef (✉)
Department of Geology and Geophysics, College of Science, King Saud University, KSA, Riyadh, Saudi Arabia
e-mail: mymohamed@ksu.edu.sa

M. Youssef
Faculty of Science, Department of Geology, South Valley University, Qena, Egypt

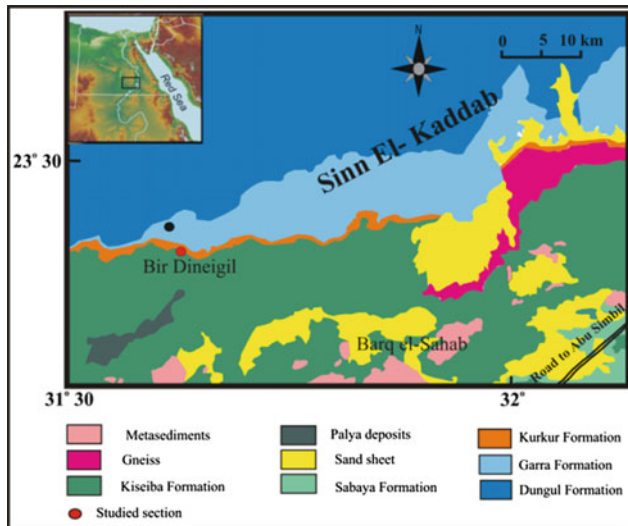


Fig. 1 Geological and locative map of the studied area, south western desert, Egypt

Subsection	Long	Lat
BDA	31° 37' 24" E	23° 24' 25" N
BDB	31° 36' 24" E	23° 24' 55" N
BDC	31° 36' 17" E	23° 24' 52" N
BDD	31° 37' 11" E	23° 24' 41" N
BDE	31° 37' 17" E	23° 24' 46" N

The present study is based on 73 samples collected from ~43 m interval at the section near Dineigil well (Bir Dineigil). The standard technique for foraminiferal study was used. The fraction 125–630 μm was investigated both qualitatively and quantitatively under binocular stereomicroscope in King Saud University.

3 Results

The Benthic foraminiferal assemblages of Paleocene in the studied interval are typically dominated by the Midway-type fauna [1]. The absence of the Velasco-type fauna [1] indicates that the Dineigil Area was not deeper than 100 m during Paleocene. It is a result compatible with that of [13]. The absence of larger foraminifera, with depths less than 50 m, and the common planktonic foraminifera through the studied interval indicates that the area was not shallower than 50–75 m according to Speijer et al. (1996). Some recorded species (e.g. *Bulimina midwayensis*, *Cibicidoides alleni* and *Osangularia plummerae*) have upper depth limit of 50–100 m [17]. The foraminiferal distribution of the Palaeocene sequence from Dineigil area is inferred to be deposited in a range from middle to outer neritic environment (50–100 m depth).

The cluster analysis (Multivariate statistical package version 3.1) of benthic foraminifera in the Dineigil section resulted in three clusters (A, B, C). These clusters are not only bathymetrically defined but also reflect eutrophic and oxygen conditions (Fig. 3). Cluster (A) includes taxa with high frequencies (e.g. *Neoeponides duwi*, *Lenticulina* spp., *Stainforthia* spp., and *S. eleganta*). These taxa suggest inner-middle neritic environments. They represent eutrophic and low oxygen conditions see Fig. 2.

The benthic species in cluster (B) have high dominance through the studied interval. They are characterized by wide depth range. Cluster (C) species (e.g. *P. quadrata*, *G. girardanus*, *V. scrobiculata*, *L. applinae*) are prevailing. They are indicative of the high food and low oxygen environments (Fig. 3).

4 Discussion

4.1 Southern Tethyan *Neoeponides duwi* Bio-Event

The *Neoeponides duwi* (Fig. 4) is exclusively Paleocene species [7]. In Egypt, *N. duwi* ranges from the Danian to the Selandian [12]. An abundant occurrence of the *Neoeponides duwi* was recorded in the latest of the Danian interval with a maximum abundance of 97% of the benthic assemblage. The benthic foraminiferal assemblages in the shallow areas of central and southern Egypt around Danian/Selandian transition consists of a combination of the peak of the *Neoeponides duwi* occurrence and a high common occurrence of the *Siphogenerinoides eleganta*, costate lenticulinids, and *Stainforthia* spp. (e.g. [11, 12], Bronneman et al. 2009, [14]). The common occurrence of the costate lenticulinids in the same interval of the studied section (6–63%) indicates that the *Neoeponides duwi* is dissolution-resistant [15]. The *Neoeponides duwi* had the capacity to repopulate the anoxic seafloor during the temporal oxygenation events [12]. The *Neoeponides duwi* event corresponds to a rapid sea-level fall with an estimation of ~50 m or less amplitude as it is also indicated by the low P/B ratio [6, 12, 15]. In the studied interval the *Neoeponides duwi* is associated with the benthic fauna as it is mentioned above. It is an indication of the deposition in shallow food-rich and oxygen-depleted environments.

4.2 Paleoenvironments

The fluctuations of the diversity and abundance of benthic foraminifera in the studied area clearly indicate the range of the middle to outer neritic open marine settings in the Paleocene. The foraminiferal assemblage is dominated by

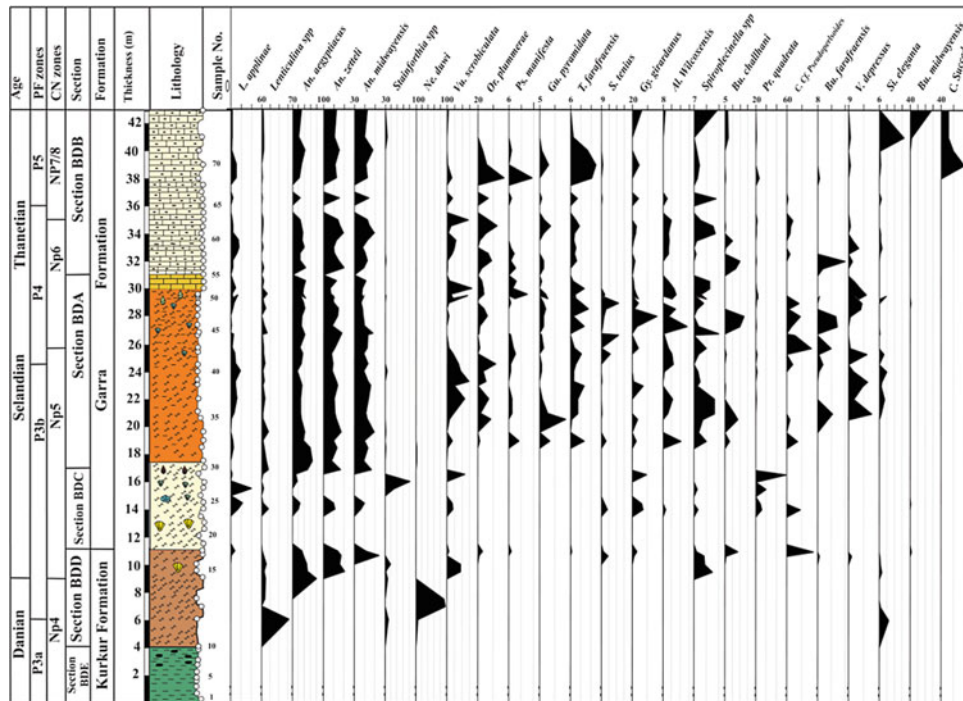


Fig. 2 The frequencies of benthic foraminiferal species recorded in the studied interval

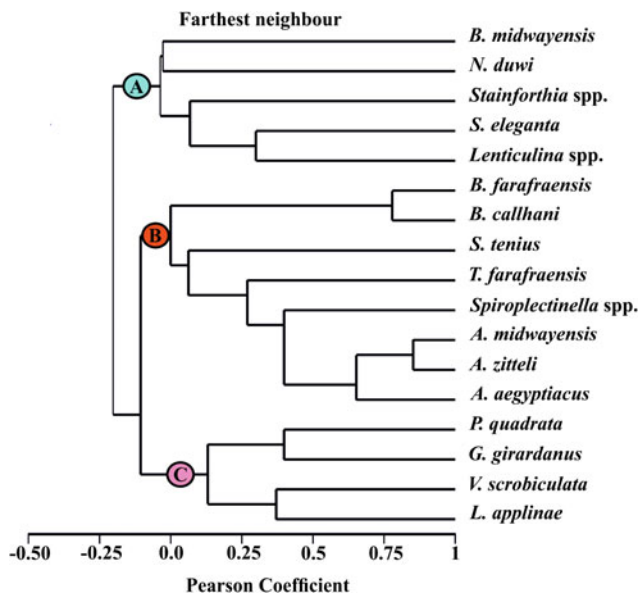


Fig. 3 Shows the Dendrogram resulting from the cluster analysis of benthic foraminifera in Dineigil section (species with >5% frequency only)

the Midway-type fauna and is characterized by the absence of deep Velasco-type fauna. The Inner shelf environments were reported from the southern part of the Western Desert (e.g. [10, 11, 19]). The distribution of the *Neoepionides duwi* seems to be limited to inner and middle neritic environments (e.g. [11, 12, 15]). The Danian/Selandian interval in the

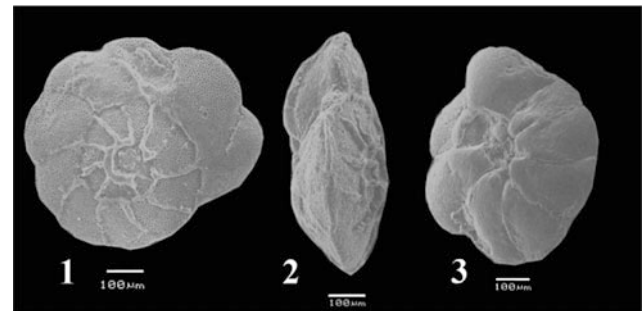


Fig. 4 *Neoeponides duwi*, BDD subsection, sample:3

South-Western desert is characterized by submerged paleo-highs. These successions include the Kurkur Formation which is characterized by sandy limestone. However, it lacks foraminifera. The Latest Danian event (LDE) coincides with the eustatic sea-level fall terminated by a regional hiatus across the Danian/Selandian boundary associated with tectonic uplift in the Western Desert (e.g. [6, 10]).

5 Conclusion

The Benthic assemblages extracted from seventy-three rock samples from the Paleocene interval in Dineigil area are typically dominated by the Midway-type fauna (e.g., *Loxostomoides applinae*, *Cibicoides alleni*, *C. succedens*, *Bulimina midwayensis*, *Siphogenerinoides eleganta*, *Osangularia*

plummerae. The Velasco-type fauna of Paleocene (e.g. *Angulogavelineela avnimelechi*) are absent. A range from a middle to outer neritic environment (50–100 m depth) prevailed during the deposition of Paleocene sediments in Dineigil area. The *Neoeponides duwi* event corresponds to a rapid sea-level fall. It suggests that *Neoeponides duwi* thrives in specific, oxygen-depleted food-rich and environments.

Acknowledgements This work is supported by King Saud University, Deanship of Scientific Research, College of Science Research Center.

References

- Berggren, W., Aubert, J.: Paleocene benthonic foraminiferal biostratigraphy, paleobiogeography and paleoecology of Atlantic-Tethyan regions: midway-type fauna. *Palaeogeogr. Palaeoclimatol. Palaeoecol.* **18**, 73–192 (1975)
- Berggren, W., Alegret, L., Aubry, M.-P., Cramer, B., Dupuis, C., Goolaerts, S., Kent, D., King, C., Knox, R., Obaidalla, N., Ortiz, S., OudaKh, Sabour A., Salem, R., Senosy, M., Soliman, M., Soliman, A.: The Dababiya corehole: Upper Nile Valley, Egypt: preliminary results. *Austrian J. Earth. Sci.* **105**, 161–168 (2012)
- Bernaola, G., Baceta, J., Etzebarria, X.: Evidence of an abrupt environmental disruption during the mid-Paleocene biotic event (Zumaia section, western Pyrenees). *Geol. Soc. Am. Bull.* **119**, 785–795 (2007)
- Bolle, M.P., Tantawy, A., Pardo, A., Adatte, T., Burns, S., Kassab, A.: Climate and environmental changes documented in the upper Paleocene to lower Eocene of Egypt. *Eclogae Geol. Helv.* **93**, 33–51 (2000)
- Bornemann, A., Schulte, P., Sprong, J., Steurbaut, E., Youssef, M., Speijer, R.: Latest Danian carbon isotope anomaly and associated environmental change in the southern Tethys (Nile Basin, Egypt). *J. Geol. Soc. Lond.* **166**, 1135–1142 (2009)
- Farouk, S., El-Sorogy, A.: Danian/Selandian unconformity in the central and southern Western Desert of Egypt. *J. Afr. Earth Sci.* **103**, 42–53 (2015)
- Hewaïdy, A.: Biostratigraphy and paleobathymetry of the Garra-Kurkur area, southwest Aswan, Egypt. Middle East Research Center Ain Shams University. *Earth Science Series*, vol. 8, pp. 48–73 (1994)
- Issawi, B.: Review of upper Cretaceous-lower tertiary stratigraphy in central and southern Egypt. *Bull. -Am. Assoc. Pet. Geol.* **56**, 1448–1463 (1972)
- Khalil, H., Al Sawy, S.: Integrated biostratigraphy, stage boundaries and Paleoclimatology of the Upper Cretaceous-Lower Eocene successions in Kharga and Dakhala Oases, Western Desert Egypt. *J. Afr. Earth Sci.* **96**, 220–242 (2014)
- Luger, P.: *Stratigraphie der marinen Oberkreide und des Alttertiärs im südwestlichen Oberrhein-Becken (SW-Ägypten) unter besonderer Berücksichtigung der Mikropaläontologie, Palökologie und Paläogeographie*. Berliner Geowissenschaftliche Abhandlungen **63**, 151 (1985)
- Schnack, K.: *Biostratigraphie und fazielle Entwicklung in der Oberkreide und im Alttertiär im Bereich der Kharga Schwelle, Westliche Wüste, Southwest Ägypten*. Ph. D. Thesis Nr. 151, Universität Bremen, Bremen, 142 pp (2000)
- Speijer, R.: Danian–Selandian sea-level change and biotic excursion on the southern Tethyan margin. In: Wing, S.L., Gingerich, P. D., Schmitz, B., Thomas, E. (eds.) *Causes and Consequences of Globally Warm Climates in the Early Paleogene: Geological Society of America, Special Paper*, vol. 369, pp. 275–290 (2003)
- Speijer, R., Schmitz, B.: A benthonic foraminiferal record of Paleocene sea level and tropic/redox conditions at Gebel Aweina, Egypt. *Palaeogeogr. Palaeoclim. Palaeoecol.* **137**, 79–101 (1998)
- Sprong, J., Youssef, M., Bornemann, A., Schulte, P., Steurbaut, E., Stassen, P., Kouwenhoven, T., Speijer, R.: A multi-proxy record of the latest Danian event at Gebel Qreiya, Eastern Desert Egypt. *J. Micropalaeontol.* **30**, 167–182 (2011)
- Sprong, J., Kouwenhoven, T., Bornemann, A., Schulte, P., Stassen, P., Steurbaut, E., Youssef, M., Speijer, R.: Characterization of the latest Danian event by means of benthic foraminiferal assemblages along a depth transect at the southern Tethyan margin (Nile Basin, Egypt). *Mar. Micropaleontol.* **86–87**, 15–31 (2012)
- Tantawy, A., Ouda, Kh., Von Salis, K., El Din, M.S.: Biostratigraphy of Paleocene sections. In: Schmitz, B., Sundquist, B., Andreasson, F. (eds.) *Early Paleogene Warm Climates and Biosphere Dynamics*, GFF, vol. 122, pp. 163–165 (2000)
- Van Morkhoven, F.P., Berggren, W., Edwards, A.: Cenozoic cosmopolitan deep-water benthic foraminifera. *Elf -Aquitaine Mem*, vol. 11, 421 (1986)
- Westerhold, T., Röhl, U., Donner, B., McCarren, K., Zachos, J.: A complete high-resolution Paleocene benthic stable isotope record for the central Pacific (ODP Site 1209). *Paleoceanography* **26**, PA2216 (2011)
- Youssef, M.: *Micropaleontological and stratigraphical analyses of the Late Cretaceous/Early Tertiary succession of the Southern Nile Valley (Egypt)*, Bochum, Germany. Published online, Ph. D. Thesis (2003). <http://www.netahtml/Hss/Diss/MohamedMohamedYoussefAli/diss.pdf>
- Zachos, J., Dickens, G., Zeebe, R.: An early Cenozoic perspective on greenhouse warming and carbon-cycle dynamics. *Nature* **451**, 279–283 (2008)

Upper Eocene (Priabonian) Larger Foraminifera from the Deh-Rashti Section, Rafsanjan City, Southeastern Iran

Tayebeh Ahmadi

Abstract

An Upper Eocene diagnostic larger foraminiferal assemblage is described and illustrated from carbonates of Deh-Rashti section, west of Rafsanjan, southeast of Iran. Thirteen taxa of benthic foraminifera were identified. This assemblage is characterized by the species *Nummulites fabianii retiatus* (Prever), *Asterigerina rotula* (Kaufmarm), *Praerhapydionina* cf. *huberi*, *Fabiania* sp., *Pellatispira* aff. *Madaraszi*, *N. striatus*, *Alveolina* sp., *Spherogypsina* sp., *Gypsina marianensis*, *Eorupertia magna* (Le Calvez), *Neorotalia* sp., *Elphidium* sp., *Pyrgo* sp. Based on the stratigraphic distribution of the well-known foraminifers, the *Nummulites fabianii* Taxon-range Zone of larger foraminifera was established. The existence of a large number of relatively elongate A-form *Nummulites* suggests low turbulence, oligotrophic water of middle-outer shelf palaeoenvironments of tropical to subtropical oceans.

Keywords

Larger foraminifera • Priabonian • Nummulites • Rafsanjan

1 Introduction

The Tertiary outcrops are significantly widespread around the Rafsanjan city, southeastern Iran. Most of these are Eocene rocks which conform to a volcano-sedimentary complex. Volcanic rocks belong to the Urmia-Dokhtar Magmatic Belt (Fig. 1a) and consist of basaltic andesite, andesite, trachyte and trachy-andesite and pyroclastic

deposits [1]. The lower and the middle-upper successions of the Eocene are varied in thickness and location but mainly consist of marine limestone and marl with subordinate sandstone. Although sedimentary deposits spread widely in the area, no comprehensive study has been conducted on these deposits so far. Most of the previous examinations were devoted to igneous rocks. The present study is a detailed investigation on the Deh-Rashti region, west of Rafsanjan.

2 Geological and Geographical Settings

The Deh-Rashti section is located in the vicinity of Deh-Rashti village (30°13'57.5"N; 55°48'49"E;), 30 km west of Rafsanjan (Fig. 1b). The section is mapped in the Rafsanjan quadrangle map of Iran [1] and structurally belongs to the Central Iran Zone (Urumia-Dokhtar belt).

The section consists of approximately 58 m of cream, fossiliferous limestones and sandy limestones which overlay the lower Eocene volcanics with no conformity.

3 Results

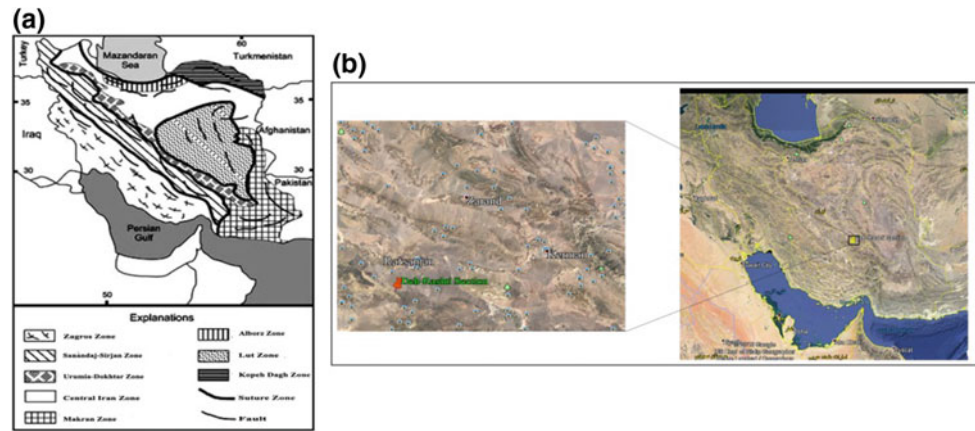
3.1 Biostratigraphy

The following thirteen genera and species (Pl. 1) were identified in the studied section:

Nummulites fabianii retiatus (Prever), *Asterigerina rotula* (Kaufmarm), *Praerhapydionina* cf. *huberi*, *Fabiania* sp., *Pellatispira* aff. *Madaraszi*, *N. striatus*, *Alveolina* sp., *Spherogypsina* sp., *Gypsina marianensis*, *Eorupertia magna* (Le Calvez), *Neorotalia* sp., *Elphidium* sp., *Pyrgo* sp.

T. Ahmadi (✉)
Department of Geology, Payame Noor University (PNU),
P.O.BOX 19395-3697 Tehran, Iran
e-mail: t.ahmadi@pnu.ac.ir

Fig. 1 a- General map of Iran showing eight geologic zones [6] and b- Location of the studied section in southeast Iran



They represent one biozone which is described below. The Paleogene biozonation proposed by [2] was employed in this research and was compared with the biozonation of [3].

Nummulites fabianii Taxon-Range Zone

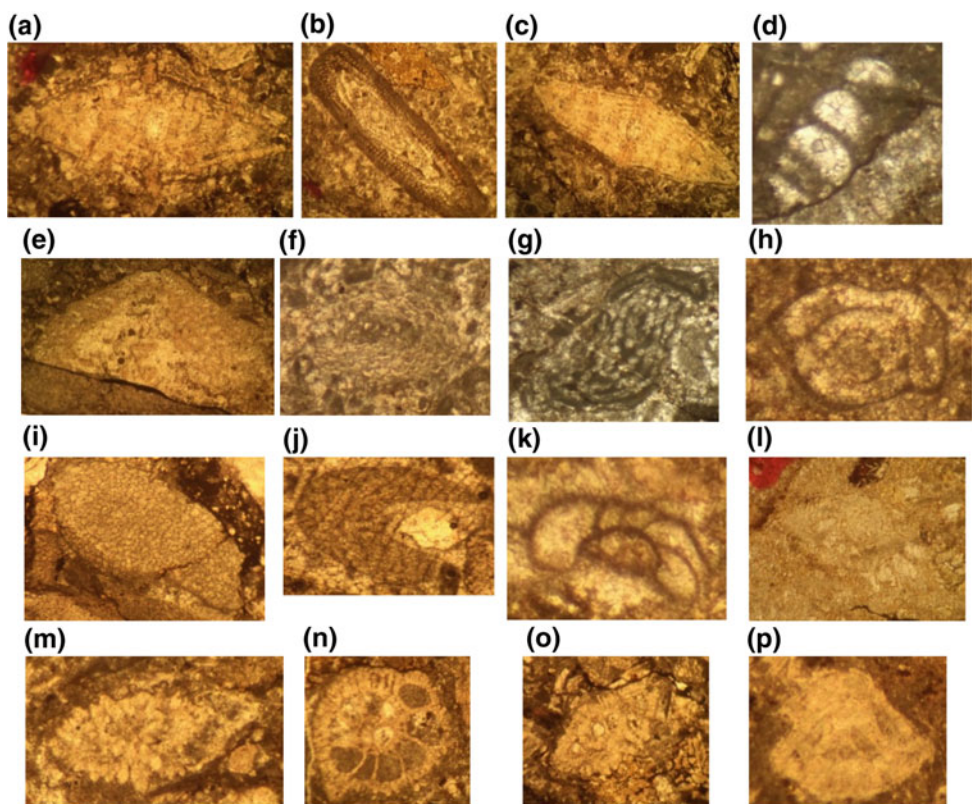
This biozone has been determined according to the presence and the domain of the *Nummulites fabianii* species. This biozone was dated to the Late Eocene (Priabonian) age which is equivalent to the SBZ19–SBZ20 Zones of [3].

3.2 Palaeoecology

Larger benthic foraminifera (LBF) are of the most important constituents to the modern, ancient tropical and shallow-marine sediments [4]. They are a useful tool for the reconstruction of the palaeoenvironmental and palaeoecological conditions of deposition.

The morphology, distribution and reproductive strategy of these organisms are influenced by the environmental

Plate 1 a, b and c- *Nummulites fabianii retiatius* (Roveda), d- *Praerhapydionina* cf. *huberi*, e- *Fabiania* sp. f- *Gypsina* sp., g- *Alveolina* sp., h- *Pyrgo* sp., i- *Gypsina marianensis*, j- Hook-shaped *Gypsina*, k- *Elphidium* sp., l, m- *Pellatispira* aff. *madaraszi*, n- *Eorupertia magna* (Le Calvez), o- *Neorotalia* sp, p- *Asterigerina rotula* (Kaufmann)



factors. With reference to the [4] foraminifera with robustness, the ovate tests and thick walls are dominated in shallow water; whereas, the flatter and thinner test are represented in deeper water.

Trevisani and Papazzoni [5] identified two different morphotypes of *Nummulites fabianii* which are distributed with respect to the environmental conditions in the thickening-coarsening upward cycles of Venetian Alps (northern Italy). The flat form (*N. fabianii retiatus*; D/T ratio average 2.8) is a characteristic of deeper marl facies. However, the more robust form (*N. fabianiiifabianii*; D/T ratio average 2.1) is restricted to shallower carbonate facies.

A/B ratio is another important factor that is controlled by the depth of the environment. Asexually-produced, A-form dominated fossil communities which are likely to have taken place in the shallowest or deepest parts of the depth range of a particular species while B-forms are most common in intermediate intervals of a specific depth range of a particular species. In the studied section, the A forms of *N. fabianii* group with large, flat and thin test (D/T ratio average 3) are the most important contributors of the studied section. They indicate deposition in middle-outer shelf where low levels of light and water energy are available.

Foraminifera are poikilothermic organisms. Thus, any changes in the ambient water temperature effect on their communities. The algal symbiont-bearing LBF have similar distribution to tropical and subtropical organisms such as corals and mangroves [4]. They are adapted to stable oligotrophic conditions. The symbiont-bearing LBF are major bio-components of the studied section which most of them belong to the rotaliids group. The rotaliids are stenohaline organisms. They are adapted to marine normal salinity.

4 Conclusion

Eocene deposits in west of Rafsanjan are composed of a carbonate unit which overlies the lower-middle Eocene volcanics with no conformity. A diverse assemblage of the benthic foraminifera was identified in this unit. One biozone was recognized on the basis of vertical distribution of these taxa along the stratigraphic column *Nummulites fabianii* of the Taxon-Range Zone. The palaeoenvironmental distribution of foraminiferal assemblages and the depositional conditions have been reconstructed (Plate 1).

References

1. Dimitrijevic, M.D., Dimitrijevic, M.N., Djordjevic, M.: Geological map of Rafsanjan (1/100000). Geol. Surv. Iran, sheet b7150 (1971)
2. Schaub, H.: Nummulites et Assilines de La Tethys Paleogene, Taxinomie, phylogenese et biostratigraphie. Memoires Suisses de Paleontologie, 104–236 (1981)
3. Serra-Kiel, J., Hottinger, L., Caus, E., Drobne, K., Ferrandez, C., Jauhri, A.K., Less, G., Pavlovec, R., Pignatti, J., Samsó, J.M., Schaub, H., Sirel, E., Strougo, A., Tambareau, Y., Tosequella, J., Zakrevskaya, E.: Larger foraminiferal biostratigraphy of the Tethyan Paleocene and Eocene. Bulletin de la Société Géologique de France **169**(2), 281–299 (1998)
4. Beavington-Penney, S.J., Racey, A.: Ecology of extant Nummulitids and other larger benthic foraminifera application in palaeoenvironmental analysis. Earth Sci. **67**, 219–265 (2004)
5. Trevisani, E., Papazzoni, C.A.: Palaeoenvironmental control on the morphology of *Nummulites fabianii* (Prever) in the Late Priabonian parasequences of the Mortisa Sandstone (Venetian Alps, northern Italy). Riv. Ital. Paleontol. Stratigr. **102**(3), 363–366 (1996)
6. Berberian, M., King, G.C.P.: Towards the paleogeography and tectonic evolution of Iran. Can. J. Earth Sci. **18**, 210–265 (1981)

The Tortonian–Messinian Transition in Saïss basin, South Rifian corridor (Morocco), Biostratigraphical and Paleoenvironmental Implications

Soukaina Targhi, Nadia Barhoun, Naima Bachiri Taoufiq, Mohamed Achab, and Abdallah Ait Salem

Abstract

The Saïss basin has long been the subject of numerous geological studies owing to its paleogeographic location in the western part of the South Rifian—Corridor that linked the Mediterranean to the Atlantic during the Tortonian–early Messinian (Cirac in *Mémoires de l’Institut de Géologie du bassin d’Aquitaine* 21:1–287, 1987 [3]; Wernli in *Notes Et Mémoires du Service géologique du Maroc* 331:1–270, 1988 [9]; Zizi in *Triassic–Jurassic extension and Alpine inversion in the northern Morocco*, pp 87–101, 1996 [10]). The Miocene–Pliocene sedimentary series deposited in Saïss basin have recorded the different biostratigraphic events, environmental, tectonic and eustatic factors that preceded the Messinian salinity crisis. The current data on the closure of the North and South Rifian corridors are conflicting and it cannot explain the thick evaporitic series accumulated during the Messinian salinity crisis (Capella et al. in *Earth Sci. Rev.* S0012–8252:30217–30219, 2018 [2]; Flecker et al. *Earth Sci. Rev.* 150:365–392, 2015 [4]). Does exist any other communication links between the Atlantic and the Mediterranean Sea? To resolve this issue, it must be established an accurate framework to the studied basin, delineated the vegetation evolution during the Tortonian–Messinian. Therefore, it may redound to understanding all

environmental, climatic and eustatic events that led to the Messinian salinity crisis, also to typify communications evolution between Atlantic and Mediterranean gateways across the southern Rifian corridor during the Upper Miocene.

Keywords

Saïss basin • Palynology • Biostratigraphy • Southern rifain corridor • Marine and continental environments • Tortonian–Messinian boundary

1 Introduction

The Miocene–Pliocene biostratigraphic data, vegetation and climate still incompletes; the only study that currently exists is that of Barhoun and Bachiri Taoufiq [1]. In order to specify a chronostratigraphical framework of Saïss basin deposits, and then get continuous vegetation and climate recording, a biostratigraphical study associated with a palynological study had proven necessary.

2 Materials and Methods

The borehole sediments derived from Saïss basin site belonging to southern rifian corridor. The area under study is located precisely in the western part of Saïss basin, at 20 km west of Meknes (33.8741–5.7534). All biostratigraphic Sampling used was muds/marls facies, 57 samples of sediment were processed using standard micropaleontological methods. It has been washed and sifted on a column of four mesh sieves successively in 63, 100, 160 and 250 μm . 300 individuals picked and identified from the 160 μm fraction. The samples were processing using standard palynological technique; the chemical treatment begins by

S. Targhi (✉) · N. Barhoun · N. Bachiri Taoufiq
Faculty of Sciences Ben M’Sik, Hassan II-Mohammedia
University, Sidi Othmane, BP7955 Casablanca, Morocco
e-mail: targhi.sokaina@gmail.com

M. Achab
Institute of Scientific Research, University Mohammed V-Souissi,
Ibn Batouta Avenue, Rabat, Morocco

A. Ait Salem
National Office of Hydrocarbons and Mines (ONHYM),
5 Avenue Moulay Rachid, Rabat, Morocco

adding hydrochloric acid (HCl) with a concentration of 20%, followed by hydrofluoric acid (40%) for the removal of carbonates and silicates component, a hot HCl was used to remove fluorosilicates each acid treatment was followed by neutralization with distilled water. After the chemical treatment all samples must be sift to remove the fine fraction, using a sieve with a mesh size of 10 μm . Before assembly slides, the obtained residues were usually liquefied with glycerin.

3 Results

3.1 Biostratigraphic Results

Foraminiferal assemblages are abundant and well diversified throughout the studied section. The planktono-benthic ratio pointed out that planktonic foraminifera dominate benthic foraminifera; it altered between 50% and 70%. A total of 34 planktonic species were identified. The keeled *Globorotalia* are well represented in relation to not keeled *Globorotalia*. Those are represented by the *G. menardii* group at the Tortonian and by *G. miotumida* group at the Messinian. The age of the biostratigraphic events identified is deduced from the correlation with the magnetostratigraphic and astronomical scale of Lourens et al. [5] (Figs. 1 and 2).

3.2 Palynological Results

Plant landscapes and climate: Pollen analysis reveals a diversified flora, composed of elements living today in

intertropical regions, subtropical to temperate-warm regions of America and Asia, alongside elements still living in Europe today and in Mediterranean regions. The representative elements of sub-desert environments and open plant formations, generally xeric, achieve high percentages.

Marine environment: The abundance of terrigenous inputs proves that the Ain Lorma drilling environment was epicontinental. Pollens and spores dominate dinocysts. The predominantly neritic dinocyst assemblage consists essentially of *Spiniferites spp.*, *Polysphaeridium zoharyii...* Oceanic taxa (*Impagidinium spp.*) are poorly represented (Fig. 3).

4 Discussion

The biochronology adopted for this presence work is grounded on marker species concept whose first, last regular occurrence or coiling changes. The biostratigraphic events identified were correlated with the magnetostratigraphic and astronomical scale of Lourens et al. [5]. We have determined the succession of four biostratigraphic events, from the bottom to the top:

- (1) LCO *Globorotalia menardii* S: corresponds to the disappearance or reduction of the group *Globorotalia menardii* with sinister winding (7.51 Ma);
- (2) FCO *Globorotalia menardii* D, marked by the, sometimes, abundant presence of the group *Globorotalia menardii* with dexter winding (7.35 Ma);
- (3) The replacement of the group *Globorotalia menardii* by the other one of *Globorotalia miotumida* S (7.24 Ma).

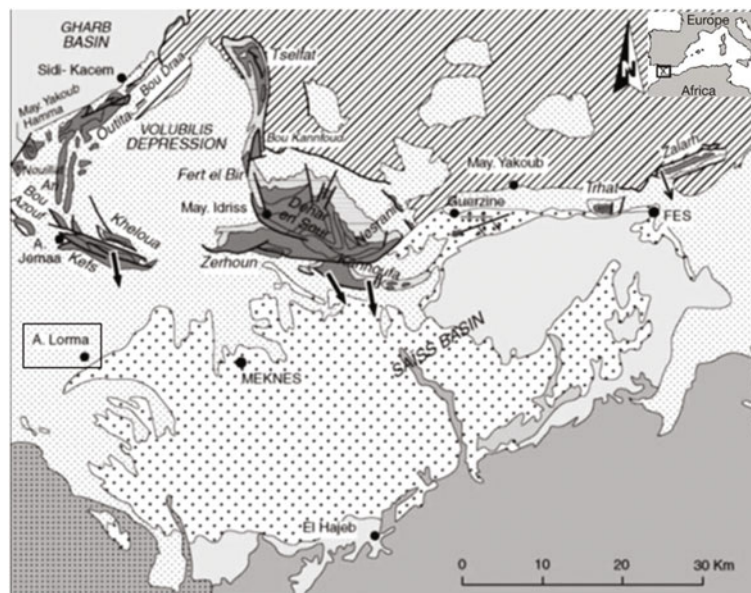


Fig. 1 Geographical and geological location of the studied area

tropical to subtropical and xeric on the coastal plain. Lower Messinian was slightly drier than Upper Tortonian.

In the Upper Tortonian, the site must have belonged to the external platform with small fluctuations. At the Tortonian–Messinian limit, there is a fall in dinocysts and an increase in land input. This could indicate a trend from the marine environment towards an internal shelf environment (IN). In Lower Messinian, the marine environment corresponds to an external platform (ON) with trends towards a medium internal platform.

The predominance of warm taxa reflects that the thermal conditions of the water surface were warm to subtropical.

5 Conclusion

A reliable analysis combines biochronologic and palynologic records for Ain Lorma (Sais basin). The bio-events recognized may be correlated with other adjacent Atlantic basins of the Western and Eastern Mediterranean sea, on the other hand; the biostratigraphy of the upper Tortonian and lower Messinian based on planktonic foraminifera events survey, is formally defined between 7.51 and 7.18 Ma.

The assemblages of dinoflagellate cysts, spores and pollens show that the continental inputs dominate the marine ones. The abundance of neritic dinoflagellate cyst and the rarity of the oceanic taxa explain that the deposition environment was neritic. Similarly, these assemblages indicate that the surface water was warm. The importance of the terrestrial inputs makes it possible to associate the sedimentary environment to an epicontinental one.

At the upper Tortonian, the distality markers indicate an external platform. At the Tortonian/Messinian boundary, there is a fall in the dinocysts and an increase in the terrestrial inputs. The marine environment at the Lower Messinian was an external platform type with trends towards an internal environment.

The vegetation cover is open and dominated by herbaceous plants that colonize the lower altitudes while trees grow at the medium altitudes. The climate is hot and humid in the middle altitude and dry in the low plain.

References

1. Barhoun, N., Bachiri Taoufiq N.: Événements biostratigraphiques et environnementaux enregistrés dans le corridor sud rifain (Maroc septentrional) au Miocène supérieur avant la crise de salinité messinienne. *Geodiversitas* **30**(1), 21–40 (2008)
2. Capella, W., et al.: Palaeogeographic evolution of the late Miocene Rifian Corridor (Morocco): Reconstructions from surface and subsurface data. *Earth Sci. Rev.* **S0012–8252**(17), 30217–30219 (2018)
3. Cirac, P.: Le bassin sud-rifain occidental au Néogène supérieur. Évolution de la dynamique sédimentaire et de la paléogéographie au cours d'une phase de comblement. *Mémoires de l'Institut de Géologie du bassin d'Aquitaine* **21**, 1–287 (1987)
4. Flecker, R., et al.: Evolution of the late Miocene Mediterranean–Atlantic gateways and their impact on regional and global environmental change. *Earth Sci. Rev.* **150**, 365–392 (2015)
5. Lourens, et al.: The Neogene period. In: Gradstein, F., Ogg, J., Smith, A. (eds.) *A Geologic Time Scale*. Cambridge University Press, London, pp. 409–440 (2004)
6. Parker, W.K., Jones, T.R., Brady, H.B.: On the nomenclature of the foraminifera, Part XII. The species enumerated by d'Orbigny in the “*Annales des Sciences Naturelles*”, vol. 7, pp. 1826. *Ann. Mag. Nat. Hist. Ser 3* **16**(3), 15–41 (1865)
7. SUC, J.P.: Flores Néogènes de méditerranée occidentales. *Climat et paléogéographie. Bull. Centres Rech. Explor-Prod. Elf-Aquitaine*, **10**(2), 477–488 (1986)
8. Sierro, F.J., et al.: The Abad composite (SE Spain): a Messinian reference section for the Mediterranean and the APTS. *Palaeogeogr. Palaeoclimatol. Palaeoecol.* **168**(1), 141–169 (2001)
9. Wernli, R.: Micropaléontologie du Néogène post-nappes du Maroc septentrional et description systématique des foraminifères planctoniques. *Notes Et Mémoires du Service géologique du Maroc* **331**, 1–270 (1988)
10. Zizi, M.: Triassic–Jurassic extension and Alpine inversion in the northern Morocco. In: Ziegler, P.A., Horvath, F. (eds.) *Peri-Tethys Memoir 2: Structure and Prospects of the Alpine Basins and Forelands*. *Mem Mus Nat Hist Nat, Paris*, pp. 87–101 (1996)



Early Pliocene Gastropods of Southern Pacific Coast of Mexico: Taxonomy and Paleogeography

Catalina Gómez-Espinosa, Claudia Ortíz-Jerónimo,
Luis Antonio Flores-de-Bois, and Oscar Talavera-Mendoza

Abstract

Gastropods mollusk from Punta Maldonado Formation (Pliocene age) were collected and identified. The studied area is located in the Southern Pacific Coast of Mexico precisely in the Panamic Malacological Province. The taxonomy of the malacofauna are revised, the distribution in the Recent Age are analyzed and their precise location over time are recorded. Forty-nine species belonging to thirty-two genera are identified, from them three species: *Conasprella armiger* (Crosse, 1858), *Solenosteira cf. dalli* (Brown & Pilsbry, 1911) and *Crepidula convexa* Say, 1822 are part of the recent Caribbean Malacological Province while *Enaeta barnesii* (Gray, 1825) has not been previously registered for the Guerrero Coast. The distribution of the gastropods during the Pliocene shows the relics of the fauna before the closure of the Isthmus of Panama.

Keywords

Marine gastropods • Early pliocene • Pacific ocean
Punta Maldonado • Guerrero Mexico

1 Introduction

The patterns of the circulation between the Pacific Ocean and the Gulf of Mexico have been drastically modified during the Cenozoic Era and the current distribution of mollusc associations reflects these changes.

During the Pliocene, there was a reconfiguration of the ocean gateways. The formation of the Isthmus of Panama produced modern patterns of the oceanic Pacific and the Atlantic circulation. It was a pivotal event that was a turning

point in the pale circulatory model driving global oceanic reorganization. It influenced the biogeography of both marine and continental fauna [1].

The purpose of this paper is to communicate the presence of marine gastropods in the Pacific coast of Southern Mexico during the Early Pliocene age, their taxonomy and biogeography. This study contributes to the understanding of the conformation of the current malacological provinces. A province is a large and continuous portion of water in which the oceanographic parameters are sufficiently similar and because of which it is inhabited by specific mollusk species [2].

Shallow water mollusk associations are sensitive to many variables with a temperature being the most important for the purposes of regional analyses. The thermal gradients are the ones that fundamentally determine the disposition of the malacological provinces nowadays. The available evidence indicates that the same happened in the past [3].

Punta Maldonado Formation in Guerrero State is actually included in the “Panamic Province”. However, the hypothesis that is proposed is that during the Pliocene there were some remains of the “Caribbean Province”.

2 Materials and Methods

Punta Maldonado Formation is named for the nearest village. It is located in the southern part of Guerrero State in the Costa Chica Region, Guerrero State, Pacific coast of Mexico. Lithologically, it is composed of sandstone and siltstone with an early age of the Pliocene (Piazian) between 5.3 and 3.6 Ma [4]. Member VI contains abundant fossil remains including foraminifera, ostracoda, mollusks (gastropods, bivalves and scaphopodes), fish otoliths and fragments of vertebrates. Gastropods are so well preserved to the point that many of them retain some of their original coloration.

Gastropods mollusk were collected and identified. Their taxonomy was revised. Their classification is in agreement with Bouchet and Rocroi [5] and WoRMS [6].

C. Gómez-Espinosa (✉) · C. Ortíz-Jerónimo
L. A. Flores-de-Bois · O. Talavera-Mendoza
Escuela Superior de Ciencias de la Tierra, Universidad Autónoma
de Guerrero, 40323 Taxco El Viejo, Guerrero, Mexico
e-mail: c_gomez@ciencias.unam.mx

The distribution process in the Recent was analyzed. Their precise location over time was recorded.

3 Results

Forty-nine species belonging to thirty-two genera of marine gastropods are identified from the silty member of the Punta Maldonado Formation: *Amaea brunneopicta* (Dall, 1908), *A. ferminiana* (Dall, 1908), *Architectonica nobilis* Röding, 1798, *Calyptraea mamillaris* Broderip, 1834, *Cancellaria darwini* Petit, 1970, *C. gemmulata* G. B. Sowerby I, 1832, *C. indentata* G. B. Sowerby I, 1832, *C. jayana* Keen, 1958, *Carinodrillia hexagona* (Sowerby I, 1834), *C. duplicata* (Sowerby I, 1834), *Conasprella arcuata* (Broderip & G. B. Sowerby I, 1829), *C. armiger* (Crosse, 1858), *Conus fergusonii* P. B. Sowerby II, 1873, *Crepidula convexa* Say, 1822, *Crucibulum lignarium* (Broderip, 1834), *C. monticulus* Berry, 1969, *Distorsio deccusata* (Valenciennes, 1832), *Enaeta barnesii* (Gray, 1825), *Epleura muriciformis* (Broderip, 1833), *Fusinus* sp., *Glyphostoma thalassoma* Dall, 1908, *Grandiconus* sp., *Hindsiclava hertleini* Emerson & Radwin, 1969, *H. militaris* (Reeve, 1843), *Hipponix pilosus* (Deshayes, 1832), *Knefastia olivacea* (Sowerby I, 1834), *Knefastia* sp., *Lottia acutapex* (S. S. Berry, 1960), *Miraclothurella mendozana* Shasky, 1971, *Natica broderipiana* Récluz, 1844, *Oliva* sp., *Olivella volutella* (Lamarck, 1811), *Pristiterebra tuberculosa* (Hinds, 1844), *P. glauca* (Hinds, 1844), *Polinices intemeratus* (Philippi, 1853), *Polystira nobilis* (Hinds, 1843), *P. picta* (Reeve, 1843), *Solenosteira cf dalli* (Brown & Pilsbry, 1911), *Stramonita biserialis* (Blainville, 1832), *Strombina fusinoidea* Dall, 1916, *Strombinoturris crockeri* Hertlein & A. M. Strong, 1951, *Subcancilla attenuata* (Broderip, 1836), *Terebra armillata* Hinds, 1844, *T. elata* Hinds, 1844, *T. lucana* Dall, 1908, *Trajana perideris* (Dall, 1910), *Triplofusus princeps* (G. B. Sowerby I, 1825), *Turritella leucostoma* Valenciennes, 1832 and *T. radula* Kiener, 1843.

4 Discussion

Despite the planktonic dispersal of the mollusk larvae, the marine gastropods species exemplify the biogeographic differentiation that occurred on both sides of the Central American isthmus [7, 8]. From the species identified, three have not been recorded for the Recent Epoch in the Pacific Coast. *Conasprella armiger* (Crosse, 1858), *Solenosteira cf dalli* (Brown & Pilsbry, 1911) and *Crepidula convexa* Say, 1822 are considered as marine gastropods from the Atlantic Ocean. *C. convexa* is a native species of the North-American Atlantic coast, from Canada to Quintana Roo (México) [9].

The present distribution of *C. convexa* in the Pacific coast is because of the Oyster farming. The introduction and settlement of this species are closely related to the American oysters (*Crassostrea virginica*, Gmelin, 1791) farming since the 1940's [10]. In the recent, they have spread worldwide throughout the northern hemisphere while the distribution of *C. armiger* in the present is from Florida (USA) to Surinam [11]. In the case of *S. dalli*, it is a species reported from the Miocene of Panama (Gatun Formation) [12].

The presence of *Enaeta barnesii* (Gray, 1825) is also remarkable because although it belongs to the Panamic Malacological Province, it has not been registered for the Guerrero Coast during the Recent (Flores-Garza *com. pers.*)

5 Conclusion

Forty-nine species belonging to thirty-two genera of marine gastropods are identified from the silty member of the Punta Maldonado Formation, Guerrero State, Mexico.

During the Pliocene, the gastropod fossil assemblage present in the South Pacific coast of Mexico (Punta Maldonado, Guerrero) still show affinities with the Caribbean Malacological Province because of the presence of the species *Solenosteira cf dalli*, *Conasprella armiger* and *Crepidula convexa*. It is the result of the uncomplete closure of the Isthmus of Panama and the planktonic dispersion of the larvae.

Acknowledgements This study was supported by SEP-PROMEP Project "Aplicación de los moluscos (bivalvos y gasterópodos) del Neógeno (Plioceno) como proxies para cuantificar los efectos a mediano plazo del cambio climático en las zonas costeras en Guerrero, México". We want to thanks to Dr. Rafael Flores-Garza, UAEM, UAGro and Dra. Martha Reguero Reza, ICMYL, UNAM for their help with the taxonomy.

References

- Schmidt, D.N.: The closure history of the Central American seaway: evidence from isotopes and fossils to models and molecules. In: Williams, M., Haywood, A.M., Gregory, F.J., Schmidt, D.N. (Eds.), *Deep-Time Perspectives on Climate Change: Marrying the Signal from Computer Models and Biological Proxies*. The Micropalaeontological Society, Special Publications, pp. 429–444. The Geological Society, London (2007)
- Conchylineth: Seashells distribution. <http://www.conchylineth.com/page23.php?Page=23&Level=2>. Accessed 24 Apr 2018
- Martínez, R., Del Río, C.: Las provincias malacológicas miocenas y recientes del Atlántico sudoccidental. *An. Biol.* **24**, 121–130 (2002)
- Juárez-Arriaga, E., Carreño, A.L., Sánchez-Zavala, J.L.: Pliocene marine deposits at Punta Maldonado, Guerrero state. Mexico. *J. South Am. Earth Sci.* **19**(4), 537–546 (2005)

5. Bouchet, P., Rocroi, J.R., Frýda, J., Hausdorf, B., Ponder, W., Valdes, A., Warén, A.: A nomenclator and classification of gastropod family-group names. *Malacologia* **47**(1–2), 1–368 (2005)
6. WoRMS: The World Register of Marine Species. <http://www.marinespecies.org/>. Accessed 27 Apr 2018
7. Vermeij, J.: Distribution, history, and taxonomy of the thais clade (gastropoda: muricidae) in the Neogene of tropical America. *J. Pal.* **75**(3), 697–705 (2001)
8. Landau, B., DaSilva, C.M., Vermeij, J.: Pacific elements in the Caribbean Neogene gastropod fauna: the source-sink model, larval development, disappearance, and faunal units. *Bull. Soc. géol. Fr.* **180**(4), 249–258 (2009)
9. Collin, R.: Another last word on *Crepidula convexa* and a description of *C. ustulatulina* sp. nov. (Gastropoda: Calyptraeidae) from the Gulf of Mexico. *Bull. Mar. Sci.* **70**(1), 177–184 (2002)
10. Carlton, J.T.: Introduced marine and estuarine mollusks of North America: an end-of-the-20th-century perspective. *J. Shellfish Res.* **11**(2), 489–505 (1992)
11. Sunderland, K.: Caribbean Conidae. *American Conchologist* **18**(3), 14–15 (1990)
12. Florida Museum: Fossils of Panama. https://www.floridamuseum.ufl.edu/panama-pire/fossils-of-panama/solenosteira_dalli.htm. Accessed 14 June 2018

Composition of the Pliocene Meiofauna from Punta Maldonado Formation, Guerrero (Mexico)

Frank Raúl Gío-Argaez, Catalina Gómez-Espinosa, Luis Antonio Flores-de-Bois, Delfina Cruz-Flores, and Sergio Salgado-Souto

Abstract

The objective of this study is to report Punta Maldonado's most representative species of the Pliocene meiofauna which is identified in the coastal sediments, located between Oaxaca and Guerrero states along the Pacific Ocean, Mexico. Punta Maldonado's marine terraces are constituted by three lithostratigraphic units: the bedrock is fine-grained marine sandstone which is uncomfortably overlain by continental deposits made up of fine-grained sandstone. However, the youngest deposits are made up of a sequence that consists of humus and sandstone beds. The marine strata in Punta Maldonado must be considered as a new lithostratigraphic unit of the Cenozoic era which has not been formally described. The taxonomic identification of 21 foraminifera and 8 ostracods genera corresponds to the early Pliocene (Piacenzian). The analysis of the meiofauna has allowed us to retrieve corals, crustacean remains, echinoderm spicules, molluscs (gastropods, pelecypods and scaphopods) and six genera of fish otoliths. The ecological relationships of these biota will be interpreted to a better understanding of the shallow marine biocenosis in the Pacific Mexican Coast during the Pliocene.

Keywords

Pliocene • Meiofauna • Pacific ocean • Mexico

F. R. Gío-Argaez (✉)

Instituto de Ciencias del Mar y Limnología, Universidad Autónoma de México, 04510 Coyoacán, Mexico City, Mexico
e-mail: raulgio@cmarl.unam.mx

C. Gómez-Espinosa · L. A. Flores-de-Bois · S. Salgado-Souto
Escuela Regional de Ciencias de la Tierra, Universidad Autónoma de Guerrero, 40323 Taxco el Viejo, Guerrero, Mexico

D. Cruz-Flores

Facultad de Ciencias, Universidad Nacional Autónoma de México, 04510 Coyoacan, Mexico City, Mexico

1 Introduction

Meiofauna is a collective name for one of the most diversified communities of the marine realm including small organisms, unicellular protists and multicellular metazoans that live in aquatic sediments [2]. Meiofaunal organisms are smaller than macrofauna and larger than microfauna with a size between 500 μm to 64 μm . The division of the fauna on the basis of size is real as species in the benthic communities have a genuine bimodal size distribution [4].

Even though the meiofauna is the best example of the most diversified group in the marine realm, this group represents an often neglected component of the marine biodiversity [1]. It is generally poorly studied.

Among the different categories of organisms, meiofauna offer several advantages for the study of the marine benthic ecosystems because their abundance, diversity, distribution and their sensitivity to abiotic factors as temperature, salinity, hydrodynamic and sedimentary processes, sediment grain size, oxygenation level and food availability [6].

2 Materials and Methods

The described otoliths in the following section have been obtained from Punta Maldonado Formation, Guerrero State, Mexico. Punta Maldonado's marine terraces are constituted by three lithostratigraphic units: the bedrock is a fine-grained marine sandstone which is unconformably overlain by continental deposits made up of fine-grained sandstone; whereas, the youngest deposits are made up of a sequence that consists of humus and sandstone beds.

The marine strata in Punta Maldonado must be considered as a new lithostratigraphic unit of the Cenozoic era which has not been formally described. For the detailed description of the lithology, reference is made to Juárez-Arriaga et al. [3].

For the purpose of this study, a mesh aperture of 63 μ was used to sieve the sediments. The obtained samples were reviewed under a microscope, separated for taxa, measured and photographed in a microscope. Then, the samples were taxonomically identified. The morphometric measurements of the otoliths follow Schwarzhans [5].

3 Results

The Meiofauna in Punta Maldonado is composed by foraminifers, ostracods, bivalves and gastropods protochonch, scaphopods, corals, crustacean remains, echinoderm spicules and fish otoliths.

Some of them cannot be identified because there are very young stages as the corals and molluscan protochonch while the others (crustaceans and echinoderm spicules) are only fragments that cannot be recognized at the family level.

The rest of the samples were identified to genus level. The number of the genera identified for each taxonomic group are in the Table 1.

Between the foraminifers a remarkable presence of the species *Globorotalia humerosa* (Takayanagi and Saito 1962), *Planulina exorna* (Phleger and Parker 1951), *Eponides parantillarum* (Galloway and Heminway 1941) and *Orbulina universa* (d'Orbigny 1839). From the ostracods to species level were identified *Cyprideis currayi* (Swain 1967), *Trachyleberidea henryhowei* (McKenzie and Swain 1967) and *Cytherella ovularia* (Swain 1967).

The scaphopoda are represented by two genera that correspond to *Dentalium* Linnaeus, 1758 and *Cadulus* Philippi,

1844. The otoliths genera identified correspond to *Opisthonema* Gill 1861, *Prionotus* Lacepède, 1801, *Gymnothorax* Bloch, 1795, *Sparisoma* Swainson, 1839 and *Deltentosteus* Gill, 1863 (see Fig. 1).

4 Discussion

The four classical branches of the Palaeontology are Micropaleontology, Paleobotany, Invertebrate Palaeontology and Vertebrate Palaeontology. With the study of the meiofauna of Punta Maldonado, the examinations of three of these branches are included. The foraminifera and the ostracoda that are considered as part of the micropaleontology, Mollusca from the Invertebrate Palaeontology and fish otoliths from the Vertebrate Palaeontology.

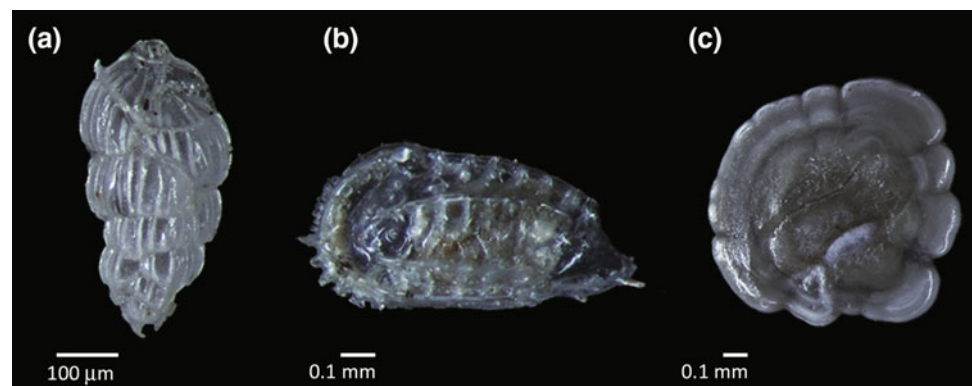
The study of these organisms will give us a more complete perspective about the biotic composition of the marine biocenosis during the Pliocene in the Pacific Coast of Mexico. The interpretation of the ecological relationships between these communities will be very helpful to understand the trophic chain and even the speculation of the existence of some organisms that did not leave a fossil record.

In the specific case of the otoliths, it is assumed that the presence of the predators of fishes, just like seals or marine lions, which in the Recent after eating the fishes defecate otoliths that is the part that cannot be digested. It is suggested that this situation was a possibility in the deposits studied because no more fish remains have been found.

Table 1 Meiofauna genera number per taxa identified from the Pliocene of Punta Maldonado, Guerrero

Taxa	Number of genera identified
Foraminifera	21
Ostracoda	8
Mollusca scaphopoda	2
Chordata osteichthyes	5

Fig. 1 Image showing some of the more representative species **a** *Uvigerina excellens* Todd, 1948 foraminifer **b** *Trachyleberidea henryhowei* McKenzie and Swain, 1967 ostracod **c** *Soarisoma cretense* (Linnaeus, 1758) fish otolith



5 Conclusion

The meiofaunal assemblage of the Pliocene in Punta Maldonado are composed of foraminifera, ostracoda, cnidarian (corals), mollusca (gastropoda, bilvalvia and scaphopoda), echinodermata and chordata (osteichthyes).

Corals, moluscan gastropods and bivalves and echinoderm spicules were not possible to identify taxonomically. Foraminifera are represented by 21 genera. From them, six were identified to species level. Ostracoda are represented by 8 genera. Only three from them have been identified to species level. Mollusca scaphopoda are represented by 2 genera. From the Osteichthyes exclusively represented by fish otoliths, five genera were identified.

The study of the meiofauna fossil will give us the opportunity to reconstruct some of the paleoecological relationships and abiotic factors during the Pliocene in the Pacific Coast of Mexico.

Acknowledgements This study was supported by SEP-PROMEP Project “Aplicación de los moluscos (bivalvos y gasterópodos) del Neógeno (Plioceno) como proxies para cuantificar los efectos a

mediano plazo del cambio climático en las zonas costeras en Guerrero, México”.

References

1. Curini-Galletti, M., Artois, T., Delogu, V., De Smet, W.H., Fontaneto, D., et al.: Patterns of diversity in soft-bodied meiofauna: dispersal ability and body size matter. *PLoS ONE* **7**(3), e33801 (2012)
2. Giere, O.: *Meiobenthology. The Microscopic Motile Fauna of Aquatic Sediments*. 2nd edn. Springer, Berlin (2009)
3. Juárez-Arriaga, E., Carreño, A.L., Sánchez, J.L.: Pliocene marine deposits at Punta Maldonado, Guerrero state, Mexico. *J. S. Am. Earth Sci.* **19**, 537–546 (2005)
4. Somerfield, P.J., Warwick, R.M.: *Meiofauna techniques*. In: Eleftheriou, A. (ed.) *Methods for the Study of Marine Benthos*, 4th edn. Wiley-Blackwell Ltd, Oxford (2013)
5. Schwarzhans, W.: A comparative morphological study of the Recent otoliths of the genera *Diaphus*, *Idiolychnus* and *Lobianchia* (Myctophidae). *Palaeo Ichthyologica* **13**, 41–82 (2013)
6. Zepilli, D., Sarrazin, J., Leduc, D., Martínez, P., Fontaneto, D., et al.: Is the meiofauna a good indicator for climate change and anthropogenic impacts? *Mar. Biodivers.* **45**(3), 505–535 (2015)

Part IV
Sedimentology

Gravel Bed River Scouring Analysis Downstream of Block Ramps

Karol Plesiński and Artur Radecki-Pawlik

Abstract

The paper describes the scouring process of a river bed downstream of block ramp hydraulic structures. The scour depth of the river bed downstream of the block ramps was calculated by using several different empirical formulae from the literature. The calculated results were verified with the measured results collected during the field measurements. The current paper presents the most appropriate formulae for the comparison of the scouring results with the obtained field measurements. It was found that the calculated values of scouring are usually much higher than those observed in the field. The most important aim of this paper is to verify the obtained empirical formulae for scouring downstream of block ramps based on the results of the field measurements.

Keywords

Bed erosion • Bed scour • Empirical formulae • Block ramp

1 Introduction

Determining the bed river scour is an extremely difficult issue. The most reliable methods are based in the simulation of the designed structure on the physical model in the laboratory and in the simulation on the numerical model [1–4]. However, such studies are time-consuming, labor-intensive and the data obtained from the laboratory may differ from those of the existing ones in the field. Another method to

K. Plesiński (✉)
Department of Hydraulic Engineering and Geotechnics,
University of Agriculture in Krakow, Mickiewicza Street 24/28,
30-059 Krakow, Poland
e-mail: k.plesinski@ur.krakow.pl

A. Radecki-Pawlik
Cracow University of Technology, Institute of Structural
Mechanics, Warszawska Street 24, 31-155 Krakow, Poland

determine the size of the bed river scour is the result based on calculation with used empirical formulas. Such data were calculated by using different formulas giving very different results which may lead to some errors in predicting scour.

2 Methods

The conducted research gave two types of structures: cascade block ramp on Poniczanka Stream and concrete block ramp on Raba River. The main construction element of these structures is the apron slope. Both block ramps don't have energy dissipation basin (Fig. 1).

Before and after the flood, cross-sections were done on Porębianka Stream and Raba River. The longitudinal profile of the section was analyzed (Fig. 1). The measured places were located at certain distances from the block ramp. For each set of the series, the actual depth of the scour bed was obtained.

By using the empirical formulas, the theoretical maximum depths of the scour were calculated and then compared with the real size in order to determine which calculated formulas give the nearest results.

The following were used for the analysis formulas: Eggenberger, Jaeger, Lacey, Chividini, Mason, Martins, Veronese, Chan Min Wu, Whittaker and Jäggi, Pagliara, Volkarta and Ślizowski [5–12]:

$$\text{Eggenberger formula: } h_{max} = w \cdot \frac{h_d^{0.5} q^{0.6}}{d_{90}^{0.3}} - h_d$$

Jaeger formula:

$$h_{max} = 0,55 \left[6 \cdot h^{0,25} \cdot q^{0,25} \cdot \left(\left(\frac{h_d}{d_{90}} \right)^{1/3} - h_d \right) \right]$$

$$\text{Lacey formula: } h_{max} = 0,475 \cdot \left(\frac{Q}{f} \right)^{1/3}$$

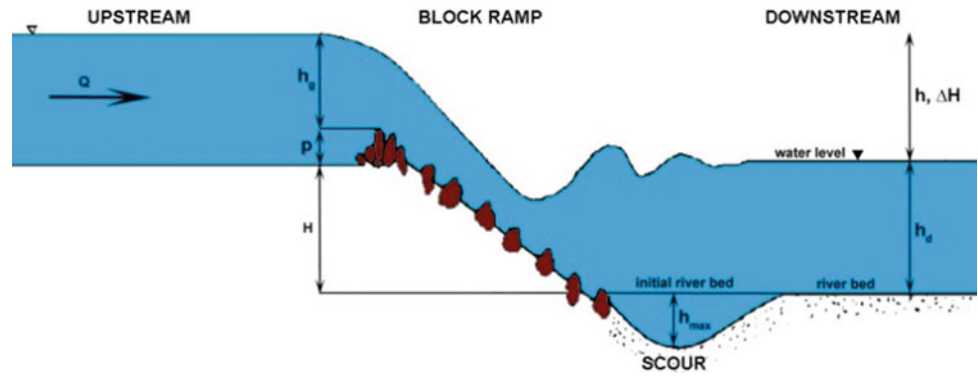
$$\text{Chividini formula: } h_{max} = k \cdot Z^{0,5} \cdot h$$

$$\text{Mason formula: } h_{max} = 3,27 \cdot q^{0,6} \cdot h^{0,15} \cdot h_d^{0,05} \cdot g^{-0,3} \cdot d^{-0,1}$$

$$\text{Martins formula: } h_{max} = 1,5 \cdot q^{0,6} \cdot h^{0,1}$$

$$\text{Veronese formula: } h_{max} = 1,9 \cdot q^{0,54} \cdot h^{0,225}$$

Fig. 1 Scheme of block ramp and river bed scour



Chian Min Wu formula: $h_{max} = 1,18 \cdot q^{0,51} \cdot h^{0,235}$

Whittaker & Jäggi formula:

$$h_{max} = 1,31 \cdot q^{0,5} \cdot v^{0,5} - 7,125 \cdot d_{90}$$

Pagliara formula: $h_{av} = 0,58 \cdot U_{84}^{-0,55} \cdot I^{0,75} \cdot Fr_{d50}$,

$$h_{max} = (1 + 1,75 \cdot Fr_{d50}^{-1,75}) \cdot h_{sr}$$

$$\text{Volkart formula: } h_{max} = 1,25 \cdot \frac{q^{1/2} \cdot I^{1/2} \cdot L^{3/2}}{d_{90}^{1/2}} \cdot \frac{\rho_w}{(\rho_s - \rho_w) \cdot g^4}$$

$$\text{Ślizowski formula: } h_{max} = \frac{(a_0 + a_1 Q + a_2 I + a_3 \Delta H)}{100}$$

where:

h_{max} —maximum depth scour [m],

h_{av} —average depth scour [m],

$h, \Delta H$ —different water level between upstream and downstream ($h_g - h_d$) [m],

Q —calculated discharge [$m^3 \cdot s^{-1}$],

q —unit discharge [$m^2 \cdot s^{-1}$],

h_d —water depth in downstream [m],

$d, d_{16}, d_{50}, d_{84}, d_{90}$ —sediment diameter [m].

w —coefficient, according to Zástěry (1984) its value will be equal 0.45, so according to Vicent (1968), we should calculate from equation: $w = \frac{(h'_{max} + h_d) \cdot d_{90}^{0,4}}{h^{0,5} \cdot q^{0,6}}$ [-],

I —drop of block ramp [-],

k —safety coefficient [-],

U_{84} —uniform sediment coefficient: $U_{84} = \sqrt{\frac{d_{84}}{d_{16}}}$ [-],

Fr_{d50} —densimetric Froude's number: $Fr_{d50} = \frac{v}{\sqrt{g \cdot d_{50}}}$ [-],

Table 1 Calculation values of maximum depth scour h_{max}

Empirical formulas	Poniczanka stream		Raba river	
	h_{max} [m]—maximum scour depth calculation	Deviation from field value [m]	h_{max} [m]—maximum scour depth calculation	Deviation from field value [m]
Eggenberger	3.59	+2.84	2.50	+1.63
Jaeger	8.81	+8.06	7.61	+6.74
Lacey	2.07	+1.32	2.44	+1.57
Chividini for:				
$k = 1$	1.23	+0.48	0.98	+0.11
$k = 2$	2.46	+1.71	1.97	+1.10
$k = 3$	3.69	+2.94	2.95	+2.08
Martins	3.32	+2.57	2.69	+1.82
Veronese	4.26	+3.52	3.39	+2.52
Chian Min Wu	2.57	+1.82	2.06	+1.19
Mason for:				
d_{50}	4.97	+4.21	4.13	+3.26
d_{90}	5.17	+4.43	3.95	+3.08
Whittaker & Jäggi	3.85	+3.10	3.43	+2.56
Pagliara	1.03	+0.28	0.58	-0.29
Volkart	6.40	+5.65	4.51	+3.64
Ślizowski	0.54	-0.21	0.87	0.00

v —average velocity was measured before the scour [$\text{m}\cdot\text{s}^{-1}$],
 g —gravity [$\text{m}\cdot\text{s}^{-2}$],
 L —length of block ramp [m],
 ρ_s —sediment density [$\text{kg}\cdot\text{m}^{-3}$],
 ρ_w —water density [$\text{kg}\cdot\text{m}^{-3}$],
 Z —drop numer: $Z = \frac{q}{(g\cdot h^3)^{0.5}}$ [-],

f —sediment function, measured from equation: $f = 1,75 \cdot d_{90}^{0.5}$ [-],

a_0 —coefficient: $a_0 = -0,0005 \pm 0,0006$

a_1 —coefficient: $a_1 = 1,6010 \pm 0,0740$

a_2 —coefficient: $a_2 = 0,1552 \pm 0,0120$

a_3 —coefficient: $a_3 = 0,0389 \pm 0,0300$

3 Results and Discussion

In Table 1, the results of maximum depth scour are shown. They were calculated by using a few empirical formulas. The real depth of the measured scour in the field was equal to $h_{\max} = 0.75$ m on the Poniczanka Stream and $h_{\max} = 0.87$ m in the Raba River. The use of the above formulas made it possible to obtain very diverse values.

4 Conclusion

The paper can be concluded as follows:

1. The formulas for calculating the maximum depth scour of the river bed below the block ramps give the best results are the Ślizowski formula, Pagliara formula and Chividini for $k = 1$ (deviation from the real value to ± 0.50 m). The remaining formulas should not be used to calculate the bed river scour because they give very high and sometimes unrealistic results.
2. The use of the empirical formulas for the theoretical maximum depth scour leads us to obtain inaccurate results. They are only partially similar to real values. These values can be used for comparative analyzes of different kinds of block ramps.
3. The worst results for depth scour were obtained from the following formulas: Jeager, Voklart, Veronese, Whittaker & Jäggi, Chividini (for $k = 3$) (≥ 2 m), Eggenbergea and

Martins. These equations should be categorically avoided in order to calculate the maximum depth scour.

4. The obtained results are local. Other results can be observed below the other kinds of block ramps and particularly in different river channel.

References

1. Sattar, A.M.A., Plesiński, K., Radecki-Pawlik, A., Gharabaghi, B.: Scour depth model for grade-control structures. *Journal of Hydroinformatics* **20**(1), 117–133 (2018)
2. Pagliara, S., Radecki-Pawlik, A., Palermo, M., Plesiński, K.: A Preliminary Study of field scour morphology downstream of block ramps located at river bends. [in:] Bung, D., Tullis, B. (eds.) 7th IAHR International Symposium on Hydraulic Structures, Aachen, Germany, 15–18 May 2018, Utah State University, <https://doi.org/10.15142/T39352>.
3. Plesiński, K., Pachla, F., Radecki-Pawlik, A., Tatara, T., Radecki-Pawlik, B.: Numerical 2D simulation of morphological phenomena of a block ramp in Poniczanka stream: Polish Carpathians [in:] Bung, D., Tullis, B. (eds.) 7th IAHR International Symposium on Hydraulic Structures, Aachen, Germany, 15–18 May 2018, Utah State University, <https://doi.org/10.15142/T31M17>.
4. Plesiński, K., Radecki-Pawlik, A., Wyżga, B.: Sediment Transport Processes Related to the Operation of a Rapid Hydraulic Structure (Boulder Ramp) in a Mountain Stream Channel: A Polish Carpathian Example [in:] Heininger, P., Cullmann, J. (eds.) *Sediment Metters*, : 39–58. Springer, Koblenz (2015)
5. Dąbkowski, S.L., Skibiński, J., Żbikowski, A.: The hydraulic bases of water-reclamation projects. PWRiL, Warsaw [in Polish] (1982)
6. Pagliara, S.: Influence of sediment gradation on scour downstream of block ramps. *J. Hydraul. Eng.-ASCE* **133**, 1241–1248 (2007)
7. Pagliara, S., Palermo, M.: Scour control and surface sediment distribution downstream of block ramps. *J. Hydraul. Res.* **46**(3), 334–343 (2008)
8. Pagliara, S., Radecki-Pawlik, A., Palermo, M., Plesiński, K.: Block ramps in curved rivers: morphology analysis and prototype data support of design criteria for mild bed slopes. *River Res. Appl.* **33** (3), 427–437 (2017)
9. Sindelar, C.: Design of a Meandering Ramp, Ph.D. Thesis, Technische Universität Graz (2011)
10. Ślizowski, R.: Increased roughness Rapids as an element used for stabilization of mountains streams. *Prace Komisji Geodezji i Inżynierii Środowiska. PAN. Krakow* (2004)
11. Ślizowski, R., Radecki-Pawlik, A.: Verification of formulae for calculating scour below hydraulic structure using laboratory results. *Acta Scientiarum Polonorum: Formatio Circumiecus* **2** (2), 25–34 [in Polish] (2003)
12. Zástěra, Z.: Block ramps. *Hydroprojekt O.Z., Rezortni Ukol R-4, Brno* [in Czech] (1984)

Diagenesis and Reservoir Quality of Glacio-Lacustrine Sandstones: An Example from the Upper Carboniferous-Lower Permian Al Khlata Formation in Wadi Daiqa, Northern Oman

Mohamed A. K. El-Ghali, Nasayaba Al-Hinai, Kothar Mandhari, and Junaid Khan

Abstract

Controls on the diagenesis of ancient glaciogenic sandstone reservoirs are still poorly-constrained. This study examines and documents the types, the spatial and the temporal distribution of diagenetic alterations and their subsequent impact on reservoir quality of sandstones from the outcropped Late Carboniferous, glacio-lacustrine Al Khlata Formation in Wadi Daiqa, Northern Oman. An integration of textural and petrographic with geochemical analysis revealed that sandstones have undergone various diagenetic histories during eo- and mesogenetic stages. Eodiagenetic alterations are dominated by mechanical compaction and rarely by kaolinization of chemically unstable framework grains such as feldspars, micas and calcite cements. In contrast, mesodiagenesis is extensively dominated by the occurrence of the chemical compaction, quartz overgrowths, illitization of grains coating clay and micas and rarely calcite cements. Paragenetic sequence revealed that compaction has played significant role than cementation in destroying porosity and thus reservoir quality. Such an extensive compaction (mechanical and chemical) and scarcity of early cementation are attributed to the high rate of sedimentation due to glacier retreat and melting. The availability of meteoric waters as a result of glacier melting was responsible for silicate framework grains dissolution and kaolinite formation.

Keywords

Glacial • Diagenesis • Sandstone • Reservoir quality Al khlata

1 Introduction

The parameters controlling diagenesis and their subsequent impact on reservoir quality of ancient glaciogenic sandstones are still poorly understood and thus less documented in literature [1, 2]. The Late Carboniferous-Early Permian Al Khlata Formation of the Haushi Group is related to the third glacial event in the Arabian Plate. The glacially Al Khlata Formation sandstones are important hydrocarbon reservoirs in Oman. This study aims to explore and understand the controlling parameters on types and distributions of diagenetic alterations and their subsequent impact on reservoir quality of Al Khlata Formation sandstones. The study is carried out on the well-exposed Late Carboniferous Al Khlata Formation section represented by a glacio-lacustrine facies in Wadi Daiqa (i.e. distal part), Northern Oman [3].

2 Materials and Methods

Sixty sandstone samples have been collected from the well-outcropped, Late Carboniferous [3], Al Khlata Formation in Wadi Daiqa, North Oman. Thin sections were prepared for all the samples in order to introduce detailed textural and petrographic examination. The textural analysis was performed by taking 100 measurements for each thin section along the longest axes to determine the grain size and sorting. The modal composition was obtained for all thin-sections by counting 300 points per each one. JEOL JSM-7600F Scanning Electron Microscope (SEM) equipped with digital imaging system, EDS and BSI was used to investigate the habits and the textural relationships of diagenetic minerals on 15 selected sandstone samples. The samples were coated with a thin layer of gold and examined under an acceleration voltage of 15 kV and current beam of wavelength $4.5 \times 10^{-11} \text{A}^\circ$. XRF and XRD analysis were also performed on 15 powdered sandstone samples for whole rock geochemistry and mineral composition, respectively.

M. A. K. El-Ghali (✉) · N. Al-Hinai · K. Mandhari · J. Khan
Sultan Qaboos University, Al-Khod, 123, Sultanate of Oman
e-mail: melghali@squ.edu.om; ; mohamed.elghlali@gmail.com

3 Results

3.1 Sandstones Texture and Modal Composition

The studied Al Khlata Formation sandstones are commonly very fine-, to medium-grained, to rarely coarse-grained and are well-sorted to rarely poorly-sorted. The sandstones are quartz-arenite to sublith-arenite in composition. The framework grains are dominantly mono-crystalline quartz and less commonly polycrystalline quartz. Feldspars occur in small amounts and are commonly potassium feldspars, microcline and orthoclase. Lithic fragments are more abundant than feldspars but less than quartz. They are mainly volcanic and sedimentary fragments in origin. Mica minerals, muscovite and biotite are present in trace amounts where muscovite dominates over biotite. Matrix is dominantly clay-sized and less commonly silt-sized of quartz and mica grains.

3.2 Diagenetic Minerals

The sandstones of Al Khlata Formation are subjected to various degrees of diagenetic alterations dominantly mechanical and chemical compaction and less commonly dissolution of chemically unstable detrital silicate grains and formation of kaolinite, quartz overgrowths; illitization of micas, grain coating clays and calcite cements (Figs. 1a–j). However, mechanical compaction is evidenced by grains rearrangement as well as bending and deformation of micas in between of ridged detrital grains. In contrast, chemical compaction is observed by the presence of concave-convex, straight and sutured inter-granular contacts (Figs. 1a–c). Chemical compaction is predominant where micas occur along the interface of detrital quartz grains and also where the grains are coated partly or entirely by clays.

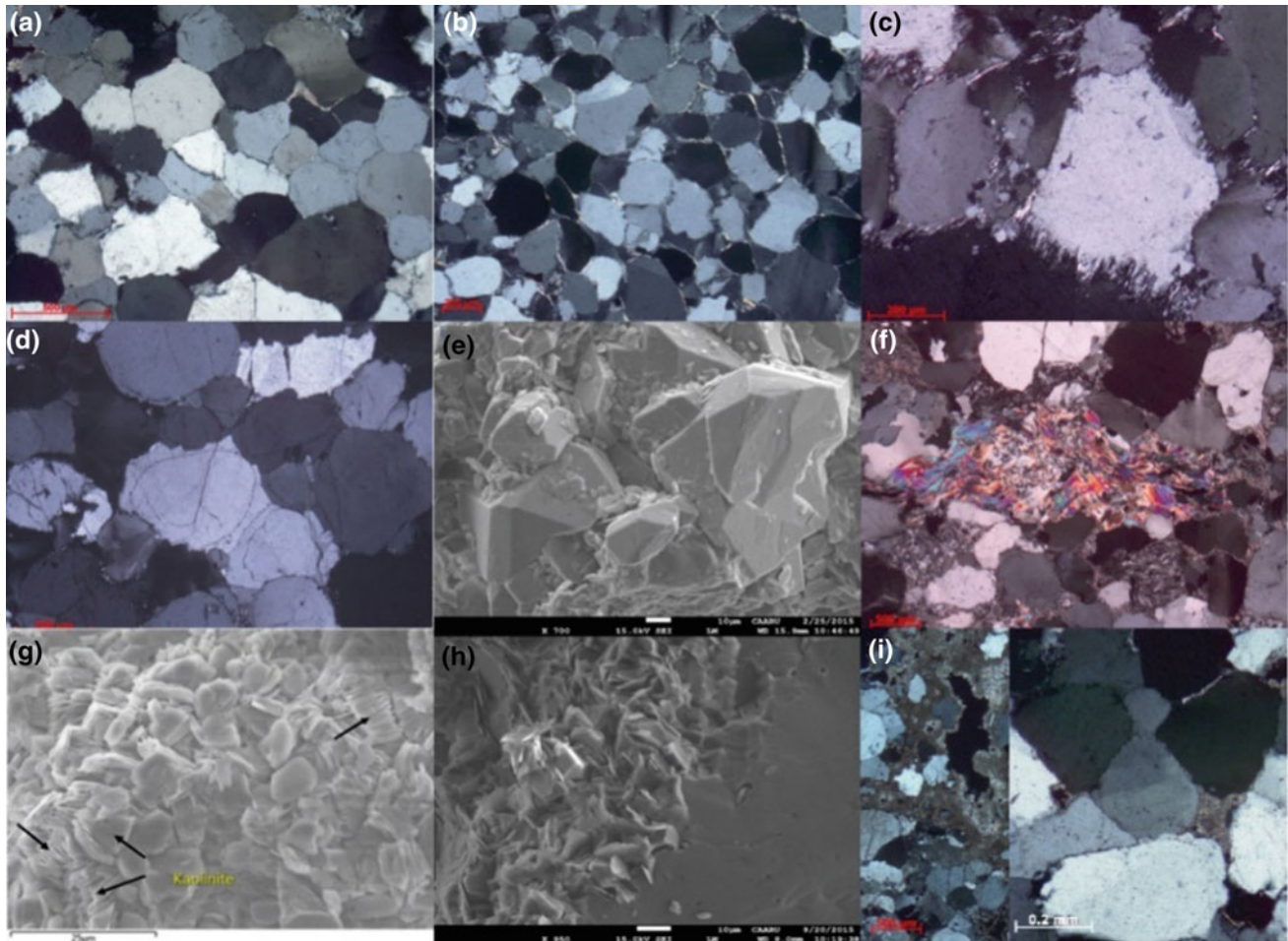


Fig. 1 Photomicrograph (crossed polarizers) and SEM images showing **a–c** point-, concave-convex, straight and sutured contact and development of mechanical and chemical compaction, **d–e** syntaxial quartz overgrowths around the detrital quartz grains, **f** expanded texture of micas into adjacent pores which is associated with kaolinite

formation, **g** booklet-like texture of kaolinite, **h** flake-like texture of illite which is engulfed by and thus predates quartz overgrowths, **i** microcrystalline calcite cements filling large intergranular pores, **j** coarse-crystalline calcite cements filling small intergranular pores after quartz overgrowths

Chemical compaction is extensively predominant in fine- to medium-grained than coarse-grained sandstones.

Quartz cements occur commonly as euhedral to subhedral, syntaxial overgrowths and rarely as microcrystalline around detrital quartz grains (Figs. 1d–e). Quartz overgrowths occur as thick to thin continuous to discontinuous envelop around clean or discontinuously clay coated quartz grains. Quartz overgrowths are common in medium- to coarse-grained than fine-grained sandstones. Microcrystalline quartz developed as small crystals on detrital quartz grains which may be coalesced to form well-developed syntaxial overgrowths that envelope detrital quartz grains.

Authigenic clays occur as kaolinite and illite (Figs. 1f–h). However, kaolinite is observed under the optical microscope as kaolinitized micas exhibiting the expanded accordion-like texture that fill the adjacent inter-granular pores. SEM examination has shown the presence of booklet-like texture of kaolinite (Fig. 1g). In contrast, illite occurs as hair- to flake-like texture around detrital quartz grains and in some cases, engulfed by quartz overgrowths (Figs. 1b, c and h) and as illitized micas.

Calcite cements are the least encountered diagenetic alteration and occur as scattered patches of microcrystalline and coarse-crystalline that fill large and small intergranular pores, respectively (Fig. 1i–j). However, the coarse crystalline calcite, in some cases, engulfs and thus postdates quartz overgrowths (Fig. 1j).

4 Discussion

The abundance of fine- to medium-grained and well-sorted sandstones and scarcity of chemically unstable silicate grains such as feldspars and micas support that Al Khlata Formation in Wadi Daiqa were deposited at a distal part in relation to the glacier core [3]. Long-distance transportation of sandstone grains by running waters over 100 s of kilometers from the glacier core (South Oman) to a more distal parts (i.e. Wadi Daiqa-North Oman) is responsible for grain abrasion and thus reduction in size and dissolving of chemically unstable silicate grains.

The occurrence of variable degrees of mechanical and chemical compaction in the studied sandstones is attributed to the scarcity and sometime lack of early cementation and increasing the rate of sediment supply [1, 2]. Increasing the rate of sediment supply is enhanced by glacier melting and release of huge amounts of sediments. Glacier melting and

thus meteoric waters availability is accounted for chemically unstable silicate grains dissolution and kaolinite formation [1, 2]. Scarcity and in some cases, lack of early cementation and occurrence of clays and micas along the quartz grains interface promoted pressure dissolution during progressive burial [1, 4]. Pressure dissolution was associated with the release of silica and thus quartz overgrowths formation [4].

5 Conclusion

Studying the glacio-lacustrine sandstone reservoirs of the Late Carboniferous-Early Permian Al Khlata Formation in Wadi Daiqa, Northern Oman revealed that diagenetic alterations are primarily controlled by grain size, mineral composition, rate of sediment supply and availability of meteoric waters. Mechanical and chemical compactions are the most dominant diagenetic process. This process is enhanced by high rate of sediment supply which was associated with glacier melting as well as fine- to medium-grained sandstones, the presence of clays and micas around and along the interface of quartz grains. Availability of meteoric waters owing to glacier melting was responsible for chemically unstable detrital silicate grains dissolution and kaolinite formation.

Acknowledgements The authors acknowledge Sultan Qaboos University, Oman for the Internal Research Grant [IG/SCI/ETHS/15/04].

References

1. El-Ghali, M.A.K., Mansurbeg, H., Morad, S., Al-Aasm, I., Ramseyer, K.: Distribution of diagenetic alterations in glaciogenic sandstones within a depositional facies and sequence stratigraphic framework: evidence from the Upper Ordovician of the Murzuq Basin. SW Libya. *Sediment. Geol.* **190**, 323–351 (2006)
2. El-Ghali, M.A.K., Tajori, K.G., Mansurbeg, H.: The influence of transgression and regression on the spatial and temporal distribution of diagenetic kaolin in the Upper Ordovician glaciogenic sandstones within a sequence stratigraphic framework, Murzuq Basin. SW Libya. *J. Geochem. Explor.* **89**, 87–91 (2006)
3. Heward, A.P., Penney, R.A.: Al Khlata glacial deposits in the Oman Mountains and their implications. *Geol. Soc. Lond. Spec. Publ.* **392** (1), 279–301 (2014)
4. Morad, S., Ketzer, J.M., De Ros, F.: Spatial and temporal distribution of diagenetic alterations in siliciclastic rocks: implications for mass transfer in sedimentary basins. *Sedimentology* **47** (Suppl. 1), 95–120 (2000)

Stromatolitic Origin of Laminar Crusts in Palustrine Environments (Pleistocene of Borj Edouana Unit, Northwestern Tunisia)

Ildefonso Armenteros, Naoufel Ghannem, and Kamel Regaya

Abstract

The Pleistocene Borj Edouane in NW Tunisia unit consists of two principal facies associations: (1) calcrete-palustrine-laminar crust facies and (2) microbialites. The laminar crusts consist of millimeter-thick couples (ranging from 0.7 to 3 mm thick) of light (from 0.4 to 2 mm) and dark (from 0.2 to 1 mm) laminae. The laminar alternation represents the succession of events with biological remains under quite hydrodynamic conditions (dark laminae) and of slight erosion and transport episodes by thin water sheets and/or eolian activity (detrital phases, light laminae). The presence of intervening intraclastic-oidal layers indicate erosive processes and the action of weak sheet flows. The laminar crusts were developed in marginal palustrine environments.

Keywords

Laminar crust • Palustrine • Stromatolitic
Spherulite • Pleistocene

1 Introduction

Carbonate laminar crusts are facies commonly linked to calcrete profiles in several situations [1] and in some instances have been referred to carbonate palustrine environments [2]. They are attributed to different origins, namely

edaphic precipitation at the top of a massive horizon of calcrete accumulation, rhizogenic formation at subsuperficial soil levels and stromatolitic-like origin on free-surfaces. The mechanisms of formation for similar structures can be different and their identification should be lean on a comprehensive study including facies association and facies relationships (both at field and micromorphological scales). In the current study case, laminar crusts associated with carbonate palustrine facies will be analyzed.

2 Geological Setting and Methods

The continental carbonate unit of Borj Edouana (Mid-Late Pleistocene) is located in the northwest of Tunisia (Lat. 35° 57' and 35° 55' N and Long. 8° 23' and 8° 24' E) [3], southward of Kef and westward of Tajerouine towns. It forms part of the central filling of the El Gara basin and lies unconformably on the carbonate Cretaceous series. Geologically, it is located at the transition between the central and northern Tunisian paleogeographic domains. Seven laminar crust samples were studied by using petrographic microscope and SEM.

3 Results

3.1 Carbonate Facies of Borj Edouana Unit

The Borj Edouana unit has a maximum thickness of 4 m. It was deposited gradually on a marginal unit tabular to lenticular beds of conglomerates and sandstones in the western, south-western and north-eastern basin margins. The middle western part of the unit consists of massive calcretes, palustrine limestones and laminar crusts that forms an association of facies [4]. This association passes upward and toward the middle eastern part of the unit to tabular beds of lacustrine microbialites consisting of planar stromatolite and oncolite facies.

I. Armenteros (✉)
Salamanca University, 37071 Salamanca, Spain
e-mail: ilde@usal.es

N. Ghannem · K. Regaya
Faculty of Science of Bizerte, University of Carthage, 7021
Zarzouna, Tunisia

3.2 Laminar Crusts

The laminar crusts are well represented in the north and southern borders of the unit. Crust bearing levels correspond to light brown and to pale orange colored tabular limestone beds from 0.15 m to 0.40 m thick. In the northern areas of the unit, they crown a sequence formed from the base to the top by three units: (1) Chalky limestone bed (5–15 cm thick) with irregular gradual boundary with the overlying level. It consists of micrite micro-nodules rich in silt-sized quartz grains and with very scarce gastropod fragments. It is similar to the ‘croûte tuffeuse’ of the French literature for Maghreb-ian Quaternary calcretes [5, 6]. (2) Coarsely stratified nodular limestone bed (30–60 cm thick) that passes through an irregular transitional contact to the upper level. This change can be marked by an intraclastic pebbly bed. The nodular bed shows a typical clotted-peloidal texture favored by curved brecciation including gastropod fragments as described elsewhere (palustrine facies) [4]. (3) Limestone bed apparently massive that includes the laminar crusts. It is characterized by the presence of laminated facies a few millimeters thick. It is interspersed with facies of similar thickness made up of palustrine brecciated microtextures and/or ooidal-intraclastic textures. These facies correspond respectively to the “croûte zonaire” and “croûte en dalle (≈perlitique)” of the classical Mediterranean carbonate crust profiles [6, 7]. The second and the third units of the sequence can show asymmetrical undulations with a wavelength reaching up to 2 m and the laminar crust bed can be fractured in the form of irregular polygons (generally pentagons) from a few cm to 30 cm in diameter. We focus the description on the laminar and ooidal-intraclastic layers.

Laminated crusts show adaptations to the substrate morphology and may achieve antigravitatory and vertical dispositions. In some cases, the sets of laminae are unconformable (Fig. 1a). In hand specimen view, the laminar facies commonly show millimeter-thick couples (from 0.7 to 3 mm thick) of light (from 0.4 to 2 mm) and dark (from 0.2 to 1 mm) laminae that correspond to the alternation of light and dark brown laminae under microscope (Fig. 1b). The dark laminae are massive. They show micro-wavy morphology and principally consist of micrite including diffuse filaments and elliptical to circular sections of spherulites 20–60 µm in diameter. The latter can be arranged in botryoidal spherulite aggregates and in undulating ribbon-like morphologies and semicircular coronas (these average 200 µm in diameter). They are formed by palisades of perpendicular-arranged prismatic calcite crystals (20–30 µm thick). The lighter laminae consist of a silt-sized clotted-peloidal texture (*calcisiltite*) richer in silt-sized quartz grains. Within the lighter laminae, a thinner similar laminar alternation (averaging 200 µm thick) can occur showing a corrugated lamination formed by discontinuous to anastomosed wisp-like dark laminae (about 30–50 µm thick) resembling filament traces and that show humps upward.

The laminated layers (from 2 to 5 mm thick) can alternate with slightly thicker ooidal-intraclastic layers where most intraclasts are formed by micrite mudstones with silt-size quartz grains and scarce gastropod remains. Both laminae show rapid changes of thickness and wedge-edge lateral terminations even at the scale of thin section. One common type of ooidal-intraclastic facies is characterized by ooidal grains 30 µm to about 1 mm in diameter. Ooid nuclei are commonly muddy peloidal-intraclastic particles with

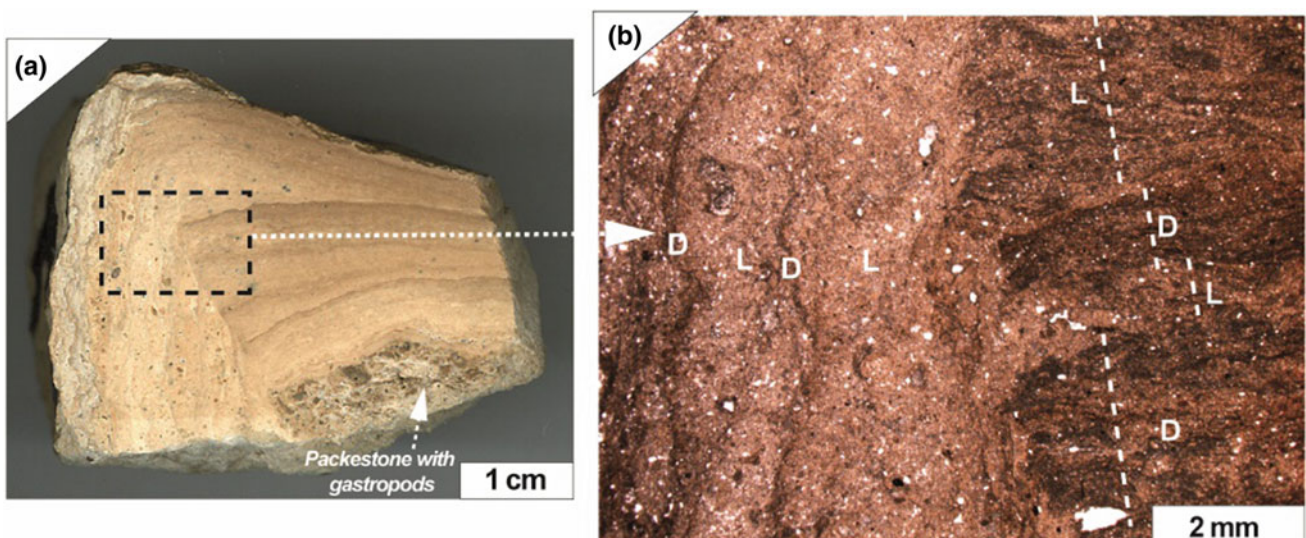


Fig. 1 a Two unconformable sets of laminar crusts (polished slab) and b detail of alternation of dark (D) and light laminae (L) (Thin section under parallel nicols)

silt-sized quartz crystals and dispersed gastropod fragments. Others are formed by compound ooids and fossiliferous Cretaceous lithoclasts.

4 Discussion

The stromatolitic genesis of the laminated layers is supported by the alternation of the dark spherulite-rich micritic laminae and the lighter detrital laminae that indicates the rhythmic repetition of phases with biological activity in quiet conditions and detrital phases implying slight erosion and transport by thin water sheets and/or eolian activity. The development of the rhythms needs the cover of a water lamina, at least intermittently, and they may represent seasonal wet-dry cycles. The close association with brecciation features, erosive surfaces, the presence of detrital particles and gastropod fragments reinforce that they were deposited on a free surface intermittently covered by a thin water film. This fact explains the source for carbonate that may be supplied in dissolution and as silt-sized particles transported by runoff and wind both from the surrounding Cretaceous outcrops (i.e., lithoclasts) and intrabasinal peripheral sediments (i.e., intraclasts). The interlaminated intraclastic-ooidal layers represent deposition under low-velocity tractive currents. It is difficult to understand the interlamination of sorted ooidal textures (with gastropods fragments and silt-size peloids and quartz grains) and laminar layers with biogenic aquatic remains as formed in the soil interior. Therefore, we propose that the ooids in the study unit are particles likely formed in the interface water-floor of very shallow ponds (puddles) subjected to intermittent drying. The similarity between the cortical lamination and the laminar crusts seems to propose a similar origin with binding of clay- to silt-sized particles. The presence of spherulitic fabrics is indicative of the biological control in the accretional construction of the laminar crusts [8]. Favorable conditions for the laminar crust development are not entirely known. However, the close association with palustrine facies and the above described features lead to the consideration of drying-wetting episodes with intermittent thin water cover within marginal low-energy palustrine sub-environments marked by episodic level changes.

5 Conclusion

The Pleistocene Borj Edouana unit forms part of the El Gara basin filling in Kef province, northwest Tunisia. It consists of two facies associations: (1) Calcrete palustrine-crust laminar facies and (2) Microbialites. The laminar crusts constitute singular facies of the former association. They show millimeter-thick couples (ranging from 0.7 to 3 mm thick) of light (from 0.4 to 2 mm) and dark (from 0.2 to 1 mm) laminae that represent the alternation of phases with biological activity in quiet conditions (dark laminae) and detrital phases (light laminae) resulting from slight erosion and transport by thin water sheets and/or eolian activity. The interbedded intraclastic-ooidal layers imply erosive processes and the action of weak sheet flows. These laminar crusts were developed in marginal palustrine environments.

Acknowledgements This work was supported by the Ministry of Higher Education and Scientific Research of Tunisia and MINECO CGL2014-54818-P.

References

1. Semeniuk, V., Searle, D.J.: Distribution of calcrete in Holocene coastal sands in relationship to climate, southwestern Australia. *J. Sediment. Res.* **55**(1), 86–95 (1985)
2. Armenteros, I., Daley, B.: Pedogenic modification and structure evolution in palustrine facies as exemplified by the Bembridge limestone (late Eocene) of the Isle of Wight, southern England. *Sediment. Geol.* **119**, 275–295 (1998)
3. Ben Haj Ali, M., Jédoui, Y., Dali, T., Bensalem, H., Memmi, L.: Carte géologique de la Tunisie au 1/500 000. Service des Mines, de l'industrie et de l'Energie, Tunis, Tunisie (1985)
4. Ghannem, N., Armenteros, I., Riahi, C., Regaya, K.: The lacustrine carbonate in the El Gara basin (Mid-Late Pleistocene, NW Tunisia). *Sociedad Geologica de Espana, Geo-Temas.* **16**(2), 621–624 (2016)
5. Durand, J.H.: Les croûtes calcaires et gypseuses en Algérie: formation et age. *Bulletin Sci Géol France.* **7**(5), 959–968 (1963)
6. Vogt, T.: Croûtes calcaires: types et genèse. Dissertation Thèse, Université Louis Pasteur, Strasbourg. 239 p. (1984)
7. Regaya, K.: Origine stromatolithique des croûtes zonaires quaternaires de Tunisie en contexte aride à semi aride. *Notes Service Géologique, Tunisie.* **70**, 21–38 (2003)
8. Verrecchia, E.P., Freytet, P., Verrecchia, K.E., Dumont, J.L.: Spherulites in calcrete laminar crusts: biogenic CaCO₃ precipitation as a major contributor to crust formation. *J. Sediment. Res.* **A65**, 690–700 (1995)

Sedimentary Characteristics of the Fourth Member of Cretaceous Nenjiang Formation in the Southern Songliao Basin, Northeast of China

Jinkai Wang, Jinliang Zhang, and Jun Xie

Abstract

The lithology of the fourth member of the Cretaceous Nenjiang formation (K_2n_4) in southern Songliao Basin is mainly mudstone. The proportion of sandstone is about 10% which is mainly composed of lithic feldspar sandstone. The carbonate content of sandstone is very high with an average of 25%. The clay minerals are mainly illite/montmorillonite (I/M) mixed layer. In the studied area, 9 single lithofacies types and 5 combination lithofacies types were identified and described in detail. The subfacies type of K_2n_4 in the studied area is delta front which includes four microfacies: underwater distributary channel, mouth bar, sand sheet and interdistributary. During this period, the lake basin gradually shrank, the delta continued to push south, and the sand bodies were lingual to the south with their thickness gradually decreasing.

Keywords

Songliao basin • Sedimentary • River delta
Rock facies

1 Introduction

The Songliao basin is located in the warm humid climate during the Cretaceous period. The Nenjiang formation is a large lake—delta sedimentary strata formed during the second lake flooding periods. It is also the period of its decline from extreme prosperity [2]. According to the literature, researchers usually study the facies from the large scale. They think that the K_2n_4 formation is a single prograding sequence. However, the researcher of the present study subdivides this formation and finds that there are still two short retrogradations (K_2n_3 , K_2n_1) under the large progradation background. Many researchers have carried out conventional sedimentary facies studies which were but detailed in the studied area [5]. This paper is an attempt to characterize lithofacies by single and combination lithofacies research. It is also an establishment of a comprehensive discriminant sequence of lithofacies. In addition, there is no unified standard for the deposition model of K_2n_4 especially for the studied area. This paper has solved these problems systematically and established an accurate sedimentary model.

2 Materials and Methods

The studied area (H168 block) is located in Jilin province of China. All the used data in this paper were gathered with the well coordinates and the well deviation. Logging data body, core and various analysis and laboratory data are all derived from Jilin Oilfield Research Institute, PetroChina. Using these data, the sequence and the system tract study was carried out firstly in the paper. The sequence stratigraphic framework of K_2n_4 was established. Then, the source direction and sedimentary environment are determined. The single and the composite lithofacies model are established. Finally, the sedimentary model of the studied area was established. This research is systematic and meticulous.

J. Wang (✉) · J. Zhang · J. Xie
College of Earth Science and Engineering, Shandong University of Science and Technology, Qingdao, 266590, China
e-mail: wangjk@sdust.edu.cn

J. Wang · J. Xie
Laboratory for Marine Mineral Resources, Qingdao National Laboratory for Marine Science and Technology, Qingdao, 266237, China

J. Zhang
Faculty of Geographical Science, Beijing Normal University, Beijing, 100875, China

3 Results

3.1 Lithologic Characteristics

The lithology of K₂n₄ formation is mainly mudstone (Fig. 1b), argillaceous siltstone, siltstone and fine sandstone. The mudstone content is about 90%. The sandstone is mainly lithic feldspar sandstone (quartz 45%, feldspar 39%, debris 16%) (Fig. 1a). The sandstone interstitial material includes mud, carbonate and clay minerals (I/M mixed layer (Fig. 1d), kaolinite (Fig. 1e), illite (Fig. 1f) and chlorite (Fig. 1g)). I/M mixed layer has the highest content, reaching

55% (Fig. 1c). It shows that the hydrodynamic conditions are weak but later the diagenesis is strong.

3.2 Lithofacies Characteristics

(1) Single Lithofacies

Nine types of single lithofacies were identified in the delta facies according to the characteristics of rock fabric, bedding and grain order of the studied area. These lithofacies include massive fine sandstone facies (FIM), trough cross bedding

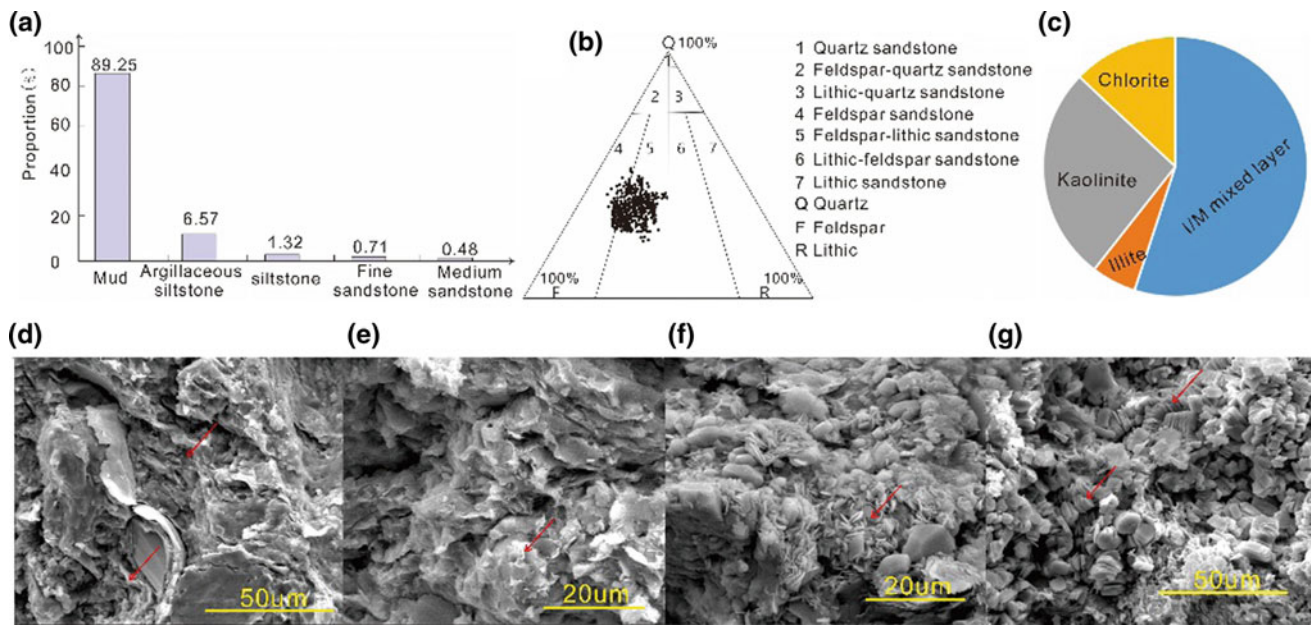


Fig. 1 Characteristics of lithologic and porosity

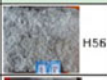
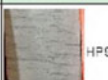
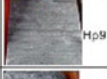

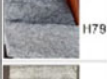
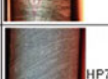



lithofacies		Sedimentary structure	Rock	Sedimentary facies	lithofacies		Sedimentary structure	Rock	Sedimentary facies
FIM	Fine sand facies	Massive bedding	 H56	Underwater distributary channel	PR	Argillaceous siltstone facies	Ripple bedding	 HP9	Inter distributary
FIT	Fine sand facies	Trough cross-bedding	 Hp9	Underwater distributary channel	SIC	Siltstone facies	Ripple bedding Lenticular bedding	 H79	Inter distributary Sand sheet
FIO	Fine sand facies	Oblique bedding	 H79	Mouth bar	SiR	Siltstone facies	Ripple bedding	 HP7	Inter distributary Sand sheet
FIL	Fine sand facies	Oblique bedding	 H79	Sand sheet	MH	Mudstone facies	Horizontal bedding	 H56	Inter distributary
SI	Inverse grading sand facies	Graded bedding	 H158	Mouth bar					

Fig. 2 Single lithofacies types

sandstone facies (FIT), oblique bedding fine sandstone facies (FIO), low-angle cross-beddings fine sandstone facies (FIL), inverse graded sandstone facies (SI), ripple cross lamination fine sandstone facies (PR), ripple cross lamination and lenticular bedding siltstone facies (SiC), ripple cross lamination siltstone facies (SiR), horizontal bedding mudstone facies (MH) [3] (Fig. 2).

(2) Combination Lithofacies

Nine single lithofacies were recombined and five lithofacies combination types were identified according to the observation and the description of the cores [1, 4]. These combined lithofacies types include MH-FIT-TIO-SiC-MH, MH-FIT-FIO-FIT-FIO-MH, MH-SI, MH-SiC-FIO-FIT-MH and MH-SiC-MH-PR-MH. These lithofacies combination types coincide with the sedimentary facies types (Fig. 3).

3.3 Lithofacies Characteristics

The subfacies type of K_2n_4 in the studied area is delta front. It includes four microfacies: underwater distributary channel (Fig. 4a), mouth bar (Fig. 4b), sand sheet (Fig. 4c) and interdistributary (Fig. 4d). Microfacies have a good correspondence with lithofacies and logging facies.

4 Discussion

At the early stage of the K_2n_4 , the basement tectonic activity in the southern Songliao Basin gradually weakened. The lake basin was uplifted. The sand body gradually developed from north to south. Later, the lake shrank and the delta continued to move south. This paper abandons the conventional study methods of other researchers and adopts the method from rock

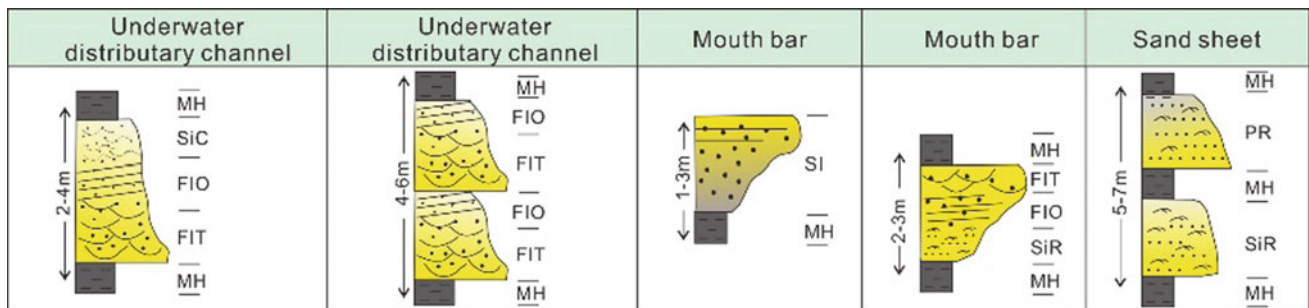


Fig. 3 Combination lithofacies types

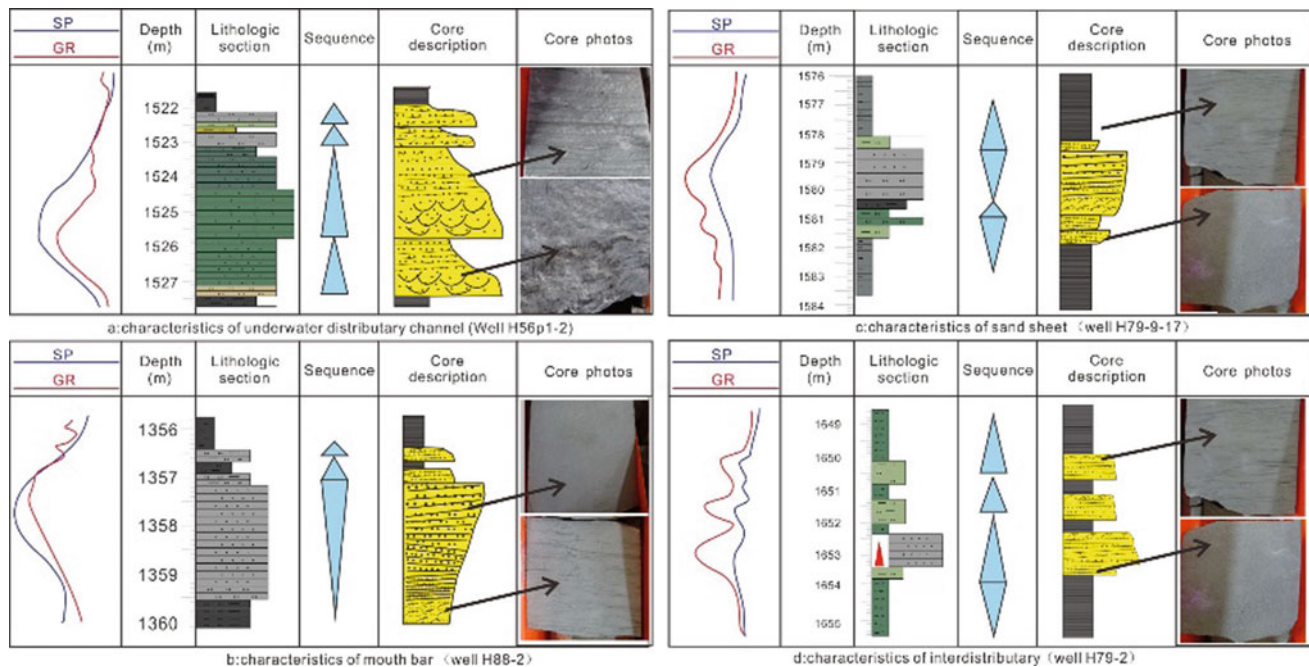


Fig. 4 Microfacies correspondence with lithofacies and logging facies

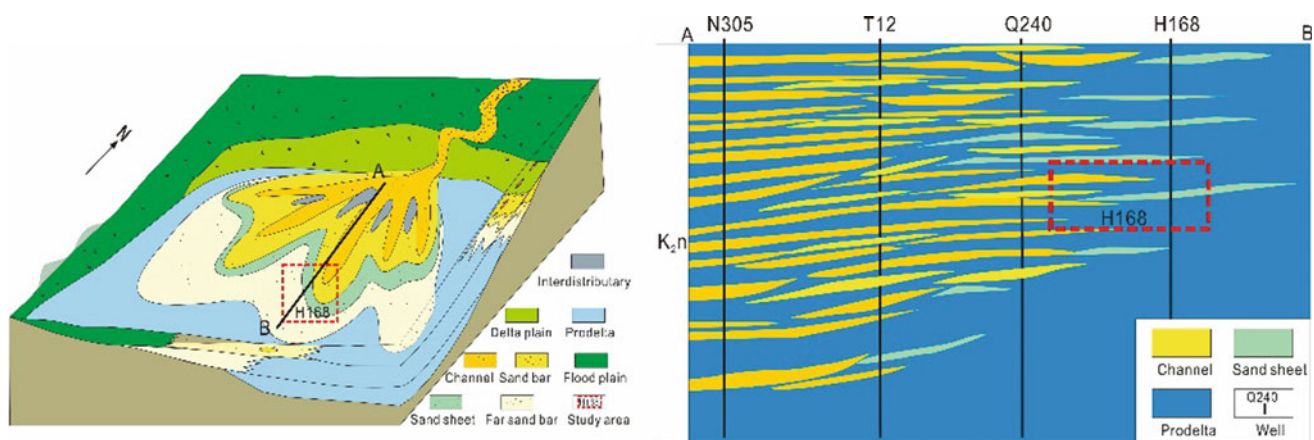


Fig. 5 Sedimentary model of delta front

facies to sedimentary facies which provides an important basis for the accurate characterization of sedimentary facies. The sand bodies in the studied area are lingual to the south whose thickness gradually decreases (Fig. 5).

5 Conclusion

- (1) The main sandstone type of K_{2n_4} is siltstone. Its particle is very thin. Its porosity and permeability are very low. The clay minerals are mainly *I/M* mixed layer.
- (2) Nine single lithofacies types were identified within the studied cores which can be combined into five combination lithofacies types.
- (3) The subfacies of the K_{2n_4} is river delta front. The microfacies includes underwater distributary channel, mouth bar, sand sheet and interdistributary.

References

1. Ding, F., Zhang, J., Xie, J.: Fine description of structure and sedimentary microfacies of Li32 block of Lijin oilfield, Dongying depression. *China. Arab. J. Geosci.* **7**(5), 1693–1704 (2014)
2. Huang, W., Zhang, S., et al.: Sequence structure and sedimentary evolution of Nenjiang formation in Songliao Basin. *Acta Sedimentologica Sin.* **31**(5), 920–927 (2013)
3. Kallepalli, A., Richardson, M.: Digital shoreline analysis system-based change detection along the highly eroding Krishna-Godavari delta front. *J. Appl. Remote Sens.* **11**(3), 36011–36018 (2017)
4. Li, J., Zhang, J., et al.: Architecture and facies model in a non-marine to shallow-marine setting with continuous base-level rise. *Mar. Pet. Geol.* **68**, 381–393 (2015)
5. Liu, L., Zhang, J., Wang, R., et al.: Facies architectural analysis and three-dimensional modeling of Wen79 fault block, Wenliu oilfield, Dongpu depression, China. *Arab. J. Geosci.* **9**(18), 714 (2016)

The Dolomitization in the Deltaic System of Meloussi Formation (Upper Berriasian-Valanginian) in Jebel Meloussi (Central Tunisia)

Najwa Khlifi, Jamel Tourir, and Anna Travé

Abstract

The present work aims at studying the dolostones of the Meloussi Formation (Upper Berriasian-Valanginian) in Jebel Meloussi (Central Tunisia) which is considered as a paleodeltaic system M'Rabet [1]. The study is based on the analysis of dolostones sampled along the Khanguet Zebbag section. Various analyses have been achieved on the dolomite samples in order to reconstruct the environment and the mechanisms of dolomitization. The dolostones include alternating regressive sandy dolomites and transgressive fossiliferous dolomites. The optic microscope and SEM observations show three main petrotypes of dolomite: replacive dolomicrite (P1) associated to the sandy dolostones beds, recrystallized subhedral dolomicroparite (P2) and cementing euhedral dolosparite (P3) associated to the fossiliferous dolostones. The P1 petrotype resulted from mixing waters dolomitization during the regressive intervals and delta progradation as shown by the significant concentration of Fe and Mn and the negative values of $\delta^{18}\text{O}$ and $\delta^{13}\text{C}$. The P2 resulted from a late burial recrystallization but it should have been initially developed in a rather marine environment during the transgressive intervals and the delta retrogradation as testified by the high amount of Sr, Na and Mg *versus* low amount of Fe and Mn and by the slightly negative $\delta^{18}\text{O}$ and $\delta^{13}\text{C}$. The P3 represents late burial dolomite cement resulting from dolomite precipitation within marine water as attested by the very high concentration of Sr and Na in comparison with those of Fe and Mn and the moderately negative to positive $\delta^{18}\text{O}$ and $\delta^{13}\text{C}$.

Keywords

Dolomite • Dolomitization • Petrotypes
Geochemical and isotopic analyses • Paleodelta
Meloussi formation • Upper Berriasian-Valanginian
Jebel meloussi • Central tunisia

1 Introduction

Dolomite and dolomitization are the subject of several discussions. They also raise many debates because of the numerous controversies of their origins as well as the mode of genesis of the mineral 'dolomite'. The study of the Lower Cretaceous dolomites in particular has neither been examined since M'Rabet [1], nor reviewed by any worker and nor considered as the subject of any other research work. In spite of several works already carried out on dolomites in Tunisia, no work has been particularly achieved on dolomitization in deltaic environments.

The Meloussi Formation (Upper Berriasian-Valanginian) in Jebel Meloussi (Central Tunisia) is an appropriate example of a paleodelta system (deltaic littoral platform) where dolostones alternate with sandstones [2]. The aim of the present study is to characterize the dolostones of the Meloussi Formation in order to reconstruct the environment and the mechanisms of dolomitization in a deltaic sedimentary setting.

2 Materials and Methods

The analyses of the dolomite of the Meloussi Formation are based on an analytical method which consists of the observation of the dolomite at different scales from the field to the scanning electron microscope (SEM), DRX mineralogy, electronic microsonde geochemistry and mass spectrometry isotopic ($\delta^{18}\text{O}$ and $\delta^{13}\text{C}$). The different systems tracts in the

N. Khlifi (✉) · J. Tourir
Sfax University, 3029 Sfax, Tunisia
e-mail: najwakhlifi1@gmail.com

A. Travé
Barcelone University, 08028 Barcelone, Spain

Meloussi Formation have been defined from the analysis of the lithofacies associations.

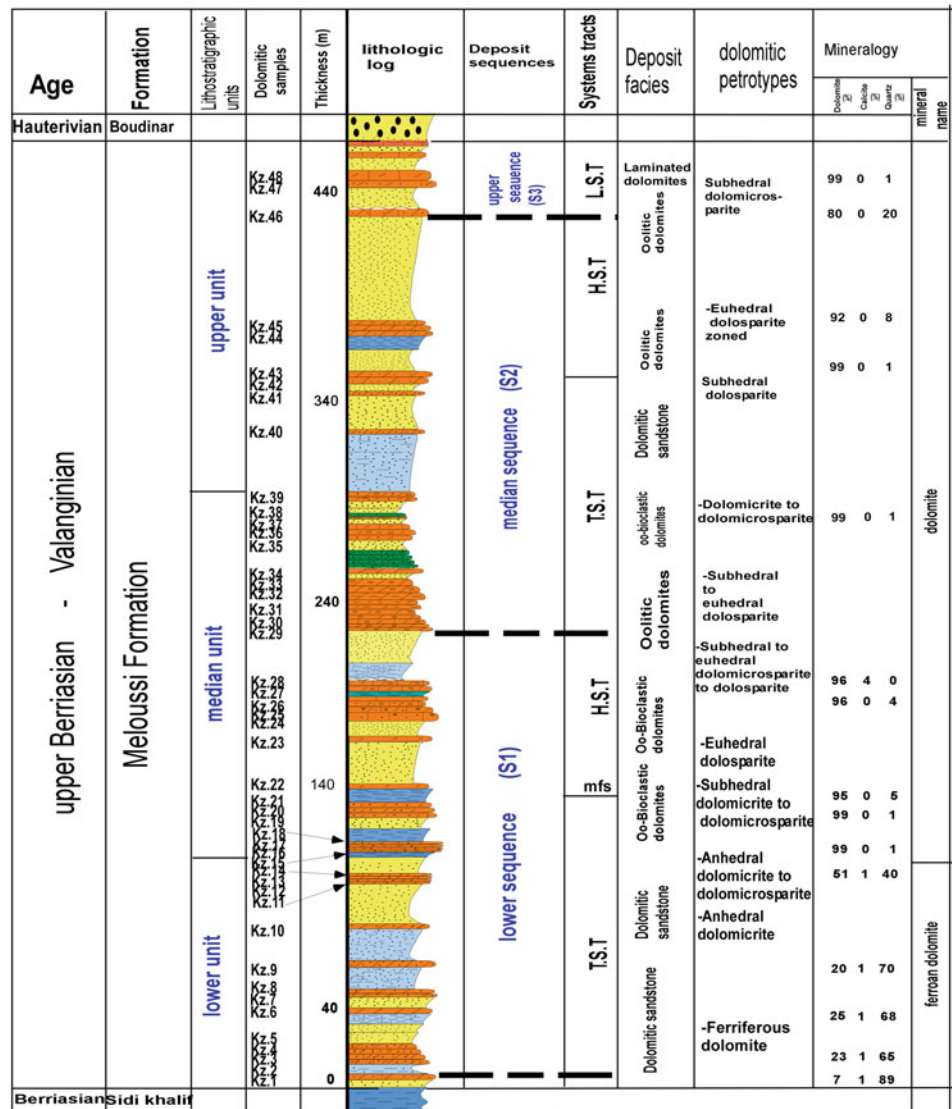
3 Results

According to the field examination, the dolostones of the Meloussi Formation include three lithostratigraphic units in which dolostone beds alternate with sandstones and clays. The dolostone intercalations show, in fact, an alternation of sandy and fossiliferous dolomites. The optic and SEM observations of the dolomites show three main petrotypes

[3, 4]: (i) P1 sandy dolomiticrite which occurs mainly in the lower and middle units of the Meloussi Formation especially in the sandy dolostone beds, (ii) P2 turbid subhedral dolomicrosparite and (iii) P3 limpid euhedral dolosparite. Both occur mainly in the middle and upper units especially in the fossiliferous dolostone beds.

According to the mineralogical, geochemical and isotopic analyses (Fig. 1), the petrotype P1 consists of a ferroan dolomite with significant concentration of Fe (65535 to 79840 ppm) and Mn (2542 to 3797 ppm) *versus* low content of Sr (118 to 250 ppm), Mg (82394 to 88848 ppm) and Na (24 to 250 ppm) and negative values of $\delta^{18}O$ (-3.74 to -6.01

Fig. 1 Sequence stratigraphy, dolomitic petrotypes and mineralogy of the Meloussi Formation (Jebel Meloussi)



PDB) and $\delta^{13}\text{C}$ (-5.71 to -6.89 PDB). The petrotype P2 is a dolomite rich in Sr (270 to 280 ppm), Na (250 to 450 ppm) and Mg (117800 to 119369 ppm) with low content of Fe (3938 to 24488 ppm) and Mn (200 to 2064 ppm) and with moderately negative $\delta^{18}\text{O}$ (-4.93 to -5.89 PDB) and $\delta^{13}\text{C}$ (-1.93 to -2.58 PDB). The petrotype P3 is a dolomite with high content of Sr (250 to 369 ppm), Mg (102359 to 120756 ppm) and Na (220 to 807 ppm) in comparison with those of Fe (7791 to 8133 ppm) and Mn (575 to 991 ppm) and moderately negative to positive $\delta^{18}\text{O}$ (-2.33 PDB) and $\delta^{13}\text{C}$ (1.12 PDB).

4 Discussion

The petrotype P1 corresponds probably to a replacive dolomicrite, the geochemical and isotopic attributes of which are indicating a dominantly meteoric mixing waters dolomitization [1, 5]. In addition, this dolomite is rich in detrital siliciclastic material which suggests regressive conditions and progradation of the Meloussi delta during marine low stand and high stand. The petrotype P2 with turbid subhedral crystals resulted from burial re-crystallization, even though its geochemical and isotopic signature suggests that they have been initially developed according to a dominantly marine mixing waters dolomitization. In addition, the significant marine fossils associated with the P2 dolomites suggest dolomitization during transgressive intervals and deltaic retrogradation. The petrotype P3 shows limpid euhedral dolomite, which may have been related to late burial precipitation [6] with marine connate water, as shown by the geochemical and isotopic composition of this dolomite.

5 Conclusion

The paleodeltaic dolostones of the Meloussi Formation in Central Tunisia show different attributes indicating that the dolomitization occurred during two stages under different conditions:

- Sandy dolomite: is a replacive dolomicrite that occurred during the regressive progradational deltaic evolution.
- Fossiliferous dolomite: is a burial re-crystallized dolomite that initially developed during the transgressive retrogradational deltaic evolution.

References

1. M'rabet, A.: Differentiation of environments of dolomite formation, lower Cretaceous of central Tunisia. *Sedimentology* **28**, 331–352 (1987)
2. Burolet, P.F.: Contribution à l'étude stratigraphique de la Tunisie Centrale. *Ann. Mines Geol, Tunis*, N **18**, 345 (1956)
3. Gregg, J.M., Sibley, D.F.: Epigenetic dolomitization and the origin of xenotopic dolomite texture. *Jour. sedim. Petrology* **54**(3), 908–931 (1984)
4. Grimaldi, M.H.: Types pétrographiques associés aux différents stades de genèse d'une dolomie tidale polyphasée: la dolomie de Mano. 1^{er} Congrès Français de sédimentologie, Paris, Novembre 1987, pp. 193–194 (1987)
5. Badiozamani, K.: The Dorag dolomitization model-application to the middle ordovician of Wisconsin. *J. Sed. Petrology*. **43**(4), 965–984 (1973)
6. Touir, J., Soussi, M., Troudi, H.: Polyphased dolomitization of a shoal-rimmed carbonate platform: example from the middle Turonian Bireno dolomites of central Tunisia. *Cretac. Res.* **30**(3), 785–804 (2009)

Integrated Sequence Stratigraphy of the Middle Jurassic (Bajocian-Callovian) Chiltan Formation in the Lower Indus Basin, Pakistan

Sajjad Ahmad, Abdul Wahab, Suleman Khan, Muhammad Sadiq, Kamil Qureshi, and Zaid Khan

Abstract

Detailed sedimentological analysis of the Jurassic (Bajocian-Callovian) Chiltan Formation has been accomplished from the Middle Indus Basin, Pakistan. We have discriminated six different microfacies that deciphered a carbonate barrier-inlet shelf platform depositional setting. These facies represented the lagoonal tidal inlets (CHF 1 facies), carbonate shoals (CHF 2 facies), fore shore (CHF 3 facies), supra tidal (CHF 4 facies), wash over fans (CHF 5) and near shore (CHF 6 facies) setting. The record of the smaller benthic foraminifera (*Lenticulina subalta*, *lenticulina vobulus* and *planularia protracta*) confirms a middle Jurassic (Bajocian-Callovian) age of the unit. This biostratigraphic calibration suggests that the deposition of the Chiltan Formation correspond to a second order cycle (17 Ma) which encompasses a composite transgressive systems tract and various third order cycles and systems tracts. The long and short term sea level fluctuations show a close match with global sea level curve.

Keywords

Jurassic • Indus basin • Sequence stratigraphy
Pakistan

1 Introduction

The studied area is located in the north-eastern part of the Middle Indus Basin (Fig. 1) which comprises several units formed during Middle Jurassic to Pliocene. The Chaman Fault bounds the Sulaiman fold and thrust belt to the north and west; whereas, the Indus plain marks the southern and eastern limits of the active fore deep basin.

S. Ahmad (✉) · A. Wahab · S. Khan · M. Sadiq · K. Qureshi
Z. Khan
Department of Geology, University of Peshawar, KPK, Peshawar,
25000, Pakistan
e-mail: Dr.s_ahmed@uop.edu.pk

In this study we have combined fieldwork investigations and a detailed petrographic analysis for the microfacies characterization, depositional environments, and the sequence interpretation of the Chiltan Formation.

2 Materials and Methods

The detailed outcrop investigation resulted in the construction of a composite stratigraphic log and detailed petrography (based on the study of the rock samples). The microscopic analysis of the carbonate rock samples is based on the identification of microfacies types that can be identified by using the limestone composition, depositional texture and fossil distribution of specific samples. The sequence stratigraphy is based on the integration of sea level changes deduced from the facies interpretations supported by the foraminiferal biostratigraphic framework.

3 Results

3.1 Facies and Paleoenvironments

Various facies have been recognized which represent deposition under shallow shelf conditions (Tidal flats) as seen in the Dampier basin, North West shelf, Australia. The Chiltan Formation has been deposited on a carbonate barrier inlet system (shelf) as it mainly consists of pure limestone facies. The bioclastic peloidal grainstone facies (CH F1) was deposited in the lagoonal tidal inlets and the mudstone facies (CH F4) shows a supra tidal environment. The deposition of miliolid bearing intraclastic peloidal grainstone facies (CH F5) occurred in the wash over fan and spicules bearing peloidal ooidal grainstone (CH F2) facies dominated the carbonate shoals. The ooidal peloidal intraclastic grainstone facies (CH F3) have indicated the fore-shore while the bioclastic intraclastic peloidal grainstone facies (CH F6) were being deposited in the near-shore zone (Fig. 2).

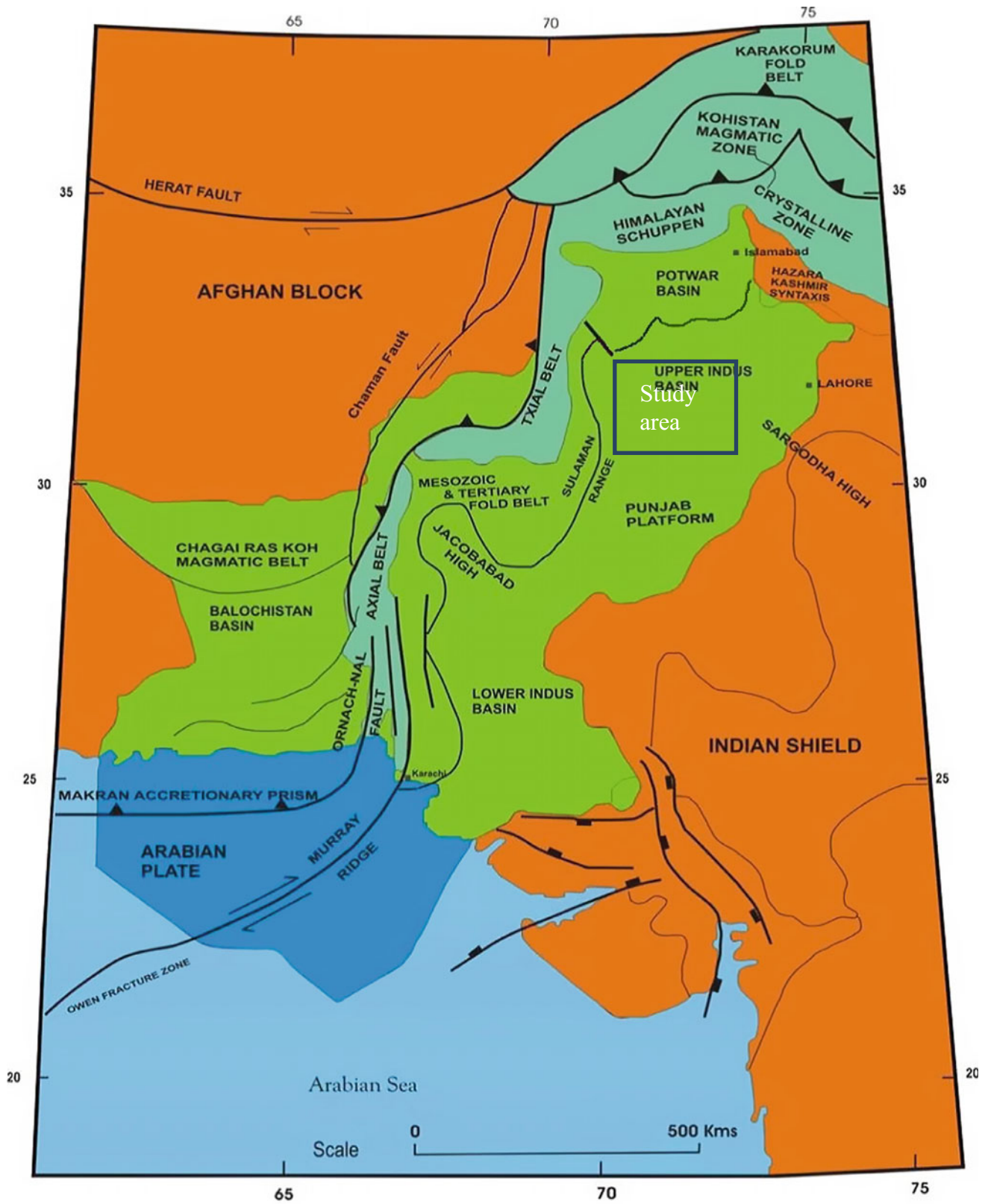


Fig. 1 Inset shows the location map of the study area within the Middle Indus Basin

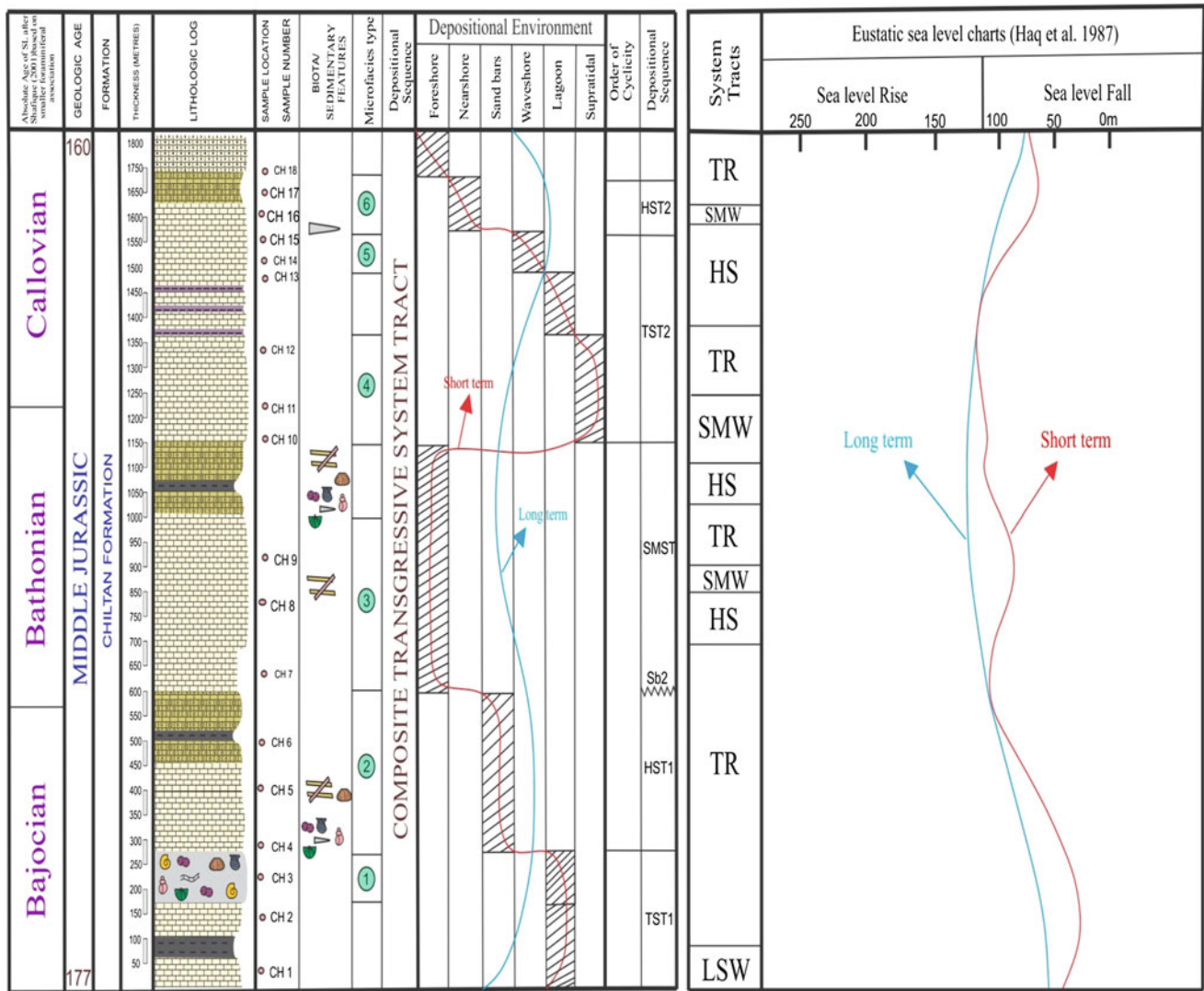


Fig. 2 The composite sequence stratigraphic chart is based on the integration of outcrop data (Lithostratigraphic logs), facies information, depositional settings, nature of depositional cycles, sequences, systems

tracts and comparison of relative and eustatic sea level during Bajocian-Callovian time in the study area

4 Discussion

The Chilton Formation is characterized by a variety of faunal constituents that include smaller benthic foraminifera, echinoderms, bivalves, gastropods, sponge spicules, brachiopods, algae, and radiolarians. However, on the basis of smaller benthic foraminifera, the Chilton Formation was assigned a middle Jurassic (Bajocian-Callovian) age. The *Lenticulina subalta*, *lenticulina vobulus* and *planularia protracta* association was recognized from the Chilton Formation which is a characteristic fauna of the Bajocian-Callovian age. Based on these data, the Chilton Formation is interpreted to have been deposited during a time span of 17 Ma. The numerical ages are assigned and

the second order of cyclicity is interpreted. The relative sea level curve of the Chilton Formation is constructed by the recognition of various facies types and its depositional settings. In long term, the sea level curve of the Chilton Formation corresponds to one episode of sea level rise. This is recognized as a second order cycle which consists of composite transgressive tract systems. In the short term, the relative sea level curve shows two episodes of sea level rise and fall of a third order cycle. In long term, a sea level rise in the Bajocian and fall during the Bathonian followed by a rise in the Callovian. It is noted that it extends to the Oxfordian (Fig. 2). In long term, the global sea levels remained generally low in the middle Jurassic, rising somewhat in the Bajocian but falling again in the late Bathonian. The trend reversed itself in the Callovian. The long-term sea level

continued to rise through the Oxfordian it reaches the peak in the Kimmeridgian (Fig. 2).

5 Conclusion

The sea level fluctuations observed in the Chilton Formation are in harmony with the long term global fluctuations [1]. In short terms, two episodes of sea level rises and falls have been observed in the Chilton Formation

while the Haq curve [1] contains three episodes of rise and fall. The absence of one episode of sea level rise and fall in the Chilton Formation may be attributed to the local tectonics.

Reference

1. Haq, B.U., Hardenbol, J., Vail, P.R.: Chronology of fluctuating sea levels since the Triassic. *Science* **2**(35), 1153–1165 (1987)

Factors Controlling Oncoid Distribution in the Inner Areas of a Late Kimmeridgian Carbonate Ramp (Northeast Spain)

Cristina Sequero, Beatriz Bádenas, and Marcos Aurell

Abstract

The factors controlling the oncoïd distribution in the interior areas of a latest Kimmeridgian shallow carbonate ramp were examined based on a detailed sedimentological and petrographic analysis of the upper sequence of the Higuieruelas Formation (Iberian Basin, Northeast Spain). Four types of oncoïds are defined: small micrite-dominated type I and II oncoïds are generally found in low proportion in all sub-environments (from backshoal/washover, lagoon to intertidal). Large *Bacinnella*-dominated type III and IV oncoïds predominate in low-energy lagoonal areas. Variable energy water, oligotrophic conditions and probably low sedimentation rates controlled oncoïd growth and distribution, thus highlighting their potential as palaeo-environmental proxies.

Keywords

Oncoids • Lagoon • Carbonate ramp • Latest kimmeridgian • Iberian basin

1 Introduction

Different types of marine oncoïds and their palaeo-environmental significance have been described in the Late Jurassic [1, 2, 5, 8]. In this work, the different oncoïd types occurring abundantly in the interior areas of a latest Kimmeridgian carbonate ramp (Higuieruelas Formation, Iberian

Basin, Northeast Spain) are studied in detail in order to decipher the main environmental factors involved in the formation of the different oncoïd types and their distribution.

2 Sedimentological Setting and Methodology

The shallow-water domains of the latest Kimmeridgian of the Iberian Basin (Fig. 1a) are represented by the oncolitic limestones of the Higuieruelas Formation. This work concerns the upper (10–16 m thickness) shallowing-upward sequence of the unit (Fig. 1b), exposed in an outcrop area of 1 × 2 km in extent. Facies analysis was based on a detailed sedimentological field description of 14 closely logs and petrographic description of rock samples in 438 polished slabs and 111 thin sections.

The palaeoenvironmental interpretation by Sequero et al. [7] provides the sedimentological framework for the detailed analysis of oncoïds presented here (Figs. 1b and 2a). Five facies encompassing from intertidal to shallow subtidal lagoon and backshoal areas were distinguished (Fig. 2a). Oncolitic and oncolitic-stromatoporoid wackestone to packstones with local patches of stromatoporoids, predominate in the sheltered lagoon. Backshoal/washover peloidal wackestone to grainstones represent resedimented sediment from distal oolitic-peloidal and oncolitic-dominated shoals. Peloidal mudstone to grainstones with fenestral porosity and gastropod-oncolitic wackestone to grainstones are accumulated in intertidal areas with small ponds.

C. Sequero (✉) · B. Bádenas · M. Aurell
University of Zaragoza, Zaragoza, Spain
e-mail: csequero@unizar.es

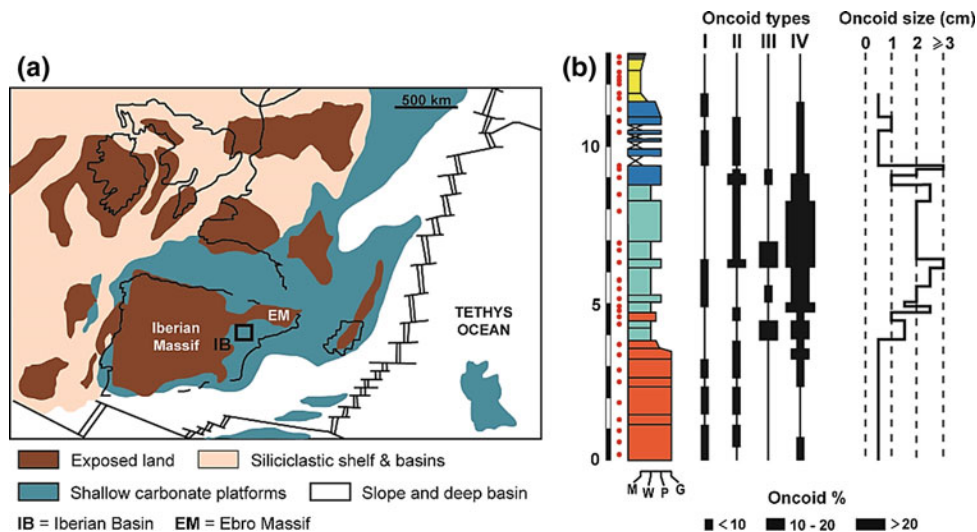


Fig. 1 a Paleogeographic distribution in western Europe during the late Kimmeridgian (adapted from Dercourt et al. [3]) indicating the location of the studied area. b Vertical facies distribution in the

uppermost sequence of the Higuieruelas Formation (log M7 from Sequero et al. [7]), showing the vertical distribution of oncooid types and size (legend for facies in Fig. 2a)

3 Oncooid Distribution and Controlling Factors

Four types of oncooids (type I, II, III and IV; [2]) show a preferential distribution and relative abundance within the intertidal to shallow subtidal areas have been recognized (Figs. 1b and 2). Type I and II oncooids are present in all facies in very low proportion. They are spherical to elliptical and few millimeters to 1 cm in size. The cortex is formed by micritic laminae (type I, Fig. 2b, A) and micritic laminae with organism-bearing laminae of *Bacinella irregularis* (type II, Fig. 2b, B). Type III oncooids are common in oncolitic facies. They are up to 3 cm in size and from sub-elliptical to spherical with undulated surfaces (Fig. 2b, C). The cortex is formed by an alternation of micritic and organism-bearing (mostly *Bacinella-Lithocodium* association) laminae. Type IV oncooids are abundant in oncolitic facies, and also common in oncolitic-stromatoporoid and pond facies. They display irregular shapes with lobate contours ranging from a few millimeters to 7 cm in size (Fig. 2b, D). They are exclusively formed of mostly *Bacinella-Lithocodium* meshwork. Large type IV oncooids are found in oncolitic facies.

The interaction of the different palaeo-environmental factors controlled the oncooid growth and distribution in the studied inner ramp. Shoals protecting the lagoon controlled the occurrence of low-energy conditions which are favorable for the development and abundance of large type IV oncooids in the lagoon; whereas, micrite-dominated type I and II oncooids were probably resedimented by storms and distributed throughout the inner ramp domain. Low siliciclastic input and probable low sedimentation rates contributed to the generation of the *Bacinella-Lithocodium* association that characterize type III and IV oncooids [6], since these cyanobacteria indicate oligotrophic levels, medium-level salinity and high-transparent waters [4].

4 Conclusion

The spatial distribution obtained for the oncooids in the inner areas of a latest Kimmeridgian carbonate ramp highlights that oncooids constitute a useful tool for the high-resolution palaeo-environmental studies. Large *Bacinella*-dominated type III and IV oncooids predominate in the inner areas of a sheltered lagoon, where low-energy conditions, low siliciclastic input and probably low sedimentation rates

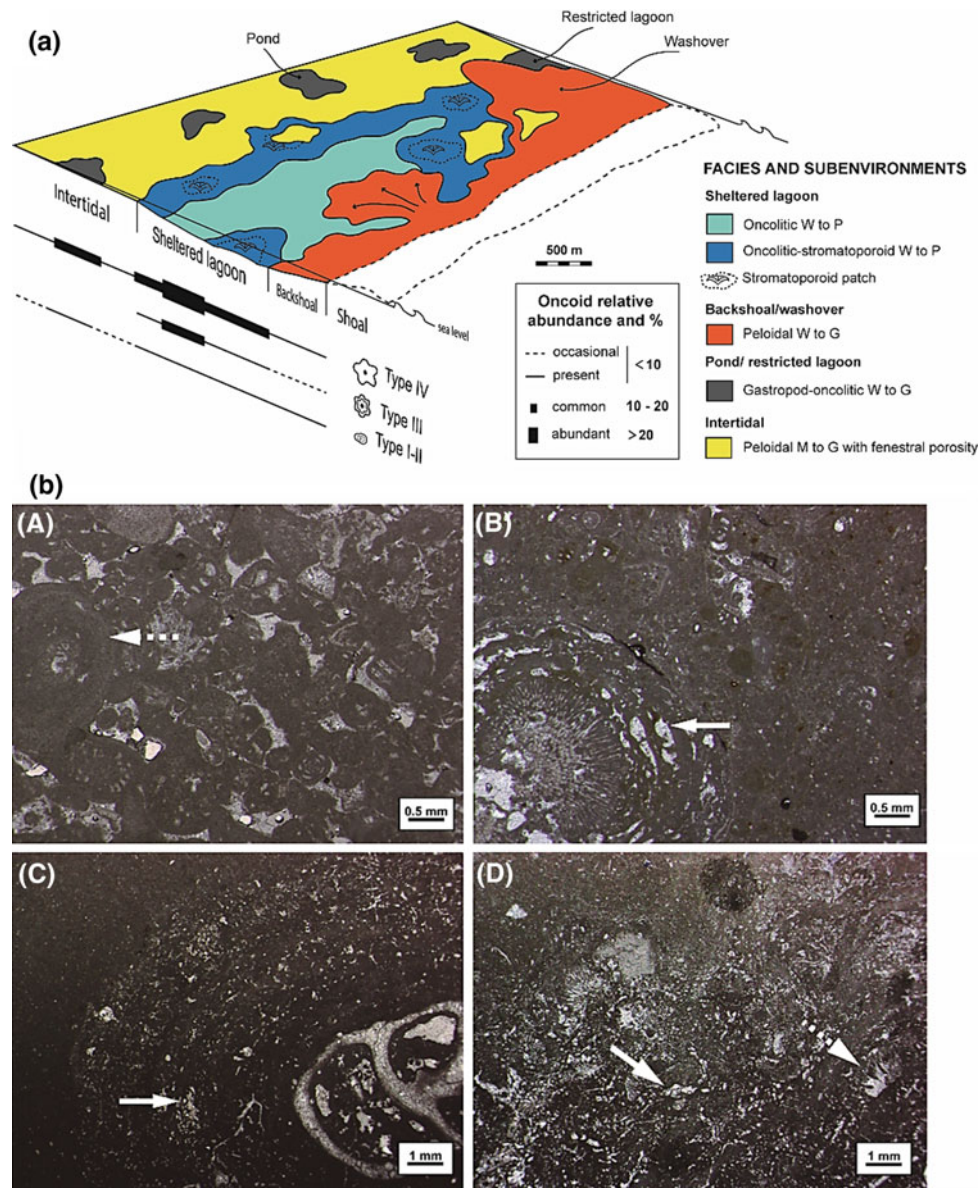


Fig. 2 a Facies distribution in the sedimentary model proposed for the studied carbonate inner ramp [7], and abundance of different oncooid types. b A–D Thin section images in plane polarized light of oncoids:

type I (A, dashed arrow), type II (B), type III (C) and type IV (D) oncoids. Note the *Bacinella* (white arrows in B–D) and *Lithocodium* (dashed arrow in D)

contributed to the extensive growth of cyanobacteria. Type I and II oncoids, which are present in all sub-environments in very low proportion, are probably resedimented by storms.

Similar palaeo-environmental interpretations are found for oncoids studied in the Late Jurassic [1, 2, 8], where the lateral and vertical distribution of oncoids through small-scale depositional sequences is also congruent with relative sea-level changes or variations in the platform morphology [8].

References

1. Bádenas, B., Aurell, M.: Facies model of shallow-water carbonate ramp based on distribution of non-skeletal grains (Kimmeridgian, Spain). *Facies* **56**, 89–110 (2010)
2. Dahanayake, K.: Sequential position and environmental significance of different types of oncoids. *Sediment. Geol.* **20**, 301–316 (1978)
3. Dercourt, J., Ricou, L., Vrielynck, B.: Atlas Tethys palaeoenvironmental Maps. CCGM, Paris (1993)
4. Flügel, E.: *Microfacies of Carbonate Rocks: Analysis, Interpretation and Application*. Springer, Berlin (2004)

5. Gygi, R.A.: Structure pattern of distribution and paleobathymetry of late Jurassic microbialites (stromatolites and oncoids) in northern Switzerland. *Eclogae Geol. Helv.* **85**, 799–824 (1992)
6. Leinfelder, R.R., Nose, M., Schmid, D., Werner, M.: Microbial crusts of the Late Jurassic: composition, palaeoecological significance and importance in reef construction. *Facies* **29**, 195–230 (1993)
7. Sequero, C., Bádenas, B., Aurell, M.: Facies mosaic in the inner areas of a shallow carbonate ramp (Upper Jurassic, Higuerales Fm, NE Spain). *Facies* **64**, 9 (2018)
8. Védryne, S., Strasser, A., Hug, W.: Oncoid growth and distribution by sea-level fluctuations and climate (Late Oxfordian, Swiss Jura Mountains). *Facies* **53**(4), 535–552 (2007)

Diagenetic Evolution of Upper Jurassic-Lower Cretaceous Berdiga Formation, NE Turkey: Petrographic and Geochemical Evidence

Merve Özyurt, Ihsan S. Al-Aasm, and M. Ziya Kirmaci

Abstract

Upper Jurassic-lower Cretaceous Berdiga Formation crops out extensively in NE Turkey. The host carbonates at Eski Gümüşhane section are pervasively dolomitized by fabric-destructive and fabric-preserving replacive dolomites (RD). These dolomites are Ca-rich and non-stoichiometric ($\text{Ca}_{56-58}\text{Mg}_{42-44}$). They have highly variable but low $\delta^{18}\text{O}$ (-11.38 to -4.05% V-PDB) and $\delta^{13}\text{C}$ (0.69 to 3.13% V-PDB) values, radiogenic $^{87}\text{Sr}/^{86}\text{Sr}$ ratios (0.70753 to 0.70884), extremely high Fe (2727 – 21053 ppm) and Mn (1548 – 27726 ppm) contents. Microcrystalline quartz cement, dolomite cement and the scattered euhedral pyrite minerals (average $5\ \mu\text{m}$) are also observed in the dissolution porosity of replacive dolomites. This study demonstrates that these carbonates have undergone a complex diagenetic history from shallow to deep burial associated with syn-sedimentary extensional tectonic activity during the Albian–Aptian and later with the hydrothermal emplacement of the polymetallic mineralization during the Eocene.

Keywords

Diagenesis • Carbonates • Berdiga Formation • NE turkey

1 Introduction

Late Jurassic-early Cretaceous Berdiga Formation is composed of platform carbonates well exposed in NE Turkey which is known as one of the best examples of the

M. Özyurt (✉) · M. Ziya Kirmaci
Department of Geological Engineering, Karadeniz Technical University, 61080 Trabzon, Turkey
e-mail: merveyildiz@ktu.edu.tr

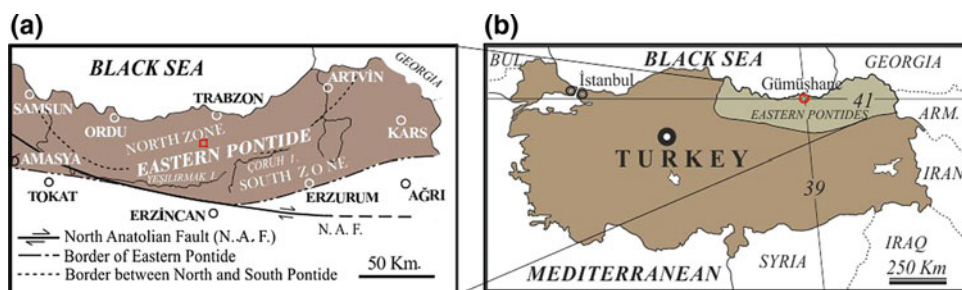
M. Özyurt · I. S. Al-Aasm
Department of Earth and Environmental Sciences, University of Windsor, 401 Sunset Avenue, Windsor, ON N9B 3P4, Canada

metallogenic provinces in the Alpine-Himalayan belt. Berdiga Formation, which is affected by the pervasive dolomitization, was examined by many researchers in terms of its stratigraphic, lithologic and structural attributes [1 and many others]. However, little effort has been made to understand the origin of the dolomitization. Although Berdiga Formation hosts important economic mineralizations in Eski Gümüşhane area, there has not been any attempt to understand the evolution of the hydrothermal fluids related to polymetallic mineralizations. The aim behind this study is, simply, to decipher the origin and the diagenetic evolution of the dolomites in the formation. We report the petrographic investigations, the geochemical analyses and the microthermometric results of the dolomite samples as well as the petrographic and fluid inclusion analyses of quartz which co-exist with the pyrite minerals.

2 Methods

The samples of the current study were collected from Eski Gümüşhane section in Gümüşhane (NE Turkey) where polymetallic deposits occur as veins and lenses within the Berdiga Formation in proximity to its upper contact with the overlying formation (Fig. 1a, b). They were examined under a polarizing microscope to evaluate the diagenetic and the microfacies types. Microfacies types were described and interpreted based on the textural and/or the compositional characteristics [2–5]. Stable isotope analyses ($\delta^{18}\text{O}$ and $\delta^{13}\text{C}$) of selected samples were conducted at Fakultät laboratories of the Friedrich-Alexander Universität Erlangen-Nürnberg (FAU). Carbonate powders were reacted with 100% pure phosphoric acid at $70\ ^\circ\text{C}$ by using a Gasbench II connected to a Thermo Fisher Delta V Plus mass spectrometer. All values are reported in per mil relative to V-PDB.

Fig. 1 Location of study area (a and b)



3 Results

A variety of diagenetic processes were observed in the Berdiga carbonates. A paragenetic sequence is presented in Fig. 2 based on petrographic observations, cross-cutting relationships and geochemical considerations. Three different types of the replacive dolomite textures are recognized: (1) Microcrystalline planar-s dolomite with crystal size ranging from 25 to 50 μm replacing micritic matrix (Mcd); (2) Fabric-preserving, fine to medium crystalline planar-s dolomite (Fpd) and (3) Fabric-destructive medium to coarse crystalline planar-s dolomite with crystal size ranging from 100 to 150 μm (Fdd). Mcd occurs prior to Fpd and Fdd formed during the early stage of burial history. This dolomite crosscuts by microstylolites and low amplitude stylolites cut across Fpd and Fdd. All replacive dolomites are Ca-rich and non-stoichiometric ($\text{Ca}_{56-58}\text{Mg}_{42-44}$). They have highly variable but low $\delta^{18}\text{O}$ (from -11.38 to -4.05‰) and $\delta^{13}\text{C}$ (from 0.69 to 3.13 ‰) values, radiogenic $^{87}\text{Sr}/^{86}\text{Sr}$ ratios (from 0.70753 to 0.70884), extremely high Fe (2727–21053 ppm) and Mn (1548–27726 ppm) contents. Moreover, Fe and Mn values show enrichment from core to the overgrowth rim of coarse crystalline dolomite. Authigenic quartz with crystal size ranging from 5 to 30 μm is generally observed along the stylolitic dissolution and secondary vuggy porosity within dolomites. Scattered pyrite with crystal size (2–5 μm) is the second noncarbonate mineral observed within dolomites and it commonly co-exists with the microcrystalline quartz. Primary fluid inclusions in Fdd dolomite are quite small (3–6 μm in size). They commonly have two-phases. Homogenization temperatures in cloudy cores ranged from 85 to 170 $^{\circ}\text{C}$ and those distributed along the growth rims ranging from 160 to 230 $^{\circ}\text{C}$ for replacive dolomite. However, dolomite cement and quartz cement show a higher range of Th values from 200 to 240 $^{\circ}\text{C}$ and from 230 to 250 $^{\circ}\text{C}$, respectively.

4 Discussion

Berdiga Formation was generally deposited on the inner platform environment and the facies produced in such an environment ranging from non-laminated mudstone to foraminiferal grainstone/packstone. At the time of deposition,

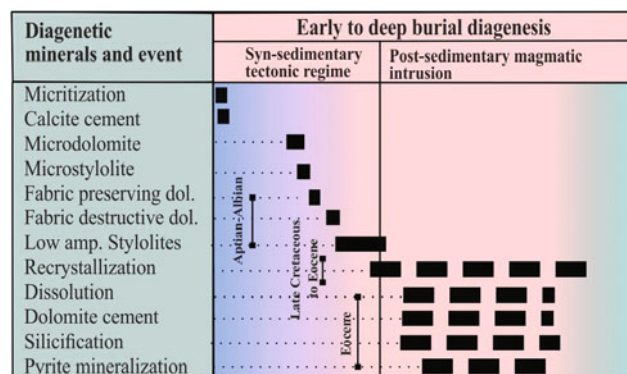


Fig. 2 Paragenetic sequence of the Berdiga Formation

diagenesis was initiated by micritization and early cementation. This was followed by the dolomitization of the mudstone facies at a shallow burial. Pervasive dolomitization occurred at the intermediate burial stage. Such a large-scale dolomitization generally necessitate high amounts of magnesium source in order to pervasively replace the host limestone [6]. Magnesium source can be provided by the dewatering of thick shale sequences during burial compaction [3]. However, large sources of Mg in the underlying formation are not apparent in the study area and also the early to medium stage of chemical compaction in the form of stylolites crosscuts all dolomite types. Hence, the burial compaction model cannot explain the origin of the pervasive dolomites. The lack of the primary evaporite minerals and the negative shift in $\delta^{18}\text{O}$ values imply that the hypersaline dolomitization model can also be ruled out. Therefore, Mg source for the pervasive dolomitization can be supplied by considerable volumes of seawater funneled through the main fault zone to the facies with high porosity and permeability (Fig. 3). The majority of $\delta^{13}\text{C}$ values for pervasive dolomite are in agreement with the range reported late Jurassic-early Cretaceous seawater values suggesting that carbon was derived internally from the same seawater or host carbonates [7]. Low $\delta^{18}\text{O}$, radiogenic $^{87}\text{Sr}/^{86}\text{Sr}$ ratios, extremely high Fe and Mn contents may have been sourced from the hydrothermal fluids during the recrystallization. The recrystallization of the pervasive dolomites probably occurred later during the deeper burial diagenetic stage

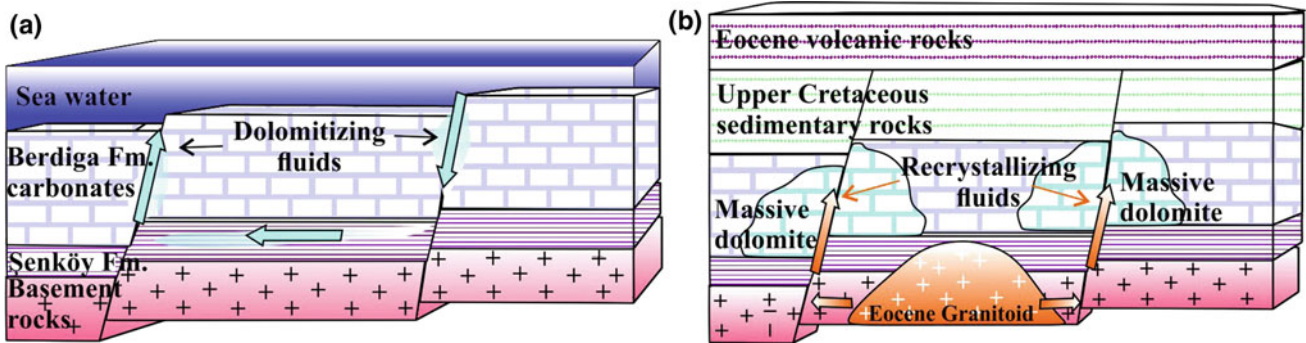


Fig. 3 Schematic model of the dolomitization **a** and recrystallization **b**

associated with Eocene intrusion and their related economic mineralization. Moreover, the enrichment of Fe and Mn and fluid inclusion homogenization temperatures (from 160 to 230 °C) from core to the overgrowth rim of the coarse crystalline dolomite also suggest that the replacive dolomites have been recrystallized by hydrothermal fluids associated with polymetallic mineralization under high-temperature domain (Fig. 3). At the same time, dissolution, silicification and pyrite mineralization affected the massive dolomite during the emplacement of the polymetallic mineralization as evidenced by the fact that quartz and co-existing pyrite occur along stylolites. The majority of the homogenization temperature values (average 250 °C) of the fluid inclusions in quartz are consistent with Th of the fluid inclusions in the overgrowth rim of the dolomites and the Cd dolomite.

5 Conclusion

The petrographic and the geochemical data indicate that the diagenetic evolution of the Berdiga carbonates involve complex alterations occurring at early shallow burial (micritization, calcite cementation), shallow to intermediate (dolomitization associated with syn-sedimentary extensional tectonic activity during to Albian–Aptian) and intermediate to deep burial (recrystallization, dissolution, silicification and pyrite mineralization) associated with the hydrothermal

emplacement of the polymetallic mineralization during Eocene (Fig. 3a and b).

Acknowledgements The authors thank Karadeniz Technical University (Project no: FBA-2015-5160) and TÜBİTAK (Project no: 115Y005, ÇAYDAG and International PhD Research Scholarship Program-2214-A-BİDEP) for their financial support. ISA acknowledge the support from NSERC.

References

1. Kirmacı, M.Z., Koch, R., Bucur, J.I.: An early Cretaceous section in the Kırcaova area (Berdiga Limestone, NE-Turkey) and its correlation with platform carbonates in W-Slovenia. *Facies* **34**, 1–22 (1996)
2. Dunham, R.J.: Classification of carbonate rocks according to depositional textures (1962)
3. Durocher, S., Al-Aasm, I.S.: Dolomitization and neomorphism of Mississippian (Visean) upper debolt formation, blueberry field, Northeastern British Columbia: geologic, petrologic, and chemical evidence. *Am. Assoc. Petrol. Geol. Bull.* **81**(6), 954–977 (1997)
4. Sibley, D.F., Gregg, J.M.: Classification of dolomite rock textures. *J. Sediment. Res.* **57**(6) (1987)
5. Flügel, E.: *Microfacies Analysis of Carbonate Rocks. Analysis, Interpretation and Application*. Springer, Berlin (2004)
6. Warren, L.: Dolomite: occurrence, evolution and economically important associations. *Earth-Sci. Rev.* **52**, 1–81 (2000)
7. Veizer, J., Ala, D., Azmy, K., Bruckschen, P., Buhl, D., Bruhn, F., Jasper, T.: $^{87}\text{Sr}/^{86}\text{Sr}$, $\delta^{13}\text{C}$ and $\delta^{18}\text{O}$ evolution of Phanerozoic seawater. *Chem. Geol.* **161**(1–3), 59–88 (1999)

Rudist Mud Mounds and Biostromes from Upper Cretaceous of Istria (Croatia)

Alan Moro, Alceo Tarlao, and Giorgio Tunis

Abstract

In addition to biostromes which are the most common paleo-environmental appearance of rudist congregations, in Upper Cretaceous of Istria, rare rudist mud-mounds were investigated. The aim of this work is to present the appearance of rudist congregations with respect to the lithofaces characteristics of paleo-environment. Rudist congregations could appear within both mud mounds and biostromes in relatively shallow subtidal. They are the result of the interaction of the accommodation space adequate to the thriving for radiolitids and carbonate sedimentation rate. The shallowing and the decrease of accommodation space are indicated in mud mounds by thin sheets of densely packed F–R with fragments of radiolitids at the top of beds together with lateral migration of congregations within mud mound marked by flanks. They are visible as lamination. In case when radiolitid congregations thrive in shallower subtidal paleo-environment with less accommodation space, they appear through biostromes.

Keywords

Rudists • Mud mound • Biostrome • Upper Cretaceous Istria • Croatia

1 Introduction

During the Upper Cretaceous, the Adriatic Dinaric Carbonate Platform (ADCP) was characterized by shallow-water peritidal depositional conditions. It was interrupted by two drowned platform events [5, 9]. Rudists which thrive in such paleo-environment were elevators, sediment dwelling [3] radiolitids and hippuritids. They are preserved mostly as in situ toppled biostromal congregations [7] from floatstone to rudstone textural characteristics [1, 2]. Besides this most common appearance through biostromes, in Upper Cretaceous of Istria radiolitid congregations which form rare rudist mud-mounds, were investigated. The aim of this work is to present paleo-environmental characteristics of such mud mounds and biostromes.

2 Stratigraphic Settings

The investigated localities are Upper Cenomanian (Premantura locality) and Middle Turonian age (Škokovac and Mrlera localities) according to the benthic foraminifers *Chrysalidina gradata* D'Orbigny, *Moncharmontia appeninica* (De Castro) and *Pseudocyclamina sphaeroidea* Gendrot. Macrofossils are radiolitid species *Radiolites trigeri* Bayle, *Radiolites peucetius* Parona, *Radiolites lustitanicus* (Bayle) [6], *Radiolites praesauvagesi* Toucas and *Biradiolites* cf. *rotundatus* Pleničar [8]. These deposits located at the area of cape Mrlera, cape Premantura and Škokovac Island in Southernmost part of Istrian peninsula preceded or succeeded Lower Turonian drowned platform event [4].

3 Results

In all successions, there are lateral and vertical exchange of floatstones–rudstones (F–R) and packstones–grainstones (P–G). Besides the whole shells and fragments of radiolitids,

A. Moro (✉)
Faculty of Science, Department of Geology, University of Zagreb,
Horvatovac 102A, 10000 Zagreb, Croatia
e-mail: amoro@geol.pmf.hr

A. Tarlao
Gruppo Speleologico Monfalconese, Via Valentinis, 134,
I - 34074 Monfalcone, Italy

G. Tunis
Dipartimento Di Matematica E Geoscienze, Università Di Trieste,
Via Weiss, 2, 34127 Trieste, Italy

other most common particles are benthic foraminifers, pellets and peloids.

Premantura profile is 10.2 m thick. It is composed of P–G and F–R. The thickness of beds ranges from 2 to 110 cm. At the 7.6 m of succession, 110 cm thick radiolitid F–R congregation which form mud mound.

The Mrlera profile is 9.7 m thick. It consists of laminated and non-laminated P–G and radiolitid F–R which could appear as intercalations within P–G. The thickness of beds ranges from 20 to 80 cm. At the 7.2 m of succession, two 80 cm thick radiolitid F–R congregations which form biostromes are laterally in exchange with P–G. Uppermost part of the radiolitid F–R which characterize thin sheet of densely packed F–R with small fragments of radiolitids.

Škokovac locality comprises 12.8 m thick succession of P–G and radiolitid F–R. Bed thickness ranges from 20 to 70 cm. At the beginning of succession, upper bedding plane of P–G are bio-turbated. At 4.88 m of succession biostromal radiolitid congregations with R–F texture laterally form mud mound. Tops of radiolitid F–R congregations are marked with thin sheet of densely packed radiolitid fragments. Laterally, the rudist congregations' flanks are as visible as lamination.

4 Discussion

Mud mounds are extremely rare on ADCP in comparison with the presence of biostromes. Here, the investigated successions, partly as mud mounds and partly as biostromes, are most probably the result of the interaction of the

available accommodation space and carbonate sedimentation rate which determine their formation (Fig. 1).

At Premantura locality radiolitid F–R congregations form mud-mound which are laterally in exchange with P–G beds. The same textural type and absence of depositional structures within mud-mound imply that they are a result of a relatively lower rate of carbonate sedimentation and larger accommodation space.

The Škokovac locality characterizes the mud mound, where the limitation of accommodation space visible as bedding within mud mound, are marked by thin F–R sheets of radiolitid fragments. Flanks of migrating radiolitid congregations within mud mound are marked by lamination.

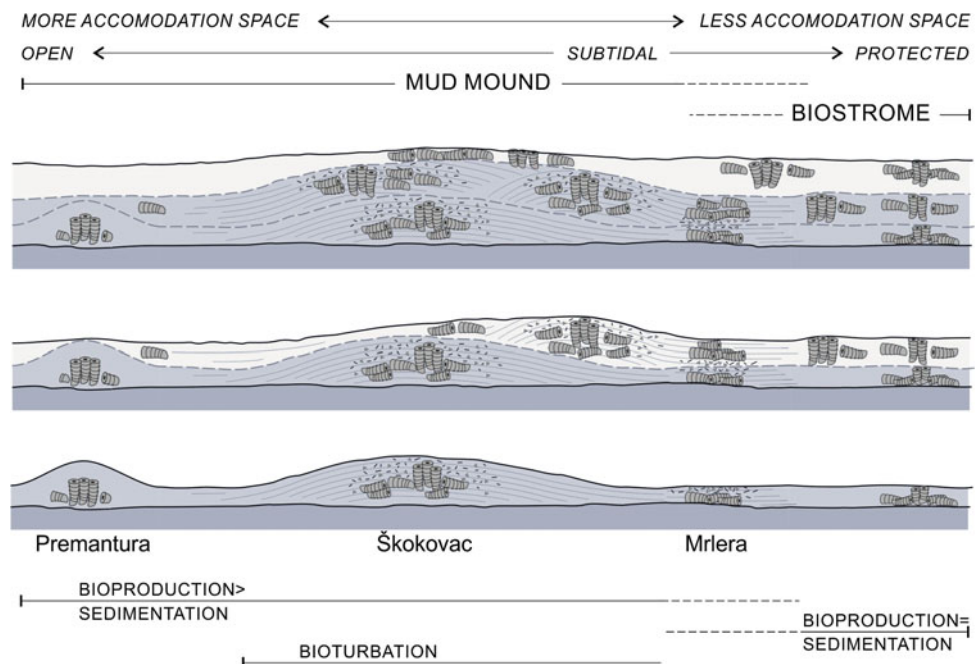
Rudist congregations of Mrlera locality with F–R texture in lateral exchange with P–G indicate, together with densely packed F–R sheet of radiolitid fragments at their top, the limitation of accommodation space as well as the top of the bed within the shallowest part of the subtidal. As a result, the radiolitid congregations form biostrome.

5 Conclusion

In the light of the conclusion that can be pointed out and based upon paleo-environmental analysis of the Premantura, Mrlera and Škokovac successions:

1. Mud mounds and biostromes, which appear in shallow subtidal, are the result of the interaction of accommodation space and the rate of carbonate sedimentation. Relatively deeper subtidal paleo-environments with

Fig. 1 Schematic lateral and vertical successions of rudist mud mounds and biostromes of Southern Istria



larger accommodation space enable the radiolitid congregations to form mud mounds while the shallower paleo-environment with less accommodation space characterizes the formation of biostromes.

2. On the one hand, the shallowing of the subtidal paleo-environment and the decrease of accommodation space are indicated by thin sheets of densely packed fragments of radiolitids at the top of beds.

References

1. Dunham, R.J.: Classification of carbonate rocks according to depositional texture. In: Ham, W.E. (ed.) *Classification of Carbonate Rocks. A Symposium*. American Association of Petroleum Geologists Memoir, vol. 1, pp. 108–171 (1962)
2. Embry, A.F., Klovan, J.E.: A late Devonian reef tract on Northeastern banks Island, NWT. *Bull. Can. Pet. Geol.* **19**, 730–781 (1971)
3. Gili, E., Masse, J.P., Skelton, P.W.: Rudists as gregarious sediment dwellers, not reef-builders, on Cretaceous carbonate platforms. *Palaeogeogr. Palaeoclimatol. Palaeoecol.* **118**, 245–267 (1995). [https://doi.org/10.1016/0031-0182\(95\)00064-X](https://doi.org/10.1016/0031-0182(95)00064-X)
4. Moro, A.: Stratigraphy and paleoenvironments of rudist biostromes in the Upper Cretaceous (Turonian-upper Santonian) limestones of Southern Istria, Croatia. *Palaeogeogr. Palaeoclimatol. Palaeoecol.* **131**, 113–131 (1997). [https://doi.org/10.1016/S0031-0182\(96\)00144-7](https://doi.org/10.1016/S0031-0182(96)00144-7)
5. Moro, A., Skelton, P.W., Čosović, V.: Palaeoenvironmental setting of rudists in the Upper Cretaceous (Turonian-Maastrichtian) adriatic carbonate Platform (Croatia), based on sequence stratigraphy. *Cretac. Res.* **23**, 489–508 (2002). <https://doi.org/10.1006/cres.2002.1017>
6. Polšak, A.: Kredna makrofauna južne Istre (Macrofaune Crétacée de l'Istrie meridionale (Yougoslavie). *Paleontologia Jugoslavica*, HAZU, Zagreb, vol. 8, pp. 1–219 (1967)
7. Skelton, P.W., Gili, E.: Paleocological classification of rudist morphotypes. In: Sladić-Trifunović, M. (ed) *Rudists, Proceedings, First International Conference on Rudists*. Beograd, 1988, Union of Geological Societies of Yugoslavia, Memorial Publication, Beograd, pp. 71–86 [delayed publication; authors reprints issues 1991] (2002)
8. Steuber, T.: A palaeontological database of rudist bivalves (Mollusca: Hippuritoidea, Gray 1848). www.paleotax.de/rudists/intro.htm (2002)
9. Vlahović, I., Tišljarić, J., Velić, I., Matičec, D.: Evolution of the adriatic carbonate platform: palaeogeography, main events and depositional dynamics. *Palaeogeogr. Palaeoclimatol. Palaeoecol.* **220**, 333–360 (2005). <https://doi.org/10.1016/j.palaeo.2005.01.001>

Early Cretaceous Oceanic Anoxic Events in Rudist-Bearing Succession, North Egypt

Yasser Salama and Gouda Abdel-Gawad

Abstract

The $\delta^{13}\text{C}$ curve of the Late Barremian-Late Albian rudist-bearing succession of Gabal Raghawi, in north Sinai, can be subdivided into 22 characteristic Carbon segments (C1–C22). The $\delta^{13}\text{C}$ record from the studied section is consistent with that previously documented in other sections of the Tethyan realm. This correlation allows us to place the Barremian-Aptian boundary at the positive shift in $\delta^{13}\text{C}$ at the contact between Carbon segments C1 and C2. The Oceanic Anoxic Event 1a (OAE1a), represented by the segments C3–C6, is recognized below the Early-Late Aptian boundary and is identified in different Tethyan sections at the *D. forbesi* Zone. The Aptian-Albian boundary is located above the *Acanthohoplites nolani* horizon within the Oceanic Anoxic Event 1b (OAE1b). During the early Late Albian, the positive Carbon isotope excursion at the topmost of C15 and C16–C17 segments shows similarities to the segments C16–C17 of the Tethys and corresponds to the Oceanic Anoxic Event 1c (OAE1c). The OAE1d occurred directly below the Albian/Cenomanian boundary within the *Mortoniceras inflatum* Zone.

Keywords

Cretaceous • North Sinai • Carbon isotopes • Anoxic events

1 Introduction

Carbon isotope ($\delta^{13}\text{C}$) stratigraphy has been established to be a valuable tool for global stratigraphical correlation of the Cretaceous deposits [1–3]. The curve of the Aptian-Albian carbon-isotope record of Tethyan sections has been subdivided in a series of segments that seem to be reproduced

globally [4–6]. In this work, the Carbon-isotope data from the Late Barremian through the Late Albian Risan Aneiza and Halal formations provide the first detailed Carbon isotope curve for this interval in north Sinai. In this study, carbon isotopic investigations of the lower Cretaceous succession were done at a sufficient resolution to observe the onset of the oceanic anoxic events.

2 Methods

The Late Barremian-Late Albian Carbon isotope record has been studied from 90 limestone samples collected from Risan Aneiza and Halal formations in the Gabal Raghawi section in north Sinai. Petrographic screening of the samples for any diagenetic features was also carried out by using a petrographic microscope. The analyses were limited to the mudstone and wackestone carbonate rocks. Carbon isotope ratios were determined at the Stable Isotope Laboratory in the University of Miami. Results are reported in the δ notation in parts per thousand or ‘Per mil’ (‰) relative to Vienna Pee Dee Belemnite (VPDB) international standard.

3 Results

The results of the isotopic analysis are illustrated in Fig. 1 and Table 1. The $\delta^{13}\text{C}$ curve can be subdivided into 22 characteristic segments in northern Sinai section. The chemostratigraphic segments defined in the previous studies [4–6] can be easily identified. In the uppermost Barremian segment C1, the $\delta^{13}\text{C}$ curve shows an increase from 0.37‰ to 3.89‰. However, segment C2 shows no significant trend. The $\delta^{13}\text{C}$ values fluctuate between 0.93‰ and 3.89‰. Moreover, the negative carbon excursion ($\delta^{13}\text{C}$ –2.29‰) characterized the boundary between segments C8 and C9. An abrupt negative carbon isotopic shift (C3–C6; C11–C12; C16–C17; C19–C20) is the marker for the onset of OAE1a, OAE1b, OAE1c and OAE1d (Fig. 1).

Y. Salama (✉) · G. Abdel-Gawad
Geology Department, Faculty of Science, Beni-Suef University,
Beni Suef, Egypt
e-mail: yasser.salama@science.bsu.edu.eg

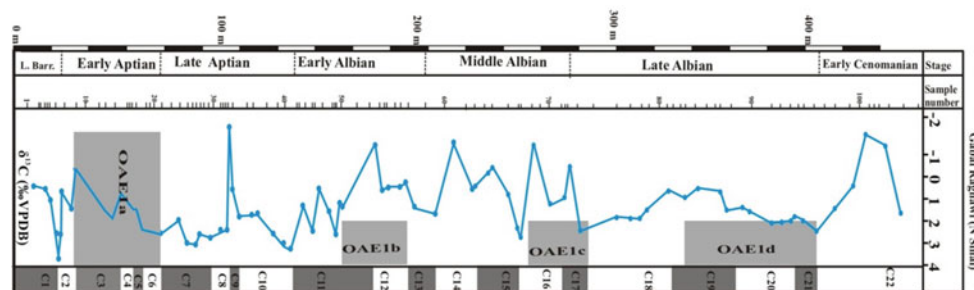


Fig. 1 Carbon isotope curve showing the isotopic expression of the oceanic anoxic events in the lower Cretaceous deposits at Gabal Raghawi, North Sinai. C-isotope segments compiled from [4, 5 and 6]

Table 1 Carbon stable isotope results from the lower Cretaceous of north Sinai

Sample no.	$\delta^{13}\text{C}$ ‰	Sample no.	$\delta^{13}\text{C}$ ‰	Sample no.	$\delta^{13}\text{C}$ ‰
1	0.37	29	2.45	59	1.82
2	0.53	31	2.17	60	-1.62
3	1.00	32	-2.29	61	0.40
4	2.76	33	0.54	63	-0.02
5	3.89	35	1.97	64	-0.80
6	2.76	36	1.86	65	0.82
7	0.93	37	1.82	66	2.09
8	1.27	38	2.45	67	2.75
9	-0.49	39	2.99	68	-1.49
11	1.75	40	3.18	70	1.26
12	1.79	41	1.13	72	0.98
13	0.90	43	2.45	73	-0.56
14	1.43	44	0.26	75	2.52
15	1.49	46	1.55	76	1.80
16	1.93	47	2.49	77	1.89
18	2.34	48	1.09	78	1.92
19	2.32	49	1.22	79	1.76
20	2.33	52	-1.71	82	0.60
22	1.81	53	0.80	84	0.94
23	3.02	54	0.43	85	0.64
24	3.03	56	0.37	88	0.82
25	2.70	57	0.33	89	1.51
28	2.70	58	1.21	90	1.42

4 Discussion

The recorded Oceanic Anoxic Event 1a (OAE1a) is located from the Carbon-isotope negative excursion represented at segment C3 to the positive Carbon segment C6 [4] below the Early-Late Aptian boundary of Iran [3] and above sequence boundary Apt4 of the Pacific Guyots [7]. The OAE1a

corresponds to the early Aptian ammonite *D. forbesi* Zone. The Aptian-Albian boundary has been placed at the top of segment C10. The onset of the negative Carbon isotope excursion of the C11–C12 segments represents the early Albian Oceanic Anoxic Event 1b (OAE1b). The onset of the negative carbon isotope excursion of the OAE1c is located at segments C16 and C17 which are similar to C16–C17 of Italy [6]. The Late Albian OAE1d is also associated with a positive carbon isotope shift peaking at the Albian-Cenomanian boundary within the ammonite *Mortoniceras inflatum* Zone.

5 Conclusion

Carbon isotope stratigraphy was used to improve the stratigraphic correlation and the age determination of the examined studied section. The Late Barremian-Late Albian Carbon isotope records of the studied section show a good correlation with those previously described from the Tethys. In other words, the Barremian-Aptian boundary is placed at the positive Carbon isotope peak above the contact between C1 and C2 Carbon segments of the Risan Aneiza Formation at Gabal Raghawi. Moreover, the Cretaceous Oceanic Anoxic Events (OAE1a-d) coincide with a negative followed by a positive Carbon excursions and display a correlation with those recorded from the reference Carbon curves reported elsewhere.

References

1. Arthur, M.A., Dean, W.E., Pratt, L.M.: Geochemical and climatic effects of increased marine organic carbon burial at the Cenomanian/Turonian boundary. *Nature* **335**, 714–717 (1988)
2. Jarvis, I., Gale, A.S., Jenkyns, H.C., Pearce, M.A.: Secular variation in Late Cretaceous carbon isotopes: a new $\delta^{13}\text{C}$ carbonate reference curve for the Cenomanian-Campanian (99.6–70.6 Ma). *Geol. Mag.* **143**, 561–608 (2006)
3. Vincent, B., van Buchem, F.S.P., Bulot, L.G., Immenhauser, A., Caron, M., Baghbani, D., Huc, A.Y.: Carbon-isotope stratigraphy, biostratigraphy and organic matter distribution in the Aptian-Lower

- Albian successions of southwest Iran (Dariyan and Kazhdumi formations). *GeoArabia Spec. Publ.* **4**(1), 139–197 (2010)
4. Menegatti A., Weissert, H., Brown, R.S., Tyson, R.V., Farrimond, P., Strasser, A., Caron, M.: High-resolution $\delta^{13}\text{C}$ stratigraphy through the Early Aptian 'LivelloSelli' of the Alpine Tethys. *Paleoceanography* **13**, 530–545 (1998)
 5. Bralower, T.J., Cobabe, E., Clement, B., Sliter, W.V., Osburn, C.L., Longoria, J.: The record of global change in mid-cretaceous (Barremian-Albian) sections from the Sierra Madre, Northeastern Mexico. *J. Foramin. Res.* **29**, 418–437 (1999)
 6. Luciani, V., Cobianchi, M., Jenkyns, H.C.: Albian high-resolution biostratigraphy and isotope stratigraphy: the CoppadellaNuvola pelagic succession of the Gargano Promontory (Southern Italy). *Eclogae Geologicae Helveticae* **97**, 77–92 (2004)
 7. Röhl, U., Ogg, J.G.: Aptian-Albian eustatic sea-levels. *Spec. Publ. Int. Assoc. Sedimentol.* **25**, 95–136 (1998)

Late Cretaceous Transgressive-Regressive Cycles Including Rudist-Rich Units in Central Tunisia

Mohamed Hédi Negra and Jalel Jaballah

Abstract

In central Tunisia, Upper Cretaceous deposits including rudist-coral carbonates are generally transgressive upon Lower Cretaceous formations that mainly consist of siliciclastic deposits sometimes associated to neritic and to emergent carbonates [1]. A regional sequence boundary separates the Upper Aptian emergent series and the Upper Albian transgressive deposits. On the basis of the rudist-rich carbonates used as a “facies reference”, the identification of transgressive-regressive cycles within the Upper Cretaceous series has helped a lot to establish correlations at regional and global scales.

Keywords

Late cretaceous • Rudist-rich carbonates • Third order cycles • Sea level changes

1 Introduction

The identification of the depositional cycles in the stratigraphic record of Late Cretaceous carbonate platforms constitutes a tool that could help to recognize the main events stimulating the growth of these platforms. The correlation of these cycles at a global scale, which uses the rudist-rich carbonates as a “facies reference”, could confirm the role of sea level changes in the development and/or the demise of rudist-rich carbonates. The main objective of this study is to situate the position of the rudist-rich facies within these cycles and to establish correlations of the identified cycles at regional, mediterranean and global scale.

M. H. Negra (✉)
Faculty of Sciences of Tunis, University of Tunis El Manar, Tunis,
Tunisia
e-mail: hedi.negra@fst.utm.tn

J. Jaballah
College of Petroleum Engineering and Geosciences, King Fahd
University of Petroleum and Minerals, Dhahran, Saudi Arabia

2 Methods

The present study was based on field work including detailed geological mapping, sections logging and sequence analyses. In this regard, 5 sections were logged in Jebel el Kebar and Jebel Meloussi. Petrographical analyses have been conducted on 300 thin sections in order to determine the composition and microfacies characteristics. For additional biostratigraphical precisions, microfauna (e.g., benthic and planktonic foraminifera) have been extracted from soft marly sediments. Concerning the rudist-rich bodies, detailed mapping in Jebel el Kebar area has allowed us to establish a detailed subdivision based on changes in geometry and composition.

3 Results

Rudist-rich carbonates are frequent in Late Cretaceous series outcropping in the Sidi Bouzid area especially in Jebel el Kebar and locally in Jebel Meloussi. In Jebel el Kebar, rudist-rich units appear in the Cenomanian C Member of the Zebbag Formation, the Late Cenomanian Gattar Member of the Zebbag Formation and in the Middle Turonian upper Bireno Member. In addition, coral-rich units are included in the Coniacian Douleb Member and rudist-coral rich limestones are included in the Campanian Merfeg Formation. In Jebel Meloussi, rudist-rich units were recently observed in the Cenomanian C Member of the Zebbag Formation. In this respect, the distribution of the rudist-rich carbonates appears in both the regressive and the transgressive parts of the successions of the transgressive-regressive cycles.

3.1 The Rudist-Rich Units in Regressive Successions

In regressive successions, rudist-rich units are identified in the Cenomanian C Member of the Zebbag Formation. The

coral-rich units are recognized in the Middle Turonian upper Bireno Member and in the Late Turonian-Coniacian Douleb Member.

In Jebel el Kebar and Jebel Meloussi, a Cenomanian succession directly starts on a transgressive surface overlying the Aptian Kebar continental Formation. In Jebel Meloussi, the transgressive surface underlined by conglomeratic carbonates directly overlies emergent Aptian Orbata dolostones.

In both cases, the transgressive surface is directly overlain by the Cenomanian A and B Zebbag units which are rich in entire and joined bivalves. The latter are directly overlain by rudist-rich carbonates showing joined entire rudists mainly represented by radiolitids. The rudist-rich carbonates vertically change to high energy carbonates rich in oolites, changing above to the tidal-flat facies including bioturbated, laminated stromatolith-rich carbonates with mud cracks and, locally, gypsum.

In the Middle Turonian upper Bireno Member and in the Late Turonian-Coniacian Douleb Member, coral-rich units constitute the upper part of the regressive successions.

3.2 The Rudist-Rich Units in Transgressive Successions

In the transgressive successions, rudist-rich units are identified in the Late Cenomanian Gattar Member. The rudist-coral rich limestones are recognized in the Campanian Merfeg Formation.

In Jebel el Kebar and Meloussi, the Late Cenomanian Gattar rudist-rich units (with directly overlying tidal-flat carbonates) express a regional transgression at least at the Sidi Bouzid area. They start with bioclastic carbonates overlain by lensoid bodies rich in entire and joined rudists (*Durania arnaudi*; [2]). The lower part of this 3rd order transgressive successions includes deepening-upward 4th and 5th order cycles, changing in the upper part to shallowing-upward cycles ending with emergent carbonates and evaporates. Above, a following cycle starts with pelagic marls of the Turonian Aleg Formation.

In Jebel el Kebar, the Campanian Merfeg rudist-coral rich limestones [3] are directly deposited on an erosional surface, locally conglomeratic, suggesting a transgressive phase. The Merfeg Formation shows the superposition of three deepening-upward cycles starting with rudist-rich micritic limestones and ending with pelagic marls.

4 Discussion

- Transgressive successions comprising rudist-rich facies were also described in Algeria [4] during the Late

Cenomanian. In fact, rudist-rich carbonates mark the first marine inundation overlying coastal lagoonal deposits, tidal-flat restricted carbonates and local evaporates. This marine event starts under relatively high energy conditions.

- Regressive successions comprising rudist-rich deposits were also described in Jebel Bireno [5] where they constitute regressive shallowing upward cycles comparable to those of a Late Highstand System Tract [6, 7]. Similar Turonian cycles were also identified in Algeria in the eastern atlastic domain [4] and other areas at the Tethyan margin [8, 9].

5 Conclusion

During the Late Cretaceous, the Central Tunisia was covered by extended platforms. The rudist-rich carbonates generally occupied the margins of these platforms or local horsts. However, sea-level changes have caused obvious modifications on the depositional systems. The main Cenomanian transgressive event has stimulated the development of rudist-rich carbonates. The Turonian rudist-rich carbonates were deposited during subsequent shallowing conditions. Since the Late Turonian, transgressive deposits, especially marlstones, have tended to seal the irregular paleotopography affected, at least locally, by middle Turonian extensional tectonic movements. This partial drowning of carbonate platforms linked to a sea level rise was already identified in other localities of the African Tethyan margin. Global platforms drowning appear more significant during the Campanian transgression which has led to a dramatic change of sedimentation that is mainly represented by pelagic marls and fine-grained chalky carbonates.

References

1. Heldt, M., Lehmann, J., Bachmann, M., Negra, M.H., Kuss, J.: Increased terrigenous influx but no drowning: palaeoenvironmental evolution of the Tunisian carbonate platform margin during the Late Aptian. *Sedimentology* **57**(2), 695–719(25) (2010) (Wiley-Blackwell)
2. Razgallah, S., Philip, J., Thomel, G., Zaghbib-Turki, D., Chaabani, F., Ben Haj Ali, N., M'rabet, A.: La limite Cenomanien-Turonien en Tunisie centrale et méridionale: Biostratigraphie et paléoenvironnements. *Cretaceous Res.* **15**, 507–533 (1994)
3. Negra, M.H., Skelton, P.W., Gili, E., Valdeparas, F.X., Argles, T.: Recognition of massive Upper Cretaceous carbonate bodies as olistoliths using rudist bivalves as internal bedding indicators (Campanian Merfeg Formation, Central Tunisia). *Cretaceous Res.* **66**, 177–193 (2016)
4. Herkat, M.: Geodynamic Evolution of the North African Atlas Belt. *Geomorphology and Plate Tectonics*. Nova Science Publishers, Inc. (2009)

5. Zagrarni, M.F., Boughdiri, M., Snoussi, A.: Sequence stratigraphy and paleogeography reconstruction of the reference Lower-Middle Turonian successions of Jebel Biréno (Central Tunisia): a semi-quantitative approach. *Arab. J. Geosci.* (2016). <https://doi.org/10.1007/s12517-016-2349-2>
6. Scott, R.W.: High resolution North African Cretaceous stratigraphy: status. NATO Advanced Research Workshop, 13–18 May 2002, Tunisia. North African Cretaceous rudist and coral formations and their contributions to carbonate platform development- Nato Sciences Series (2003)
7. Haq, B.U., Al-Qahtani, A.M.: Phanerozoic cycles of sea-level change on the Arabian platform. *GeoArabia* **2**, 127–160 (2005)
8. Gili, E.: Paleoecological significance of rudist constructions: a case study from les Collades de Basturs (Upper Cretaceous, south-central Pyrenees), *Geol. Rom.* **28**, 319–325 (1992)
9. Philip, J., Babinot, J.F., Tronchetti, G., Fourcade, E., Guiraud, R., Bellion, Y., Herbin, J.P., Combes, P.J., Cornée, J.J., Dercourt, J., Ricou, L.E.: Late Cenomanian (94–92 Ma). In: Dercourt, J., Ricou, L.E., Vrielynck, B. (eds.) *Tethys Palaeoenvironmental Maps, Explanatory Notes*. Gauthier-Villars, Paris, pp. 153–178 (1993)

Sedimentology and Petrophysics of Turonian-Coniacian Rudist Rich-Reservoir Rocks, Offshore Tunisia

Senda Boughalmi, Mohamed Hédi Negra, Yves Géraud, Sonia Ben Alaya, and Danièle Grosheny

Abstract

The Turonian-Coniacian rudist-bearing carbonates are characterized by their good quality as reservoir rocks. They produce oil and gas in several fields in eastern onshore and offshore of Tunisia. These rudist-rich facies are featured by a developed porosity (intragranular, intergranular, intercrystalline and matrix porosity especially between micritic grains). In terms of reservoir properties, the highest values of helium-porosity (reaching 24%) and nitrogen-permeability (reaching 1200 mD) were measured in rudist-rich carbonates. In addition, some diagenetic features such as dolomitisation and dissolution have created additional pores and have clearly enhanced the reservoir potential of these rudist-rich carbonates. On the other side, some diagenetic processes such as cementation, silicification and compaction have led to the destruction of the pore system and the decrease of porosity and permeability values.

Keywords

Late-cretaceous • Rudist-bearing reservoir rocks • Tunisia • Sedimentology • Petrophysics

1 Introduction

In Tunisia, Turonian-Coniacian rudist-bearing carbonates occur in Central and South East Tunisia along a NW-SE trend from Kasserine to the northern part of the Gulf of Gabes. During Turonian-Coniacian period, this area is occupied by shallow-marine platform carbonates. However, changes in facies and thickness are obvious along this trend [1].

From a petroleum system angle, the Late Cretaceous rudist-bearing carbonates, especially those of the Turonian-Coniacian (Douleb Member) and belonging to the Turonian-Early Campanian Aleg Formation, are known for their good reservoir quality. In fact, they are productive in several sectors of Tunisia, notably in the region of Sfax and the Gulf of Gabes [2] and more specifically in several oil fields especially those of Guebiba, Gremda, El Ain, Rheimoura and Miskar [3].

The present study is based on core sedimentological and petrophysical analyses of a proven carbonate reservoir producing gas in the Gulf of Gabes (Tunisia Offshore).

The basic aims of this paper are to characterize the rudist-rich carbonate reservoirs by means of the above mentioned analyses.

2 Materials and Methods

The present study is based on sedimentological and petrophysical analyses on samples taken from a well located area in the Northeast of the Gulf of Gabes approximately 110 km at the east-southeast of Sfax. Sedimentological study is based on a macroscopic analysis in order to recognize the main sedimentological features of ten cores covering 170 m of series. This study is also pivoted on microscopic analyses particularly by using an optical microscopy and Scanning Electron Microscopy (SEM). Concerning with the petrophysical examination, the study consists in the measurements of the helium-porosity and the nitrogen-permeability.

S. Boughalmi (✉) · M. H. Negra
Faculté des Sciences de Tunis, Université Tunis El Manar,
Campus Universitaire, 2092 Tunis, Tunisia
e-mail: sendaboughalmi@gmail.com

Y. Géraud · D. Grosheny
Université de Lorraine, CNRS, GREGU, Ecole Nationale
Supérieure de Géologie, 54000 Vandoeuvre lès Nancy, France

S. Ben Alaya
Entreprise Tunisienne d'Activités Pétrolières (ETAP), Charguia II,
2053 Tunis, Tunisia

For the helium porosity, the “UltraPore™300” helium porosimeter is used. Regarding the gas permeameter “UltraPerm™ 400”, the Darcy’s law to determine the permeability from the measured gas flow rate and the upstream and downstream pressures is used.

3 Results and Discussion

3.1 Sedimentological Study

Based on the sedimentological study of the Turonian-Coniacian cores, three distinct lithological units are highlighted which show the following characters from base to top:

- Unit 1 (U1): A carbonate unit mainly composed of rudist-rich limestones intercalated by two laminated dolomitic layers. Within this unit, rudists could be entire and joined or fragmented and associated to other bioclasts.
- Unit 2 (U2): An anhydritic unit intercalated by a thin layer of packstone texture containing peloids, some benthic foraminifera and echinoderm debris.
- Unit 3 (U3): A fine-grained unit composed of micritic facies, partly argillaceous.

3.2 Petrophysical Study

Porosity and permeability are the two main petrophysical parameters which control the movement and the storage of the fluids in rocks. They are the main petrophysical parameters that characterize a carbonate reservoir.

The relationship between the porosity and the permeability of the Coniacian samples (Douleb Member) is presented in a logarithmic graph (Fig. 1). The distribution of the different points indicates the degree of influence of the porosity on the permeability. It shows that there is a good correlation between these two petrophysical parameters.

Four Rock-types are defined according to the porosity-permeability relation established in the Fig. 1:

- The rock-type **RT1** regroups the grainstones with small peloids and rudist-debris (MF2; porosity values between 21 and 24% and permeability values between 21 and 360 mD).
- The rock-type **RT2** shows a medium to good reservoir quality (porosity between 14 and 19%; permeability between 15 and 1200 mD). It regroups four microfacies and packstone with large rudist-debris and peloids (MF6), dolomitized packstone rich in entire and fragmented rudists (MF1), dolomites (MF9) and

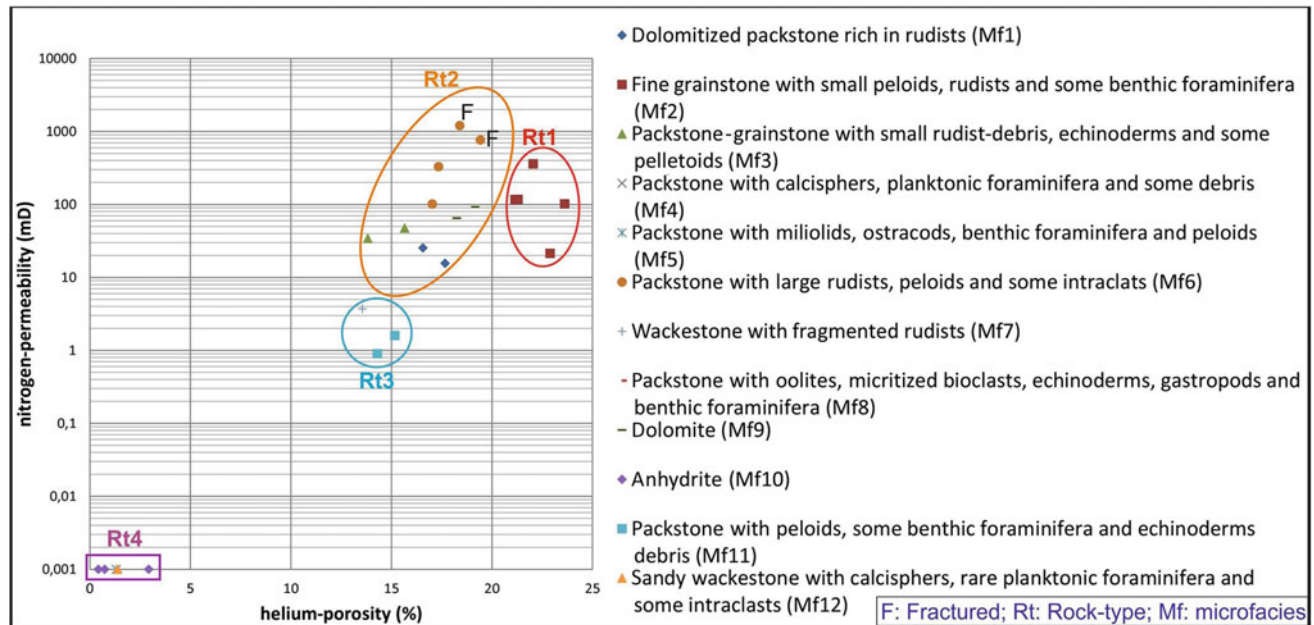


Fig. 1 Correlation between Helium-porosity and nitrogen-permeability of Douleb member rocks

packstone-grainstone with small rudist-debris associated to echinoderm-debris and peloids (MF3).

- The rock-type **RT3** shows a medium reservoir quality (porosity between 13 and 15%; permeability between 0.9 and 4 mD). It regroups wackestones with fragmented rudists and packstone with peloids (MF7), echinoderm-debris and benthic foraminifera (F11).
- The rock-type **RT4** regroups the fine micritic facies (MF4, MF5, MF8 and MF12) and anhydrites (MF10). It shows low to negligible porosity and permeability values, respectively from 0.3 to 2.93% and <0.01 mD (apparatus measurement limit).

3.3 Relationship Between Petrophysical Properties and Microfacies Characteristics

Samples that belong to the rock-types RT1, RT2 and RT3 show an evolution of the permeability parallel to that of the porosity. Figure 1 shows that porosity and permeability generally increase and decrease simultaneously. These three distinguished groups are mainly composed of rudists. They are characterized by a complex porous system that include matrix, intercrystalline (Fig. 2a), intergranular (Fig. 2a, c, d) and intragranular (Fig. 2a, b, d) porosities. Microscopic study has shown that RT1, RT2 and RT3 rocks are mainly

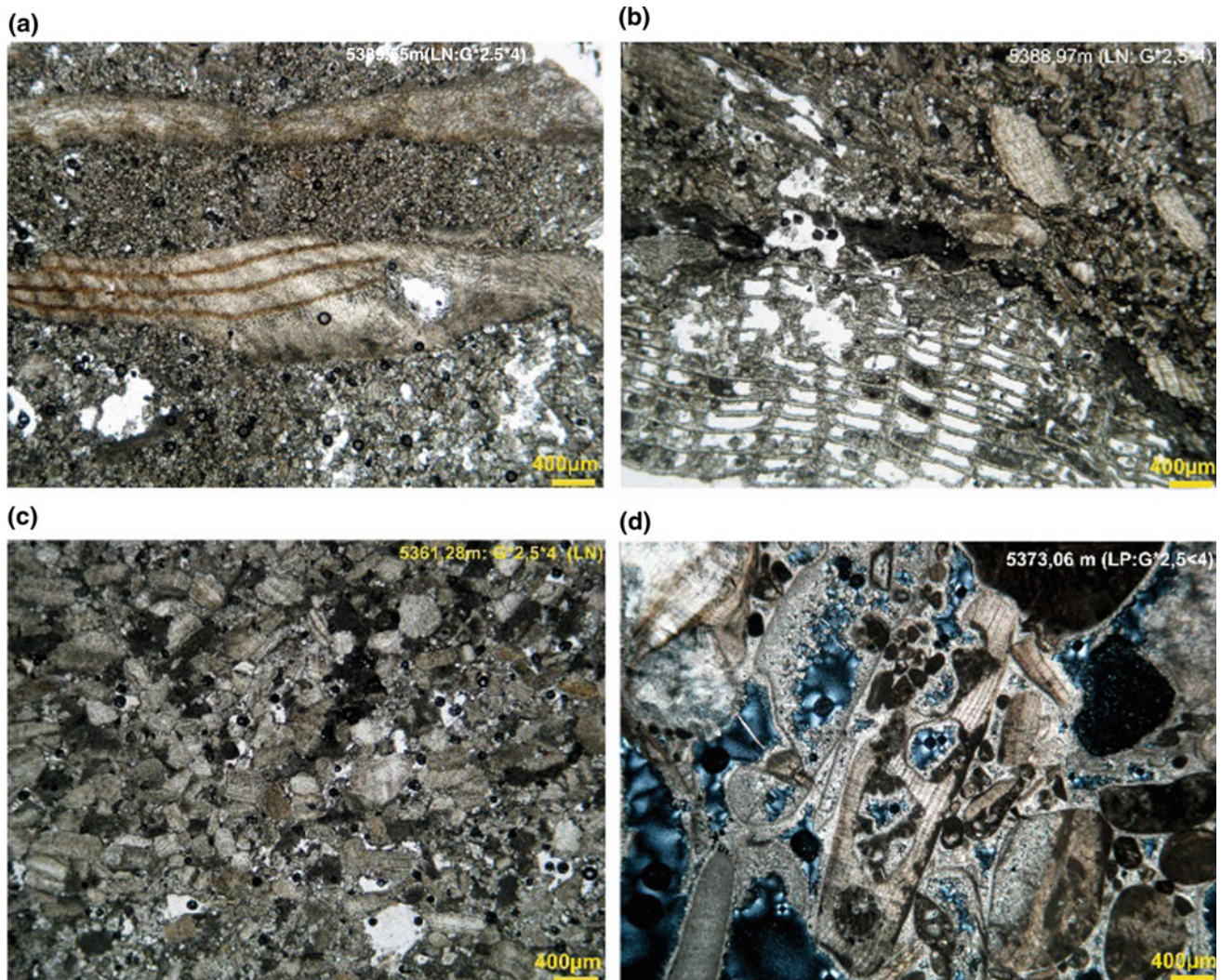


Fig. 2 The different and main rudist-rich microfacies at the studied well; **a**, dolomitized packstone rich in rudist-debris (Hippuritidae) showing an intergranular, intragranular and intercrystalline porosity; **b**, packstone rich in rudists (Hippuritidae and Radiolitidae)

showing an important intragranular porosity; **c**, grainstone with small rudist-debris and peloids showing an intergranular porosity; **d**, packstone with large rudist fragments and peloids showing an important intergranular and intragranular porosity

affected by dissolution and matrix dolomitization that create a significant secondary porosity (intercrystalline and/or moldic). Rocks which have the highest porosity show an intermediate to good permeability, especially in the fractured layers (MF6).

The rock-type (RT4), which characterizes the summital part of the series, is represented by a horizontal straight line where the porosity values slightly increase. However, the permeability remains constant and negligible (<0.01 mD). The RT4 regrouping micritic facies also including pyrite crystals and phosphatic grains are affected by strong compaction with the development of numerous stratiform stylolithes. In addition to compaction, these facies are modified by silicification processes that are expressed by automorphic quartz crystals particularly occurring within the matrix. These diagenetic processes, which involve cementation of the pores, decrease the porosity and permeability of these facies.

4 Conclusion

From a petroleum perspective, it seems that only the first carbonate unit (U1) of the Douleb Member is of petroleum interest. It can be considered as a reservoir layer. At this unit, the rock-type RT1, which regroup fine grainstones containing small and well sorted rudist-debris and peloids (Mf2),

present the best petrophysical characteristics (porosity and permeability).

In this study, the compilation of petrophysical results associated with sedimentological analyses shows that porosity is under the influence of the texture of the sediment (the highest porosity values are measured within the fine-grained microfacies) and the diagenetic phenomena. Matrix dolomitization and dissolution are the main diagenetic processes which improve the porous system (porogenesis); whereas, it is completely destroyed by compaction, silicification and cementation.

References

1. Jaballah, J.: Les series du Crétacé supérieur (Albien-Campanien inférieur) en Tunisie Centrale Meridionale. Caractères sédimentaires et intérêt économique. Thèse Doc. Tunis. University, 289 p. (2017)
2. Lansari, F., Hammouda, F., Negra, M.H.: The Upper Cretaceous carbonate facies in Central-Eastern Tunisia: Electrofacies, sedimentary characters and economic implications. In: Proceedings of the 10th Tunisian Petroleum Exploration & Production Conference. Entreprise Tunisienne d'Activités Pétrolières (ETAP), pp. 67–91. EPC. 26, Tunis (2006)
3. Zagarni, M.F., Negra, M.H., Melki, S.: Turonian rudist-coral limestones in Jebel Biréno, Central Tunisia. In: Gili, E., Negra, M. H., Skelton, P. (eds.) North African Cretaceous Carbonate Platform Systems, pp. 111–128. Kluwer Academic Publishers, Amsterdam (2003)

Depositional Facies, Sequence and Diagenesis of the Middle-Upper Eocene in Jebel Cherahil (Central Tunisia)

Zahra Njahi-derbali and Jamel Tourir

Abstract

This paper is set out to study the Cherahil Formation (middle-upper Eocene) in Jebel Cherahil. In this area, the Cherahil Formation is subdivided into three lithostratigraphic units: the lower, the middle and the upper Cherahil members. The field examination and microscope observation of thin sections and the DRX clays mineralogy allowed us to distinguish six depositional facies (marly and five carbonate facies) that have been developed broadly within a shallow water carbonate platform with episodes of open marine conditions and others of restricted lagoon conditions. The depositional environment was subjected to variable continental inputs. According to the vertical variation of the depositional facies and the examination of the discontinuity surfaces, the Cherahil Formation may be subdivided into eight third-order depositional sequences. Each one of them includes transgressive and high-stand systems tract developed in a platform setting. Moreover, the sequence boundaries generally consist of erosive surface that corresponds to superimposed subaerial exposure surface and transgressive surfaces. The sea level fluctuation has, in addition, controlled the carbonate diagenesis, in particular dissolution.

Keywords

Cherahil formation • Diagenesis • Sequence stratigraphy • Carbonate • Depositional facies

1 Introduction

The sedimentology of the middle-upper Eocene sedimentary successions in central Tunisia was discussed in several studies Bismuth et al. 1978; El Waer [4]; Ben Ismail-Latrache [2] including the marine deposits of the Cherahil formation in its type locality [1, 8, 9]. These authors discussed the depositional environment of Cherahil Formation in Jebel Cherahil and in central Tunisia by using different approaches: depositional facies, paleontology and paleoecology of ostracods. In the present study, a more detailed study of the middle upper Eocene Cherahil Formation in Jebel Kabbara area (south Jebel Cherahil) is provided. In particular, the purpose of this paper is to study the depositional environment, diagenesis and sequence stratigraphy of Cherahil Formation in this area.

2 Materials and Methods

A detailed section was logged, sampled and described in the Cherahil Formation along the southern Jebel Cherahil (Jebel Kabbara). Eleven shale samples and forty three carbonate rock samples were collected and examined in the laboratory. The analyses include sediment texture examination and X-ray Diffraction analysis. Thin sections of carbonate rocks were prepared and described under the petrographic microscope based on the classification of Dunham [3]. Eleven oriented clay fraction for X-ray Diffraction analysis were prepared for each shale sample. These typically include: airdried sample, heating to 550°C, for kaolinite destruction and dehydration of smectite which potentially hide chlorite peaks and treatment by ethylene glycol in order to reveal expandable clay minerals [6]. The classical sequence stratigraphy terminology is followed in the present study [5, 7].

Z. Njahi-derbali (✉) · J. Tourir
Laboratory 3E, National School of Engineers of Sfax,
University of Sfax, PB 1173 3038 Sfax, Tunisia
e-mail: zahra.njahi@gmail.com

3 Results

3.1 Lithostratigraphy

The Middle–Upper Eocene Cherahil Formation in Jebel Kabbara is 92 m thick. It is arranged into an alternation of lumachellic limestones and marls rich in foraminifers and ostracods. Based on the dominant litho-facies, the Cherahil Formation can be subdivided into three units: the Lower Cherahil member (dominated by marly facies with intercalated limestones), the Middle Cherahil member (dominated by lumachellic carbonates with intercalated marly levels) and the Upper Cherahil member (dominated by marls at the base and limestones at the top).

3.2 Depositional Facies

Two depositional facies types have been defined in Cherahil formation: argillaceous and carbonate facies.

The marly facies is characterized by the presence of variable proportions of smectite, kaolinite and illite. The smectite is characterized by important proportions which reveal an arid palaeoclimates. The kaolinite and the illite are characterized by significant proportions that reveal a wet climate.

The carbonate facies type includes five sub-facies: (i) coquina and lumachellic limestone that developed within a lagoonal restricted environment (ii) mudstone with pellets indicating an infralittoral lagoonal environment (iii) sandy mudstone indicating infralittoral lagoonal environment exposed to continental imputes (iv) wackestone-packstone with bryozoans and green algae that indicate an open marine infralittoral to circalittoral environment (v) bioclastic wackestone with benthic and planktonic foraminifera that developed within a circalittoral environment.

3.3 Early Diagenesis Features

The microscopic observation of the Cherahil formation carbonates shows various early and late diagenetic features. In particular, the main early diagenetic features are materialized by dissolution, carbonate cementation, micritisation and microperforation. The dissolution vug is micrometric to millimetric and is associated with geopetal internal sediment. They are mainly located under the emersion surfaces. The carbonate cements consist of a micrometric frange of CaCO₃ microsparite coating some dissolution vug wall.

3.4 Sequence Stratigraphy

According to the depositional facies variation and to the field examination of unconformity surfaces, eight third-order depositional sequences were identified in the studied formation (Fig. 1). These sequences include only transgressive and high-stand systems tract. They are generally bounded by subaerial exposure surfaces.

4 Discussion

According to the vertical variation of the depositional facies of Cherahil formation in Jebel Kabbara, this formation may be subdivided into different depositional systems tract. In addition, according to the field examination, these systems tract may be arranged into eight depositional sequences bounded with erosive surfaces. The early dissolution features observed under these surfaces may result from meteoric diagenesis which may be related to a sea-level fall and subsequent subaerial exposure of the shelf. Considering the total duration of the middle and upper Eocene (15.3 Ma), the overage duration of each sequence is of (1.9 Ma). Then, the studied depositional sequences may be considered as third-order sequences [7].

Taking into account, the paleogeography of Tunisia during the Eocene and according to which central Tunisia should have correspond to an inner shelf domain, it seems logical that the studied sequences start with the transgressive interval and end with the high-stand systems tract. The transgressive intervals show generally marine fossiliferous marls with benthic and planktonic foraminifera that developed within infralittoral and circalittoral environment. The high-stand systems tract consist of alternating marls and carbonate beds. From bottom to top, the high-stand carbonate beds vary from mudstone-wackestone rich in benthic and planktonic foraminifera that developed in infralittoral domain to lumachellic wackestone-packstone and end with oyster-rich lumachells that developed in lagoonal environment.

5 Conclusion

The middle upper Eocene Cherahil Formation deposit occurred within the inner shelf domain of central Tunisia. These deposits include eight third-order depositional sequences. Each one of them is composed of a transgressive interval and high-stand systems tract. These sequences are bounded by subaerial exposure surfaces.

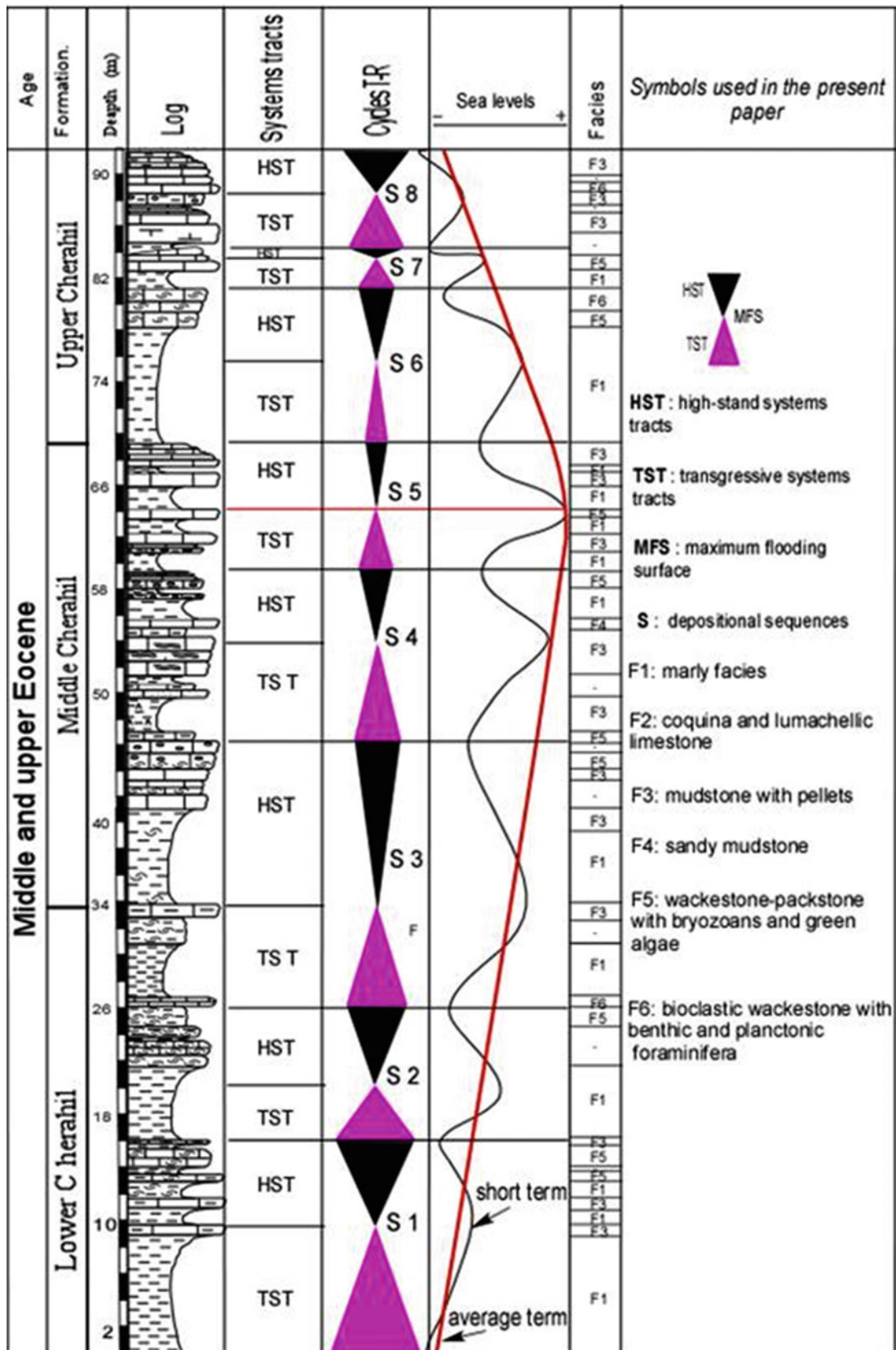


Fig. 1 Sequence stratigraphy of the Cherahil formation in Jebel Kabbara (South Jebel Cherahil)

References

1. Amami-Hamdi, A., Dhahri, F., Saïd-Benzarti, R.: Middle to Upper Eocene ostracod fauna of central Tunisia and Pelagian Shelf: examples of Jebel Bargouand the Gabes Gulf. *Arab. J. Geosci.* **7**(4), 1587–1603 (2014)
2. Ben Ismail-Latrache, K.: Précision sur le passage Lutétien-Bartonnien dans les dépôts éocènes moyens en Tunisie centrale et Nord-orientale. *Rev. Micropaléontol.* **43**, 3–16 (2000)
3. Dunham R.J.: Classification of carbonate rocks according to depositional texture. In: Ham, W.E. (eds.) *classification of carbonate rocks*. Mem. Amer. Ass. Pétr. Géol. Tulsa **1**, 108–120 (1962)
4. El Waer, A.A.: Tertiary and Upper Cretaceous Ostracoda from NW off-shore Libya. Their Taxonomy, Biostratigraphy and Correlation with adjacent. *Earth Sciences Society Libya, Tripoli*, p. 445 (1992)
5. Haq, B.U., Hardenbol, J., Vail, P.R.: Mesozoic and Cenozoic chronostratigraphy and cycles of sea-level change. *Soc. Econ Paleont. Min.* **42**, 71–108 (1988)
6. Hardy, R., Tucker, M.: X-ray powder diffraction of sediments. In: Tucker, M. (ed.) *Techniques in sedimentology*, pp. 191–228. Scientific Publications, Blackwell (1988)
7. Vail, P.R., Audemard, F., Bowman, S.A., Eisner, P.N., Perez-Cruz, C.: The stratigraphic signatures of tectonics, eustasy and sedimentology. An overview. In: Einsele, G., et al. (eds.) *Cycles and events in stratigraphy*, pp. 617–659. Springer, Berlin (1991)
8. Burolet, P.F.: Contribution à l'étude stratigraphique de la Tunisie centrale. Ph.D Thesis Paris. *Annales des Mines et de la Géologie, Tunis.* **18**, p. 350 (1956)
9. Comte, D., Dufaure, P.: Quelques précisions sur la stratigraphie et la paléontologie Tertiaire en Tunisie Centrale et Centro-Orientale, du Cap Bon au Mazzouna. *Livre Jubilaire M. Solignac. Annale des Mines de la Géologie* **16**, 97–115 (1973)
10. Bismuth, H., Kelj, A.J., Oertli, H.J., Szczechura, J.: The genus *Loculi-cytheretta* (Ostracoda). *Bulletin Centre de Recherche, d'Exploration et de Production, Elf-Aquitaine* **2**(2), 227–263 (1978)

Paleozoic Reservoir Systems in the Ghadames and Jefarah Basins, Tunisia

Adel Jabir, Adrian Cerepi, Corinne Loisy, and Jean-Loup Rubino

Abstract

Twenty eight wells with its geological well reports and well logs from the Paleozoic reservoirs of the Ghadames and Jefarah basins (Libya) illustrate how reservoir properties changes laterally and vertically through time (from a proximal to a distal setting). The reservoirs in the study area are spread over a large range of siliciclastic succession with the prospective section extending from Cambrian to the Permian. Six stratigraphic cross sections through the study area have been reconstructed to illustrate the vertical and lateral reservoir extensions. It was noted that the reservoir properties vary laterally and vertically between the proximal and distal deposits with the average porosity decreasing towards the distal part of the basin.

Keywords

Ghadames basin • Jefarah basin • Paleozoic • Sandstone reservoirs • Porosity

1 Introduction

The Ghadames basin is an intra-cratonic one of about 350.000 km² located in the northwestern part of Libya. It is bounded to the north by the Nafusah Uplift, to the south by

the Al Qarqaf Arch and finally to the west it extends into Algeria. To the east, the boundary is not clearly defined where it overlaps with the western flank of the Sirte basin. The Jefarah basin covers an area of 15.000 km². It is a complex faulted zone that forms a terrace between the Nafusah uplift to the south and the offshore Sabrata basin to the north. It extends westwards into Tunisia at the north of the Dahar Uplift (Fig. 1).

The purpose of the present work is to study the overall characteristics of the reservoirs in the Paleozoic succession in the Ghadames and Jefarah basins. The Paleozoic in the study area contains many reservoir units (including the Cambrian Hasawnah Formation, Middle Ordovician Hawaz Formation, Upper Ordovician Mamouniyat Formation, from Middle to Upper Silurian Akakus Formation, Lower Devonian Tadrart Formation, and Upper Devonian Tahara Formation).

In this study, six cross sections in the Paleozoic succession have been constructed based on 28 reference wells crosscutting the Paleozoic reservoirs from the Cambrian up to the Permian. Depending on the available data, two wells in each cross section have been analysed representing respectively a proximal and distal setting with the aim to assess the lateral changes with regard to reservoir properties.

2 Methodology and Database

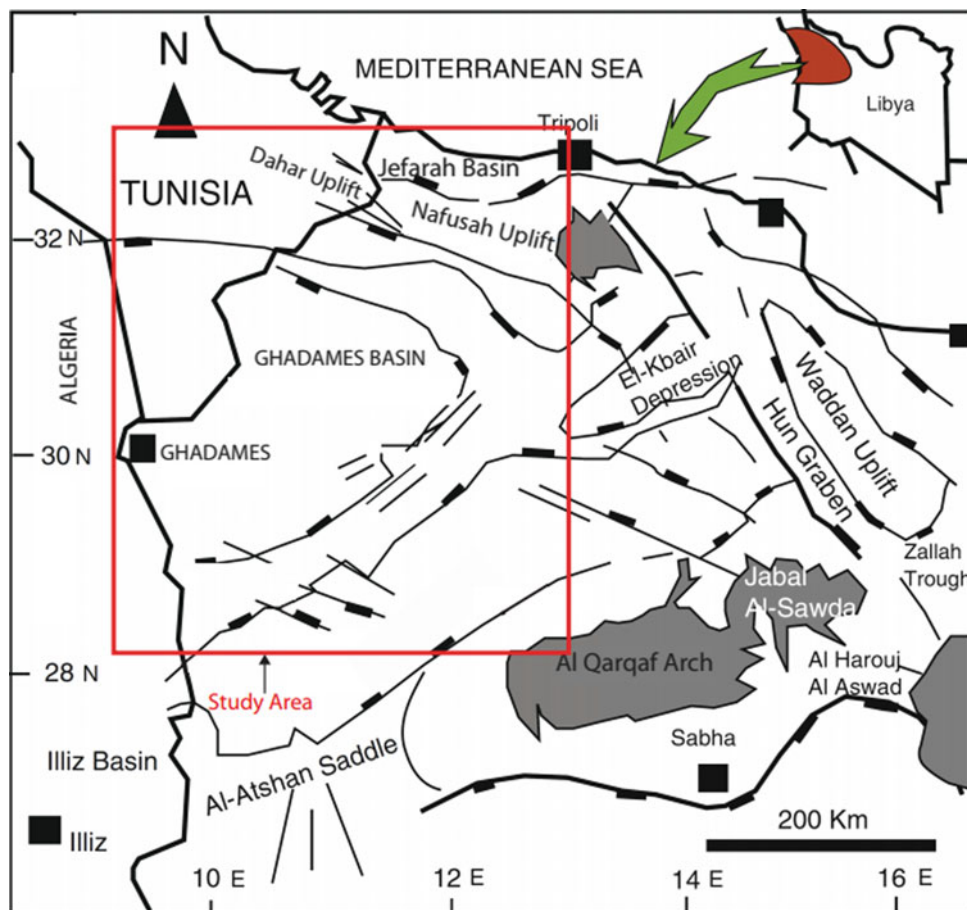
Twenty eight wells were used in the establishment of five cross-sections. Forty core samples have been analyzed in the laboratory. Fifteen of them are representative for the Cambro-Ordovician period in well SN-1. Nineteen are representative for the same period in well ST-1. The six remaining samples representing the Lower Akakus Formation in well J1-NC100.

To get an accurate porosity value, using density, sonic, resistivity and neutron logs depends on the available data from some wells JLog version 4 (Petrophysical software) which has been used to estimate the porosity value for each

A. Jabir (✉) · A. Cerepi · C. Loisy
EA 4592 Géoresources et Environnement, ENSEGID—
Bordeaux-INP, 1 allée Fernand Daguin, 33607 Pessac
Cedex, France
e-mail: abngaber@yahoo.com

J.-L. Rubino
Total CSTJF, Avenue Laribau, 64018 Pau Cedex, France
e-mail: jeanloup.rubino@total.com

Fig. 1 Geological map showing location and boundaries of the Ghadames Basin and Jefarah basin. (Modified after [2, 3])



reservoir and PETREL (Schlumberger software 2014 version) for constructing the stratigraphic correlation models.

3 Results and Discussion

The characteristics of the Paleozoic reservoirs (Cambrian—Permian) in the Ghadames and Jefarah basins were studied. A summary of the Silurian is presented briefly.

The Akakus Formation is the main Paleozoic reservoir in the study area. Two wells have been studied from the SE-NW cross section relying on six wells. They represent the sandstones of the Akakus Formation (Fig. 2).

Well HH1-NC7A (Fig. 2) located in the southern part of Ghadames basin is about 560 m in thickness. It predominantly consists of an interbedding of sandstones, siltstone and shales. They were considered as proximal parts of the fluvial setting (Its proximity to the source). The average porosity values have been calculated by basing on deep and

shallow resistivity and sonic Wyllie and AFF with a value of salinity 5.6 g/l.

The distal well in the cross section is J1-NC100. It is located 243 km NW of the well HH1-NC7A and is located in the central Ghadames basin (Fig. 2). In the well J1-NC100, the Akakus Formation is represented by silty shales, siltstones and clayey sandstones with about 692 m in thickness. The formation waters in the Akakus Formation in this well have salinity values varying between 232 and 317 g/l.

4 Discussion

The middle part of this reservoir formation, in the well HH1-NC7A, has a thickness of 300 m (Figs. 2 and 3). This part shows a range of different depositional environments which are dominated by proximal shelf and fluvial deposits. The average porosity is around 16.8% (as inferred from deep

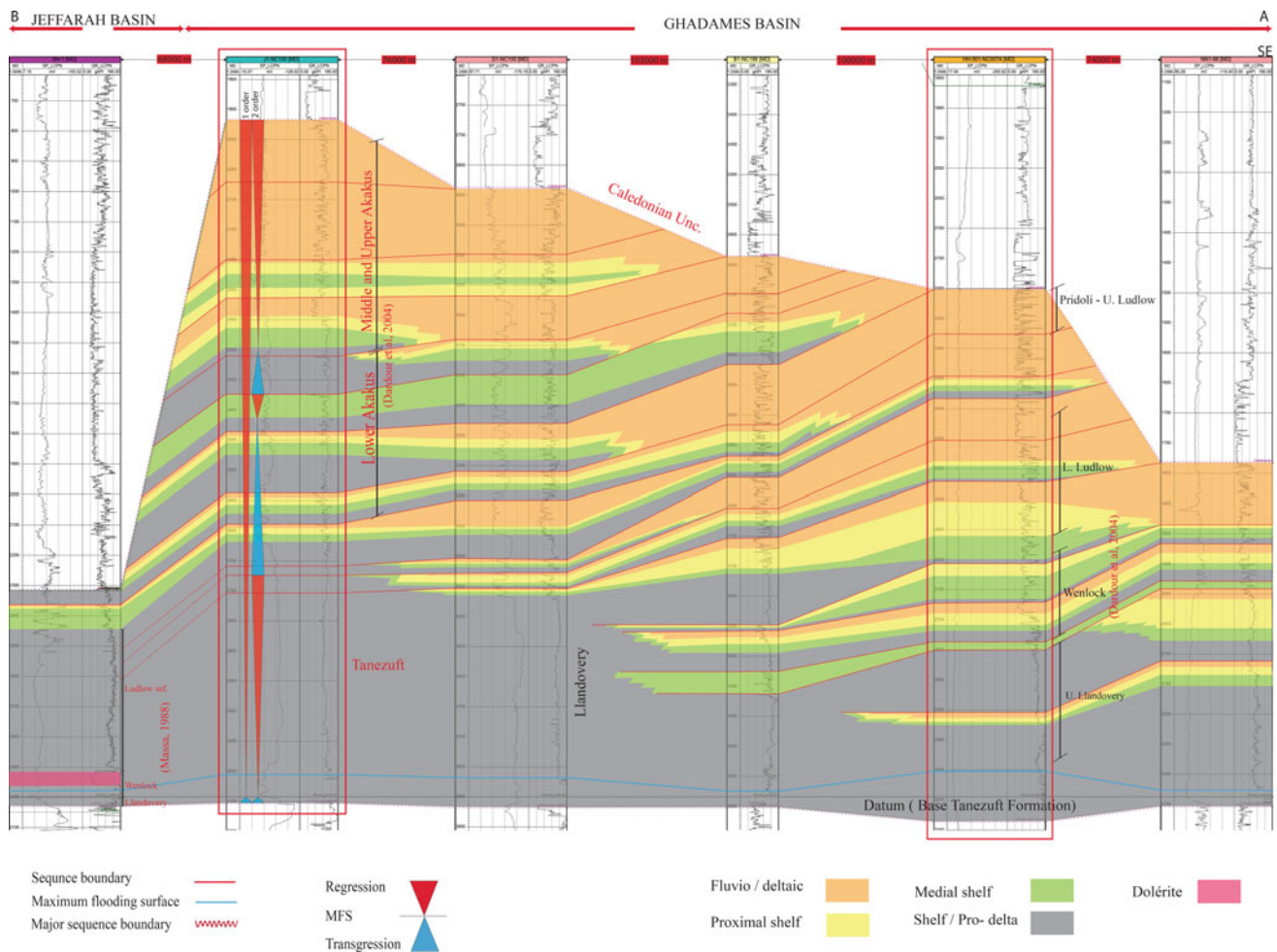


Fig. 2 SE—NW cross section of the Silurian Akakus formation through the Ghadames and Jefarah basins illustrating the depositional environment and sequence stratigraphy

resistivity logs). The same part, in the well J1-NC100, reaches about 160 m in thickness (Figs. 2 and 3). This part is dominated by a spatial span from fluvial-deltaic to medial shelf deposits. The average porosity, (as inferred from deep resistivity logs), is around 8.3%.

The upper part of this reservoir, in well HH1-NC7A, is with a thickness of 110 m (Figs. 2 and 3). It is dominated by fluvial deposits [1]. The average porosity, (as inferred from deep resistivity logs), is 9.1%. The same part, in well J1-NC100, reaches about 232 m in thickness (Figs. 2 and 3). This part is dominated by a range from proximal and distal

deltaic to fluvial deposits. The average porosity is around 7.2%. It is based on the deep resistivity logs.

It was noted that the Akakus reservoir displays convenient petrophysical properties in the southern and central parts of the basin. This is due to the reservoir properties which vary laterally and vertically between the proximal and distal deposits with the average porosity decreasing towards the distal part of the basin. It can be explained by the fact that the Akakus sandstones display a succession prograding from the southeast to the northwest that can be subdivided into a lower, middle and an upper unit [2].

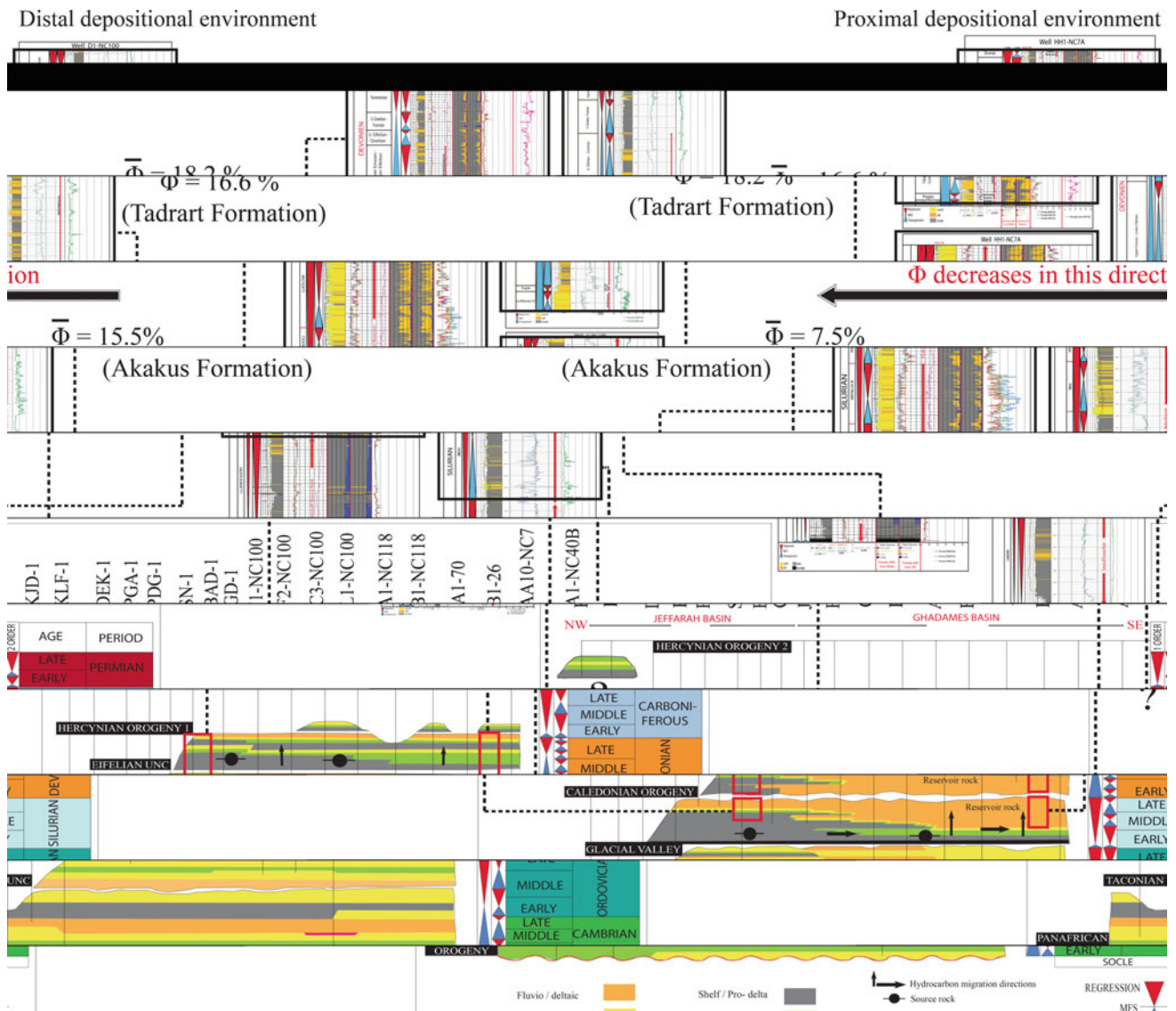


Fig. 3 Relation between stratigraphic, sedimentary, depositional environments and reservoir properties of the Paleozoic series in the Ghadames and Jefarah basins

5 Conclusion

This study is based on the available well logs that served to construct the cross sections which are representing each period of the Paleozoic. Once two wells were selected in each cross section, a proximal or distal location with respect to its location in the basin is represented. The average porosity changed according to the sedimentary facies. The Paleozoic reservoirs of Ghadames and Jefarah basins have convenient petro-physical properties at the central and the south-east which decreases to the northwest of the basins (Fig. 3).

References

1. Dominique, M.: Paléozoïque de Libye occidentale: stratigraphie et paléogéographie. Thesis Sci., University Nice, France, p. 514 (1988)
2. Khaled, E.: Geology and hydrocarbon occurrences in the Ghadames Basin, Algeria, Tunisia, Libya. In: Macgregor, D.S., Moody, R.T.J., Clark-Lowes, D.D. (eds.) Petroleum Geology of North Africa. Geol. Soc. London, Sp. Publ., 132, pp. 109–129 (1998)
3. Muftah, K., Sadoon, M.: Impact of depositional facies on the distribution of diagenetic alterations in the Devonian shoreface sandstone reservoirs, Southern Ghadamis Basin, Libya. Sediment. Geol. **329**, 62–80 (2015)

The Albian-Cenomanian Transition in Central Tunisia: Insights from Jebel Mrhila

Etienne Jaillard, Jean-Louis Latil, and Naser Raisossadat

Abstract

Three sections of the Albian-Cenomanian boundary have been studied in Jebel Mrhila of Central Tunisia. The Upper Albian succession directly overlies Aptian dolomites. It exhibits two depositional sequences and belongs to the *M. fallax* (?) to *S. africana* zones. The top of the Upper Albian series is eroded by a major discontinuity reflecting a major sea level drop. Deposition resumed in earliest Cenomanian times (*N. carcitanense* and *S. schlueteri* subzones) with two sequences of condensed sandy marls and dolomites. Both are capped by phosphate layers which are overlain by thick outer shelf marls (Early Cenomanian). Comparison with other areas suggests that during the Albian-Cenomanian transition, northern Central Tunisia acted as a bypass zone between the emergent southern areas and the northern basinal domain.

Keywords

Albian-Cenomanian transition • Sedimentology • Ammonites • Tunisia

1 Introduction

The Albian stage is one of the longest of Mesozoic times and records many oceanographic and geodynamic events. It is, however, still poorly known in the Tethyan region probably because of its monotonous and clayey lithology.

E. Jaillard (✉) · J.-L. Latil
ISTerre-IRD, University of Grenoble Alpes, CS 40700,
38058 Grenoble Cedex 9, France
e-mail: Etienne.Jaillard@Univ-Grenoble-Alpes.fr

J.-L. Latil
GREGB, Le Maupas, 05300 Lazer, France

N. Raisossadat
Faculty of Sciences, Department of Geology,
University of Birjand, 79/615 Birjand, Iran

Central Tunisia offers opportunities to study this period since it offers convenient exposures and fossiliferous successions. This work is a focus on the Albian-Cenomanian transition in Jebel Mrhila and its comparison with other areas of Central Tunisia.

2 Geological Background

During the Cretaceous, Tunisia is part of the South-Tethyan passive margin which deepens northward. In this framework, Central Tunisia represents the transition from a little subsiding, southern platform domain recording frequent emergence periods, to a subsiding, northern, outer shelf to basin domain. Albian deposits are represented by the carbonated Hameima Fm of earliest Albian age [1] which are overlain by the marly Fahdene Fm of Early Albian to Cenomanian age [2].

In Jebel Mrhila, the Albian succession directly overlies the Aptian dolomites and the Albian-Cenomanian boundary is roughly represented by a laterally extensive sandy dolomite bed. Three sections have been studied in Jebel Mrhila, from sedimentological and biostratigraphical points of view.

3 Results

3.1 Sedimentology

Five sedimentary discontinuities have been identified (Fig. 1). The first discontinuity (D1) is the brecciated, karsted and mineralized surface of the Aptian dolomite which corresponds to the long-lasting post-Aptian emergence period. D2 is a scoured erosional surface overlain by sandy carbonates containing reworked lithoclasts. D3 is either marked by an erosional surface at the base of a coarsely sandy dolomitic bed or underlies sandy dolomitic marl bearing reworked pebbles. D4 and D5 are marked by mineralized surfaces (hard-grounds) at the top of massive beds.

Each is overlain by a bioturbated, glauconite- and phosphate-rich marl beds. The hard-grounds are interpreted as hiatuses (D4 and D5) while the phosphate levels indicate condensed sedimentation interpreted as transgressive surfaces.

These discontinuities define transgressive-regressive depositional sequences (Fig. 1). The first one (S1) is made of glauconite-rich and laminated/rippled calcareous sandstones grading upward into dolostone capped by algal laminae. S2 is a thinning up series of clayey marl with thin calcareous beds. S3 begins with dolomitic sandstone rich in phosphate and glauconite containing open marine fauna and ends up with massive beds of sandy dolomite. S4 comprises bioturbated phosphate-rich marl (D4) overlain by sea urchin bearing marl and capped by a bed of sandy dolomite locally laminated and rippled. S5 begins with a bioturbated phosphate-rich marl bed (D5) overlain by a thick series of Lower Cenomanian marl [3].

3.2 Ammonite Biostratigraphy

Although the standard Albian-Cenomanian boundary is defined by planktic foraminifera, ammonite zones is used in the following discussion.

S2 yielded numerous ammonites that allow us to identify the Late Albian *Mortoniceras (Subschloenbachia) rostratum* and *Mortoniceras (Subschloenbachia) perinflatum* zones.

The *Mortoniceras (Mortoniceras) fallax* Zone may be present in S1. At the top of the sequence, the disappearance of the specimens of the *Mortoniceras* genus suggests the *Stoliczkaella (Shumarinaia) africana* Zone which contains the standard Albian-Cenomanian boundary.

S3 contains heteromorph ammonites and its upper part yielded a species of the *Mantelliceras* genus. This led us to ascribe its lower part to the *Neostlingoceras carcitanense* Subzone and its upper part to the *Sharpeiceras schlueteri* Subzone: both of earliest Cenomanian age. The specimens of *Mantelliceras* from S4 and from the base of S5 indicate the *Sharpeiceras schlueteri* Subzone.

4 Discussion

East of Jebel Mrhila (Jebel Zaouïa), oyster-bearing marl directly overlies the Aptian dolomites. They are overlain by rudistid-rich limestone. Southwest of Jebel Mrhila (Jebel Selloum), the top of the Late Albian marl exhibits emergence features [4, 5], and is overlain by high energy, coarse bioclastic calcarenites, interpreted as tidal, shelf margin deposits [5]. In both cases, ammonites [5] indicate that these deposits are coeval with the S5. Thus, they give evidence of a hiatus of the lowermost Cenomanian deposits (S3 and S4).

West of Jebel Mrhila (Jebel Semmama), the Late Albian marl is overlain by variably thick and cross bedded bioclastic limestones [4]. They are interpreted as channelized [5]. Their top yielded latest Albian foraminifera and ammonites [5]. Northwest of Jebel Mrhila (Oued Azreg), the Late Albian marls

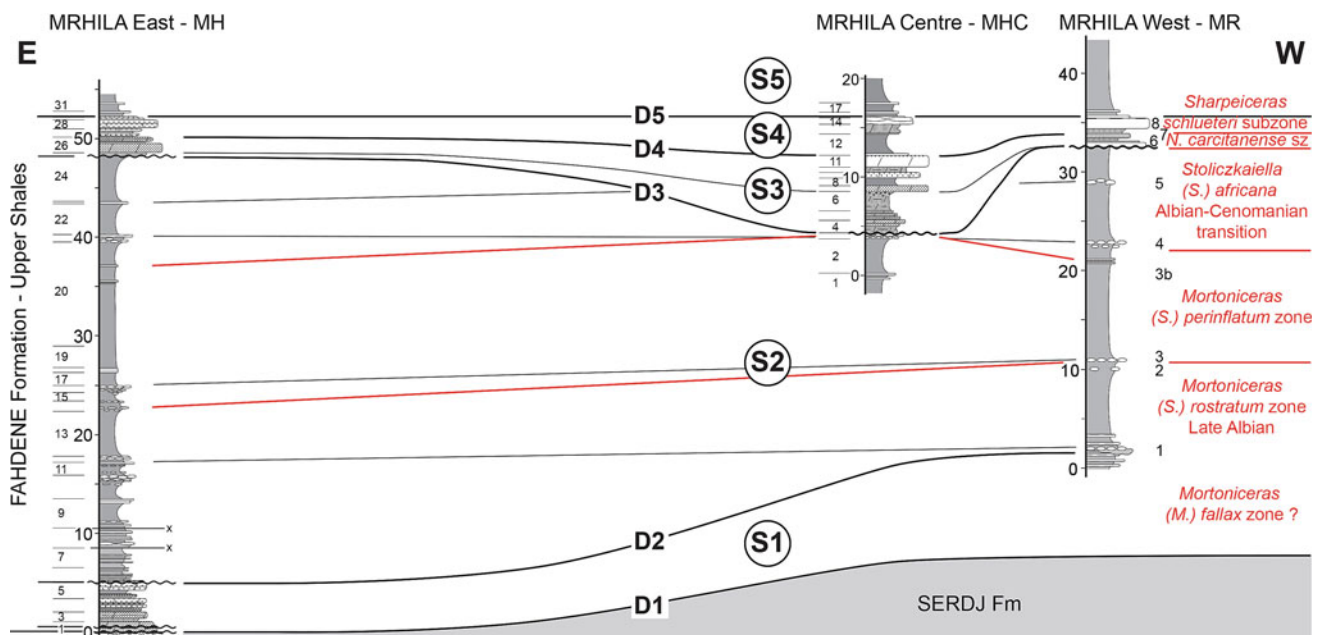


Fig. 1 The Albian-Cenomanian transition in Jebel Mrhila

are scoured by scattered, shallow channels infilled by phosphate-rich deposits of earliest Cenomanian age. They are interpreted as shelf margin wedge deposits [6] and coeval with our S3 and S4. Farther NW (Oued Zerga), the Albian-Cenomanian transition is marked by thickening-, then thinning-upward alternations of marl and limestone (80 m) rich in ammonites and radiolarians containing scarce rudistids [7]. The base of these alternations marks a noticeable shallowing of the environment and is interpreted as a sequence boundary of terminal Albian age. The transition from thickening- to thinning-upward trends may represent a transgressive surface.

These comparisons show that earliest Cenomanian (S3 and S4) deposits are only preserved in Jebel Mrhila and NW of it. To the East and South, Early Cenomanian beds directly overly either Aptian dolomite (E) or Late Albian marls (S). Moreover, the earliest Cenomanian deposits are thin (<10 m) and preserved mainly in channels in Jebel Mrhila and in Oued Azreg. However, they are thicker (\approx 50 m) and not channelized farther NW. This suggests that (1) the Albian-Cenomanian transition is marked by a drastic sea level drop which triggered the emergence and erosion of the southern Central Tunisia. (2) While channels were caved in northern Central Tunisia, which acted as a NW-deepening bypass zone between emergent and basin zones, in the earliest Cenomanian, incipient sea level rise was associated with significant marine currents (upwellings?). It favored the deposition of condensed phosphate-rich layers in northern Central Tunisia. (3) In the Early Cenomanian, sea level was high enough to allow deposition of outer shelf marls in northern Central Tunisia, high energy and locally channelized shoreline deposits farther South.

In Algeria and Morocco, although no sedimentological studies have been carried out on this interval, Upper Albian biogenic shelf limestones (Kechoula Fm of Morocco) are overlain by oyster-rich marls. They are ascribed to the Cenomanian [8–10]. Thus, they support the occurrence of a significant regional Late Albian regression followed by an Early Cenomanian transgression.

5 Conclusion

Sedimentological and biostratigraphic studies of the Albian-Cenomanian transition in Jebel Mrhila allow us to propose that (1) this transition is marked by a significant sea level drop, (2) during low sea level, northern Central Tunisia acted as a bypass zone between emergent zones to the E and S, and basin zones to the W and N, and (3) sea level rise allowed deposition first (earliest Cenomanian) of condensed phosphate-rich beds in channels of the bypass zone and then, of outer shelf marls in the bypass zone and shoreline deposits in the previously emergent southern areas (Early Cenomanian).

References

1. Chihaoui, A., et al.: Stratigraphy of the Hameima and Lower Fahdene formations in the Tadjerouine area (Northern Tunisia). *J. Afr. Earth Sci.* **58**, 387–399 (2010)
2. Burolet, P.F.: Contribution à l'étude stratigraphique de la Tunisie Centrale. *Ann. Mines Géologie* **18**, 350 (1956) (Tunis)
3. Pervinquier, L.: Etude géologique de la Tunisie centrale. de Rudeval Publ, Paris (1903)
4. Bismuth, H., et al.: Etude sédimentologique et biostratigraphique du Crétacé moyen et supérieur du Djebel Semmama (Tunisie du Centre Nord). *Cret. Res.* **3**, 171–185 (1982)
5. Philip, J., et al.: Organisation et évolution sédimentaires d'une marge de plate-forme carbonatée: l'Albien-Cénomanien de Tunisie centrale. *Géol. Méditerran.* **15**, 155–169 (1989)
6. Robaszynski, F., et al.: Le Cénomanien de la région de Kalaat Senan (Tunisie centrale): Litho-biostratigraphie et interprétation séquentielle. *Rev. Paléobiologie* **12**, 351–505 (1993)
7. Jaillard, E. et al.: Albian sedimentation in the Tadjerouine area. *Géologie Alpine, sér. Colloques Excursions* **5**, 105–124 (2005)
8. Emberger, J.: Esquisse géologique de la partie orientale des Monts des Oulad Nail. *Serv. Carte géol. Algérie Bull.* **27**, 410 (1960)
9. Vila, J.-M.: La chaîne alpine de l'Algérie orientale et des confins algéro-tunisiens. *Thesis Sci. Univ. P. et M. Curie, Paris* p. 60 (1980)
10. Ambroggi, R.: Etude géologique du versant méridional du Haut Atlas occidental et de la plaine du Souss. *Notes et Mém. Serv. Géol. Maroc* **157**, 321 (1963)

Sequence Stratigraphic Analysis of the Middle Paleocene-Middle Eocene in the Sulaimani District (Kurdistan Region), North Iraq

Fadhil Ameen and Fawzi Mardan

Abstract

The Paleocene-Eocene sequence is of great importance as oil reservoir in the Kurdistan region (North Iraq). Seven studied sections have been selected at the boundary between the high and low folded Zagros zones. The successions are represented by the mixed siliciclastic-carbonates of the Kolosh and Sinjar formations overlain by red clastics of the Gercus Formation. Three facies associations were identified from Paleocene age strata in addition to three planktonic foraminifera biozones (P3, P4 & P5) and shallow benthic zone SBZ.5 & 7. However, the shallow benthic zone 9 & 10 are identified from three facies associations from Eocene strata. The Paleocene Eocene Thermal Maximum (PETM) is evidenced by the disappearance of the deep benthic foraminifera and the decrease of the planktonic foraminifera associated with notable increase of large foraminifera. The studied sequences indicate the presence of one 2nd order depositional cycle that includes six 3rd order cycles. It is in turn subdivided into ten 4th order depositional sequences. Sequence boundary type one recorded in the base and the top of the studied sequences. All in all, the facies associations and biostratigraphic data point to a shallowing upward sequence from relatively deep marine flysch (Kolosh Formation) to ramp carbonates (Sinjar Formation) and then to red molasses of the Gercus formation or evaporites of the Sagerma unit which almost reflects six stages of the foreland evolution, from Middle Paleocene to Middle Eocene time.

Keywords

Paleocene • Eocene • Flysch • Nummulites • Sequence boundary

1 Introduction

The majority of the Paleocene-Eocene Nummulites bear limestones of the Tethys basin act as important oil reservoirs in Iran, Kuwait, Oman, Egypt, Libya, Tunisia and possibly the Kurdistan region. Therefore, they are the main subject of this study. The sandwiched carbonate-clastics sequence (represented by the Kolosh-Sinjar-Gercus and Pila Spi formations) of the Paleogene foreland basin is manifested by several facies associations of different depositional settings. It indicates possible global correlation with sequence boundaries. The convergent lines of evidences (sedimentological, stratigraphic, paleontological and structural) are integrated with detailed field work in order to postulate the depositional setting evolution and the role of subsidence and climatic changes in the basin analysis. It may be useful as a key solution for other parts of the Kurdistan region. The sequence boundaries, system tracts, 3rd and 4th order cycles of recognized sequences are determined and correlated with the global curves of Haq [1], Sharland et al. [2] and Emery and Myers [3]. The lithostratigraphic, biostratigraphic units, chronostratigraphic sequences and stratigraphic subdivisions of the Middle Paleocene-Middle Eocene strata are also clarified along different geological, structural and tectonically domains.

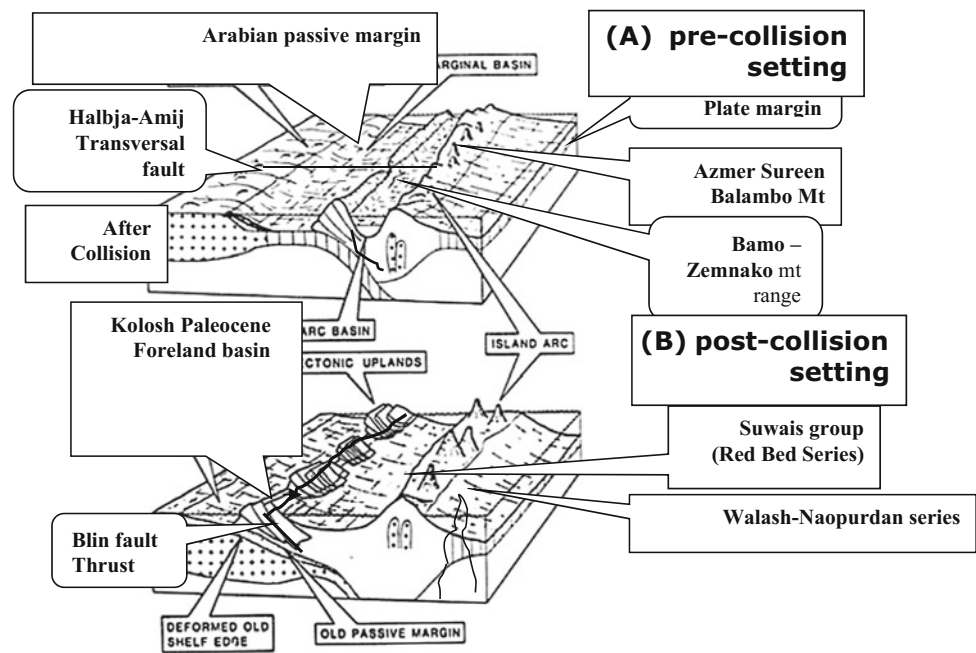
2 Methodology

Using a base map and global positioning system, (GPS), integrated with the detailed field works, the lithostratigraphic units are plotted and mapped by using MapInfo program version (7.5). Accordingly, seven sections and field data were

F. Ameen (✉)
Sulaimani University, New Campus Qiyasan 511, Sulaymaniyah,
Iraq
e-mail: Flawal@mail.com

F. Mardan
Kirkuk University, Baghdad Main Road, Kirkuk, Iraq

Fig. 1 Kolosh Foreland Basin site between Arabian and Iranian plates margins Pre- A and post-collision settings **B**



CRATONIC BASIN & EXTENSIONAL MARGIN SETTING

sampled from each stratum. They are followed laterally and vertically. About (778) samples were collected from all selected sections for lithofacies, biofacies, sedimentary structures, diagenetic processes and ichnofacies analysis. Samples are also prepared for planktonic and benthonic foraminiferal identifications using classical cooking methods.

3 Results

Six facies associations are recorded in this study based on several types of sedimentary structure of different scales supported by macro and microfossils data as well as field measurements. Almost flysch facies associations are recognized in the Kolosh Formation of Paleocene age. The outer ramp – middle ramp and inner ramp facies association FA.3 is rich in large *Nummulites* of Middle Eocene age (Lutetian). The facies association FA.4 represents outer shelf, middle shelf and inner shelf environments. It consists of mixed siliciclastics and carbonates assigned to the Early Eocene (Ypresian) Sinjar formation. The red molasse facies association FA.5 marks the lower part of the Gercus formation while the carbonate and evaporites facies association FA.6 represents the lower part of the Sagerma Formation. The biostratigraphic zones are recorded as follows: A- Paleocene planktonic zonation: *Morozovella angulata* zone (P 3); *Planorotalites pseudomenardii* zone (P 4) *Morozovella velascoensis* partial range zone (P 5) AL-Mutwali [4], B- Paleocene shallow benthic zonation: *Alveolina aramaea aramaea* zone SBZ.5; *Alveolina*

pasticillata zone SBZ.6; *Nummulites frassi* *Nummulites deserti* zone SBZ.6. B- Eocene zonation: The recorded Eocene shallow benthic zone is: A- Early Eocene (Ypresian) Zones. shallow benthic zone SBZ 8, *Nummulites exilis* zone, shallow benthic zone SBZ 9, *Nummulites globules* shallow benthic zone SBZ.10 -*Alveolina aragonensis* -*Alveolina oblonga* or/ Shallow benthic zone SBZ 10 *Nummulites planulatus* zone. B- Lutetian zones shallow benthic zone SBZ 13. *Assilina spira*, *Discocyclina archaici*. Shallow benthic zone SBZ 14. *Nummulites gizhensis*, *Nummulites discorbinus* and *Nummulites beneharnensis*. Shallow benthic zone SBZ 15. *Nummulites millecaput*, *Assilina gigantea* and *Discocyclina pulcra*.

4 Discussion

The progressive shallowing upward trend of the studied sections are distinguished by the variation of the midway fauna to Velsoco planktonic type and by the Tethyan fauna type that emphasize the great lowering of the sea level changing from depth that exceeds 250 to few 10 s and finally to zero. The upward shallowing is marked by P/B ratio decreases, dominance of proximal facies, coarser siliciclastic, and appearance of the coral and algae. It also precisely emphasizes the paleoecological variations. The paleoecological conditions during the Paleocene might be essentially controlled by paleobathymetric condition. Finally, the increasing temperature terminates all the planktonic and benthonic foraminiferal associations, at the Paleocene/Eocene boundary. Figure 1

shows the pre-collision and post-collision set up of the Paleocene (Kolosh) foreland basin set up.

5 Conclusion

The sequence stratigraphic analysis points to one 2nd order cycle, six 3rd order cycles, and ten 4th order cycles. The Kolosh marine siliciclastics and mixed siliciclastic and carbonates provide a record of two 3rd order cycles. The first 3rd order cycle indicates the early to middle Paleocene TST with retrograding and aggrading stacking pattern. The maximum flooding surface (MFS) of the paleogene age (Pg10) at the Selandian/Thanetian boundary overlies the first cycle. Sequence boundaries of type one are recorded at the Cretaceous/Tertiary boundary and at the Paleocene/Eocene (Thanetian/Lutetian) boundary. They are represented by incised valleys. The middle Paleocene and middle Eocene depositional cycles were characterized by depocenter shifting, shelf-margin progradation and depositional system evolution. The global phenomenon called Paleocene-Eocene thermal maximum (PETM) is recognized in the studied sections by the mass extinction of the deep benthic

foraminifera and great decrease of the planktonic foraminifera. It is associated with the appearance of large Thanetian foraminifera. Anoxic condition may be responsible for the pyrite infilling of the planktonic tests and the increases of the carbonates bed emphasis with the increasing temperature. The appearance of the extraordinary Paleocene gastropods in distinct massive limestone at the Paleocene/Eocene boundary (55.0 my) seems to confirm the hypothesis above”.

References

1. Haq, B.U: Sequence stratigraphy, sea level change and significance for the deepsea. In: MacDonald, D.I.M. (ed.) Sedimentation Tectonics and Eustasy. Int. Assoc. Sediment. Spec. publ. 12, 3–39 (1991)
2. Sharland, P.R., Ratmond, A., Casey, D.M., Daris R.B., Hall, S.H., Hewerd, A.P., Horbury A.D., Simmons, M.D: Arabian plate sequence stratigraphy. *Geo. Arabia Spec. Pub.* 2 (2001)
3. Emery, D., Myers, K.: Sequence stratigraphy. Blackwell Sci. 210 (1996)
4. Al-Mutwali, M.M.A.: Paleocene-early Eocene benthic foraminifera biostratigraphy and paleocology of Kolosh formation, shaqlawa area, Northeastern Iraq. *Iraqi J. Earth Sci.* I(2), 12–24 (2001)

Palynological study of the Pliensbachian-Toarcian transition of the Traras Mountains (northwestern Algeria)

Louisa Samar, Abbas Marok, and Choukri Soulimane

Abstract

A palynological study of the Late Pliensbachian-Early Toarcian deposits in the Traras Mountains (NW Algeria) identified sporomorphs (spores and pollen grains) associated with acritarchs and algae unknown in this Algerian basin at this time. Seeking to characterize the Pliensbachian-Toarcian transition, the results of qualitative and quantitative analysis of pollen assemblages generated new stratigraphic information on the lower limit of Bayada beds which have already been established by ammonites, brachiopods and foraminifera.

Keywords

Traras mountains • Algeria • Pliensbachian • Toarcian • Palynology

1 Introduction

The Traras Basin (Fig. 1a) has been the subject of several studies: structural [1], biostratigraphic and sedimentological [2] which allowed it to be integrated palaeogeographically into the Tlemcenian field. During the Pliensbachian-Toarcian transition, the Traras basin was marked by major paleo-environmental and paleo-oceanographic changes. They were correlated with the events of the western Tethys. In particular, we cite sea level variations, carbonate production crisis, $\delta^{13}\text{C}$ and $\delta^{15}\text{N}$ geochemical disturbances and an anoxic ocean event (T-OAE) [3–5]. In the present work, and through the study of two sections (Benzerka and Mellala, northern part of the Traras basin) (Fig. 1a), we provide

information for the first time on the palynological components of the Lias in Algeria. The systematic inventory of the different palynomorphs (spores, pollen grains, acritarchs and algae) aims to characterize the Pliensbachian-Toarcian transition as far as possible.

2 Stratigraphic Framework

As part of the Tlemcenian domain, the two selected sections (Figs. 1b, c) will be described in detail.

2.1 Benzerka Sect. (32, 65 m Thick) (Fig. 1b)

This section shows the following lithostratigraphic succession.

Tisseddoûra Limestone Fm. (5.90 m): it is represented by brecciated limestones, bioclastics, followed by clay limestones. Upwards, it changes to marl-limestone alternations. The macropaleontological content (*Tetrahynchia ageri* and *Spiriferina* sp.), on the one hand, and micropaleontological ones (namely the benthic foraminifera *Lingulina tenera carinata*, *Lenticulina acutiangulata* mg. *Lenticulina*, *Lenticulina*, *Lenticulina gottengensis* mg. *Lenticulina*, *Marginulina prima*, *Spirillina infima*, *Bolivina liasica*, *Lingulina tenera tenera*), on the other hand, give a Late Pliensbachian age (Algovianum Zone).

Bayada Fm. (26.75 m): it is essentially a marl-limestone alternation (Late Pliensbachian-Early Toarcian) (Emaciatum-Levisoni Zones).

2.2 Mellala Sect. (47 m Thick) (Fig. 1c)

Located a few meters from the road (Ghazaouet-Nadroma), the Mellala section is represented essentially by the “Bayada Beds” which consist of marl and limestone alternation. The lithostratigraphic succession shows from bottom to top:

L. Samar
Division Technologies et Développement (DTD), Sonatrach,
Avenue du 1er Novembre, Boumerdès, Algeria

A. Marok (✉) · C. Soulimane
Department of Earth and Univers Sciences, University
of Tlemcen, B.P. 119 Tlemcen, Algeria
e-mail: a_marok@yahoo.fr

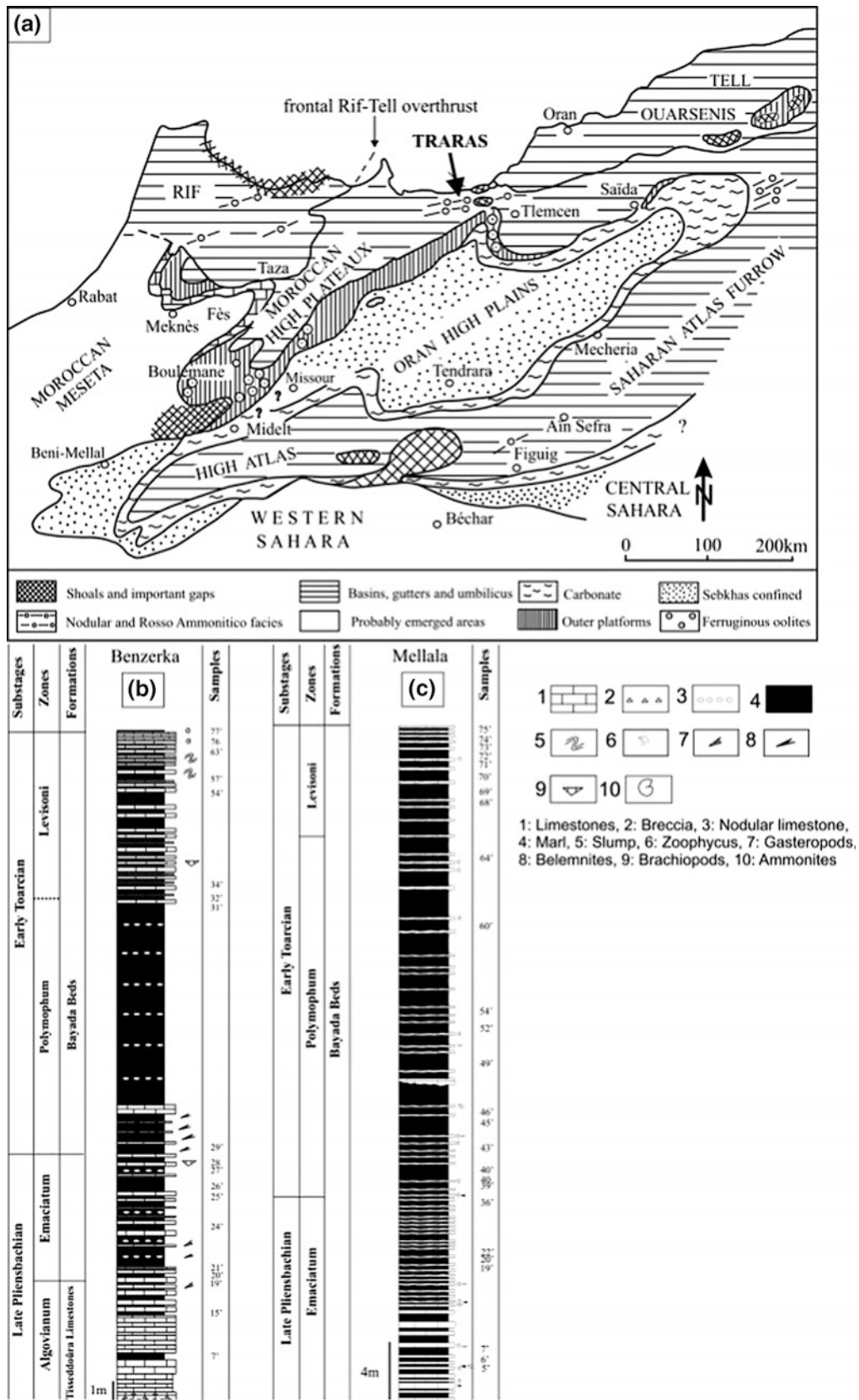


Fig. 1 Location map of the study area (a) (after [3]) and stratigraphic column of the Benzerka and Mellala sections (b and c)

- 6.20 m: alternation of marls and decimeter-thick beds of well-stratified marly limestone, very rich in ammonites, belemnite rostra and brachiopods.
 - 7.80 m: alternation of marls and centimeter-thick beds of marly limestone with nodular appearance. The rich macrofauna is mainly represented at the top by the ammonite, *Paltarpites paltus* and *Dactyloceras (Eodactylites) pseudocommune* indicating the transition between the Late Pliensbachian (Emaciatum Zone) and the Early Toarcian (Polymorphum Zone).
 - 25.25 m: alternation of marls and centimeter to decimeter-thick beds of marly limestone with a nodular appearance. Note the presence at the base of zoophycus and some brachiopods and ammonites.
 - 07.75 m: marls and centimeter to decimeter-thick beds of marly limestone.
- Note that the stratigraphy of this section was described by Elmi et al. (2009). For example, brachiopod-associated ammonites and foraminifera were used to date the Late

Fig. 2 Distribution of palynomorphs in the Benzerka section

		Samples	Spores										Pollen grains							Acritarchs	Algae			Incertae Sedis					
			<i>Rotverrisporites tenuis</i>	<i>Cyathidites australis</i>	<i>Cyathidites minor</i>	<i>Verrucosisporites</i> sp.	<i>Reticulatisporites castellatus</i>	<i>Reticulatisporites</i> sp.	<i>Lycopodiumsporites reticulatum</i>	<i>Lycopodiumsporites clavatooides</i>	<i>Lycopodiumsporites</i> sp.	<i>Zonalapollenites</i> sp.	<i>Perinopollenites</i> sp.	<i>Classopollis</i> sp.	<i>Classopollis torosus</i>	<i>Inaperturopollenites</i> sp.	<i>Araucariacites liasicus</i>	<i>Araucariacites</i> sp.	<i>Spheripollenites subgrammidatus</i>	<i>Spheripollenites</i> sp.	<i>Exesipollenites</i> sp.	<i>Cerebropollenites</i> sp.	<i>Monosulcites</i> sp.		<i>Micrhystridium</i> sp.	<i>Tasmanites</i> sp.	<i>Typhodiscus</i> sp.	<i>Botryococcus</i> sp.	<i>Prasinophytes</i> sp.
Early Toarcian	Levisoni	Bz57'		■			■										■	■		■			■				■		
		Bz54'					■										■								■	■			
		Bz34'		■			■	■	■			■	■				■		■					■	■			■	
		Bz32'					■												■								■	■	
	Polymorphum	Bz31'	■	■				■											■						■	■	■		
		Bz29'											■	■	■											■			
	Late Pliensbachian	Emaciatum	Bz27'												■				■						■				
			Bz26'												■														
			Bz25'					■				■	■				■		■	■	■	■				■	■		
			Bz24'											■	■					■					■	■	■	■	■
		Bz21'		■					■			■	■	■	■	■	■	■	■	■	■	■			■		■	■	
		Bz20'		■	■	■					■	■	■	■	■	■	■				■	■			■		■	■	
		Algovianum	Bz19'																	■						■	■		■
	Bz15'							■	■						■			■	■	■	■			■		■	■	■	
Bz7'	■					■					■	■						■					■			■	■		

Pliensbachian (with the Emaciatum Zone) and the Early Toarcian (with the Polymorphum and Levisoni Zones).

3 Analysis of Palynological Assemblages

Quantitative analysis showed a predominance of the terrestrial elements represented by spores and pollen grains along the Late Pliensbachian- Early Toarcian interval (Figs. 2 and 3). Thus, we have been able to note the following quantitative variations:

- Of the Late Pliensbachian (Algovianum-Emaciatum Zones): the “Tissedouira Limestones” (Algovianum Zone), the ten (10) samples of the Benzerka section yielded spores and pollen grains consisting of: *Rotverrusporites tenuis*, *Reticulatisporites* sp., *Zonapollinites* sp., *Araucariacites liasicus*, *Lycopodiumsporites reticulatum*, *Classopollis* sp., *Inaperturopollenites* sp., *Spheripollenites subgranulatus*, *Spheripollenites* sp., *Exesipollenites* sp., *Cerebropollenites* sp., associated with an acritarch, *Micrhystridium* sp. and the algae: *Tasmanites* sp., *Tycthodiscus* sp., *Prasinophytes* sp. and forms whose determination remains unfortunately very difficult (*Incertae Sedis*). In addition, the palynological residues of eighteen (18) samples from the Bayada Beds (Emaciatum Zone) contained palynological assemblages consisting of spores and pollen grains (*Varirugosisporites* sp., *Leiotriletes* sp., *Lycopodiacidites* sp., *Calamospora* sp., *Piloseporites* sp., *Deltoidospora* sp., *Callialasporites segmentatus*, *Bennettitaepollinites* sp.). Acritarchs and algae are represented (*Tasmanites puntatus*, *Leiosphaeridia* sp., *Crassosphaera* sp., *Tapajonites* sp., *Umbellasphaeridium* sp., *Baltisphaeridium* sp., *Acanthodiacrodium* sp.).
- In the Early Toarcian (Polymorphum-Levisoni Zones): the “Bayada Beds”, in the Polymorphum Zone produced a relatively poor palynological assemblage, which included some spores and pollen grains (*Reticulatisporites* sp., *Verrucosisporites* sp., *Lycopodiumsporites* sp., *Rotverrusporites tenuis*, *Lycopodiacidites* sp., *Spheripollenites* sp., *Classopollis* sp., *Inaperturopollenites* sp., *Araucariacites* sp.), associated with scanty and diversified algae (*Tasmanites puntatus*, *Tasmanites* sp., *Leiosphaeridia* sp., *Botryococcus* sp., *Prasinophytes* sp.) and indeterminate forms (*Incertae Sedis*). Acritarchs are completely absent. Moreover, in the Levisoni Zone, the palynological association is dominated by spores and pollen grains: *Cyathidites minor*, *Cyathidites australis*, *Reticulatisporites castellatus*, *Reticulatisporites* sp., *Lycopodiumsporites clavatoides*, *Lycopodiumsporites*

sp., *Classopollis* sp., *Classopollis torosus*, *Araucariacites* sp., *Spheripollenites subgranulatus*, *Spheripollenites* sp., *Exesipollenites* sp., *Cerebropollenites* sp., *Inaperturopollenites* sp. accompanied by acritarchs (*Micrhystridium* sp., *Umbellasphaeridium* sp., *Baltisphaeridium* sp., *Acanthodiacrodium* sp.) and algae (*Tasmanites* sp., *Tycthodiscus* sp., *Leiosphaeridia* sp., *Prasinophytes* sp.).

4 Conclusion

The qualitative and quantitative results of the palynological assemblages found in the Pliensbachian-Toarcian interval show that the boundary between the Algovianum Zone and the Emaciatum Zone is marked by the appearance of a group of sporomorphs consisting of *Cyathidites minor*, *Verrucosisporites* sp., *Monosulcites* sp., *Lycopodiumsporites clavatoides*, *Zonalappollenites* sp., *Classopollis* sp., *Araucariacites liasicus*, *Araucariacites* sp., *Monosulcites* sp., *Reticulatisporites castellatus*. The boundary between the Polymorphum Zone and the Levisoni Zone is distinguished by the appearance of taxa: *Cyathidites australis*, *Lycopodium* sp., *Classopollis torosus* and *Botryococcus* sp. This palynological study, carried out for the first time in Algeria, allowed us to identify 14 (fourteen) pteridophyt spores, 15 (fifteen) gymnosperm pollen genera, 4 (four) acritarchs and 08 (eight) algae that show a great similarity with palynomorphs found in some northern and southern Tethyan basins.

References

1. Guardia, P.: Géodynamique de la marge alpine du continent africain d'après l'étude de l'Oranie nord-occidentale. Université de Nice, France, Thèse Doctorat d'Etat (1975)
2. Ameur, M.: Histoire d'une plate-forme carbonatée de la marge sud-téthysienne: l'autochtone des Traras (Algérie occidentale) du Trias supérieur jusqu'au Bathonien moyen. Documents des Laboratoires de Géologie de Lyon **150**, 1–339 (1999)
3. Elmi, S., Marok, A., Sebane, A., Alméras, Y. : Importance of the Mellala section (TrarasMountains, north-western Algeria) for the correlations of the Pliensbachian-Toarcian boundary. *Volumina Jurassica* **4**, 158–160 (2009)
4. Reolid, M., Marok, A., Sebane, A.: Foraminiferal assemblages and geochemistry for interpreting the incidence of Early Toarcian environmental changes in North Gondwana palaeomargin (Traras Mountains, Algeria). *J. Afr. Earth Sc.* **95**, 105–122 (2014)
5. Soulimane, C., Reolid, M., Marok, A.: Ostracod assemblages from the uppermost Pliensbachian and Lower Toarcian of the Traras Mountains (Tlemcen Domain, north Algeria). *Arab. J. Geosci.* **10**(393), 1–24 (2017)



Stratal Geometries and Patterns: A New Lower-Upper Cretaceous Depositional Model of the Levant Shelf, Syria

Hussam Ghanem and Hans-Joachim Kuss

Abstract

The thickening of the Aptian-Cenomanian deposits of the central part of Syria indicates that the Levant platform of Syria was subdivided into intrashelf basin settings surrounded by shallow ramps. A high resolution sequence stratigraphic model has been established for the Aptian-Cenomanian succession in the north Levant margin that allows us to demonstrate detailed facies patterns in the transition zone from inner ramp to intra-shelf basin. This comparison recommends an excellent opportunity to distinguish between the qualified control of sedimentary supply and accumulation on the depositional geometries of twelve 2nd and 3rd order Aptian to Early Turonian sequences.

Keywords

Syria • Intrashelf • Levant • Aptian-Cenomanian Sequences

1 Introduction

Cretaceous shallow marine carbonates in Syria were formed in the so-called Levant platform located at the northern edge of the African-Arabian plate. The objectives of the present work are: (1) to analyze and correlate the Aptian to Turonian sedimentary successions in outcrops from the South Palmyrides and the Coastal Range and boreholes of Ad-Daww and Homs depressions and Latakia ridge within a sequential stratigraphic framework.

Reconstructing the paleogeography of the Levant platform includes the structuration in major sub-basins of the platform during Aptian to Turonian. In this context, the present study concentrates on stratigraphic and seismic interpretations in addition to the linked impact of the basin

modeling and the interpreting of the variety of outer ramp settings during the compression processes on the Cretaceous evolution of the north Aribian plate [10] (Fig. 1).

2 Depositional Setting

The Aptian—Turonian succession is subdivided into three subsurface formations (Rutba, Hayan, Judea formations). They are correlated with the adjacent age-equivalent formations from outcrops of South Palmyrides (Palmyra sand, Zbeideh, Abou Zounar, Abtar, and Halabat formations) and Coastal Range (Slenfeh, Bab Abdallah, Hannafyah, and Aramo formations) [1, 2, 4, 5] (Fig. 2).

3 Results and Discussion

3.1 Depositional Environments and the Paleogeography

12 depositional sequences are extended from Aptian to Early Turonian of the studied area. They are bounded by four characteristic hiatus in South Palmyrides and 3 in Coastal Range. Thus, they yield specific depositional and biotic compared to gamma ray response. The two 2nd order Aptian sequences of the Levant Platform is characterized by humid climatic conditions [7, 9] and supports the sedimentologic changes from carbonate to siliciclastic environments (Rutba and Palmyra sandstone formations [1], Fig. 2). Comparable facies variations from sandstone to shale are observed in the tidal to outer ramp in Coastal Range (Bab Jannah formation).

By contrast, the Albian-Cenomanian carbonate lithologies reflect arid climates, as indicated by four albian and five Cenomanian 2nd to 3rd order sequences. They accumulate the prevailing limestones, dolomites and marls from neritic to open marine including several evaporitic intervals in the intrashelf basins (Homs and Ad-Daww) which specify the environment. The bio- sequence stratigraphy of the

H. Ghanem (✉) · H.-J. Kuss
Department of Geoscience, Bremen University, PO Box 330440
28359 Bremen, Germany
e-mail: ghanem@uni-bremen.de

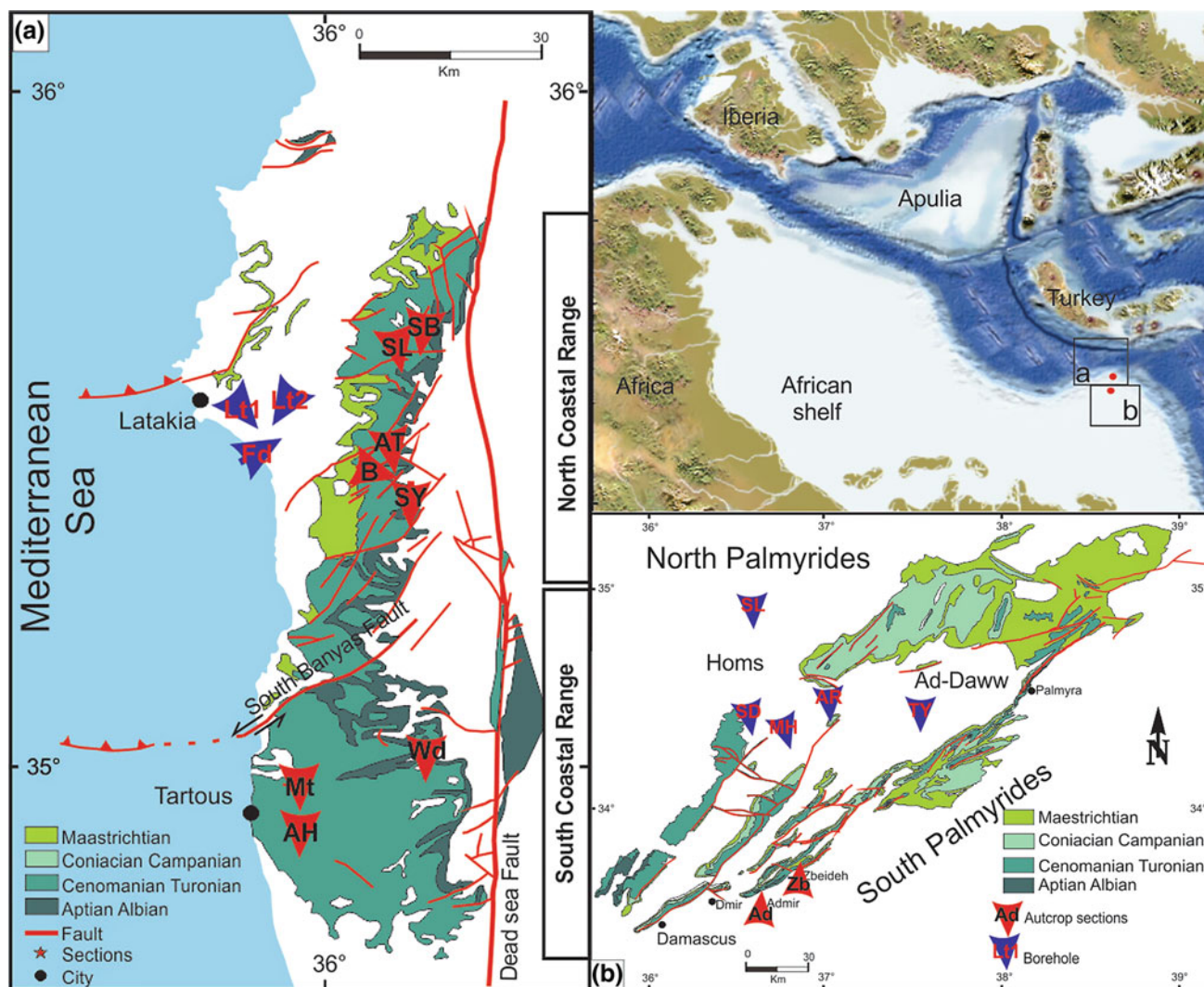


Fig. 1 Regional Palaeogeographic map of the North Arabian Plate during Aptian to Turonian after Blakey (<http://jan.ucc.nau.edu/rcb7/midcretmed.jpg>), figures a, b represent simplified maps of the

Cretaceous rocks of the studied areas of the Eastern Mediterranean margin (Coastal Range and Palmyrides)

Aptian-Early Turonian formations from Coastal Range to the South Palmyrides transect [4] exhibit a conspicuous thickening of the shallow marine Albian succession, compared to Zbeideh, Ain Elbeida outcrops and Hayan subsurface formations, at the Ad-Daww and Homs depressions. This is also confirmed by seismic interpretations (Fig. 3). Thus, it indicates deposition in a shallow marine inner-shelf basin. Similar thickness trends were observed for the Cenomanian succession (Figs. 2 and 3).

Deep marine limestones occurred especially during the Late Albian upper most Zbeideh, Hayan, and Ain Elbeida Formations in both Palmyrides and Coastal Range. They were overlain by neritic Cenomanian carbonates of Slenfah, lower Abou Zounnar, and lowermost Judia Formations. Rapid deepening depositional environments occur in Albian-Turonian platform areas. They are represented by pelagic

black shales, marls and marly limestones of the Judea, Hallabate in Latakia Ridge, Bab Abdallah, and Aramo Formations (Coastal Range) [2]. They are overlain by dolostones (Abter, Halabat, and upper Judia of Palmyrides Formations) and limestones which reflect protected lagoonal, tidal deposition and rudist banks in Ain Elbeida. They are, in turn, overlain by the deep marine deposits before the upward shallowing of the Late Turonian in the Coastal Range Aramo Formation [6, 4, 5], (Figs. 2 and 3).

3.2 Basin Evolutions and Regional Implications

The north Levant platform of the Mid-Cretaceous contains several sedimentary stages on the basin evolution, thickening to the central part of Syria (Homs and Ad-Daww depressions).

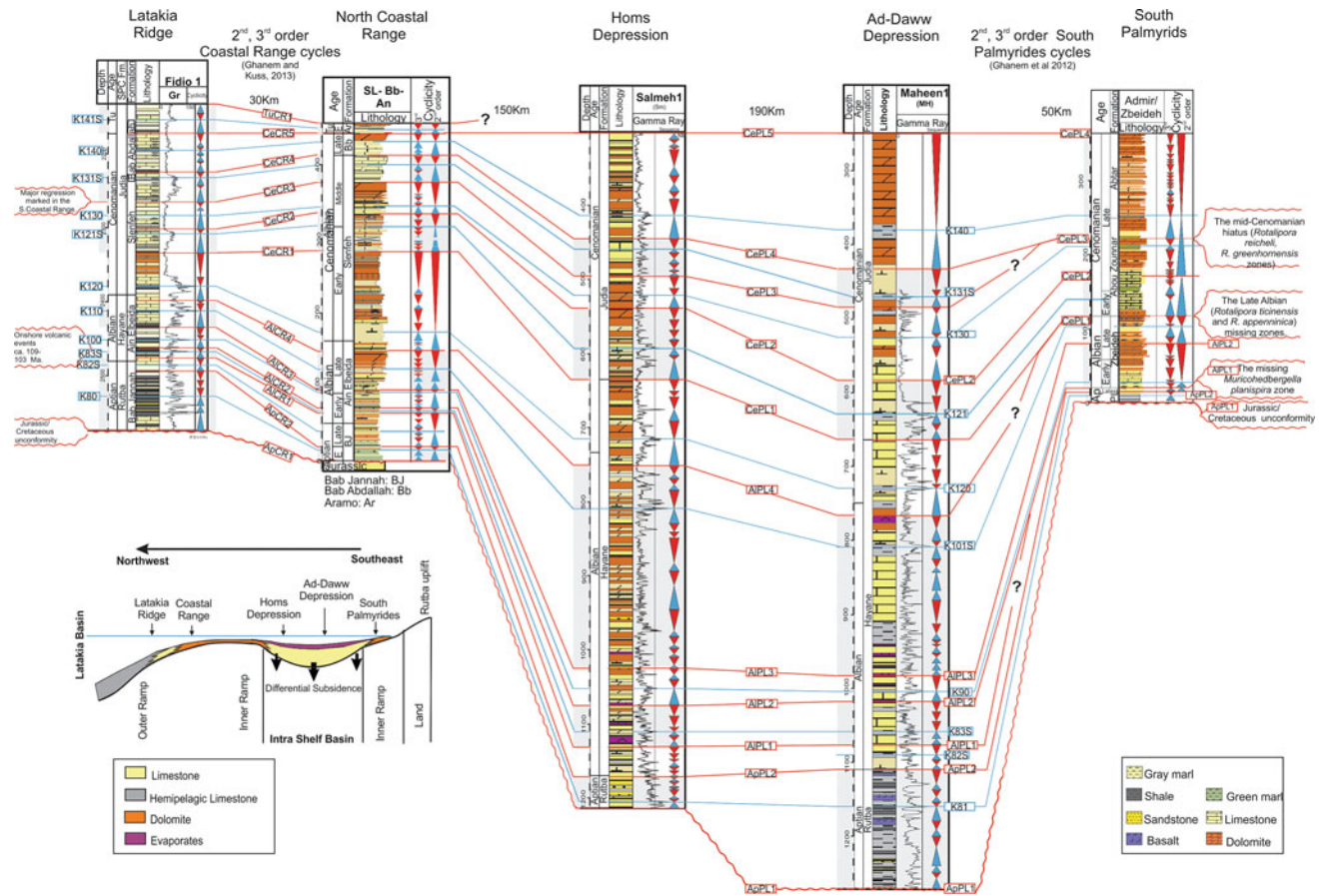


Fig. 2 Correlation of the sequences in the Aptian- Turonian successions of the Coastal Range and South Palmyrides (Ghanem et al. 2012, [5] with subsurface data of the Ad-Daww and Homs Depression and the

Latakia Ridge (see also transect A-B in Fig. 3). Sequence boundaries in red and maximum flooding surfaces in blue

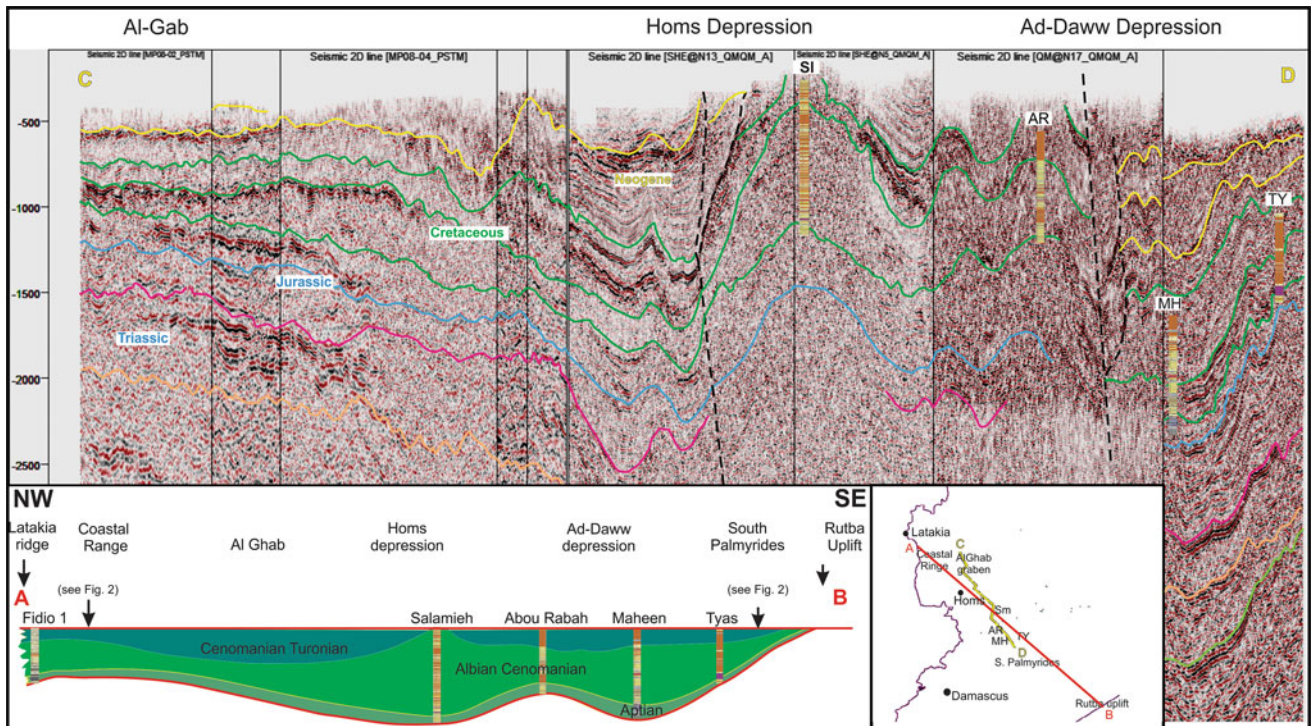


Fig. 3 Seismic section from South Palmyrides to AlGhab graben crossing Homs and Ad-Daww depressions

Following the Aptian siliciclastic/carbonate deposits, the thickening toward of AlPI3-AIPI4, CePI4 Ad-Daww and Homs sequences demonstrate higher subsidence rate in the Ad-Daww and Homs intrashelf basin settings. They are dominated by carbonates, intercalated with evaporitic deposits, towards the basin axis (Figs. 2, 3). The big thickness variation of the studied section is comparable to the Early Cretaceous mantel plum [8] and (Albian-Campanian) compression activities in the North Arabian Plate [3, 10]. Seismic interpretations support that the current Ad-Daww and Homs subbasins overlay subsiding areas.

4 Conclusion

The variations of the accommodation space favor progradation/retrogradation belts of different deepening-up and shallowing up sequences. The palaeoenvironmental position extended from inner ramp carbonates and open lagoonal to outer ramp (e.g. in the Latakia Ridge). The correlation along an S-N transect of West Syria allows us to reconstruct the platform configuration and to estimate the palaeogeographic evolution of the Palmyrides and the Coastal Range during the Aptian—Early Turonian. Several key episodes of the platform development that point to different Aptian, Albian, Cenomanian and Turonian platform stages of the North Levant have been distinguished. The correlation with major tectonic events and marginal progradation/retrogradation will be discussed.

The accumulation rate of the Ad-Daww and Homs intra-shelf basins was subsequently realized by the progradation of the evaporation when carbonate production exceeded the accommodation rates in the surrounding inner ramp environments. Increasing subsidence rates are postulated as major driving processes that caused the change from a flat ramp system to an intra-shelf basin. Both Ad-Daww

and Homs intrashelf basins were initiated when a rapid sea level rise exceeded the carbonate production and subsequent accumulation over the platform interior.

References

1. Brew, G., Barazangi, M.: Tectonic and geologic evolution of Syria. *GeoArabia* **6**(4), 289–318 (2000)
2. Caron, C., Mouty, M.: Key elements to clarify the 110 million year hiatus in the Mesozoic of eastern Syria. *GeoArabia* **12**(2), 13–36 (2007)
3. Gardosh, M.A., Garfunkel, Z., Druckman, Y., Buchbinder, B.: Tethyan rifting in the Levant Region and its role in Early Mesozoic crustal evolution. *Geol. Soc. Lond. Spec. Publ.* **341**(1), 9–36 (2010)
4. Ghanem, H., Mouty, M., Kuss, J.: Biostratigraphy and Carbon-isotope stratigraphy of the uppermost Aptian to Late Cenomanian strata of the Southern Palmyrides. *Georabia* **17**(2), 155–184 (2012)
5. Ghanem, H., Kuss, J.: Stratigraphic control of the Aptian—Early Turonian sequences of the Levant Platform (Northwest Syria—Coastal Range). *Georabia* **18**(4), 85–132 (2013)
6. Mouty, M., Al-Maleh, A.K.H., Abou-Laban, H.: Le Crétacé moyen la chaîne des Palmyrides (Syrie centrale). *Geodiversitas*, Paris **25**, 429–443 (2002)
7. Philip, J.: Peri-Tethyan neritic carbonate areas: distribution through time and driving factors. *Palaeogeogr. Palaeoclimatol. Palaeoecol.* **196**(1–2), 19–37 (2003)
8. Segev, A., Sass, E., Schatner U.: Age and structure of the Levant Basin, Eastern Mediterranean. *Earth Sci. Rev.* **182**, 233–250 (2018)
9. Stampfli, G.M., Borel, G.D.: A plate tectonic model for the Paleozoic and Mesozoic constrained by dynamic plate boundaries and restored synthetic oceanic isochrones. *Earth Planet. Sci. Lett.* **196**, 17–33 (2002)
10. Wood, B.: Whole Lithospheric Folding as a Mechanism of Basin Formation and Tectonic Implications for Gondwana Evolution: Evidence from the Palmyride Trough, Syria. *APPG Annual Convention and Exhibition*, p. 30176 (2011)

Foraminiferal and Geochemical Input to OAE 2 Event at Jebel Bou Arif (Aures, Eastern Algeria)

Abdia Touahria, Abdelmoumen Garah, Abbes Sebane, and Fatiha Hadji

Abstract

To highlight the anoxic event (OAE2) in the Aurès, a multidisciplinary study was conducted on the northern slope of Jebel Bou Arif (Aurès) where the sedimentation is marked by (1) marl-limestone deposits rich in bivalves and echinids and by foraminiferal limestones of the lower Turonian represented by *Whiteinella archeoretacea* [1], *Helvetoglobotruncana Helvetica* [2], *Heterohelix* sp. Microfacial analysis coupled with foraminiferal counting results, for quantitative and qualitative analyzes to calculate bioeonic indices, demonstrated periods of basin instability. Two peaks of faunal renewal were observed. The first occurred at the Cenomanian-Turonian passage. It coincides with the anoxic event OAE₂ and the second during the Middle Turonian. The interpretation of the geochemical results (CaCO₃, TOC: Total Organic Carbon, $\delta^{13}\text{C}$ and $\delta^{18}\text{O}$) indicates the presence of an important anoxic phase that starts in the *Whiteinella archeoretacea* zone and increases at the base of the *Helvetoglobotruncana helvetica* zone. The presence of organic matter associated with the evolutionary response of benthic foraminifera preceding the $\delta^{13}\text{C}$ isotopic signal explains a well-marked transgressive regime.

Keywords

Cenomanian • Turonian • Aures • OAE2
Foraminifera • Geochemistry

1 Introduction

The study concerns Bou Arif Mountain of Cenomanian-Turonian (C-T) age which is located in the northwestern part of Batna city [3]. It constitutes a part of the outcropping formation of the autochthonous Auresian in the north of Batna Mountains.

Observations and results of the various lithological, biostratigraphic, micropaleontological, palaeoecological and geochemical analyzes can contribute to the palaeoenvironmental and paleogeographic studies of the study area. They make it possible to draw certain conclusions on the geodynamic events and the tectono-eustatic control of the southern margin of this basin.

Few studies carried out do not take into account the concepts of modern chemostratigraphy on the characterization of deposits rich in organic matter. The aim of this study is to understand the parameters that can control the evolution of sedimentary systems and to perceive the relationship between the distribution of rich in organic matter levels in time and space during the C-T transition.

2 Materials and Methods

A multidisciplinary study was conducted on a section of the North slope of Jebel Bou Arif, located North of the Timgad Basin [3], in a sedimentary series of marls and limestone rich in microfauna (Fig. 1). Forty four samples were collected and subjected to several laboratory analysis techniques for analysis. Concerned parameters were the organic matter (OM), by loss on ignition, CaCO₃ (%), dolomite, quartz and

A. Touahria (✉) · A. Garah · A. Sebane
Faculty of Earth and Universe Sciences, Laboratory GeoBaBise,
University of Oran 2, Bir El Djir, Algeria
e-mail: touahria_abdia@yahoo.fr

F. Hadji
Département of Earth and Universe Sciences SNV-STU Faculty,
Tlemcen University, PO Box 119 Tlemcen, Algeria

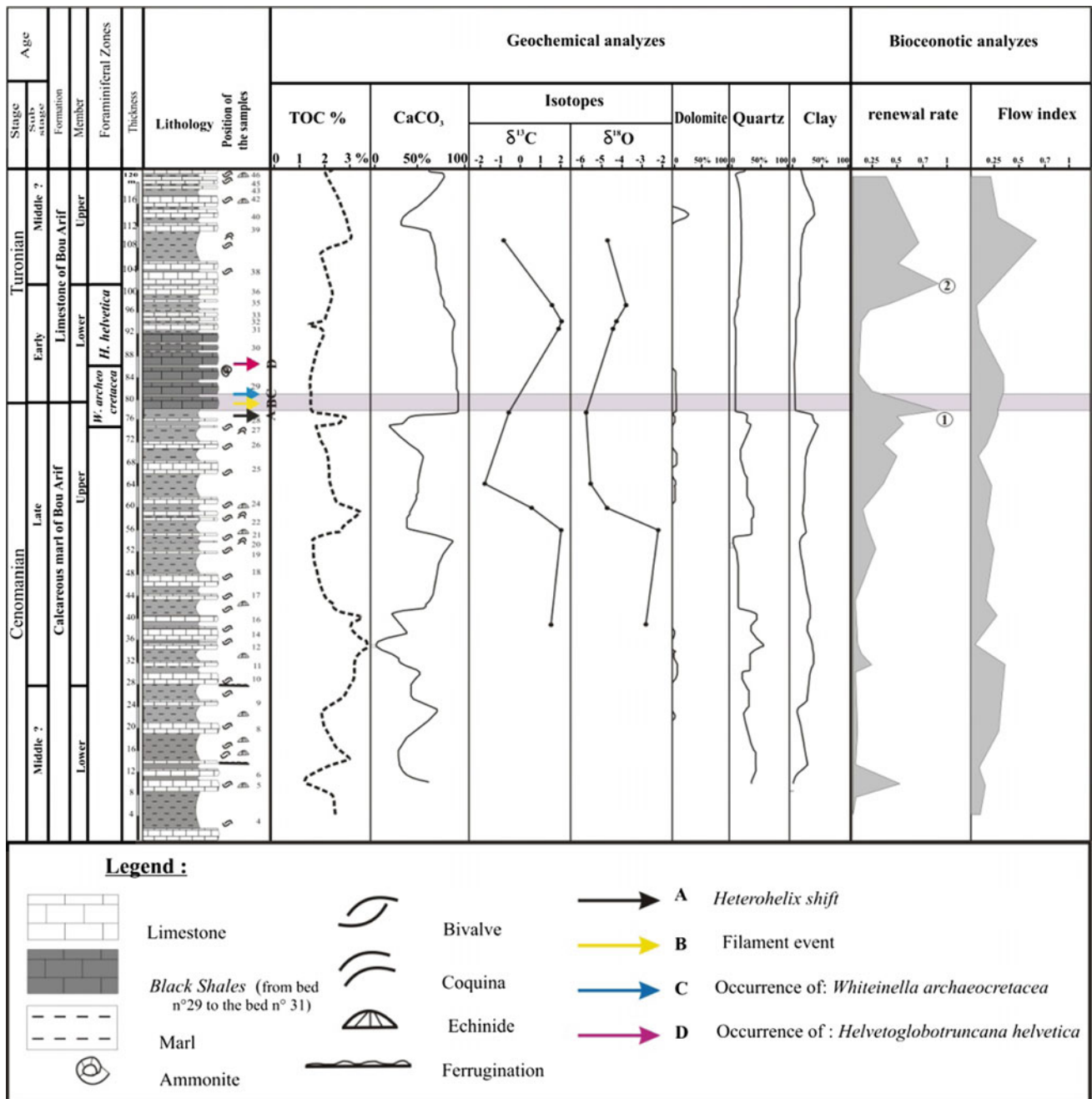


Fig. 1 Lithostratigraphy, sample location and geochemical and biocenotic variations

clays by X-ray diffractometry (XRD). Nine of them concerning the C-T transition stable isotopes (¹³C and ¹⁸O) by mass spectrometry. Foraminifera's determination, which were released after washing and sieving under a continuous water jet, were done under binocular loupe and polarizing microscope. The method used to compute the biocenotic indices is that of Jarvinen [4]. It makes it possible to calculate the rates of winding, unwinding and the renewal of foraminifera.

3 Results

3.1 Lithostratigraphy and Biostratigraphy

The study series is subdivided into two formations with different lithological and palaeontological characteristics. The first formation is of the cenomanian age. It is composed of marl-limestone deposits rich in bivalves and echinides.

The second is marked by a mainly calcareous sedimentation with lower Turonian microfauna (foraminifera) (Fig. 1).

The microfacies analysis allows us to distinguish several biosedimentary facies that show well-known biostratigraphic events of the C-T passage.

The sequence of these biosedimentary deposits has yielded several microfaunal tools highlighting the C-T transition which can be recognized by the rich levels of planktonic foraminifera of the lower Turonian such as *Whiteinella archeoretacea* [1], *Helvetoglobotruncana Helvetica* [2], *Heterohelix* sp [5].

Variations in unwinding and winding indices are related to instability periods recorded in the basin. Two renewal peaks were observed along the sedimentary series. The first one occurred at the C-T passage while the second at the middle Turonian. These paleo-ecological changes explain the well-marked sea transgression in the study area (Fig. 1).

3.2 Paleo-Ecology

The reconstitution of the depositional environment and the fluctuations of the physicochemical and trophic parameters of the sea bed were based firstly on the observed microfacies analysis and secondly on the results of the qualitative and quantitative foraminiferal analyzes.

3.3 Geochemistry

The geochemical data interpretation (CaCO_3 , TOC and $\delta_{13}\text{C}$ and $\delta_{18}\text{O}$) during the late Cenomanian-Early Turonian chronological interval indicates the presence of an important anoxic phase that starts at the *Whiteinella archeoretacea* zone and increases at the base of the *Helvetoglobotruncana helvetica* zone (Fig. 1).

3.4 Results

The outcropping series in Bou Arif Mountain from Cenomanian to lower Turonian shows a transgressive

evolution that evolves from an internal platform to the basin edge. During the late Cenomanian and Early Turonian, a transgression led to OAE₂ and the black shales deposits.

4 Discussion

The evolution analysis of the benthic foraminifera shows sensitivity to water depth and anoxia. The response to environmental conditions precedes the variation of the $\delta_{13}\text{C}$ isotopic signal (Fig. 1).

5 Conclusion

The sedimentary, the micropaleontological and the geochemical data synthesis indicated a confined environment suffering from anoxia which was usually accompanied by organic matter presence. The ^{18}O and ^{13}C results of the C-T interval coincide with one of the Cretaceous oceanic anoxic events defined by Schlanger and Jenkyns [6].

References

1. Pessagno, E.A. Jr.: Upper Cretaceous planktonic foraminifera from the West Gulf Coastal Plain. *Paleontographica amer.* **5**, 245–445 (1967)
2. Bolli, H.M.: Zur stratigraphie der oberen Kreide in den hoheren helvetischen Decken. *Ecologiae Geologicae Helveticae* **37**, 217–328 (1945)
3. Vila, J.M.: Carte géologique de l'Algérie au 1/200 000, feuille de Constantine (P-Q; 3–4), avec notice explicative détaillée. Publ. Comm. Serv. Carte géol. Algérie/SONATRACH (1977)
4. Jarvinen, O.: Geographical gradients of stability in European land bird communities. *Oecologia* **38**, 51–69 (1979)
5. Bengtson, P.: Turonian stage and substage boundaries. *Bull. Inst. Royal, Sci. Nat. Belgique, Sci. Terre* (66), 69–79 (1996)
6. Schlanger, S.O., Jenkyns, H.C.: Cretaceous oceanic anoxic events: causes and consequences. *Geologie en Mijnbouw* (55), 179–184 (1976)

Carbonate Deposit Microfacies and Carbonatogenesis of Abiod Formation (Campanian/Maastrichtian) in Jebel Kebar (Central Tunisia)

Manel Zidi, Jamel Tourir, Frédéric Boulvain, and Abderrazak El Albani

Abstract

The present work aims to study the origin of limestones and carbonatogenesis of the Abiod Formation (Campanian Maastrichtian) in Jebel Kebar area (Central Tunisia). This work is based on the examination of a geological section in Jebel Kebar area. The polarizing microscopic observation of thin sections of limestone allowed us to determine four depositional facies: (i) Planctonic foraminifera-rich mudstone-wackestone, (ii) Calci-sphera-rich mudstone, (iii) Bioclastic-bioturbated mudstone and (iv) Bioturbated mudstone, which is developed in turn in open circalittoral, circalittoral and infralittoral environments. These different carbonate facies correspond respectively to Transgressive and Regressive systems tracts that determine carbonate depositional sequences. The SEM observation shows that the Abiod Formation limestone is essentially micritic with three kinds of micrite (i) biotrital micrite (ii) Chemical micrite (chemical precipitation) and (iii) Biological micrite (bacteria product?). The biotrital micrite is the most represented in the studied limestones in comparison with the other kinds of micrite. The mineralogy, calcimetry, geochemical element concentrations and magnetic susceptibility (SM) show cyclic vertical changes which are related to the deposit facies (systems tracts) variation

in the same way the maximum carbonate production rates are related to the transgressive intervals and mainly resulted from the biotrital micrite accumulation. Accordingly, it seems that the carbonatogenesis was at least in part controlled by the sea-level fluctuation.

Keywords

Facies • Carbonatogenesis • Bacteria
Campanian maastrichtian • Jbel kebar

1 Introduction

carbonate deposits. Almost all of the oceanic carbonate production is directly (CaCO₃-rich shells accumulations) or indirectly (bacteria precipitation of CaCO₃) of biological origin. It may also be the result of inorganic precipitation, (Sorby 1879; Boquet et al. 1973; Tucker 1992; [1]; Baskar et al. 2006). The main objective of the present work is to study the origin of limestones and the carbonatogenesis controlling factors in the rudist-rich Abiod Formation (Campanian/Maastrichtian) in Jebel Kebar area (Central Tunisia), using different analyses of these limestones.

2 Geographic, Geological Settings and Methodology

The Abiod Formation limestone (Campanian-Maastrichtian) is studied in the Jebel Kebar area (Central Tunisia). This formation is underlain by the upper marls of the Aleg Formation (Santonian) and overlain by the silty clay of the Segui Formation (Mio-Pliocene), (Khessibi 1978; Negra 1994). This Formation consists of rudist-rich limestone deposits.

The study of the Abiod Formation is based on the examination of a geological section in the Jebel Kebar area. Depositional facies and carbonate petrography analyses are

M. Zidi (✉) · J. Tourir

Faculty of Sciences of Sfax, Road Soukra, km 3.5,
3038 Sfax, Tunisia

e-mail: manel.zidi@gmail.com

M. Zidi · J. Tourir

Laboratory 3E, National Engineering School of Sfax,
Road of Soukra km 4, 3018 Sfax, Tunisia

F. Boulvain

Laboratory Pétrologie sédimentaire B20, Boulevard du Rectorat
15, Liège University, Sart Tilman, 4000 Liège, Belgium

A. El Albani

University of Poitiers, UMR 7285-IC2MP, UFR SFA,
Bât. Sciences Naturelles, 5, rue Albert Turpin,
86073 Poitiers Cedex, France

based on polarizing microscope and SEM observations of limestone samples. Mineralogy analysis, calcimetry test, geochemical analysis and magnetic susceptibility (SM) have been applied in order to respectively evaluate carbonate mineralogy, CaCO₃ rates, the Ca, Mg, Fe, K and Mn concentrations and the magnetic signal (MS).

3 Results

In the studied section, the Abiod Formation is about 65 m thick, and can be subdivided into three lithostratigraphic units: lower, middle and upper. The Abiod Formation limestone includes three distinct carbonate facies:

- F1: Planctonic foraminifera-rich mudstone-wackestone, occurs mainly in the median unit of the Abiod Formation (KB26 to KB47) it indicates a circalittoral environment with medium to low hydrodynamic energy.
- F2: Calcisphaera-rich mudstone, occurs mainly in the lower unit of the Abiod Formation (KB1 to KB25) it indicates a circalittoral environment with low to moderate hydrodynamic energy.
- F3: Bioclastic-bioturbated mudstone, occurs in the upper unit of the Abiod Formation (KB66 to KB 72) it indicates an open-marine infralittoral environment.

- F4: Azoic bioturbated mudstone, characterizes the upper unit of the Abiod Formation (KB48 to KB65). It indicates a relatively restricted infralittoral domain.

The vertical changes of previous deposit facies determined different deposit systems tracts that may be arranged into 5 Transgressive/Regressive depositional sequences, [2].

The SEM observation shows that the studied limestones are mainly characterized by mudstone-wackestone textures and composed of micritic particles. At least, three kinds of micrite particles, which can have been resulted from different origins, are recognized:

Biotrititic micrite: detrital carbonate particles which consists of nano-fossils (calcisphaera, coccoliths) and fine-grained bioclasts (ostracods, rudists, foraminifers), Negra et al. [3], they are the most common in the studied limestones. This kind of micrite is mainly associated with the calcisphaera and foraminifers-rich facies.

Chemical micrite: carbonate particles resulting from inorganic precipitation of CaCO₃: $\text{CaCO}_3 + \text{CO}_2 + \text{H}_2\text{O} \rightleftharpoons \text{Ca}^{++} + 2 \text{HCO}_3^-$, which are related to carbonate saturated marine waters, with low rates of dissolved CO₂. This micrite is mainly associated to azoic limestone facies.

Biological micrite: Association of carbonate particles which are showing biological micro-structures comparable to bacterial fabrics. Three kinds of presumed bacterial

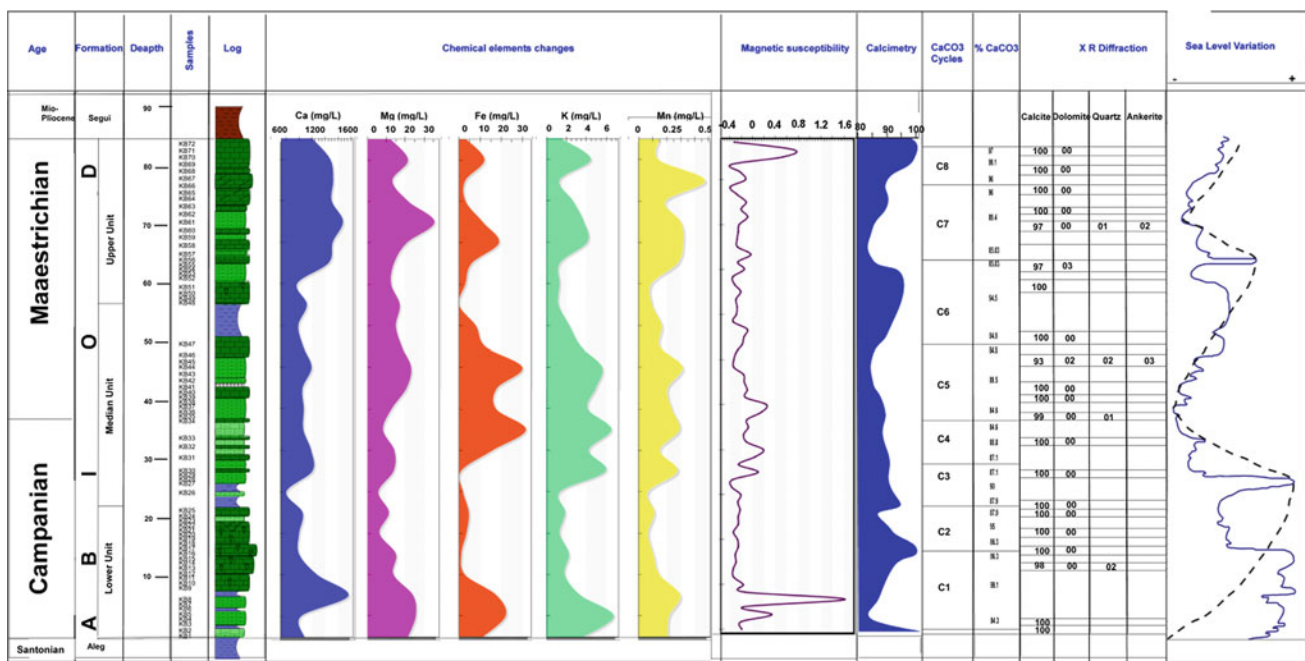


Fig. 1 X R Diffraction, Calcimetry test, Geochemical analysis and Magnetic Susceptibility of the Abiod Formation in Jebel Kebar area

structures: rods, rounded structures and filaments. They are the least common among the studied kinds of micrite. The biological micrite is associated mainly with F4 and F3 facies.

The vertical distribution of these kinds of micrite in the Abiod Formation shows that the biotrital micrite is related to the transgressive facies whereas the chemical micrite characterizes the regressive limestones.

The XRD mineralogy and calcimetry test show that the limestone of the Abiod Formation is very rich in calcite with 100% of CaCO₃ in some samples. The CaCO₃ concentrations are vary with the systems tracts which illustrate the role of eustatic fluctuations in the carbonatogenesis such as the high concentrations of carbonates are recorded in the transgressive intervals of the eustatic cycles (Fig. 1).

The magnetic susceptibility (SM) and the chemical major elements concentrations are correlative with the systems tracts such as high concentrations of Fe are recorded in the regressive intervals of the eustatic cycles, whereas the high concentrations of Ca and Mg are recorded in the transgressive intervals. As for MS, it is mainly negative in the transgressive interval of the eustatic cycles, and positive in the regressive interval of the eustatic cycles.

4 Discussion

According to their components and textures, the deposit facies determines to different systems tracts. Indeed, F1 and F2 represent transgressive systems tracts whereas F3 and F4 correspond to regressive systems tracts.

The vertical variation of these systems tracts determines 5 depositional sequences controlled by 5 short-term transgressive/regressive eustatic cycles that can be regrouped into 2 long-term eustatic cycles. To determine the marine transgression and regression and their magnitude the associated microfossils and textures of limestone are considered. In addition the local sea-level change curve was correlated with the global eustatic curve (Haq et al. 1988). This assumption is supported by the vertical variations through Abiod Formation of mineralogy, calcimetry, magnetic susceptibility and geochemical concentrations of the limestones. Indeed, the high rates of CaCO₃ and the high

concentrations of Ca and Mg are recorded in the transgressive intervals whereas the low rates of CaCO₃ and the high concentrations of Fe are recorded in the regressive interval of the eustatic cycles. The significant amounts of the biotrital micrite in the study of limestones show the important role of the associated rudist buildups which played as a biotrital micrite feeder of the sedimentary environment. It appears that carbonatogenesis materialized by the maximum of CaCO₃ levels is favored by the marine transgression where the multiplication of calcareous organisms (planktonic foraminifers, calcisphaera, inoceramids, rudists) is the most important. As for the presumed bacterial micrite, many workers in the world [4] affirm that the carbonatogenesis can be achieved the bacterial activities (bio-precipitation)

5 Conclusions

The present study of the Abiod Formation limestones in Jebel Kebar allowed us to lead a discussion not only about the origin of limestone deposits and the possible role of bacteria in the carbonatogenesis but also the significant role of the associated calcareous organisms as carbonate producers. The carbonatogenesis of Abiod Formation limestones was controlled by the sea level fluctuation and the transgressive interval are the most favorable for carbonatogenesis.

References

1. Collin, P.Y., Loreau, J.P., Courville, P.: Depositional environments and iron ooid formation in condensed sections (Callovian-Oxfordian, south-eastern Paris basin, France): *Sedimentology* **52**, 969–985 (2005)
2. Tour, J., Zaghbib-Turki, D.: Effets des oscillations eustatiques couplées à une tectonique synsédimentaire sur la marge sud de la Téthys au Sénonien: exemple du Jebel M'rhila, Tunisie centrale. *Creataceous Res* **5**, 675–695 (2004)
3. Negra, M.H, F.: Upper cretaceous platform-derived conglomerates in Central Tunisia: significance and genesis mode. In: Gili, E., Negra, M.H., Skelton, P.W. (eds.) *North African Cretaceous Carbonate Platform Systems*. NATO Science Series, IV/28, pp. 129–141 (2003)
4. Sushmitha, B., Baskar, R., Mauclaire, L., McKenzie, J.: Role of microbial community in stalactite formation, Sahastradhara caves, Dehradun. India. *Curr. Sci.* **88**, 1305–1308 (2006)

The Eocene–Oligocene Climate Transition in the Southern Tethys: Calcareous Nannofossil Response and Element Geochemistry

Jihede Haj Messaoud, Chokri Yaich, Johannes Monkenbusch, and Nicolas Thibault

Abstract

The late Eocene—Early Oligocene transition is characterized by the transient changes in the environmental conditions from greenhouse to icehouse controlled by the onset of the major Antarctic glaciation phase (~34 Ma). The effects of this major climatic transition in Earth history have not been studied so far in the southern Tethys. Here, we present new data from the Ain Rahma section (Northeastern Tunisia, Cap Bon peninsula) across the Late Eocene—Early Oligocene. Calcareous nannofossil biostratigraphy permits an excellent detection of the paleoclimatic events of this transition. Hand-held X-ray Fluorescence (HH-XRF) analysis is used to show changes in detrital elements across the transition (Fe, Si, Al, Zr). Two major changes are recorded in the studied interval corresponding to the Eocene/Oligocene transition 1 event (EOT1) and to the Oi-1 glaciation event. Both depicted by important shifts in detrital elements and calcareous nannofossil assemblages.

Keywords

Southern tethys • Eocene oligocene boundary
Calcareous nannofossil • Trace elements
Paleoclimate

J. H. Messaoud (✉) · J. Monkenbusch · N. Thibault
Department of Geosciences and Natural Resource Management,
University of Copenhagen, Øster Voldgade 10, 1350 Copenhagen
C, Denmark
e-mail: jhm@ign.ku.dk

J. H. Messaoud · C. Yaich
Sfax National Engineering School, University of Sfax, Soukra
Road km 4, Road of the Airport km 0.5, PB 1178 3038 Sfax,
Tunisia

J. H. Messaoud · C. Yaich
Laboratory of Sediment Dynamics and Environment, Sfax
National School of Engineers, University of Sfax, PB 1173 3038
Sfax, Tunisia

1 Introduction

Calcareous nannoplankton species are largely controlled by temperature and water mass conditions [2]. Therefore, they react to climate fluctuations as well as variation in surface water nutrient amount. In this study, calcareous nannofossils have been used as proxies for the reconstruction of the paleoenvironmental conditions around the Eocene-Oligocene transition on the margin of the southern Tethys (Tunisia). These paleontological data are compared to major and trace element geochemistry acquired via hand-held XRF in order to provide more reliable interpretations of the environmental changes.

2 Results

2.1 Calcareous Nannofossil Results

A total of 32 samples with a spacing of 20 cm were examined. They have led to the identification of 24 calcareous nannofossil species. *Coccolithus pelagicus*, *Coccolithus eopelagicus*, *Reticulofenestra dictyoda*, *Cyclicargolithus floridanus* and *Ericsonia formosa* are the dominant components of the assemblage at the Ain Rahma section (Fig. 1). Rapid declines of abundance nannoplankton diversity are obvious around 6 m and 14 m. Following the work of Agnini et al. [1], *D. saipanensis*, *C. subdistichus*, *E. Formosa* and *R.umbilicus* are the key species for the biohorizons of the study interval and allowed the identification of three Calcareous Nannofossil Zones: The Helicosphaera compacta Partial Range Zone (CNE21) from Top *Discoaster saipanensis* to the Base common of *Clausicoccus subdistichus*. The *Ericsonia formosa* *Clausicoccus subdistichus* Concurrent Range Zone (CNO1) covering the interval from Base common *C. subdistichus* to Top *E. Formosa* and the *Reticulofenestra umbilicus* Top Zone (CNO2).

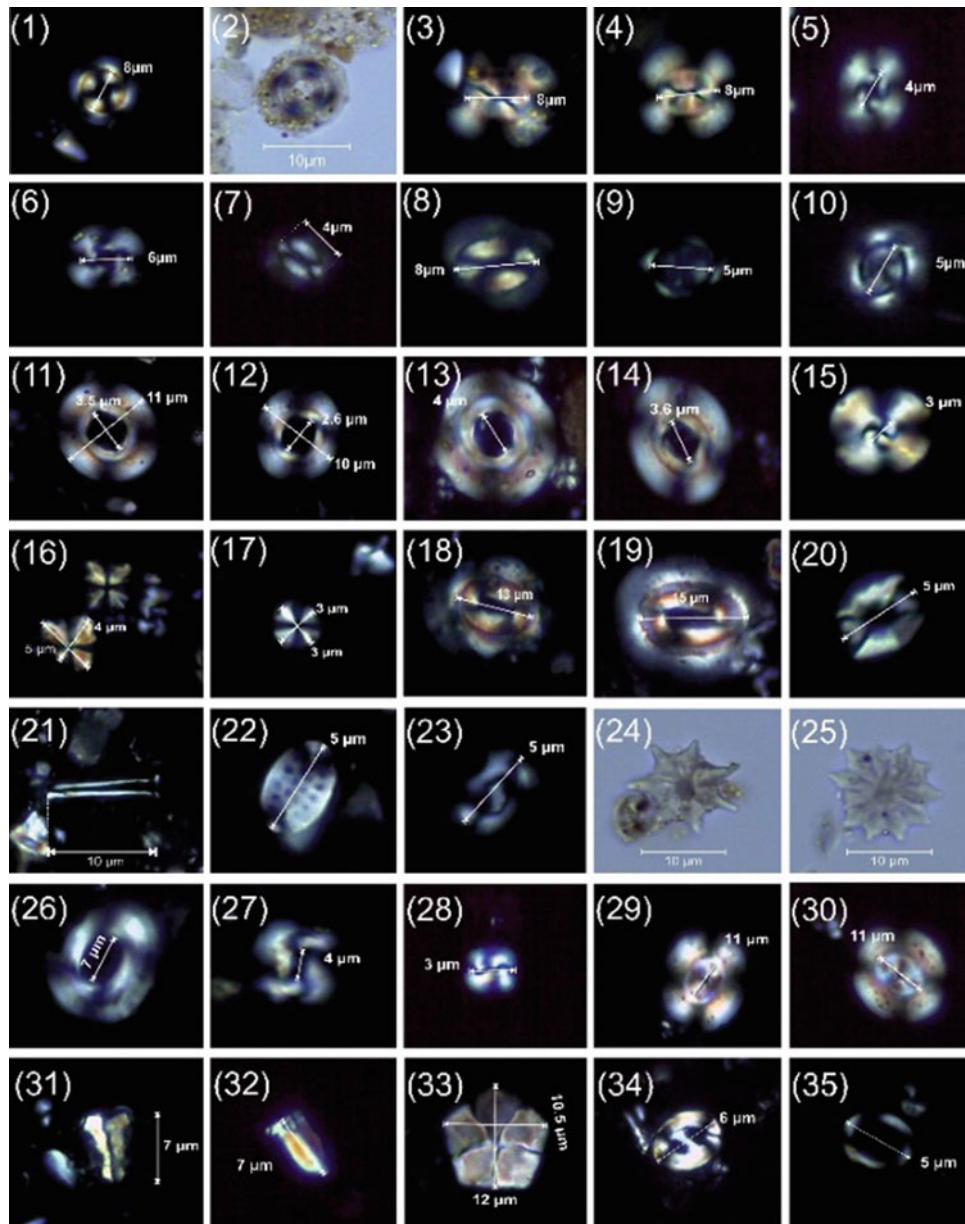


Fig. 1 Microphotographs of selected calcareous nanofossils from the Ain Rahma section. Scale is indicated on each picture. 1. *Ericsonia formosa*, crossed nicols 0° . 2. *Ericsonia formosa*, parallel nicols 0° . 3, 4. *Dictyococcites bisectus*. 5, 6. *Cycliscardolithus floridanus*. 7, 8. *Coccolithus pelagicus*. 9, 10. *Clausicoccus subdistichus*. 11, 12. *Reticulofenestra umbilicus*. 13, 14. *Reticulofenestra hillae*. 15. *Cycliscardolithus lumnis*. 16. *Sphenolithus moriformis*. 17. *Pontosphaera*

exilis. 18, 19. *Coccolithus eopelagicus*. 20. *Lanternithus minutus*. 21. *Blackites spinosus*. 22. *Pontosphaera multipora*. 23. *Helicosphaera bramlettei*. 24. *Discoaster saipanensis*. 25. *Discoaster barbadiensis*. 26. *Reticulofenestra dictyoda*. 27. *Reticulofenestra dictyoda* with narrow central area. 28. *Reticulofenestra minuta*. 29, 30. *Reticulofenestra stavensis*. 31, 32. *Zygrhablithus bijugatus*. 33. *Braarudosphaera bigelowii*. 34. *Helicosphaera reticulata*. 35. *Coronocyclus nitescens*

2.2 Palaeoecological Results

PCA on the coccoliths results distinguish between three assemblages directed by two factorial factors plotted on the PCA (Fig. 2). The first (47.9%) factor shows a good correlation with *I. recurvus*, *L. minutus* and *C. pelagicus* and an anti-correlation with *S. moriformis*; *D. saipanensis* and *D. barbadiensis*. The second axis (24.9%) is in good correlation with *B. bigelowii*, *C. lumnis* and *C. floridanus*.

3 Discussion

The change in nanoplankton includes the decline of the warm water *Discoaster* spp. and the increase of cool water—nearshore species such as *I. recurvus*, *C. pelagicus*, *L. minutus* and *Z. bijugatus*. Extinctions of warm water taxa and size variations (*S. moriformis*, *C. floridanus*...) are detected. Statistical analyses based on nanofossil

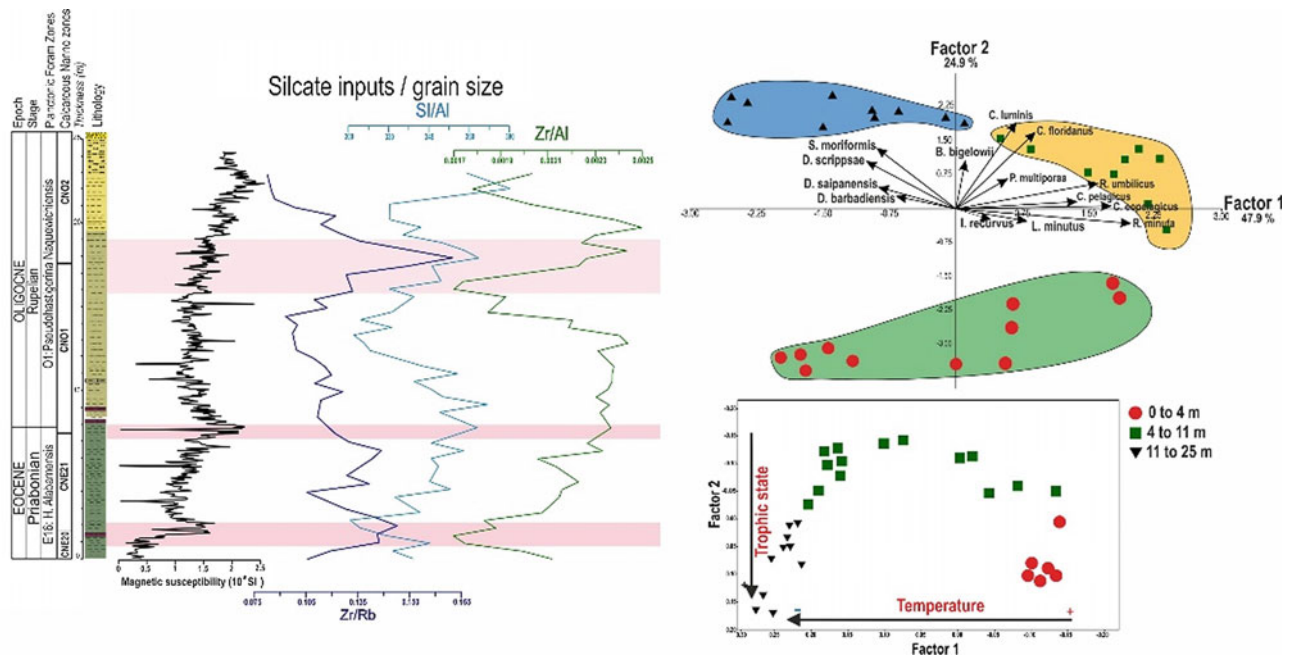


Fig. 2 Traces elements with Principal component analysis (PCA) with the Q-mode non-metric multidimensional scaling analysis

assemblage distinguish between three ecological groups: a warm water and oligotrophic nannoplankton association in the Late Eocene which indicates fully open marine connections. A group of transition is represented by temperate-cool water taxa. A third group corresponds to a nearshore nannoplankton assemblage across and after the EOT. Cool water, eutrophic conditions and enhanced terrestrial influx are inferred in the interval dominated by this third association. Detrital elements (Si, Fe, Al), grain size proxies (Zr/Rb) spots the CNO1/CNO2 and the CNE20/CNE21 limits while the EOT is not well expressed.

4 Conclusion

Our study documents the major shift in calcareous nannofossil assemblages across the Eocene–Oligocene transition along the southern margin of the western Tethys. A drop in

nannofossil species diversity, coupled with high abundances of eutrophic cool-water taxa, indicate a gradual increase in surface water nutrient from continental runoff across the transition. The eustatic sea level fall, related to the onset of Antarctic glaciation, led to surface-water cooling and to the increase of continental weathering in Tunisia, which in turn, favored the thriving of eutrophic cool water species.

References

1. Agnini, C., Fornaciari, E., Raffi, I., Catanzariti, R., Palike, H., Backman, J., Rio, D.: Biozonation and biochronology of Paleogene calcareous nannofossils from low and middle latitudes. *Newsl. Stratigr.* **47**(2), 131–181 (2014)
2. Persico, D., Villa, G.: Eocene–Oligocene calcareous nannofossils from Maud Rise and Kerguelen Plateau (Antarctica): palaeoecological and palaeoceanographic implications. *Mar. Micropaleontol.* **52**, 153–179 (2004)

Sedimentology and Geochemistry of the Chouabine Phosphate Succession (Upper Paleocene-Lower Ypresian) in El Guettar Area (Gafsa Region, Central Tunisia)

Wejdène Slimène, Jamel Tourir, Lotfi Khélil, Zied Saïid,
and Nabil Fatteh

Abstract

This work is set out to conduct a sedimentological and geochemical study of the phosphate series in Oued Tarfa section in El Guettar area (east Gafsa region) in order to characterize the phosphate deposits and reconstruct the phosphatogenesis environment. The studied phosphate series corresponds to the Chouabine Formation (Upper Paleocene–Lower Eocene) which is underlain by the uppermost dolomitic bed of the Selja Formation (Lower Paleocene). It is also overlain by the carbonate cliff of the Kef Eddour Formation (Lower Eocene). The series mainly includes nine phosphate layers alternating with limestones and marls. The latter intercalations are themselves intercepted with 5–10 cm-thick phosphate horizons. The total rock major element contents show an alternation of phosphate layers relatively rich in MgO and Na₂O with low concentrations of Fe₂O₃ and SiO₂ that may be related to transgressive open-marine environment and sandy phosphate layers rather poor in MgO and Na₂O with significant concentrations of Fe₂O₃ and SiO₂ that may have been developed in regressive prograding littoral environment. The open marine phosphates are richer in P₂O₅ than the littoral sandy ones.

Keywords

Phosphates • Geochemistry • P₂O₅
Phosphatogenesis environment • Chouabine formation
Upper Paleocene–Lower eocene • Oued Tarfa section
El guettar area • Central tunisia

1 Introduction

Since 1885, research on phosphate deposits in Tunisia has greatly expanded in terms of stratigraphy, mineralogy, paleontology, sedimentology, and geochemistry. Among the pioneering works in this field, we mention those of Sassi [6], Chaabani [4, 5], Bélayouni [3], Beji-Sassi [1, 2], Zaïer [7]. However, no study was carried out on the phosphate deposits in the El Guettar area especially in Oued Tarfa locality (east Gafsa region).

The Oued Tarfa section is located on the northwest side of Jebel Chemsî, few kilometers east of the village of El Guettar and east of Gafsa region (Fig. 1). It is bordered to the north by the chain of Gafsa (Jebels Ben Younes and BouRamli), to the south by the chain of North Chotts (JebelsMorra, Askar, Berda, Atra) and to the west by the Algerian border.

2 Methods

The present study is based on the examination of 63 samples recovered from the Oued Tarfa geologic section at the southwestern end of Jebel Chemsî flank (Fig. 1) complemented by microscopic observation of thin-section microfacies and geochemical analyzes of major and trace elements as well as the determination of P₂O₅ levels to evaluate the economic potential of this phosphate series.

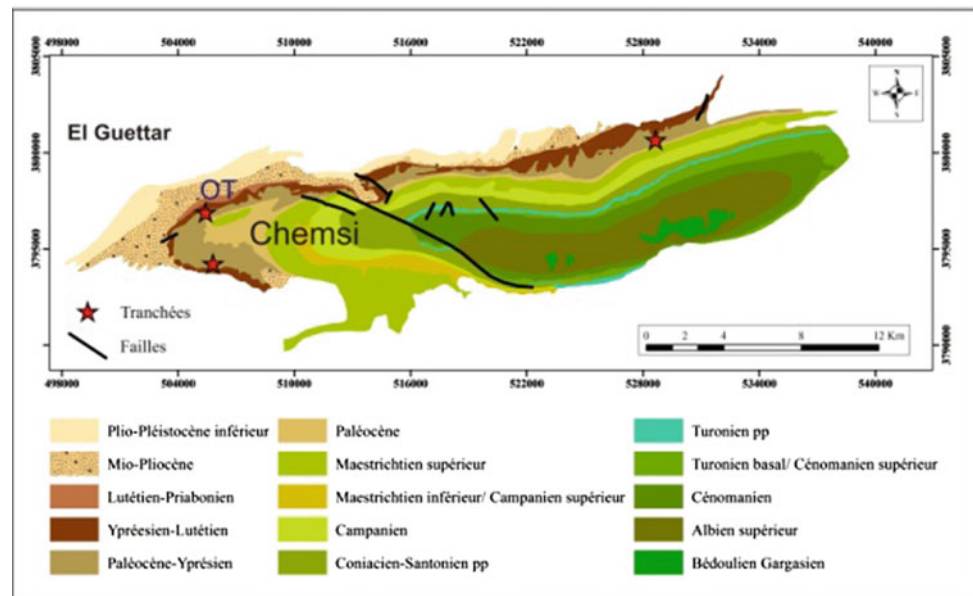
3 Results

The field examination of the Chouabine Formation in Oued Tarfa section shows 9 phosphate layers (1–9) which are alternating with layers devoid of phosphate. Layer 6, in particular, is very thick (4 m) in comparison with its stratigraphic equivalent in the Gafsa–Metlaoui region.

W. Slimène (✉) · J. Tourir
Laboratory Water Energy Environment,
Faculty of Sciences of Sfax, Road Soukra km 3.5, 3029 Sfax,
Tunisia
e-mail: wejdenslimen36@gmail.com

L. Khélil · Z. Saïid · N. Fatteh
Phosphate Company, Road Bayech, 2100 Gafsa, Tunisia

Fig. 1 Simplified geological map of Jebel Chemsî and location of the Oued Tarfa section. (extract from the geological map of El Ayecha 1/500,000)



The petrographic analysis of the studied carbonate and phosphate beds allowed us to distinguish six deposit facies, three of which are phosphate-rich: Facies 1: dolomitic sandstone with phosphatized grains—Facies 2: bioturbated wackestone mudstone with phosphate fillings—Facies 3: phosphate-rich grainstone packstone—Facies 4: mudstone with oyster debris—Facies 5: bioclastic wackestone packstone with pellets—Facies 6: bioclastic grain stone pack stone. In the following, we only consider the phosphate-rich facies.

- Facies F1: characterizes the levels OT6 and OT56 of the series. It is a slightly sandy dolomitic with phosphatized bioclasts and well-sorted fine quartz grains. These deposits are relatively rich in MgO associated to medium concentrations of SiO₂ and Na₂O with no negligible Fe contents (Fig. 2). Such attributes indicate a continent-influenced marine environment with relatively low hydrodynamic energy.
- Facies F2: occurs in the levels OT23, OT42, OT44 and OT51. It is characterized by bioturbated wackestone-mudstone with burrows filled with phosphatized and non-phosphatized pellets, ooids, coprolites and bioclasts. The quartz grains are rare and very fine. These deposits are significantly rich in Fe₂O₃ (Fig. 2). The bioturbation traces are synonymous of marine environments with O₂-rich waters that should have increased the biomass. The quite high concentration in Fe₂O₃ associated with this facies suggests that this environment was subjected to continental inputs. However, the presence of the significant phosphate grains filling the burrows suggests the presence of hypoxic marine bottom waters in the basin which are necessary for phosphate preservation.

- Facies F3: it characterizes, in particular, the levels OT45 and OT49 of the phosphate series. It consists of a phosphate-rich grainstone-packstone associated with well-sorted fine quartz grains, phosphatized pellets and coprolites. These deposits are richer in SiO₂ than in MgO (Fig. 2). Such features suggest a high-energy littoral marine environment that received terrigenous detrital material.

On the other hand, the facies F3 phosphate deposits show different P₂O₅ concentrations which vary according to the deposition facies (Fig. 2).

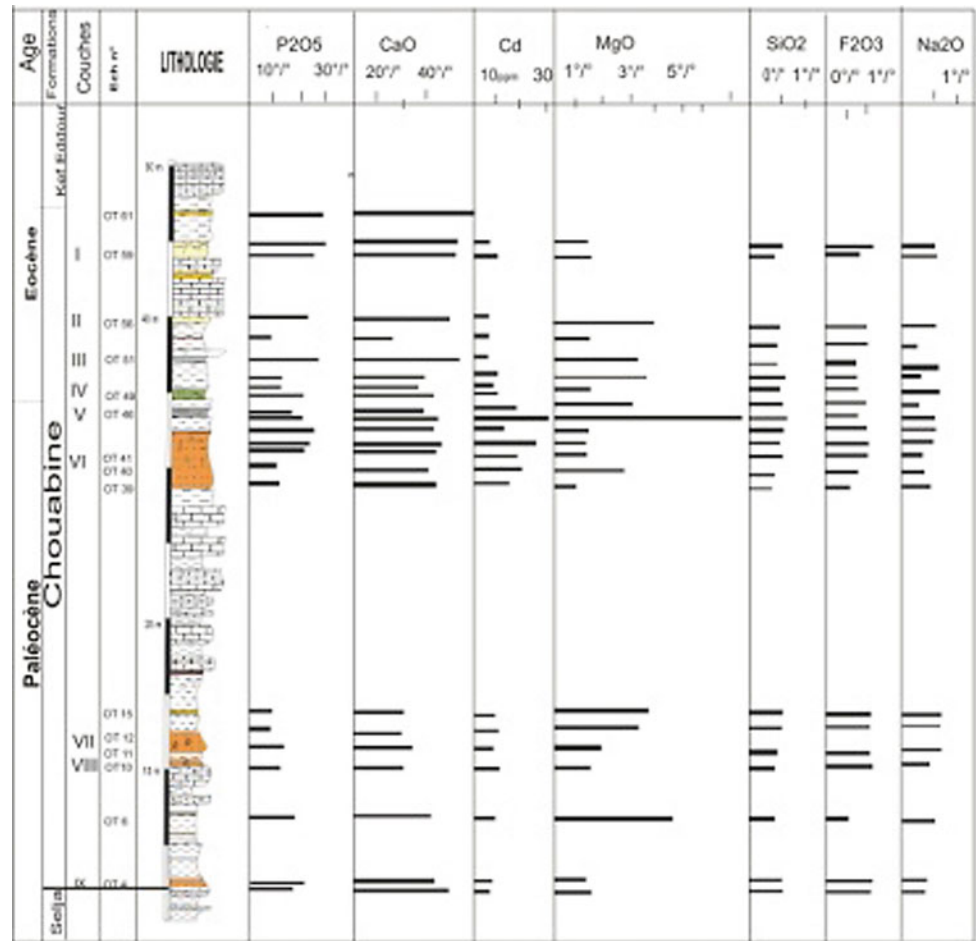
4 Discussion

The facies F2 phosphate-rich deposits are the richest in P₂O₅ (from 28 to 30%). Then, it seems that the O₂-rich marine environments that have not been exposed to significant detrital inputs are the most favorable for phosphatogenesis. Nevertheless, the preservation of the phosphates requires stratified marine waters with hypoxic ones on the bottom of the basin.

The Facies F3 phosphate-rich sandy deposits are less rich in P₂O₅ (from 17 to 20%) which shows that when the high-energy littoral marine environments are exposed to important detrital siliciclastic inputs become less favorable to phosphatogenesis and much less to their preservation in sediments.

The phosphatogenesis cycle recorded in the Chouabine Formation in the El Guettar region was intercepted by the deposition of limestones or marls devoid of phosphate.

Fig. 2 Chemical composition of Oued Tarfa phosphorite



It indicates that the episodes of the environmental conditions are adverse to phosphatogenesis and phosphate preservation.

5 Conclusion

The present study shows, for the first time, that the Chouabine Formation in the El Guettar area (central Tunisia) includes nine phosphate layers with high economic potentials. The P_2O_5 concentrations are more important in phosphate-rich beds related to open marine transgressive environment than those having been developed under regressive prograding environments.

References

1. Béji-Sassi, A.: Pétrographie, minéralogie et géochimie des sédiments phosphatés de la bordure orientale de l'île de Kasserine (Tunisie). Thèse de 3ème cycle : Géologie, Sédimentologie, Université d'Orléans, France (1984)
2. Béji-Sassi, A.: Les phosphates dans les bassins paléogènes de la partie méridionale de l'Axe Nord-Sud (Tunisie). Thèse Doct. Etat, Univ. Tunis II, Tunisie (1999)
3. Bélayouni, H.: Etude des la matière organique dans la série phosphatée du bassin deGafsa-Métlaoui (Tunisie): application à la compréhension des mécanismes de la phosphatogenèse. Thèse Doct. ès Sci. Univ. Orléans, France (1983)
4. Chaabani, F.: Les phosphorites de la coupe-type de FomThelja (Métlaoui-Tunisie). Une série sédimentaire séquentielle à évaporite du Paléocène, 131 p. Thèse 3ème cycle ULP, Strasbourg (1978)
5. Chaabani, F.: Dynamique de la partie orientale du bassin de Gafsa au Crétacé et au Paléogène: Etude minéralogique et géochimique de la série phosphatée Eocène, Tunisieméridionale. Thèse Doc. Etat. Univ. Tunis II, Tunisie (1995)
6. Sassi, S.: La sédimentation phosphatée au Paléocène dans le Sud et le Centre Ouest de la Tunisie. Thèse Doct. ès Sci. Univ. Paris-Sud Orsay, France (1974)
7. Zaïer, A.: Evolution tectono-sédimentaire du bassin phosphaté du centre-ouest de la Tunisie. Minéralogie, pétrographie, géochimie et genèse des phosphates. Thèse de Doct. èsScien., Université de Tunis (1999)

Thin-Bedded Turbidites of the Numidian Flysch, North Africa and Southern Europe

Dorrik Stow, Sami Riahi, Bouabdellah Menzoul, Urval Patel, Bayonle Omoniyi, and Melissa Johansson

Abstract

The Numidian Flysch (Oligocene-Miocene) is a mud-rich deepwater system dominated by thin-bedded and very thin-bedded turbidites. Preliminary study of the equivalent series in Sicily, Tunisia, Algeria and southern Spain reveal a similar range of mud, silt and sand-rich facies in each locality. They are commonly associated with thick-bedded turbidites and the deepwater massive sandstone facies association. They were deposited by low-concentration turbidity currents in a slope setting which shows a general shallowing-upward trend. Attribute and sequence characteristics indicate deposition in channel-abandonment, channel-levee, open slope and lobe architectural elements, for which we infer a series of separate basins and input points along the 2000 km extent of the Numidian Flysch system. Intensive bioturbation in parts are indicative of the interbedded hemipelagites and, possibly, contourites, although evidence for interaction with along slope currents during closure of the Tethys Ocean is yet to be elucidated. While the sand-rich turbidites represent good potential for hydrocarbon reservoirs, any exploration must take the dominance of thin-bedded turbidites into account.

Keywords

Numidian flysch • Thin-bedded turbidites
Attribute indices • Deepwater • Continental slope

D. Stow (✉) · B. Omoniyi
Heriot-Watt University, Edinburgh, EH14 4AS, Scotland, UK
e-mail: d.stow@hw.ac.uk

S. Riahi
Faculté Des Sciences de Tunis, CP2092 Tunis, Tunisia

B. Menzoul
University of Tlemcen, Fg Pasteur BP. 119, Tlemcen, Algeria

U. Patel
Heriot-Watt University, Putrajaya, Malaysia

M. Johansson
Geode Energy, Cardiff, UK

1 Introduction

The Numidian Flysch is a deepwater succession of Upper Oligocene to Lower Eocene age that outcrops over some 2000 km from southern Italy, across northern Africa, to southern Spain [1, 7, 13, 14]. It is best known for its thick-bedded sandstone turbidites and associated deepwater massive sandstone assemblage [4, 8, 11] which represent good outcrop analogues for the subsurface architecture of hydrocarbon reservoirs. Very little attention has been paid to the extensive fine-grained, mud-rich facies which are generally dominant but may be poorly preserved at outcrop and/or covered with vegetation. This study, therefore, focuses on these fine-grained sediment facies as observed in the Numidian Flysch of selected localities in Sicily, Tunisia, Algeria and Spain.

2 Sediment Facies and Succession

Detailed logging at 4 localities in Sicily and 4 localities in Tunisia have provided the bulk of the data for this contribution. The total thickness of the section measured ranged from 400 m to over 2000 m, although the thicker successions show clear evidence of thrust repetition of the stratigraphic sequence. These sections are complemented by the preliminary data from one locality in Algeria and two in southern Spain.

At least 20 individual facies are recognised across all localities. These can be represented as five main facies groups: (1) conglomerates and pebbly sandstones, (2) massive and structured sandstones, (3) interbedded sandstones/siltstone and mudstones, (4) mudstones with minor siltstones, and (5) chaotic (i.e. slumped and contorted units). There is a wide range of variation in the proportion of these different groups in each of the measured sections. In general, the proportion of mudstones is between 38 and 79%, the interbedded

sandstone–mudstone group between 8 and 18%. A further 4 and 24% is covered with vegetation or scree slope but most of this is likely mud-rich. When detailed logs have been measured through sand-dominated successions, the two facies groups (3 and 4) range from 10 to 54% compared with the sandstone and conglomerate groups that may reach up to 90% in parts. The new observations in the current study, combined with previous works, enable the clear interpretation of these facies as turbidites, mass-flow deposits and minor hemipelagites.

2.1 Facies Characteristics

Fine-grained facies groups 3 and 4 are characterised by medium beds (0.1–0.3 m thick), thin beds (0.03–0.1 m) and very thin beds (<0.03 m) or laminae. In some parts of the thick mudstone sections, bedding is indistinct. Normally, graded beds are common with sharp and erosive bases and a sequence of internal sedimentary structures. Bouma's [2] sequences are present in medium/thin beds (thin-bedded turbidites, TBTs) whereas Stow's [12] sequences are typical of thin and very thin beds (very thin-bedded turbidites, VTBTs). In both cases, partial sequences are most common. Grain size ranges from fine sand to silt and to clay. It shows from moderately good to poor sorting. The sandstone composition shows a quartz-dominated mineral assemblage with minor feldspar, muscovite mica and rock fragments. Polycrystalline quartz is the principal lithic grain type. There is a restricted heavy mineral assemblage characterized by zircon, tourmaline, rutile and opaque minerals. Glauconite and calcareous bioclastics are locally present. Few data exist on mineralogy of the mudrocks. However, chlorite, illite and kaolinite have all been noted in addition to a quartz-rich silt fraction. A diverse trace fossil assemblage is a characteristic of the TBT and mud-rich parts of the succession recently documented in detail for the Numidian Flysch in Tunisia [9].

The attribute indices [6] within these thin and very thin-bedded turbidites have not been quantified. However, preliminary estimates show a range from high values of Net-to-Gross and Sand Connectivity indices (>0.7) for some zones of closely-spaced and amalgamated TBTs within channel and lobe elements to much lower values (<0.3) for the isolated silt-laminated mudrock facies more typical of an open slope setting.

2.2 Sequences and Elements

Both small and medium-scale vertical sequences of bed thickness variation are present within the fine-grained turbidites. Symmetrical and thickening-up sequences (over a span from 5 to 15 m) are likely to represent depositional

lobes. Thinning-up sequences (over a span from 5 to 15 m) are recognized at the tops of thick-bedded and coarse-grained channel-fill successions. They are likely to indicate channel abandonment. Elsewhere, irregular and symmetrical to asymmetrical, small-scale sequences (ranging from 1 to 5 m) of mainly TBTs and VTBTs are indicative of levee, channel margin, interchannel and open slope environments. The regular bed-thickness variation is probably due to compensation cycles.

The thick and very thick-bedded coarse-grained facies typically occur in more blocky sequences associated with channel fill. Amalgamated channel elements locally exceed 100 m in thickness and laterally extend to a span from 1 to 2 km. further work are still required on the lateral extent of TBT and VTBT beds.

3 Discussion

This study is the first published attempt to document the nature of fine-grained facies as the dominant part of the Numidian Flysch succession, across North Africa and southern Europe. Although the data is preliminary at this stage, three significant aspects are emphasized:

Depositional processes The majority of fine-grained facies are turbidites deposited by low-concentration turbidity currents and/or by spillover from channelized higher concentration flows. They are best described as TBTs and VTBTs with reference to the Bouma and Stow facies models [10]. Parts of the interbedded mudrock facies are likely to be hemipelagites while some early work also suggested reworking by bottom currents. This would fit with the progressive closure of the Tethys Ocean at that time and probable intensification of through-flowing bottom currents [5]. Further work is required to establish evidence for contourites.

Depositional environments The processes and deposits along the 2000 km extent of the Numidian Flysch have close similarities. They are best interpreted as part of the deepwater slope system with a series of localized input points and downslope channels. Overall, there appears to be a shallowing upwards of the depositional environment from late Oligocene into early Miocene. Although there is some evidence for a European provenance [3], most authors favour supply from North Africa [13].

Petroleum significance Hydrocarbon exploration both onshore and offshore North Africa has considered the Numidian Flysch thick-bedded, coarse-grained facies as a potential reservoir target. It is important to note that such reservoirs are likely to be encased in fine-grained slope facies which may provide excellent seals for stratigraphic

trapping as well as leading to over-pressure and injection of sandstone dykes into the surrounding mudrock. Some of the TBT facies also have good attribute indices that would render them as potential secondary reservoir targets.

References

1. Benorman, O., Naim, A., Schamel, S.: Sources and dispersal of mid-Cenozoic clastic sediments. *Boll. Soc. Geol. Ital.* **38**, 54–65 (1987)
2. Bouma, A.H.: *Sedimentology of Some Flysch Deposits: A Graphic Approach to Facies Interpretation*. Elsevier, Amsterdam (1962)
3. Fildes, C., Stow, D.A.V., Patel, U., Milton, J.A., Riahi, S., Soussi, M., Marsh, S.: European provenance of the numidian flysch in northern Tunisia. *Terra Nova* **22**, 94–102 (2009)
4. Johansson, M., Braakenberg, N.E., Stow, D.A.V., Faugères, J.C.: Deep-water massive sands: facies, processes and channel geometry in the Numidian Flysch, N Sicily. *Sediment. Geol.* **115**, 233–266 (1998)
5. Kahler, G., Stow, D.A.V.: Turbidites and contourites of the paleogene lefkara formation, Southern cyprus. *Sediment. Geol.* **115**, 215–232 (1998)
6. Omoniyi, B., Stow, D.A.V., Gardiner, A.R.: Characterisation of thin-bedded turbidites in the North Brae field. *AAPG Memoir* **115**, 95–107 (2018)
7. Raoult, J.F.: Géologie du centre de la chaîne numidique (Nord du Constantinois, Algérie). *Mém. Soc. Géol.* **121**, 163 (1974).
8. Riahi, S., Uchman, A., Stow, D.A.V., Soussi, M., Boukhalfa, K., Ben Ismaïl-Latrache, K.: Stratigraphy, sedimentology and structure of the Numidian Flysch thrust belt in Northern Tunisia. *J. Afr. Earth Sci.* **57**, 109–129 (2010)
9. Riahi, S., Soussi, M., Boukhalfa, K., Ben Ismaïl-Latrache, K., Stow, D.A.V., Khomsi, S., Bedir, M.: Deep-sea trace fossils of the Oligocene–Miocene Numidian Formation, Northern Tunisia. *Palaeo. Palaeo. Palaeo.* (2014)
10. Stow, D.A.V., Omoniyi, B.: Thin-bedded turbidites: overview and petroleum perspective. *AAPG Memoir* **115**, 45–57 (2018)
11. Stow, D.A.V., Johansson, M.: Deep-water massive sands: nature, origin and hydrocarbon implications. *Mar. Petrol. Geol.* **17**, 145–174 (2000).
12. Stow, D.A.V.: Late quaternary stratigraphy and sedimentation on the Nova Scotian outer continental margin. Ph.D. thesis, Dalhousie University, Canada (1977)
13. Thomas, M., Bodin, S., Redfern, J., Irving, D.: A constrained African craton source for the Cenozoic Numidian Flysch: implications for the paleogeography of the western Mediterranean Basin. *Earth Sci. Rev.* **101**, 1–23 (2010)
14. Wezel, F.C.: Numidian Flysch: an oligocene to early miocene continental rise deposit of the african platform. *Nature.* **228**, 275–276 (1970).

Deepwater Sediment Facies and Sole Marks of the Numidian Flysch, Algeria

Bouabdellah Menzoul, Dorrik Stow, Mohammed Adaci, Miloud Benhamou, Hicham Mahdjoub Araibi, Mustapha Bensalah, and Madani Benyoucef

Abstract

The sedimentology of the Numidian Flysch (Upper Oligocene) of the Ouarsenis Mountains, Northwest Algeria, is presented here for the first time. The outcrops of the Forêt des Cèdres section comprise thick and very-thick bedded sandstones as the dominant facies. They are interbedded with more minor mudstones. Five distinct facies have been identified including: (1) massive sandstone, (2) normally-graded sandstone, (3) parallel-laminated sandstone, (4) siltstone, and (5) mudstone. The range of the observed bedding and facies characteristics can be interpreted as resulting from deepwater gravity flow processes. Many sole marks are present on the bases of the overturned sandstone beds including groove casts, flute marks, gutter casts, longitudinal ridge and furrow marks, mud ripples, and frondescant marks. A new type of flute-mark structure is documented here for the first time on the base of medium-grained sandstone beds. These features are designated as *curved flute marks*. It is suggested that they result from the flow interaction with an obstacle or irregular relief on the seafloor in the path of a strong turbidity current. Similar features have been generated in laboratory simulations by Dzulynski [4].

Keywords

Numidian flysch • Turbidite • Massive sandstone • Sole structures • Curved flute

B. Menzoul (✉) · M. Adaci · M. Bensalah
University of Tlemcen, Abi Ayad Abdelkrim street Fg
Pasteur BP. 119, Tlemcen, Algeria
e-mail: menzoul.bouabdellah@hotmail.fr

D. Stow
Heriot-Watt University, Edinburgh, EH14 4AS, Scotland, UK

M. Benhamou · H. Mahdjoub Araibi
University of Oran 2, BP. 1015, El Mnaouer, Oran, Algeria

M. Benyoucef
University of Mascara, 29000 Mascara, Algeria

1 Introduction

The Numidian Flysch in Algeria is characterised by deep sea turbiditic sandstone and mudstone deposits of Upper Oligocene to Lower Burdigalian age [2, 3, 7, 10] (Mattauer 1954 in [8]). This study focuses on the sediment facies and their distinctive suite of sole mark structures as observed in the Numidian Flysch of the Ouarsenis Mountains of NW Algeria. The study area is located 7 km northwest of the town of Theniet El Had, and 50 km northeast of Tissemsilt, in the Nature Reserve of the Forêt des Cèdres.

2 Sedimentary Succession Results

2.1 Vertical Succession

The total section measured at the Forêt des Cèdres section is 56 m thick of which sandstone beds are the dominant facies (50 m thick in total) and intercalated with more minor mudstones (6 m thick in total). Following careful examination of the sedimentary structures and the other way-up criteria, it is found that this series is overturned. On the basis of a slight variation in bed thickness and facies associations, the section has been subdivided into two parts: (1) the lower set, dominated by thick to very-thick bedded sandstones with minor mudstone; and (2) the upper set with medium to very thick-bedded sandstones and thicker intercalated mudstone units.

2.2 Sedimentary Facies

The Forêt des Cèdres section comprises an alternation of sandstone (dominant) and mudstone. Preliminary data on the sandstone composition shows a quartz-dominated mineral assemblage with minor feldspar, muscovite mica and polycrystalline quartz. There is a restricted heavy mineral

assemblage characterized by zircon, tourmaline, glauconite and opaque minerals. Five distinct facies are identified on the basis of bed thickness, sedimentary structures, grain size and textures including: (1) massive sandstone, (2) normally-graded sandstone, (3) parallel-laminated sandstone, (4) siltstone and (5) mudstone.

2.3 Process Interpretation

The range of bedding and facies characteristics observed in the Forêt des Cèdres section can be interpreted as resulting from deepwater gravity flow processes [9] (Stow et al. 1996). The massive (structureless) sandstone facies (Facies 1) are very similar to the deepwater massive sands described by Stow and Johansson [12] deposited from high-concentration turbidity currents and/or sandy debris flows. The graded and laminated sandstone facies (Facies 2 and 3) show typical partial Bouma sequences as a result of deposition from medium and low-concentration turbidity currents. The siltstone and mudstone facies (Facies 4 and 5) show typical partial Stow sequences and/or Bouma Te divisions. They probably result from deposition by low-concentration turbidity currents. Some of the mudstone facies (Facies 5), or marly mudstones, are without any clear sedimentary structures. However, they are with a high degree of bioturbation which may be the result of hemipelagic deposition.

Nevertheless, further work is needed to distinguish between these and muddy turbidites.

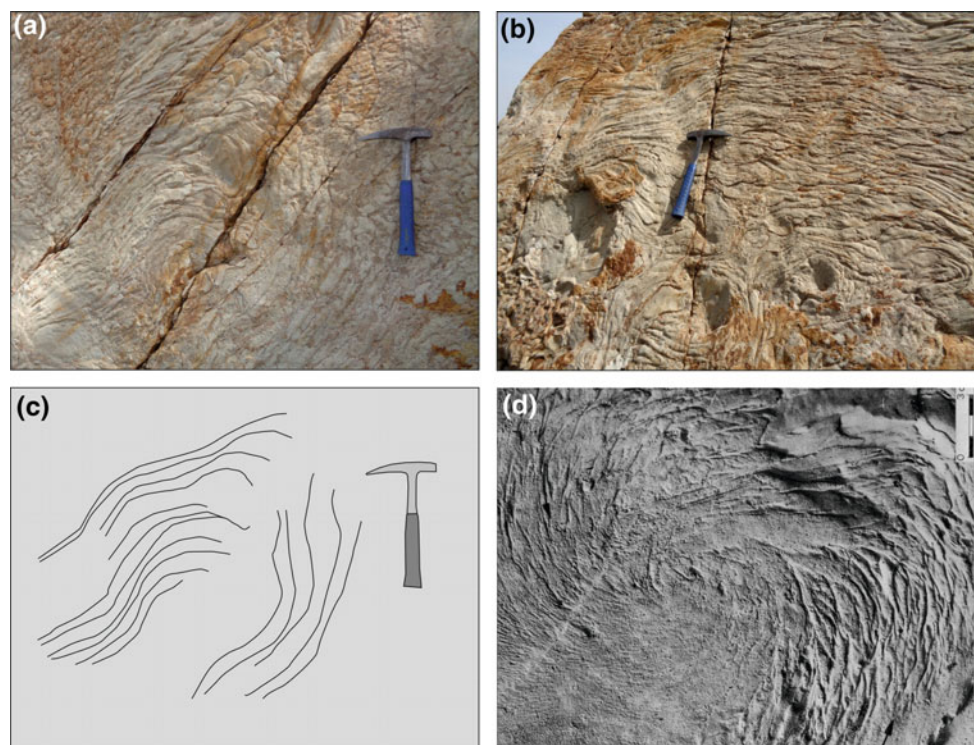
3 Sole Marks

The Forêt des Cèdres section is very rich in a range of different sole marks. They are clearly seen on the bases of the overturned beds including the sole structures common at the base of sandstone beds with the inclusion of groove casts, flute marks, longitudinal ridge and furrow structures, mud ripples and frondescant marks.

4 Curved Flute Casts (Fig. 1)

These scour structures appear to be very similar to the normal flute marks but are asymmetrical to curve in shape. In some cases, they form almost a spiral pattern or diagonal arrangement. They are preserved on the base of the medium-grained sandstone beds, in the lower part of the Forêt des Cèdres section and occur in 2% of the sandstone beds. The following sections describe the common scour marks and the observed tool marks. They are characterized by a longitudinal and parallel furrow ending with a curved nose as for normal flutes. They range from 3 to 30 cm in length, from 1 to 5 cm in width and from 0.5 to 2 cm in

Fig. 1 a, b panoramic photograph of the curved flute structure; c detail of (a); d structure obtained experimentally by Dzulynski (1965) described as asymmetrical flute



depth. It is believed that this paper is the first documentation of their occurrence in the field.

Similar features have been generated in laboratory simulations by Dzulynski [4], although they are much smaller in scale and with a more distinct spiral shape. These were the result of changing the orientation of the vortex axis towards the horizontal. After his experiments, he concludes that the oblique or diagonal arrangement of asymmetrical flutes appeared when the flow of the current was curved [1]. It is suggested that the curved flutes recorded in the Forêt des Cèdres section were formed by turbidity currents in which the development of large-scale and powerful eddies was caused by an upstanding obstacle to the flow path or by a marked irregularity of the bottom morphology. The presence of irregularities on the bottom like bumps or obstacles can cause local acceleration of the flow which gives rise to a flow separation and a local change in flow direction.

5 Discussion

This study is the first published account of the Numidian Flysch succession where it outcrops as a thrust nappe in the Ouarsenis Mountains in the far external part of the Greater Kabylies. The succession of the examined deepwater facies are similar to those documented in earlier studies of the Numidian Flysch in Algeria (e.g. Gelard [5]), northern Tunisia [11] and Sicily [6]. They also represent a clear example of the globally widespread deepwater massive sandstone facies association as documented by Stow and Johansson [12]. Very thick-bedded structureless sandstones are common typically with basal erosion, fluid-escape structures and mud clasts. These characterize rapid deposition and consequent water escape from high-density turbidity currents. The sole structures common at the base of sandstone beds including groove casts, flute marks, longitudinal ridge and furrow, mud ripples and frondescant marks also indicate turbidite sedimentation. A new type of flute-mark structure has been highlighted for the first time in this section.

It is designated as a *curved flute*. These structures are similar in some respects to the asymmetrical flutes of Allen [1] and to the much smaller-scale spiral flute-like features generated in laboratory simulations by Dzulynski [4].

References

1. Allen, J.R.L.: Transverse erosional marks of mud and rock: their physical basis and geological significance. *Sediment. Geol.* **5**, 167–385 (1971)
2. Bizon G., Hoyez B.: Données stratigraphiques sur les formations sous-numidiennes en Algérie. *C.R. Acad. Sci.*, vol. 289, pp. 655–658 (1979) (Paris)
3. Durand Delga, M., Magne, J.: Données stratigraphiques et micropaléontologiques nouvelles sur le Numiditique de l'Est de Cordières bétiques. *Revue de micropaléontologie*, vol. 1/3, pp. 155–175 (1958) (Espagne)
4. Dzulynski, S., Walton, E.K.: *Sedimentary Features of Flysch and Greywackes: Developments in Sedimentology*, vol. 7, 274 p. Elsevier, Amsterdam (1965)
5. Gélard, J.P.: Géologie du Nord-Est de la Grande Kabylie. *Mém. géol. Univ. Dijon*, vol. 5, 335 p., 98 fig., 19 pl., 2 pl. h.t. (1979) (France)
6. Johansson, M., Braakenberg, N.E., Stow, D.A.V., Faugères, J.C.: Deep-water massive sands: facies, processes and channel geometry in the Numidian Flysch, N Sicily. *Sediment. Geol.* **115**, 233–266 (1998) (Italy)
7. Lahondere, J.C., Feiberg, H., Hac.: Datation des grès Numidiens d'Algérie orientale: Conséquences structurales, *C.R. Acad. Sci.* 289, vol. 4, pp. 383–386 (1979) (Paris)
8. Mattauer M.: Etude géologique de l'Ouarsenis oriental (Algérie) *Bull. Serv. Géol. Monographie Régionale*, vol. 17, 534 p. (1958) (Algérie)
9. Pickering, K.T., Hiscott, R.N.: *Deep Marine Systems, Processes, Deposits, Environments, Tectonics and Sedimentation*. Wiley (2016)
10. Raoult, J.F.: Géologie du centre de la chaîne numidique (Nord du Constantinois, Algérie). *Mém. Soc. Géol.*, t. 111, n 121, 163 p. (1974) (France)
11. Riahi, S., Patel, U., Soussi, M., Stow, D.A.V., Croudace, I., Fildes, C., Ben Ismaïl Latrache, K., Boukhalfa, K.: The Onshore Tunisia Numidian Flysch: Petrography, Geochemistry and Reservoir Characteristics. *EAGE Tunisia, extended abstracts*. Tunisia (2009)
12. Stow, D.A.V., Johansson, M.: Deep-water massive sands: nature, origin and hydrocarbon implications. *Mar. Pet. Geol.* **17**, 145–174 (2000)

Part V

Tectonics and Sedimentation

Evaluation of Sediment Transport Rate of the Kizilirmak River Basin on the Tectonically Active North Anatolian Fault Zone (NAFZ), Turkey

Gulcan Sarp

Abstract

In this study, sediment transport rate of the Kizilirmak River basin located in the tectonically active North Anatolian Fault Zone (NAFZ) is evaluated in order to determine the effects of the NAFZ on the Kizilirmak basin sediment transport rate. Vegetation covers the basin area is extracted from the LANDSAT ETM data by using Normalized Difference Vegetation Index (NDVI). On the other hand, topographic attributes (elevation, slope, curvature, and water catchment) were obtained from Digital Elevation Model (DEM) to detect areas associated with sediment transport and accumulation. GIS was used to extract topographic profiles along with the Kizilirmak River and attributes as well as for the implementation of the stream power index (SPI), topographic wetness index (TWI), sediment transport index (STI) and channel width. The relation with the derived indices and NAFZ is determined by integrating hot and cold spot clusters of indices values mapped with Getis-Ord G_i^* statistics. According to the derived results which highlighted hot and cold spots of the index values helped to identify the relation between sediment transport rate of the basin area and NAFZ.

Keywords

Sediment transport rate • Kizilirmak River
NAFZ • Getis-Ord G_i^* statistics

1 Introduction

Morphometric indices commonly used to determine the degree of Quaternary tectonic activity have been associated with the erosional and the depositional processes related

G. Sarp (✉)
Department of Geography, Süleyman Demirel University,
32260 Isparta, Turkey
e-mail: gulcansarp@sdu.edu.tr; gulcansarp@gmail.com

with fluvial systems. These indices give information about the geomorphological elements of the land according to the level of the tectonic activity. Morphometric indices based on river parameters can give relevant evidence on the Quaternary tectonic activity of the structures of Keller and Pinter [1] as an example. The morphometric analysis is performed effectively through the measurement of the linear, aerial, relief, the gradient of channel network and contributing ground slope of the basin [2, 3]. A broadly accepted principle of morphometry is that of the drainage basin morphology which reflects the level of the tectonic activity over time as specified by previous studies [4, 5, 6].

2 The Studied Area

The Kizilirmak, also known as the Halys River, is the longest river which originates and ends in Turkey. The Kizilirmak flows for a total of about 1,150 km. The Kizilirmak basin is located in the eastern part of Central Anatolia (Fig. 1).

3 Methods of the Study

The primary objective of this study is to determine the effects of the NAFZ on the Kizilirmak basin sediment transport rate. The applied methodology consists of four different stages as summarized in the Fig. 2. In the first stage drainage network, slope, TWI, sediment transport rate of the basin area and channel width of the Kizilirmak River are extracted from the ASTER DEM data. In the second stage, the vegetation cover of the basin area is extracted from Landsat ETM data by using the soil-adjusted vegetation index. In the final stage, the relation among the DEM derived derivatives, lithological units, fault lines and sediment transport rate are evaluated by using the Getis-Ord statistics.

Fig. 1 Location map of the Kizilirmak Basin area

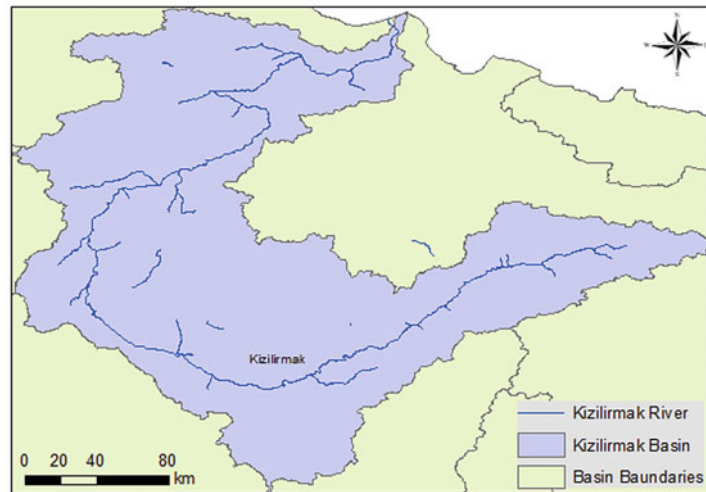
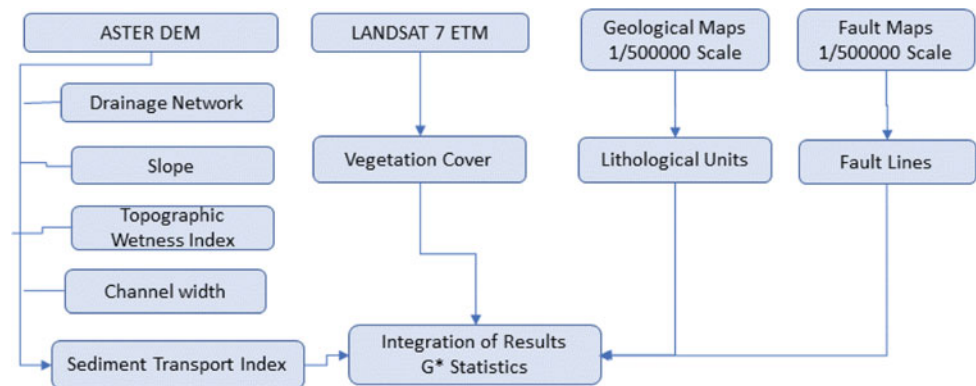


Fig. 2 Method of the study



4 Results and Discussion

The slope map of the basin area is generated from the ASTER DEM data. According to derived results, slope values range from 0° to 80° .

The Topographic Wetness Index (TWI) is usually used to compute the topographic control on the hydrological processes [7]. This index involves the upslope contributing area (a) a slope raster and a couple of geometric functions. TWI values represent drainage depressions. Low TWI values

represent crests and ridges. On the other hand, the high values represent valley bottoms. Sediment transport index (STI) is derived from a unit stream-power theory; whereas, in the current study, it is used to determine the flow power of each unit area.

According to the derived results, TWI values range from 1 to 15. High TWI index values are mainly concentrated along the areas where the sediment transport rate is high. On the other hand, drainage density is high in the northern and central part of the basin area where the rate of the erosion is also high. Vegetation cover is low where the rate of the

erosion is low. The channel width of the Kizilirmak river is extracted from DEM data and changes in the width values on erosion are very significant and mostly dependent on discharge, slope, lithological properties and tectonic activity of fault lines.

The evaluation of the lithological units and the fault lines with the sediment transport rate by using G_i^* statistics also reveal a consistency in the areas where high low sediment transport rate indicate clusters.

5 Conclusion

According to the derived results the hot and cold spots of the index values are highlighted by G_i^* statistic which helped to identify the relation between sediment transport rate of the basin area and NAFZ. In the tectonically active zones TWI, the channel width and drainage density reveal strong relation with the sediment transport rate. The clustered distribution of the index values is mainly placed near the active fault zones which reveal the high rate of the sediment transport in the basin area.

References

1. Keller, E.A., Pinter, N.: Active Tectonics. Earthquakes, Uplift and Landscape, 2nd edn. Prentice Hall, Upper Saddle River (2002). (E. E.U.U.)
2. Nag, S.K., Chakraborty, S.: Influence of rock types and structures in the development of drainage network in hard rock area. *J. Indian Soc. Remote Sens.* **31**(1), 25–35 (2003)
3. Magesh, N.S., Chandrasekar, N., Kaliraj, S., A GIS based automated extraction tool for the analysis of basin morphometry. *Bonfring Int. J. Ind. Eng. Manag. Sci.* **2**(1), 32–35 (2012)
4. Strahler, A.N.: Hypsometric (area-altitude) analysis of erosional topography. *Geol. Soc. Am. Bull.* **63**, 1117–1142 (1952)
5. Cox, R.T.: Analysis of drainage-basin symmetry as a rapid technique to identify areas of possible quaternary tilt-block tectonics: an example from the Mississippi Embayment. *Geol. Soc. Am. Bull.* **106**, 571–581 (1994)
6. Hurtrez, J.E., Sol, C., Lucazeau, F.: Effect of drainage area on hypsometry from an analysis of small-scale drainage basins in the Siwalik hills (central Nepal). *Earth Surf. Process. Landform* **24**, 799–808 (1999)
7. Sørensen, R., Zinko, U., Seibert, J.: On the calculation of the topographic wetness index: evaluation of different methods based on field observations. *Hydrol. Earth Syst. Sci.* **10**, 101–112 (2006)

Paleoseismological Indices Recognized in the Great Kabylia Region (Algeria)

Nadia Sidi Said, Azzeddine Benhamouche, Sahra Aourari, Djamel Machane, and Sid Ali Kechid

Abstract

The continental Quaternary and coastal deposits of Great Kabylia show typical deformation of paleoseismicity including paleoliquifaction (sismoslumps, thixotropic wedges, dish), boulders and coastal uplift. The aim of the present study is to characterize the deformations as indications of paleoseismicity and to reveal the existence of the traces of the historical earthquakes that would have affected the region of Neogene Tizi Ouzou basin. Field observations indicate that these deformations exist in several areas of Great Kabylia. In fact, the traces of paleoseismicity have been found in the Quaternary deposits of the Neogene Tizi Ouzou basin in the southern part and also on the coast in its northern part. Among the arguments that demonstrate the seismic origins are: the thixotropic nature of deformations as well as presence of the notches at different levels of the coast. They are good indications of coastal uplift.

Keywords

Quaternary • Paleoliquifaction • Notches • Coastal uplift • Tizi ouzou basin

1 Introduction

The Great Kabylia belongs to the western Peri-Mediterranean Alpine domain (Fig. 1) which also includes a southern branch represented by the sections of the Rif (Morocco), Tell (Algeria and Tunisia) and the Sicilian-Calabrian Arc (Italy).

N. S. Said (✉) · A. Benhamouche · S. Aourari · D. Machane
CGS, National Centre of Research Applied for Earthquake
Engineering, 01 Kaddour Rahim Street, Hussein Dey, BO 255
Algiers, Algeria
e-mail: nadsidisaid@yahoo.fr

S. A. Kechid
FSTGAT, USTHB University Sciences and Technology of Houari
Boumediene, Algiers, Algeria

It extends further towards the North West in the Betic Cordilleras in Spain. In large Kabylia, the neogenic post-nappe sedimentary series [4], the associated magmatic formations, the underlying water table structure, the ante-nappe Miocene and the MKO have been subjected to multiple deformations ranging from the Middle Miocene to current. The Tellian Atlas that extends from the Algerian margin to the South Atlas flexure is the seat of a high density of population, installed around basins such as those of Mitidja, Mleta, El-Habra, Cheliff, Guelma, Tizi Ouzou, Soummam, Hodna, etc. The weak to moderate seismic activity that characterizes the region of Great Kabylia is punctuated by violent and destructive earthquakes, Boumerdès of May 21, 2003 ($M = 6.8$). Despite this occasionally destructive seismic activity, the region of Greater Kabylia remains little known at the seismotectonic and geodynamic levels. Moreover, until the eve of the Boumerdès earthquake, most of this seismicity was linked to some tectonic structures whose seismogenic potential is still not proven, notably the Thénia fault [4] and the fault Zemmouri [5, 6].

2 Paleoseismological Indices

The field investigations were undertaken in the Plio-Quaternary deposits in order to highlight the traces of the historical earthquakes recorded in the sediments on the basis of the indirect indices such as traces of the uplifts of the marine terraces.

The traces of the ancient earthquakes have been found in a number of sites in Tizi Ouzou region (Fig. 2). These traces of paleoseismicity mark the induced effects by earthquakes with magnitudes more than 5.5 [1].

2.1 Seismites

In Timnouarth site in Tizi Rached locality, Southern Tizi Ouzou, paleoliquifaction indicators have been observed in

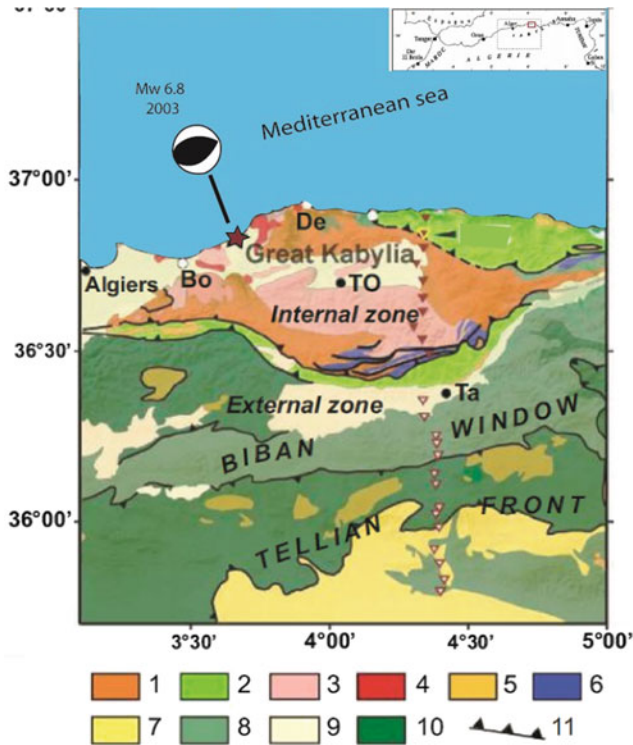
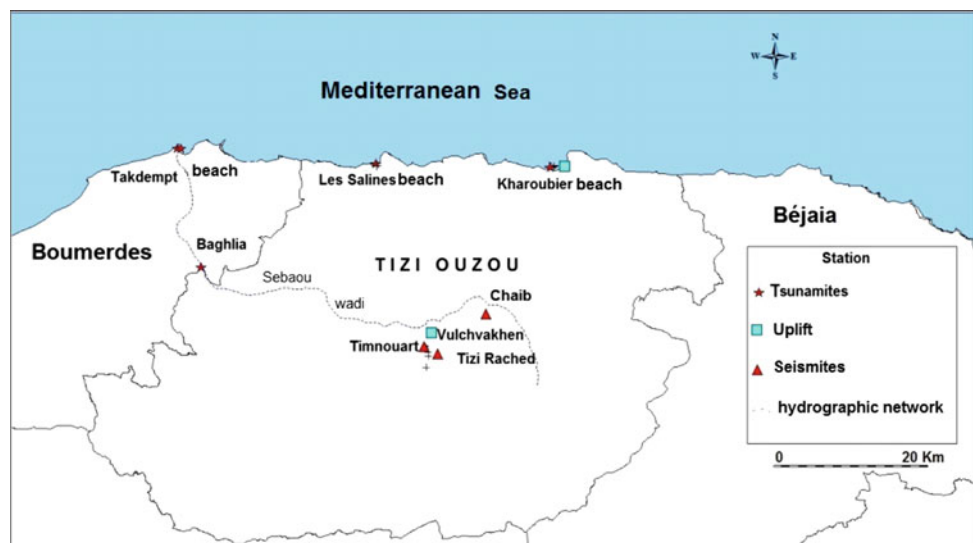


Fig. 1 Simplified geological map (modified from [8]). 1: Kabylia Oligo-Miocene, 2: Flysch nappe, 3: Basement (Paleozoic included), 4: Calcalkaline magmatism, 5: Numidian nappes, 6: Trias and Jurassic limestones, 7: Tellian forchain (Miocene), 8: Autochthonous formations, 9: Post-Miocene formations, 10: Tellian nappes, 11: Major anomal contact. TO: Tizi Ouzou, BO: Boumerdes

the ancient Quaternary (Villafranchian) deposits, near the limit between Neogene Tizi Ouzou basin and Cristal-liphllian basment. The Villafranchian [3] outcrop which

Fig. 2 Map of distribution of sites with indices of paleoseismicity



reveals the paleoliquifactions figures is composed of more granular sandy levels with sandstone intercalations. In detail, the indicators observed can be grouped into three types according to the following nomenclature: thixotropic bowls, dish structures and sismoslumps (Fig. 3).

2.2 Discussion

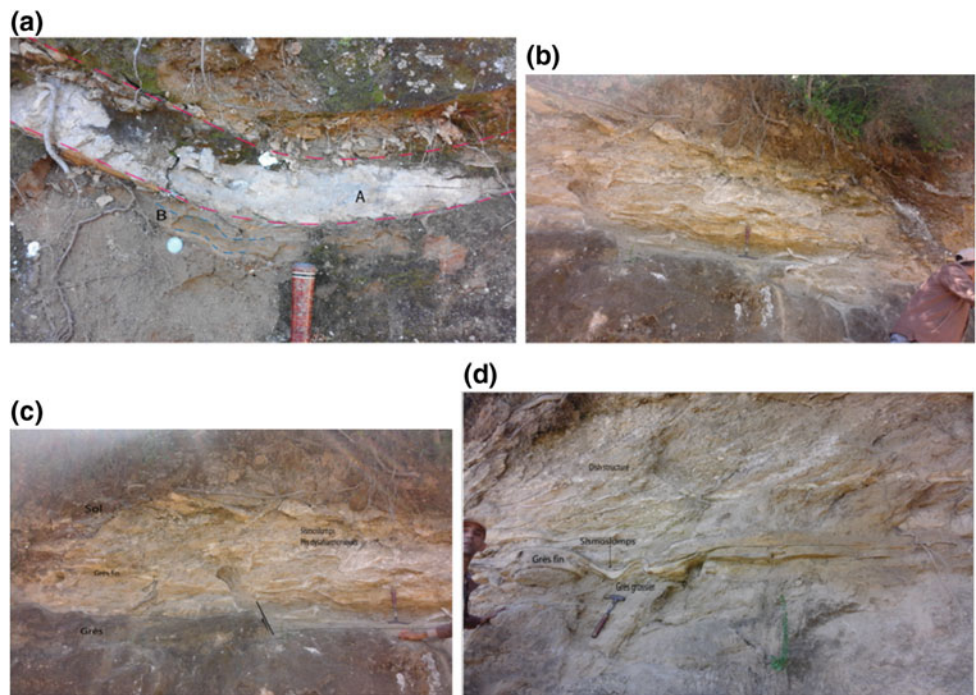
For the liquefaction of the non-cohesive sediments, many sedimentologists favor other causes such as the shock of the waves [2], the action of a high turbulence flood with strong tractive current or during the collapse of a granular material along with a slope [7].

- In the Timnouarth region, they are found in a floodplain environment (fine deposits capped with carbanate crusts). It is a quiet environment with no slope.
- In the center of the basin, these deformations are outcropping at the southern shore of Wadi Sebaou in a region where the slope is relatively low as evidenced by the meandering shape of the Wadi.

2.3 Coastal Uplift

The Algerian coast is the seat of a compressive tectonic regime resulting from the rapprochement of the African and Eurasian plates. This dynamic is responsible for the seismicity of the entire northern margin. In Boumerdes May 2003 a strong earthquake affected the coastal region between Great Kabylia and Algiers the effects of which are manifold.

Fig. 3 Thixotropic trough seismites, **b** Sismoslumps, **c** seismites of sismoslumps type and subsidence fault, **d** Seismites of type dish structure and sismoslumps, in quaternary deposits of Timnouarth site (Tizi Rached)



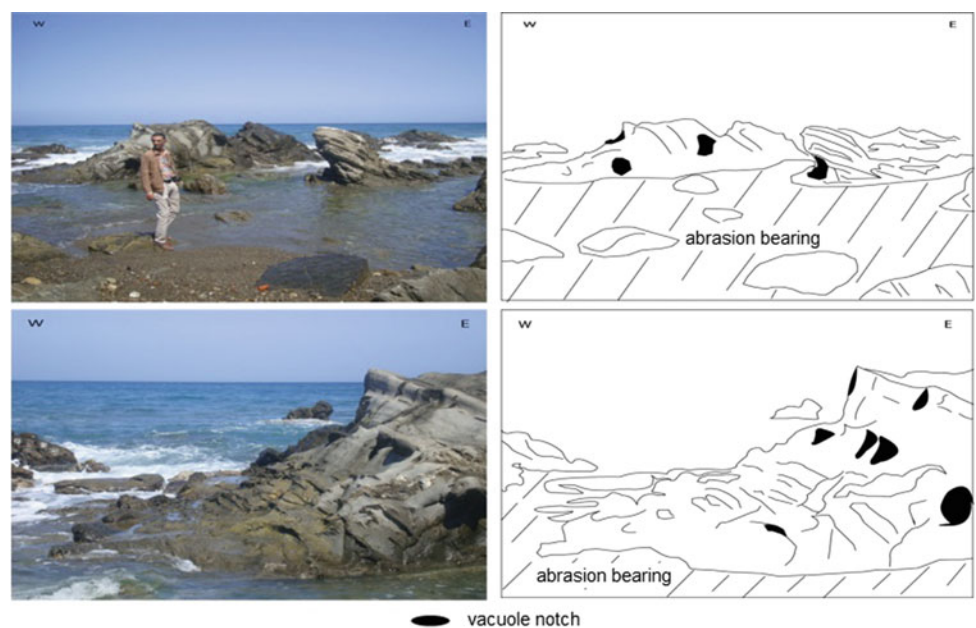
The morphology is dramatically modified with a decline of the coastline over ten kilometers due to a coastal uplift approaching 0.8 m [5].

In the region of Azeffoun, the coastal uplift is manifested by the change of the line of the coast and especially by the presence of notches in the rocky part of the Caroubier beach. In this case, Fig. 4 is very instructive because it shows a block that bears the traces of three successive uprisings in the form of very sharp notches.

Inside Tizi Ouzou basin, Benhassaine [3] signaled an uplift of fluvial terraces, in the Oued Sebaou Valley, particularly at Taqerravth-n Vouchvatsen.

On the littoral side, the author has also reported the presence of four stepped flats rich in estuarine deposits that she assimilates to marine terraces. These are terraces of 140 m, 50 m, 12 m and 5 m, on the left bank of the Oued Sebaou near Tadmaït and in the Takdempt beach in Baghliia locality.

Fig. 4 Coastal uplift during the Quaternary period in the Azeffoun region highlighted by a series of three notches and abrasion bearing



3 Conclusion

The paleoseismicity within the Neogene basin of Tizi Ouzou is manifested by uplift of fluvial terraces of the Sebaou Wadi valley and the paleoliquefaction indicators on its left bank of the Sebaou Wadi. It is difficult to attribute this paleoseismicity to the supposed active faults located at sea to the North or to the South Kabyle fault located in the south because of the large distance separating these faults from the different sites marked by the traces of the historical earthquakes or at least because of the short period of the historical seismicity covered by the catalogs of seismicity.

The deformations in soft sediments are depicted as those in the Tizi Ouzou basin and as seismites outcrop in river deposits.

In both cases, the sedimentological causes mentioned above cannot be applied to the structures observed because of their depositional environment (relatively quiet medium with no steep slope). A seismic shock is the most plausible cause for the formation of these structures and their qualification of seismites is rightly so.

References

1. Ambraseys, N.N.: Descriptive catalogues of historical earthquakes in the Eastern Mediterranean and the Middle East; Revisited. In *Historical Seismology*, pp. 25–39 (2008)
2. Benhamouche, A., Nedjari, A., Bouhadad, Y., Machane, D., Oubaiche, E., Sidi Said, N.: Field evidence of seismites in Quaternary deposits of the Jijel (Eastern Algeria) coastal region. *J. Seismol.* (2015). <https://doi.org/10.1007/s10950-013-9384-1>
3. Benhassaïne, M.: Recherche sur les modes du relief et les formations superficielles dans la vallée de l'oued Sebaou (Grande Kabylie, Algérie), Thèse de doctorat, université de Paris I, France (1980)
4. Boudiaf, A.: Etude sismotectonique de la région d'Alger et de la Kabylie (Algérie) Utilisation des modèles numériques de terrain (MNT) et de télédétection pour la reconnaissance des structures tectoniques actives : contribution à l'évaluation de l'aléa sismique. Thèse de doctorat, Université de Montpellier II, France (1996)
5. Maouche, S., Meghraoui, M., Morhange, C., Belabbes, S., Bouhadad, Y., Haddoum, H.: Active coastal thrusting and folding, and uplift rate of the Sahel Anticline and Zemmouri earthquake area (Tell Atlas, Algeria) *Tectonophysics* **509**, 69–80 (2011)
6. Meghraoui, M.: Coastal uplift and thrust faulting associated with the Mw = 6.8 Zemmouri (Algeria) earthquake of 21 May, 2003. *Geophys. Res. Lett.* **31**(19) (2004)
7. Plaziat, J.C., Ahmamou, M.: Les différents mécanismes à l'origine de la diversité des séismes, leur identification dans le Pliocène du Saïss de Fès et de Meknès (Maroc) et leur signification tectonique. *Geodinamica Acta* (Paris) **11**, 183–203 (1998)
8. Wildi, W.: La chaîne tello-rifaine (Algérie, Maroc, Tunisie): Structure, stratigraphie et évolution du Trias au Miocène. *Rev. Géol. Dyn. Géog. Phys.* **24**, 201–297(1983)

New Insights of the Early Cretaceous Syn-Rift Sedimentation in the Mecella Structure (Northeastern Atlas of Tunisia): Geodynamic Evolution

Nejla Sekatni Aïch and Mohamed Gharbi

Abstract

Detailed stratigraphy and facies analysis of the Early Cretaceous successions outcropping in the Mecella structure (Northeastern Tunisian Atlas), integrated with a structural analysis, allowed us to characterize the evolution of an intraplateau basin. A syn-rift tectonic is associated with the development of the major synsedimentary normal fault systems producing the tilted blocks basin geometry in Northeastern Tunisian Atlas. Incised sandy turbidite canyon, soft-sediment deformational structures mainly represented by slumps, down-slope sliding of ancient deposits and halokinetic activity are the main features of a syn-rift intraplateau basin. The close up of this intraplateau basin history occurred in the Hauterivian and Barremian stages by the installation of a condensed shallow water carbonate platform on the higher structures. The biostratigraphic results and the facies analysis of the resedimented Triassic series allow us to ascribe the halokinetic activity to the Upper Valanginian.

Keywords

Early cretaceous • Intraplateau basin • Syn-rift tectonic
Halokinetic activity • Mecella structure

1 Introduction

Different models of extensional basin formations have been related to rifted margins. These rifted basins were derived from the strike-slip movement like the pull-apart basins or the normal faults bounding horsts and grabens structures in the tilted blocks models. The Tethyan realm offers numerous examples of the intraplateau basins during the Mesozoic [2]; Casero et Roure [1, 4]. These basins display a strict relationship between sedimentary facies and syn-sedimentary faults. During the Early Cretaceous, the Mecella structure (Northeastern Tunisian Atlas) was submitted to a rifting phase attested by a depth modification in the sedimentation and the environments associated with the syn-sedimentary and the halokinetic activities, resedimentations, soft-sediment deformation structures and incised sandstone turbidite canyon.

Based on detailed stratigraphic, sedimentological and syn-sedimentary tectonic analysis, the aim of the present study is to illustrate the main features of the Early Cretaceous pelagic series of the syn-rift phase in the Mecella structure basin.

2 Geological Setting

The Mecella structure basin is located in the northeastern part of the Tunisian Atlas foreland which constitutes the northeastern segment of the southwest–northeast-trending Atlas fold-and-thrust belt. This range is itself a result of the collision of the African and the European plates during the Cenozoic tectonic inversion. It constitutes a part of the alpine chain of the Africa named “the Maghrebides belt”. Our study area is located approximately east of the Jebel Djouf syncline (itself located east of the Jebel Oust structure), southwest of the Ressay structure, northeast of the Zaghouan, and northwest of the Jebel sidi Zid syncline structure. The Jebel Mecella corresponds to a segment of the

N. Sekatni Aïch (✉)

Faculté des Lettres et des Sciences Humaines de Sousse,
Department of Geography, Université de Sousse, Sousse Ryadh,
Sousse, 4029, Tunisia
e-mail: sgatinejla@yahoo.fr

M. Gharbi

Geo-resources Laboratory, Centre de Recherches et des
Technologies des Eaux de Borj Cedria, B.P 273 Soliman, 8020,
Tunisia
e-mail: mohamed.gharbi@certe.mrt.tn

famous Zaghouan Thrust Belt considered the front of the Atlasic Alpine Range.

The field geology, facies and basin analysis and stratigraphic correlations are the main methodologies used to recognize the stratigraphic successions and to characterize their sedimentological and environmental setting. Numerous thin sections have been analyzed by using the petrographic microscope and applying the Dunham classification of the microfacies. The dating and the correlations of the lithological units were based on ammonites and foraminifera biozonations.

3 Results

3.1 Stratigraphy and Facies Analysis

Two sections were logged bed by bed and sampled for the sedimentological and the biostratigraphic analysis in the study area. They display from base to top:

- Lower Valanginian: represented by dominantly greenish clay where few grey thin-bedded pelagic mudstone-wackestone are interlayered. The overall thickness is more than 130 m. The fossil content consists of abundant ammonites (rich in *Olcostephanus (Olcostephanus) atherstoni*. Sharpe pinpoints the Karakaschiceras inostranzewi Zone of latest Early Valanginian age), gastropods, aptychus and belemnite fragments, planktic foraminifera, radiolarian and sponge spiculae.

This succession suggests a deep open marine environment.

- Upper Valanginian: The transition to the Upper Valanginian age is marked by the uplift of a discontinuous reef-type Tithonian deposits. It shows a morphology in the topography. The Upper Valanginian serie displays greenish poorly-fauna detrital clay units with few intercalations of thin grey bedded wackestone limestone. This unit is characterized at the base by a 12 m thick calciturbidite succession filling a submarine canyon. The ichnofacies analysed in this fine-grained sandstone and siltstone suggests a terrace to inner levee depositional environment of the distal canyon [3]. A salt deposit is interlayered within the Upper Valanginian unit. It consists of a 4 m thick Triassic succession formed by the mass of red, green and grey gypsiferous clays, sandstone and carbonate with erosive conglomeratic base which reworks the Valanginian clay. Following this Triassic resedimented unit, abundant slumping structures and gravity slide of the Upper Tithonian resedimentation took

place. The top of the Upper Valanginian series was marked by a 1.5 m thick yellow-darkish detrital limestone rich in ammonite molds indicating the Valanginian, phosphate, glauconite and quartz grains. These beds are correlated in the two logged sections and are interpreted as maximum flooding deposits following a transgressive phase at the end of the Upper Valanginian period.

The petrographic analysis shows abundant dissolution features and epikarsts affecting the Upper Tithonian beds resedimented in the Upper Valanginian series. The epikarsts are filled by Upper Valanginian pelagites during the transgressive phase.

- Hauterivian: it occurs with the variable thickness in the two logged sections (from 3.5 to 21 m). It is dominated by shales bearing planktonic foraminifera. It consists of the argillaceous deposits with the intercalation of the few slumped limestone beds. The top of the succession is marked by a 50 cm thick condensed glauconitic, phosphating and ammonites bearing sandy limestone bed which marks the maximum flooding surface. The presence of *Hedbergella hauterivica* confirms a Hauterivian age.
- Barremian: in the two sections, the Barremian deposits display low thickness in comparison with other areas. They consist of wackestone-limestone with thin argillaceous intercalation rich in foraminifera (*Epistomina*, *Lenticulina* and especially *Marginolapsis djaffaensis* dating the Barremian). Sandy limestone beds mark the top of this section and the argillaceous intercalation are rich in ferruginous oolites indicating the installation of a shallow carbonate platform.

3.2 Syndimentary Tectonics

The dynamic sedimentary of the Early Cretaceous series in the Mecella structure shows an intraplatform basin characterized by an irregular sea floor. The geometry and the facies variations of this basin are related to the regional extensional tectonics during the synrift period. Syndimentary features recorded in the study area (slumps, sealed normal faults, thickness variation, resedimented blocs...) are governed by an extensional tectonic regime associated with slumps structures which allow us to consider the Mecella structure basin as part of the Southern Tethyan rifted continental margin [5].

The unfolded slump axis (MAM Method) and the unfold poles of axial planes (APM method) give the same paleoslope direction with WSW-trending paleoslope during Upper Valanginian time. The back-tilted fault diagrams

show a ~WNW to ~NE- extension during the Early Cretaceous time which indicates that NW-, N- and NE-trending faults remain active during the Valanginian. This fault system is interpreted as an inherited normal fault during the development of the Valanginian intraplateau basin related with the southwest submarine slope. The Hauterivian-Barremian series shows numerous small scale syn-sedimentary normal faults preserved within argillaceous sediments. During the Hauterivian-Barremian, the Mecella basin is affected by normal faulting locally characterized by a ~NE-trending minimum stress axis (σ_3).

4 Interpretations and Conclusion

Based on several stratigraphic, sedimentological and tectonic features, the Mecella structure is interpreted as an intraplateau basin experiencing an Early Cretaceous synrift stage. The facies analysis highlighted the evolution of different depositional environment during the Early Cretaceous controlled by synsedimentary normal fault tectonics.

The Lower Valanginian, well dated by ammonites during this study, was characterized by pelagic clay deposits corresponding to an open deep marine basin. From the Lower to the Upper Valanginian, the sedimentary basin of the Mecella is governed by an extensional tectonic regime associated with synsedimentary normal faulting. The tectonic activity was accompanied by an important halokinetic activity which is responsible for the uplift of the Tithonian reef and the disturbance of the topography of the sea floor. An instable sea bottom occurs during the Upper Valanginian. It was active up to the Barremian. The tectonic instability during the Upper Valanginian gives way to poorly fossiliferous deposits with often mineralized foraminifera incised

sandstone turbidite submarine canyon. The soft-sediment deformational structures are mainly represented by slumps associated with the down-slope sliding of reef-type Tithonian deposits. Sandy limestone beds overlie all these deposits. This synsedimentary tectonics was characterized by thicker pelagic succession in the depressions (during the Upper Valanginian) and condensed deposits in the structural height (Hauterivian and Barremian). The install of a condensed shallow carbonate platform ends up the intraplateau basin evolution. Such a geodynamic evolution went from deep water basin to a condensed shallow platform and passed by slope area characterizing the syn-rift systems. It generated many intraplateau basins separated by small horst areas. The biostratigraphic framework of this study allows us to date the halokinetic rise as Upper Valanginian.

References

1. Basilone, L., Gasparo Morticelli, M., Lena, G.: Mesozoic tectonics and volcanism from Tethyan rifted continental margins in western Sicily. *Sediment. Geol.* **226**, 547 (2010)
2. Bosellini, A.: Progradation geometries of carbonate platforms: examples from the Triassic of the Dolomites, Northern Italy. *Sedimentology* **31**, 1–22 (1984)
3. Callow, R.H.T, McIlroy, D., Kneller, B., Dycstra, M.: Integrated ichnological and sedimentological analysis of a Late Cretaceous submarine channel-levee system: the rosario formation, Baja California, Mexico. *Mar. Pet. Geol.* **41**, 277–294 (2013)
4. Casero, P., Roure, F.: Neogene deformations at the Sicilian-North African plate boundary. In: Roure, F. (ed.) *Peri-Tethyan Platforms*, pp. 27–50. Editions Technip, Paris (1994)
5. Naji, C., Gharbi, M., Amri, Z., Masrouhi, A., Bellier, O.: Temporal and spatial changes of the submarine Cretaceous paleoslope in Northern Tunisia, inferred from Slump folds analysis. In: *Proceedings of the Geologists' Association*, vol. 129, pp. 40–56 (2018)

The Main Late Cretaceous Tectonic Episodes Controlling the Deposition of Rudist-Rich Platform Carbonates in Central Tunisia

Jalel Jaballah and Mohamed Hédi Negra

Abstract

In the Sidi Bouzid area (Central Tunisia), the Late Cretaceous sedimentation was controlled by tectonic movements that occur during two main episodes. A first active episode occurs during the Cenomanian-Early to Middle Turonian interval, the second tectonic instabilities start at the Campanian. Between these two active periods, a quieter episode marks the Late Turonian-Early Campanian interval. During the latter, a relatively homogeneous sedimentation mainly represented by marlstones and argillaceous limestones tend to seal the irregular paleotopography inherited since the previous period of extensional tectonic movements. This relatively quiet period appears marked, in contrast, by a sea level rise mainly related to a generalized transition. Similar events were also described abroad in other localities of the Tethyan margin (Philip in *Palaeogeogr Palaeoclimatol Palaeoecol* 196:19–37, 2003 [8]).

Keywords

Central tunisia • Late Cretaceous • Tectonic control
Rudist-rich carbonates

1 Introduction

In Central Tunisia, rudist-bearing carbonates are deposited at some intervals of the Late Cretaceous especially at the Late Cenomanian, the Middle Turonian, the Coniacian and the Campanian. During these periods, extended platforms are

covering the whole of Central Tunisia (Fig. 1). The deposited platform shallow marine carbonates are separated by pelagic marls suggesting a clear deepening of the environment deposition. The main purpose of our paper is to emphasize the role of tectonic movements and sea-level changes in the development/drowning of these platforms. On the basis of recorded tectonic and sedimentary features, we will try to reconstitute the chronology of significant tectonic events and sea level changes [2, 3].

2 Materials and Methods

This study was conducted based on field works including sections logging and sequence analysis. A detailed mapping has focused on the Late Cretaceous series in Jebel el Kébar. Petrographic study has been conducted to define microfacies and depositional environments. Detailed observations have concerned the main faults with a special focus on the typical features indicating syndepositional tectonic activities.

3 Results

Rudist-rich carbonates preferentially occupy the platform margins [8] and some elevated areas such as horsts. In fact, extensional tectonic movements are mainly recorded by tilted blocks [7] and syndepositional features oriented parallel with NW–SE; E–W; NNE–SSW trending normal faults (Fig. 2).

- During a first tectonic episode which occurs during the Late Cenomanian-Early to Middle Turonian interval, the sea floor was compartmented into a series of tilted blocks [5, 7]. In Jebel el Kébar, several types of blocks were identified [4]. According to their depositional environment, three types of blocks corresponding to shallow marine, deep marine and subsiding blocks were determined. These

J. Jaballah (✉)
King Fahd University of Petroleum & Minerals, College of
Petroleum Engineering & Geosciences, Dhahran, Saudi Arabia
e-mail: jalel.jaballah@kfupm.edu.sa

M. H. Negra
University of Tunis El Manar, Faculty of Sciences of Tunis,
UR Pétrologie Sédimentaire et Cristalline, Tunis, Tunisia

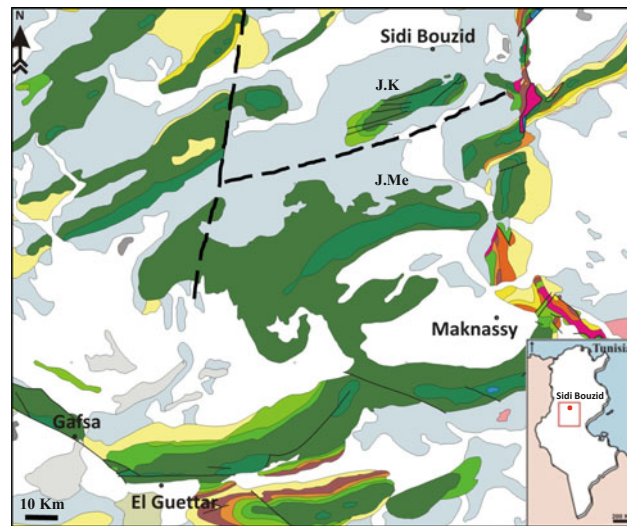


Fig. 1 Location map showing Jebel el Kébar (J.K) and Jebel Meloussi (Me), central Tunisia

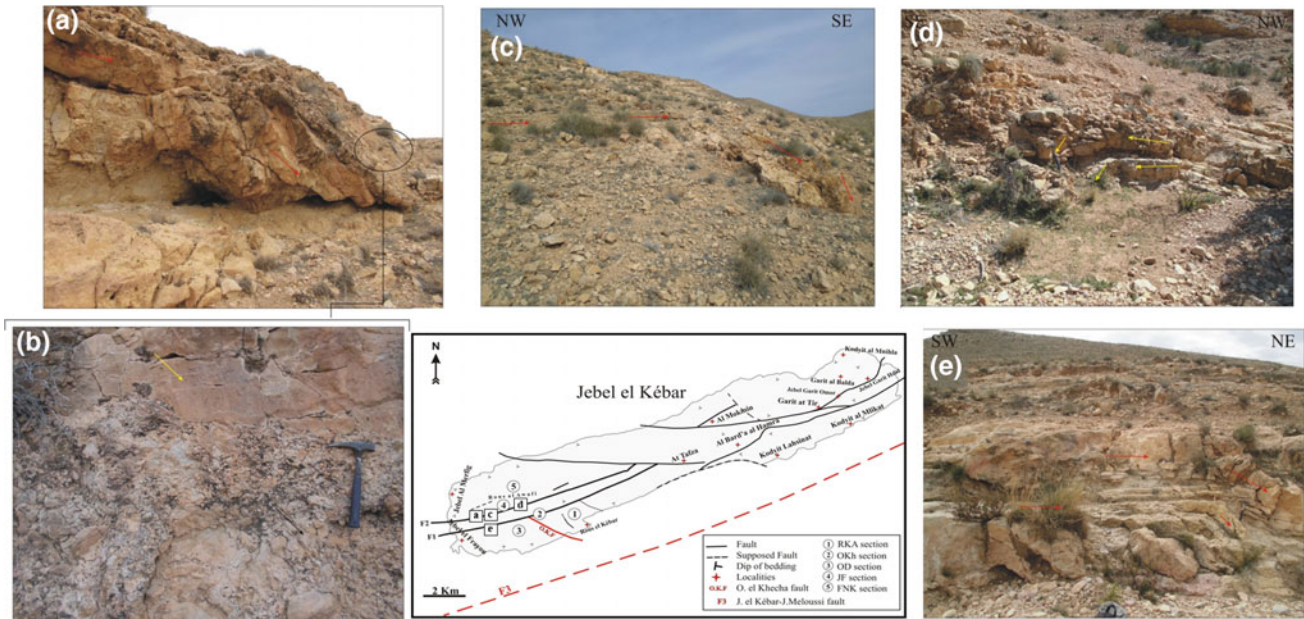


Fig. 2 Tectonic features associated to NE-SW faults in Jebel el Kébar

blocks are separated by normal faults sensibly oriented NW-SE to N-S.

- During a second active episode (Campanian), platforms are frequently disintegrated into conglomeratic carbonates essentially represented by mass-flow deposits. In Jebel el Kébar, most of the rudist-rich platform carbonates are fragmented into debris flow deposits [6] in which rudist-rich boulders and olistoliths are enveloped by a micritic pelagic matrix suggesting a clear deepening of platforms comparatively to those of previous periods.

More to the North, in deeper environments, Campanian tectonic instabilities are also common [1].

4 Conclusions

During the Late Cretaceous, the sedimentation of platform rudist-rich carbonates was certainly influenced by significant events expressed by tectonic instabilities especially

extensive tilting movements and sea-level changes that occurs in Central Tunisia. Periods marked by a sea level rise, such as during the Late Turonian-Early Campanian interval, are favorable to the deposition of deep marine transgressive deposits that tend to seal the paleotopographic irregularities (grabens, half grabens, horsts, tilted blocks, etc.) created during the Late Cenomanian-Early to Middle Turonian tectonic activities.

References

1. Bey, S., Kuss, J., Premoli Silva, I., Negra, M.H., Gardin, S.: Fault-controlled stratigraphy of the Late Cretaceous Abiod formation at Ain Medheker (Northeast Tunisia). *Cretac. Res.* **34**, 10–25 (2012)
2. Haq, B.U., Al-Qahtani, A.M.: Phanerozoic cycles of sea-level change on the Arabian platform. *GeoArabia* **2**, 127–160 (2005)
3. Hardenbol, J., Thierry, J., Farley, M.B., et al.: Mesozoic and Cenozoic sequence chronostratigraphic framework of European Basins. In: de Graciansky, P.-C., et al. (eds.) *Mesozoic and Cenozoic Sequence Stratigraphy of European Basins*. SEPM Special Publication, vol. 60, pp. 3–13 (1998) (Chart 5, “Cretaceous Chronostratigraphy”)
4. Jaballah, J., Negra, M.H.: Stratigraphical and sedimentary characters of Late Cretaceous formations outcropping in central and southern Tunisia, Tethyan southern margin. *J. Afr. Earth Sci.* **124** (2016), 289–310 (2016)
5. Kadri, A., Essid, M., Merzeraud, G.: Kasserine Island boundaries variations during the Upper Cretaceous-Eocene (Central Tunisia). *J. Afr. Earth Sci.* (2015). <https://doi.org/10.1016/j.jafrearsci.2015.07.027>
6. Negra, M.H., Skelton, P.W., Gili, E., Valdeparas, F.X., Argles, T.: Recognition of massive Upper Cretaceous carbonate bodies as olistoliths using rudist bivalves as internal bedding indicators (Campanian Merfeg Formation, Central Tunisia). *Cretac. Res.* **66**, 177–193 (2016)
7. Ouali, J., Martinez, C., Khessibi, M.: Caractères de la tectonique crétacéenne distension au Jebel Kébar (Tunisie Centrale): ses conséquences. *Géodynamique* **1**, 3–18 (1986)
8. Philip, J.: Peri-Tethyan neritic carbonate areas: distribution through time and driving factors. *Palaeogeogr. Palaeoclimatol. Palaeoecol.* **196**, 19–37 (2003)

Lower Albian Sequence Stratigraphy of the South Tethyan Margin: The Tajerouine Area, Tunisia

Abir Chihaoui, Etienne Jaillard, and Jean-Louis Latil

Abstract

Central Tunisia, part of the South-Tethyan passive margin, is marked by the transition from the southern stable Sahara platform, to the open marine Tethyan basin and to the North. Detailed biostratigraphic and sedimentological studies of the Early Albian succession in the El Kef-Tajerouine area allowed us to define five depositional sequences which are well correlated in Central Tunisia. They give evidence of the drowning of the Aptian-earliest Albian platforms and the diachronic SE-ward back-stepping of the shelf facies. Tectonic synsedimentary deformation began in the earliest Albian, increased in intensity throughout the Early Albian and culminated with the Middle Albian sedimentary hiatus.

Keywords

Central tunisia • Albian • Carbonate platform
Sequence stratigraphy

1 Introduction

During the Lower Cretaceous, the central part of Tunisia was dominated by carbonate and mixed platform deposits. The sedimentation was mainly represented by massive limestones deposits such as “*The limestones of the Serdj Formation*” [1]. Across the Aptian–Albian boundary, the sedimentation record a huge change that led to the demise of the platform. This change in the paleogeographic framework

A. Chihaoui (✉)
Department of Earth Sciences, University of Gabès, Gabès,
Tunisia
e-mail: abir.chihaoui@gmail.com

E. Jaillard · J.-L. Latil
University of Grenoble Alpes, ISTerre-IRD, CS 40700,
38058 Grenoble cedex 9, France

J.-L. Latil
G.R.E.G.B, Le Maupas, 05300 Lazer, France

from carbonate and mixed platforms to open marine environment of Central Tunisia during the Aptian–Albian was not only the result of local and regional events but also of eustasy (The Albian transgression).

The current study deals with the evolution of the northern part of Central Tunisian platform, in the Tajerouine area, during the Albian transgression. The main aims of this study are: to recognize the environmental evolution of this transition zone and to understand the relative influence of global transgression and local factors (tectonic) in the evolution of the Central Tunisian platform.

2 Materials and Methods

In the Tajerouine area, four sections were studied (Fig. 1).

The collection of ammonites allowed us to define regional biozones which provide the biostratigraphic framework of this study [2]. Detailed analysis of microfacies and biotic assemblages led to establish the environmental evolution, to identify the discontinuities, to define the sequences and to attain the correlations throughout the study area supported by biostratigraphy. Field observations allowed us to identify the synsedimentary tectonic structures such as deformed strata, slumps, erosional surfaces, olistholiths or normal faults precisely dated by ammonites from the involved or surrounding beds.

3 Results

3.1 Stratigraphy/Regional Biozonation

In the Tajerouine area, the Albian transgression is represented by the Hameïma and Fahdene Formations that are overly an Aptian carbonate shelf (Serdj Formation). The Hameïma Formation is represented by mixed, clastic-carbonate and shelf deposits with benthic fauna (orbitolinids, pectinids and oysters) that characterize a shelf

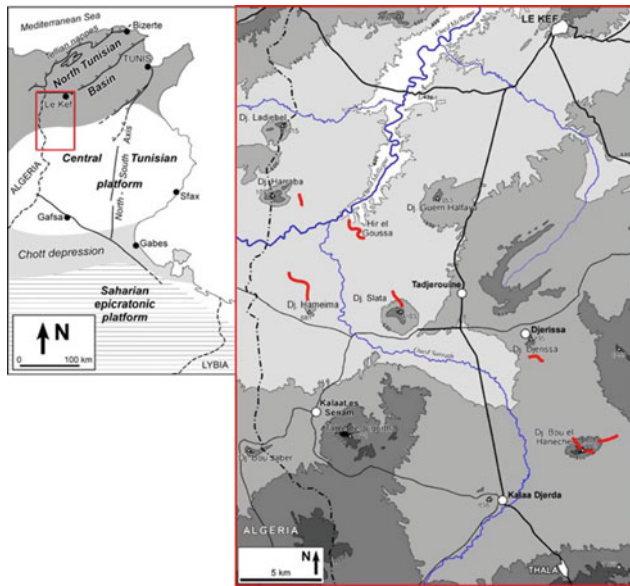


Fig. 1 Study zone and location of the main sections

environment. The Fahdene Formation is represented by marls and shales. Then, it is interpreted to have been an open marine environment [3].

Ammonite collections allowed us to define a regional biozonation establishing:

- An earliest Albian age of the Hameïma Formation
- The evidence for a sedimentary hiatus in most of the middle Albian.

3.2 Sedimentology

In the lower part of the succession, the nature of deposits and their biotic assemblages and microfacies [3] characterize shallow marine environments which progressively change to deep water marine environments and deposits during the Albian transgression. The biotic assemblages show that The Central Tunisian Platform was a gently low-energy Northward-dipping ramp sheltered from energetic marine processes although the moderate shelf currents were active especially during low sea level periods. They were marked by erosional discontinuities.

3.3 Sequence Stratigraphy

Five third-order depositional sequences were identified. The first two sequences (SA1 and SA2) correspond to shelf

deposits and are separated by karstified surfaces indicating temporal sea-level lowstand. They can be subdivided into minor depositional sequences capped by karstified surfaces which can be correlated regionally (Fig. 2). The three overlying sequences (SA3–SA5) were deposited in an open marine environment characterized by marls and fine-grained limestones deposits. Above submarine erosional surfaces marked by the presence of reworked nodules (sequence boundaries), carbonated lowstand systems tracts with benthic faunas are overlain by dark shales within which the maximum flooding surfaces are locally marked by pyritized or phosphatic ammonites. Highstand systems tract deposits are usually reduced.

Regional correlations between the lower parts of the studied successions (Fig. 2) show an inversion of the topography and bathymetry in addition to the progressive demise of the platform. The latter is illustrated by the diachronism of the base of the Fahdene Formation from the Northwest to the Southeast.

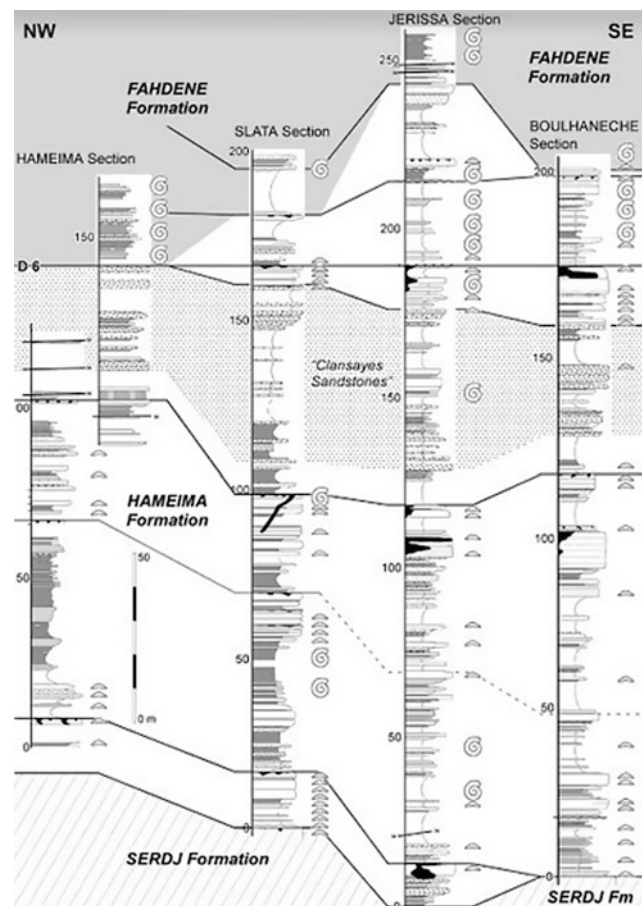


Fig. 2 Regional correlation of the studied successions in the Tajoine area

4 Discussion

The evolution of microfacies and biotic assemblages through time gives evidence of the evolution from carbonates bearing benthic fauna and exposure surfaces of shallow marine environment to ammonite-rich marl with marly limestone beds of open marine environment [3, 4]. The recognition of the third order sequences allows regional correlations and gives evidence of the regional demise of the platform due to the transgression, accordingly evidencing the importance of eustasy. However, the regional tectonics also had a major role in the evolution of the study area. The topographic and bathymetric inversions in the Hameïma Formation indicate a strong link with this tectonic event. Synsedimentary tectonic deformation affecting the studied area began during the earliest Albian, increased throughout the Early Albian and culminated during the Middle Albian hiatus in relation to halokinetic activity [3, 5, 6].

5 Conclusion

In the Tadjerouine area, five third-order depositional sequences were identified. The first two sequences (earliest Albian, *tardefurcata* zone) correspond to shelf deposits and are separated by karstified surfaces. The three overlying

sequences (Early Albian) were deposited in an open marine environment. Detailed study of biotic assemblages and microfacies and the correlations of the studied successions give evidence of the demise of the carbonate platform. This evolution did not happen at the same time throughout the studied area. It highlights the parts of both local tectonic and global eustasy factors.

References

1. Burolet, P.F.: Contribution à l'étude stratigraphique de la Tunisie Centrale. *Annales des mines et de la géologie* **18**, 345 (1956)
2. Latil, J.-L.: Lower Albian ammonites from Central Tunisia and adjacent areas of Algeria. *Revue de Paléobiologie, Genève* **30**, 321–429 (2011)
3. Chihaoui, A.: La transgression albienne dans la région de Tadjerouine en Tunisie Centrale: Stratigraphie, Sédimentologie et Tectonique synsédimentaire. Thèse de Troisième cycle, Université Joseph Fourier, pp. 290 (2009)
4. Chihaoui, A., Jaillard, E., Latil, J.L.: Stratigraphy of the Hameïma and lower Fahdene Formations in the Tadjerouine area (Northern Tunisia). *J. Afr. Earth Sci.* **58**, 387–399 (2010)
5. Jaillard, E., Dumont, T., Ouali, J.: The Albian tectonic “crisis” in Central Tunisia: Nature and chronology of the deformations. *J. Afr. Earth Sci.* **85**, 75–86 (2013)
6. Jaillard, E., et al.: Albian Salt tectonics in Central Tunisia: Evidence for an Atlantic-type passive margin. *J. Afr. Earth Sci.* **135**, 220–234 (2017)

Stratigraphic Differentiation of the Zagros Foreland Basin Sequence, Kurdistan Region, (Northern Iraq): Impacts on Oil Accumulations

Basim Al-Qayim

Abstract

Field examinations of surface and subsurface stratigraphic data from 50 localities and wells from NE Iraq are used to revise and differentiate the Arabian margin sequence and Zagros foreland basin evolution. The stratigraphic arrangement of megasequences AP₉, AP₁₀, and AP₁₁ of the Arabian plate stratigraphy is revised and chronostratigraphically correlated across the different parts of the basin. Their bounding surfaces are revised according to regional extent unconformities and associated hiatuses. Backstripping analysis is attempted to support stratigraphic differentiation.

Keywords

Zagros • Iraq • Sequence • Cretaceous Tertiary • Stratigraphy • Arabian margin

1 Introduction

The stratigraphic sequence of the Zagros foreland basin systematically records the Upper Cretaceous—Neogene active margin history of the Arabian plate Al-Qayim et al. [1]. The processes include the ophiolite-radiolarite emplacement and the associated flexure of the Arabian Plate margin, the foreland basin infilling and inversion, the Miocene collision and the Pliocene- Pleistocene suturing Jassim and Goff [2], and Homke et al. [3]. The recorded sedimentary series of the basin at the foredeep, forebulge, and the backbulge areas are subdivided by major unconformities and their correlative conformities into three major sequences. These sequences include the full record of the AP₉, AP₁₀ and AP₁₁ megasequences of the Arabian plate Sharland et al. [4].

B. Al-Qayim (✉)
Department of Geology, Sulaimani University, Kurdistan Region,
Sulaimaniah, Iraq
e-mail: basim.alqayim@univsul.edu.iq

2 Materials and Methods

The recognized megasequences were examined at fifty localities (outcrop sections and wells) from the Zagros fold and thrust belt in northern Iraq. The compiled data includes field examinations and surface stratigraphic sections, well logs, rock samples and geophysical data. Examinations and analyses include backstripping analysis of subsidence history, facies modeling and lithostratigraphic correlation.

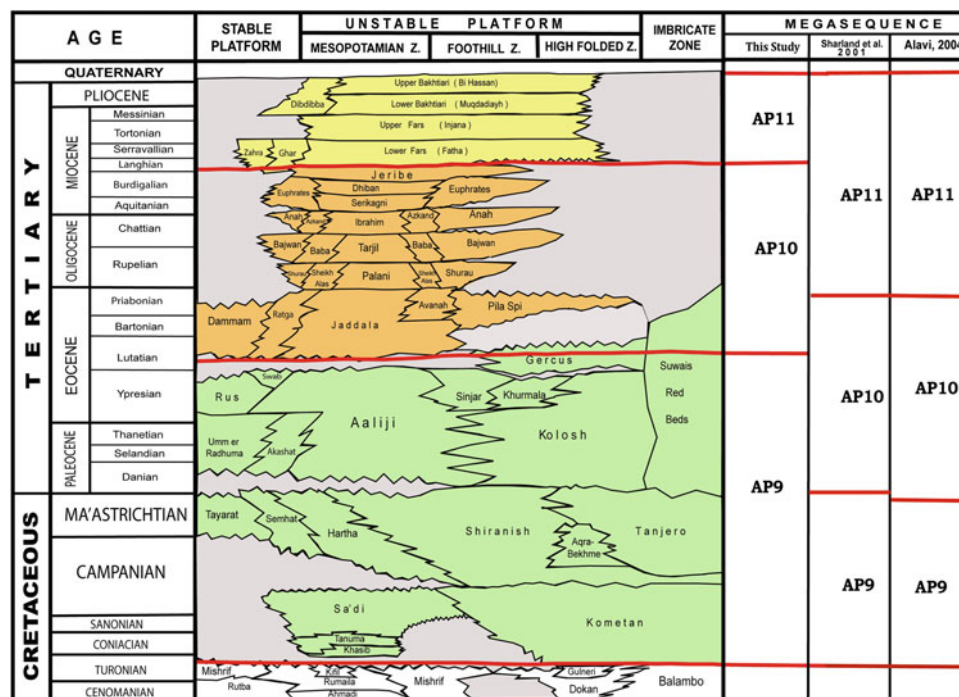
3 Results

The investigation results lead to reconsider the tectonostratigraphic setting, subdivision as well as the sequence differentiation of the series. The stratigraphic differentiation and the position of the major bounding surfaces were revised based on stratigraphic relations among correlated stratigraphic sections, extension and hiatus of the cross-basin unconformity surfaces and tectonostratigraphic stage of the basin evolution. Other considerations includes: changes in tectonic regime and basin architecture, basin subsidence history, the shifting of depocenter and the nature of basin filling. The revised sequences and the shift of bounding surfaces are shown in Fig. 1.

4 Discussion

The lower sequence (AP₉) represents the Zagros proto-foreland basin which is developed upon flexural descending plate margin in response to the obduction of the radiolarite-mélange suites. The age of the bounding unconformities are Mid -Turonian at the base and Early Bartonian at top. The latter boundary is verified by the deposition of the continental red siliciclastic molasse sediments of the Gercus Formation with thick extensive conglomerate horizon on top (at the folded zone) and part of the Suwais Red Beds (at the

Fig. 1 The chronostratigraphic chart of the Zagros foreland basin sequence with the revised boundaries of the arabian plate megasequences



imbricate zone). Additional reference came from biostratigraphic dating of the gap between the Gercus and the Pila Spi formations equivalents on the Iranian side of the basin suggest a large hiatus between the two units Homke et al. [3]. This sequence includes from bottom to top: deep marine carbonates (Kometan and Shiranish Fm.) and thick sequence of deep marine turbidites thick sequence; Tanjero and Kolosh Fm. Al-Qayim [5]. Basin inversion and shoaling is evidenced by the occurrences of the reefal and shoal carbonates punctuating the upper parts of the flysch sequences including the Aqra-Bekhme Fm. (Maastrichtian), and Sinjar and Khurmala (Upper Paleocene–Lower Eocene) (Fig. 1).

The second sequence (**AP₁₀**) is represented by a sagging interior basin developed under subdued tectonics with mild subsidence Al-Qayim [6]. This led to the development of a carbonate-dominated seaway over the Arabian margin which lasted from the Bartonian to the late Burdigalian. Sequence includes the Bartonian- Priabonian platform carbonate of the Pila Spi Formation, the Oligocene Kirkuk Group (Nine Carbonate-dominated formations), the Lower Miocene shelf carbonates of the Euphrates and the Serikagni, Dhiban and Jeribe Formations. The upper boundary is a wide-spread Late Burdigalian unconformity marked by the extensive Basal Fars Conglomerate.

Finally, a marine to continental and siliciclastic-dominated sequence (**AP₁₁**) is developed in a syn-collisional overfilled foreland basin of the so called “Mesopotamian Foredeep”. The sequence is developed from Langhian to the Quaternary times. This sequence is represented by the Fars (Fatha and

Injana formations.), and the Bakhtiari (Mukdadiyah and Bai Hassan formations) Groups.

The stratigraphic architecture, the mixed carbonate siliciclastic facies and the succeeding foreland folding of these successive sub-basins effectively contributes to the distribution of sources, reservoirs, seals and the structural traps of this hydrocarbon-rich basin.

5 Conclusions

The examination of 50 outcrops and well sections from the Zagros foreland basin of northeastern Iraq reveals important reviews which invoke the revision of the Arabian Plate sedimentary evolution. The stratigraphic arrangement of Megasequences **AP₉**, **AP₁₀** and **AP₁₁** is revised and their bounding surfaces are revised according to the regional extent unconformities and the associated hiatuses.

References

- Al-Qayim, B., Omer, A., Koyi, H.: Tectonostratigraphic overview of the Zagros Suture Zone, Kurdistan Region, Northeast Iraq. In: *GeoArabia*, vol. 17, pp. 109–156 (2012)
- Jassim, S.Z., Goff, T.: Phanerozoic development of the Northern Arabian plate. In: Jassim, S.Z., Goff, J.C. (eds.) *Geology of Iraq*. Dolin, Prague and Moravian Museum, Brno, 341 p. (2006)
- Homke, S., Vergés, J., Serra-Kiel, J., Bernola, G., Sharp, I., Garcés, M., Montero-Verdu, I., Karpuz, R., Goodarzi, M.H.: Late

- Cretaceous-Paleocene formation of the proto-Zagros foreland basin, Lurestan province, SW Iran. *Geol. Soc. Am. Bull.* **121**, 963–978 (2009)
4. Sharland, P.R., Archer, R., Casey, D.M., Davies, R.B., Hall, S.H., Heward, A.P., Horbury, A.D., Simmons, M.D.: Arabian plate sequence stratigraphy, *GeoArabia Special Publication 2*, Gulf PetroLink, Bahrain, 371 p., with 3 charts (2001)
 5. Al-Qayim, B.: Evolution of flysch basin along the Northeastern margin of the Arabian plate. In: Abed and Others (Eds.) *Geology of Jordan and Adjacent Areas*. (Geocom III), Amman, pp. 347–372 (1994)
 6. Al-Qayim, B.: Sag-Interior Oligocene Basin of North-central Iraq: Sequence Stratigraphy and Basin Overview. *GEO 2006 Middle East Conference and Exhibition, Bahrain, Abstract book* (2006)

Paleogene Calciclastic Deposits in Southern Tunisia

Moez Ben Fadhel, Mohsen Henchiri, Njoud Gallala, Rim Zammali, Ahlem Amri, Asma Chermiti, and Mohamed Ben Youssef

Abstract

The Paleogene outcrops of the abandoned open pit mine near El Mdhilla, Gafsa display calciclastic deposits encased in phosphorite-rich marls and limestone alternations of Chouabine Formation. Lithostratigraphic investigation of the quarry sections allows recognizing chaotic lenticular bodies that spread uniformly within Ypresian layers. The individual lens is concave up in cross section. The lens width range from 9 to 12 m; whereas, the height ranges between 1 and 3 m. These lenticular bodies are composed of skeletal-rich (*Ostrea*, bivalve shells, e.g. pecten) and coarse-grained sediments with low amount of mud (calcirudite). Thin sections analysis shows mixed depositional environments indicated by high-energy grainstone (mostly bivalve shell fragments) and intertidal sediment textures. The sediments originated from isolated carbonate platform via submarine gravity flow processes and redeposited in the phosphorite-rich basin. The predominance of coarse-grained sediment textures indicates that the carbonate platform, probably made up of organogenic limestone, allows steep slope paleotopography. Textural analysis of calciclastic deposits shows that

the sediment main source is related to the Late Paleocene carbonate/lagoonal platform of Thelja Formation. The formation of these calciclastic deposits involves submarine erosion process that stripped lithified sediments from submarine uplifted the carbonate platform edge and slope controlled by the conjunction of tectonic activity (e.g. normal faults) and possibly low sea level. Rockfalls along faulted escarpments (platform margin) are not excluded to produce calciclastic deposits since that grain shape roundness indicates little transport of sediments.

Keywords

Southern Tunisia • Paleogene • Calciclastic submarine deposits • Carbonate platform slope • Gravity mass flow

1 Introduction

The ancient calciclastic submarine deposits have been studied over different intervals of the geological time and several deposition models have been established [1–4]. These slope-derived deposits have received particular attention as potential hydrocarbon reservoirs [5, 6].

Recent investigations of paleogene outcrops exposed near the Mdhilla open pit mines including lithostratigraphy and thin sections analysis have provided new data dealing with submarine mass movement occurring during the early Eocene.

2 Geological Setting

The study area is located in the Gafsa phosphatic basin, South-West of the M'Dhilla town near the El Khasfa anticline. The Paleocene to early Eocene lithostratigraphic column are composed of from base to top by: (1) The Thelja Formation: bioclastic carbonate bed with interbedded oyster, marly and gypsum-rich bed dated as [7] and references

M. B. Fadhel (✉)

Research Laboratory of Environmental Science and Technologies,
Higher Institute of Sciences and Technology of Environment,
University of Carthage, Borj Cedria, 2050, Tunisia
e-mail: moez.benfadhel@gmail.com

M. Henchiri · R. Zammali

Faculty of Sciences of Gafsa, Gafsa University, Sidi Ahmed
Zarroug, Gafsa, 2112, Tunisia

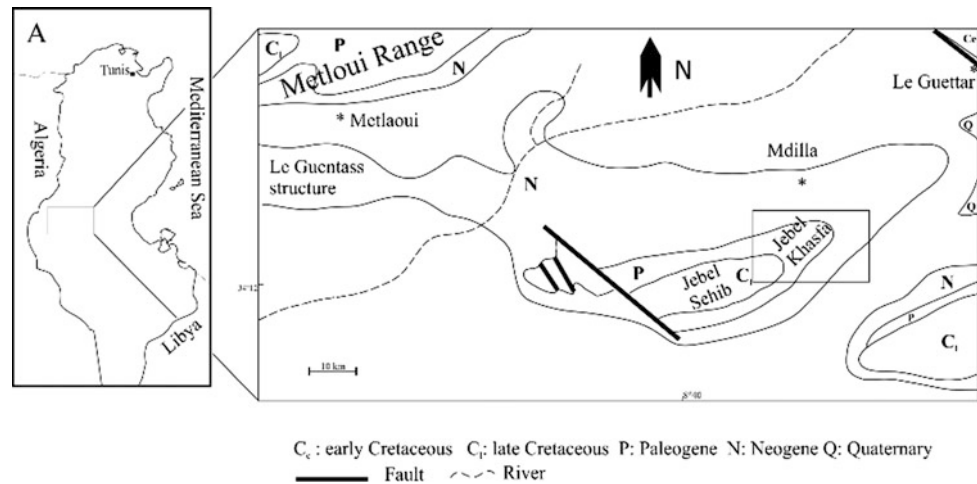
N. Gallala

Civilization Department, High Institute of Theology Tunis,
University of Ez Zitouna, Tunis, 1008, Tunisia

A. Amri · A. Chermiti · M. B. Youssef

Water Researches and Technologies Center Borj-Cedria
Technopark, Tourist Route of Solman Nabeul, PO-box No 273
Soliman, 8020, Tunisia

Fig. 1 Localization of the study area (Modified after El [10])



therein) (2) The Chouabine Formation is a phosphatic-rich marl and limestone alternations including siliceous-rich beds of the late Paleogene to the Eocene age (3) The Kef Eddour formation is composed of two thick bioclastic and dolomitized limestone beds with interbedded phosphorites-rich chalk and micritic concretions dated as early Eocene (Fig. 1).

3 Results

3.1 Lithostratigraphy

The lenticular bodies are encased in a green marly interval of the Chouabine Formation upper part overlain by a drape composed of phosphorite green shale and siliceous limestone. The top is composed by a highly bioturbated interval.

The lenticular bodies display skeletal-rich (*Ostrea*, bivalve shells, e.g. pecten) and coarse-grained lenses with low amount of mud (calcirudite). They are widely distributed in the upper part of Chouabine Formation. The individual lens is concave up in cross section. The lens width ranges from 9 to 12 m; whereas, the height ranges from 1 to 3 m (Photos 1 and 2).

3.2 Thin Sections Analysis

Twenty samples have been collected from base to top of the calciclastic bodies. Thin sections analysis shows high-energy grainstone texture mostly composed of bivalve shells. Some thin sections show oyster shells associated with fenestral fabrics and laminated algal structures (Photos 3 and 4).

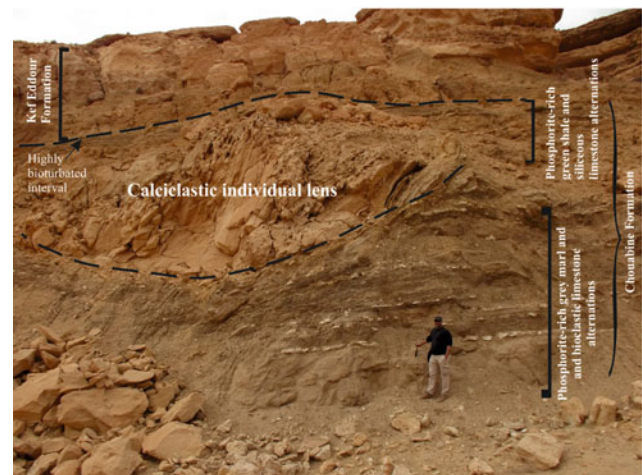


Photo 1 Lithostratigraphy and stratigraphic position of the calciclastic sediment bodies



Photo 2 Sediment texture of calciclastic bodies. Note the skeletal-rich facies (calcirudite)

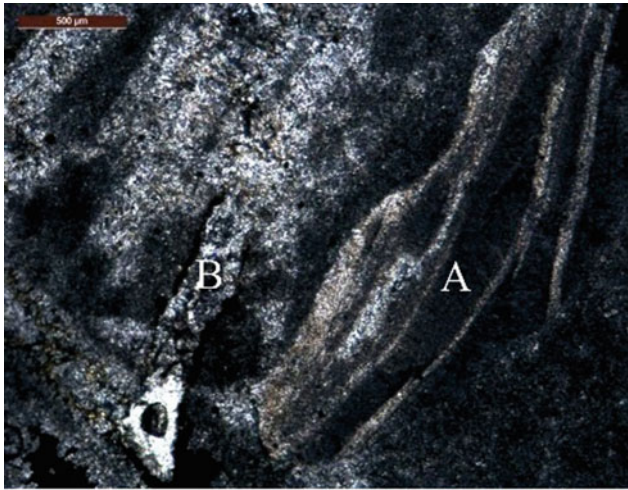


Photo 3 Thin section showing grain-supported texture. Note the presence of bivalve shells partially micritized (A). Some neomorphosed shell fragments were filled by sparry calcite (B)

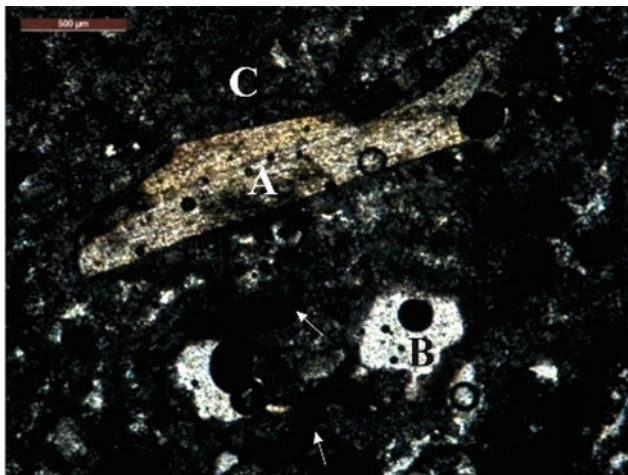


Photo 4 Thin section dense fenestral fabric associated with oyster shells (A) and peloids (white arrow). The cavities are irregular somewhat elongated in shape (B) (birds eyes structures). Laminated algal structures are visible above the oyster shells (C)

4 Discussion

The presence of the different environment microfacies shows that sediments were mixed and reworked. The biogenic debris content indicates a sediment source related to the Thelja carbonate/lagoonal platform.

The deposits originated from a carbonate platform via submarine gravity flow processes. They were redeposited in the phosphorite-rich basin. The predominance of the

coarse-grained sediments texture indicates carbonate platform probably made up of organogenic limestones which favors steep slopes [8].

The transport and the formation of the calciclastic lenticular bodies involve submarine erosion process that stripped sediments from Thelja submarine uplifted carbonate platform edge and slope controlled by tectonic activity (normal faults) in conjunction with sea level changes occurring during the Early Eocene [9]. Sea level drop below the platform edge in addition to steep slopes induce slope instabilities and mass transport processes [2, 8]. Rockfalls along faulted escarpments (platform margin) are not excluded to produce calciclastic deposits since that grains shape and roundness analysis indicates little transport of sediments.

5 Conclusion

The field investigations and the microfacies analysis of the paleogene outcrops of the M'dhilla area provided new data about the depositional processes in the Gafsa Basin. The textural and the lithostratigraphic analysis of the calciclastic deposits probably related to mass transport of lithified rocks (rockfalls), encased in hemipelagic phosphorite-rich beds, indicate that the main source of the sediment supply may correspond to the Thelja carbonate/lagoonal platform. The organogenic components characterizing the Thelja Formation carbonate/lagoonal platform has favored steep slope. The carbonate platform was subjected to submarine collapse events related to the conjunction of the tectonic activity and possibly sea level lowstand during the Early Eocene.

References

1. Cook, H.E., Hine, A.C., Mullins, H.T.: Platform margin and deep water carbonates. Society of Economic Paleontologists and Mineralogists (1983)
2. Shanmugam, G., Moiola, R.J., Damuth, J.E.: Eustatic control of submarine fan development. In: Submarine Fans and Related Turbidite Systems, pp. 23–28. Springer, New York, NY (1985)
3. Watts, K.F., Garrison, R.E.: Sumeini Group, Oman—evolution of a Mesozoic carbonate slope on a south Tethyan continental margin. *Sediment. Geol.* **48**(1–2), 107–168 (1986)
4. Payros, A., Pujalte, V.: Calciclastic submarine fans: an integrated overview. *Earth Sci. Rev.* **86**(1–4), 203–246 (2008)
5. Coniglio, M., Dix, G.R.: Carbonate slopes. Facies models: response to sea level change, pp. 349–373 (1992)
6. Rong, H., Jiao, Y., Wu, L., et al.: Architecture and evolution of calciclastic marginal slope fans of the Ordovician carbonate platform in the Yijianfang outcrop of the Bachu area, west Tarim Basin. *AAPG Bull.* **97**(10), 1657–1681 (2013)

7. Kocsis, L., Ounis, A., Baumgartner, C., Pirkenseer, C., Harding, I. C., Adatte, T., Chaabani, F., Neili, S.M.: Paleocene–Eocene palaeoenvironmental conditions of the main phosphorite deposits (Chouabine Formation) in the Gafsa Basin, Tunisia. *J. Afr. Earth Sci.* **100**, 586–597 (2014)
8. Einsele, G.: *Sedimentary basins: evolution, facies, and sediment budget*, 2nd edn., Springer Science & Business Media (2013)
9. Bouaziz, S., Barrier, E., Soussi, M., Turki, M.M., Zouari, H.: Tectonic evolution of the northern African margin in Tunisia from paleostress data and sedimentary record. *Tectonophysics* **357**(1–4), 227–253 (2002)
10. Ahmadi, R., Mercier, E., Ouali, J.: Growth-strata geometry in fault-propagation folds: a case study from the Gafsa basin, southern Tunisian Atlas. *Swiss J. Geosci.* **106**(1), 91–107 (2013)



Lower to Middle Miocene Deposits of North-East Tunisia: Implied Facies Evolution and Tectonic-Sedimentary Control

Nadia Gaaloul, Wissal Ghazzay, and Saloua Razgallah

Abstract

This work was the result of a scientific collaboration between the faculty of sciences of Tunis (FST) Tunis –El Manar University (which provides the logistic support) and the Lundin Petroleum Tunisia (which provides wells and seismic data). It aims to study the response of the Miocene sedimentary systems, in the North-East of Tunisia, to the global events occurring during sedimentation. Miocene deposits organization is complex and evolved in time and space. It is characterized by pedogenetic alteration, great sedimentary supply with frequently, bad preservation and stratigraphic lacuna. In this context, a multidisciplinary approach integrating biostratigraphy, facies analysis, interpretation of depositional environments and seismic correlations has been adopted. It has allowed us to mark the distribution and the thickness of the facies (petroleum objects) and to understand the general evolution of sedimentary systems related to tectonic, eustatic and climatic events that they have been recorded. The compilation of the data shows that several modifications of the depositional environments, during the Burdigalian-Langhian period, have occurred in the studied area. Two transgressive events are recognized and major discontinuities have been highlighted. The sudden changes of thickness and the individualization of the Miocene microbasins are arguable in favor of a tectonic control.

Keywords

North-East Tunisia • Lower to Middle Miocene Facies • Eustatism • Tectono-sedimentary model

1 Introduction

In Mediterranean and surrounding area, the Cenozoic corresponds to a compressive period materialized by folding phases and filling of basins. The North-Eastern Tunisian province is situated on the southern border of the Mediterranean basin. It corresponds to a favorable area in order to study the Cenozoic geological series including the Lower and Middle Miocene series studied here. Energetic and hydrogeological potentialities of the Miocene sedimentary series attract general interest [1, 2].

The main objectives of the present work are:

- A sedimentological and paleontological investigation in surface outcrops and wells are performed both to assess the facies distribution and the spatio-temporal correlation and to identify the environmental changes linked to relative sea level variations.
- A seismo-tectonic approach is pursued in order to detect the faults that affected the subsurface sedimentary sequences and guided the morpho-structuration of the region.

The studied area covers the Grombalia-Bouficha region and the North part of the Gulf of Hammamet (Fig. 1). The investigated Miocene lithostratigraphic succession is represented from the base to the top for the following formations: Fortuna/Ketatna/Messiouta formations, Oued Hammem Formation, Aïn Grab Formation, Mahmoud/Begonia formations, Beglia/Birsa formations, and Saouaf Formation.

The geological framework corresponds to a succession of NE-SW anticlines and synclines extending from Cap Bon peninsula to the pelagian sea (Fig. 1). In fact, the Gulf of Hammamet is affected by several tectonic corridors: N90-120 El Haouaria and Maamoura corridors and the N160-170 Enfidha corridor.

N. Gaaloul (✉) · W. Ghazzay · S. Razgallah
Faculty of Sciences of Tunis, Department of Geology, University
of Tunis El Manar, Tunis, 1060, Tunisia
e-mail: nadiagaaloul1@gmail.com

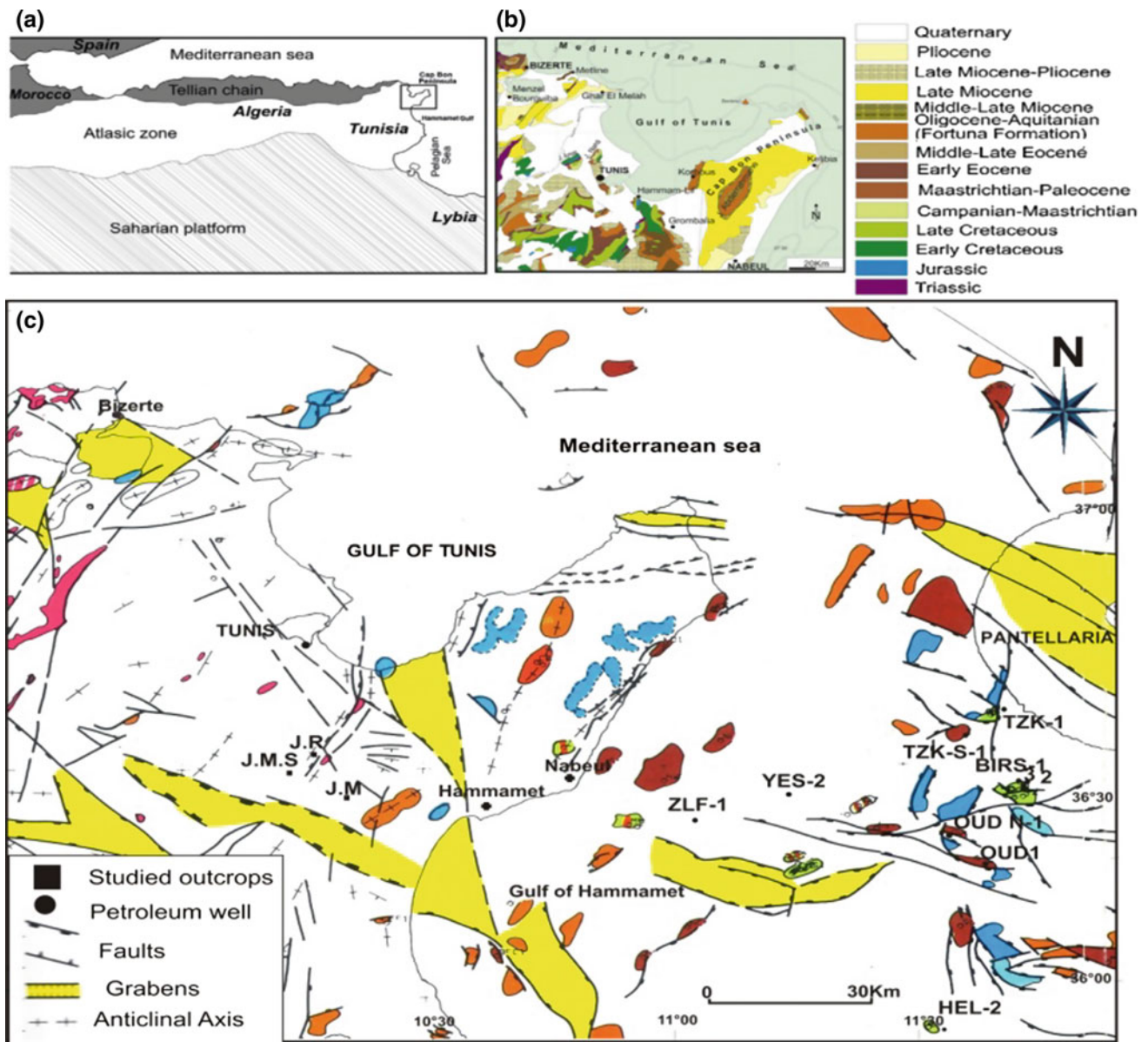


Fig. 1 Geodynamical and geological setting of the study area (Cap Bon Peninsula and Hammamet Gulf): **a** structural setting of North Africa in the Mediterranean domain; **b** geologic map of the onshore outcrops of northeastern Tunisia; **c** structural map of the onshore and

offshore areas showing the main surface and subsurface tectonic features ([4, 2] modified). This map shows the position of the outcrop section and the used petroleum wells

2 Methods

From the Lower to the Middle Miocene deposits have been studied in three outcrop sections of the Grombalia-Bouficha area (Ressas, Msalla, Menchar) and five wells drilled in the Gulf of Hammamet (Birs, Oudna, Zelfa, Halk El Menzel and Tazarka) (Fig. 1c). Based on direct field observations (Lithology, Sedimentary figures, discontinuities, fauna.), a

detailed litho-sedimentological description was carried out. A total of 498 samples were collected. In laboratory, the studies were conducted by using the classic methods that include:

- Examination of thin sections by optical microscopy to ascertain their texture and components.
- X-ray diffraction for the identification and the measurement of clays minerals.

- Granulometric analysis to characterize grain size of sandy samples by using classic indicators (M_z : mean grain size, Q : median value, SK_i : skewness index).
- Identification of paleontological content and species identifications of the microfauna (foraminifera and ostracoda) under the binocular loupe and the microflora (pollen) under optical microscope
- The interpretation of seismic sections (seismic lines) is based on seismic stratigraphic concepts.

3 Results

3.1 Facies and Related Depositional Environments

The biostratigraphic and the sedimentological analyses allowed us to identify the lithostratigraphic succession of the studied formations. The Biozones and the palynozones were also defined. The establishment of the corresponding zones for each formation led us to the identification of the timing of the deposition and the existence of stratigraphic lacuna.

Several facies and depositional environments were identified. Their evolution, during the Lower to Middle Miocene, can be summarized as follows:

- A continental alluvial plain where soils and xeric vegetation (corresponding to the red silty clay facies of the Messioua Formation and the base of the Ketatna Formation or the sandy bodies of the top of the fortuna Formation) were developed. This continental episode marks the end of the regressive cycle of the Oligo-Aquitania in the Bouficha-Grombalia region and the Gulf of Hammamet
- An inner-ramp where reef tendency is clear (limestones, with algae and corals, of the upper part of the Ketatna Formation).
- A shallow marine environment evolving to an offshore one during the Burdigalian to the early Langhian (suggested by the green glauconitic clays with planktonic and benthic microfauna of the Oued Hammam Formation). It is noted that the transgressive character of the series of the upper part of the Ketatna Formation and its coeval-laterally Oued Hammam Formation allowed us to deduce the first eustatic rise period of the Early Langhian in the Eastern part of the Cap Bon peninsula and the Gulf of Hammamet.
- Sandy limestone facies with pectinidae and echinoderma (Ain Grab Formation) indicate a sea level rise related to

the Middle Miocene transgression. The transgressive surface corresponds to a regional unconformity.

- Clays, rich in planktonic microfauna, change laterally to sandy bars (Mahmoud Formation and/or Lower and Middle Birsa) related to a transition from an open marine environment to a coastal marine environment. The Ain Grab limestones and the clayey Mahmoud Formation indicate the mainly transgression phase of the Middle and the Late Langhian in Eastern Tunisia.
- A predominantly siliciclastic facies (Beglia Formation and/or Upper Birsa Formation) reflect a marine environment with the continental influences and the beginning of the regressive cycle of Serravallian.

3.2 Correlation and Tectonic Control

The sedimentological correlation of outcrops (Grombalia and Bouficha regions) and drilled wells (Gulf of Hammamet) allowed us to have an overview of the facies distribution and the geometry of the sedimentary bodies. The presence of several major discontinuities, changes of thickness, rapid facies changes (e.g. Gulf of Hammamet) and absence by erosion or non-deposition of some lithostratigraphic units (Ketatna, Ain Grab) reveal the imprint of syndimentary tectonics.

The interpretation of the structural profiles of the Gulf of Hammamet has conducted to the identification of the microbasins structures bordered by normal faults corresponding to a succession of subsident zones (grabens) and high zones (horsts). This kind of structuring is generated by normal and strike-slip NE–SW trending faults [3]. Based on the lithostratigraphic correlation and the structural profiles analysis, it seems that the morpho-structuring of the Gulf of Hammamet has widely guided sedimentation during Lower to Middle Miocene.

4 Discussion

This study highlights the impact of the sea level fluctuations and the tectonic movements on the deposition of sediments and the facies evolution. Two eustatic pulsations have been identified in Lower to Middle Miocene.

The individualization of the subsident grabbens (where sediments are mostly argelaceous) was guided by the tectonics.

Other phenomena, such as climatic changes, could interplay on the control of the sedimentary processes. In fact, the paleosols and the high energy fluvial deposits found

especially in the continental formations (Messiouta, Ketatna, Beglia) denote hot and humid atmospheric conditions. The presence of lignite (at the base of the Saouaf Formation) shows biostatic- rhexistatic periods.

Consequently, it is necessary to find more detail of the interaction of the tectonic, eustatism and climate in order to precise the role of each factor. Palynological studies could also be beneficial.

5 Conclusion

From the Lower to the Middle Miocene deposits describing the outcrop formations from the Grombalia-Bouficha area and the petroleum wells of the Gulf of Hammamet show several sedimentary facies changes.

Three kinds of depositional environments were defined: (i) marine environments (characterized by clays with planktonic microfauna), (ii) mixed environments, where limestones or sandstones with benthic foraminifera and mollusca, are identified and (iii) a continental area where vegetation could be present.

The correlation of the different sections shows that the sedimentation is controlled by regional and global factors: tectonic, eustatism and climate.

The tectonics has mastered the structuring into subsident microbasins and horsts. Eustatic variations have permitted the deposition of clays, the individualization of bounding unconformities and a great supply of sediments. Climate phenomena are more significant in continental areas where hot and humid atmospheric conditions justify the generation of fluvial deposits and paleosols.

References

1. Ben Salem, H.: Contribution à la connaissance de la géologie du Cap Bon: stratigraphie, tectonique et sédimentologie. Thèse 3^{ème} cycle, Université de Tunis-II, Tunis, Tunisie, 203 p. (1992)
2. Gharsalli, R., Zouaghi, T., Soussi, M., Chebbi, R., Khomsi, S., Bédir, M.: Seismic sequence stratigraphy of Miocene deposits related to eustatic, tectonic and climatic events, Cap Bon Peninsula, northeastern Tunisia. *Comptes Rendus Geosci.* **345**, 401–417 (2013)
3. Bédir, M., Arbi, A., Khomsi, S., Houatmia, F., Aissaoui, M.N.: Seismic tectono-stratigraphy of fluvio-deltaic to deep marine Miocene silicoclastic hydrocarbon reservoir systems in the Gulf of Hammamet, northeastern Tunisia. *Arab. J. Geosci.* **9**(19), 1–33 (2016)
4. Ben Ferjani, A., Burolet, P., Mejri, F.: Petroleum geology of Tunisia ETAP. 194 p. (1990)

Geologic Origins of the North American Shale-Gas Revolution: Can it Happen Elsewhere?

Frank R. Ettensohn

Abstract

The “shale-gas revolution” has been a largely North America phenomenon despite efforts to transfer it to other countries with likely gas-shale resources. Understanding how this “revolution” has occurred on North America may be critical in duplicating it elsewhere as in North Africa and the Middle East. North America holds in excess of 30 major shale-gas basins most of which reflect the influence of plate tectonics. From Ordovician to Tertiary, continental-margin orogenies and rifting events were crucial in generating not only large, mostly undeformed, basin repositories for the shales, but also conditions favorable for organic-rich shale deposition. Time and place (paleogeography and paleoclimate) were also important. Developmental factors having to do with culture, population, economics, and technology, along with detailed characterization of the shales and careful planning, can be just as significant as the geologic factors. Hence, the situation in North America reflects more of an evolution of understanding than any kind of revolutionary change. Whether or not a similar alignment of factors, like those that have occurred in North America, can happen elsewhere is uncertain; but thus far, the evidence suggests that it is unlikely.

Keywords

Shale-Gas revolution • North America • Plate tectonics • Basin repositories • Organic-Rich shale • Paleogeography • Paleoclimate • Developmental factors

1 Introduction

The inception of the “shale-gas revolution” in the United States in about 2008 quickly made the United States one of the leading gas and oil producers in the world. One of the important outgrowths of this revolution was the attempt to transfer it to other countries so that they could develop energy independence and use cleaner fuels. In an attempt to do this, the United States EIA [1] developed estimates of possible shale-gas and shale-oil resources for many countries around the world including several from North Africa and the Middle East. Although they had a stimulating effect, many of these assessments proved to be problematic. Assessment continues in several countries at present. However, only Canada and China have been successful at producing commercial amounts of shale gas.

A review of these developments suggests that the North American revolution is not really a revolution at all. It is rather a series of unusual achievements associated with unique geologic and developmental factors. The developmental factors are related to culture, economics, and long-term planning as a consequence of the oil embargo of the U.S. in the mid-1970s. This fact will only be briefly mentioned. More importantly, the critical geologic factors that facilitated a revolution gas shale will be examined.

2 Geologic Setting of North America

The origin of large accumulations of organic-rich shales, capable of producing shale gas, is still a subject of controversy and the suggested origins are many and complex. However, I will argue that another more basic factor may be the accessibility of appropriate basin repositories for deposition of the suspended organic matter that is nearly always present in epicontinental and pericontinental waters [2]. The formation of these basins and their infilling with organic-rich shales, from which the North American unconventional

F. R. Ettensohn (✉)
Department of Earth and Environmental Sciences,
University of Kentucky, Lexington, KY 40506-0053, USA
e-mail: fettens@uky.edu

oil-and-gas shales originated, are mostly related to plate tectonics. Geologically, North America has greater than 30 major shale-gas basins (Fig. 1) whose shales range in age from Ordovician to Tertiary. The presence of so many basins in part reflects the large size and stability of the continent during nearly 500 Ma of development since Laurentia (North America) separated from the Rodinian supercontinent at about 760–680 Ma. Moreover, large-scale deformation of the continent, which began by Early Ordovician time, occurred only at the continental margins, and in the process, produced the many inland foreland, intracratonic, and yoked basins that became repositories for the organic-rich sediments generated during basin formation. Orogenies on the Cordilleran (four orogenies), Ouachita and Appalachian

(four orogenies) margins created several foreland basins through deformational loading, a tectonic process that in most cases created circumstances favorable for the production of dark, organic-rich shales as parts of normal foreland-basin stratigraphic sequences. Hence, formation of organic-rich black shales is probably inherent in the development of most foreland basins [3]. Moreover, continued deformational loading during orogeny invariably led to the yoking (joining) of foreland and intracratonic basins, which allowed the depositional setting for black shales to migrate into adjacent basins. In several cases, successive, overlapping foreland basins generated very economic stacked plays. In addition, during Paleozoic and Mesozoic time, when most organic-rich sediments were deposited in North American

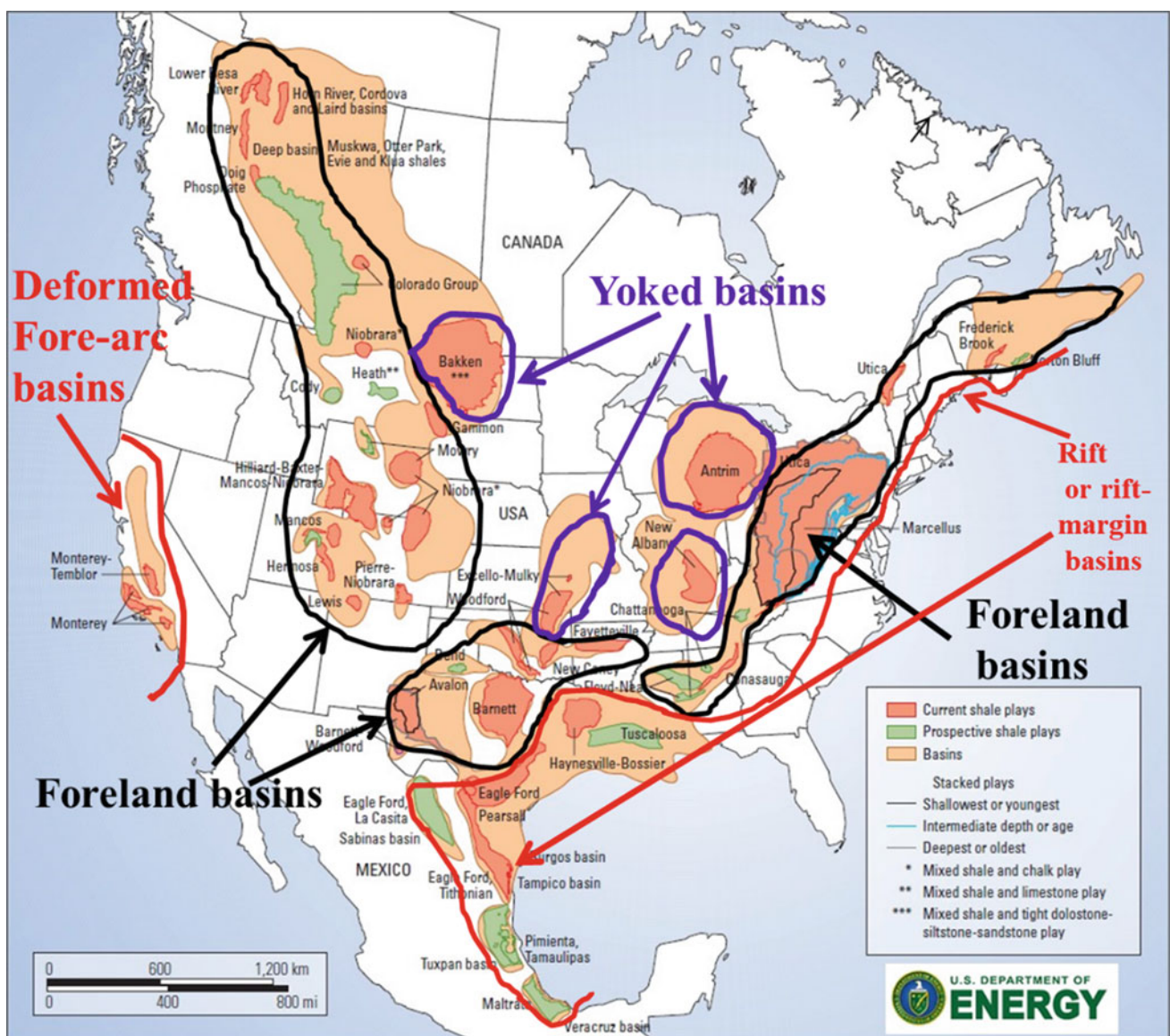


Fig. 1 Major North American gas-shale basins, highlighting the various types of basins containing gas shales (U.S. Department of Energy)

basins, parts of the continent with major basins were located in the tropics or subtropics where warmth and increased sunlight enhanced organic-matter productivity during both greenhouse and icehouse climates. During the breakup of Pangea in Triassic–Jurassic time, additional repositories were created in the form of rift and rift-margin basins along the eastern and southern continental margins of North America (Fig. 1). Along the western margin of North America in California, dark, organic-rich shales also accumulated in Cenozoic forearc and extensional/transensional basins.

3 Developmental Factors

As important as geological factors were, developmental factors since 1975 have been of equal importance. One of the most important factors includes more than 40 years of research into the nature of eastern and central U.S. gas shales. As a result of the oil embargo of the U.S. in the mid-1970s, these shales were extensively characterized. The importance of this kind of understanding cannot be underestimated. Economic factors can be just as important and include private ownership of subsurface resources, population distribution, the presence of nearby markets, abundant water, adaptable political and social institutions as well as technological factors that reflect the work of many small independent operators, supporting contractors and infrastructure.

4 Conclusion

Understanding the origin of the North American shale-gas “revolution” is critical if any part of it is to be repeated in other countries. Four contributing geologic factors include:

(1) a large continental area that was stable for periods of time long enough for shale basins to develop; (2) restriction of deformation to continental margins and the resulting development of large inland basins with homogeneous geologic parameters that can guarantee predictable drilling results; (3) largely undeformed basins with simple geology; and (4) basin development at places and times (paleogeography and paleoclimate) that facilitate the high production of organic matter. Developmental factors include detailed characterization of shale resources, private ownership of subsurface rights, availability of water resources, technology, distribution of population and markets relative to basin resources, adaptable political and social institutions and the availability of independent operators, supporting contractors and infrastructure.

As it has been noted, the situation in North America reflects more of an “evolution” of understanding than a “revolution.” Whether or not the same association of factors that developed in North America can occur elsewhere, is uncertain. Although it is believed that several countries will go on to produce shale gas and oil, similar “revolutions” in other parts of the world are probably unlikely.

References

1. Energy Information Agency (EIA): EIA/ARI World Shale Gas and Shale Oil Resource Assessment. U.S. EIA, Washington, D.C. (2013)
2. Effensohn, F.R.: Assembly and dispersal of Pangea: large-scale tectonic effects on coeval deposition of North American, marine, epicontinental, black shales. *J. Geodyn.* **23**(3/4), 287–309 (1997)
3. Effensohn, F.R.: The Appalachian foreland basin in eastern United States. In: Miall, A.D. (ed.) *The Sedimentary Basins of United States and Canada, Sedimentary Basins of the World*, vol. 5, pp. 105–179. Elsevier, Amsterdam (2008)

Part VI

Geomorphology—Quaternary Geology

Thermodynamic Consideration on Volcanic Landforms

Naoto Kaneko and Hiroyuki Nagahama

Abstract

Based on the first law of thermodynamics in the view point of non-equilibrium thermodynamics, the concept of entropy is expressed in terms of the probability of various states and treatments of the distribution of energy. From the general hypothesis of forming volcanoes by physical constraints, typical shape for the longitudinal profiles of volcanoes is determined which enables us to observe in the field or map. Weathering and erosion are insufficient to determine the shape, height, and geometries of volcanoes. However, solutions become possible by introducing the concept that the distribution of energy tends toward the most probable. This solution leads to a theoretical definition of the thermodynamics and geometry of volcanic landforms that agrees closely with field observations. The most probable state for certain physical systems can also be illustrated by Lorentz plot. The average longitudinal profiles and angle of repose were so derived. They have the properties implied by the theory. The regularity derived from the average longitudinal profiles has some of the principal properties demonstrated by the concept of entropy. Specifically, the height of volcano and distance from its summit are exponentially inversely-proportional.

Keywords

Entropy • Volcanic landform
 Non-equilibrium thermodynamic
 Digital elevation model (DEM) • Angle of repose

1 Introduction

The fact that over 20% of the area of the foundation of the Japanese archipelago is covered with volcanic ejecta is requesting us to learn about the formation of volcanic archipelago and mitigation of disaster. We have theoretically clarified the formation patterns of accretionary prisms and folds which are the foundation of the Japanese archipelago [1]. In our previous research [1], we mentioned the deformation of the ground material from the viewpoint of internal friction angle and rheology which also enables us theoretically to derive the volcanic slope topography from the thermodynamic granular behavior by [2, 3]. Interestingly, the angle at the time of the deformation failure of the granular body is related to the formula of bearing capacity force (field of soil mechanics) when considering the volcano as a structure [4, 5]. This old-finding established by Japanese Army's survey technology about 90 years ago was newly discussed by using the digital elevation model (DEM) in this study.

2 Theoretical Background

When discussing the continuous mechanics and thermodynamics in a unified manner, we need to formulate the law of thermodynamics by the concept corresponding to the fundamental law of motion (the field theory). From the first law of thermodynamics, the change of internal and total kinetic energy is expressed by force and heat. Here, taking the example of slope failure and rock deformation, the deformation of the plastic body is irreversibly irrespective of the speed of process. Hence, the change in the thermodynamic state of the object involves an increase in the positive rate of entropy production (non-negativity, by [2]):

$$\rho \dot{e} \geq \sigma_{ij} \dot{\epsilon}_{ij} + q_{i,i} + \rho r \geq 0, \quad (1)$$

N. Kaneko · H. Nagahama (✉)
 Department of Earth Science, Tohoku University, 6-3 Aoba,
 Aramaki Aoba-ku, Sendai, Japan
 e-mail: h-nagahama@m.tohoku.ac.jp

where ρ is density, e internal energy per unit mass, σ_{ij} stress, ε_{ij} strain, q_i heat flux, r heating value from internal heat source per unit mass. Based on the variational inequality in non-equilibrium thermodynamics, Niiseki and Satake [2] induced the minimum energy principle of Rowe [3]'s equation which expresses the stress-dilatancy equation in granular mechanics. From the compatibility condition of force balance and displacement among granular materials, Rowe theoretically obtained

$$-\frac{\sigma_1 \dot{\varepsilon}_1}{2\sigma_3 \dot{\varepsilon}_3} = K = \tan^2\left(\frac{\pi}{4} + \frac{\varphi}{2}\right) = \frac{1 + \sin \varphi}{1 - \sin \varphi}, \quad (2)$$

where subscript indicates the direction by triaxial-compressed, and K is energy ratio, φ internal friction angle (or can interpret as angle of repose: stable inclination). Now, when applying Eqs. (1) and (2) to the field of fracture mechanics, crack faces of granular bodies such as ground materials are formed so as to maximize the rate of energy release. When the volume strain rate is constant by plastic deformation with respect to Eq. (2), we can introduce the concept of bearing capacity as stress ratio, so

$$y = \frac{1 - \sin \varphi}{1 + \sin \varphi} e^{-\pi \tan \varphi}, \quad (3)$$

where $y = (z_l - z_d)/(H' - z_d)$ is function of elevation (z_l, z_d and H' are heights: Fig. 1). Interestingly, Terada [4] based on previous research [5] argued that the form of several volcanoes on Eq. (3). From the above, we cleared that there is a thermodynamic background in the shape of the volcano which is regarded as a group of granular bodies. Accordingly, we derived the ridgeline of volcano which is considered theoretically as golden ratio from non-equilibrium thermodynamics in this study.

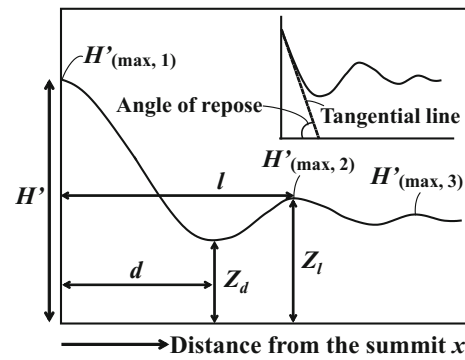


Fig. 1 Schematic volcanoes

3 Methods

We carried out Digital Elevation Model and nonlinear analysis on volcanoes of Japan that may cause disasters in the future. By Terada's method (16 azimuths and 40 km from the summit, and minimize from each other's volcano), longitudinal profile of volcano was created. We used KASHMIR 3D as DEM software (10 m resolution) and a 1/25000 topographic map of Japan Geographical Survey Institute which gave the following parameters with respect to height and distance from the summit (Fig. 1).

4 Results and Discussion

The average longitudinal profile of the volcano can be represented by the typical curve as shown in Fig. 1 and Table 1. The tangential line of ridgeline by DEM representing the critical angle in the vicinity of the summit was set. We interpreted the

Table 1 Results of DEM to volcanoes

Name of volcano (detail)	Heights parameter			Distance parameter		Elevation function $y = (Z_l - Z_d)/(H' - Z_d)$	Actual degree φ_a (°)	Theoretical degree φ_r (°)
	H' (m)	Z_d (m)	Z_l (m)	d (km)	l (km)			
Yoteizan (Siribesi)	1819	234	513	7.5	27.0	0.176	25.4	18.8
Hokkaido-Komagatake	1002	96	253	8.3	16.3	0.173	14.0	19.0
Tarumaesan	967	187	323	9.3	19.9	0.174	11.0	18.9
Nasudake (Tyausudake)	1856	572	703	25.3	30.6	0.102	14.8	24.2
Harunasan (Kamongatake)	1286	426	563	9.9	18.7	0.159	14.6	19.8
Akagisan (Kurobiyama)	1772	596	697	12.4	15.1	0.086	19.8	25.8
Hakoneyama (Kamiyama)	1368	247	315	12.4	14.9	0.061	15.6	28.9
Fujisan (Kengamine)	3709	516	608	23.4	25.3	0.029	33.7	35.3
Daisen (Kengamine)	1626	229	391	16.9	32.0	0.116	14.9	23.0
Sakurajima (Ontake)	1041	3	165	6.9	24.3	0.156	17.0	20.0
Asosan (Takadake)	1523	601	699	9.1	14.4	0.106	14.3	23.8
Kirishimayama (Karakunidake)	1626	270	352	17.0	21.7	0.060	13.8	29.1

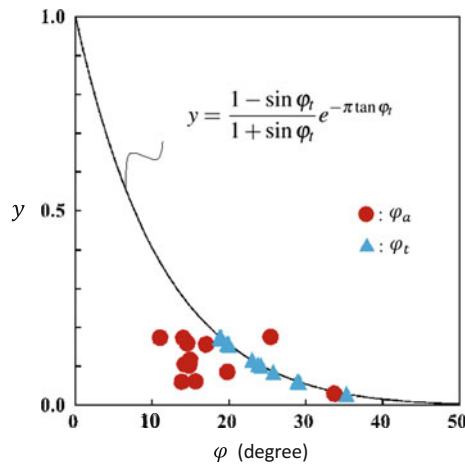


Fig. 2 Correlation with y and φ

analyzed actual φ_a as angle of repose of the mountain. We determined φ_t from Eq. (3) by [4]. φ_t represents the repose angle that the volcano can theoretically obtain from the heights and distance parameter based on the idea of force support [5]. As a result, φ_a was smaller than φ_t except Yoteizan (only one of which has not erupted since the history). Then, we point out two reasons why φ_a is smaller than φ_t : (i) effects of erosion and weathering, (ii) using of more sophisticated tools (DEM). Therefore, we clear the shape of volcanoes which is determined under the boundary as shown in Fig. 2.

Next, we used the so-called Lorentz plot, in which $H'_{(\max,n)}$ is given to one peak in the longitudinal profile as shown in Table 2 and Fig. 3, and the ratio of the next peak $H'_{(\max,n+1)}$ is repeatedly recorded, where H' is height of the summit

Table 2 Results of Lorentz plot

Name of volcano (detail)	a
Yoteizan (Siribesi)	0.92
Hokkaido-Komagatake	0.83
Tarumaesan	0.90
Nasudake (Tyausudake)	0.69
Harunasan (Kamongatake)	0.98
Akagisan (Kurobiyama)	0.69
Hakoneyama (Kamiyama)	0.90
Fujisan (Kengamine)	0.76
Daisen (Kengamine)	0.64
Sakurajima (Ontake)	0.70
Asosan (Takadake)	0.84
Kirishimayama (Karakunidake)	0.67

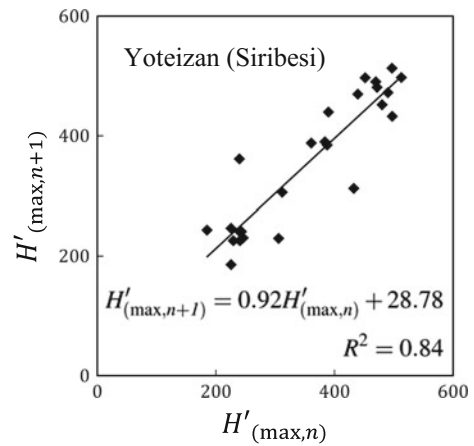


Fig. 3 One of the examples

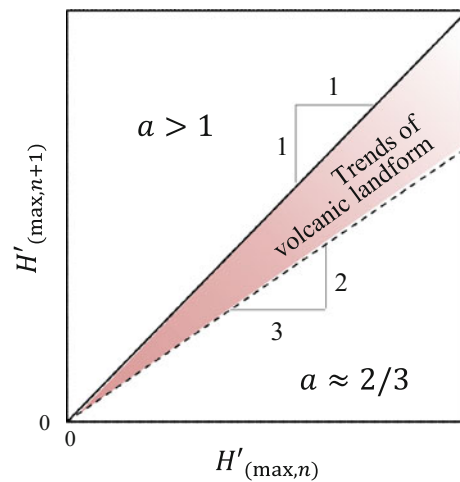


Fig. 4 Range of volcanic landform

($H'_{(\max,1)} = H'$) and a is inclination. Based on the results of Lorentz plot, Fig. 4 shows the approximate straight line obtains the range of about 0.6–1. Then, when calculating the difference equation, we can find out that the height of mountains decreases exponentially as the distance x increases:

$$H'_{(\max,n)} = H' e^{b(n-1)} = H' e^{bx}, \quad (4)$$

where $b (= a - 1; \text{always negative})$ expresses the range of form of volcanoes and mountains. Namely, b is determined by φ . This finding is consistent with the previous study [6] which pointed out that the height of mountains is in the maximum entropy state.

5 Conclusion

We reveal the shape of the volcanoes of Japan by longitudinal profile. The ridgeline can show the height decreases exponentially as the distance x increases. Volcanoes could be classified as a typical form so that we can give some unified parameters with respect to length and angle. Then, we point out an actual angle of repose of the Japanese volcanoes is smaller than theoretical one because of mainly weathering and erosion. As a result, we can mention that forming volcanoes have clearly trends by each peak including its summit. Finally, these facts found in this paper agree theoretically with the first law of thermodynamics and Rowe's stress-dilatancy equation.

References

1. Kaneko, N., Muto, J., Nagahama, H.: Plasticity index effects on mechanical bifurcation: soils and soft-sediment deformation. *GEOMATE* **13**(36), 19–25 (2017)
2. Niiseki, S., Satake, M.: Derivation and discussion on Rowe's principle of energy ratio minimum. In: Proceedings of the Annual Conference JMCE, 3rd edn., vol. 36, pp. 5–6 (1981, in Japanese)
3. Rowe, P.W.: The stress-dilatancy relation for static equilibrium of an assembly of particles in contact. *Proc. R. Soc. A.* **269**(1339), 500–527 (1962)
4. Terada, T.: On the form of volcanoes. *Bull. Eqk. Res. Inst., Univ. Tokyo.* **7**(2), 207–221 (1929)
5. Reissner, H.: Zum Erddruckproblem. In: Proceedings of the 1st International Congress Applied Mechanics, Delft, pp. 295–311 (1924)
6. Leopold, L.B., Walter, B.L.: The concept of entropy in landscape evolution. In: Geological Survey Professional Paper, pp. A1–20 (1962)

Quantitative Study of the Geomorphic Evolution of Shilin County, Yunnan Province, China, Based on Classic Theory and Method

Yuhui Li and Zhiqiang Ding

Abstract

Geographical cycle, hypsometric (area-altitude) analysis, sequence of karstic evolution and DEM analysis supported by geographical information system are used to quantify the geomorphic evolution of Shilin county territory of China Yunnan for an integral protection of stone forest reserve. The area-altitude curves and integrals of Shilin county territory, elevation zones and their inner depressions demonstrate that the Shilin county territory is a characteristic of a rejuvenating geomorphic structure at a late period of mature stage. The evolutionary dynamics represent an interplay of the faulted-blocks motion and Bajiang erosion base level control which made the original monadnock karst planation plateau into four levels of elevation terrains with different topographic features. The curve and the integral of the subarea and depressions in elevations ranging between 1700 and 1900 m demonstrates that the geomorphic structure is a complex of a vertical layer structure of the stone forest and the horizontal step structure because of mixing karst vertical reduction and horizontal erosion.

Keywords

Geomorphic evolution • Hypsometric analysis
Geographical information system • Stone forest
Water and soil resource • Karst reserve

1 Introduction

Surficial morphology attracts geoscientists, the traditional geomorphic theories and the methods such as geographical cycle, sequence of karstic evolution, hypsometric (Area–Altitude) analysis. They have been widely used with the aid

of new technology such as DEM analysis of Geographical Information System [1–3]. The problem is to quantitatively study the heterogenous regions in geomorphic factors, processes and structure for an integral protection of various reserves such as the geopark and the world natural heritage sites. For this reason, The Shilin County Territory of China Yunnan Province is chosen for that.

2 Regional Setting of Shilin County and Methods

2.1 Regional Settings

Shilin county with an area of 1777.1 km², 24°30′N–25°03′N, 103°10′E–104°40′E and elevation ranging between 1476 m and 2613 m is located in Yunnan province of the south west China and a subtropical karst plateau There are four groups of strata including the Neoproterozoic erathem in the north of shilin county, the Lower Paleozoic one in the west, the Upper Paleozoic in the middle and the Cenozoic. The world famous stone forest was mainly developed in the Permian carbonatite. What was discovered was that the stone forests/teeth were baked by basalt and covered by the Paleogene Lunan group which made Yunnan stone forests considered to experience the complicated, long history of evolution and paelogeographical changes [4]. The geological structures are, respectively, the NNE–SSW Shizong-Mile fault in the east side, the N–S Jiuxiang-Shiyakou fault in the west and the wandering Weize-Wenbishan fault in the middle. The relief here is high in the northern, western and eastern of the Shilin County. The low is in the middle and the southwest. The Bajiang river flows across the Shilin County from the north tip to the southwest. The faults and Bajiang river divided the Shilin County territory into four terrains: the structural erosion karst plateau middle mountain in the eastern side, the structural erosion karst plateau middle mountain in the west side, the north–south rolling karst hills called as

Y. Li (✉) · Z. Ding
Yunnan Normal University, Kunming, 650500, China
e-mail: li.yuhuihui@ynnu.edu.cn

Jiupanshan and the karst slope complex which is composed of the karst depressions and the stone forests in the middle and the Lunan River basin in the southwest.

2.2 Materials and Methods

The data of Shilin County's digital elevation model (DEM) are taken from the Geospatial data Cloud of Computer Network Information Center of the Chinese Academy of Sciences (<http://www.gscloud.cn>) and the spatial resolution of the subpixel images which is of thirty meter. The method is to use the spatial analytical tools of the geographical information system for statistical analysis of the mean elevation, relieves, gradients, hypsometric curves and integrals of the Shilin County, the subareas and the inner depressions of elevation with the following ranges of <1700 m, 1700–1900 m, 1900–2100 m, >2100 m with the Excel technology.

3 Results

3.1 Relief, Gradient and Landform Zones of the Shilin County

The relative altitude difference (relief) in most area of the Shilin County is ≤ 100 m with the maximum gradient of 69.8° and the mean one of 10.8° . The Shilin County territory can be divided into four landform units: the structural erosion and dissolution middle mountain making up of 25.7% of the county area in the east and the west side of Shilin County, the cone clusters and the depressions of 18.8% and the karst plateau depressions of 37.9% in the middle eastern part; the gentle karst slope with hill depressions and stone forest of 12.2% and the river basin (Lunan basin) of 5.4%.

3.2 Stone Forests, Depressions and Underground Rivers

The stone forests mainly distribute in the gentle karst slope in the subarea ranging in elevation between 1700 and 1900 m where there are the boundary of the Bajiang River basin and the Jiupanshan west slope and there are numerous underground rivers. There are typically four kinds of stone forests: the pinnacle-shaped stone forest, the most typical one, the column-shaped one the pagoda-shaped one, the mushroom-shaped one as well as the irregular shaped ones. There are also the fossilized stone forest baked by basalt, the paleo-stone forest covered by Paleogene clastic rocks and the stone forest at developing conditions. The stone forests

occur respectively in the karst depressions, valley, basin and on hilltop. The stone forests differently occur in the north part and the south one of the Shilin Park. In the north, the stone forests distributes in sites with an elevation of over 1800 m. In the south ones, they distribute in sites of an elevation below 1800 m. The baked or covered stone forests were exposed in some gullies and depressions. The vertical layers of stone forests from the hill top to the bottom of the depressions or gullies coexist with the horizontal step landforms group from the karst plateau surface to karst springs in the boundary between the river basin and the karst hill slope.

3.3 Hypsometric Analysis Results of Shilin County Territory

The area-altitude curve of the Shilin County territory is of a left upend straight raise, middle gentle, right end steep bend with an integral of 0.3936. The curve of the depressions is an incline with middle raise and right end bend. The integral is 0.4702. The results give the fact that the Shilin County's geomorphic evolution is of rejuvenation at the late mature stage of the balanced period. The hypsometric analysis results of the elevation subzones further describe the geomorphic structure and the evolutionary process of the Shilin County. The curve of the elevation subzone from 1700 to 1900 m is a reserve 'S'-shaped curve of upside raise, middle dip straight and downside concave. The integral is 0.4949. The curve of the depressions of the subzone is of obvious upside raise bend with the integral of 0.6919. The curve of the subzone is in an elevation of over 2100 m. It is a middle concave incline with an integral of 0.3097. The curve and the integral of the depressions of the zone were not produced because of the least depressions. For the subzone of elevation ranging between 1900 to 2100 m, the curve is a reverse concave 'S'-shaped with the integral of 0.1367. For the depressions of the subzone, they are a concave decline line of 0.383.

4 Discussion

The different results of the Strahler hypsometric analysis in montane terrains, structural subareas, drainage basin range, lithological zones and different scales have been discussed for their causes and implications [5, 6]. The elements of the different results are of geomorphic process, original topography and affecting factors. As for the Shilin County, the different results can be explained in the similar way. Firstly, the curves and integrals of the whole Shilin county territory and inner depression demonstrate the Shilin County

topographic structure and its dynamic process. The topographic composition is 25.7% area of the fluctuant plateau mountain in high and lower altitude and 74.3% area of the gentle karst monadnock plateau and depressions in middle elevation zone. The cause of such geomorphic structure is the dynamic process that three groups of the faults made the original paleo-karst monadnock planation plateau into three faulted-blocks terrains and then Bajiang river provides an erosion level for development of the present topographic pattern under the regional uplift during the Shilin physiographic plateau-Bajiang period^[15-16]. The curves and integrals of the elevation subareas give some details of the structure and their process. They demonstrate the geomorphic evolution of the same period and the heterogeneous structure. For example, the curves and integrals of the sub-area and depressions in elevation ranging between 1700 and 1900 m reflects the mixing process of the karst vertical reduction with horizontal erosion. It means that the rainfall firstly leeching, centering in lower sites and finally flowing into the underground rivers and again appearing as springs. Meanwhile, the caprocks of basalt and clastic rocks were eroded off and the buried stone forest reappeared or continued to develop. Such process does not only coincide with both the features of Bajiang drainage basin's karst complete infiltration and the hydrogeological structure of the plateau planation landform turning to karst hills and depression [7] but also with Davis's geographical cycle's relationship among structure, process and times as well as the Cvijić's sequence of karstic evolution. The geomorphology of the Shilin county territory is a synergistic result of structure, erosional dynamics and mixing process of surficial runoff and the underground river.

5 Conclusion

The hypsometric analysis is an effectively quantifying way for a geomorphic evolution of the heterogeneous regions with the aid of the modern DEM technology. The topography of the Shilin County territory is at the rejuvenating evolution of later mature stage and characteristic of the same period and heterogeneous structure. The unique Yunnan stone forests are the result of a mixing process of the karst vertical reduction with the horizontal erosion under the suitable geological settings.

References

1. Wei, L.U.O.: Hypsometric analysis with a geographic information system. *Comput. Geosci.* **24**(8), 815–821 (1998)
2. Leonowicz, A.M., Jenny, B., Humi, L.: Automatic generation of hypsometric layers for small-scale maps. *Comput. Geosci.* **35**, 2074–2083 (2009)
3. Rache, C.A., Summerfield, M.A.: Scale dependence of hypsometric integrals: an analysis of Southeast African basins. *Geomorphology*, **96**, 174–186 (2008)
4. Yuhui, L., Yiguang, Y., Yongning, L., et al.: Study of paleo-environment of shilin karst (stone forest) development, yunnan, China. *Carsologica Sin.* **20**(2), 91–95 (2001)
5. Hiroo, O.: Changes in the hypsometric curve through mountain building resulting from concurrent tectonics and denudation. *Geomorphology* **8**, 263–277 (1993)
6. Hurtlez J.E., Lucazeau, F.: Lithological control on relief and hypsometry in the Herault drainage basin (France). *Earth Planet. Sci.* **328**, 687–694 (1999)
7. Liang, H., Yang, M.D., Peng, J., Chen, G.X., Wang, Z.G.: The hydrological characteristics of the karst basin in Lunan stone forest. *Carsologica Sin.* **20**(4), 24–28 (2001)

Karst Landforms as Possible Lithological and Paleo-Climatic Markers in an Unnamed Crater in Northern Sinus Meridiani, Mars

Davide Baioni

Abstract

This paper describes the possible karst landforms observed in the Light Toned Deposits (LTDs) located within an unnamed crater in northern Sinus Meridiani, an area located in the equatorial region of Mars. Morphological and morphometric surveys of the LTDs surface morphologies through an integrated analysis of the available images from the High Resolution Imaging Science Experiment (HiRISE) instrument on the Mars Reconnaissance Orbiter (MRO) were performed. The Martian landforms interpreted as a doline of karst origin resemble closely karst landforms that can be observed both in different karst terrains on Earth and in other regions of Mars. The karst landforms observed highlight the evaporitic origin of these materials and suggest a climatic change and the presence of liquid water, probably due to ice melting, during the late Amazonian age.

Keywords

Mars • Sinus meridiani • Karst landforms • Evaporate deposits • Climate change

1 Introduction

Studies based on new high-resolution images have revealed the presence of karst landforms and processes in several Martian evaporite deposits [1–3] and have highlighted the usefulness of karst landforms as lithological and paleo-climatic markers [4]. In particular, karst landforms such as doline depressions, like those on Earth are indices of solutional processes [5], and are related on Mars to the presence of soluble rocks (i.e. evaporite) and liquid water as it has been suggested in many recent works [6, 7]. Sinus

Meridiani is located near the south–western margin of Arabia Terra in the equatorial region of Mars. Crater diameters in the region vary widely, from a few metres to 100 km. Some of these craters have floors that are covered by distinct regions of light toned layered deposits. These deposits, which are also widespread in various locations in the equatorial region of Mars, are known as light toned deposits (LTDs). Among the goals of this study are to describe, for the first time, the landforms in the LTDs located within this crater in northern Sinus Meridiani, and to discuss their possible origins, as well as their lithological and paleo-climatic significance.

2 Data and Methods

Toward this end, a detailed morphologic and morphometric analyses of available images of the LTDs located within this crater in northern Sinus Meridiani was performed. Landform features were investigated through an integrated visual analysis of data from the MRO High-Resolution Imaging Science Experiment (HiRISE) and the Context Camera (CTX). The CTX images (F05_037610_1843_XI_04N003 W; G13_023382_1846_XN_04N003 W) have spatial resolutions ranging between 5.42 m and 5.83 m per pixel, and the HiRISE image analysed (ESP_032296_1845) has a spatial resolution of 54.7 cm per pixel (objects 164 cm across are resolved). Thus, the HiRISE images give enough detail to clearly observe even the smallest characteristics of the landforms. The measurement of the morphometric values of the studied depressions was performed using a GIS software measurement tool.

3 Results

The present morphological analysis revealed the presence of many shallow, rimless closed depressions of various sizes and shapes, surrounded entirely by unbroken plains.

D. Baioni (✉)
Urbino University, Campus Scientifico Sogesta,
61029 Urbino, Italy
e-mail: davide.baioni@uniurb.it

The depressions are scattered or isolated, with locations and shapes that are unrelated to the bedding plane, surface slope or tectonic lineaments (i.e. joints, faults). The depressions are randomly distributed, with no particular pattern of orientation. They display various plan forms, including rounded, elliptical, drop-like, polygonal and elongated forms. Depressions range in length from 120 to more than 550 m, while widths generally range from 80 to over 250 m. Depths span from 14 to 20 m. In some places polygonal-like karst morphology can be observed. In fact, in some areas depressions pock some parts of the surface and occupy most of its area. Here, the depressions appear to be spaced farther apart, display well defined shapes with sharp divides and have diameters that range from 15 m to more than 50 m. The major axes show very different orientations, ranging from N–S to E–W, from NE–SW to NW–SE and from ENE–WSW to NNW–SSE. Orientations appear to be unrelated to the depression location or shape. The depressions also have well-defined, continuous and sharp margins. Their sides exhibit mainly symmetrical slopes with very steep to vertical walls. They generally lack deep gravitational slope processes and fan deposits at the foot. The floors are apparently flat and have only minute differences in the accumulation of dust and/or sediment between depressions. In some cases, the floors are subdivided into smaller and shallower depressions, highlighting a second generation of depressions. Additionally, the main parameters used in the morphometric analysis of karst depressions on the Earth were calculated for the observed depressions. While the perimeter ranges from 30 to over 1,300 m, the area's covers from 85 to more than 60,000 m². The depressions have low-to-moderate elongation index values, which range from 1.02 to 3.45, while the circularity index values range from 0.48 to 0.82. The depression density values scope between 8 and 34/km².

4 Discussion

Based on a detailed analysis of the characteristics of the features described above, these morphologies are interpreted as karst depressions. The features demonstrate major contributions of karst processes, because they lack evidence of wind action or erosional features associated with the evolution of impact craters, volcanic processes, tectonism, groundwater sapping and ice-related processes. In particular, these depressions were not formed by wind deflation, mainly because they lack a dominant orientation and do not display any of features typical of the bowl-shaped hollows or slight depressions caused by deflation found on Earth. Moreover, features of the depressions do not support their formation as eroded or softened impact craters, as indicated by the following two points of evidence. Firstly, the depressions display

various plan forms that cannot be shaped by an impact, which would instead create bowl-shaped depressions characterized by a circular plan form [8]. Secondly, all of the observed depressions lack raised rims and ejecta. It is unlikely that all possible rims and ejecta deposits were totally destroyed by erosional processes. The thermokarst origin can be ruled out in this study due to the absence of other morphologies on the floor of the depressions, suggesting ice sublimation such as unsorted polygons. Instead, the studied depressions display morphometric and morphologic similarities with terrestrial dolines that commonly develop in all kinds evaporite terrains described in several regions on Earth. Additionally, they strongly resemble the evaporite dolines described recently in other regions of Mars [1–3, 6, 7].

The karstic landform features appear to be the result of water-related processes. These findings provide evidence of the presence of liquid water, probably caused by the melting of ice-rich ground and/or snow, which provide the water necessary to stimulate karstification processes. Episodic changes in Martian obliquity may explain the origin of the ice and/or snow that melted and shaped these karst landforms. Theoretical considerations about the stability of water ice and numerical simulations of climate predict that surface ice and/or snow accumulation areas may have shifted repeatedly between polar, middle, tropical and equatorial latitudes in response to changes in Martian orbital and atmospheric characteristics in the past [9, 10].

On Earth, doline landforms are considered diagnostic of the presence of karst processes and therefore they are markers of soluble rocks [5]. Moreover, on Earth the presence of polygonal karst is typical of evaporite terrains where the inherently high solubility of evaporite rocks make densely-packed depressions more easily than in carbonates [5, 11]. Thus, the doline landforms observed in the study area allow us to similarly presume that they represent a clear sign of the presence of soluble (i.e. evaporite) rocks.

5 Conclusions

Considering the morphological and morphometric similarities of features on Earth and Mars, and after discarding other possible origins, the investigated landforms in LTDs within a crater in northern Sinus Meridiani were interpreted as karst landforms. Landforms characteristics suggest that the landforms were affected by a single geologic 'wet episode', characterised by sufficient water availability due to the melting of ice or snow, followed by dry climatic conditions. The presence of karst landforms suggests a response to climatologic change requiring the presence of sufficient water for their development. They indicate that conditions in the past on Mars were much warmer than those prevailing now. Thus, these landforms are markers of climatic changes

during which water was available at this latitude in the Amazonian age. Moreover, the karst landforms highlight the presence of soluble rocks, and can therefore be used as significant lithological markers to distinguish units characterised by soluble minerals such as evaporites studied within the crater in northern Sinus Meridiani.

References

1. Baioni, D., Zupan Hajna, N., Wezel, F.C.: Karst landforms in a martian evaporitic dome. *Acta Carsologica* **38**(1), 9–18 (2009)
2. Grindrod, P.M., Balme, M.R.: Groundwater processes in Hebes Chasma, Mars. *Geophys. Res. Lett.* **37**, L13202 (2010)
3. Jackson, M.P.A., Adams, J.B., Dooley, A.R., Montgomery, D.R.: Modeling the collapse of Hebes Chasma, Valles Marineris, Mars. *GSA Bull.* **123**(7–8), 1596–1627 (2011)
4. Baioni, D., Sgavetti, M.: Karst terrains as possible lithologic and stratigraphic markers in northern Sinus Meridiani, Mars. *Planet. Space Sci.* **75**, 173–181 (2013)
5. Ford, D.C., Williams, P.: *Karst Hydrogeology and Geomorphology*. Wiley & Sons Ltd, England (2007)
6. Baioni, D., Tramontana, M.: Evaporite karst in three interior layered deposits in Iani Chaos, Mars. *Geomorphology* **245**, 15–22 (2015)
7. Flahaut, J., Carter, J., Poulet, F., Bibring, J.-P., van Westrenen, W., Davies, G.R., Murchie, S.L.: Embedded clays and sulfates in Meridiani Planum, Mars. *Icarus* **248**, 269–288 (2015)
8. De Pablo, M.A., Komatsu, G.: Possible pingo fields in the Utopia basin, Mars: geological and climatical implications. *Icarus* **199**, 49–74 (2009)
9. Madeleine, J.B., Forget, F., Head, J.W., Levrard, B., Montmessin, F., Millour, E.: Amazonian northern mid-latitude glaciation on Mars: a proposed climate scenario. *Icarus* **203**, 390–405 (2009)
10. Wordsworth, R., Forget, F., Millour, E., Head, J.W., Madeleine, J.-B., Charnay, B.: Global modelling of the early Martian climate under a denser CO₂ atmosphere: water cycle and ice evolution. *Icarus* **222**, 1–19 (2013)
11. Warren, J.K.: *Evaporites: Sediments, Resources and Hydrocarbons*. Springer, New York (2006)

Boron Characterization and Distribution in Particle-Size Fractions Separated from a Semi-arid Tunisian Soil

Ahlem Tlili, Imene Dridi, Rafla Attaya, and Moncef Gueddari

Abstract

Boron is essential for crop growth. However, it is needed in very small amounts. The range between boron deficiency and toxicity in plants is quite narrow. These stressing conditions gravely reduce the yield and the quality of many crop species. Therefore, an understanding of the factors and the reactions affecting its availability in soil is necessary. Against this framework, our research aims to determine the available boron status in a semiarid soil of Dour Ismail irrigated perimeter (North Tunisia). The objective was also to investigate B distribution in different particle size fractions throughout the soil profile. For this purpose, one pit was dug in the field plot that had not received any B fertilization. Our results showed that the highest boron amounts were recorded in deep horizons and were greatly affected by organic matters and clay contents. However, the increase in pH level and the high percentage of TCaCO_3 significantly diminished the available B contents mainly in surface horizons. The investigation of the depth boron distribution in the different particle-size fractions indicated a considerable contribution of the silt (2–50 μm) fraction (52% of the soil total available B) while the clay (<2 μm) and coarse (>50 μm) fractions seem to play a less important role.

Keywords

Available boron • Soil • Particle-size fractions

1 Introduction

Boron (B) is a micronutrient necessary for growth of all crops. It plays a key role in a diverse range of plant functions including cell division and sugar transport. B is also required for the production of nucleic acids and the development of reproductive structures [1]. In soil, B content evolves. It must be monitored frequently because of the narrow range between the levels for B deficiency and its toxicity as compared to other nutrients [2]. Therefore, the management of this nutrient is critical and appropriate B supply is necessary for obtaining better yields.

B exists in four major forms in the soil: (a) in rocks and minerals; (b) on clay surfaces and iron and aluminium oxides; (c) combined with organic matter (OM); and (d) as boric acid and B in the soil solution. Nevertheless, only a few forms are available to plants. Their determination is important for delineating the deficient soils. B deficiency is prevalent in coarse-textured acidic soils developed mainly in high rainfall zones (easily leached). Moreover, soils with low OM content and high adsorption capacity (e.g., soils with high pH and rich in clay minerals) are generally impacted by B deficiency [3]. On the contrary, B toxicity symptoms are often observed in arid and semi-arid regions owing to the use of irrigation waters high in B [3]. Currently, the major focus of the agronomists and the soil scientists is the study of B occurrence and distribution in soils through a multitude of approaches (B characterization, B fractionation, extraction techniques and methodologies...). Consequently, innumerable researchers have studied B dynamic in soil for a long time. Nevertheless, most of these studies have examined B in soil surface horizons only with little attention given to B distribution according to depth. Besides, only few researchers have investigated this issue in Tunisian soils which makes B management in such areas difficult and demands for fundamental understanding of B distribution. Against this backdrop, the present research was undertaken to better determine the available B content in a Tunisian soil

A. Tlili (✉) · I. Dridi · M. Gueddari
Faculty of Sciences of Tunis, Department of Geology,
University of Tunis El Manar, 2092 El Manar, Tunisia
e-mail: ahlemtlili@hotmail.fr

R. Attaya
Soil Resources Department, Ministry of Agriculture,
Tunis, Tunisia

of Dour Ismail irrigated perimeter (North Tunisia) as well as to investigate its depth distribution in the different particle-size fractions.

2 Materials and Methods

To conduct this study, one pit was dug in Dour Ismail irrigated perimeter situated in the Northwest of Tunisia (Béja Governorate—Goubellat delegation). Three soil samples were collected from each horizons of the profile (the four horizons were considered, see Table 1). Then, 12 samples were analyzed for the main physicochemical soil properties according to the international norms. We measured the soil pH level (NF ISO 10390), the electrical conductivity (EC) (NF ISO 11265), soil texture (NF X31-107), Total Calcium Carbonate (TCaCO₃) (NF ISO 10693), Total Organic Carbon (TOC) (NF ISO 14235), Total Nitrogen (TN) (NF ISO 11261), the Cation-Exchange Capacity (CEC) (NF X31-130) and the available B (NF X31-122). Moreover, we submitted each soil samples to a particle size fractionation to isolate coarse fraction (>50 μm), silt fraction (2–50 μm) and clay fraction (<2 μm). All separates soil fractions were quantified for their B contents.

3 Results and Discussion

3.1 Soil Characteristics

Table 1 shows the main physicochemical properties of the studied soil. The pH level was basic (≈ 8) and slightly dropped with depth. Similarly, the EC values increased as we moved from surface (1.36 dS/m) to deep layers (2.08 dS/m). The soil texture was dominated by clay-silt ($\approx 60\%$) fraction throughout the profile. The TCaCO₃ percents decreased with the increase in depth. The surface horizon of the studied soil exhibits the highest OM contents with 1.23% of TOC and 1.12% of TN. These values decreased with depth and reach respectively 0.61% and 0.60%. The CEC has the same behavior as the TOC and TN. The values varied from 30.67 meq/100 g top to 17.33 meq/100 g bottom.

3.2 Depth B Distribution

The examination of B distribution in the studied soil showed an increase in available B concentration as we moved from surface horizon (0.64 ppm) to the deep horizon (0.74 ppm). The low B values recorded in surface layers may be explained by a slight increase in pH level (8.30) and a relatively high TCaCO₃ (13.16%) amount. Indeed, B adsorption in soil depends on soil pH level. It rises between pH 6.0–8.5 and reaches the highest values around pH 9. B adsorption decreases with further pH increases [2]. Furthermore, the soils containing important amounts of lime are usually low in available B [4]. The calcium carbonate increases B adsorption by soils since it raises the soil solution pH. Several researchers observed similar result and failed to get a significant correlation between TCaCO₃ and the available B content of the soil [4]. The great B amounts recorded in deep layers correspond to a slightly enrichment in OM (1.05%) and to a great percentage of clay-silt fractions ($\approx 62\%$). Our results were in line with some earlier studies which have shown that OM [5] and clay contents [6] effect the B bioavailability.

A statistical analysis was performed to find out possible correlations between the available B contents and the studied soil properties (pH, EC, clay, silt, sand, TCaCO₃, and TOC). The results revealed a significant and positive correlation between the available B and the clay fraction ($r^2 = 0.64$ at $p < 0.05$). A similar correlation was also found by [7]. The authors revealed that fine-textured soils usually contain more available B than coarse-textured soils. Besides, the EC showed a significant and positive correlation with the available B ($r^2 = 0.53$ at $p < 0.05$). Our result agrees with those of [8] which stated that the onset of salinization is accompanied by an increase in the available B content. However, our results showed a negative relationship between the available B content and the pH level ($r^2 = -0.79$ at $p < 0.05$). This appears to correspond to the common belief that an increase in pH would increase B adsorption and consequently cause a reduction in B availability [2]. The same negative relationship was revealed between the available B and the TCaCO₃ content ($r^2 = -0.90$ at $p < 0.05$). Indeed, the calcium carbonate acts as an important B adsorbing surface in soil [4].

Table 1 Selected physicochemical properties of the studied soils

Horizons	pH	EC (dS/m)	Sand (%)	Silt (%)	Clay (%)	TCaCO ₃ (%)	TOC (%)	TN (‰)	OM (%)	CEC (meq/100 g)	B (mg kg ⁻¹)
H1	8.30	1.36	41.46	26.48	32.06	13.16	1.23	1.12	2.12	30.67	0.64
H2	8.23	1.89	37.39	23.78	38.83	12.75	0.81	1.40	1.39	25.33	0.63
H3	8.08	2.07	36.44	21.95	41.60	8.50	0.73	0.62	1.26	20.00	0.66
H4	8.05	2.08	37.91	19.16	42.93	6.25	0.61	0.6	1.05	17.33	0.74

EC: Electrical Conductivity, TCaCO₃: Total Calcium Carbonate, TOC: Total Organic Carbon, TN: Total Nitrogen, OM: Organic matter, CEC: Cation Exchange Capacity, B: Boron

The investigation of depth B distribution in the different particle-size fractions indicated a considerable contribution of the silt (2–50 μm) fraction (52% of the soil total available B) to B adsorption in soil especially in depth while the clay (<2 μm) (15%) and the coarse (>50 μm) (26%) fractions seem to play a less important role. For this latter, few studies report were in accordance with what we found [7]. The authors showed that the silt fraction had a positive but non-significant relationship with the available B ($r^2 = 0.21$). The lowest B values recorded in the clay fractions mainly in depth correspond to significant OM levels (1.05%). Indeed, B adsorption in clay surfaces decreases as OM content increases [9]. Soil OM occupies the reactive adsorption sites on clay fractions.

4 Conclusion

A variety of soil properties (organic matters and clay contents, percentage of calcium carbonate, soil pH level, and salinity) have been identified as affecting the B dynamic and distribution in soil of Dour Ismail irrigated perimeter (North Tunisia). The obtained results showed that the increase in pH level and the great percentage of TCaCO_3 significantly diminished the available B contents mainly in surface horizons. However, the accumulation of B in depth corresponds to an enrichment in OM (1.05%), to a high EC solution (2.08 dS/m) and to a high percentage of clay-silt fractions ($\approx 62\%$).

The investigation of depth B distribution in the different particle-size fractions showed a considerable contribution of the silt (2–50 μm) fraction (52% of the soil total B) to B adsorption in soil especially in depth while the clay (<2 μm) and the coarse (>50 μm) fractions seem to play a less important role. The lowest B values recorded in the clay

fractions mainly in depth correspond to significant OM levels (1.05%). Soil OM occupies the reactive adsorption sites on clay surfaces and therefore decreasing B adsorption.

In effect, a deeper understanding of the factors affecting B bioavailability in soils is essential for the assessment of B deficiency or toxicity under different conditions.

References

1. Kabu, M., Akosman, M.S.: Biological effects of boron. *Rev. Environ. Contam. Toxicol.* **225**, 57–75 (2013)
2. Goldberg, S., Corwin, D.L., Shouse, P.J., Suarez, D.L.: Prediction of boron adsorption by field samples of diverse textures. *Soil Sci. Soc. Am. J.* **69**, 1379–1388 (2005)
3. Niaz, A., Nawaz, A., Ehsan, S., Saleem, I., Ilyas, M., Majeed, A., Muhmood, A., Ranjha, A.M., Rahmatullah, Ahmed, N.: Impacts of residual boron on wheat applied to previous cotton crop under alkaline calcareous soils of Punjab. *Sci. Lett.* **4**(1), 33–39 (2016)
4. Niaz, A., Ranjha, A.M., Rahmatullah, Hannan, A., Waqas, M.: Boron status of soils as affected by different soil characteristics-pH, CaCO_3 , organic matter and clay contents. *Pak. J. Agric. Sci.* **44**(3), 428–433 (2007)
5. Raza, M., Mermut, A.R., Schoenau, J.J., Malhi, S.S.: Boron fractionation in some Saskatchewan soils. *Can. J. Soil Sci.* **82**, 173–179 (2002)
6. Sandabe, M.K., Mohamed, S.: Boron adsorption by some semi-arid soils of North Eastern Nigeria. *Int. J. Appl. Agric. Res.* **6**(1), 71–76 (2011)
7. Kumari, K., Nazir, G., Singh, A., Kumar, P.: Studies on boron fractions with different physico-chemical properties of cultivated soils of Himachal Pradesh, India. *Int. J. Curr. Microbiol. App. Sci.* **6**(6), 1547–1555 (2017)
8. Chaudhary, D.R., Shukla, L.M.: Boron status of arid soils of Western Rajasthan in relation to their characteristics. *J. Indian Soc. Soil Sci.* **52**(2), 194–196 (2004)
9. Marzadori, C., Vittori Antisari, L., Ciavatta, C., Sequi, P.: Soil organic matter influence on adsorption and desorption of boron. *Soil Sci. Soc. Am. J.* **55**, 1582–1585 (1991)

A Study of Ammonium Adsorption on Clay Soil (Siliana, Northern Tunisia)

Manel Allani, Abdessatar Hatira, and Hatem Ibrahim

Abstract

The study of the different forms of nitrogen's loss in soil has shown that there is significant ammonium fixation in clay layers which is expected to minimize water contamination. In this work, the adsorption characteristics of ammonium were studied on pure kaolinite and on clay fraction dominated by kaolinite. The characteristics of the adsorption equilibrium were measured mathematically by using the two models of Langmuir and Freundlich isotherms. And it is worthy to note as observed that the ammonium binding curves on both types of kaolinite present a similar appearance to that found by Langmuir. The initial ammonium concentration plays an important role in the adsorption's mechanism. The ammonium adsorption capacity increases with the initial concentration and with the time flow.

Keywords

Clay • Ammonium • Capacity of adsorption
Batch equilibrium study

1 Introduction

Nitrogen is one of the major constituent elements of the organic matter which is an essential component of living entities. This study reveals a dual interest angularly connected to economy and environment. In Tunisia, nitrogen fertilizers are the most important agronomic practice [6] for intensive agricultural production.

M. Allani (✉) · A. Hatira
Faculty of Sciences of Tunis, Tunis El Manar University,
2092 Tunis, Tunisia
e-mail: manel_allani@hotmail.fr

H. Ibrahim
Faculty of Sciences of Bizerte, University of Carthage,
7021 Tunis, Tunisia

An excess use of ammonium in agronomy as a chemical fertilizer causes the environmental destruction. It can also lead to degrade soil quality and especially contaminate water resources. "Thus, ammonium has been regarded as an indicator of groundwater contamination" [12]. In soils, the main colloids of the soil namely the clay and the organic fractions have the property of retaining various substances. This binding relates to several cations and in this case ammonium NH_4^+ [8]. The adsorbed ions are largely retained in exchangeable form [10]. Therefore, reducing the transformation and the movement of N compounds by adsorbent materials such as clay minerals [11] is crucial to protect the quality of the groundwater and the environment and to increase the agricultural production.

2 Materials and Methods

To develop this work, two different kinds of clays were used: a pure kaolin and a clay fraction of vertic soil (Siliana, Tunisia North) along a profile one-meter-deep divided into four typical horizons.

The experiments are carried out in a fixed column. For each sample, 2 cm in diameter and 32.5 cm in height contains 10 g of the clay fraction of each sample as macerated adsorbent in an ammonium acetate solution as a liquid phase at different concentrations (0.1 N, 0.5 N, 1 N). A tip of the tick at the bottom of the opening of the column is to prevent the passage of particles of the adsorbent. A closure (like the tap) at the bottom of the column for time management and measurements are made by the kjeldahl method after 30 min, 60 min, 180 min and 12 h: 720 min at ambient temperature. In order to determine the physicochemical properties of the clays on the field, various methods and means of identification have been used such as mineralogical, chemical and geotechnical analyzes; granulometry, X-ray diffraction (XRD), potential Hydrogen (pH) [5], electrical conductivity (EC) [3] and cation exchange capacity (CEC), The total specific surface area (SSA) are the

apparent density (D_a), the lime contents (CaCO_3) [2], phosphorus (P_2O_5), the total organic nitrogen (TON) [1] and the total organic carbon (TOC) [4].

3 Results and Discussion

3.1 Adsorbent Characterization

About the clay fraction of Siliana soil of the study site (Siliana, Tunisia of North), the analysis shows that the granulometry confirms the dominance of the clay fraction (from 48 to 62%) (Table 1), X-ray diffraction analysis was performed on all samples of each horizon along the profile shows the mineralogical components were mostly composed of kaolinite, illite and smectite.

3.2 Effect of Ammonium Concentration and Percolation Time

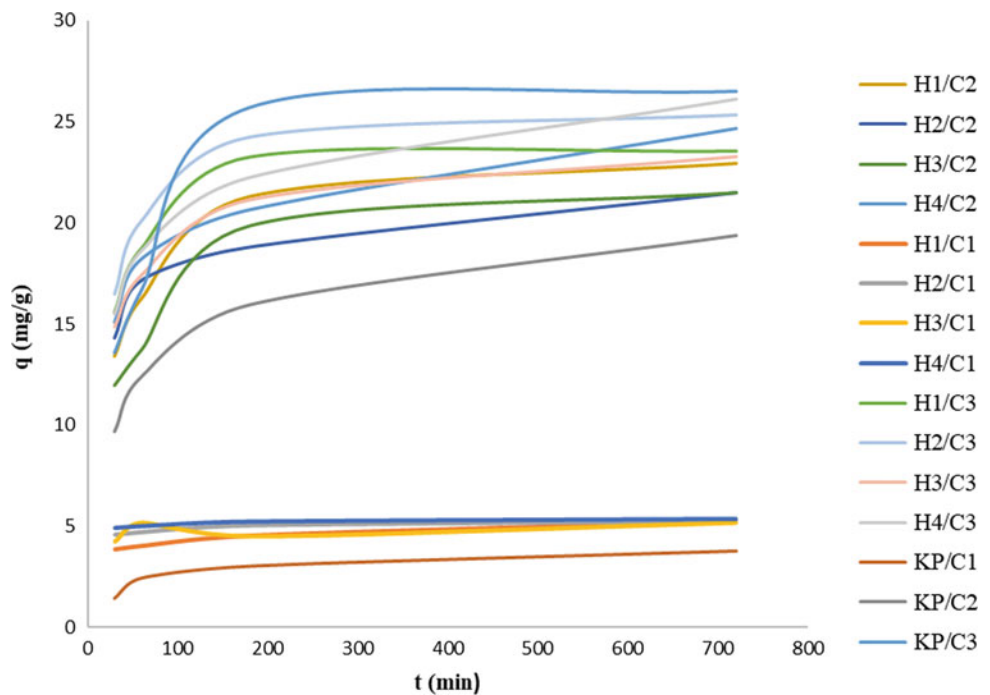
It is noted for all samples either pure kaolin or clay fraction of the soil study that the adsorption capacity (q) increases by augmenting the initial concentration of the ammonium solution. Increasing the adsorbed amount can be the result of a rise not only in the concentration of NH_4^+ but also in the electrostatic interactions on the colloids sites.

The lower the initial concentration of NH_4^+ , the lower the equilibrium time is. When concentration is higher the competition for active sites increases. This is consistent with the ion exchange surface which becomes increasingly saturated with ammonium ion. It is also noted that the adsorption capacity of NH_4^+ increased with the contact time. It has been observed that the ammonium adsorption is faster during the

Table 1 Analytical characteristics of the representative soil profile of Siliana studied area

Depth (cm)	Granulometry (%)			pH	EC ($\mu\text{s}/\text{cm}$)	CaCO_3 T (%)	CaCO_3 a (%)	OM (%)
	Clay	Silt	Sand					
0–20	48	37	15	7,47	302	25	8,79	2,53
20–50	51	38	11	7,66	239	28	8,49	1,72
50–70	55	36	9	7,79	319	32	8,78	1,91
70–100	62	25	13	7,74	245	27	7,31	1,4

Fig. 1 Effect of initial concentration and contact time on ammonium adsorption



first 180 min (Fig. 1). Then, the fixation rate becomes slow with an increasing time contact. It is caused by the rapid fixation on the outer surface of the colloids and by the presence of the unsaturated and the active sites at the beginning of the adsorption process. From the previous observations, it can be deduced that the increase in the contact time always causes the increase of the ammonium fixation on the clay samples.

In addition, the kinetics of fixation seems rapid until the equilibrium time approximate 180 min.

4 Conclusion

For clays, the most important phenomena over the retention of the cations could be the electrostatic (internal substitutions) or the chemical (dissociation of the hydroxyls) nature. The relative importance of these phenomena is linked initially with the arrangement of crystal lattices. This study has shown that in constant temperature and neutral pH close to 7, the clay fraction (Siliiana soil) can serve as a fixer for the ammonium ion. Thus, these clays can contribute to the reduction of environmental pollution when the ammonium ion is present in excess.

Also, the equilibrium time contact for all the ammonium ion concentrations was observed approximately at 180 min.

The kinetics of adsorption on pure kaolin is faster than on natural clays. The ammonium binding curves on the studied soil show a similar appearance to that found by Langmuir [9] and Freundlich [7]. It asserts that the adsorbent is expected to have a maximum adsorption capacity at the equilibrium time and all the adsorption sites which are assumed to be identical. The calculated value of the RL was obtained by $0 < RL < 1$ close to zero. This verification indicates that the data might be acceptable.

And according to the mineralogical analysis (RX), the abundance of kaolinite, illite and smectite in the different studied samples could explain the high adsorption capacity of NH_4^+ . In soil, the availability of nutrients for plant uptake depends on leaching processes of soil adsorption capacity.

Globally, the studied clay colloids can serve as a fixer for the ammonium ion can reduce its movement to aquifers and increase their availability for plants. Thus, the balance of the nitrogen compounds in natural ecosystems should be taken into account.

References

1. AFNOR: Qualité du sol: Dosage de l'azote total. Méthode de Kjeldahl modifiée- NF ISO 11261. Association Française de Normalisation, Paris (1995a)
2. AFNOR: Qualité du sol: Détermination de la teneur en carbonate; Méthode volumétrique, NF ISO 10693. Association Française de Normalisation, Paris (1995b)
3. AFNOR: Qualité du sol: Détermination de la conductivité électrique spécifique, NF ISO 11265. Association Française de Normalisation, Paris (1995c)
4. AFNOR: Qualité du sol: Dosage du carbone organique par oxydation sulfochromique, NF ISO 14235. Association Française de Normalisation, Paris (1998)
5. AFNOR: Qualité du sol: Détermination du pH, NF ISO 10390. Association Française de Normalisation, Paris (2005)
6. Dridi, I., Arfaoui, A.: Organic nitrogen distribution in seven Tunisian soil types under contrasting pedogenetic conditions. *Environ. Earth Sci.* (2017) (Springer)
7. Freundlich H.M.F.: Over the adsorption in solution. *J. Phys. Chem.* 385–471 (1906)
8. Hatem, I.: Modélisation des cycles c et n dans les Systèmes Sols-Céréales-Légumineuses, Centre international d'études supérieures en sciences agronomiques Montpellier, Université Tunis EL Manar, Faculté des Sciences de Tunis, thèse, 180 p. (2013)
9. Langmuir, I.: The constitution and fundamental properties of solids and liquids. *J. Am. Chem. Soc.* 38 (1916)
10. Manel, A., Abdessatar, H.: Cinétique de fixation de composé azoté (ammonium) sur les colloïdes argileux. Mémoire mastère, Université Tunis EL Manar, Faculté des Sciences de Tunis, Département de Géologie (2014)
11. Pansu, M., Gautheyrou, J.: Handbook of Soil Analysis - Mineralogical, Organic and Inorganic Methods. Springer (2006)
12. Shahram, S., Mohammad, A.K., Tahereh, S., Yaser, S.: Characterization, isotherm and kinetic studies for ammonium ion adsorption by light expanded clay aggregate (LECA). *J. Saudi Chem. Soc.* (2013)

Assessing Heavy Metal Distribution and Contamination of Soil in Ogere Trailer Terminal, Ogun State (Southwestern Nigeria)

Olutoyin Adeola Fashae, Adeyemi Oludapo Olusola, and Paulina Orekan

Abstract

Soil contamination is an issue of growing concern largely due to the risk it poses to the safety of the environment. This study investigated heavy metals contamination of soils at Ogere trailer terminal along the busy Ibadan-Lagos express road, Nigeria. Soil samples were collected and analyzed in the laboratory using standard techniques. Eighteen sampling sites were selected along the road as well as a control point located outside the influence of the haulage vehicle park. The concentration of nine different heavy metals: lead (Pb), cadmium (Cd), chromium (Cr), cobalt (Co), nickel (Ni), iron (Fe), copper (Cu), zinc (Zn), mercury (Hg) and arsenic (As) were assessed. Heavy metals concentration in the soil samples ranged from 0.20–9.60 mg/kg, 0.20–1.40 mg/kg, 0.20–0.25 mg/kg, 0.60–0.65 mg/kg, 0.65–1.65 mg/kg, 0.65–5.46 mg/kg, 0.76–3.13 mg/kg, 1.60–64.55 mg/kg, 0.80–43.25 mg/kg, and 12.0–65.0 mg/kg for Pb, Cd, Cr, Co, Ni, Fe, Cu, Zn, Hg and As respectively. Moreover, soil contamination levels were assessed by using the Accumulation Factor (AF) and the Integrated Pollution Index (IPI). The obtained results revealed significant positive relationship between various heavy metals concentration and their likewise with high concentration which makes the soils environmentally unfriendly. In this respect, a potential pollution risk exist which may consequentially have potential adverse impacts on the environment.

Keywords

Soil contamination • Heavy metals
Accumulation factor • Integrated pollution index

1 Introduction

Industrialization and urbanization have increased significantly in the past decades with an accompanying growth in the populations of the developing nations in Sub-Saharan countries like Nigeria. Urban growth is usually fueled by migration in a quest for better standard of living which the cities may provide [1]. Lagos, the commercial nerve center of Nigeria, for instance, is home to over 20 million inhabitants. Its proximity to the sea and the consequent location of the sea-port and other essential facilities in the city imply that haulage and other supporting services will be required to evacuate goods and the processing of commodities for export. This undeniable fact, coupled with the high population density in the city, has resulted in high congestion within and around the city. The congestion makes it difficult to secure appropriate space for tank farms and other services such as truck maintenance workshops for the haulage industry. The lack of designated parking space for trucks has led to the indiscriminate siting of tank farms within the city and in its outskirts particularly along major road corridors in the adjoining Ogun State.

The lack of an environmental consideration prior to siting these space parks results in significant adverse environmental consequences on soil, water and air. Its corollary is definitely the contamination of the soil. Therefore, there is the need for adequate information regarding the sources and potential risks concerning soil contamination in order to provide suitable remediation techniques [2]. This study seeks to assess heavy metal distribution and soil contamination in a trailer park using the example of Ogere in Southwestern Nigeria so as to determine the impact of the trailer park on the level of heavy metal concentration and soil pollution in the area.

This study was carried out on the Ogere Trailer Park which is located between kilometers 56 and 59 along Lagos-Ibadan expressway in South-western Nigeria. The

O. A. Fashae (✉) · A. O. Olusola · P. Orekan
Department of Geography, University of Ibadan, Ibadan, Nigeria
e-mail: toyinafashae@yahoo.com

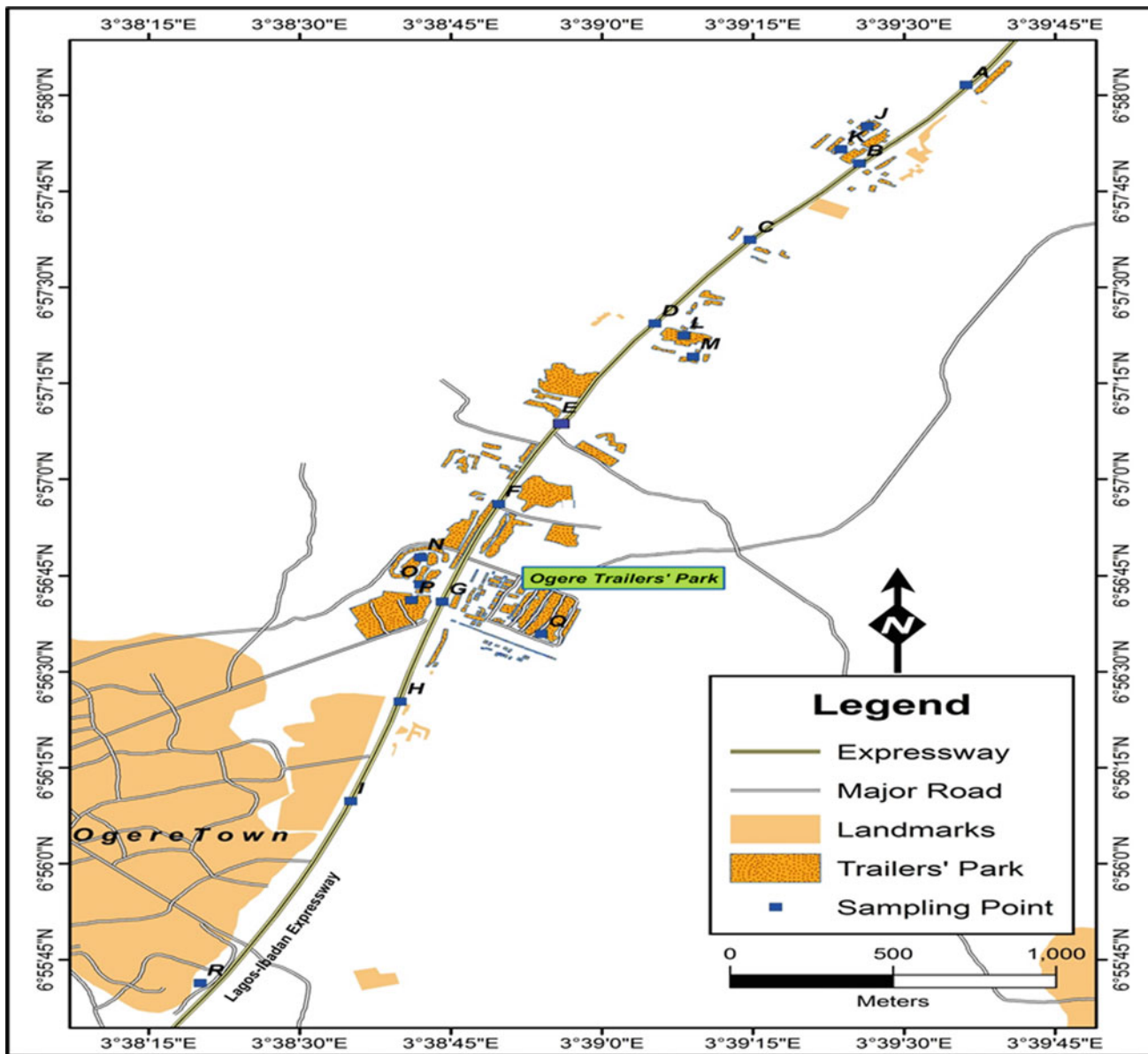


Fig. 1 Map of the Ogere haulage park, Nigeria

Table 1 Heavy metal concentration (mg/kg) in Ogere haulage vehicle park

Metals	Pb	Cd	Cr	Co	Ni	Fe	Cu	Zn	Hg	As
Mean	9.98	0.68	0.89	2.45	1.08	2.53	1.82	18.37	17.66	36.35
Std. Dev	8.23	0.40	0.65	1.63	0.31	1.13	0.72	18.61	16.31	19.02
Control	4.45	0.05	0.60	1.15	0.90	4.16	2.68	3.10	2.97	21.85

Source Author's Fieldwork, 2015

study area, which is characterized by a general lack of vegetation, is located in the moderately hot, humid tropical climatic zone of south-western Nigeria. It has a generally lowland undulating topography belonging to the coastal

sedimentary rocks of western Nigeria. It is important to note that there are several auto-mechanic workshops and several congested mini-garages within the site. All of these activities tend to have pronounced environmental impacts and are in

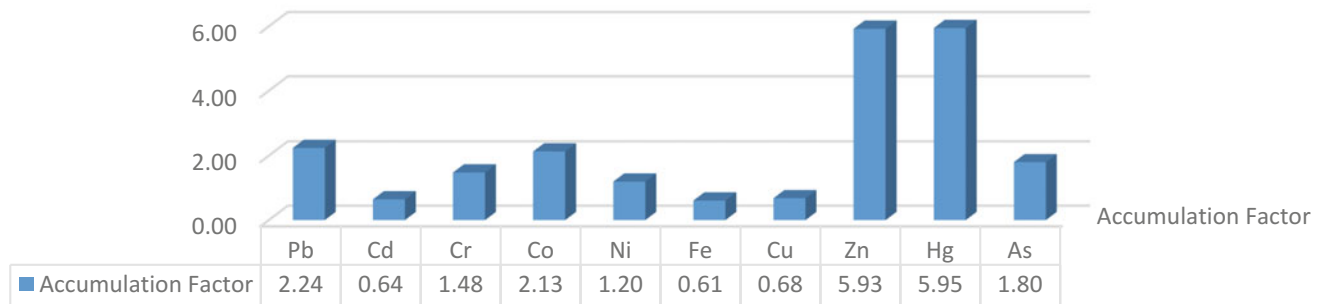


Fig. 2 Variation in accumulation factors of heavy metals at Ogere haulage park, Nigeria *Source* Author's Fieldwork, 2015

part what make the presence of the haulage vehicle park an issue of environmental concern. More often, the waste generated out of vehicle repair is not disposed appropriately. It makes the substances of the wastes come into direct contact with the soil which alter the soil properties.

2 Methods

The sampling points were located within the park itself and along the road in order to compare the distribution of metals and other properties of the soil (Fig. 1). Eighteen soil samples at a depth of 0–20 cm from the soil surface were collected by using a soil auger that had been pre-cleaned with concentrated nitric acid. Samples were collected and analysed in the laboratory by using standard field and laboratory techniques. Accumulation Factor (AF) and Integrated Pollution Index (IPI) were estimated from the concentrations so as to assess the degree of soil contamination with heavy metals.

3 Results

The average concentration of Pb, Cd, Cr, Co, Ni, Fe, Cu, Zn, Hg and As in the study area was 9.98, 0.68, 0.89, 2.45, 1.08, 2.53, 1.82, 18.37, 17.66, and 36.35 mg/kg, respectively. Thus, the trend of metals according to mean concentration is As > Zn > Hg > Pb > Fe > Co > Ni > Cu > Cr > Cd. The variation of the heavy metal concentration was due to the various haulage practices prevalent in the study area. The higher standard deviation reveals higher variations in the heavy metal distributions. While WHO has strict regulations concerning the concentration of the Arsenic in drinking water, the Canadian standard for concentration of Arsenic in agricultural, residential and industrial soil is 30 mg/kg (according to [3]). Consequently, the mean concentration value of As within the study area exceeded the permissible standard for Arsenic in the soil (Table 1).

4 Discussion

The accumulation Factor (AF) was used in the analyses of the soil sampling obtained from the study area. This was done in order to show the mean levels of the concentration of the heavy metals in the study area and their relationship to the levels of the concentration of these metals in the controlled site selected for the study. The analyses revealed Hg > Zn > Pb > Co > As > Cr > Ni > Cu > Cd > Fe in a descending order of concentration (Fig. 2) with Zn and Hg having the highest AF value of 5.93 and 5.95 respectively. This suggests a potential risk to the agricultural use of the land as it affects soil productivity by slowing the rate of the microbial action which causes a retarding of the rate of organic matter breakdown [4].

The IPI analysis was estimated in order to calculate and assess the degree of soil contamination with heavy metals within the study site. The total IPI analysis is in the order of Zn > Hg > Pb with indices as 0.52–20.82, 0.71–14.56 and 0.04–6.02 respectively. It suggests that these three metals have an extreme high pollution (IPI > 5) through making the use of the rating categorization in the studied site. The IPI was classified as;

- IPI < 1 = Low level of pollution
- IPI > 1 < 2 = Moderate level of pollution
- IPI > 2 < 5 = High level of pollution
- IPI > 5 = Extreme high level of pollution

5 Conclusion

The study confirmed that there is a higher concentration of heavy metals in the park compared to the control point where the impact of park activities is not significant. It suggests an intense soil contamination. The study, therefore, confirmed the Ogere haulage vehicle park which is indeed polluted with metals. The indices of contamination considered to be significant in terms of the degree of contamination. This contamination has anthropogenic origins which

point to the activities in the haulage vehicle park. The study is concluded with the significant potential of the negative impacts on the soil in the area as well as the potential risk to the health of the people within the area in case of exposure.

References

1. Hove, M., Ngwerume, E.T., Muchemwa, C.: The urban crisis in Sub-Saharan Africa: a threat to human security and sustainable development. *Stab. Int. J. Secur. Dev.* **2**(1), 7 (2013)
2. Worksafe, V.: Industry standard contaminated construction sites. EPA Victoria. www.Worksafe.Vic.Gov.Au, First Edition. pp. 1–28 (2005)
3. Lee, D.Y., Lee, C.: Regulatory standard of heavy metal pollutant in soil and groundwater in Taiwan. 10–17 (2011)
4. Wuana, R.A., Okieimen, F.E.: Heavy metals in contaminated soils; a review of sources, chemistry, risks and best available strategies for remediation. *Isrn Ecol.* (2011)

Spectroscopic and Chromatographic Characterization of the Composition of Organic Matter in Arid Salt-Affected Soils Under Different Vegetation Cover, Southeastern Tunisia (Gabes and Medenine)

Zohra Omar, Abdelhakim Bouajila, Jalloul Bouajila, Rami Rahmani, Houda Besser, and Younes Hamed

Abstract

In arid Tunisia, particularly in salt-affected soils, studies concerning the soil organic matter (SOM) dynamics and stability are scarce. SOM stability is closely linked to its chemical and molecular composition. This work aims to figure out the SOM composition in arid salt-affected soils, particularly in Lithosols and Solonchaks, under different vegetation cover (sorghum, millet, olive-grove, native vegetation). Ten sites were sampled from 0 to 10 and from 10 to 30 cm depth. SOM composition was assessed at functional group and molecular level by Fourier Transform infrared (FTIR) spectroscopy and Gas Chromatography Mass spectrometry (GC/MS). The results showed that, across all studied soils, the characterization of SOM by FTIR spectroscopy revealed a homogeneous composition. Polysaccharides ($1043\text{--}1032\text{ cm}^{-1}$), aliphatic ($1435\text{--}1432\text{ cm}^{-1}$) and aromatic ($1635\text{--}1621\text{ cm}^{-1}$) groups predominate the SOM's composition at different depths. Those organic compounds, known as relatively recalcitrant, enhance the SOM's stability. The GC/MS data suggest that SOM of the studied soils contains a

higher abundance (up to 30.05%) of mid chain n-alkanes (soil aliphatic fraction). Those molecules which are stable recalcitrant confirm the FTIR finding. Therefore, regardless the soil type and the vegetation cover, the SOM in arid salt-affected soils seems to be recalcitrant and stable. It consolidates the soil's potential to store the green house gases.

Keywords

Soil organic matter composition • FTIR
GC/MS • Arid salt-affected soils • Tunisia

1 Introduction

The SOM's molecular composition is a key factor in understanding soil carbon (C) dynamics because soil atmosphere C fluxes is largely determined by SOM's stability [1]. It depends on the environmental conditions, chemistry of the input material and decomposition processes all of which leave a fingerprint on SOM. It remains that it is significant necessity to enhance our baseline understanding of the SOM compositional variability especially in the world's semi-arid and arid environments [2] where soils have a high potential to sequester organic carbon despite their low stocks on organic matter. In Tunisia, almost studies focus on organic carbon stock changes in relation to soil types and properties [3, 4]. No studies exist on the chemical composition of SOM particularly in salt-affected soils despite they are widespread in the country [5]. As salinity affect the SOM's dynamics, precise comprehension of its composition is required. For this purpose, FTIR spectroscopy [6] and GC/MS [7] are used. The FTIR give insight into the nature of the chemical functions and the GC/MS provide detailed structural information on SOM. Therefore, the objective of this work is to evaluate the stability of SOM in arid salt-affected soils by characterizing its chemical composition by using FTIR and GC/MS.

Z. Omar (✉) · A. Bouajila · H. Besser · Y. Hamed
Research Unit of Geosystems, Georesources and
Geoenvironments (3G), Faculty of Sciences of Gabes,
University of Gabes, 6072 Gabes, Tunisia
e-mail: zohra.omar2012@gmail.com

J. Bouajila
Laboratoire des IMRCP UMR CNRS 5623, Faculté de pharmacie
de Toulouse, Université de Toulouse, Université Paul-Sabatier,
118 route de Narbonne, 31062 Toulouse, France

R. Rahmani
Unité de recherche «Valorisation des biomolécules actives»,
Institut Supérieure de Biologie Appliquée de Médenine,
Université de Gabès, Gabes, Tunisia

H. Besser · Y. Hamed
International Association of Water Resources in the Southern
Mediterranean Basin, Gafsa, Tunisia

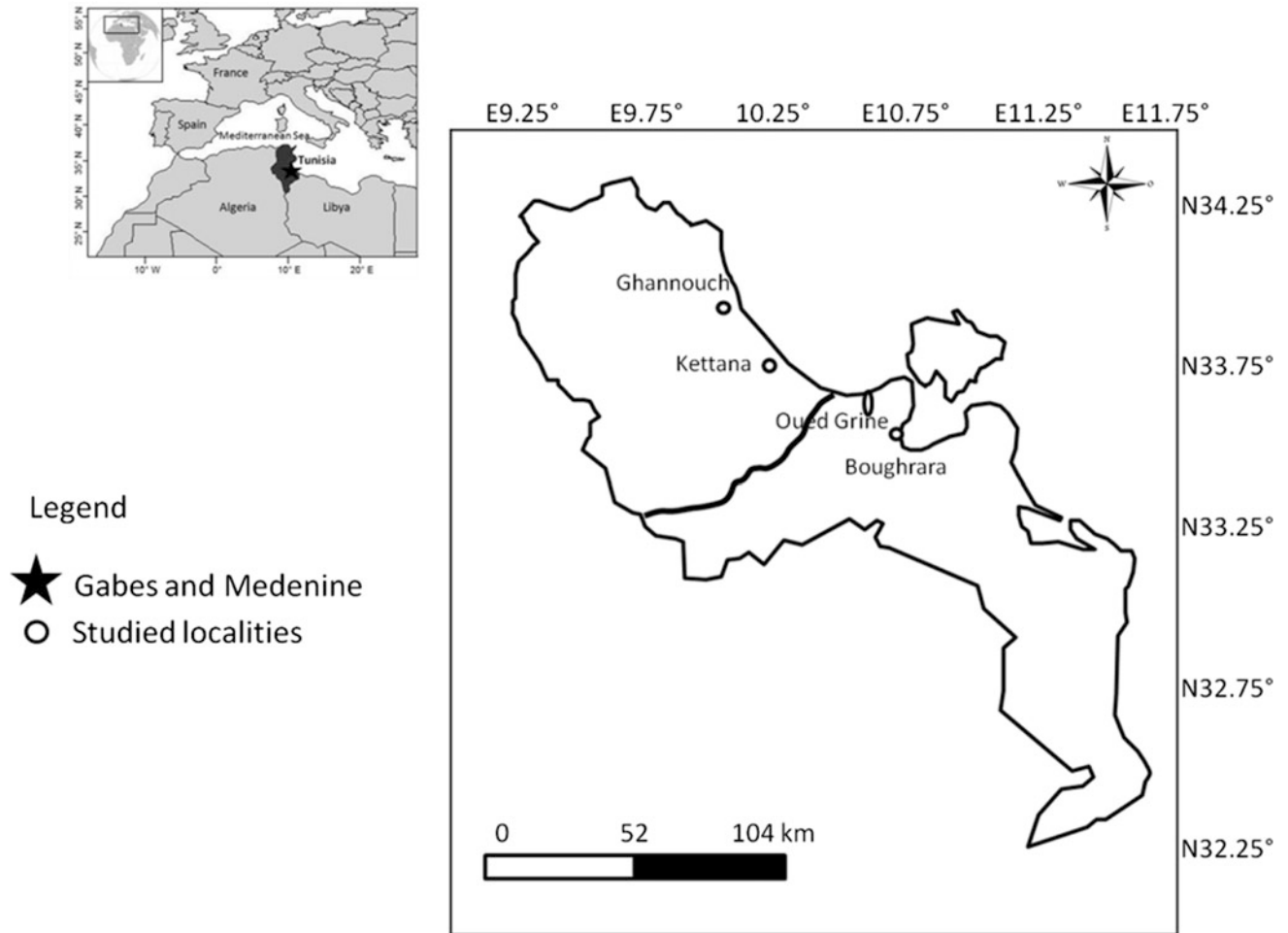


Fig. 1 Localization map of the studied area

Table 1 Mean values of soil physico-chemical properties

Site	Soil/vegetation type	Depth (cm)	Soil properties					
			pH	EC (d Sm ⁻¹)	SOM (%)	Sand (%)	Silt (%)	Clay (%)
Ghannouch	Solonchaks (Sorghum)	0–10	8	8.32	1.23	73	5	14
		10–30	7.98	7.07	1.02	68	2	14
Boughrara	Lithosols (Millet)	0–10	8.13	5.54	0.78	81	9	7
		10–30	8.11	5.06	0.61	80	12	7
Kettana	Lithosols (Olive-grove)	0–10	8.27	3.45	1.01	82	10	6
		10–30	8.27	4.4	0.95	80	11	8
Oued Grine	Solonchaks (native vegetation)	0–10	8.6	158.6	0.65	87	4	3
		10–30	8.5	64.5	0.34	85	4	3

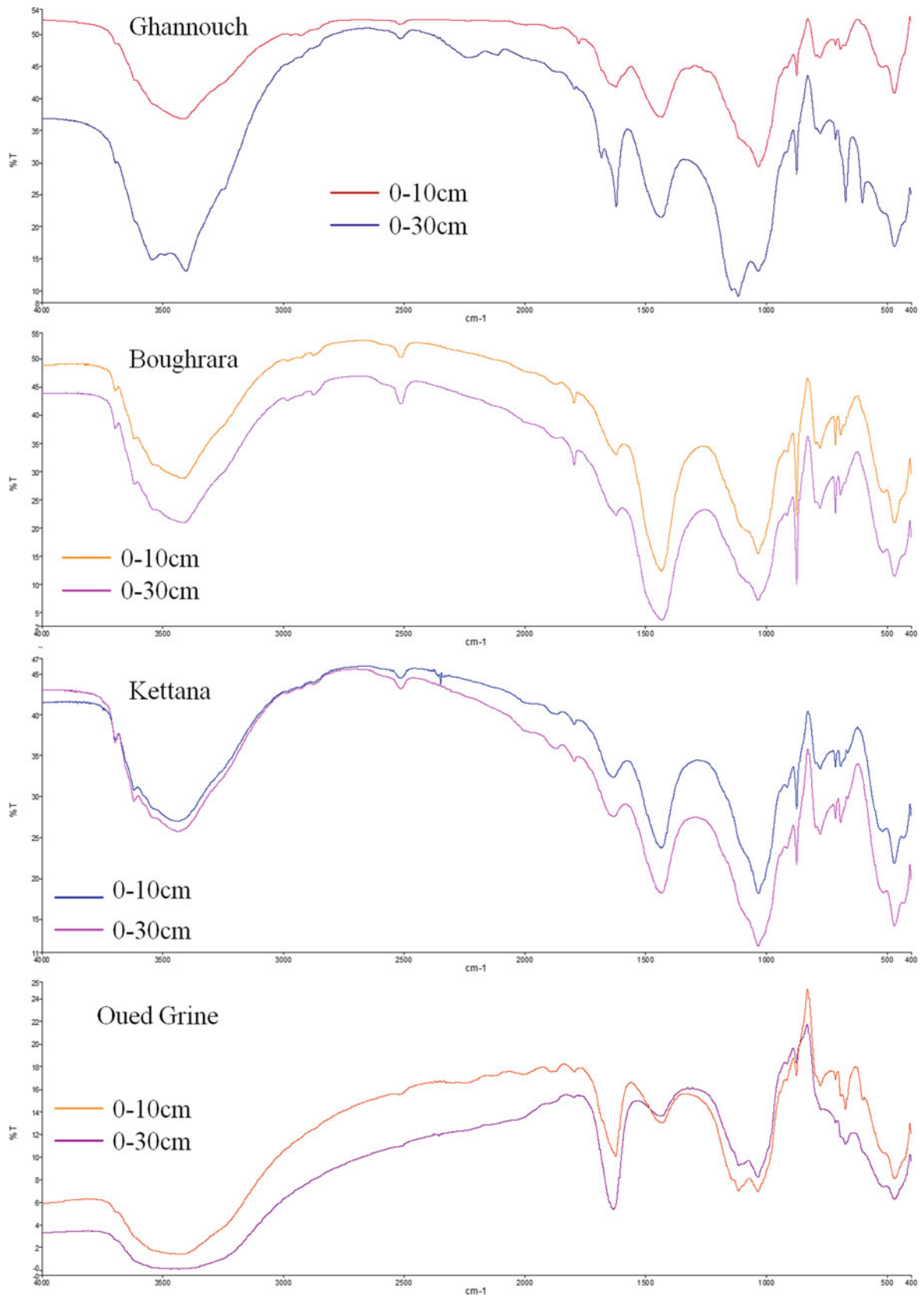


Fig. 2 FTIR spectra of the representative soil samples across all studied soils and depths

2 Materials and Methods

This study was conducted in SE Tunisia in four localities (Fig. 1) developed under an arid Mediterranean climate with different salinity and vegetation cover: Ghannouch (sorghum), Boughrara (millet), Kettana (olive grove) and Oued Grine (native vegetation). The studied soils, which are predominated by Lithosols and Solonchaks and sampled from two depths, are mainly coarse textured soils. Their electrical conductivity (EC) is slightly higher at surface layer. The same trend characterizes the SOM contents (Table 1) [8]. The FTIR spectroscopy was performed on bulk soil samples while the GC/MS characterizes the polar fraction of soil organic compounds.

3 Results

3.1 SOM Functional Groups

All FTIR spectra have a similar pattern, except those of the native soils which are relatively different (Fig. 2). They showed characteristic absorption band patterns in the frequency range of 400–4000 cm^{-1} . CH vibrations of aliphatic groups (3000–2850 cm^{-1}) and C = O stretching absorption bands are only detected in agricultural soils. Absorbance bands assigned to aromatic (1635–1621 cm^{-1}), aliphatic CH_2 (1434–1432 cm^{-1}) and polysaccharides (1043–1032 cm^{-1}) are detected at different depths in all studied soils. Characteristic bands are attributed to Si–O stretching in quartz and inorganic components are also identified.

3.2 SOM's Molecular Composition

Irrespective of the soil type and the vegetation cover, the chromatograms showed a high resemblance in SOM's molecular composition. The recognized molecules were grouped according to frequent source and chemical similarity into mid chain n-alkanes (C14–C19) and ester where their contribution increase with soil depth.

4 Discussion

The Major FTIR absorbance bands across the studied soils showed identical peak position and relatively comparable trends with depth, indicating a relatively similar molecular composition of SOM, which is in agreement with previous works [9]. For all soils, the polysaccharides and the aromatic's relative proportion (RP) decrease with depth as well as the

aliphatic CH deformation except in native soils where their RP increase with depth. The reduction of the polysaccharide with depth may reflect their rapid degradability and their affinity to organic rich layer. The intensification of the salinity at soil's upper layer hampers the microbial activity which explains the abundance of the aromatic and the aliphatic. This fact represents the stabilized and recalcitrant soil's organic components at those layers. Across the studied soils, the SOM seems to be stable. This result is confirmed by the GC/MS analysis that showed a predominance of the SOM by aliphatic-C. Aliphatics are dominated by mid chain n-alkanes, which mainly originate from plant tissues [10], are resistant to microbial degradation [11] because of their recalcitrance reflecting a relatively stable and recalcitrant SOM [12]. Thus, the SOM's composition as revealed by the GC/MS seems also to be stable confirming the finding of FTIR.

5 Conclusion

This work seems to be the first one that evaluates the SOM's composition in arid salt-affected soils of Southeastern Tunisia. FTIR and GC/MS enabled the characterization of the SOM. The SOM's functional composition is dominated by aliphatic and aromatic-C that is relatively recalcitrant compounds. Similarly at a molecular scale, the SOM is predominated by recalcitrant components suggesting that the SOM of arid salt-affected soils is relatively recalcitrant and consequently stable.

References

1. da Silva Oliviera, D.M., Schellekens, J., Cerri, C.E.P.: Molecular characterization of soil organic matter from native vegetation-pasture-sugarcane transitions in Brazil. *Sci. Total. Environ.* **548–549**, 450–462 (2016)
2. Lal, R.: Soil carbon sequestration to mitigate climate change. *Geoderma* **123**, 1–22 (2004)
3. Brahim, N., Brahim, H., Hatira, A.: Tunisian soil organic carbon stock spatial and vertical variation. *Proc. Eng.* **69**, 1549–1555 (2014)
4. Bouajila, A., Brahim, N., Gallali, T.: Rôle des différentes fractions organiques dans la stabilité structurale des sols à textures riches en sables du Nord et du Centre de la Tunisie. *Etude et Gestion des Sols* **23**, 77–90 (2016)
5. Hachicha, M.: Les sols sales et leurs mises en valeur en Tunisie. *Sécheresse* **18**(1), 45–50 (2007)
6. Yan, N., Marschner, P.: Response of microbial activity and biomass to increasing salinity depends on the final salinity, not the original salinity. *Soil Biol. Biochem.* **53**, 50–55 (2012)
7. Derenne, S., Quénéa, K.: Analytical pyrolysis as a tool to probe soil organic matter. *J. Anal. Appl. Pyrolysis* **11**, 108–120 (2015)

8. Omar, Z., Bouajila, A., Bouajila, J., Rahmani, R., Besser, H., Hamed, Y.: Soil organic matter chemical characterization and molecular composition from arid salt-affected soils under different vegetation cover from Southeastern Tunisia- A FTIR and GC/MS study. *Geoderma* (2018). Submitted
9. Dhillon, G.S., Gillespie, A., Peak, D., van Rees, K.C.J.: Spectroscopic investigation of soil organic matter composition for shelterbelt agroforestry systems. *Geoderma* **298**, 1–13 (2017)
10. Tegelaar, E.W., Hollman, G., Vandervegt, P., De Leeuw, J.W., Holloway, P.J. : Chemical characterization of the periderm tissue of some angiosperm species-recognition of an insoluble nonhydrolyzable aliphatic biomolécules (suberan). *Org. Geochem.* (23), 239–251 (1995)
11. Stewart, C.E., Neff, J.C., Amatangelo, K.L., Vitousek, P.M.: Vegetation effects on soil organic matter chemistry of aggregate fractions in a Hawaiian forest. *Ecosystems* **14**, 382–397 (2011)
12. Wang, T., Camps-Arbestain, M., Hedley, C.: Factors influencing the molecular composition of soil organic matter in New Zealand grasslands. *Agr. Ecosyst. Environ.* **232**, 290–301 (2016)

Soil Salinity Dynamic and Water Quality in a Ramsar Saline Inland Wetland: Case Study—Bazer-Sakra Sabkha, Setif (North-East Algeria)

Yacine Louadj, Ahcene Semar, Salah Belghemmaz, Nasser-Eddine Soualili, and Nazim Soualili

Abstract

Salinization affect ecosystem to a level where it cannot provide environmental services to its full potential. Therefore, understanding the dynamics of salt in the soil and the quality of water resources is of utmost importance. The aim of this study is the assessment of the dynamic of soil salinity and the quality of water (saline lake, groundwater) in RAMSAR wetland (Bazer-Sakra sabkha: northeastern Algeria). 6 water samples were sampled in April 2016) and 8 soil profiles sampled at three depths (0–20 cm, 20–40 cm; 40–60 cm) across a toposequence in April 2016 and 2017. The results show that groundwater r samples range from saline to very saline. The saline lake presents a high risk of eutrophication because of its high nitrate (128 mg/L) and phosphorus (1031 mg/L) content. For soil salinity, the results reveal two patterns of evolution in salinity profile. The first one is an evolution from shape B (High salinity in the middle) in 2016 to a salinity profile of Shape A (Ascending) in 2017. The second pattern is an evolution from a descending salinity profile (shape C) in 2016 to an ascending salinity profile (Shape A) in 2017.

Keywords

Soil salinity dynamic • Water quality • RAMSAR Inland wetland • Bazer-Sakra sabkha

1 Introduction

Salinization is the accumulation of water-soluble salts in the soil solum (the upper part of a soil profile, including the A and B horizons) or regolith to a level that impacts on agricultural production, environmental health, and economic welfare [1]. In general, salinization develops in places where the following conditions occur together: presence of soluble salts, high water table, high rate of evaporation and low annual rainfall [2]. It is projected that soil salinization is likely to be increased with future climate change scenarios like sea level rise and impact on coastal areas and rise in temperature that will subsequently increase evaporation and salinization [2]. The knowledge of soil salinity and the temporal changes of its distribution in the soil profiles can give warnings for the protection of saline habitats [3]. In this respect, the aim of this study is to understand the dynamic both in space and time of soil salinity and to assess the quality of surface water (the lake) and groundwater of the bazer-sakra saline wetland (Northeastern Algeria).

Y. Louadj (✉) · S. Belghemmaz · N.-E. Soualili
Department of Agronomic Sciences, Faculty of Life and Natural Sciences, Ferhat Abbas University, 19000 Sétif-1, Algeria
e-mail: louadj.y@univ-setif.dz

Y. Louadj · A. Semar
Department of Soil Science, Higher National Agronomic School (ENSA), 16000 Algiers, El-Harrach, Algeria

S. Belghemmaz
Valorization of Biological and Natural Resources Laboratory, Faculty of Life and Natural Sciences, Ferhat Abbas University, 19000 Sétif-1, Algeria

N. Soualili
Department of Earth Sciences, Institute of Architecture and Earth Sciences, Ferhat Abbas University, 19000 Sétif-1, Algeria

2 Materials and Methods

2.1 Description of the Study Area

Bazer-Sakra Sabkha is located in south-east of the province of El-Eulma (Sétif), in the East of Algeria. The Wetland is characterized with semi-arid climate. It is a permanent endorheic saltwater depression fed by rainwater, domestic and industrial wastewater carried by three tributaries from the nearby town of El Eulma. The wetland consists of three

Table 1 Analytical results of the groundwater samples (April 2016)

Samples	Depth (m)	pH *	EC ₂₅ * (dS/m)	Calcium (mg/L)	Chloride (mg/L)	Nitrates (mg/L)	Phosphorus (mg/L)
1	17	7.19	3.02	162.7	1420	2.652	0.793
2	107	7.48	1.22	29.85	1420	5.608	0.996
3	14	7.8	1.92	88.176	1065	6.913	0.961
4	175	7.5	2.53	76.95	1420	2.217	1.108
5	10	7.78	5.75	89.77	2130	11.782	0.540
6	12	7.83	9.66	158.71	3550	7.869	0.4

Table 2 Salinity profile dynamic (2016/2017)

	EC s.p *(2016) dS/m	EC s.p (2017) dS/m
Soil profile 1	0.484 7.856 3.995	2.38 1.18 1.44
Soil profile 6	0.957 2.673 9.447	0.729 0.545 0.624

*ECs.p: electrical conductivity of saturated paste extract

areas; the flooded central part which is devoid of vegetation. It extends along Oued El Melah. Its peripheral belt is plenty with sparse vegetation on which cattle and sheep graze. Added to that the saline wetland hosts more than 1% of the common shelduck's biogeographic population showing the importance of saline conditions for some wintering species (Ramsar 2004). According to soil taxonomy classification (2004), the soils of the wetland are mainly composed of saliorthid (northern and south of the sabkha) and calciorthid (western part of sabkha).

2.2 Sampling and Laboratory Analysis

7 Water samples had been taken from the lake or its nearby wells during the first year of the investigation (April 2016). These water samples have been characterized by measuring the Electrical conductivity EC (dS/m), pH (potentiometric method), calcium content (complexometric titration), the chloride concentration (Mohr Method) and Nitrate and Phosphorus (spectrometric measurement). 8 soil profiles have been sampled for two successive years (April 2016 and April 2017) across a toposequence N- S according to 3 sampling depths: H1 (0–20 cm), H2 (20–40 cm) and H3 (40–60 cm). The soil salinity have been assessed in this work by means of electrical conductivity (EC) with the reference method (saturated paste extract)

3 Results and Discussion

3.1 Water Quality Characterization

The results show that pH of lake water is very alkaline with a value of 9.15. Its salinity is very high with EC of 56.24 dS/m. The water of the lake reveals a high concentration of lake water with Nitrate (NO₃⁻) and phosphorus (PO₄) which are of 128 mg/L and 1031 mg/L, respectively. For the groundwater, the results of the EC and pH are summarized in the Table 1. We notice that the pH of groundwater range from 7 to 19 (S** 1) and to 9.12 (S** 4). Generally, the groundwater is slightly alkaline. The EC of these groundwater vary from 1.22 dS/m (S** 2) to 9.66 dS/m (S** 6). According to Ayers and Westcot [4], the Salinity of the groundwater is classified as follows: High salinity C3 (S** 2 et 3) and very high salinity C4 (S** 1, 5, 6 et 6).

The results show that the calcium content varies from 29.85 mg/l (S**2) to 162.7 mg/l (S**1). On the other hand, the chloride content ranges from 1065 mg/l (s**3) to 3550 mg/l (s**7). Finally, the Nitrate and Phosphorus content in the groundwater show that nitrates vary from 2.217 mg/L (S**4) to 11.78 mg/L (S **5) while the phosphorus content is lower and varies from 0.4 mg/l (S** 6) to 1.108 mg/l (S** 4).

3.2 Spatio-Temporal Variation of Soil Salinity

Salinity profile allows us to distinguish 3 trend of salinity changes with depth along the toposequence N-S. In general, the shapes of the salinity profile are: shape A (Ascendant) maximum of salinity in the surface, Shape C (descendent) whereby the maximum of salinity is in the depth, and shape B (maximum of salinity in the middle of soil profile). The overall trend in salinity profile dynamics between the two period show two patterns of evolution which are represented by the soil profile 1 and 6 (Table 2).

The Table 2 shows that the salinity profile 1 (2016) is of shape B with a maximum of salinity 7.85 dS/m at the middle of the soil profile (20–40 cm). On the other hand, the salinity profile 1 (2017) is of shape A with a maximum of salinity at the soil surface (0–20 cm) and (2.38 dS/m). However, for the salinity profile 6, the results show that the salinity profile (2016) corresponds to shape C (descending) with a maximum of EC (9,447 dS/m) at the depth (40–60 cm). On the other hand, the salinity profile (2017) is of shape A (Ascending) with a maximum of salinity at the soil surface (0–20 cm) (0.729 dS/m).

4 Discussion

The groundwater nearby the wetland is very high in soluble salts, alkaline, and calcium content. The obtained results in this study are similar to those found by Demdoum et al. [5] in the same saline wetland. There is a danger of eutrophication of the lake because of high concentration of nitrate and phosphorus. It is due to sewage and fertilizer's contamination of the lake from the city of Eulma and from the agricultural land uphill as well.

Soil salinity dynamics associated with time factor reveal a different trend despite the fact that the sampling has been done in the end of the humid season where there should be a maximum leaching of the salt. Other factor can explain this dynamic, namely, by land cover, micro-relief, water and clay content [3, 6].

5 Conclusion

This work as it is carried out on the soil salinity dynamic and water quality in an inland saline wetland (Bazer-Sakra) allowed us to show that the salinity of groundwater and eutrophication of saline lake can be detrimental to biodiversity and agriculture in its neighborhood. Irrigated crops in this region may increase the risk of salinization if specific practices (leaching and drainage) are not adopted.

References

1. Rengasamy, P: World salinisation with emphasis on Australia. *J. Exp. Bot.* **57**(5), 1017–1023 (2006)
2. Shahid, S.A., Abdelfattah, M.A., Taha, F.K.: *Developments in Soil Salinity Assessment and Reclamation Innovative Thinking and Use of Marginal Soil and Water Resources in Irrigated Agriculture*. Springer, New York (2013)
3. Herrero, J., Castaneda, C.: Temporal changes in soil salinity at four saline wetlands in NE Spain. *Catena* **133**, 145–156 (2015)
4. Ayers, R.S., Westcot, D.W.: *Water quality for agriculture*. In: *FAO Irrigation and Drainage Paper 29*, 2nd edn. Food and Agriculture Organization, Rome (1994)
5. Demdoum, A., Hamed, Y., Feki, M., Hadji, R., Djebba, M.: Multi-tracer investigation of groundwater in El Eulma Basin (northwestern Algeria), North Africa. *Arab. J. Geosci.* **8**(5), 3321–3333 (2015)
6. Tanji K.K., Yaron B: *Management of Water Use in Agriculture*. Springer (1994)

Impact of Catchments Morphology and Lithology on Stream Channels System in High Mountains of Arid Zone (Example of High Atlas, Morocco)

Elżbieta Rojan, Maciej Dłuzewski, Joanna Rotnicka, Kazimierz Krzemien, Lukasz Kokosinski, and Ewelina Niklas

Abstract

Several factors control the morphodynamics of stream channels in high mountains of arid zone. The aim of the paper was to analyze the relation between stream channels system, catchment morphology and lithology based on examples of three small catchments of ephemeral streams that are tributaries of the Dades River (High Atlas, Morocco). The research included analysis of the topographic and the geological maps, LANDSAT, Google Earth images and the geological and geomorphological field survey. The results showed that the drainage density is strongly controlled by lithology. In the catchment built of conglomerates, the density of stream channels is almost one and a half time greater than in catchments built of limestones and almost twice as large if we take into account only initial channels. Tectonics impacts the stream density to a lesser extent. Two catchments built of limestones which are strongly fissured due to joint system and some faults are characterized by much lower drainage density than the catchment built of conglomerates where signs of discontinuous deformation are sparse. The stream channels of high-order formed in conglomerates are wide and low-gradient, whereas the initial and the first-order channels are narrow, deep, and closely spaced. In catchments built of limestone, the relation is reverse.

Keywords

River channels system • Catchments morphology • Catchments lithology • High Atlas • Arid zone

1 Introduction

Although the annual rainfall in the arid zone is very small, the river channels are shaped during episodic flood events driven by high rate rainfall. Other important factors controlling the morphodynamics of river channels in high mountain regions include catchment morphology, lithology, tectonic and structural setting which control the type of the river channels and their structures [1]. In regions of arid zones, where there is no plant cover or it is of low density, these factors are particularly important [2].

The Upper Dades catchment located in Moroccan High Atlas is an excellent example of a catchment in the high mountain region of arid zone. The average long-term precipitation ranges here from 150 mm/year at the Boumalne (1526 m a.s.l.) to 203 mm/year at the Msemrir (2000 m a.s.l.) weather stations [3]. Almost all streams in this catchment are active episodically, usually several times a year, mainly in autumn (September and October) and spring (from February to April). Research carried out within northern and southern part showed that this river channel system is significantly modified at a recent time [3].

The aim of the research was to analyze the structure of the channels network within three small catchments of arid zone in relation to their morphology and lithology.

2 Settings and Methods

Taking into account the environmental features of the Upper Dades catchments, topographic maps (on a scale of 1:50 000 and 1:100 000), LANDSAT-8 and Google Earth images and DEMs, three small catchments of ephemeral streams that are

E. Rojan · M. Dłuzewski (✉) · L. Kokosinski
Faculty of Geography and Regional Studies, University
of Warsaw, Krakowskie Przedmieście 30, 00-927 Warsaw, Poland
e-mail: dłuzewski@uw.edu.pl

J. Rotnicka · E. Niklas
Institute of Geology, Adam Mickiewicz University in Poznań,
Bogumiła Krygowskiego 12, 61-680 Poznań, Poland

K. Krzemien
Institute of Geography and Spatial Management, Jagiellonian
University, Gronostajowa 7, 30-387 Kraków, Poland

Table 1 Catchments and stream channels morphology

Parameter, Indicator	Symbol	DAD1	DAD2	DAD3
Catchments				
Drainage area	A (km ²)	22.73	2.95	7.39
Perimeter	L _p	23.33	8.36	14.32
Maximum elevation	H _{max} (m a.s.l.)	2164	2455	2887
Minimum elevation	H _{min} (m a.s.l.)	1573	1720	2055
Relative elevation	ΔH (m)	591	735	832
Length	L _p (km)	9.23	3.46	6.11
Effective width	R _b (km)	2.46	0.85	1.21
Form factor	F _f (-)	0.27	0.25	0.20
Shape factor	R _s (-)	3.75	4.06	5.05
Elongation ratio	R _e (-)	0.58	0.56	0.50
Average slope	R (°)	3.66	11.99	7.76
Channels				
Total streams length	L _s (km)	198.94	17.92	39.38
Drainage density	D (km/km ²)	8.75	6.07	5.33
Length of main channel	L _k (km)	9.37	3.38	7.41
Gradient of main channel	R _k (‰)	73	254	128
Sinuosity of main channel	S (-)	1.18	1.21	1.26
Tributaries per 1 km of main channel	(-)	2.05	0.86	2.03

tributaries of the Dades river have been selected for the research. These were: (i) lower catchment DAD1, (ii) middle catchment DAD2 and (iii) upper catchment DAD3 (Table 1).

The hierarchical classification of the stream channels network was carried out according to the Strahler's stream order [4]. For the purpose of the work, the classification has been extended to a "0" order that represents very numerous initial streams. Parameters of the river channels and the catchment morphology were determined on the basis of the results of the field works as well as on the Google Earth images and DEMs developed for each of the studied catchments (DAD1–3). Lithology of the catchments was identified by means of the geological maps (on a scale of 1:50 000 [5]) and verified by field works and microscopic analysis of collected rock samples.

3 Results

3.1 Catchments and Stream Channels Morphology

The largest catchment DAD1 is characterized by the lowest average slope and greatest drainage density contrary to other studied catchments (Table 1). Form factor (F_f) achieves similar and generally small values suggesting elongated shape of the studied catchments. It is also confirmed by relatively small values of elongation ratio (R_e). As for the

mountain regions, the main channel gradient of the catchment DAD1 is relatively small. The channel gradient of the catchment DAD3 is twice as large as DAD1. The catchment DAD2 is four times larger than DAD1 (Table 1). The largest channel gradients (up to 1200‰) are observed in short, up to 1 km long, initial or first-order channels.

The results showed that drainage density decreases as the channel-order increases. The exception is the middle catchment DAD2 where the density of the third-order channels is greater than the density of the second-order channels. In all studied catchments, the percentage of 0-order channels is high and varies between 43.6 and 47.6%.

3.2 Catchments Lithology

The largest catchment DAD1 is mainly built of Neogen massive conglomerates cemented by calcium carbonate. The components of the grain framework are well rounded with a mean particle size of 15 cm. The uppermost part of the catchment is dominated by layered micritic limestones of the lower Jurassic age whose structure is responsible for graded profiles of both the river bed and banks.

The catchment DAD2 is built of lower Jurassic massive and locally undulated limestones interbedded with marlstone. Rocks are strongly fractured due to a joint system which is visible on layer surfaces exposed in the bed rock channel. It consists of two joint sets. They are perpendicular

to each other and to the layering causing blocky disintegration of rocks. It leads to the formation of steep stream banks that favor gravity mass movements and supply of angular blocks (of size up to boulders) into the channels. The dip angle of the layers varies along the channel due to numerous faults and folds.

The catchment DAD3 is dominated by oolitic, onkolitic and bioclastic limestones of the middle Jurassic age. Marlstones interbedding limestones are in minority. The differentiation of the rock types, their thickness and structures combined with monoclinical inclination of strata and folds are responsible for uneven longitudinal channel profiles.

4 Discussion and Conclusion

The streams of high mountains in dryland landscapes are of episodic nature of flow and sediment transport. They are characterized by high dynamics of channels which is strongly influenced not only by climate and hydrology but also by catchment morphology and lithology [1]. The resistance to down-cutting of the stream channels is controlled by lithology and rock structure. All these factors impact drainage pattern, channel cross-section, channel gradient, planform and longitudinal profile.

The analyzed stream channels system is strongly controlled by lithology. It is proved by high density of stream channels in the catchment DAD1, built predominantly of rocks of low resistance to physical weathering. In comparison with it, the stream channel densities in the catchments DAD2 and DAD3, built mainly of massive and layered limestones, are significantly lower. It seems that tectonics impacts the stream channels system to a lesser extent. The highest drainage density is recorded in the DAD1 catchment where signs of discontinuous deformation of conglomerates are rare. Contrary to it, rocks in the catchments DAD2 and DAD3 are strongly fissured due to joint system and faults but the drainage density is much lower than in DAD1.

Longitudinal channel profiles and gradient are controlled by lithology, dip angle and azimuth of layers and the nature of tectonic deformation. High-order channels of the catchment DAD1 are wide and of a low-gradient. The channel bed and partly the channel banks are covered by pebbles and cobbles. However, low resistance of conglomerates to physical weathering causes the covering of the valley slopes with thick regolith which, in turn, is not very resistant to fluvial erosion. Therefore, the 0- and the first-order channels are here narrow, deep, and closely spaced. Contrary to DAD1's channels, the gradient of the high-order channels in the DAD2 and DAD3 catchments is strongly influenced by the dip of limestone layers. As the regolith formed on valley slopes is here much thinner, the 0- and the first-order channels are broad and shallow. Their banks are often difficult for identification.

Acknowledgements This work was supported by the Polish National Science Centre, project No. 2011/01/B/ST10/07295.

References

1. Tooth, S., Nanson, G.: Distinctiveness and diversity of arid zone river system. In: Thomas, D.S.G. (ed.) *Arid Zone Geomorphology: Process, Form and Change in Drylands*, 3rd edn, pp. 269–300. Wiley (2011)
2. Stokes, M., Mather, A., Belfoul, M., Faik, F., Bouzid, S., Geach, M., Cunha, P., Boulton, S., Thiel, C.: Controls on dryland mountain landscape development along the NW Saharan desert margin: insights from quaternary river terrace sequences (Dadès River, South-central High Atlas, Morocco). *Quat. Sci. Rev.* **166**, 363–379 (2017)
3. Dłużewski, M., Krzemień, K., Rojan, E., Biejat, K.: Stream channel development in the southern parts of the High Atlas Mountains, Morocco. *Geografija* **49**(1), 10–21 (2013)
4. Strahler, A.: Hypsometric (area-altitude) analysis of erosional topology. *Geol. Soc. Am. Bull.* **63**(11), 1117–1142 (1952)
5. Danielli, P.: *Geological Map of Boumalne 1: 50,000*. Ministère de L'Énergie et des Mines, Direction du Développement Minier, S. E. L. C. A. Florence, Italie (2007)



Classification and Prediction of Channel Morphology Within Selected Third-Order Basins (Southwestern Nigeria)

Adeyemi Oludapo Olusola, Olutoyin Adeola Fashae, and Adetoye Faniran

Abstract

Process-form interactions as a means through which classification and prediction are better presented across river systems have received attention in mountainous regions and extra-tropical areas with (non) glacial history. However, in the low-relief areas without glacial history, detailed descriptions of basins are not as popular and widely presented as their counterparts in other climes. This research seeks to classify and predict river systems by using the Rosgen and Montgomery and Buffington framework. Seventeen third-order basins were extracted from digital elevation models (DEMs). They were validated by using topographical maps. Ten basins were picked systematically. Six were randomly selected out of them. Eighteen morphological variables using standard procedures and hydraulic equations were measured and derived at bankfull. Alongside, domains were identified and described within each basin. Step-wise discriminant analysis was performed on the entire dataset in order to identify the variables that can successfully classify the channel types. The result produced three dominant explanatory variables which are cross-sectional area, hydraulic radius and width ($CA-W-HR$). These variables successfully predicted 53% of the domains across the dataset. Hierarchical cluster analysis was performed by using $CA-W-HR$. The iteration produced five distinct groups: plane-bed-bedrock channels, partly-confined mixed channels, partly-confined bedrock channel, unconfined alluvial channels and partly-confined mixed channels void of step-pools.

Keywords

Process-form • River systems • Low-relief Mixed channels and Discriminant analysis

1 Introduction

Process-form dynamics refer to interrelationships between river morphological variables such as discharge, velocity, depth and width. It helps in the understanding and management of the rivers and their ecosystems. Process-form explanations are achieved through classification and prediction of process domains. Little or no morphological data exists on domain classes within low-relief settings of humid tropics which hinders the interpretation of the fluvial dynamics. The interactions of the processes and forms are both diverse and profound. Interrogating process-form dynamics becomes cumbersome because of the long time periods required to carve out an entire drainage basin. Hence, the geomorphologists have studied useful small-scale natural watersheds of lower orders in pristine settings and in laboratory flumes [1]. Process-Form dynamics can be investigated at the basin, at reach scale or at both scales depending on the nature of the study. Therefore, the aim of this study is to identify, classify and predict the process domains within third-order basins of Upper Ogun River Basin, Southwestern Nigeria. The Upper Ogun River Basin (UORB) provides a unique attempt to study across varying spatial scales with full characterization of the river channels which to a large extent presents an opportunity to understand the dynamics within the process-form relationships.

2 Study Area

The Ogun River basin is located in Southwestern Nigeria within the latitudes of 6° 26'N and 9° 10'N and the longitudes of 2° 28'E and 4° 8'E. This study is carried out within the Upper section of Ogun River generally called Upper Ogun River

A. O. Olusola (✉) · O. A. Fashae · A. Faniran
Department of Geography, University of Ibadan, Ibadan, Nigeria
e-mail: ao.olusola@mail.ui.edu.ng; olusolaadeyemi.ao@gmail.com

Basin (UORB). UORB (Fig. 1) constitutes the main body of the Ogun River Basin. It includes the Oyan-Ofiki river system. The confluence of the Oyan and Ogun rivers marks the boundary between the Upper-Central Basin to the north and the Lower Basin to the south. The relief is generally low. It rises gradually towards the northern part of the basin (Fig. 1). The geology of the study area is described as a rock sequence that starts with the Precambrian Basement and which consists of quartzites and biotite schist. The UORB is underlain by the metamorphic rocks of the Precambrian basement complex [2, 3]. The great majority of which are very ancient in age. This basement complex shows great variations in grain size and in mineral composition. The rocks are quartz, gneiss and schist consisting essentially of quartz with small amounts of white micaceous minerals. The remaining sections are composed of crystalline rocks of the basement complex. They consist mainly of folded gneiss, schist and quartzite complexes which belong to the older intrusive series. The Ogun River takes its source at an elevation of about 530 m above mean sea level and flows directly southwards over a distance of about 480 km before it discharges into the Lagos lagoon.

3 Methodology

Third-order basins were extracted from the shuttle radar thematic mapper (SRTM) with digital elevation data (30 m) by using ArcHydro tools in ArcGIS 10.2. they were validated by using the topographical maps (1:50,000). The basins were overlaid on geological maps covering the Upper Ogun Basin; Saki (1:250,000) and Ibadan (1:250,000) by using ArcGIS 10.2. Ten basins were systematically selected (areas with more than two lithological units (migmatites, granites and schists)) out of which six were randomly selected for the study. Eighteen river morphological variables were measured and derived at bankfull by using standard field procedures and hydraulic equations respectively across eighty-three (83) reaches within the six basins (Ogboro, Igboburo, Awon, Onikoko, Odo-Oba and Ayin). Normality test was performed on the entire variables with transformation where necessary after which they were analyzed by using descriptive statistics, step-wise discriminant analysis and agglomerative hierarchical cluster analysis by using Ward's linkage.

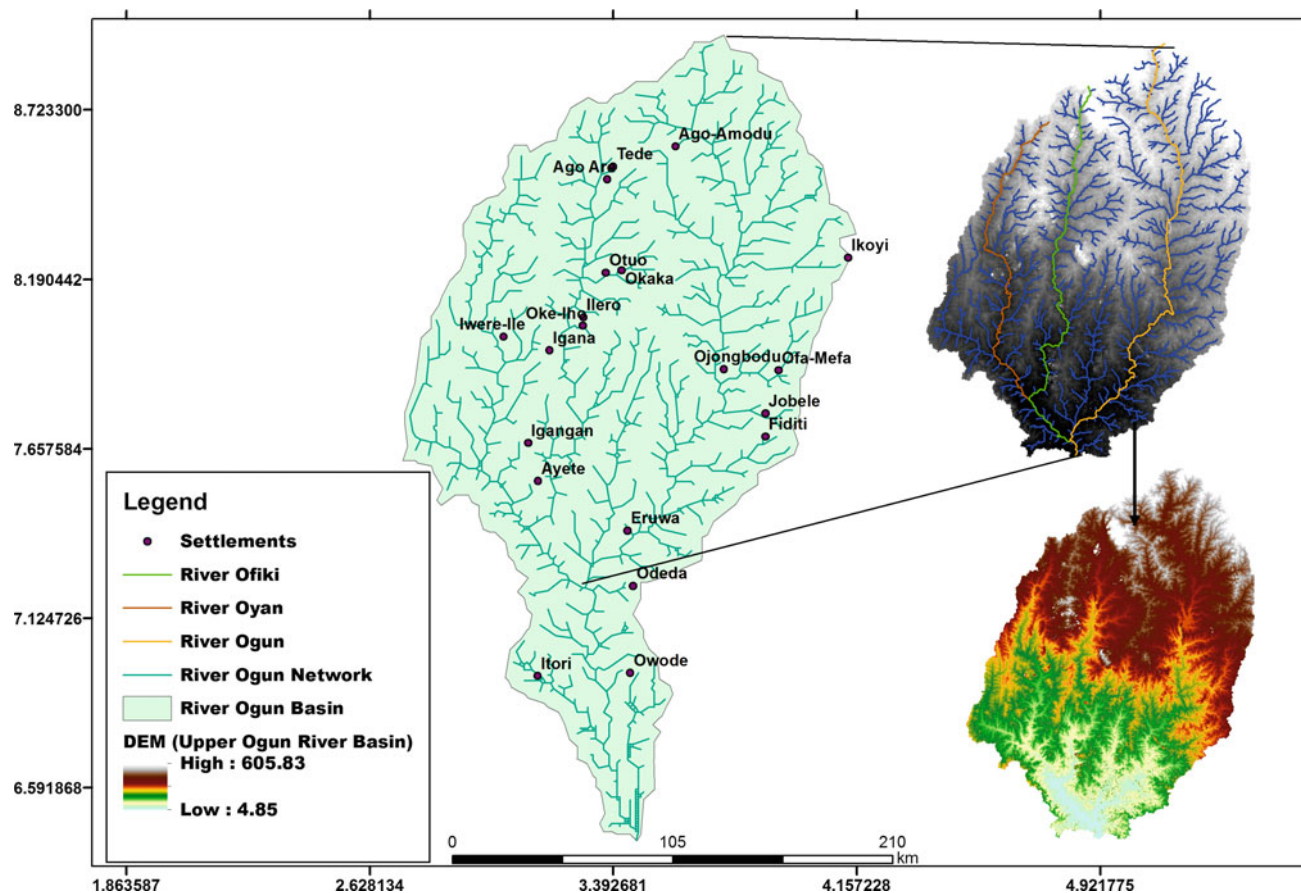


Fig. 1 Map of Ogun River Basin showing Upper Ogun extent and DEM. Source: [7]

4 Results and Discussion

River classification can be used to understand and predict sediment input, transport and storage, as well as ecological structure along and within stream segments [4]. Domain types were identified and mapped by being based on existing categories [5, 6] across the lithological units revealing a total of 42 plane-bed reaches (17 on granite, 13 on schist and 12 on migmatite); 13 pool-riffle reaches (2 on granite, 6 on schist and 5 on migmatite); 6 step-pool reaches (1 on granite, 1 on schist and 4 on migmatite) and 22 bedrock reaches (8 on granite, 1 on schist, and 13 on migmatite). In predicting channel types within the Upper Ogun River Basin, step-wise discriminant analysis was conducted on the entire dataset to determine the subset of morphological variables that best discriminate between channel types (Table 1).

The variables retained in the analysis are cross-sectional area (CA), hydraulic radius (HR) and width (W). These variables (CA–HR–W) successfully predicted and identified domains across the entire dataset with an error rate that is less than 48%. Eighty-six percent of the plane-bed reaches were correctly classified (14% incorrectly classified as pool-riffle reaches). Fifteen percent of pool-riffle reaches were correctly classified (17.7% were incorrectly classified as step-pool reaches and 77% incorrectly classified as plane-bed reaches). Fifty percent of step-pool reaches were correctly classified (16.7% incorrectly classified as pool-riffle reaches and 33.3% incorrectly classified as plane-bed reaches). Hundred percent was correctly classified as bedrock reaches. The F tests ($F < 0.005$; $\lambda > 0.75$) indicated that the cross-sectional area is by far the most significant dominant controlling variable. The explanatory variables identified in this study suggests that in attempting to predict channel types, functions developed are sensitive to individual channel types and specific stream reaches [see 4, 8, 9]. Having identified the three-dominant classification functions (Table 1), hierarchical cluster analysis was performed by using these three variables. The final number of

clusters distinguished was determined by being based on statistical analysis interpretations already discussed as well as the physical understanding of the region. Agglomerative hierarchical clustering with Ward's linkage [see 8] illustrated the clustering structure of the 83 studied reaches. The first split of cluster occurs at a distance of 20 distinguishing between largely ephemeral streams with high width–depth ratio and perennial streams with low width–depth ratio. Splitting groups at a distance of 10 produced 5 distinct groupings which are clear reflection of the overall picture of dominant reached-bed configuration present within Upper Ogun River Basin. The five distinct domain clusters produced are: M1e (Plane-bed-Bedrock channel); M5e (Partly confined mixed channel); B1 (Partly confined Bedrock channel); E5b (Unconfined Alluvial channel) and E (Partly confined mixed channel void of step-pools).

5 Conclusion

In classifying and identifying controls on the channel morphological types, the overall discriminant function is significant in that it does a good job of classifying the channel types. The entire data from the six third-order basins within Upper Ogun River Basin was used to explore the dynamics in reach-scale channel morphology. Domain clusters operating within low-relief settings of humid tropical climes are distinguished by being based on the magnitude of their width–depth ratio. Specifically, the identified discriminant variables suggested that landscape evolution and spatial distribution of domains within low-relief settings of humid tropics are closely linked to the interplay of the channel properties and geometry. The domain clusters presented a fundamental approach to compare process-form dynamics in low-relief settings and extra-tropical climes. In essence, the study presented a unified channel typology that explicitly links lithology, hydrology and reach-scale domain process. Finally, the ability to accurately predict and classify channel types has important implications for interdisciplinary studies in earth and environmental studies such as ecology, ecohydrology, hydro-geomorphology, water resources management, etc.

References

1. Olusola, A.O., Fashae, O.A.: Stream energy distribution below Eleyele Dam in Southwestern Nigeria. *Singap. J. Trop. Geogr.* **38** (3), 402–413 (2017)
2. Jones, H.A., Hockney, R.D.: The geology of part of South–Western Nigeria. *Niger. J. Min. Geol.* **3**(1&2) (1964)
3. Faniran, A.: *African Landforms*, 1st edn. Heinemann, Ibadan (1982)
4. Wohl, E., Merritt, D.: Prediction of mountain stream morphology. *Water Resour. Res.* **41**(8), 1–10 (2005)

Table 1 Stepwise discriminant analysis

Step		Tolerance	Sig. of F to remove	Wilks' Lambda
1	Cross-sectional area (m ²)	1.000	0.002	
2	Cross-sectional area (m ²)	0.363	0.000	0.958
	Hydraulic radius	0.363	0.032	0.826
3	Cross-sectional area (m ²)	0.040	0.000	0.815
	Hydraulic radius	0.057	0.001	0.779
	Width (m)	0.110	0.008	0.738

Source: [7]

5. Montgomery, D.R., Buffington, J.M.: Channel processes, classification, and response. In Naiman, R.E., Billy, R.J. (eds.) *River Ecology and Management: Lessons from the Pacific Coastal Ecoregion*, pp. 13–42. Springer, New York (1997)
6. Rosgen, D.L.: A classification of natural rivers. *Catena* **22**(3), 169–199 (1994)
7. Olusola, A.O.: Process-form dynamics of Upper Ogun River Basin, Southwestern Nigeria. Unpublished Ph.D. thesis, University of Ibadan, Ibadan, Nigeria (2019)
8. Lane, B.A., Pasternack, G.B., Dahlke, H.E., Sandoval-Solis, S.: The role topographic variability in river channel classification. *Prog. Phys. Geogr.* **41**(5), 570–600 (2017)
9. Fashae, O.A., Faniran, A.: Downstream morphologic characteristics of the alluvial section of lower River Ogun, Nigeria. *J. Environ. Geogr.* **8**(1–2), 1–10 (2015)

Pool and Riffle Sequences and Morphology of Lower Alaknanda River in Srinagar Valley (Garhwal Lesser Himalaya), India

Sapna Semwal and Devi Datt Chauniyal

Abstract

This study analyzes the pool-riffle sequences of the lower Alaknanda River within the context of mountain meandering river. It is based on the 1/50000 topographical map, CARTOSEAT1 image and field investigation. The data for 8 pools and 18 riffle of 11.5 km channel length are tabulated. The main controlling variables considered for the study are width, depth, spacing, bank full width, length and tectonic setting. The average depth of the pool is 7.75 m. The average width of the pool is 54 m while the average bank full width is 120 m. The average width and depth ratio of the pool is 7.74 which vary from 4 to 12.5. The average spacing of the pool is calculated about 1.4 km. The channel width at riffle is significantly greater than that at the pool. The trend of the regression line shows that there is a negative correlation between depth and width variables and bank full width. The results of the investigation show that the pools and riffles are controlled by longitudinal and transverse tectonic features and gradient of the river.

Keywords

Pool-riffle • Bank full • Morphology • Tectonic setting • River meander

1 Introduction

The long profile is influenced by the distribution of pool and riffle. In a flowing stream, a riffle-pool sequence develops as a stream's hydrological flow structure alternates from areas of relatively shallow to deeper water. Meandering river adjusts its channel in the plane form cross-section, and longitudinal dimensions [5]. The geomorphological research on pool and riffles has considered that these bed forms are fundamental elements of meandering stream [1, 4]. Pools represent the zone of convergent flow scour while the riffles constitute the zone of divergent flow and deposition. Most of the studies that have examined changes in pool and riffles with channel migration were in the alluvial plain [6]. Hudson [3] has established the relationship between depth of pool and radius of curvature of meander in the Mississippi River. Few studies have examined the characteristics of pool-riffle morphology within the context of mountain meandering channel particularly for the Himalayan Rivers. The lower course of Aleksandra River in Srinagar valley (Garhwali Lesser Himalaya) is a classic example of a meandering river. It represents an ideal setting to examine the adjustment of the pool and riffle morphology and the lateral migration of the river. The main objective of the present study was to investigate the pool and riffle sequences and morphology of the Alaknanda River in Srinagar valley.

1.1 Data and Methods

A variety of methods are available for the identification of pool and riffle in the meandering channel. Field study method and remote sensing data have been applied for the identification and analysis of the pools and riffles. In the first step, the 11.5 km longitudinal profile of the river was divided into three segments according to homogenous characters. In the second step, the segments were further divided into 8 reaches on the basis of 8 meander bends which

S. Semwal (✉)

Department of Geography, D.B.S. (PG) College,
Dehra Dun, 248001, India
e-mail: sapnasemwal1991@gmail.com

D. D. Chauniyal

Department of Geography, HNB Garhwal University,
Srinagar (Garhwal), 246174, India
e-mail: chauniyal_devidatt@yahoo.co.in

coincide with a change in the channel morphology and sediments. In this case, each reach was marked on the map and identified on the CARTOSEAT1 (2013) and Google images. After that, field survey was conducted for both banks of the river. The theoretical relationship between the average riffle-pool unit length and the channel width applies to the present study.

2 Results

An 11.5 km thalweg profile was constructed from Supana Dam axis to Kirtinagar Bridge. The thalweg profile was used to identify pools and riffles in the study area. About 8 pools and 18 riffles of 1 to 2 m height were identified. For most of the reach, the data reveal an uneven thalwege profile characteristics of a well developed pool-riffle sequence. The difference in spacing of pools and riffles is related to gradient, lithological changes, deformation stages, tectonic features and river material. Riffle height is a product of riffle length. Pool depth is a positive function of pool length. The average riffle height (H) is proportion of average bank full depth (h) is 0.43. Close riffle or pool is relatively high channel gradient. It shows that as the channel gradient decreases, bed form becomes flattened and pool and riffle become more systematic rather than high channel gradient [2]. The locations of pools occur at the apex of meander bend which is controlled by tectonic features and undercutting by peak discharge [4]. The spacing of pools depends also on the size of the meander bends. The results of the study demonstrate that with the increase in width of the pool and bank full width, the depth of the pool decreases. The relationship between riffle steepness (H/L) and water depth are depending upon the material on the river bed and river bank lithology. The summary data for 8 pools and 18 riffle of 11.5 km channel length are tabulated in Table 1.

Table 1 reveals that the average depth of the pool is 7.75 m which ranges between 6 and 10 m from zero crossing. There was no significance change in pool depth when comprising river length. The average width of pool is 53 m ranging from 40 to 75 m. The pool depth was strongly negative skewed as the width of the pool increases (Fig. 1). Within each reach the model value of width/depth ratio tended to fall in the interval 4–12.5. This demonstrates that many pools are asymmetrical. The average bank full width of the pool is 120.6 m which varies from 100 to 150 m. Pool depths are correlated with bank full width (Fig. 2) considering all the 8 data points. The average spacing of the pool is 1.4 km which varies from 0.5 to 3 km.

Morphology of Riffle \pm Pool sequences in the river severn, England.

An analysis of the depth of the pools and the radius of the curvature of each meander bend reveals an inverse relationship showing that the depth of pools increases with decrease in radius of curvature. However, the depth of pool is lower as the radius of the curvature is higher (Table 1). In the present case, geological structure plays a significant role in the formation of meanders, pool and riffle sequences (see discussion).

3 Discussion

In the Himalayan terrain, the riffle and the pool morphology are controlled by the channel gradient, lithology and tectonic features. With the decrease in slope, the river flows through a meandering course and both riffle and pool becomes longer and increasingly asymmetrical [2]. Pools and riffles are intricately linked to the plane forming geometry of meandering rivers. Generally, the mountain river flows through a hard rocky banks. The pools are developed along the meander apex bends and riffles are shorter and attain height. During the field work, it has been ascertained that all the

Table 1 Summary statistics of pool-riffle morphology

Segment	Reach	Pool characteristics				Bank full width/depth ratio	Width/depth ratio
		Depth (m)	Pool width (m)	Spacing (m)	B. width (m)		
Supana to Srikot	Supana	10	40	0	100	10.0	4.0
	Koteswar	8	50	1000	125	15.63	6.25
	Surasu	10	75	500	100	10.0	7.5
	Srikot	7	50	1300	130	18.57	7.14
Srikot to Ranihat	Chauras	7	45	2200	125	17.86	6.43
	Srinagar	6	60	2000	110	18.33	10.0
Ranihat to Kirtinagar	SSB	8	65	3000	150	18.75	8.13
	Sriyantra Tapu	6	75	1500	125	20.83	12.5
Average		7.75	53	1437.5	120.63	16.25	7.74

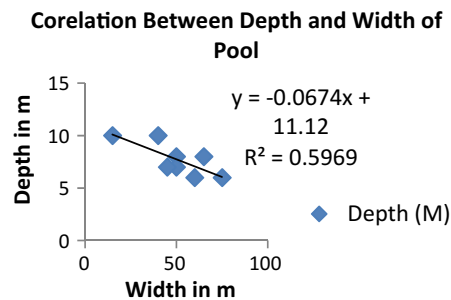


Fig. 1 Regression between D and W of pool

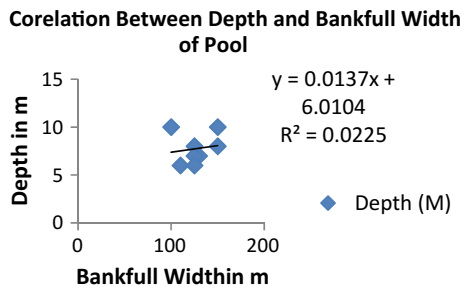


Fig. 2 Regression between D and B. full W&D

meander bends are controlled by the structural features like thrusts, faults and lineaments. In various episodes of Himalayan development, the early phase of NW–SE longitudinal features was displaced by transverse features along the river [7]. Supana and Guguli hogback features with pools in the area are the best examples. In contrast to the spacing of pools, the depth of pools increases from 6 to 10 m. The tectonic map clearly demonstrates that pools and riffles are intricately controlled by the tectonic features.

North Almora Thrust (NAT) passes through Supana village across the river. A longitudinal fault along Srikot Sweet Nala section and transverse fault is exposed along the Chauras Badkot traverse which cut across the Srikot meander. There is a 7 m deep pool under the terrace scarp. Similarly, pools are developed at Chauras suspension bridge, Srinagar meander bend at Kilkilewar, SSB meander bend at Ranihat village and at Sriyantra Tapu meander bend at Ufhald village at the junction of two tectonic features. One north–south trending transverse lineament also joins with Kiratinagar longitudinal fault at Sriyantra Tapu meander bend. Here, a 6 m deep complex type of pool has been developed. Because of the litho-tectonic control on meanders, the pools will not be migrating in short span of time at the meander bends. It is noted that the pool depth remains the same in the mountain river channel so this does not

imply that the pool depth is maintained after the occurrence of river bank erosion and lateral migration. There is no significant relationship between time and river bank erosion and pool depth of each meander bend which implies that there is considerable vertical adjustment of the thalweg with litho-tectonic control.

4 Conclusion

The river Alaknanda in Srinagar valley data proved detailed summary information on riffle and pool geometry. It is concluded that there is no significant change in the morphology of the mountain river, pool and riffle morphology. The average pool depth equal about 7 times the channel width while the average pool depth equal about 15.6 times of bank full depth. Pool depth is positive function of pool length and bank full depth. The statistical relationship between pool depth and width, and depth and bank full width demonstrate the negative correlation ship. The width and depth ratio is 2.1 times of bank full and depth ratio. Thus, these results are consistently different from the work done by previous workers. It is because of the partially alluvial and partially rock bed channel. The pools and riffles are closely associated with meander shape and size while the meanders are tectonically controlled. The crossing of major lineaments demonstrates the deeper pools at meander bends. Finally, it can be concluded that the pool and riffle morphology influenced by the tectonic features of the studied area.

References

1. Bhowmik, N.G., Demissie, M.: Bed material in pool and riffle. *J. Hydrol. Div.* **108**(10), 1227–1231 (1982)
2. Carling, P.A., Orr, H.G.: Morphology of riffle and pool sequences in the river severn, England. *Earth Surf. Process. Landf.* **25**, 369–384 (2000)
3. Hudson, P.F.: Pool-riffle morphology in an actively migrating alluvial channel: the lower Mississippi river. *Phys. Geogr.* **23**(2), 154–169 (2002)
4. Keller, E.A., Melhorn, W.N.: Rhythmic spacing and origin of pools and riffles. *Geol. Soc. Am. Bull.* **89**, 723–730 (1980)
5. Kinghton, A.D.: *Fluvial Forms and Processes*. Wiley, New York (1998)
6. Leopold, L.B.: *Fluvial Process in Geomorphology*. W.H. Freeman, San Francisco (1994)
7. Valdiya, K.S.: Reactivation of terrain defining boundary thrust in Central sector of The Himalaya: implications. *Curr. Sci.* **81**, 1418–1430 (2001)

Quaternary Fluvial Terraces of the Oued El Gourzi (Batna, NE Algeria): Sedimentology and Characteristics of the Depositional Environment

Fouad Djaiz, Nabil Defaflia, Bachir Lamouri, Abdallah Boushaba, and Imen Chairat

Abstract

Field observations and sedimentological analyses of alluvial terraces of the O. Gourzi (Batna, NE Algeria) lead us to consider sediments as dominated by clayey and silty-sandy fractions overlain by gravel and calcareous coarser fractions. Moderate CaO_3 contents would have resulted from the dissolution of the nearby carbonate relieves. They are mainly composed of Maastrichtian limestones. The distribution of the mineral fraction led us to identify 07 levels including horizons of coarse fractions alternating with layers rich in sand and silt with a roughly constant clay fraction through the stratigraphic column. Kurtosis values, frequency histograms of a prokurtic type, rarely mesokurtic, mark a constant power mode for the transport agent. Classification indices indicate poorly- to moderately sorted material, indicating a turbiditic depositional environment. Quartz grain nature and morphoscopy refer to Miocene sandstones as a potential origin. The ferruginous coating is due to the initiating pedogenesis.

Keywords

Stream terraces • Physical parameters • Sedimentology
Batna area • NE Algeria

F. Djaiz (✉) · I. Chairat
Laboratory of Mobilization and Management of Resources Water,
Institute of Earth and Universe Sciences, University of Batna 2,
Fesdis, Algeria
e-mail: djaizfou@yahoo.fr

N. Defaflia
Laboratory of Sedimentary Environments, Mineral and Water
Resources of Eastern Algeria, Faculty of Exact Sciences and
Sciences of Nature and Life, University of Tebessa, Tebessa,
Algeria

B. Lamouri
Geodynamic Laboratory and Natural Resources, University of
Biskra, Biskra, Algeria

A. Boushaba
Laboratory of Systems Integration and Advanced Technologies,
University of Dhar El Mehrez Fez, Fes, Morocco

1 Introduction

The Oued El Gourzi site of NE Algeria is located to the NE of the Batna plain and to the SW of the Mather plain, 220 km far from the Mediterranean Sea. The northern boundary of the gentle slope plain is a water sharing line between two basins: the Timgad and El Mather plains which flow to the North and North-East, respectively. To our knowledge, no sedimentological analyses were focused on the fluvial terraces of this water course. The hydrodynamic characters of transport agent and their depositional environment are still poorly known. This work attempts a first petrophysical analysis of the sediment content and granulometry of the identified levels.

2 Materials and Methods

The particle size of fine elements was performed using the growing mesh screen. Sieves were shaken by using a mechanical device (Sifter, vibrating) to separate a set of particles by their frequency statistics related to their size. The sample CaCO_3 content of less-than-2-mm sized grained was systematically evaluated by means of Bernard's calcimeter. The sediment PH was measured by using a hand-held pH meter. The morphoscopic analysis was performed after statistic interpretations of Cailleux and Tricart [1] and Le Ribault [2].

3 Results and Discussion

3.1 Stratigraphic Column

From top downwards, the stratigraphic column within El Mather's basin consists of: (i) a Mio-Plio-Quaternary covering made of clayey silty levels is associated with conglomerates and travertines; (ii) a clayey marl-limestone

horizon of a mainly Upper Cretaceous age; (iii) a lower cracked horizons of calcareous-sandstone/limestone alternations dated to Barremian. Within the quaternary terraces, field observations and the evaluation of fine fraction proportions for analyzed levels allowed us to distinguish seven sections (A to G, Fig. 1) totaling 1175 cm.

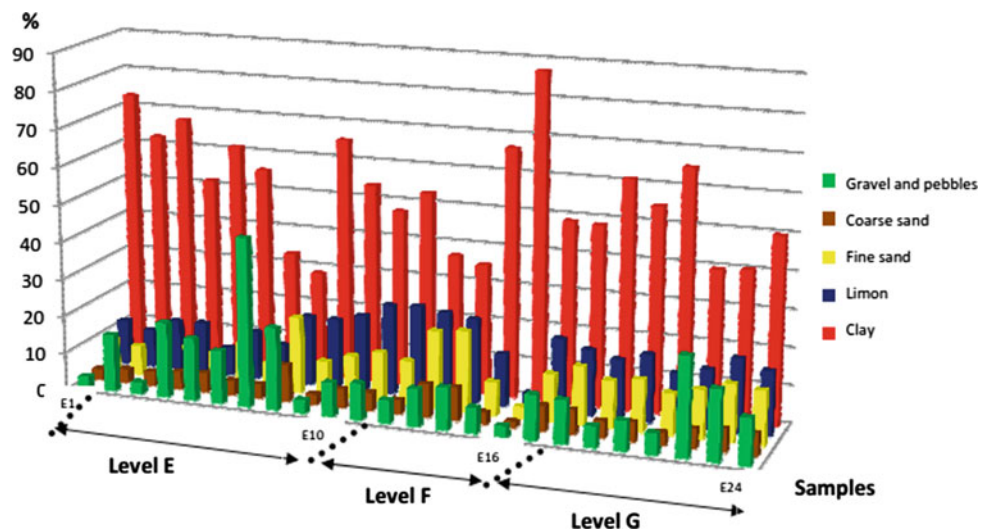
Level A (0–170 cm) is a gravel and pebble horizon with plant roots corresponding to the humus horizon. Level B (–170 to –370 cm) is of 200 cm in thickness and is characterized by a predominant clear fine matrix of yellowish clays and sands. Level C (–370 to –650 cm) is a yellowish to brownish silty and sandy horizon characterized by its rare fine elements (mainly in its middle part). Level D (–650 to –715 cm) is a clayey to sandy level. It is composed of gravels and pebbles with gastropod fragments. Level E (–715 to –865 cm) is a dark silty and sandy clay interval with gravel and pebble intercalations. Level F (–865 to –1015 cm) is of 150 cm in thickness and is separated from the overlying horizon by its reddish color and scarcity of gravel and pebbles. Level G (–1015 to –1175 cm) is of a relatively clayey texture. This horizon exhibits a higher pebble and gravel content than that of level F reddish color in its upper part. The particle size variation through the studied terrace column as well as proportions of the different particle size fractions within each level are first criteria that allowed us to distinguish two groups of the level structures: horizons rich in coarse fraction, mainly gravel, pebbles and blocks (A and C). They alternate with clay and silt-rich levels (B, E, F and G). The Granulometric analysis of the fine fraction is expressed in cumulative curves. It shows that the sediment is relatively uniformed with a high clay proportions (53.52%), silt and powder medium proportions (16,14%), low to very low percentages of fine and coarse sands (12.32% and 5.03%, respectively).

3.2 Petrophysical Characteristics

The granulometric cumulative curves of clay fractions are of a relatively constant aspect. The Mesokurtic curve of level B from the terrace upper part (Fig. 1) indicates that this horizon corresponds to immature sediments with a limited evolution over time and no particular reworking by transport [3]. The Ptokurtic curves for all the samples from the middle and lower part of the terrace are in favor of a transport mode characterized by a relatively constant energy. Samples E5, F13 and G21 of the section are mainly clayey and silty, their sediments onset in relatively calm environment conditions, after a load excess during transport speed lowering. The studied terraces of Oued El Gourzi are characterized by clayey and silty deposits with moderate grain size asymmetries towards larger sizes. They are all transported by moderate energy currents. Grain size mean values (M_z) range from 0.30 ($M_z < 1$) to 1.17 ($1.00 < M_z < 2.32$) with a preponderance of clay fractions. The sample 13 of level F ($M_z = 0.30$) reflects a high kinetic energy with a deviated asymmetry towards larger sizes in relation to a decrease in water level. On the other hand, the M_z value = 1.17 for the sample 1 of level B corresponds to a medium kinetic energy. It indicates a high asymmetry towards larger sizes. The Kurtosis values vary between 0 and 1.85 frequency histograms mainly of a protokurtic type. They are rarely mesokurtic. they make a constant power mode for the transport agent.

Asymmetry values are negative or close to zero. They vary from –0.34 to –0.87. This indicates a low energy current as the histogram is deviated towards fine fractions. Classification indices range from 0.72 to 1.01. They indicate a poorly- to moderately sorted material of a Turbidite depositional environment.

Fig. 1 Grain size and content of the terrace stratigraphic column



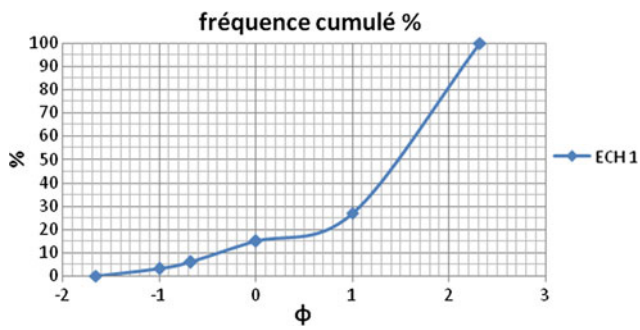


Fig. 2 The granulometric cumulative curve of clay fractions (level B)

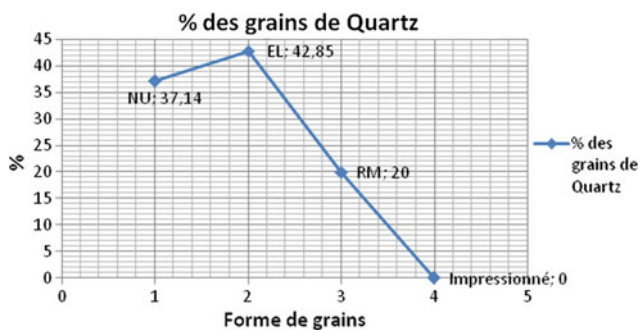


Fig. 3 Grain percentages (Ech 1 level B)

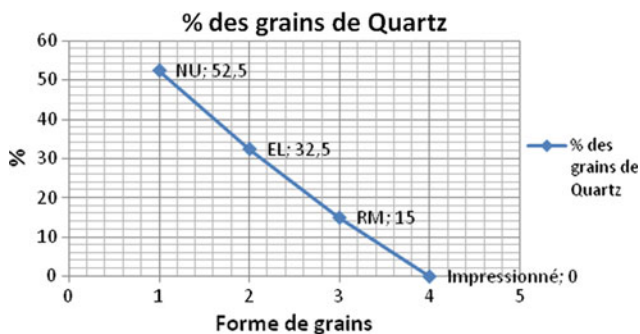


Fig. 4 Grain percentages (Ech 5 level E)

Fig. 6 Grain morphoscopy (samples 1 level B and 5 level E)

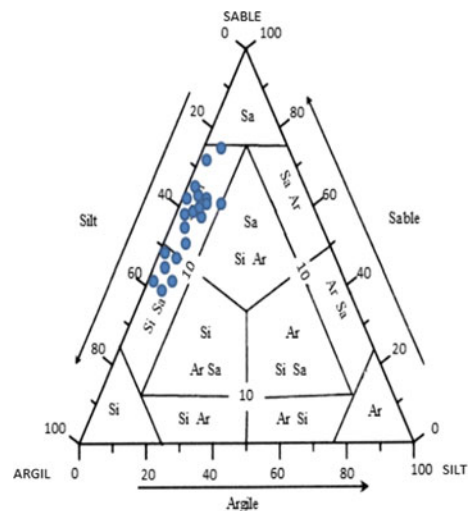
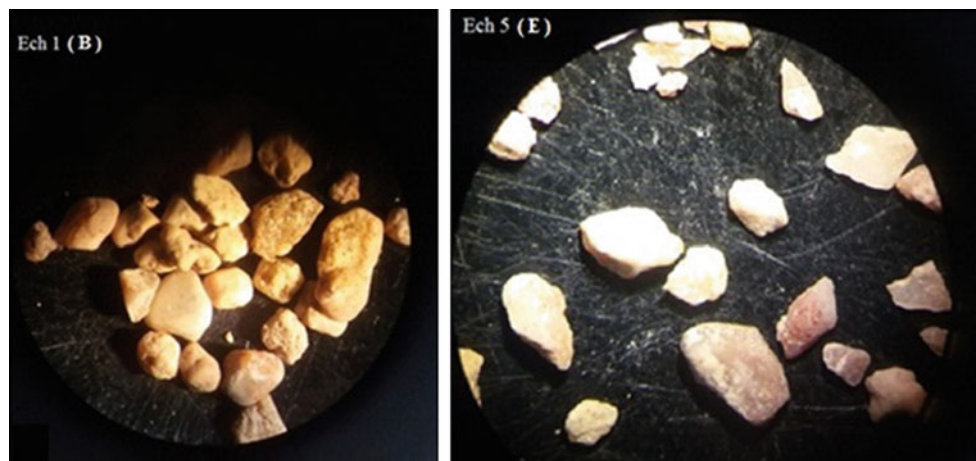


Fig. 5 Fine sediment ternary diagram

The calcium carbonate content of the different samples are relatively constant with percentage varying between 9.52 and 12.30% and with extreme values for levels G and E. The pH values encompass the value 6 and 7 that can be interpreted as related to low dissolution of carbonates.

As a complement to grain size evaluation, the morphoscopic analysis is aimed to identify and determine the percentage of shiny, unworn and round carpet grains Fig. 6 for the purpose of reconstructing the transport mode and depositional environmental characteristics. High percentages (44.97%) of blunted or under-blunted kernels (Fig. 2) characterize the levels (B, F, G) of the fluvial terrace. However, the level E exhibits a higher rate of NU grain compared to the EL grain (Fig. 4) which pleads in favor of Cretaceous neighboring limestones as a source for fluvial dynamics. Round carpet quartz grains (RM) with a percentage of 18.23% refer to Miocene sandstones as a potential origin. The ferruginous coating is due to an initiating pedogenesis Figs. 3 and 5. The ternary diagram shows that sediments consist mainly of clays and sands, with clays dominating at the top (Fig. 5).

4 Conclusion

Main physical characteristics of fluvial terrace section from the Oued El Gourzi (Batna, NE Algeria) allow us to distinguish seven stratigraphic levels. The Particle size distribution indicates that sediments span the values 1.00 and 2.32 which is due to their enrichment in clay, silt and fine sands during a water level rise. The frequency curves are leptokurtic, rarely mesokurtic. Kurtosis values vary between 0 and 1.85 and indicate a constant power mode of water. Sorting index values indicate bad-to-very bad sorting classes related to the irregularity of the transport agent energy level. The asymmetry values are negative or close to zero. Their standards vary from -0.34 to -0.87 showing that the histogram propagation is due to the fine fraction side. The classification indexes are between 0.72 and 1.01. The sediments are considered as poorly to moderately sorted. They indicate a turbiditic depositional environment. The morphoscopic evaluation of quartz grains show often blunted, shiny or sub-rounded and not worn grains. These two categories correspond to cores of almost perfect and angular shape. They give the UN the appearance of mat

surfaces. The abundance of these families of quartz grains indicates that the mode of water transport is the most important factor controlling the Oued el Gourzi remodeling evolution.

Further studies may focus on detailed sedimentological structures characterizing the studied fluvial terrace of the Oued El Gourzi first initiated here. It would be of a particular relevance to the individualization of the different steps of the terrace onset and to the main controlling factors and their relationships with neighbouring water courses at a regional scale.

References

1. Cailleux A., Tricart J.: Initiation à l'étude des sables et des galets. Centre de Documentation Universitaire, Paris, 369 p. (1963)
2. Le Ribeu.: L'exoscopie des quartz, Editions Masson, Paris, 200 pages, 170 photographies (Epuisé). THESES (1977) (LE RIBEAULT L)
3. Miskovsky.: Géologie de la Préhistoire, méthodes, techniques, applications. Association pour l'étude de l'environnement géologique de la Préhistoire. Paris, GéoPré, Presses universitaires de Perpignan, 1519 p. (2002)

Characterization of Sand Particles in Arid Areas

Abdulsalam Alhazza, Shorouq Ahmad, and Ali Al-Dousari

Abstract

Sand particles in the arid areas are an important source of silica and silicon oxide. The study of Micro-features of these particles can provide outstanding information about its history. In addition, it can show the properties of these particles. Chemical and Physical properties are considered in analyzing sand samples. This work aims to study the properties of the sand particles in an arid area. Sand particles from different locations within the same wind corridor were chosen to be analyzed. Then, some chemical and physical analysis was performed by using the Scanning Electron Microscope (SEM) and X-ray Fluorescence (XRF). The chemical and the physical study show that some quartz particles tend to be spherical and smooth. The mechanical features of the quartz particles surface mostly occur in the form of dish-shaped depressions, V-shaped pits and crescentic pits, rounded, and upturned plates.

Keywords

Sand particles • Arid areas • Micro features
Physical properties • Depressions

1 Introduction

The Sand particles feature like, composition, origin, and transport history can reflect the shape of these particles [1]. Kuenen [2] suggests, in his experimental work, that the wind

rounds 100–1,000 times are faster than the fluvial action. Goudie and Watson [3] state that when the particle is transported in water, it accumulates a very tight adherent film of water which helps to protect the particle from the impact.

Furthermore, Krinsley and Doornkamp [4] briefly mention further physical and chemical features on the quartz particles from diverse environments.

Very important information on paleoenvironmental history like the aeolian activity and the weather severity could be extrapolated from the microfeatures on sand particles exemplified by abrasion, coating, etching, and dissolution features.

Scanning electron microscope (SEM) analysis could provide very important information on the surface features to distinguish between particles from different environments [5]. It is an invalid approach to use one microfeature for the purpose of determining a paleoenvironment. A succession of environments can represent a series of events on a single sand particle or group of particles [6]. Previous studies on the aeolian sediments in different regions such as Kuwait and other places have focused on sedimentimorphic features [7–9], Iraq [11], Saudi Arabia [10], Qatar [12], Emirates [13]. The investigation of the physical properties of the aeolian sand particles has not been studied thoroughly. Therefore, the aim of this study is to fill this gap of knowledge in order to study the transportation of sand for further industrial and environmental planning purposes.

2 Methodology

A number of samples were randomly collected from the top of the surface of sand dunes and from three different areas in Kuwait (Kabd, Um Alaish, and Huwaimliah). All samples have been characterized by scanning electron microscope (SEM) according to size, shape, and mechanical damage. Also, some chemical analysis was performed by using the X-ray fluorescence (XRF) for eighteen samples for oxides.

A. Alhazza (✉) · S. Ahmad · A. Al-Dousari
Kuwait Institute for Scientific Research, Safat, 13109 Kuwait City,
Kuwait
e-mail: ahazza@kisir.edu.kw

3 Results

3.1 Physical Characterization

All the samples have been characterized by scanning electron microscope (SEM) according to size, shape, and mechanical damage. The particle size was between 258 and 304 μm . The shape of the particle is mainly rounded and ovally shaped (Fig. 1) while the physical microfeatures are mainly V-shaped pits, spherical pits, crescentic cavities, coalescing pits, dish-shaped holes, grooves, stepped cleavage planes, and sutures (curved and straight).

Figure 1 shows the dish-shaped holes and V-shaped pits which are most widely distributed features on the surfaces of the quartz particles. This depression can be found on the surface of most of the studied particle. The V-shaped and rounded pits sizes varies approximately from 5 to 50 μm . Some quartz particles show severe breakage and abrasion (Fig. 2).

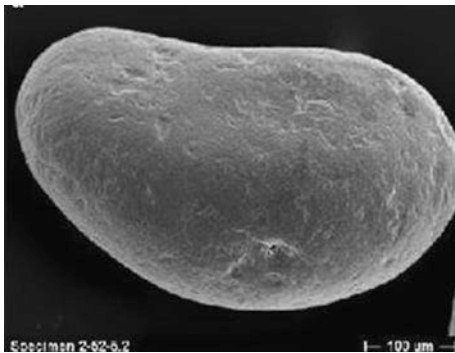


Fig. 1 Dish-shaped holes and V-shaped pits



Fig. 2 Severe breakage and abrasion

3.2 Chemical Characterization

Furthermore, the chemical characterization of the sand samples from three different locations in Kuwait was analyzed by using XRF for oxide materials. These places are (Kabd, Um Alaish, and Huwaimliah) Table 1 (a, b, and c).

Silica concentration varies from 46% minimum to 94% maximum. Other oxides were analyzed like (Na_2O , MgO , K_2O , and CaO). All these oxides have a low concentration (less than 5%) except for CaO which reaches up to 22% in some areas.

4 Discussion

The physical characterization shows mechanical features on the particles. These features were mainly damages on the corner of the particle due to the particle to particle

Table 1 XRF analysis for some oxides appears in the sand samples

Sample name	Na_2O	MgO	SiO_2	K_2O	CaO
Kabed 1	3.099	5.438	51.97	1.30	22.18
Kabed 2	0.961	0.069	93.62	1.73	0.14
Kabed 3	0.694	0.074	95.44	1.11	0.14
Kabed 4	1.34	0.138	94.25	1.12	0.34
Kabed 5	2.78	1.247	80.69	1.55	4.70
Um.7	2.184	6.016	46.87	1.01	22.58
Um.8	1.12	0.275	89.89	2.18	1.1
Um.9	1.32	0.217	91.79	1.51	0.96
Um.10	1.28	0.821	86.39	1.28	4.22
Um.11	2.744	1.947	71.5	1.38	10.76
H 13	3.004	4.551	54.82	1.28	22.06
H 14	0.369	5.197	78.77	1.96	3.05
H 15	1.04	0.386	92.6	1.34	1.03
H 16	1.778	0.882	85.82	1.31	3.67
H 17	3.388	1.776	73.18	1.43	8.63

collision during transportation. This might indicate that the particle was moved from its local place by wind. The wind plays a very important role in shaping the particles in addition to erosion especially when moved for long distances.

The chemical analysis shows the oxides materials in three different areas. In Kabd area the highest silicon Oxide concentration was 95.44% while the lowest was 51.97%. Um Al-aish area has the lowest concentration in SiO₂ (46.87%). Hamliah readings were in the middle with average concentration of 73.67%. On the other hand, the other oxides were in very low concentrations, except for CaO in some places which reaches to 22% for all the three areas.

5 Conclusion

The characterization of the sand particle in arid areas shows that these particles contain a high content of silica which reaches up to 95% in some areas. Other oxide materials (NaO₂, MgO, K₂O, CaO) were detected in low concentrations except for CaO in some places where it reaches to 22%. In addition, it shows some other physical features occurring from the movement of these particles due to the transportation from one place to another. Wind erosion and collision between particles remove the corners and provide upturned plates around fractures and breaks.

References

1. Pye, K., Tsoar, H.: *Aeolian Sand and Sand Dunes*, p. 396. Unwin Hyman, London (1990)
2. Kuenen, P.: Experimental abrasion-eolian action. *J. Geol.* **68**, 427–449 (1960)
3. Goudie, A.S., Watson, A.: The shape of desert sand dune grains. *J. Arid Environ.* **4**, 185–190 (1981)
4. Krinsley, D., Doornkamp, J.: *Atlas of Quartz Sand Surface Textures*. Cambridge University Press, Cambridge (1973)
5. Culver, S.J., Bull, P.A., Campbell, S., Shakesby, A., Whalley, W. B.: Environmental discrimination based on grains surface textures: a statistical investigation. *Sedimentology* **30**, 129–136 (1983)
6. Krinsley, D.H., Funnell, B.M.: Environmental history of quartz sand grains from the lower and middle Pleistocene of Norfolk, England. *Q. J. Geol. Soc. Lond.* **121**, 435–461 (1965)
7. Khalaf, F.I., Misak, R., Al-Dousari, A.M.: Sedimentological and morphological characteristics of some nabkha deposits in the northern coastal plain of Kuwait, Arabia. *J. Arid Environ.* **29**, 267–292 (1995)
8. Al-Dousari, A.M., Pye, K.: Mapping and monitoring of dunes in Northwestern Kuwait. *Kuwait J. Sci. Eng.* **32**(2), 119–134 (2005)
9. Al-Dousari, A.M., Misak, R., Ahmed, M., Al-Mutairi, M.: Characteristics of Nabkhas in relation to dominant perennial plant species in Kuwait. *Kuwait J. Sci. Eng.* **35**, 129–150 (2008)
10. Al-Fredan, M.A.: Sand dune and sabkha vegetations of Eastern Saudi Arabia. *Int. J. Bot.* **4**(2), 196–204 (2008)
11. Al-Janabi, K.Z., Jawad Ali, A., Al-Taie, F.H., Jack, F.J.: Origin and nature of sand dunes in the alluvial plain of southern Iraq. *J. Arid Environ.* **14**(1), 27–34 (1988)
12. Embabi, N.S., Ashour, M.M.: Barchan dunes in Qatar. *J. Arid Environ.* **25**(1), 49–69 (1993)
13. El-Sayed, M.I.: The nature and possible origin of mega-dunes in Liwa, Ar Rub' Al Khali, UAE. *Sediment. Geol.* **134**(3–4), 305–330 (2000)

Aeolian Sand Transport Rate Over Windward and Lee Slopes of Small Reversing Dunes, Southern Morocco

Maciej Dłuzewski and Joanna Rotnicka

Abstract

Several factors affect the aeolian sand transport rate over reversing dunes. In arid zone poor in vegetation, the most important factors are effective wind direction in relation to the dune crest and the inclination of the windward slope. The objective of this paper is to analyze the variation in sand transport rate over such dunes under wind events differing in the direction of the incident wind including winds blowing from the direction of the former lee side. The research was carried out in the dune field of the Coude du Dra region (southern Morocco) where small reversing dunes, up to 3 m high, are numerous. In the case of wind blowing from the direction of low-angle slope, the sand transport rate increased tenfold between dune toe and crest when wind speed was well above the threshold value and around 25 times when wind speed was slightly greater than the threshold value. When the wind direction reversed and the steep lee slope became a windward slope, the sand transport rate at the dune crest was greater than in the previous case. It was caused by strong sand deflation that occurred at the dune crest due to its kinked profile.

Keywords

Aeolian sand transport • Reversing dunes
Amplification factor

1 Introduction

The airflow, which transports the sand above dunes surface, is significantly influenced by the dune topography. In the windward side, streamline is compressed and airflow acceleration takes place. Contrary to that, in the lee side, the flow expands and/or separates resulting in flow deceleration. The aeolian sand transport rate over a reversing dune surface depends mainly on: (i) wind direction in relation to the dune crest which controls acceleration of the near surface airflow and (ii) inclination of the windward slope which in the case of such dunes may reach angle up to 30° [1]. In arid zone, others factors such as grain size and petrographic composition of sand, sand moisture and vegetation are of secondary importance. Surface crusting is important only locally [2].

There were some research on sand transport rate within the reversing dunes but they have documented it under wind one-direction events [3, 4]. Therefore, the aim of present study was to analyze the variation in sand transport rate over small reversing dunes under wind events differing in the direction of incident wind: (i) from windward side, (ii) from former lee side and (iii) parallel to the dune crest.

2 Settings and Methods

The research was carried out in the Coude du Dra region, southern Morocco, where bimodal wind regime occurs. Measurements were made on 3 dunes in 3 different wind seasons. The studied dunes were between 2 and 3 m high. Their windward and lee slopes were about 13–15 m and 3–4 m long, respectively. The windward slope profile was concave-convex with an inclination changing from 5 to 7° above the dune toe, through 10–12° in the middle part of the slope to 5° in the upper part of the slope. Lee slope inclination equaled to 20–30°. Dunes were built of sand composed mainly of quartz and ferruginous-clayey clasts. Surface sand samples collected during the study averaged

M. Dłuzewski (✉)
Faculty of Geography and Regional Studies, University of
Warsaw, Krakowskie Przedmieście 30, 00-927 Warsaw, Poland
e-mail: dłuzewski@uw.edu.pl

J. Rotnicka
Institute of Geology, Adam Mickiewicz University in Poznań,
Bogumiła Krygowskiego 12, 61-860 Poznań, Poland

2.17 phi (224 μm) in diameter and was moderately sorted (0.87 phi on average) and symmetrically skewed (0.006 on average).

On each dune, a set of 4 anemometers was deployed within both windward and lee slopes at 1 m above dune surface and a reference mast was placed on the flat interdune area. Wind speed and direction were recorded every second. The sand transport rate Q ($\text{kg}/\text{m}/\text{s}$) was measured by means of 10 passive vertical sand traps 0.5 m in height, divided into 40 compartments, each 1 cm wide and 1.27 cm high [5]. The sand traps were arranged along the transect perpendicular to the dune crest.

3 Results

3.1 Airflow Acceleration

In the case of studied small reversing dunes, the amplification factor (A_z) equaled from 1.11 to 1.68. When wind blew normal to the crest, from the direction of windward slope, amplification factor reached the greatest value. When the angle between wind direction and dune crest (angle of attack) decreased slightly, the value of amplification factor decreased significantly. If wind blew from the former lee side direction, the amplification factor was in the range of values calculated for winds blowing from the direction of low angle windward slope. It means that in the case of small reversing dune bed slope impacts the streamline acceleration to a small extent. The lowest value of amplification factor was obtained for wind direction parallel to the dune crest. The results also showed that in the case of wind direction normal to the dune crest, the amplification factor decreases as wind speed increases.

3.2 Sand Transport Rate

In the case of crest-normal wind events when wind blew from the direction of low inclined dune slope, the mass flux generated by airflow acceleration reached the largest values at the crest (Fig. 1a). On the lee side, where airflow slowed down, the mass flux considerably decreased. When wind reversed and blew from the direction of former lee slope the mass flux at the dune crest was on average greater than when wind blew from the opposite side (Fig. 1b). On the lee side (former windward side) the decelerated airflow transported significantly less sand. During events of winds oblique or parallel to the crestline, when airflow acceleration was minimal, the sand transport rate on the stoss and lee side was almost equal. The maximum value recorded at the crest was usually only slightly greater than in other parts of the dune.

The results showed that sand transport rate at the dune crest correlates well with the wind speed but when wind approaches the dune crest from the direction of former steep lee slope, the sand transport rate at the crest (at given wind speed) is higher than the transport generated by wind blowing from the direction of low-angle slope.

4 Discussion

Although research on reversing dunes dates back to the end of XIX century [6] and despite the fact that this type of dunes occurs in almost every sand desert, process of their formation and particularly variations in sand transport rate over them are still far from understood. It may be caused by fast change of dune shape as wind direction reverses.

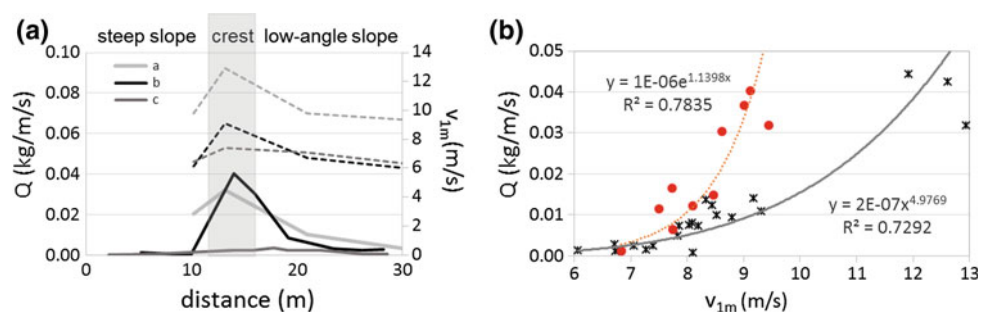


Fig. 1 a Variation in wind speed v_{1m} (dashed lines) and sand transport rate Q (solid lines) measured along the transect normal to the dune crest during different wind events: a—wind from the low-angle slope direction, b—wind from the steep slope direction, c—wind parallel to

the crest. b Relationship between wind speed and sand transport rate at the dune crest for wind approaching the dune crest from the steep (circles) and low-gradient (cross signs) slopes

The sand transport over not kinked windward slope of reversing dune is similar to that over transverse dunes. It depends on flow acceleration which, for crest transverse wind, is of a magnitude of around 1.5 [7]. However, the present study showed that such airflow acceleration may cause great differences in sand transport rate. It increased tenfold between dune toe and crest when wind velocity was well above the threshold value and around 25 times when wind velocity was slightly greater than the threshold velocity. Both values are higher than values documented by others studies [4]. These differences resulted from the decrease of wind speed at the dune toe which is well documented phenomenon and results in deposition of coarser grain in the lower part of windward slope [3]. When the wind velocity is around threshold value, almost all sand transported to the dune is also deposited in this zone. The unsaturated airflow moving up the stoss slope has a great potential to deflate sand from the dune surface and as the airflow accelerates the sand transport intensity increases. Therefore, the differences in sand transport rate between dune toe and crest are so great. At the lee side of a transverse dune, the airflow decelerates and sand transport rate decreases by up to 90%. This value coincides with values obtained by Walker [3] who concluded that a significant amount of sediment transported over the dune crest moved as fallout.

Much more complex is the variation in sand transport rate when the wind direction reverses and the steep lee slope becomes a windward slope. In this case, the same flow acceleration recorded at the dune crest resulted in sand transport rate greater than in the case of wind blowing from the opposite direction of low inclined slope. This does not necessarily mean that sand transport rate depends on slope inclination but rather that the strong sand deflation occurs at the dune crest when the direction of wind change of a 180° which is a common process in a reversing dunes.

5 Conclusion

The paper presents results of sand transport rate measurements made both during the reversing process of transverse dune and during the phase of transformed dune symmetry. The main conclusions are: (i) the amplification factor reached the lowest values in the case of wind parallel to the dune crest; whereas, in the case of wind blowing from the directions of low-angle and steep slopes direction, these values were greater and in similar range, (ii) wind blowing up the steep windward slope (former lee slope) generated the sand transport whose rate at the dune crest was on average much greater than in the case of wind blowing up the low-angle windward slope and (iii) wind blowing parallel to the dune crest generated transport whose rate was several time smaller than in all other cases.

Acknowledgements The research has been supported by the National Science Center, Poland, project No. 2016/23/B/ST10/01700.

References

1. Hardisty, J., Whitehouse, R.J.S.: Evidence for a new sand transport process from experiments on Saharan dunes. *Nature* **332**, 532–534 (1988)
2. Zobeck, T.M.: Abrasion of crusted soil: influence of abrader flux and soil properties. *Soil Sci. Soc. Am. J.* **55**(4), 1091–1097 (1991)
3. Walker, I.J.: Secondary airflow and sediment transport in the lee of a reversing dune. *Earth Surf. Proc. Land.* **24**, 437–448 (1999)
4. Dong, Y., Hesp, P.A., Namikas, S.: Flow dynamics and sediment transport over a reversing barchan, Changli, China. *Geomorphology* **278**, 121–127 (2017)
5. Rotnicka, J.: Aeolian vertical mass flux profiles above dry and moist sandy beach surfaces. *Geomorphology* **187**, 27–37 (2013)
6. Cornish, V.: On the formation of sand dunes. *Geogr. J.* **9**(3), 278–309 (1897)
7. Parsons, D.R., Walker, I.J., Wiggs, G.F.S.: Numerical modelling of flow structure over idealized transverse aeolian dunes of varying geometry. *Geomorphology* **59**, 149–164 (2004)

Grain Size Analysis for the Study of Wave Energy in the Vicinity of Breakwaters: Case of the Coast of Ain Taya (Algiers)

Mohamed Bouhmadouche, Yacine Hemdane, and Farid Atroune

Abstract

Some studies have allowed us to understand hydrosedimentary dynamics of the eastern Algerian continental shelf where the aspects of morphology, hydrodynamism and erosion were underlined (Bouhmadouche and Hemdane in *Environ Earth Sci* 75 (10) 2016, [1]). The aim of this paper is to understand the impact of “hard” coastal protections of Ain Taya (Algiers) on the hydro-sedimentary balance. The granulometric analysis of sediments is essential for this study to be conducted. This study made it possible to obtain some information concerning the forcing of coastal waves, currents and coastal erosion. In addition, this study provided insight of the impact of the coastal protection (installed on the Ain Taya coast) on the coastal dynamics of the region surrounding the breakwaters of the study area. These “hard” coastal protections disturb sedimentary dynamics and marine hydrodynamics. Therefore, the dimensioning of the coastal protection structures should be based on the hydrosedimentary balance regulating the coastline and beaches.

Keywords

Coastal erosion • Grain-size • Coastal protections • Waves and currents • Ain taya

1 Introduction

Today, several industrial, port and tourist activities are concentrated at the level of these coastal zones which are subject to an anthropic constraint. These anthropogenic

pressures have in many cases led to a decline in the shoreline threatening coastal populations. The coast of Algiers is characterized by a strong urbanization making this coast vulnerable to marine erosion. Consequently, heavy coastal protections have been installed in some places of the coast of Algiers to stop coastal erosion. The basics of this work are to study the nearshore sedimentological characteristics of the Ain Taya coast where breakwaters and groins were built to stop the erosive effect of the waves. This study is based on the analysis of the grain-size parameters to interpret both the sediment transport and the potential marine energy acting near the breakwaters of the study area. Indeed, an understanding of the nearshore sediment transport is necessary for coastal engineering and coastal erosion (including coastal flood) studies. The study of grain size can help to understand sediment transport in the nearshore area. Thus, grain size trends may contain information on sediment transport [2].

2 Methods

Twenty-two bottom sediment samples were collected in the nearshore of Ain Taya (Surcouf). These samples were taken in water depths ranging from 0 to 20 m. The surficial sediments were taken by using Van Veen grab. Sampling was carried on a relatively large surface layer (approximately 20 cm) in order to study the recent residual transports. The sediment is placed in a sieve with a mesh size of 40 μm where it is rinsed with tap water. Rinsing ends when the wash water from the sieve becomes clear. The sediment is then dried in an oven at 60 °C during 48 h. In addition to the conventional method of particle size analysis (sieves),

M. Bouhmadouche (✉) · Y. Hemdane · F. Atroune
Laboratoire Géo-Environnement, Faculté des Sciences de la Terre,
Géographie et Aménagement du Territoire, Université Houari
Boumediene, BP 32, El-alia, Algiers, Algeria
e-mail: mbouhamadouche@gmail.com

the laser particle size technique is used to compare some samples whose fine fractions are important. Grain-size parameters were calculated by using the equations of Folk [3]. The determination of grain size indices allows us to look for a quantitative expression of the grain size distribution and to try, among other things, to reconstruct the dynamics of sediment inputs [4].

3 Results

The overall observation of the spatial distribution of the sediments shows that the three granulometric parameters (Mean size, Sorting, Skewness) show differences between the shallows and the offshore (see Fig. 1). The results indicate that the average grain size tends to become finer offshore and the coarse particles are mainly observed on the shallows. On the other hand, globally, the sorting improves as the depths become more important. It is noted that the sorting becomes significantly worse near breakwaters in the study area.

Finally, the observation of the asymmetry of the grains shows that it tends, generally, towards the fines in the vicinity of the breakwaters.

4 Discussion

Results show that sediments tend to become finer offshore the studied area. However, it should be noted that grain size becomes larger near the breakwaters. This situation could be induced by strong mobilization of sediments in the swash zone (see Fig. 1). In addition, the observation of the sorting parameter shows that it improves markedly offshore because of the weakness of hydrodynamism which tends, generally, to become weaker offshore. Indeed, the friction of the waves on the bottom is more important on the nearshore than on the deep waters. On the other hand, it is important to emphasize that sorting becomes unfavorable in the vicinity of breakwaters. These results are consistent with those obtained from the analysis of mean grain size. The observed sorting near

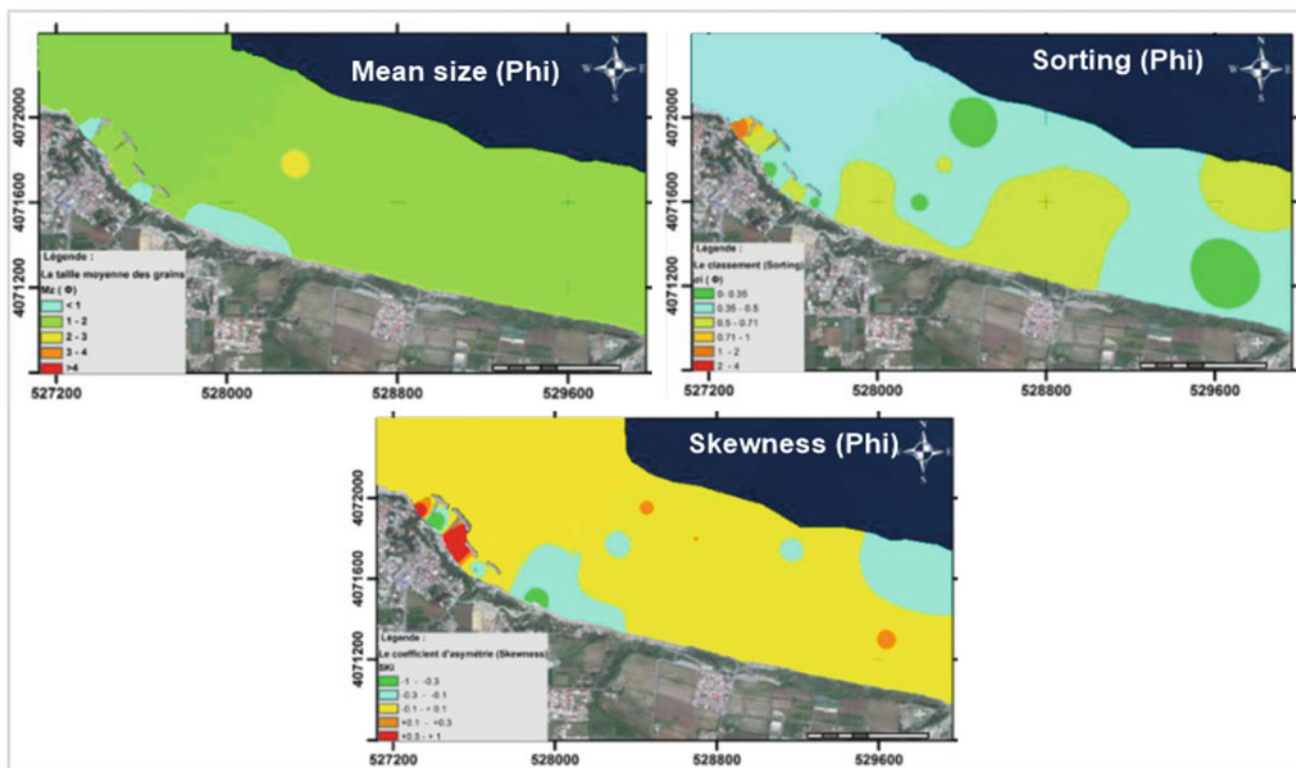


Fig. 1 Spatial variations of grain-size on the coast of Ain Taya

the tears could be dependent on the strong energy induced by the friction of the waves on the shoals. This probably explains why sediments could be transported from these unfavorable sorting areas to much better others. Indeed, the vector of sediments transport points from the higher sorting coefficient towards the lower sorting value [5].

5 Conclusion

This study highlights the importance of the grain analysis to understand the erosive energy of the waves near the breakwaters. The results indicate that these heavy structures disturb sedimentary dynamics and marine hydrodynamics. Therefore, the dimensioning of the coastal protection works should be grounded on the hydrosedimentary balance regulating the coastline and beaches. In addition, it is important to complete these results with meteorological conditions in order to have

a suitable understanding of the sedimentary dynamics based on spatial variations of the grain-size parameters.

References

1. Bouhamadouche, M., Hemdane, Y.: Erosion of a sandy coast: continuous follow-up of the coastal groynes of protection in Boumerdes (Algeria). *Environ. Earth Sci.* **75**(10) (2016). <https://doi.org/10.1007/s12665-016-5665-7>
2. Gao, S., Collin, M.B., Lanckneus, J., De Moor, G., Van Lancker, V.: Grain size trends associated with net sediment transport patterns: an example from the Belgian continental shelf. *Mar. Geol.* **121**(1994), 171–185 (1994)
3. Folk, R.L.: *Petrology of Sedimentary Rocks*, p. 182. Hemphili Publication, Company, Austin Texas (1974)
4. Chamly, H.: *Recherches sur la sédimentation argileuse en Méditerranée*. Thèse d'état, Univ. d'Aix-Marseille, 401 p. (1971)
5. Gao, S.: A Fortran program for grain-size trend analysis to define net sediment transport pathways. *Comput. Geosci.* **22**(4), 449–452, 199 (1995)

Recent Geochemical and Grain Size Distribution of Terrestrial Sediment in Coastal Area from the Watershed of Medjerda River, Gulf of Tunis

Thouraya Benmoussa, Oula Amrouni, Laurent Dezileau, Gil Mahé, Domenico Chiarella, and Saâdi Abdeljaouad

Abstract

The geochemical and grain size analysis were carried out on surface and down core sediments from the present-day alluvial-coastal plain of the Medjerda River, Gulf of Tunis, Tunisia. The aim of this paper is to characterize the geochemical and grain size distribution of sediments and its relationship with the hydrodynamics extreme events occurring during the last century. Using a multi proxy approach, six turbidities layers have been identified in down core sediment (i.e. TL-1, TL-2, TL-3, TL-4, TL-5, TL-6, TL-7 and TL-8) characterized by multimodal grain size distribution. The terrestrial sediment which feeds the northern coastal of the Gulf of Tunis is characterized by very fine-grained sediment (clay and silt). The geochemical signature shows a highly concentration of Rb, Ti, Zn and Pb. The Medjerda River is the mainly source of silts and clay sediment. Besides, the mining pollution (Zn and Pb) is relatively strong in the coastal area, especially during the great floods events of Medjerda watershed

recorded in the 1953; 1957; 1969 and 1973. Even during high frequency events, the sediments are devoid of any coarse fraction.

Keywords

Coastal • Medjerda river • Extreme floods
Turbidities layers • Mining pollution

1 Introduction

Rivers are sources of water for social and economic development with the alluvial plain of offering a relatively flat area for urban and agricultural activities. However, human societies have to deal with the fact that the flow of water in river basins is never constant. An often high flow of water during the extreme floods events is one of the more types of natural disasters. Moreover, the sediment leaching from the watershed causes coastal contamination through urban, industrial and agricultural discharges. Rivers are considered as the principal sediment delivery toward the marine environments and are closely depended on the climatic and the human pressure [1, 2]. The Medjerda River basin in NE-Tunisia is one of the largest basins in the northern zone of Africa. It is located in the northern bay of the Gulf of Tunis between 37°10'N–10°16'E and 37°55'N–10°18'E. The aim of the present study is to characterize the recent geochemical and grain size distribution of the terrestrial sediment in coastal area.

2 Settings and Analytical Methods

We collected short cores sediment core (CEM-1; 168 cm) at the new delta of Medjerda River. Six surface samples were collected at the coastal area (MED-2, MED-3, MED-North, O10, and O20) and the sediment deposits of the riverbanks of Medjerda (MED-1). The grain size analysis was carried

T. Benmoussa (✉) · S. Abdeljaouad
Laboratory of Energetic, Mineral Resources and Environment,
Faculty of Sciences of Tunis, University of Tunis El-Manar,
Tunis, Tunisia
e-mail: benmoussa_thouraya@yahoo.fr

O. Amrouni
Laboratory of Marine Environment, National Institute of Marine
Sciences and Technologies, Salammbô, Tunisia

L. Dezileau
Laboratoire Morphodynamique Continentale et Côtière,
University of Caen, Caen, France

G. Mahé
UMR HydroSciences Montpellier/IRD, Montpellier, France

D. Chiarella
University of London, Royal Holloway, Egham, TW20 0EX, UK

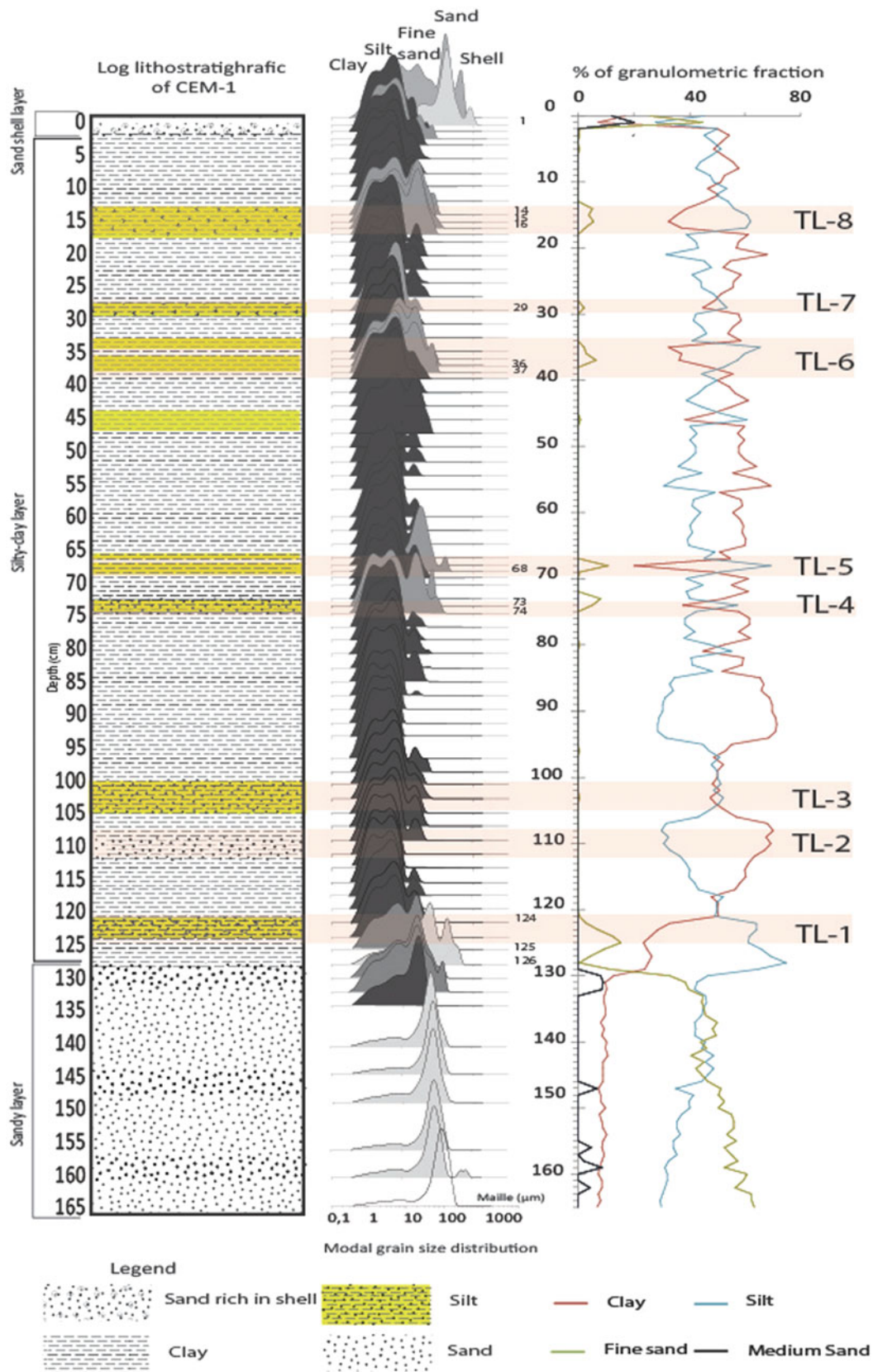


Fig. 1 The litho stratigraphic log description and grain size distribution on down core sediment. Unit-1: Major Sand layer facies; Unit-2: Major silt-clay facies; Unit-3: Major Sand/shell facies. TL-1, TL-2

TL-3 TL-4 TL-5 and TL-6: Turbidity layers formed by heterogeneous facies (Silt, Clay and sand)

out by using the Backman Coulter LS 13 320. A semi-quantitative geochemical analysis was performed by using the X-ray fluorescence (XRF) mobile. To flow the trace terrestrial sediment geochemically, the Zn/Fe; Pb/Fe and Zr/Fe inter-elements ratios have been used. This method provides the advantage to be insensitive to dilution and matrix effects [3].

3 Results

3.1 Spatial and Temporal Grain Size Distribution and Turbidities Layers Identification

3.1.1 Litho Stratigraphic and Sedimentological Description of Turbidity Layers

The results of the grain size distribution of down core sediment are summarized in the Fig. 1. The CEM-1 core sediment shows litho stratigraphic and grain size variability. The down core was roughly divided, from bottom to top, into three major units of granulometric facies: fine sand, silt-clay and medium sand/shell. In the silt-clay facies, 6 coarser turbidities layers are identified from TL-1, TL-2, TL-3, TL-4, TL-5, TL-6, TL-7 and TL-8. These TL layers consist of fine-grained sediments showing multimodal grain size distribution.

3.1.2 Spatial Grain Size Distribution

The Sand/Shell facies of CEM-1(0 and 1 cm depth) is characterized by multimodal grain size distribution. In particular, it is composed of medium sand (200–315 μm) and shells (1200 μm). The riverbanks deposits (MED-1) display medium sand with no occurrence of shell fractions. The sandy beach sediment (MED-2, MED-3 and MED-Nord) is characterized by unimodal grain size distribution with medium sand (250–315 μm). The submarine samples (O10 and O20) collected in the near shore zone display a unimodal grain size distribution with fine sand (100–125 μm).

3.2 Geochemical Tracer's Evolution of Sediment Sources

The geochemical evolution of sediment in the different environments is summarized in the Fig. 2. The Rb and Ti show strongly concentration in the river banks sediment, Flood deposits of Medjerda River and deltaic deposits (silt-clay unit of CEM-1. Pb and Zn have distinguished peaks at 125 cm; 35.56 and 259.36 ppm at 73 cm: 14.98 and 95.45 ppm at 68 cm: 98.96 and 174.91 ppm at 37 cm: 130.51 ad 185.13 ppm at 29 cm depth: 31.23 and 103.03 ppm and 16 cm depth: 20.86 and 110.94 ppm, respectively. The Zr shows a similar evolution compared to the calcium (Ca). in addition, the Zr is significantly

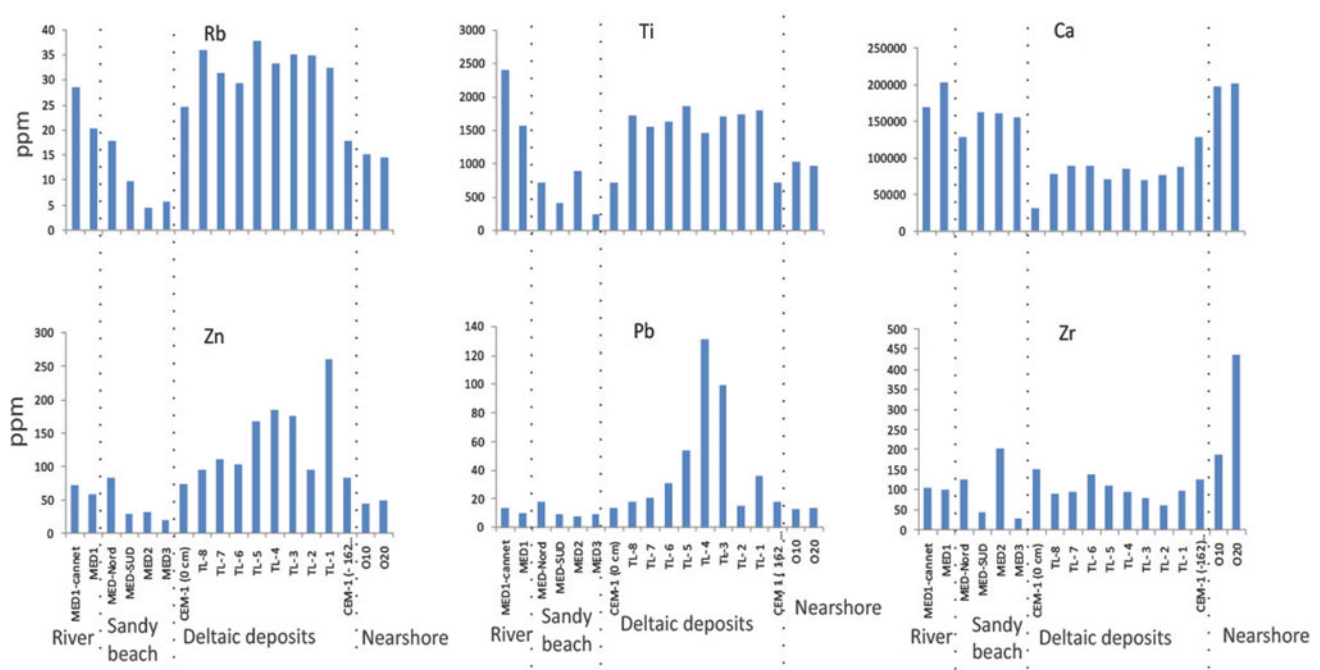


Fig. 2 The geochemical elements evolution of the Rubidium (Rb), the Titanium (Ti) the calcium (Ca), the Zinc (Zn), the Lead (Pb) and the Zirconium evolution in the sediments samples in the River, sandy beach, deltaic deposits and the nearshore of the Medjerda river coast

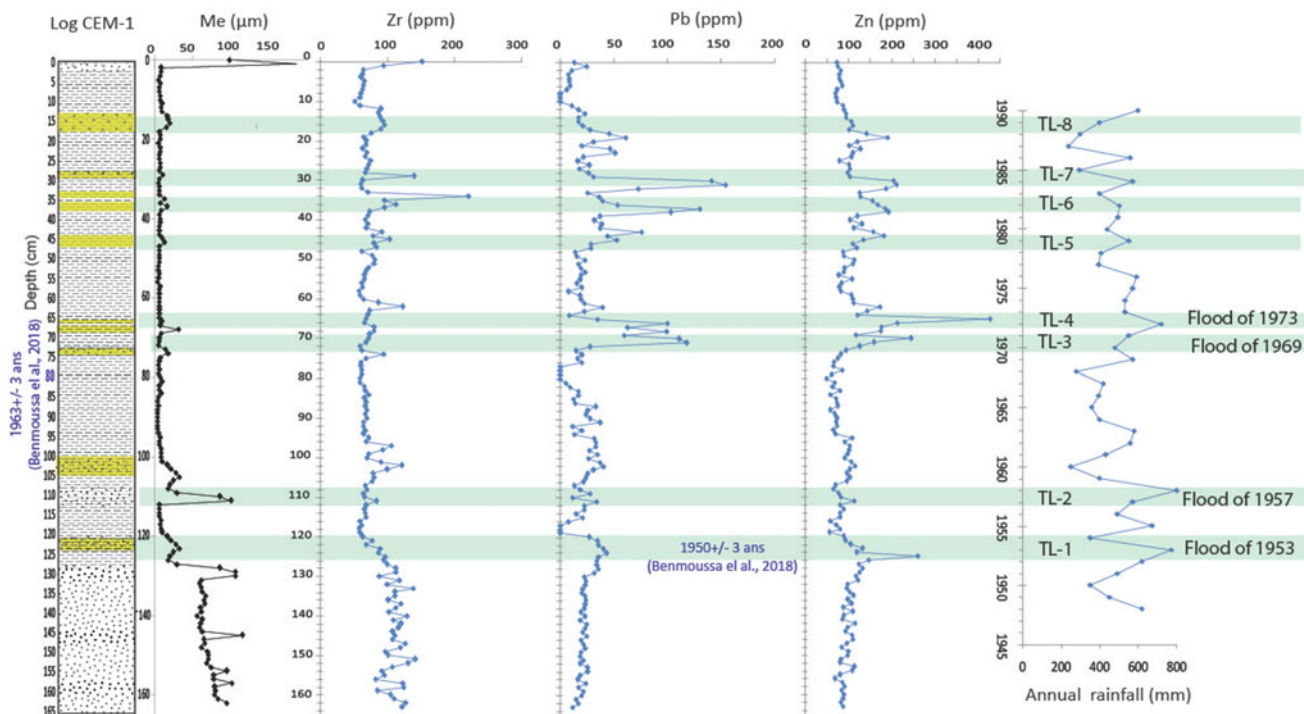


Fig. 3 The extreme floods identification based on litho stratigraphic log, median grain size (Me); geochemical elements concentration peaks and historical annual rainfall

important in the recent sandy beach (top of the CEM-1; 151.33 ppm) and the nearshore sediment (O10; 187.41 ppm and O20; 437.95 ppm). Finally, the Ca decreases from 200,346 in the nearshore sediment to 77,790 ppm in the turbidity layers.

4 Discussion

The grain size analysis of surface samples reveals that the coarser deposits present in river consist of heterogeneous medium sand. The sediment of sand beach and the near shore deposits are characterized by unimodal grain size distribution with medium sand. The deltaic deposit is mostly represented of heterogeneous multimodal sediment. However, the turbidity layers are characterized by multimodal grain size distribution. They are formed by three main grain size facies (clay, silt and very fine sand). The geochemical analysis of the surface and core sediments shows that the marine sediments source is represented by Ca and Zr and particularly the basal sand of cores. The Rb, Ti, Zn and Pb constitute the terrestrial sediment source. Silt and clay are generally rich in terrigenous elements. The level peaks of ETM (Pb, Zn) are associated with fine terrestrial sediment (clay and silt). The strongly concentration of Zr is associated with turbidity layers and the surf zone

deposits (O20). The Zr is generally associated with aeolian transport deposits [4]. Zr is a heavy metal that requires a strong dynamic energy to be mobilized in the coastal area. The multi proxy results (Fig. 3) reveal that the turbidity layers are characterized by terrestrial sediment source and strongly mining contamination of Zn and Pb. Accordingly, we associate the turbidity layers with high floods events. Based on previous results of [5] completed by the historical annual rainfall, we associate the TL-1; TL-2; TL-3 and TL-4 to four exceptional floods of Medjerda (1953, 1957, 1969 and 1973) (Fig. 3). These events caused the leaching of old mining discharges into the Medjerda watershed responsible for the coastal sediment contamination of Pb and Zn since 1950.

5 Conclusion

The terrestrial sediment which feeds the northern coast of the Gulf of Tunis is characterized by the very fine-grained sediment (clay and silt). The geochemical signature of the terrestrial sediment is characterized by highly concentration of Rb, Ti, Zn and Pb. The Medjerda River is the mainly source of silts and clay sediment for the northern coast of the Gulf of Tunis. Even during high frequency events, the sediments are devoid of any coarse fraction. Besides, the mining pollution

(i.e. Zn and Pb) is relatively strong in the coastal area especially during the great floods episodes of watershed leaching of Medjerda River.

References

1. Flemming, B.W., Hansom, J.D.: Estuarine and coastal geology and geomorphology—A synthesis, In: Wolanski, E., McLusky, D.S. (eds.) *Treatise on Estuarine and Coastal Science*, vol. 3, pp. 1–5. Academic Press, Waltham (2011)
2. Syvitski, P.M., Kettner, A.: Sediment flux and the anthropocene. *Phil. Trans. R. Soc. A* **369**, 957–975 (2011). <https://doi.org/10.1098/rsta.1010.0329>
3. Croudace, I.W., Rindby, A., Rothwell, R.G.: ITRAX: description and evaluation of a new multi-function X-ray core scanner. *Spec. Publ. Geol. Soc. Lond.* **267**, 51–63 (2006)
4. Affouri, A., Dezileau, L., Kallel, N.: Extreme flood events reconstruction during the last century in the El Bibane lagoon (Southeast of Tunisia): a multi-proxy approach, *Clim. Past Discuss.* (2016). <https://doi.org/10.5194/cp-2016-40>
5. Benmoussa, T., Amrouni, O., Dezileau, L., Mahe, G., Saâdi, A.: Impact of the Medjerda Sedimentary Fluxes on the Morphodynamic Equilibrium of the Northern Coast of the Gulf of Tunis (Medjerda-Raoued coast), *PIAHS*, vol. 377. Port Elizabeth, South Africa (2018). <https://doi.org/10.5194/piahs-377-77-2018>

Multidisciplinary Approaches for the Study of Sediment Discharges to the Mediterranean Sea to Mitigate the Impact of Climate and Anthropogenic Activities on Coastal Environments

Oula Amrouni, Gil Mahé, Saâdi Abdeljaouad, Hakim Abichou, Abdallah Hattour, Nejmeddine Akrouf, Chrystelle Bancon-Montigny, Thouraya Benmoussa, Kerim Ben Mustapha, Lassâad Chouba, Domenico Chiarella, Michel Condomines, Laurent Dezileau, Claudine Dieulin, Nadia Gaaloul, Ahmed Ghadoum, Abderraouf Hzami, Nabil Khelifi, Samia Khsiba, Fatma Kotti, Mounir Medhioub, Hechmi Missaoui, François Sabatier, Alberto Sánchez, Alessio Satta, Abdelaziz Sebei, and Wième Ouertani

Abstract

The present work is based on The RYSCMED project supported by PHC-UTIQUE 2016–2018 (16G 1005–34854QC). The RYSCMED is an interdisciplinary project which gathers different disciplines (e.g. sedimentology, hydrology, geochemistry, ecology, paleontology, biochemistry, archeology) to quantify the sediment flow of the land-sea. This research aims at identifying coastal sediment dynamics (via the sand supply sources; i.e.

Medjerda River) and hydrodynamic parameters to understand the local environmental problems in an urbanized coastal framework. The outcome is expected to produce original and new findings about the link between dams, river hydrology and sediment origin to the sea with the impact of climate and anthropogenic activities on the coastal geomorphology and ecosystem sensitivity. The main scientific outcome will be addressed to the socio-economic actors to implement necessary solutions for remediating the Mediterranean coastal vulnerability.

O. Amrouni (✉) · A. Hattour · K. B. Mustapha · L. Chouba
A. Hzami · S. Khsiba · H. Missaoui · W. Ouertani
National Institute of Marine Science and Technologies, 2025
Salammbô, Tunis, Tunisia
e-mail: oula.amrouni@instm.mrt.tn; ; oulaamrouni@gmail.com

G. Mahé · C. Dieulin · F. Kotti
UMR HydroSciences Montpellier, IRD, 34090 Montpellier,
France

S. Abdeljaouad · N. Akrouf · T. Benmoussa · N. Gaaloul
A. Sebei
Faculty of Sciences, Campus Universitaire 2092, Tunis, Tunisia

H. Abichou
Faculty of Human and Social Sciences of Tunis, University
of Tunis, Tunis, Tunisia

C. Bancon-Montigny
University of Montpellier, 34090 Montpellier, France

D. Chiarella
Department of Earth Sciences, Royal Holloway, University
of London, Egham, TW20 0EX, UK

M. Condomines · L. Dezileau
University of Caen-Normandie, 14032 CAEN cedex 5, Caen,
France

Keywords

RYSCMED · Mediterranean · Medjerda River ·
Sediment · Coast · Sensitivity

A. Ghadoum
Department of Underwater Archaeology, National Institute
of Cultural Heritage, Tunis, Tunisia

N. Khelifi
GEOMAR Helmholtz Center for Ocean Research Kiel, 24148
Kiel, Germany

M. Medhioub
Sfax University, 3029 Sfax, Tunisia

F. Sabatier
Aix-Marseille University, SCHUMAN, 13628 Aix-en-Provence,
France

A. Sánchez
Centro Interdisciplinario de Ciencias Marinas, La Paz, Baja
California Sur, Mexico

A. Satta
University of Cagliari, DICAAR, Via Marengo 2, 09123 Cagliari,
Italy

1 Introduction

The coastal areas of the Mediterranean Sea are densely inhabited and produce a valuable part of the national incomes of many countries. However, land-sea areas have suffered since the last 100 years from increased salinity, changes in geomorphology, coastline regression, coastal biodiversity reduction and increased pollution of ecosystems mostly driven by the high number of dams which reduce water and sediment flows to the sea by storing a great part of them inland. This situation is worsened by both a sustained rainfall reduction and the sea-level rise due to the worldwide temperature increase. Indeed, Mediterranean areas are among the most vulnerable environments in the world due to the potential impact of climate changes [1, 2]. In this scenario, North Africa and the Middle East are the most vulnerable areas [3, 4] in the face of this global problem. They urgently need a protection of their coastal landscapes.

Many initiatives have been developed in recent years to improve the knowledge on this rapidly changing overpopulated environment and to enhance an international cooperation around the Mediterranean. However, only few programs deal with the full continuum from the river basins to the coastline. They still less involve many countries from the South and East Mediterranean regions.

Hence, multidisciplinary approaches for the study of sediment discharges to the Mediterranean Sea to mitigate the impact of climate and anthropogenic activities on coastal environments should contribute to a better understanding of the coastal areas.

The RYSCMED project has been implemented in the pre-estuarine and coastal field of the most driven river, i.e. the Medjerda in the bay of the Gulf of Tunis (Western Mediterranean, Tunisia) (Fig. 1). Actually, the low Medjerda Delta, which is the main agricultural region in Tunisia and hosting industrial and fishing activities, is perceived as

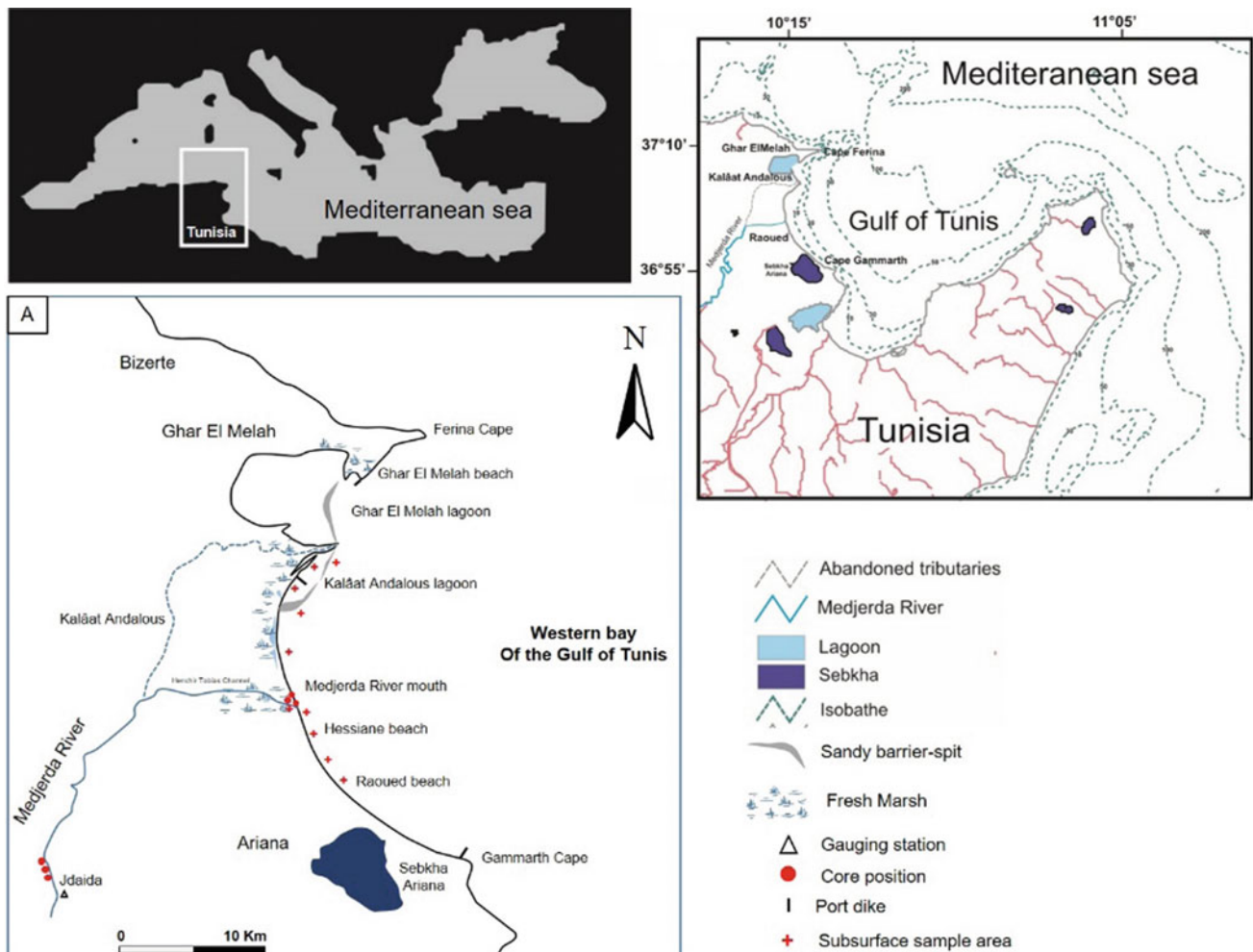


Fig. 1 The location map of the study field area of the depositional deltaic system of Medjerda River, western bay of the Gulf of Tunis (Tunisia, Mediterranean). A/Sampling position of the core and coastal subsurface sediment reconstruction

the highly vulnerable area to sea-level rise scenario. The main tributary system of the Medjerda River discharges up to 30 g.l^{-1} of sediment load during floods for an annual total of 20,400 tons of which 10% is composed of sand [5]. However, the sedimentary contributions to the coastal zone from the Medjerda River is still unknown. It is also the aim of the RYSCMED project to provide the quantitative amount of sediment yield from the Medjerda River to the sea via the coastal zone during the last 50–100 years.

2 Methods

We propose to analyze the sediment inlet fluctuation in regard of events recorded on the inland basins: dam constructions, changes in agricultural practices and in population in order to create a sediment transfer model to the sea.

The used data used are based on sediment discharges from large rivers and sediment subsurface samples and three cores in the pre-estuarine zone, downstream of the last dams and far enough three cores from the coast to avoid marine influence in order to assess the impact of the reduction of sediment transport from the upper basins to the coastal area since the past 50–100 years (Fig. 1a).

The River mouth nearshore, lagoon and dredged sediment were subject to sedimentological, mineralogical, geochemical and floristic analyses (campaign carried out from 2016 to 2018). Sedimentological multi approaches were based on the identification of different Sedimentary Types (ST). Accordingly, grain size indexes (i.e., Mz, SKI and Ku), Sediment Trend Analysis (STA) modeling tools were applied to define the seasonal sediment transport pathways throughout the nearshore of the Medjerda Delta. Both sediment cores were subjected to multiproxy approaches (major and trace elements and dating radiometric ^{210}Pb and ^{137}Cs). Surface sediment of the Medjerda River and nearshore sediment undertook geochemical study.

The evolution of the coastline of Medjerda was also estimated by satellite images carried out from SPOT1, SPOT4 and Sentinel A2 imageries (from 1936 to 2016 surveys). They were completed by the aerial and topographic surveys (missions: 1900, 1936, 1948, 1952, 1974, 1984, 1988, 1999 and 2016). The lagoon system of Kalâat Andalous (and the fishing harbor inside) was subject to ecosystemic study. We also used Fauna and flora as biologic tools to characterize physical and chemical parameters of coastal and paralic environments. The investigations were based on the study of the sedimentological facies, a floristic (Environmental Quality Ratio of macrophytes, EXCLAME index), faunistic identification and geochemical analysis (As, Cd, Cr, Cu, Ni, Pb, Zn).

3 Results

3.1 Hydroclimatic and Sedimentological Evolution

The result of the lower valley and the coastal area cores' analysis show a succession of sedimentary layers that likely correspond to different flood deposits that succeeded on this site. The dating with Pb and Cs of the cores shows that the selected area is an important deposition area. The thickest layers of sedimentary deposits were related to the exceptional events. They are mainly concentrated on the lower part of the core and are predominantly composed of sands. Since the construction of the Sidi Salem dam in 1981, all cores presented mostly a succession of small layers of fine material (silt or clay) without any sand deposits in the downstream river bed. A strong decrease in the accumulation rate of sediment was observed based on the length of the flood units and the number of years between flood events. A lower sedimentation rate (about 2.3 cm y^{-1}) is observed between 1982 and 2015 while it was much more important between 1963 and 1981 (about 4.75 cm y^{-1}) and around 10 cm.y^{-1} between 1950 and 1962 (Fig. 2a).

Sedimentological results show a fluvial dominance marked by silt and clay deposits rich in terrigenous chemical elements since the 1950. Seasonal nearshore sediment dynamics show that grain size distribution (GSD) and Sediment Trend Analysis (STA) model pathways are determined by cross-shore geomorphology, location of the sediment-cell, seasonal incident wave and local terrestrial supply.

The geochemical signature shows a highly concentration of Rb, Ti, Zn and Pb. Sediment deposit facies associated to the geochemical component and the $^{137}\text{Cs}/^{210}\text{Pb}$ radiometric dating of recent alluvial deposits confirm the shoreline retreat due to terrestrial sediment reduction (Fig. 2b).

3.2 Temporal Evolution of the Shoreline

The temporal shoreline evolution is established according to the aerial surveys from 1900 to 2016. Although the general trends of the shoreline reveal an increased rate, the meso-scale qualitative monitoring displays a nonlinear shoreline and plain flood evolution. Three periods can be individualized:

1. The natural beach progression between 1900 and 1952
2. The shoreline progression at the mouth of the new artificial channel from 1952 to 1981 ($+13 \text{ m} \pm 0.15 \text{ m y}^{-1}$)

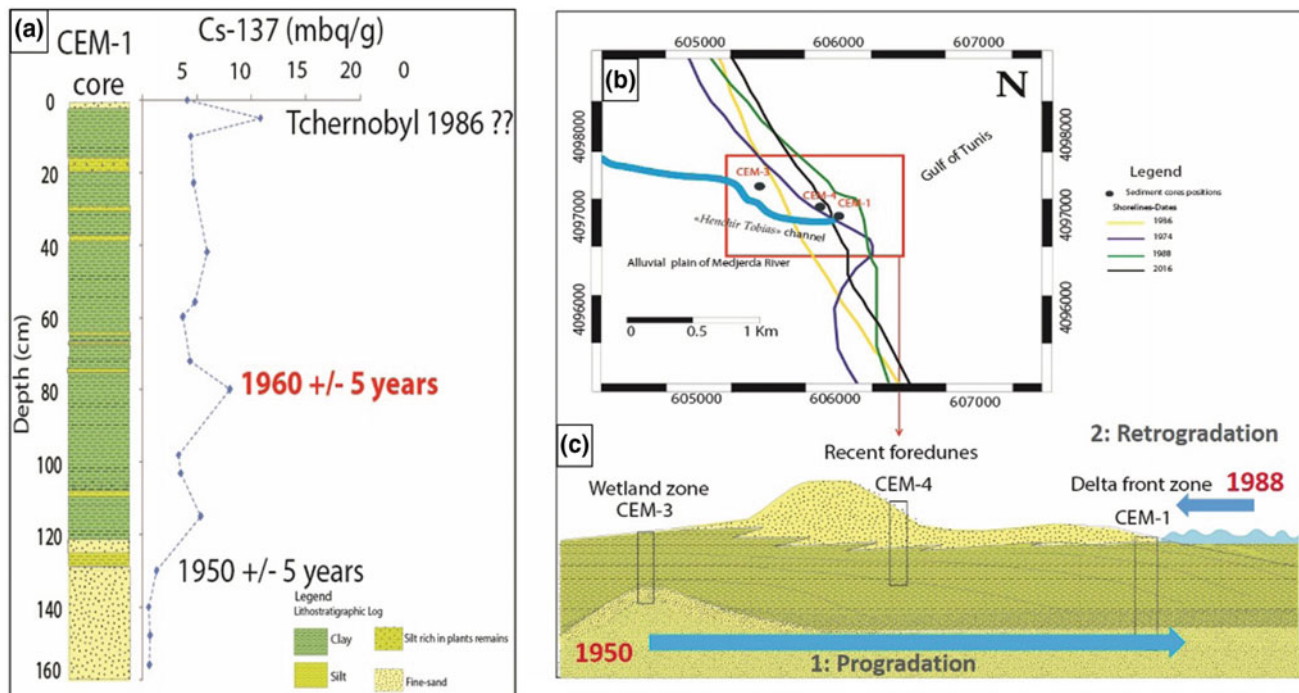


Fig. 2 a The downcore grain size distribution of the CEM-1 carried out on the delta front and the geochronology by using ^{137}Cs activity-depth profiles. b The shoreline evolution analysis at the mouth of the new Medjerda River during the 1936–2016 period. c The diagram

synthesis of morphological changes involving the development and the retrogradation of the new delta of Medjerda River during the XXth century

3. The shoreline retreat rate after the man-made construction comprised between 1981 and 2016 ($-20 \text{ m} \pm 0.15 \text{ m y}^{-1}$). The progradation and retrogradation of the Medjerda Delta during the XXth century is strongly influenced by an anthropogenic factor (Fig. 2c).

3.3 Ecological Study of the Wetland System

Spatial Kalâat Andalous sediment distribution revealed that the central lagoon area is dominated by fine sand and silty sediments. Medium sand is located mainly on the north and at the south-eastern part of the lagoon. Floristic study revealed the existence of 12 species among which five reference species whose percentage is equal to 26%. Reference species are *Cymodocea nodosa*, *Zostera nolti* (marine phanerogams), *Cystoseira barbata*, *Cystoseira compressa*, *Dictyota dichotoma* (macrophytes; brown algae). This low percentage may reveal an environment quality loss and an eutrophication of the lagoon water. The latter is proved by the EXCLAME index which is equal to 0.24 indicating that the lagoon water is in a poor state. The study of microfauna and specially foraminifera has permitted to distinguish several associations related to hydrodynamic context. Some are of coastal marine affinity. Others are more tolerant to stress

conditions. The richness of the reworked species in some samples of the lagoon denotes a strong continental impact in this humid area.

Dredged sediment of Kalaât Andalous lagoon are dominated by silts and clays, dark black in colour and relatively enriched in organic matter (with a TOC value of 1.30%) and sulphur compounds. However, the sediments are moderately contaminated by inorganic and organic pollutants except for Cd which is present in relatively highly amounts (2.85 ppm) over the standard amounts generally found in the sediment.

3.4 Geochemical Characterization of the Delta-Coast Sediment Yield

The trace metals (Zn, Cd, Cu, Cr and Ni) analysed in sub-surface sediments along the Medjerda River tributaries and along the coast are relatively high. Lead contents vary from 12 to 46 ppm. The zinc concentrations vary from 2 to 71 ppm while the cadmium concentrations vary from 0.56 to 4 ppm (mean of 1.2 ppm). The chromium contents are between 46 and 178 ppm (mean of 98 ppm). The copper contents vary from 27 to 67 ppm while the nickel concentrations vary from 14 to 51 ppm (mean of 30 ppm). The Kalâat Andalous lagoon-habour sediment reveals a variable concentration of the MTE component (Al, Fe, Zn, Ni, Co,

Cu et Pb, As) which respectively varies from 0,5 to 5,5%; 0,8 to 2,5%; 29 to 158 ppm; 7 to 29 ppm; 2 to 9 ppm; 3 to 31 ppm, 7 to 70 ppm and 4 to 15 ppm.

4 Discussion

The RYSCMED project outcomes confirm a variable sensitivity of the deltaic transition area of the sea-level rise. Morphosedimentary quantitative distribution reveals a change in the fluvial deposits facies feeding the deltaic plain with a decreasing grade and shortage of the sedimentary inputs towards the sea [6]. About 10 dams have been created on the Medjerda basin, among which the largest one is Sidi Salem, with more than 1 billion m³ not far from the sea. This has a major impact on the hydrosedimentary regime downstream and undergone significant changes in the morphology of the lower depositional deltaic valley and the coastal area (i.e., reduction in average rates and in volumes of solid transport, altered pattern of seasonal flows).

Sedimentological studies indicate that the western bay of the Gulf of Tunis is characterized by two sediments facies: (i) mud coming from the discontinuous supplies of rivers and (ii) sandy sediments originating from the continuous reworking of erosion of the cliffs and coastal drift throughout beach during storm events.

The dominance of clay deposits over sandy facies on the beaches results from the impact of the dam construction. Only the finer grain size fractions can feed the coast. The actual sediment balance of the Gulf of Tunis coast shows a shoreline retreat under the coarser sediment deficit blocked by upstream dam construction [7]. Archaeological surveys and remains around the site of the ancient paleo bay of Utica, the eldest sister of Carthage, confirm a rapid change and shift in the shoreline [8].

That initiates a regressive sequence of deltaic deposits over spatial and temporal variability in facies and process in response to the fluvial and the marine controls [9].

The textural facies of the coastal system sandy components (river mouths, sandy spits, submarine sandbars) are modified towards very fine to silty sediments. They become contaminant traps. Fluvial inputs, reduced in volume and size, work as a pollutant vector (trace elements) to adjacent beaches through coastal currents. The contaminant burden to protected areas (lagoon, bays) is related to the anthropogenic and natural component inputs. The heavy metals present in river-coast sediment have two origins: a natural source “natural background” and an anthropogenic origin. The high levels detected are mainly related to human activities (i.e., mining activities) [10]. The study of wetland ecosystems

associated to estuary areas via biotops and biocenosis showed the high degree of coastal ecosystem sensitivity to human activities.

5 Conclusion

The reduction in sediment discharge to the littoral caused by the dam is the principal cause of the negative sediment budget leading to a shortage of sand sediment on the coast closest to the delta and to the dominant erosion of the coastline. The nearshore enrichment of mud particles carried by waves and tide current contaminates strongly the coastal ecosystem.

The vulnerability of the coastal areas to the sea-level rise will be better addressed due to the new integrated approach of the sediment yields. The link with the experience of the Tunisian and French observatories will help the countries to develop Mediterranean environmental monitoring on the long term, which is crucial to provide answers to a large array of environmental questions, in relation with socio-economic and governance issues. The focused goal of the RYSCMED outcome is addressed to the implantation of Nature Based Solution to enhance urbanized Tunisian coast resilience.

References

1. WCRP: The World Climate Research Programme Accomplishment Report (2013)
2. Saab, N., Sadik, A. (eds.): AFED: Arab Environment: Sustainable Development in a Changing Arab Climate. Annual Report of Arab Forum for Environment and Development, Beirut, Lebanon. Technical Publications (2016)
3. I.H.E.E., Ingénierie de l'Hydraulique, de l'Équipement et de l'Environnement, 2007. Etude de la vulnérabilité environnementale et socio-économiques du littoral tunisien face à une élévation accélérée du niveau de la mer due aux changements climatiques et identification d'une stratégie d'adaptation. Ministère de l'Environnement et du Développement Durable. Rapport définitif, Phase I (2007)
4. El Raey, M.: Impact of Sea Level Rise on the Arab Region (2012)
5. Esonni, N.: Etude de la dynamique des sels nutritifs et des métaux lourds en relation avec relation avec la sédimentologie et l'hydrodynamique dans le large du Golfe de Tunis. Thèse de Doct., Univ. Tunis II, Fac. Sci. de Tunis, p 229 + annexes (1998)
6. Kotti, F., Dezileau, L., Mahé, G., Habaieb, H., Bentkaya, M., Dieulin, C., Amrouni, O.: Etude de l'impact des barrages sur la réduction des transports sédimentaires jusqu'à la mer par approche paléohydrologique dans la basse vallée de la Medjerda. Proc. IAHS 377, 67–76 (2018)
7. Hzami, A., Amrouni, O., Romanescu, G., Stoleriu, C.C., Mihu-Pintilie, A., Abdeljaouad, S.: Satellite images survey for

- the identification of the coastal sedimentary system changes and associated vulnerability along the western bay of the Gulf of Tunis (northern Africa). *Proc. IAHS* **377**, 83–89 (2018)
8. Delile, H., Abichou A., Gadhoun A., Goiran J-Ph., Pleuger E., Montchambert J-Y., Wilson A., Fentress E., Quinn J., Ben Jerbania I., Ghazzi F.: The geoarchaeology of Utica, Tunisia: the paleogeography of the mejerda delta and hypotheses concerning the location of the ancient harbor. *Georhcaeology Int. J.* **30**, 291–306 (2015)
 9. Benmoussa, T., Amrouni, O., Dezileau, L., Mahé, G., Abdeljaouad, S.: The sedimentological changes caused by human impact at the artificial channel of Medjerda-River (Coastal zone of Medjerda, Tunisia). *Proc. IAHS* **377**, 77–81 (2018)
 10. Helali, M.A., Added, A., Zaaboub, N., Oueslati, W.: Géochime des métaux lourds dans les sédiments marins de surface du delta de l'Oued Medjerda. *RME* **3**, 487–498 (2009)